

GEOPHYSICAL SURVEY REPORT - ARTIFICIAL ISLAND AREA OF INVESTIGATION

103783-ENN-MMT-SUR-REP-SURWP AEI
REVISION A | FOR USE
APRIL 2022

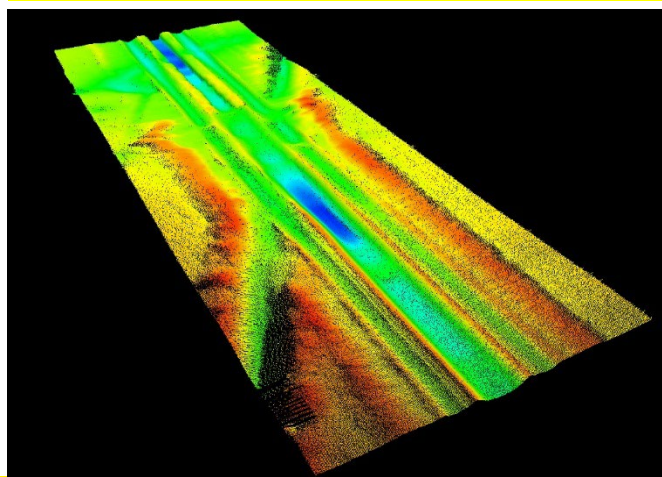


ENERGINET

ENERGY ISLANDS - NORTH SEA ARTIFICIAL ISLAND

GEOPHYSICAL SURVEY FOR OFFSHORE
WIND FARMS AND ENERGY ISLAND

NORTH SEA
MAY-AUGUST 2021



REVISION HISTORY

REVISION	DATE	STATUS	CHECK	APPROVAL	CLIENT APPROVAL
A	2022-04-20	Issue for Use	DP	KG	
02	2022-01-17	Issue for Client Review	DO	KG	
01	2022-01-16	Issue for Internal Review	DO	KG	

REVISION LOG

DATE	SECTION	CHANGE
2022-04-20	Various	As per client comments received on 2022-02-17.

DOCUMENT CONTROL

RESPONSIBILITY	POSITION	NAME
Content	MMT Senior Data Processor	Andrew Stanley / Clayton Summers / Chris Bulford
Content	MMT Geologist	Jack Turner / Jeshua Guzman Castro
Content	MMT Senior Geologist	Sophie Clark
Content	MMT Project Geophysicist	Gerald Bishop / Hanna Åkerblom
Content	GeoSurveys Interpreter Reviewer / Principal Interpreter	Ana Maia
Content	GeoSurveys Onshore Team Coordinator	Bruno Simao
Content	GeoSurveys Deputy Project Manager	Miguel Oliveira
Content	Geosurveys Project Manager / Deputy Project Manager	Henrique Duarte / Jhonny Miranda
Content / Check	MMT Project Report Coordinator	David Oakley / Darryl Pickworth
Check	MMT Document Controller	Pontus Frost / Rebecca Österberg
Approval	MMT Project Manager	Karin Gunnesson

TABLE OF CONTENTS

1 	INTRODUCTION.....	15
1.1	PROJECT INFORMATION	15
1.2	SURVEY INFORMATION	17
1.3	SURVEY OBJECTIVES	17
1.4	SCOPE OF WORK	17
1.4.1	DEVIATIONS TO SCOPE OF WORK	18
1.5	PURPOSE OF DOCUMENT	18
1.6	REPORT STRUCTURE	18
1.6.1	GEOPHYSICAL SURVEY REPORT	19
1.6.2	CHARTS	19
1.7	REFERENCE DOCUMENTS	20
1.8	AREA LINE PLAN	22
1.8.1	2D UHRS REFERENCE LINES.....	22
1.8.2	2D UHRS MAIN AND CROSS LINES	24
1.8.3	GEOPHYSICAL MAIN AND CROSS LINES	25
1.8.4	SURVEY BLOCKS.....	26
2 	SURVEY PARAMETERS	28
2.1	GEODETIC DATUM AND GRID COORDINATE SYSTEM	28
2.1.1	ACQUISITION.....	28
2.1.2	PROCESSING	28
2.1.3	TRANSFORMATION PARAMETERS	28
2.1.4	PROJECTION PARAMETERS	29
2.1.5	VERTICAL REFERENCE	29
2.2	VERTICAL DATUM.....	30
2.3	TIME DATUM.....	31
3 	SURVEY VESSELS	32
3.1	M/V NORTHERN FRANKLIN.....	32
3.2	M/V RELUME	33
3.3	OPERATIONAL SUMMARY	34
4 	DATA PROCESSING AND INTERPRETATION METHODS	36
4.1	BATHYMETRY	36
4.2	BACKSCATTER.....	40
4.3	SIDE SCAN SONAR	40
4.4	MAGNETOMETER	42
4.5	SEISMIC - 2D UHRS	45
4.6	SUB-BOTTOM PROFILER - INNOMAR.....	45
5 	PROCESSED DATA QUALITY.....	48
5.1	BATHYMETRY DATA	48
5.2	BACKSCATTER DATA	57
5.3	SIDE SCAN SONAR DATA	62
5.4	MAGNETOMETER DATA.....	66

5.5	SEISMIC 2D UHRS DATA QUALITY ANALYSIS	67
5.5.1	FEATHERING	69
5.5.2	SIGNAL & NOISE ANALYSIS.....	69
5.5.3	SOURCE RECEIVER OFFSETS.....	72
5.5.4	STREAMER GROUP BALANCING	73
5.5.5	INTERACTIVE VELOCITY ANALYSIS.....	74
5.5.6	CDP FOLD	75
5.5.7	BRUTESTACK	76
5.5.8	GEOM OUTPUT	77
5.6	SEISMIC 2D UHRS DATA PROCESSING OFFICE.....	78
5.7	SUB-BOTTOM PROFILER DATA – INNOMAR	78
6 	BACKGROUND DATA AND CLASSIFICATIONS	81
6.1	SEABED GRADIENT CLASSIFICATION	81
6.2	SEABED SEDIMENT CLASSIFICATION	81
6.3	SEABED FEATURE / BEDFORM CLASSIFICATION	83
6.4	SUB-SEABED GEOLOGY CLASSIFICATION	85
6.5	GRAB SAMPLE CLASSIFICATION.....	91
7 	GEOLOGICAL FRAMEWORK.....	92
8 	RESULTS.....	97
8.1	GENERAL	97
8.2	BATHYMETRY.....	97
8.2.1	PROFILE 1	100
8.2.2	PROFILE 2.....	102
8.2.3	SLOPE ANALYSIS.....	104
8.3	SURFICIAL GEOLOGY AND SEABED FEATURES.....	108
8.3.1	SEABED SEDIMENTS.....	108
8.3.2	MOBILE SEDIMENTS.....	111
8.3.3	BOULDERS	115
8.3.4	TRAWL MARKS.....	116
8.3.5	OTHER - AREAS OF INTEREST	118
8.4	CONTACTS AND ANOMALIES.....	119
8.5	EXISTING INFRASTRUCTURE (CABLES AND PIPELINES)	120
8.6	SEISMOSTRATIGRAPHIC INTERPRETATION	123
8.6.1	SUB-SEABED GEOLOGY – GEOMODEL	123
8.6.2	SEISMIC UNIT U05	130
8.6.3	SEISMIC UNIT U10	132
8.6.4	SEISMIC UNIT U20	139
8.6.5	SEISMIC UNIT U25	147
8.6.6	SEISMIC UNIT U30	156
8.6.7	SEISMIC UNIT U35	162
8.6.8	SEISMIC UNIT U40	169
8.6.9	SEISMIC UNIT U50	177
8.6.10	SEISMIC UNIT U60	177

8.6.11	SEISMIC UNIT U70	183
8.6.12	SEISMIC UNIT U85	192
8.6.13	SEISMIC UNIT U90	198
8.6.14	SEISMIC UNIT UKS.....	204
8.6.15	BASE SEISMIC UNIT BSU	214
8.6.16	SUMMARY AND DISCUSSION.....	216
8.7	SEABED HAZARDS	217
8.7.1	GRADIENTS	217
8.7.2	MOBILE SEDIMENT AND BEDFORMS.....	217
8.7.3	BOULDERS	217
8.7.4	EXISTING INFRASTRUCTURE AND WRECKS	218
8.8	SUB-SEABED HAZARDS.....	218
8.8.1	SEDIMENT DEFORMATION.....	218
8.8.2	BURIED CHANNELS AND TUNNEL VALLEYS.....	234
8.8.3	SOFT SEDIMENTS AND ORGANIC-RICH DEPOSITS.....	237
8.8.4	COARSE SEDIMENTS / GRAVEL BEDS / BOULDERS	251
8.8.5	TILL DEPOSITS.....	255
8.8.6	FLUID FLOW AND GAS FEATURES.....	255
8.8.7	LACUSTRINE SEDIMENTS	256
8.9	ARCHAEOLOGY CONSIDERATIONS.....	259
8.10	GRAB SAMPLE SUMMARY	259
9	CONCLUSIONS.....	262
10	RESERVATIONS AND RECOMMENDATIONS	264
11	REFERENCES.....	265
12	DATA INDEX	268

APPENDICES

APPENDIX A	LIST OF PRODUCED CHARTS.....	270
APPENDIX B	CONTACT AND ANOMALY LIST	270
APPENDIX C	GRAB SAMPLE LAB REPORT	270
APPENDIX D	2D UHRS PROCESSING REPORT	270

LIST OF FIGURES

<i>Figure 1 Overview of survey scopes performed.....</i>	<i>16</i>
<i>Figure 2 Line plan – 2D UHRS reference lines</i>	<i>23</i>
<i>Figure 3 Line plan – 2D UHRS main and cross lines.....</i>	<i>24</i>
<i>Figure 4 Line plan - geophysical main and cross lines within the Artificial Island survey area.....</i>	<i>25</i>
<i>Figure 5 Overview of survey block divisions within the Artificial Island survey area.....</i>	<i>26</i>
<i>Figure 6 Overview of the reporting tiles within the Artificial Island survey area.</i>	<i>27</i>
<i>Figure 7 Overview of the relation between different vertical references.</i>	<i>30</i>

Figure 8 M/V Northern Franklin	32
Figure 9 M/V Relume	33
Figure 10 Workflow MBES processing	37
Figure 11 Example of division of MBES data acquisition in BM3 and BM4	38
Figure 12 Artificial Island survey area contour export parameters	39
Figure 13 Exported contours with 50 cm interval over the Artificial Island survey area	39
Figure 14 Workflow side scan sonar processing (1 of 2)	41
Figure 15 Workflow side scan sonar processing (2 of 2)	42
Figure 16 Data example for Northern Franklin from B3	43
Figure 17 Data example for Relume from B3	43
Figure 18 Workflow MAG processing (1 of 2)	44
Figure 19 Workflow MAG processing (2 of 2)	44
Figure 20 Workflow SBP processing (1 of 2)	46
Figure 21 Workflow SBP processing (2 of 2)	47
Figure 22 Cross section through the Artificial Island survey area	49
Figure 23 Standard deviation at 95% confidence interval for the Artificial Island survey area	50
Figure 24 Example of MBES data acquired in good weather with a relatively stable sound velocity ...	51
Figure 25 Example of MBES data acquired in area with variable sound velocity	52
Figure 26 QC surfaces highlighting steep slopes in the Artificial Island survey area	53
Figure 27 Total Vertical Uncertainty surface for the Artificial Island survey area	54
Figure 28 Total Horizontal Uncertainty surface for the Artificial Island survey area	55
Figure 29 Example of anomaly in MBES caused by pycnocline	56
Figure 30 Overview of backscatter normalised values for the MMT OWF survey area	58
Figure 31 Backscatter mosaic with artefacts within the Artificial Island survey area	59
Figure 32 Outer beam busts visible in the Relume data, within the Artificial Island survey area	60
Figure 33 Beam busts caused by excessive vessel motion and/or bubble entrainment	61
Figure 34 Example of good high frequency SSS data from block BM01	62
Figure 35 Example 1 high frequency SSS data from BM01 displaying a striping effect	63
Figure 36 Example 2 high frequency SSS data from BM01 displaying a striping effect (highlighted) ..	63
Figure 37 Example of high frequency SSS data from BM01 displaying a pycnocline	64
Figure 38 Example of high frequency SSS data from BM01 displaying a pycnocline (highlighted)	64
Figure 39 Example of low frequency SSS data from BM01 displaying less pycnocline	65
Figure 40 SSS coverage plots for each of the survey blocks	65
Figure 41 Pie chart illustration of Average Altitudes, Percentages and Distances	66
Figure 42 Magnetometer profile showing low background noise level for Northern Franklin	67
Figure 43 Magnetometer profile showing low background noise level for Relume	67
Figure 44 Processing workflow applied to the seismic lines	68
Figure 45 Feathering plot calculated for the line BM3_OWF_E_2D_07560	69
Figure 46 Main noise sources identified in the working limit noise test	70
Figure 47 Main noise sources identified while in production, Relume	70
Figure 48 Fugro Pioneer shooting while in SIMOPS	71
Figure 49 Frequency spectrum comparison between background noise and sparker signal	71
Figure 50 Channel domain showing the calculated offsets	72
Figure 51 Profile BM4_OWF_E_2D_08820 in channel domain, showing the calculated offsets	73
Figure 52 Profile BM5_OWF_E_2D_15540 in channel domain, showing the calculated offsets	73
Figure 53 Ghost reflection in channel domain with flatten seabed	74
Figure 54 Velocity Analysis display for line BM3_OWF_E_2D_07770	75
Figure 55 Trace fold values plotted on the top of stacked sections	76
Figure 56 Brutestack for line BM4_OWF_E_2D_10080_01	77
Figure 57 Innomar data showing achieved penetration of 10 m	79
Figure 58 Innomar data showing limited penetration area where holocene unit exceeds 10 m	79
Figure 59 Raw Innomar data showing vertical striping Sparker interference	80
Figure 60 Processed Innomar data showing improved signal to noise ratio	80
Figure 61 Major Danish structural elements	92
Figure 62 Regional geological map	93
Figure 63 The Quaternary glaciations and overview of Quaternary valleys in northwest Europe	94

Figure 64 General stratigraphy model of the geology in the eastern Danish North Sea.....	95
Figure 65 Overview of the bathymetry data.	98
Figure 66 Profiles across the Artificial Island survey area showing depth relative to DTU21 MSL.	99
Figure 67 MBES data with profile showing steepest slope of the Artificial Island survey area.	100
Figure 68 MBES data with profile showing deepest depth of the Artificial Island survey area.	101
Figure 69 MBES data with profile showing shallowest depth of the Artificial Island survey area.	102
Figure 70 MBES image depicting gentle slope from the Artificial Island survey area.	103
Figure 71 Overview of slope gradients across the Artificial Island survey area.	105
Figure 72 Bedform feature (Other-Area of Interest) with slope angles up to 44°.	106
Figure 73 High slope areas within the Artificial Island survey area.	107
Figure 74 Seabed sediments within the Artificial Island survey area.	109
Figure 75 SSS data showing sediments of GRAVEL and coarse SAND and SAND.	110
Figure 76 SSS data showing varying sediments within the Artificial Island survey area.	110
Figure 77 Distribution of mobile bedforms in the Artificial Island survey area.	112
Figure 78 High frequency SSS example of ripples 0.5 -2 m wavelength.	113
Figure 79 MBES DTM image in T13, within the Artificial Island survey area, showing ripples.	113
Figure 80 High frequency SSS mosaic showing sand waves.	114
Figure 81 Distribution of individual boulders in the Artificial Island survey area.	115
Figure 82 High frequency SSS data showing trawl marks in GRAVEL and coarse SAND.	116
Figure 83 Distribution of trawl marks in the Artificial Island survey area.	117
Figure 84 SSS data example of an area of interest.	118
Figure 85 SSS data showing possible exposed TAT-14 cable.	120
Figure 86 Map overview of possible cable exposure.	121
Figure 87 Existing cable (from client) crossing the Artificial Island survey area.	122
Figure 88 Seabed of the MMT OWF survey area.	124
Figure 89 Seabed of the Artificial Island survey area.	125
Figure 90 General sub-surface architecture of survey.	127
Figure 91 General sub-surface architecture of the Central sector.	128
Figure 92 General sub-surface architecture of the South sector.	129
Figure 93 Map showing the lateral extent of U05.	130
Figure 94 Depth below seabed of H05.	131
Figure 95 Thickness of unit U05.	132
Figure 96 Map showing the lateral extent of U10.	133
Figure 97 Depth below seabed of H10, corresponding to the thickness of unit U10.	134
Figure 98 General facies of Seismic Unit U10, and the character of horizon H10 (light green).	135
Figure 99 Oblique facies of U10, overlaid by a package of sub-horizontal parallel reflectors.	136
Figure 100 Internal facies of Seismic Unit U10, and horizon H10 (light green).	137
Figure 101 Grid overlay from interpretation of H10 as interpreted on the Innomar SBP.	138
Figure 102 Map showing the lateral extent of H20.	140
Figure 103 Depth below seabed of H20.	141
Figure 104 Thickness of unit U20.	142
Figure 105 Seismic facies of seismic Unit U20, and the character of horizon H20 (dark green).	143
Figure 106 Channel facies of Seismic Unit U20, with a high negative amplitude reflector at the top.	144
Figure 107 Two distinct facies of Unit U20: channel facies at the base; basin facies at the top.	145
Figure 108 Grid overlay from interpretation of H20 as interpreted on the Innomar SBP.	146
Figure 109 Map showing the lateral extent of U25.	148
Figure 110 Depth below seabed of H25.	149
Figure 111 Thickness of unit U25.	150
Figure 112 General facies of Seismic Unit U25 within the central basin.	151
Figure 113 Facies of Seismic Unit U25 and the SW limit of the central basin.	152
Figure 114 U25 facies at transition from the central basin to the narrower N-S basin in the south.	153
Figure 115 Facies of Seismic Unit U25 and the SE limit of the central basin.	154
Figure 116 Grid overlay from interpretation of H25 as interpreted on the Innomar SBP.	155
Figure 117 Map showing the lateral extent of U30.	157
Figure 118 Depth below seabed of H30.	158
Figure 119 Thickness of unit U30.	159

Figure 120 General facies of Unit U30, and the character of horizon H30 (orange).....	160
Figure 121 H30 truncating the underlying deposits.....	161
Figure 122 Map showing the lateral extent of U35.....	163
Figure 123 Depth below seabed of H35.....	164
Figure 124 Thickness of unit U35.....	165
Figure 125 General facies of Seismic Unit U35, and the character of horizon H35 (yellow).	166
Figure 126 General facies of Seismic Unit U35, truncating the units below.	167
Figure 127 The complex composite facies of Seismic Unit U35.....	168
Figure 128 Map showing the lateral extent of U40.....	170
Figure 129 Depth below seabed of H40.....	171
Figure 130 Thickness of unit U40.....	172
Figure 131 Spatial distribution of the different types of channels identified for Seismic Unit U40.	173
Figure 132 General facies of Type A channels of Seismic Unit U40.	174
Figure 133 General facies of Type A channels of Seismic Unit U40.	175
Figure 134 General facies of Type D channels of Seismic Unit U40.	176
Figure 135 Map showing the lateral extent of U60.....	178
Figure 136 Depth below seabed of H60.....	179
Figure 137 Thickness of unit U60.....	180
Figure 138 General facies of Seismic Unit U60, and the character of horizon H60 (red).....	181
Figure 139 General facies of Seismic Unit U60, and the character of horizon H60 (red).....	182
Figure 140 Map showing the lateral extent of U70.....	184
Figure 141 Depth below seabed of H70.....	185
Figure 142 Thickness of unit U70.....	186
Figure 143 Spatial distribution of the major incisions identified for Seismic Unit U70.	187
Figure 144 General facies of a U-shaped channel of Unit U70.....	188
Figure 145 General facies along the length of a channel of Seismic Unit U70.....	189
Figure 146 Composite facies of a U70 channel.	190
Figure 147 Composite facies of the intersection area of U70 channels.....	191
Figure 148 Map showing the lateral extent of U85.....	193
Figure 149 Depth below seabed of H85.....	194
Figure 150 Thickness of unit U85.....	195
Figure 151 General facies of Seismic Unit U85, and the character of horizon H85 (hot pink).	196
Figure 152 General facies of Seismic Unit U85, and the character of horizon H85 (hot pink).	197
Figure 153 Map showing the lateral extent of U90.....	199
Figure 154 Depth below seabed of H90.....	200
Figure 155 Thickness of unit U90.....	201
Figure 156 General facies of Seismic Unit U90, and the character of horizon H90 (cyan).	202
Figure 157 General facies of Seismic Unit U90, and the character of horizon H90 (cyan).	203
Figure 158 Map showing the lateral extent of horizon KSA.	205
Figure 159 Depth below seabed of horizon KSA.	206
Figure 160 Thickness of unit UKSA.	207
Figure 161 Map showing the lateral extent of horizon KSB.	208
Figure 162 Depth below seabed of horizon KSB.	209
Figure 163 Thickness of unit UKSB.	210
Figure 164 Seismic Unit UKSA deformation below H70_CH_08 incision.....	211
Figure 165 Complex and chaotic facies of Seismic Unit UKSA.	212
Figure 166 Less intensely deformed sediments, delineated by horizon.	213
Figure 167 Thickness of Base Seismic Unit BSU.	214
Figure 168 General facies of the Base Seismic Unit.....	215
Figure 169 Different levels of deformation observed within the site.....	219
Figure 170 Seismic profile displaying minor folding and faulting affecting the BSU sequence.	220
Figure 171 Seismic profile displaying small scale faults within a thrust complex.	221
Figure 172 Seismic profile displaying large scale faults within a thrust complex.....	222
Figure 173 Seismic profile displaying intense deformation within a thrust complex,	223
Figure 174 Map displaying all the interpreted faults in the site.	225
Figure 175 Thrust complex of Seismic Unit UKSA.....	226

Figure 176 Deformation and faults within the Seismic Unit UKS	228
Figure 177 Subsidence area bounded by large normal faults in the northern limit of the area.	230
Figure 178 Structural map of the base of the Chalk deposits (GEUS),	231
Figure 179 Extensional features below a U70 valley (H70_CH_08).	233
Figure 180 Composite surface from the addition of all base horizons of units U10 to U70.	235
Figure 181 Map of the composite surface.	236
Figure 182 Lateral extent of the negative impedance contrasts deposits within U10.	238
Figure 183 Depth below seabed of GHZ_SK_U10.	239
Figure 184 Lateral extent of the negative impedance contrasts deposits within U20.	240
Figure 185 Depth below seabed of GHZ_SK_U20.	241
Figure 186 Lateral extent of the negative impedance contrasts deposits within U25.	242
Figure 187 Depth below seabed of GHZ_SK_U25.	243
Figure 188 Lateral extent of the negative impedance contrasts deposits within U30.	244
Figure 189 Depth below seabed of GHZ_SK_U30.	245
Figure 190 Lateral extent of the negative impedance contrasts deposits within U35.	246
Figure 191 Depth below seabed of GHZ_SK_U35.	247
Figure 192 Lateral extent of the negative impedance contrasts deposits within U60.	248
Figure 193 Depth below seabed of GHZ_SK_U60.	249
Figure 194 Negative impedance contrasts at the top of U20.	250
Figure 195 Map showing the lateral extent of GHZ_Gravel.	252
Figure 196 Depth below seabed of GHZ_Gravel.	253
Figure 197 Possible coarse layer within U35.	254
Figure 198 Lateral extent of the interpreted lacustrine deposits (horizon GHZ_Lacustrine).	256
Figure 199 Depth below seabed of horizon GHZ_Lacustrine.	257
Figure 200 Interpreted glaciolacustrine deposits on the upper levels of Seismic Unit U40.	258
Figure 201 Location plot of grab sample material types within the Artificial Island survey area.	260

LIST OF TABLES

Table 1 Project details.	15
Table 2 Deviations from the SOW during survey (M/V Northern Franklin).	18
Table 3 Reference documents.	20
Table 4 Line parameters (Artificial Island area of investigation).	22
Table 5 Survey line breakdown (Artificial Island area of investigation).	22
Table 6 Geodetic parameters used during acquisition.	28
Table 7 Geodetic parameters used during processing.	28
Table 8 Transformation parameters.	28
Table 9 Official test coordinates.	29
Table 10 Projection parameters.	29
Table 11 Vertical reference parameters.	29
Table 12 Average Height comparison between DTU21 and DVR90.	30
Table 13 M/V Northern Franklin equipment.	32
Table 14 M/V Relume equipment.	33
Table 15 Survey tasks – M/V Relume.	35
Table 16 Survey tasks – M/V Northern Franklin.	35
Table 17 Gridding parameters.	45
Table 18 Summary of Average Altitudes, Percentages and Distances.	66
Table 19 Seabed gradient classification.	81
Table 20 Sediment classification.	82
Table 21 Seabed features classification.	83
Table 22 Summary of the seismic units.	86
Table 23 Summary of SSS and MBES contacts.	119
Table 24 Summary of magnetic anomalies.	119
Table 25 Summary of SBP Contacts.	120
Table 26 Distribution of interpreted seismic units present in the Artificial Island survey area.	125
Table 27 General characteristics of the large incisions within seismic unit U70.	183

<i>Table 28 Distribution of soft kick features within the survey area</i>	<i>237</i>
<i>Table 29 Grab sample summary</i>	<i>259</i>
<i>Table 30 Deliverables</i>	<i>268</i>

ABBREVIATIONS AND DEFINITIONS

AOI	Area of Investigation
BSB	Below Seabed
CM	Central Meridian
DTU21	Denmark Technical University 2021
DPR	Daily Progress Report
DTM	Digital Terrain Model
DVR90	Dansk Vertikal Reference 1990
EEZ	Exclusive Economic Zone
EI	Energy Island
EPSG	European Petroleum Survey Group
ESRI	Environmental Systems Research Institute, Inc.
ETRS	European Terrestrial Reference System
FME	Feature Manipulation Engine
FMGT	Fledermaus GeoCoder Toolbox
GIS	Geographic Information System
GMSS	Geo Marine Survey Systems
GNSS	Global Navigation Satellite System
GRS80	Geodetic Reference System 1980
GS	Grab Sample / GeoSurveys
HF	High Frequency
HiPAP	High Precision Acoustic Positioning
INS	Inertial Navigation System
IHO	International Hydrographic Organisation
IMU	Inertial Measurement Unit
ITRF	International Terrestrial Reference Frame
LF	Low Frequency
LGM	Last Glacial Maximum
WP	Work Pack – Defines survey area and requirement
MAG	Magnetometer
MBBS	Multibeam Backscatter
MBES	Multibeam Echo Sounder
MIG	Migrated
MMO	Man Made Object
MSL	Mean Sea Level
MUL	Multiple Attenuated Stack
M/V	Motor Vessel
OWF	Offshore Wind Farm
POS MV	Position and Orientation System for Marine Vessels
POSPac	Position and Orientation System Package
PPS	Pulse Per Second

QC	Quality Control
ROTV	Remotely Operated Towed Vehicle
S-CAN	Scalco Combinatorial Anti Noise
SBET	Smoothed Best Estimated Trajectory
SBP	Sub-Bottom Profiler
SOW	Scope of Work
SSS	Side Scan Sonar
STW	Speed Through Water
SVP	Sound Velocity Profile
THU	Total Horizontal Uncertainty
TPU	Total Propagated Uncertainty
TVU	Total Vertical Uncertainty
TWT	Two Way Time
UHRs	Ultra High Resolution Seismic
USBL	Ultra Short Baseline
UTC	Coordinated Universal Time
UTM	Universal Transverse Mercator
UXO	Unexploded Ordnance

EXECUTIVE SUMMARY

NORTH SEA OFFSHORE WIND FARM ARTIFICIAL ISLAND AREA OF INVESTIGATION	
INTRODUCTION	
Survey Dates	M/V Relume: 01 May to 12 June 2021 M/V Northern Franklin: 11 June to 18 August 2021
Equipment	Multibeam Echo Sounder (MBES), Side Scan Sonar (SSS), Magnetometer (MAG), Innomar Sub-bottom Profiler (SBP), 2 Dimensional-Ultra High Resolution Seismic (2D-UHRS), Sediment Grab Samples (GS).
Coordinate System	Datum: European Terrestrial Reference System 1989 (ETRS89) Projection: Universal Transverse Mercator (UTM) Zone 32N, Central Meridian (CM) 9°E
BATHYMETRY AND SEAFLOOR MORPHOLOGY	
<p>The bathymetric survey recorded water depths across the MMT OWF survey area, including the 10 km x 10 km Artificial Island survey area. Within the Artificial Island survey area, the depths varied between 25.8 m and 48.2 m (DTU21 MSL) with depths generally increasing to the east and west.</p>	
SURFICIAL GEOLOGY	
<p>The surficial geology in the area is dominated by GRAVEL and coarse SAND and SAND. Less frequently observed is muddy SAND and very rarely observed is MUD and sandy MUD.</p> <p>The GRAVEL and coarse SAND, and the SAND are more prominent in the western and central parts of the Artificial Island survey area. The muddy SAND is concentrated predominately in the northeast of the Artificial Island survey area. Infrequent and isolated patches of MUD and sandy MUD are occasionally present in the northwest of the Artificial Island survey area</p> <p>In areas of muddy SAND and sandy MUD, the seabed is usually featureless, whilst mobile bedforms occur mostly in areas of SAND or GRAVEL and coarse SAND.</p>	
SEAFLOOR FEATURES AND CONTACTS	
<p>Extensive areas of mobile sediments, including ripples, large ripples and megaripples are observed particularly in the west of the Artificial Island survey area. Some sand waves are observed in the central and northern part of the Artificial Island survey area. In the west of the Artificial Island survey area, some larger scale sandbar bedforms are observed.</p> <p>A total of 280 individual seabed contacts (181 MBES contacts and 99 SSS contacts) were detected within the Artificial Island survey area. They were classified as boulders (221) and man-made objects such as debris (51), other (6), fishing equipment (1) and wire (1). No boulder fields were observed.</p> <p>A total of 128 magnetic anomalies were detected within the Artificial Island survey area. 58 of these were individual discrete anomalies, whilst 70 anomalies were interpreted to form 8 linear anomalies, one of which corresponded to the buried TAT-14 cable.</p> <p>Evidence of trawling is found across much of the Artificial Island survey area.</p> <p>Occasional areas of interest have been identified as possible biogenic features. These areas have been assessed by a senior biologist who determined these areas of interest are unlikely to be biogenic in nature. The areas have maintained their feature in case further investigation to these areas is deemed necessary. These areas are more likely to be erosional features.</p>	

NORTH SEA OFFSHORE WIND FARM ARTIFICIAL ISLAND AREA OF INVESTIGATION	
GEOLOGY	
The Artificial Island survey area is located within a complex geologic setting. The interpreted Ground Model is based on twelve horizons that correspond to erosive surfaces and make up the base of the seismostratigraphic units.	
U05 (Holocene)	The uppermost unit (U05) is occasionally present on top of U10 and consists of fine-grained mobile sediments.
U10 (Holocene)	The uppermost unit (U10) is present at the seabed and consists of marine Holocene sand deposits. A localised internal reflector was interpreted within U10 defined as H10i (internal). H10i is a discontinuous reflector which usually highlights the boundary between transparent and non-transparent facies within U10.
U20	Infills of small basins and channels, likely in a restricted marine-tidal setting, partially associated to a subaerial fluvial system.
U25	Fine sediments: fine sands-silts (?) deposited in a relatively low-energetic setting, possibly a transgressive estuary.
U30	Fining-upward sequence, likely fluvial in nature.
U35	High energy fluvial bedforms (flash floods?), interpreted to consist of gravel and sands with enclaves of coarser-grained clasts, fining-upward (?)
U40	Drainage system of glacial melt back from the north, and outwash plains, with variable sediment content. Glacial period (Weichselian?)
U50	Not present in the Artificial Island survey area. Fine sediment deposits with boulders, possibly related to glacial drift deposit (aqua till?) or glaciolacustrine deposition (?). Glacial period (Weichselian?)
U60	High energy fluvial bedforms (flash floods?) comprising mainly sands with gravel and silt (?).
U70	Glaci-fluvial deposition, in a proglacial, sub-aerial environment (reoccupation of tunnel valley depressions by fluvial systems?), with variable sediment content. Glacial period (Weichselian?)
UKS (A)	Deformed deposits of variable sediment content. Glaciotectonism (Weichselian?):
U85	High energy fluvial (possibly outwash plain?), composed of mainly sands with gravel and silt (?). Organic-rich muds at the base.
U90	Fan delta deposits comprising mainly sands and fine sediments.
UKS (B)	Deformed deposits of variable sediment content. Glaciotectonism (Saalian?):
Base Seismic Unit	Pre-quaternary sequence – marine clays, silts to sands.
SEABED AND SUB-SEABED HAZARDS	
Seabed gradients	<p>Slope angles across the site are typically very gentle (<1°) and gentle (1° to 5°). Despite the fact that large bedforms such as sand waves and sandbars constitute a large portion of the survey area; the seafloor topography is typically gently undulating. Areas of moderate to very steep slopes are largely restricted to the edges of bedforms and the lee slopes of the most defined sand waves.</p> <p>Very steep slope angles (15° to a maximum of 73°) are associated with boulders, the edges of depressions and steep banks on the western side of the Artificial Island survey area.</p>
Mobile seabed sediments	Mobile sediments are present frequently throughout the surveyed area. The mobile sediments comprise of ripples, megaripples, large ripples, sand waves as well as larger scale sediment accumulations forming sandbars.

NORTH SEA OFFSHORE WIND FARM ARTIFICIAL ISLAND AREA OF INVESTIGATION	
Wreck	No wrecks were found within the Artificial Island survey area.
Cable	There is one buried cable (TAT-14) crossing the southern end of the Artificial Island survey area shown in the background data and detected in the MAG and SBP data.
Pipeline	According to available background data, there are no known pipelines in the area. No pipelines were observed in the survey area.
Sediment deformation	Areas of tectonization/deformation have been observed predominately within UKS. The origin of these deformed deposits is interpreted to be mainly glacial tectonics, but locally may be related to salt tectonics and gravitational deformation. Deformed deposits have geotechnical significance given their complex stress/load histories. Faults are present ubiquitous within the subsurface, and do not greatly affect sediments younger than U20.
Buried channels and tunnel valleys	Buried channels occur throughout the site. The more relevant erosive events that carved these channels correspond to the unit bases of U40, U60, and U70. A potential geo-hazard related with the channels is the sharp contrasts in physical properties between the channel infill and surrounding units.
Soft sediments and organic-rich deposits	High-amplitude, negative impedance features occur within seismic units U10 to U35, and U60. These features are interpreted to be fine sediments, most likely organic-rich muds due to their strong negative acoustic impedance.
Coarse sediments/gravel beds/boulders/tills	Coarser material, such as boulders accumulations, cobbles, and gravel lags are present in glacial deposits in the site, as well as in unit U35. These are potential hazards and may constitute a constraint on drilling and other operations.
Fluid flow and gas features	No unambiguous seismic anomalies suggesting the presence of detectable gas in the subsurface were identified in the UHRS data.
Lacustrine sediments	Lacustrine deposits were identified in the area, typically associated to unit U40.

1 | INTRODUCTION

1.1 | PROJECT INFORMATION

Energinet are developing the proposed Offshore Wind Farm (OWF) and Artificial Island in the Danish sector of the North Sea (Figure 1). MMT have been contracted to provide geophysical survey (including 2D UHRS) and grab sampling of the east part of the 3 GW OWF project site (the MMT OWF survey area) including the 10 km x 10 km Artificial Island area of investigation. The Artificial Island area of investigation is located in the southwest portion of the MMT OWF survey area. Within the Artificial Island area of investigation is the 2.5 km x 2.5 km Artificial Island project site. The Artificial Island project site has a central location on a shallow bank seabed structure and will be the focus area for detailed development of the artificial island.

The scope of work was divided into four separate Work Packs (WP).

This report covers the 10 km x 10 km Artificial Island area of investigation.

A summary of the project details is presented in Table 1.

Table 1 Project details.

CLIENT:	Energinet
PROJECT:	Energy Islands - North Sea - Artificial Island
MMT SWEDEN AB (MMT) PROJECT NUMBER:	103783
SURVEY TYPE:	Geophysical and Grab Sample offshore windfarm site survey
AREA:	Danish North Sea
SURVEY PERIOD:	May – August 2021 (covers the MMT OWF survey area and Artificial Island survey area)
SURVEY VESSELS:	M/V Northern Franklin, M/V Relume
MMT PROJECT MANAGER:	Karin Gunnesson
CLIENT PROJECT MANAGER:	Jens Colberg-Larsen

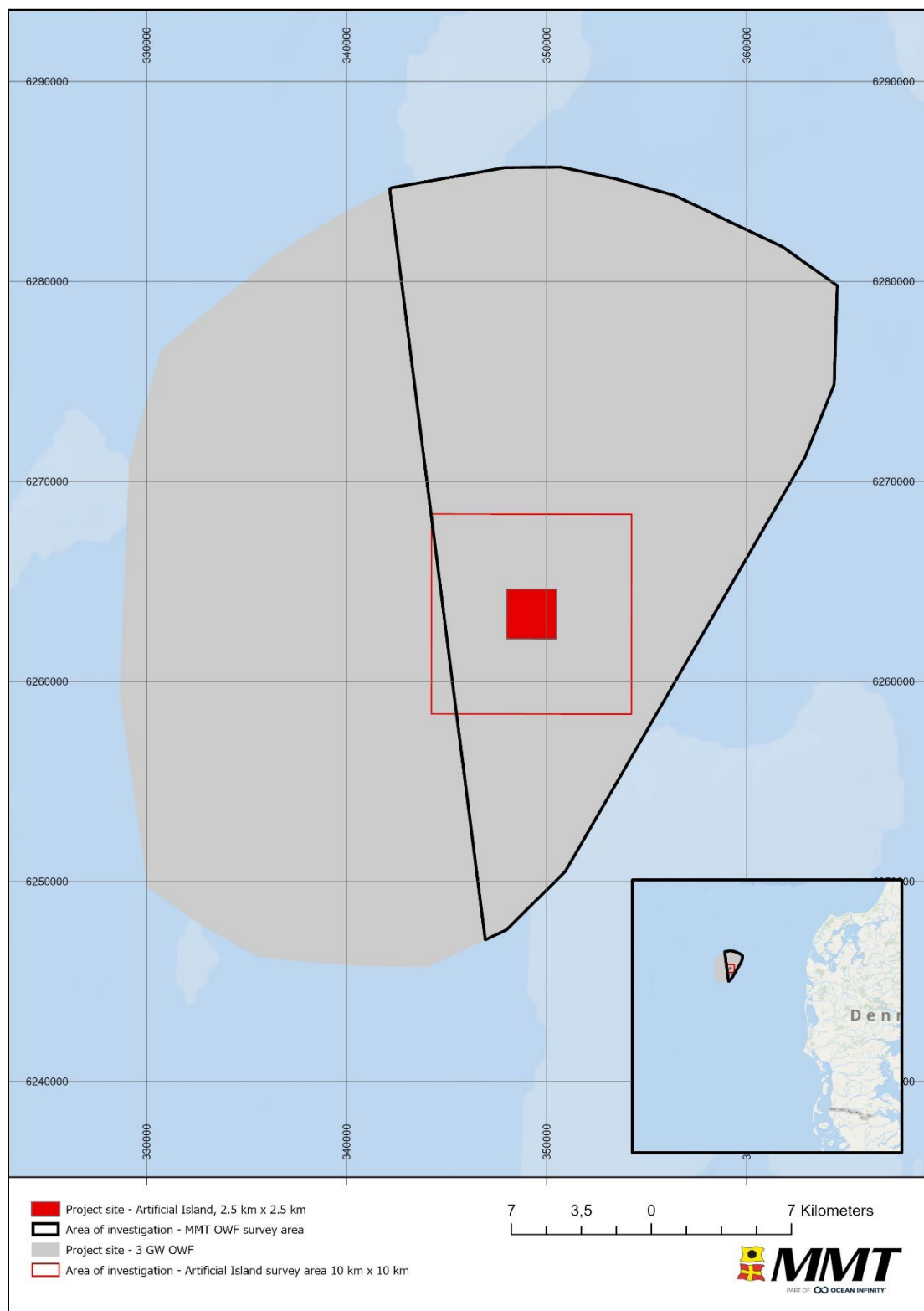


Figure 1 Overview of survey scopes performed

1.2 | SURVEY INFORMATION

The work scope comprises several tasks including:

- Project Management and Administration
- Geophysical surveys (MBES, SSS, SBP, MAG)
- 2D UHRS Survey
- Grab Sampling

The MMT OWF survey area investigation covers an approximately 526 km² area acquired by MMT and is located roughly 90 km offshore the coast of Jutland. Within the MMT area of investigation for the OWF, a 10 km x 10 km area of investigation is reported separately with particular relevance for the Artificial Island survey area and Artificial Island project site (2.5 km x 2.5 km).

This report covers the geophysical survey of the 10 km x 10 km Artificial Island area of investigation acquired by MMT with integrated grab sample data results (Appendix C). This report also integrates the 2D UHRS survey dataset acquired by GeoSurveys Ltd. (Appendix D).

1.3 | SURVEY OBJECTIVES

The survey objectives for this project were to acquire bathymetric soundings, magnetometer, side scan sonar and sub-seabed geological information within the MMT OWF survey area. The acquisition of these data sets was to provide comprehensive bathymetric soundings, seabed features maps including contact listings and shallow geological information to inform a ground model and mapping of magnetic anomalies. The interpretation of the datasets was charted and reported to inform cable route micro-routing and subsequent engineering.

The main objectives with the surveys were:

- Acquire and interpret high quality seabed and sub-seabed data for project planning and execution. As a minimum, this includes local bathymetry, seabed sediment distribution, seabed features, seabed obstructions, wrecks and archaeological sites, crossing cables and pipelines and evaluation of possible mobile sediments
- Sub-bottom profiling and 2D UHRS survey along the survey lines to map shallow geological units.
- Mapping of magnetic targets and to identify infrastructure crossings and large metallic debris.
- Ground truthing grab samples were acquired in order to aid the surficial interpretation of seabed sediments.

1.4 | SCOPE OF WORK

GEOPHYSICAL SITE SURVEY

A geophysical site survey including 2D UHR seismic survey was carried out in 2021. The survey had full coverage in the area of investigation. The survey mapped the bathymetry, the static and dynamic elements of the seabed surface and the sub-surface geological soil layers to at least 100 m below seabed.

1.4.1 | DEVIATIONS TO SCOPE OF WORK

2D UHRS AND GEOPHYSICAL SURVEY (M/V RELUME)

During the geophysical survey there were no deviations from the original SOW.

GEOPHYSICAL SURVEY AND GRAB SAMPLING (M/V NORTHERN FRANKLIN)

During the geophysical survey there were 2 deviations from the original SOW (Table 2).

Table 2 Deviations from the SOW during survey (M/V Northern Franklin).

Date	Description	Decision/Result/Conclusion
2021-08-10	Reduced Scope of work	Due to forecasted poor weather, Energinet decided to only infill 100% coverage in pycnocline areas and reduce sample amount.
2021-08-11	Reduced Scope of work	Due to forecasted poor weather, Energinet agreed to reduce the remaining GS number from 80 to approximately half in order to maximise the weather window.

1.5 | PURPOSE OF DOCUMENT

This report details the interpretation of the geophysical survey and grab sample results from the 10 km x 10 km Artificial Island area investigations.

The report summarises the conditions within the survey area with regards to; bathymetry, surficial geology and seabed features, contacts and anomalies, existing infrastructure, and subsurface geology. geo-hazard identification and interpretation has also been considered.

All data obtained from the geophysical survey and grab sample results have been correlated with each other and compared against the existing background information, in order to ground-truth the survey results.

A full list of reports is given in Table 3 (Reference Documents).

1.6 | REPORT STRUCTURE

The results from the Artificial Island survey area campaign are presented in this report:

- Artificial Island Area of Investigation Geophysical Survey Report – Includes a chart series of results. A full chart list is provided within Appendix A|.

The Artificial Island Area of Investigation Geophysical Survey Report (this report) chart series includes:

- Overview Chart
- Trackline Charts
- Bathymetry Charts
- Backscatter Mosaic Charts
- Seabed Geology Classification Charts

- Seabed Substrate Type Classification Charts
- Seabed Morphology Classification Charts
- Seabed Objects Charts
- Seabed Features Charts
- Sub-Seabed Geology Charts (Isopach)
- Sub-Seabed Geology Profile Charts (34 across the site)

1.6.1 | GEOPHYSICAL SURVEY REPORT

Attached to the report are the following appendices:

- Appendix A| List of Produced Charts
- Appendix B| Contact and Anomaly List
- Appendix C| Grab Sample Lab Report
- Appendix D| 2D UHRS Processing Report

1.6.2 | CHARTS

The MMT Charts describe and illustrate the results from the survey. The charts include an overview chart with a scale of 1:65 000, north up charts at a scale of 1:15 000 and longitudinal profile charts with a horizontal scale of 1:10 000 and a vertical scale of 1:500.

The overview and north up charts contain background data (existing infrastructure, Exclusive Economic Zones (EEZ), and wreck database) alongside survey results.

A list of all produced charts is presented in Appendix A|.

OVERVIEW CHART

Shows coastlines, EEZ, large scale bathymetric features and area of investigations.

TRACKLINE CHARTS

The actual performed survey lines are presented along with seabed grab sampling positions.

BATHYMETRY CHARTS

The bathymetry is presented as a shaded relief colour image with 1 m colour interval, overlain with contour lines (1 m (minor) and 5 m (major)) with depth labels.

BACKSCATTER MOSAIC CHARTS

The backscatter mosaic imagery is presented.

SEABED SURFACE GEOLOGY CLASSIFICATION CHARTS

The surface geology is divided into 4 different classes; MUD and sandy MUD, Muddy SAND, SAND, GRAVEL and coarse SAND and are presented as solid hatches.

SURFICIAL MORPHOLOGY CHARTS

The surface morphology is divided into 7 different classes; Ripples, Large Ripples, Megaripples, Sand Waves, Sandbars, Area of Interest and Trawl Mark Area and are presented as hatches with patterns.

SURFICIAL SUBSTRATE CHARTS

The substrate charts are divided in to six classes as per the Danish Råstof-bekendtgørelsen (BEK no. 1680 of 17/12/2018, Phase IB).

- Substrate type 1a - Sand, soft silty bottom
- Substrate type 1b – Sand, solid sandy bottom
- Substrate type 2a - Sand, gravel and pebbles, few larger stones
- Substrate type 2b - Sand, gravel and pebbles, seabed cover of larger stones 1% to 10%
- Substrate type 3 - Sand, gravel and pebbles, seabed cover of larger stones 10% to 25%
- Substrate type 4 – Stony areas and stone reefs, seabed cover of larger stones 25% to 100%

SEABED OBJECTS CHARTS

The SSS, MBES and magnetic contacts are presented.

SEABED FEATURES CHARTS

The seabed features are divided into 7 different classes; Ripples, Large Ripples, Megaripples, Sand Waves, Sandbars, Area of Interest and Trawl Mark Area and are presented as hatches with patterns

The SSS, MBES and magnetic contacts are also presented.

SUB-SEABED GEOLOGY CHARTS

Depth below seabed (BSB) for each interpreted horizon is presented as a gridded surface with contour lines and depth labels at 1 m interval.

SUB-SEABED GEOLOGY PROFILE CHARTS

A total of 14 profile charts shows interpretations of the horizons and structures across the Artificial Island survey area.

1.7 | REFERENCE DOCUMENTS

The documents used as references to this report are presented in Table 3.

Table 3 Reference documents.

Document Number	Title	Author
1100046209	Energy Island Danish North Sea Geoarchaeology and geological desk study	From Client
103783-ENN-MMT-QAC-PRO-PROJMANU-06	Project Manual	MMT
103783-ENN-MMT-QAC-PRO-CADGIS	CAD and GIS Specification	MMT

Document Number	Title	Author
103783-ENN-MMT-MAC-REP-FRANKLIN-A	Mobilisation and Calibration Report – Northern Franklin	MMT
103783-ENN-MMT-MAC-REP-RELUME-A	Mobilisation and Calibration Report – Relume	MMT
103783-ENN-MMT-SUR-REP-OPREPWPA-REVA	Operations Report MMT OWF survey area	MMT
103783-ENN-MMT-SUR-REP-SURVWPA-02	Survey Report MMT OWF survey area	MMT

1.8 | AREA LINE PLAN

The MMT OWF survey area and Artificial Island survey area line spacing and minimum parameters are detailed in Table 4.

A breakdown of the survey lines is provided in Table 5, and described in Sections 1.8.1|, 1.8.2| and 1.8.3|.

Table 4 Line parameters (Artificial Island area of investigation).

GEOPHYSICAL SURVEY SETTINGS	SCOPE
Artificial Island Area of Investigation	Ca. 100 km ²
Line spacing Geophysical Main Lines	70 m
Line spacing Geophysical and 2D UHRS Main Lines	210 m
Line spacing Geophysical and 2D UHRS Cross Lines	1000 m

Table 5 Survey line breakdown (Artificial Island area of investigation).

SURVEY LINE BREAKDOWN	SCOPE	ACTUAL SURVEYED
Geophysical Main Lines (Northern Franklin)	895.6 km/95 Lines	1019.7 km/128 Lines (includes infills)
Geophysical and 2D UHRS Main Lines (Relume)	452.6 km/48 Lines	490.1 km/48 Lines
Geophysical and 2D UHRS Cross Lines (Relume)	94.9 km/11 Lines	103.4 km/11 Lines
Geophysical Totals	1443.1 km/154 Lines	1613.2 km/187 Lines
2D UHRS Totals	547.5 km/59 Lines	593.5 km/59 Lines

Note: All 2D UHRS lines also had MBES, SSS, SBP Innomar and MAG acquired simultaneously.

1.8.1 | 2D UHRS REFERENCE LINES

Reference lines were surveyed to acquire a representative 2D UHRS seismic dataset of the MMT OWF survey area. All 2D UHRS lines also had geophysical MBES, SSS, SBP Innomar and MAG acquired simultaneously. The reference lines were selected from the seismic mainline dataset (2 mainlines and 1 intersecting crossline within the Artificial Island survey area). The dataset formed the bases of the first 2D UHRS stratigraphic model used as an interpretation guide for the entire project.

The reference lines were acquired following mobilisation and survey verification, to enable maximum time for review. A framework and strategy were then agreed with the Client prior to further interpretation

Reference lines are illustrated in Figure 2.

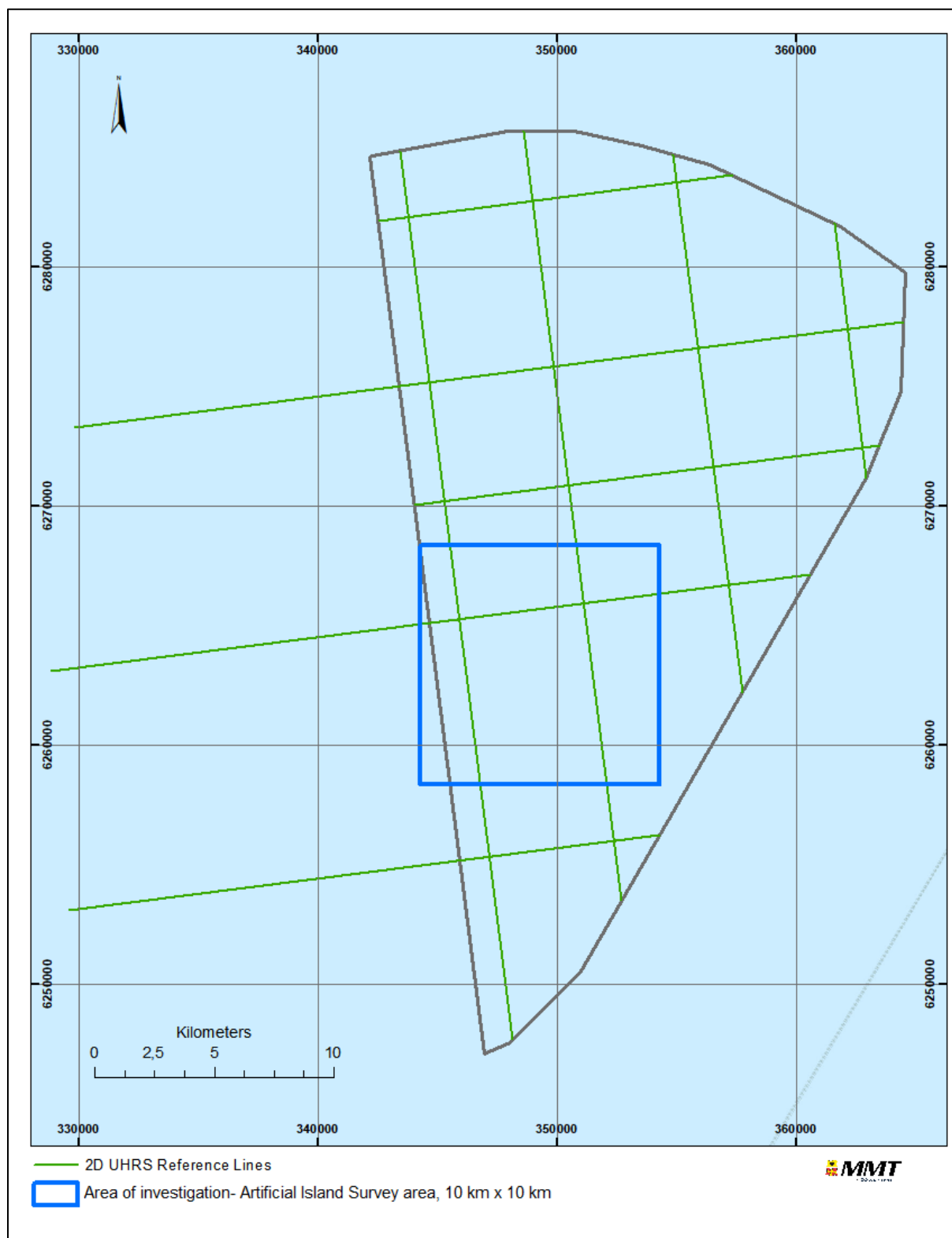


Figure 2 Line plan – 2D UHRS reference lines
 (Including geophysical data) and the Artificial Island survey area.

1.8.2 | 2D UHRS MAIN AND CROSS LINES

The MMT OWF survey area included 2D UHRS main lines (orientated north to south) and cross lines (orientated west to east). All 2D UHRS lines also had geophysical MBES, SSS, SBP Innomar and MAG acquired simultaneously.

2D UHRS main lines and cross lines are illustrated in Figure 3.



Figure 3 Line plan – 2D UHRS main and cross lines
 (Including geophysical data) within the Artificial Island survey area.

1.8.3 | GEOPHYSICAL MAIN AND CROSS LINES

The MMT OWF survey area included geophysical main lines (orientated north to south) and cross lines (orientated west to east).

Geophysical main lines and cross lines are illustrated in Figure 4.

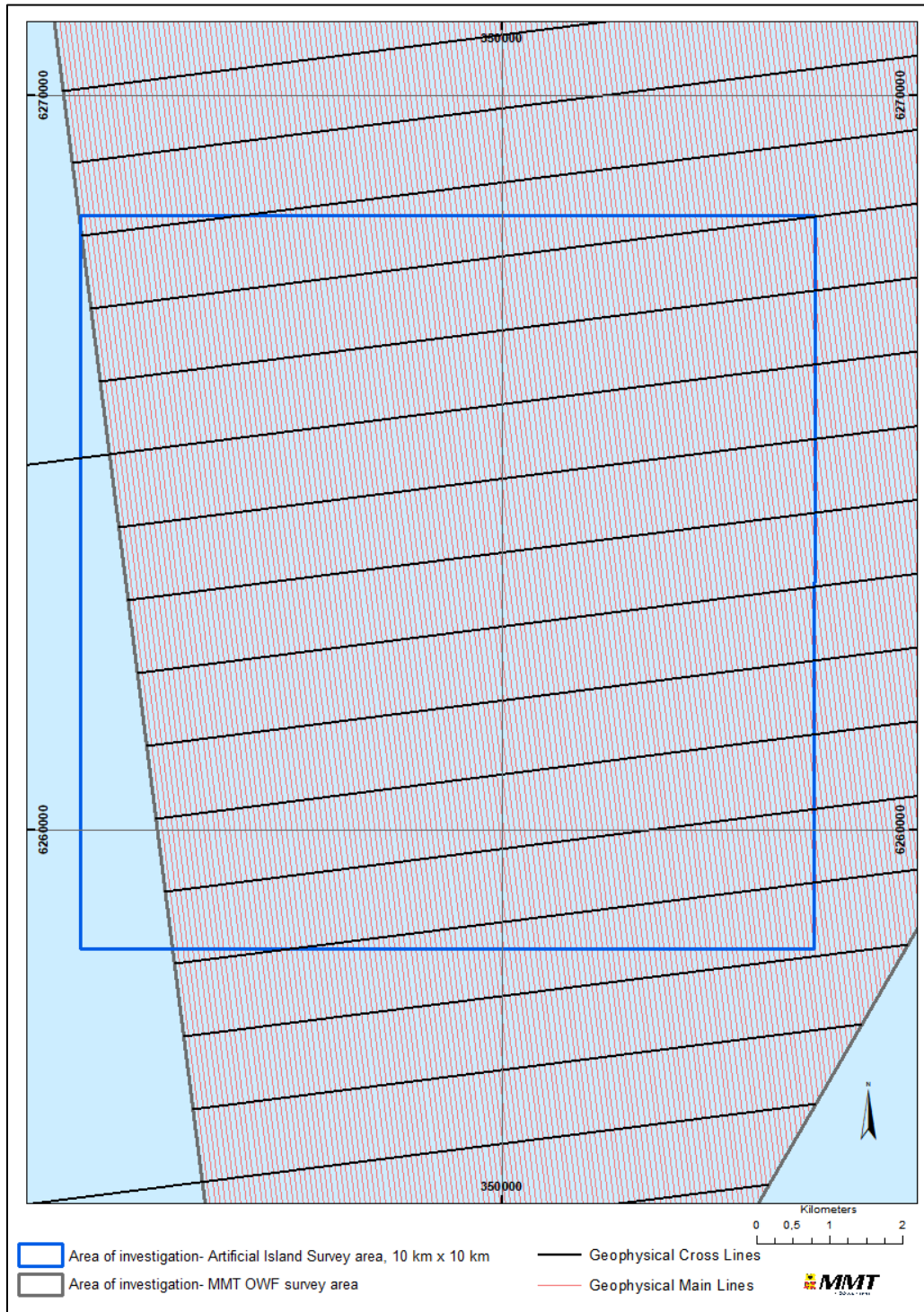


Figure 4 Line plan - geophysical main and cross lines within the Artificial Island survey area.

1.8.4 | SURVEY BLOCKS

To facilitate survey data management and survey planning, and to allow the fishing community to plan around the survey work, the MMT OWF survey area was divided into 22 smaller areas. These included six blocks for the main lines (BM1 to BM6) and four blocks for the cross lines (BX1 to BX4). The Artificial Island survey area is located within B1 to B4, and cross blocks BX3 to BX4 as shown in Figure 5. Reporting tiles were also used to aid when describing specific areas. The areas relevant for the Artificial Island Area of Investigation are shown in Figure 6. All data from the MMT OWF survey area has been trimmed to the 10 km x 10 km Artificial Island survey area boundary.

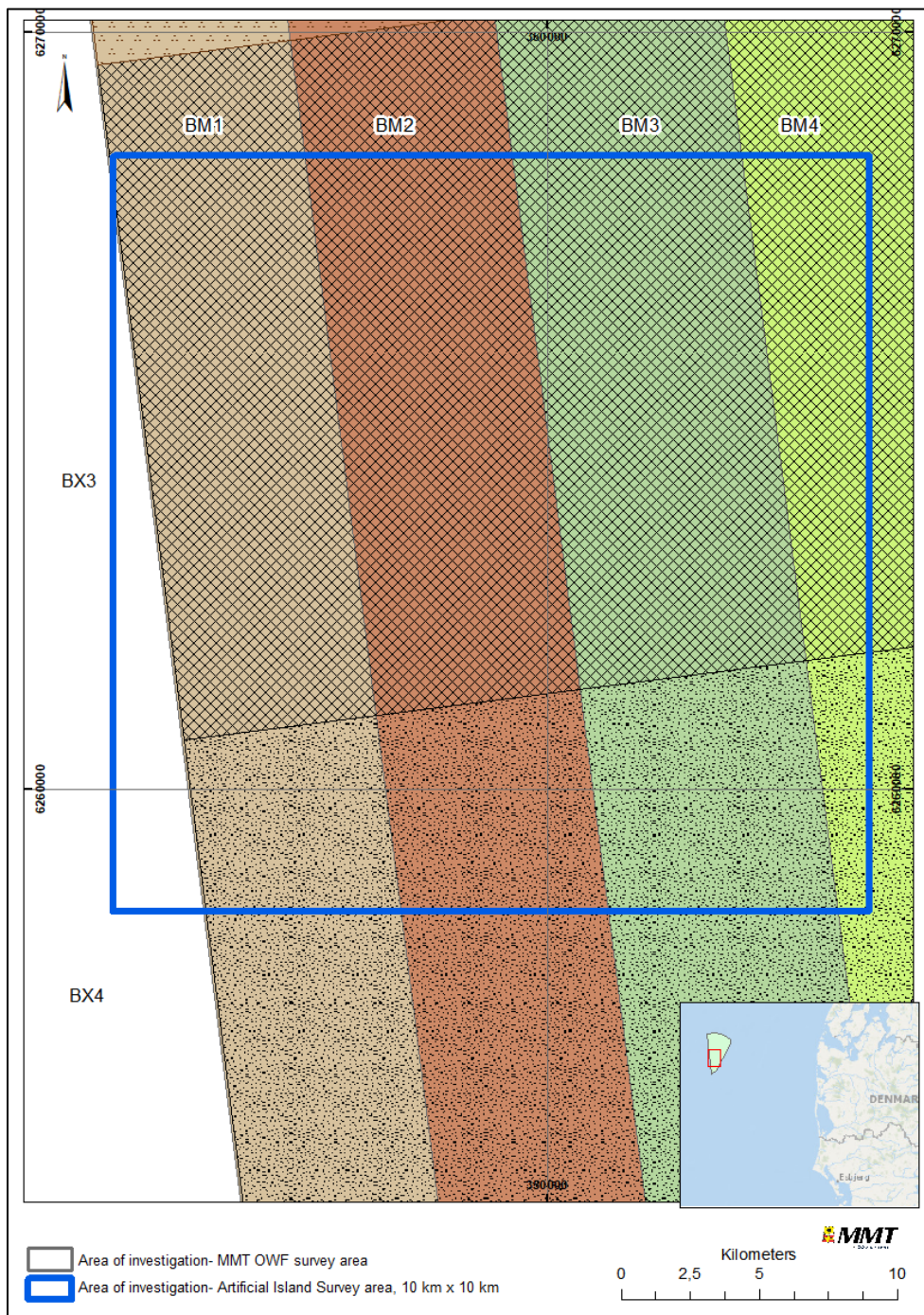
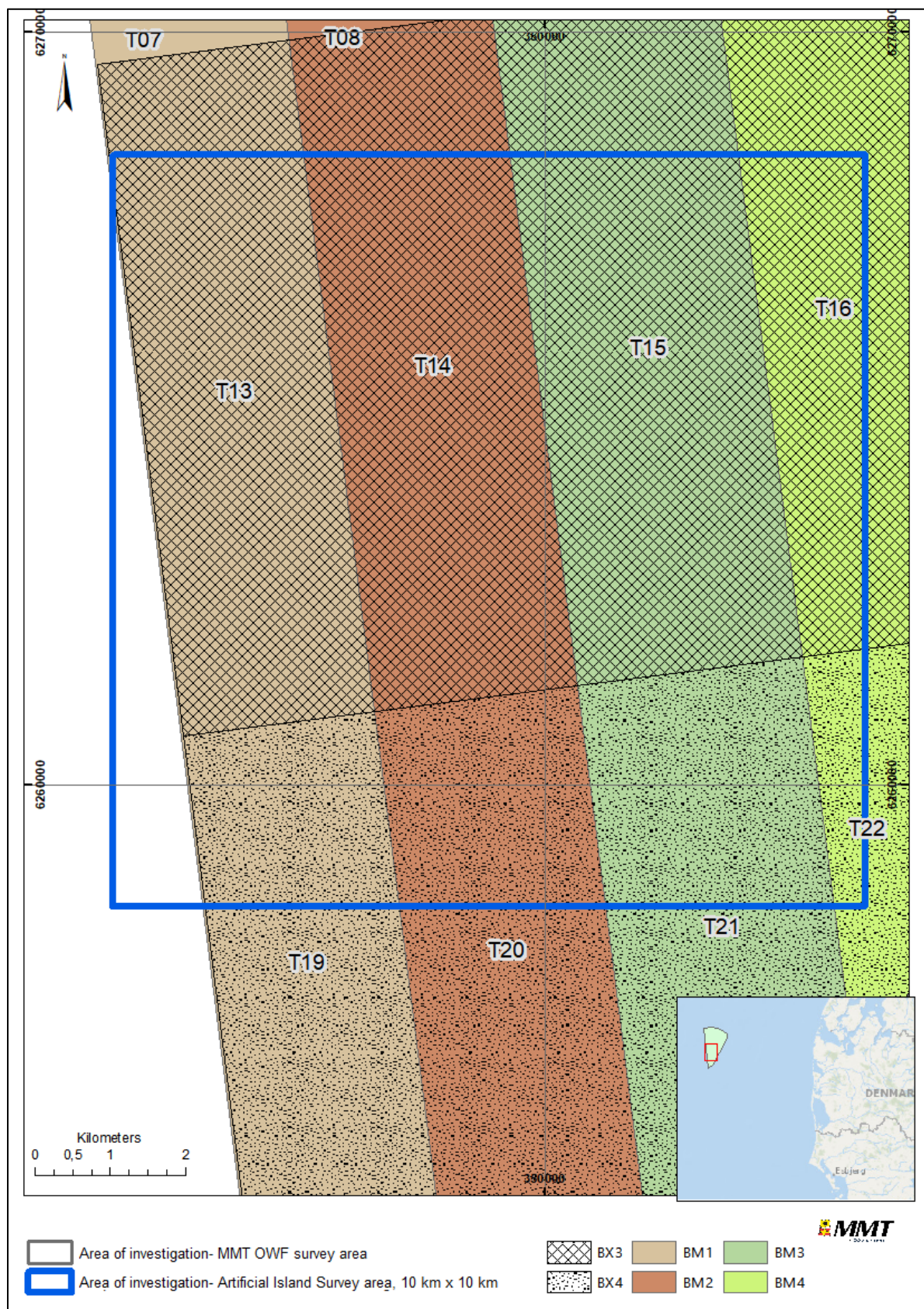


Figure 5 Overview of survey block divisions within the Artificial Island survey area.



2 | SURVEY PARAMETERS

2.1 | GEODETIC DATUM AND GRID COORDINATE SYSTEM

2.1.1 | ACQUISITION

The geodetic datum used for survey equipment during acquisition are presented in Table 6.

Table 6 Geodetic parameters used during acquisition.

Horizontal datum: WGS 84	
Datum	World Geodetic System 1984
ESPG Datum code	6326
Spheroid	World Geodetic System 1984 (7030)
Semi-major axis	6 378 137.000m
Semi-minor axis	6 356 752.3142m
Inverse Flattening (1/f)	298.257223563

2.1.2 | PROCESSING

The geodetic datum used during processing and reporting are presented in Table 7.

Table 7 Geodetic parameters used during processing.

Horizontal datum: European Terrestrial Reference System 1989 (ETRS89)	
Datum	ETRS89
European Petroleum Survey group (EPSG) Datum Code	25832
Spheroid	GRS80
Semi-major axis	6 378 137.000m
Semi-minor axis	6 356 752.314m
Inverse Flattening (1/f)	298.257222101

2.1.3 | TRANSFORMATION PARAMETERS

The transformation parameters used to convert from acquisition datum (WGS 84) to processing/reporting datum (ETRS89) are presented in Table 8.

Table 8 Transformation parameters.

DATUM SHIFT FROM WGS 84 TO ETRS89 (RIGHT-HANDED CONVENTION FOR ROTATION - COORDINATE FRAME ROTATION)	
PARAMETERS	EPOCH 2021.5
Shift dX (m)	0.10665
Shift dY (m)	0.06613
Shift dZ (m)	-0.12873

DATUM SHIFT FROM WGS 84 TO ETRS89 (RIGHT-HANDED CONVENTION FOR ROTATION - COORDINATE FRAME ROTATION)	
Rotation rX (")	-0.003409
Rotation rY (")	-0.014065
Rotation rZ (")	0.025207
Scale Factor (ppm)	0.0032

In order to verify that the transformation parameters have been correctly entered into the navigation system the following test coordinates were used (Table 9).

Table 9 Official test coordinates

UTM Zone	Datum	Easting (m)	Northing (m)	Latitude	Longitude
32	WGS84	-	-	56° 33' 00.000" N	6° 33' 00.000" E
	ETRS 89	349393.437	6269982.594	56° 32' 59.981" N	6° 32' 59.970" E

2.1.4 | PROJECTION PARAMETERS

The projection parameters used for processing and reporting are presented in Table 10.

Table 10 Projection parameters.

Projection Parameters	
Projection	UTM
Zone	32 N
Central Meridian	09° 00' 00" E
Latitude origin	0
False Northing	0 m
False Easting	500 000 m
Central Scale Factor	0.9996
Units	metres

2.1.5 | VERTICAL REFERENCE

The vertical reference parameters used for processing and reporting are presented in Table 11.

Table 11 Vertical reference parameters.

Vertical Reference Parameters	
Vertical reference	MSL
Height model	DTU21

The difference between the vertical height models (DTU21 and DVR90) are given below in Table 12. The average for each 5 km MBES grid was compared.

Table 12 Average Height comparison between DTU21 and DVR90.

AVE HEIGHT DTU21 MSL (METRES)	AVE HEIGHT DVR90 MSL (METRES)	DIFFERENCE (METRES)
40.64	40.92	0.28

2.2 | VERTICAL DATUM

Global navigation satellite system (GNSS) tide was used to reduce the bathymetry data to Mean Sea Level (MSL) the defined vertical reference level (Figure 7). The vertical datum for all depth measurements was MSL via DTU21 MSL Reduction from WGS84-based ellipsoid heights.

This tidal reduction methodology encompasses all vertical movement of the vessel, including tidal effect and vessel movement due to waves and currents. The short variations in height are identified as heave and the long variations as tide.

This methodology is very robust since it is not limited by the filter settings defined online and provides very good results in complicated mixed wave and swell patterns. The vessel navigation is exported into a post-processed format, Smoothed Best Estimated Trajectory (SBET) that is then applied onto the multibeam echo sounder (MBES) data.

The methodology has proven to be very accurate as it accounts for any changes in height caused by changes in atmospheric pressure, storm surge, squat, loading or any other effect not accounted for in a tidal prediction.

Within the Artificial Island survey area, all positions below the sea surface are referred to as **depths** in the results section of this report.

The bathymetric processing software packages EIVA NaviModel and Caris HIPS inherently stores MBES DTMs and sounding data with a positive down depth convention. Report imagery obtained from these packages show the data in this convention.

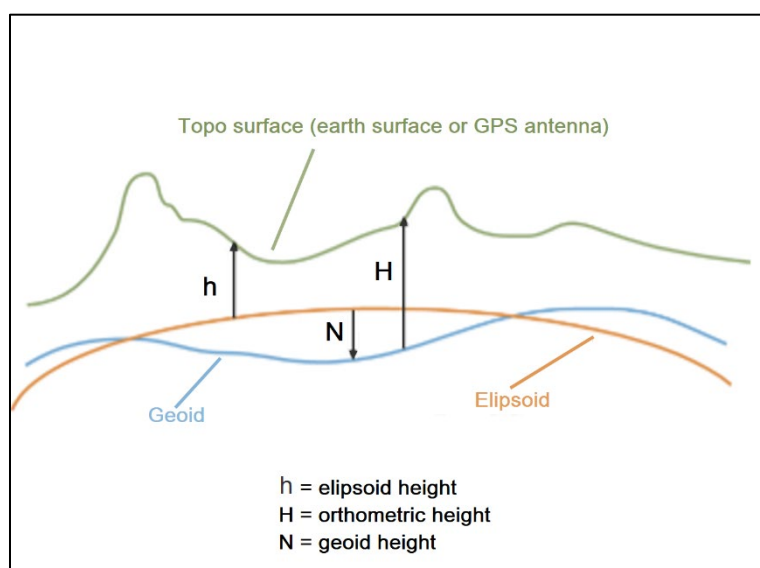


Figure 7 Overview of the relation between different vertical references.

2.3 | TIME DATUM

Coordinated universal time (UTC) is used on all survey systems on board the vessel. The synchronisation of the vessels on board system is governed by the pulse per second (PPS) issued by the primary positioning system. All displays, overlays and logbooks are annotated in UTC as well as the daily progress report (DPR) that is referred to UTC.

3 | SURVEY VESSELS

3.1 | M/V NORTHERN FRANKLIN

GEOPHYSICAL & ENVIRONMENTAL SURVEY OFFSHORE

Part of the offshore geophysical survey operation was conducted by the survey vessel M/V Northern Franklin (Figure 8). The vessel equipment is shown in Table 13.



Figure 8 M/V Northern Franklin.

Table 13 M/V Northern Franklin equipment.

INSTRUMENT	NAME
Navigational System	
Primary Positioning	Applanix POS MV 320 with C-NAV 3050 and C2 (SF2) corrections
Secondary Positioning	C-NAV 3050 and C2 (SF1) corrections
Primary Gyro and INS	Applanix POS MV 320
Underwater Positioning	iXSEA GAPS III
Surface Pressure Sensor	Vaisala Pressure Sensor
Survey Navigation Software	QPS QINSy 9.3.1
Sound Velocity	
Hull-mounted SV at MBES transducer	Valeport MiniSVS
Sound Velocity Profiler	Valeport SVX2
Geophysical Hull Mounted Equipment	
MBES	Kongsberg EM2040 Dual Head (EM2040D)
SBP	INNOMAR SES-2000 Medium 100
ROTV (towed)	
Primary Gyro and INS	iXsea Octans Nan / iXblue ROVINS
Sound Velocity Sensor	Valeport MiniSVS
Altimeter	Kongsberg MS1007

INSTRUMENT	NAME
USBL transponders	iXsea MT8
SSS	Edgetech 2200 300/600 kHz
Magnetometer	Geometrics G882
Geotechnical	
Grab sampler	Day Grab

3.2 | M/V RELUME

GEOPHYSICAL & ENVIRONMENTAL SURVEY OFFSHORE

Part of the offshore geophysical survey operation was conducted by the survey vessel M/V Relume (Figure 9). The vessel equipment is shown in Table 14.



Figure 9 M/V Relume.

Table 14 M/V Relume equipment.

INSTRUMENT	NAME
Navigational System	
Primary Positioning	Applanix POS MV 320 with C-NAV 3050 and C2 (SF2) corrections
Secondary Positioning	C-NAV 3050 and C2 (SF1) corrections
Tertiary Positioning	Veripos LD6 with Ultra corrections
Primary Gyro and INS	Applanix POS MV 320
Underwater Positioning	Kongsberg HiPAP 501 USBL
Surface Pressure Sensor	Vaisala Pressure Sensor
Survey Navigation Software	QPS QINSy v8.18.5
Sound Velocity	
Hull-mounted SV at MBES transducer	Valeport miniSVS

INSTRUMENT	NAME
Sound Velocity Profiler	Valeport MIDAS SVX2, deployed over the side as MVP
Geophysical Hull Mounted Equipment	
MBES	Kongsberg EM2040D (200-400 kHz)
SBP	Innomar Medium 100
ROTV (towed)	
Primary Gyro and INS	iXblue ROVINS
Sound Velocity Sensor	Valeport miniSVS
Altimeter	Kongsberg MS1007
DVL	LinkQuest NavQuest microDVL (600 kHz)
USBL transponders	Kongsberg MST 319
SSS	EdgeTech 2200 300/600 kHz
Magnetometer	Geometrics G882
2D UHRS System	
Sparker	Geo marine surveys systems B.V., 3 x Geo-Source stacked 200 LW
Streamer	Geo marine surveys systems B.V., Geo-Sense Ultra Hi-Res 96 channels

3.3 | OPERATIONAL SUMMARY

This section provides a summary of the operations on board the M/V Relume (Table 15) and M/V Northern Franklin (Table 16) during the MMT OWF offshore survey between 2021-05-01 and 2021-08-18. While this period covers the extents of the MMT OWF survey, within these dates will also be various operations for the 10 km x 10 km Artificial Island survey area.

For complete operational and QHSE details see the Operations Report referenced in Table 3.

M/V RELUME (AND GEOSURVEYS)

GeoSurveys (GS) and Geo Marine Survey Systems (GMSS) were contracted by MMT to provide the 2D UHRS acquisition and QC and also the onshore processing and interpretation of the data on board M/V Relume.

On 01 May 2021, M/V Relume commenced mobilisation and manning alongside Thyborøn, Denmark. Kick-off meetings and introductions to the project were held on 02 May 2021. Alongside verifications were conducted alongside Thyborøn. On 03 May 2021, M/V Relume departed port to start the offshore calibrations and verifications with the geophysical and 2D UHRS equipment.

Between 03 May and 07 May 2021, the offshore calibrations, geophysical and 2D UHRS equipment verifications were conducted.

Between 07 May and 12 June 2021, M/V Relume conducted geophysical and 2D UHRS survey operations in Lot 1, MMT OWF survey area.

On 12 June 2021, M/V Relume demobilised.

Table 15 Survey tasks – M/V Relume.

TASK	DATE	DESCRIPTION
Mobilisation	2021-05-01 – 2021-05-03	Mobilisation alongside Thyborøn, Denmark
Calibrations and verifications	2021-05-03 – 2021-05-07	Alongside Thyborøn and offshore
Geophysical Survey	2021-05-07 – 2021-06-12	Geophysical survey operations
2D UHRS Seismic Survey	2021-05-09 – 2021-06-10	2D UHRS and geophysical survey operations
Demobilisation	2021-06-12	Demobilisation alongside Thyborøn, Denmark

M/V NORTHERN FRANKLIN

On 10 June 2021, M/V Northern Franklin commenced mobilisation and manning alongside in Thyborøn, Denmark. Kick-off meetings and introductions for the project were held on the 12 June 2021. Alongside and on-site calibrations were conducted between 13 June and 17 June 2021.

Between 17 June and 16 August 2021 geophysical survey and benthic sampling was undertaken. In total 125 grab samples (from the original 150 in the SOW) were taken within the MMT OWF survey area. This was due to deteriorating weather and the need to maximise survey efficiency.

On 18 Aug 2021, M/V Northern Franklin de-mobilised in Harwich, UK

Table 16 Survey tasks – M/V Northern Franklin.

TASK	DATE	DESCRIPTION
Mobilisation	2021-01-11 – 2021-06-15	Mobilisation alongside Thyborøn, Denmark
Calibrations and verifications	2021-06-15 – 2021-06-18	Alongside Thyborøn and offshore wreck location and survey area
Geophysical Survey	2021-06-18 – 2021-08-13	Geophysical survey operations
Grab Samples	2021-07-29 – 2021-08-16	Grab sample operations
Demobilisation	2021-08-16 – 2021-08-18	Demobilisation alongside Harwich, UK

4 | DATA PROCESSING AND INTERPRETATION METHODS

4.1 | BATHYMETRY

The objective of the processing workflow is to create a Digital Terrain Model (DTM) that provides the most realistic representation of the seabed with the highest possible detail. The processing scheme for MBES data comprised two main scopes: horizontal and vertical levelling in order to homogenise the dataset and data cleaning in order to remove outliers.

The MBES data is initially brought into Caris HIPS to check that it has met the coverage and density requirements. It then has a post-processed navigation solution applied in the form of an SBET. The SBET was created by using post-processed navigation and attitude derived primarily from the POS M/V Inertial Measurement Unit (IMU) data records. This data is processed in POSPac MMS and then applied to the project in Caris HIPS.

In addition to the updated position data, a file containing the positional error data for each SBET is also applied to the associated MBES data. The positional error data exported from POSPac MMS contributes to the Total Horizontal Uncertainty (THU) and Total Vertical Uncertainty (TVU) which is computed for each sounding within the dataset. These surfaces are generated in Caris HIPS and are checked for deviations from the THU and TVU averages.

After the post-processed position and error data is applied, a Global Navigation Satellite System (GNSS) tide is calculated from the SBET altitude data which vertically corrects the bathymetry using the DTU21 MSL to GRS80 Ellipsoidal Separation model within Caris HIPS. The bathymetry data for each processed MBES data file is then merged together to create a homogenised surface which can be reviewed for both standard deviation and sounding density. Once the data has passed these checks it is ready to start the process of removing outlying soundings which can be undertaken within Caris HIPS or in EIVA NaviModel.

In the Caris HIPS workflow an average surface is derived from the sounding data and from this it is possible to remove outliers that lie at a specified numerical distance from the surface, or by setting a standard deviation threshold. Manual cleaning can also be performed using the Subset Editor tool to clean areas around features that would be liable to being removed by the automatic cleaning processes.

In the EIVA NaviModel workflow, the data is turned into a 3D model which undergoes further checks and data cleaning processes. Typically, a Scalgo Combinatorial Anti-Noise (S-CAN) filter is applied to the data to remove any outliers although some manual cleaning may also take place. This data cleaning is then written back to the data in the Caris HIPS project ready for Quality Check (QC).

In Caris HIPS the QC surfaces are recalculated to integrate any sounding flag editing that has occurred in NaviModel or within HIPS and examined to check that the dataset complies with the project specification. If the dataset passes this QC check, then products (DTMs, contours and shaded images) can be exported from either Caris HIPS or NaviModel for delivery or for further internal use.

The work flow diagram for MBES processing is shown in Figure 10.

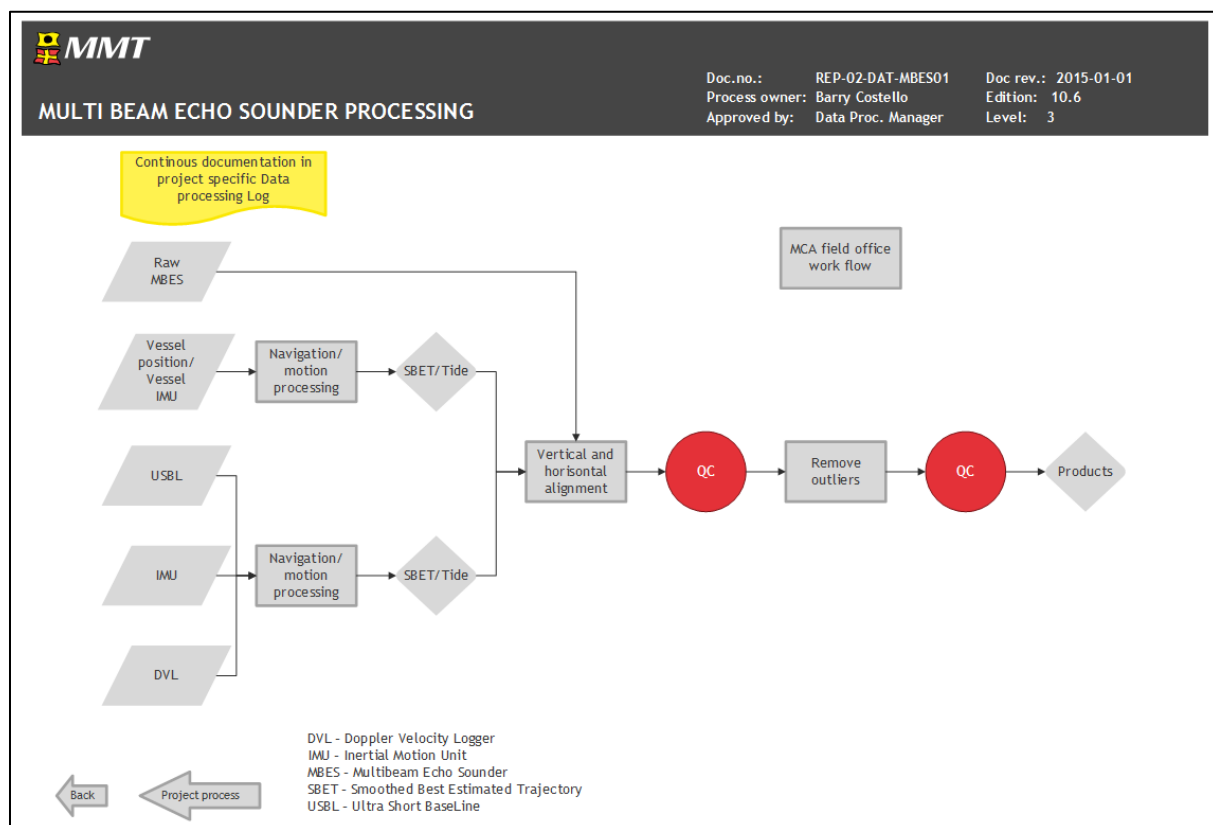


Figure 10 Workflow MBES processing.

The workflow outlines the processing that occurred on both Relume and Northern Franklin. Due to data acquisition requirements the Northern Franklin acquired MBES data for the 2D UHRS component of the survey with Relume completing the remaining Geophysical survey lines. In some instances, the vessels were processing survey lines that had no overlapping data from adjacent lines, so vertical alignment checks across the entire survey area during acquisition were not possible. During survey operations, once Northern Franklin had completed the 2D UHRS scope, she became available to assist Relume acquire the Geophysical Survey lines. An example of the pattern of survey line running can be seen in Figure 11. Here Northern Franklin was able to complete overlapping survey lines in the north eastern corner with the alternating pattern of vessels covering the majority of the survey area shown.

Both datasets were combined in the office and QC steps followed to check for vertical alignment between each vessel's MBES data.

Finally, the MMT OWF survey area MBES data was trimmed to the 10 km x 10 km Artificial Island survey area.

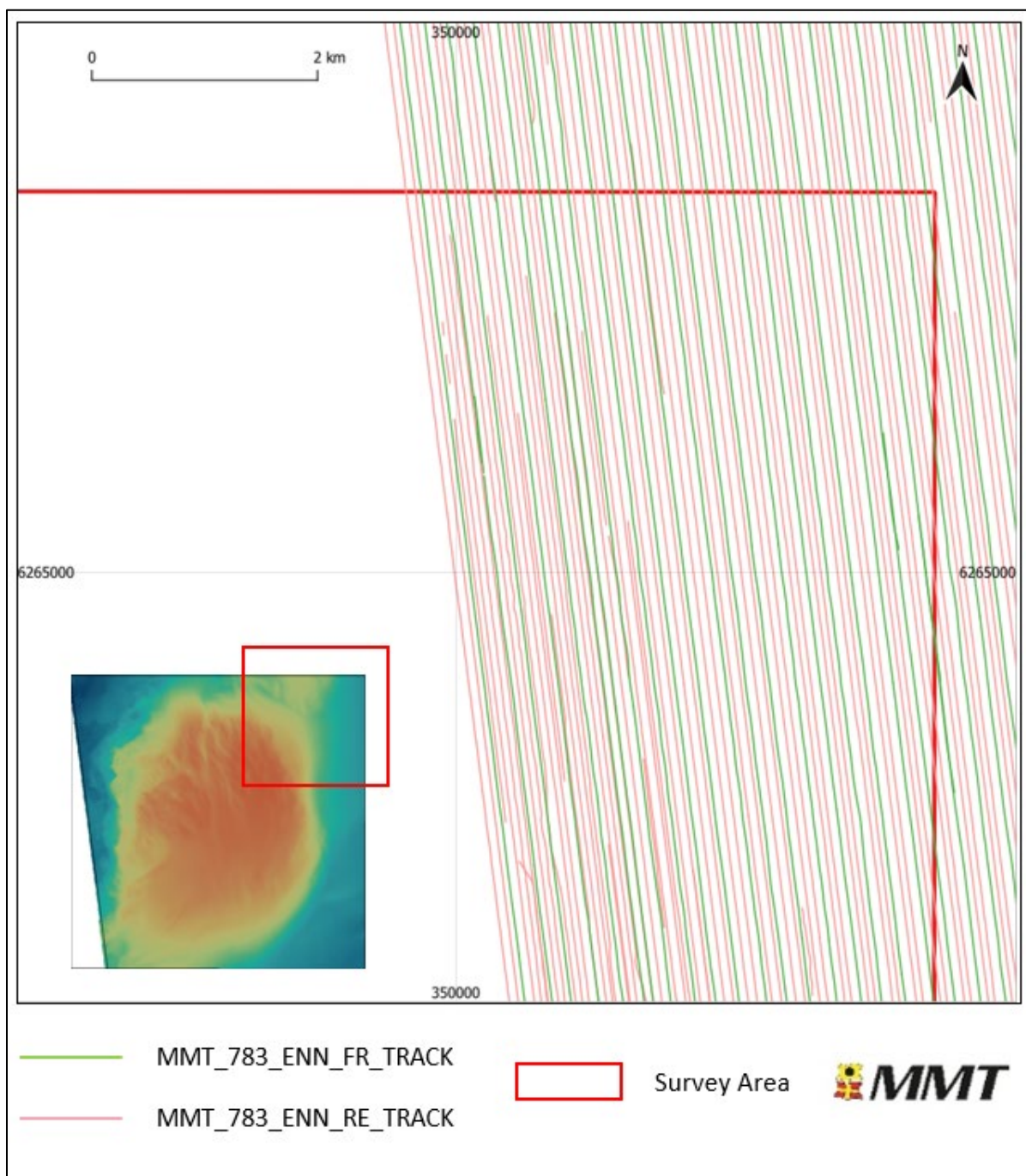


Figure 11 Example of division of MBES data acquisition in BM3 and BM4.
 Relume (orange) and Northern Franklin (green).

Bathymetric contours were generated from the 1 m DTM in combination with scaling factors applied to generalise the contours to ensure the charting legibility. The contour parameters used are shown in Figure 12 and the exported contours presented over the DTM is shown in Figure 13.

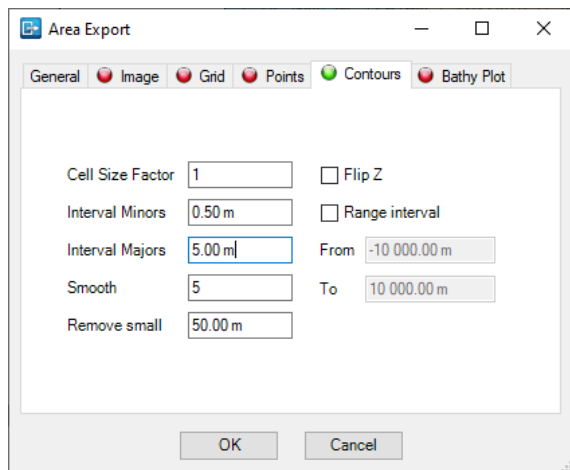


Figure 12 Artificial Island survey area contour export parameters.

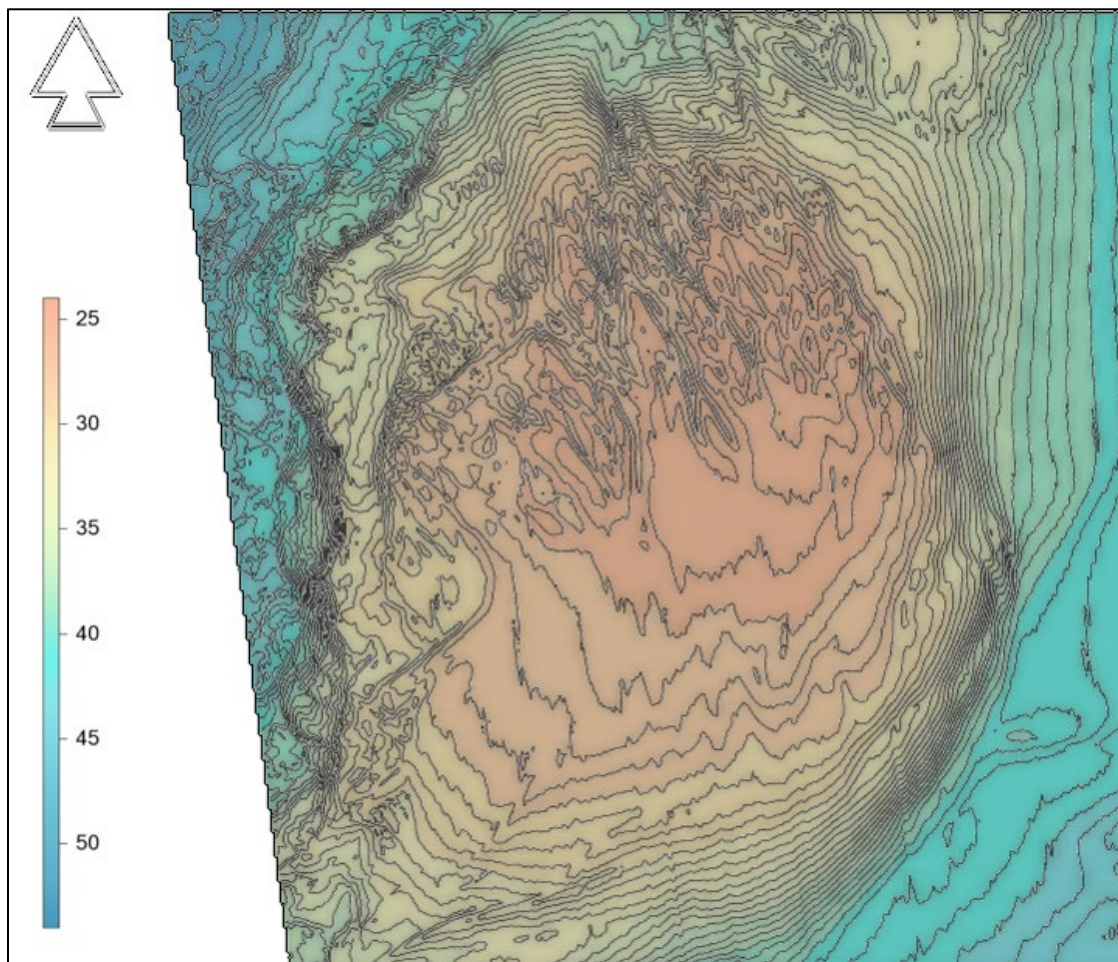


Figure 13 Exported contours with 50 cm interval over the Artificial Island survey area. Navimodel depth convention is positive down.

4.2 | BACKSCATTER

MBES backscatter data was processed on both Relume and Northern Franklin using QPS Fledermaus GeoCoder Toolbox (FMGT). The aim of this process was to provide information of sediment boundary positions to the geologists on-board. Since the two vessels were not obtaining 100% sea floor coverage individually the data from each vessel needed to be combined in the office after acquisition was completed. Products generated on the vessel could then be used as an interim dataset for the surficial geology interpretation and contact picking whilst final backscatter processing was taking place.

The final processing was performed for the Artificial Island survey area. Data from both Northern Franklin and Relume were processed in the same FMGT project to optimise the blending of overlapping data from the two vessels. Survey lines that run obliquely to the main survey line direction are excluded to reduce the presence of artefacts in areas that already have 100% coverage.

FMGT reads the intensity of each returned ping and applies a sequence of normalising algorithms to account for the variations in intensity generated by vessel motion, beam angle and high frequency, along track variability. In addition, FMGT effectively back-calculates other intensity changes generated by any automatic changes to the EM2040D (MBES) operating settings and results in a homogenous grayscale backscatter mosaic that accurately represents the spatial variations in seafloor sediments.

ASCII files containing XY and backscatter intensity (XY+i) were exported from FMGT at 0.5 m resolution and these were re-projected using Feature Manipulation Engine (FME) to the project coordinate system. The ASCII files were merged before being clipped to 2 km x 2 km grid tiles using the Tile Schema (783_Energinet_TileSchema_ETRS89_32N_2KM). These XY+i ASCII files were used to create tiled 32bit FLT GeoTiffs for delivery and import to ArcGIS. The XY+i files were also used to create RGB GeoTiff image. Finally, the MMT OWF survey area backscatter data was trimmed to the 10 km x 10 km Artificial Island survey area.

4.3 | SIDE SCAN SONAR

SSS processing and interpretation was conducted within SonarWiz. Prior to importing raw SSS JSF files the water sound velocity at towing depth was confirmed and updated within the SonarWiz import settings. The raw SSS data was then imported into SonarWiz without the application of any gains, and the following QC/processes were conducted:

1. Navigation data QC'd and any occasional spikes removed
2. Seabed auto tracked, QC'd and manually adjusted if necessary
3. User controlled gains applied to the data and manually adjusted to enhance seabed sediment contrasts and seabed features
4. SSS data QC'd against MBES data by locating features/contacts clearly distinguishable in both data sets and comparing appearance and position
5. Coverage QC'd and any gaps flagged and infilled in order to meet client coverage requirements

The SSS processing workflow is outlined in Figure 14 and Figure 15.

The processing was conducted with the following objectives:

- To classify seabed surface sediments
- To classify mobile bedforms and other potential hazards
- To identify natural and anthropogenic seabed features
- To detect contacts
- To detect cables and pipelines

The interpretation of SSS geo-boundaries was conducted within SonarWiz and AutoCAD software. Within SonarWiz geo-boundaries were digitised as features and exported as DXF files. For digitisation in AutoCAD, SSS mosaics were exported from SonarWiz loaded into AutoCAD and line and polygon features mapped. Before the mosaic were exported as a GeoTiffs, the files were arranged so the best available data is uppermost. The nadir was made transparent in order for data in overlapping files that cover the nadir gap to be seen. This process is conducted for both high frequency (HF) and low frequency (LF) data sets.

The geo-boundaries (interpreted changes in surface geology) were reviewed against backscatter, MBES and magnetometer (MAG) grid data so an integrated interpretation was obtained based upon all available data. Seabed sediment classifications were also reconciled against the geotechnical grab sample (GS) results. Interpretations were QC'd and finalised by a Senior Geologist.

The interpretation of SSS contacts was initially conducted within SonarWiz. The SSS data was viewed in digitising mode and man-made objects were digitised. Wrecks/cables were correlated to existing databases. Contacts were initially picked using an auto-picking algorithm in NaviModel. Based on the results, boulder fields were delineated in AutoCAD according to the boulder field classification provided. Once boulder field polygons were generated, the boulders within them were filtered to remove boulders less than 1 m in either dimension. Remaining contacts were then QC'd against the mosaics and MBES, and any missing contacts were added using SonarWiz. The contact list was then correlated to MAG.

The MMT OWF survey area SSS data and contact lists were then trimmed to the 10 km x 10 km Artificial Island survey area.

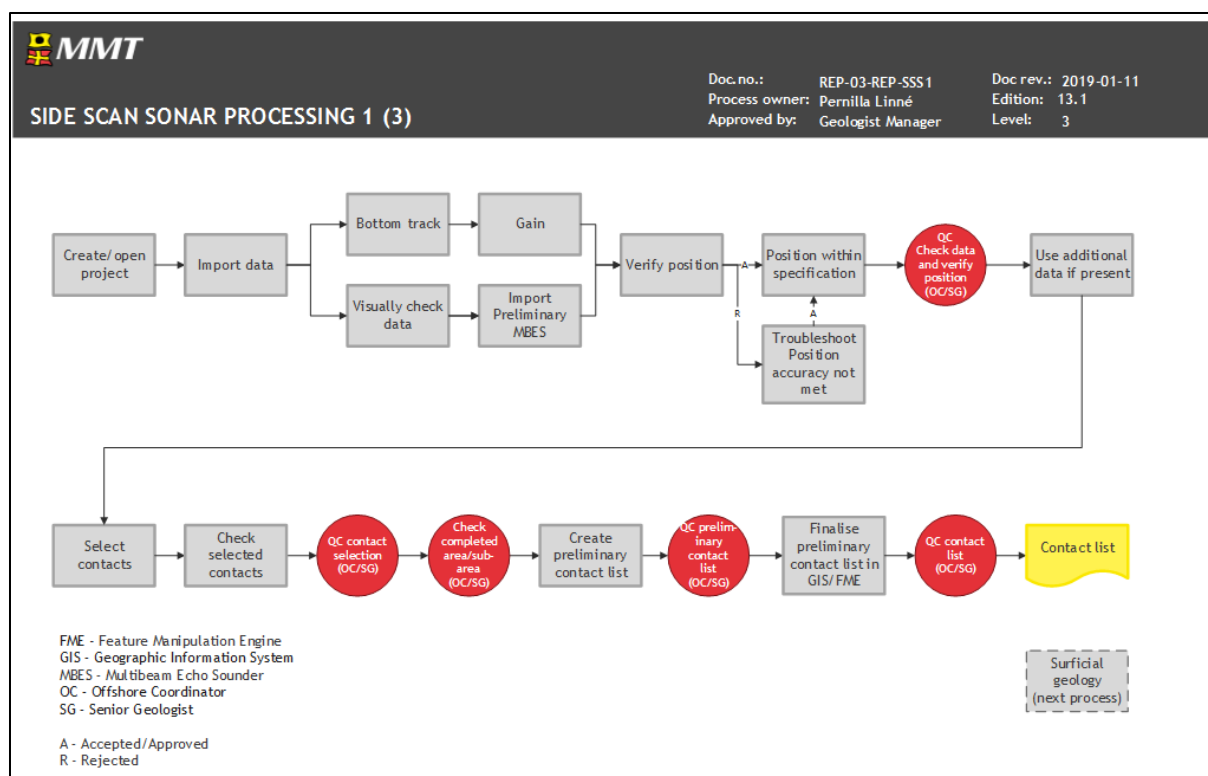


Figure 14 Workflow side scan sonar processing (1 of 2).

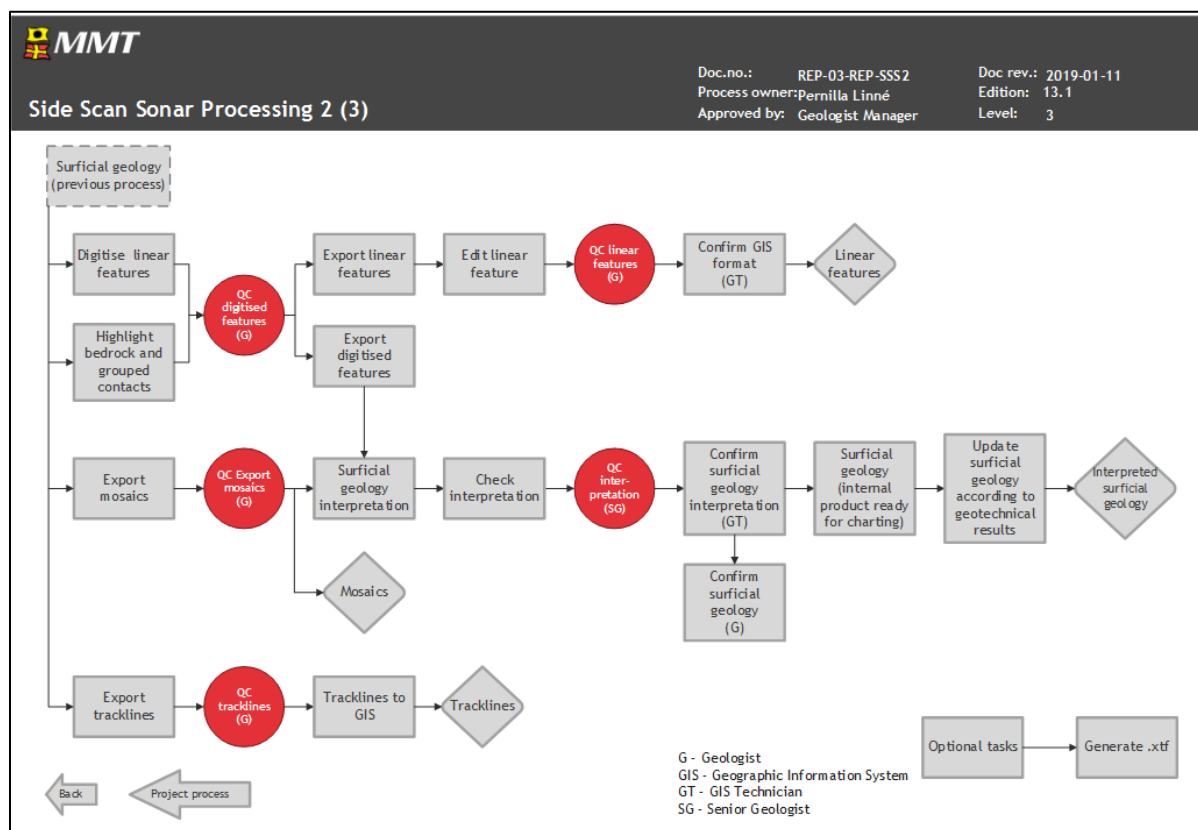


Figure 15 Workflow side scan sonar processing (2 of 2).

4.4 | MAGNETOMETER

MAG data was processed and interpreted within Oasis Montaj software.

Navigation is despiked removing outliers through a set distance from the navigational trend, after a manual check is performed and additional spikes are removed as needed. Small gaps are interpolated and bigger navigational gaps are flagged for infill. 100 samples are interpolated: at 4 knots survey speed with a sample rate of 10 Hz, approximately 20m is the maximum interpolation distance. Once the navigation has been despiked a small rolling statistic smoothing filter is applied.

Altitude, depth and motion is despiked removing outliers through a set value that incorporates real data for each sensor but excludes spikes as these vastly differ from the real data, after a manual check is performed and additional spikes removed as needed. Once despiked a small rolling statistic smoothing filter is applied for each sensor.

The raw MAG data was de-spiked using a pre-set cut off value of 45000 nT and 56000 nT to remove occasional spikes. To generate the regional background field, a series of four filters were used. The regional background field was then subtracted from the total field to generate the residual field.

Applied filters to generate background:

- Non-linear filter 1; Width = 60, Tolerance = 1.2
- Non-linear filter 2; Width = 30, Tolerance = 0.5
- Non-linear filter 3; Width = 15, Tolerance = 0.25
- Non-linear filter 4; Width = 7, Tolerance = 0.125

Example of the filter result can be seen in Figure 16 for Northern Franklin and Figure 17 for Relume.

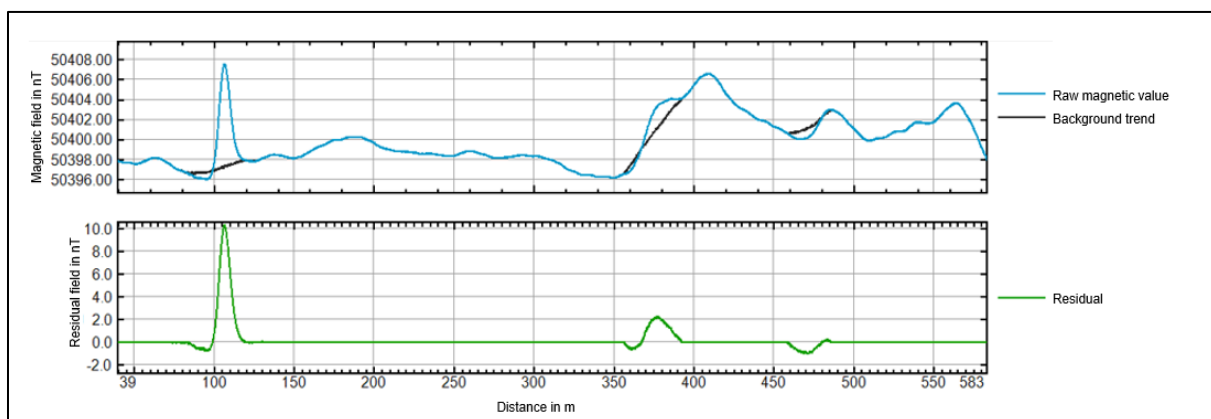
The same set of filters were used over the whole dataset to remove the regional background field.

No altitude correction has been performed on the magnetic data set.

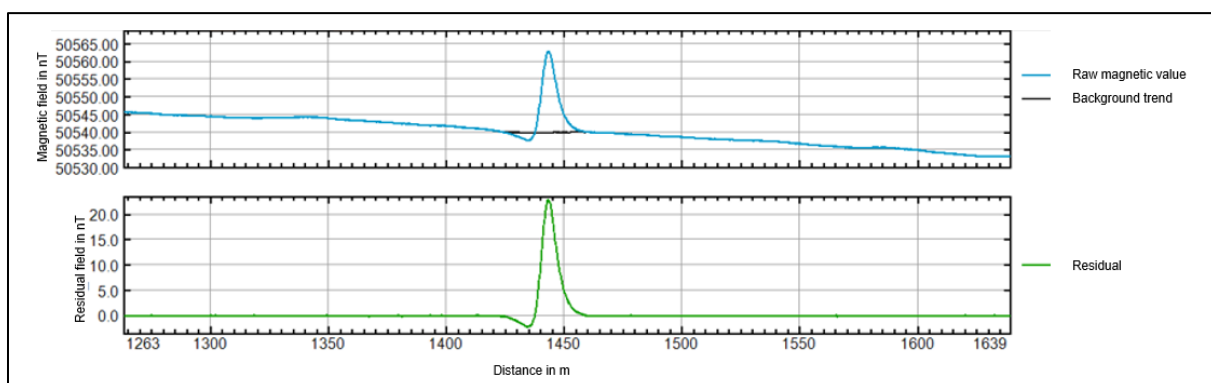
Each file was individually studied for anomalies. The criteria for magnetic anomalies is 10 nT (peak to peak). However, clear anomalies below the threshold have also been picked.

Once an anomaly was identified a comparison was carried out between the different sensor information available (altitude, depth, motion and quality) to determine if the anomaly is real or induced by low quality or rapid changes in MAG movement. Once an anomaly was confirmed to be real the location was added to a database and the anomaly's amplitude and wavelength was manually measured. Once completed, each picked anomaly was individually Quality Checked to confirm stored values.

The MMT OWF survey area MAG contacts lists were then trimmed to the 10 km x 10 km Artificial Island survey area.



*Figure 16 Data example for Northern Franklin from B3.
 Raw, processed background trend and the resulting residual signal of the magnetometer data.*



*Figure 17 Data example for Relume from B3.
 Raw, processed background trend and the resulting residual signal of the magnetometer data.*

The general workflow of the MAG processing is outlined in Figure 18 and Figure 19.

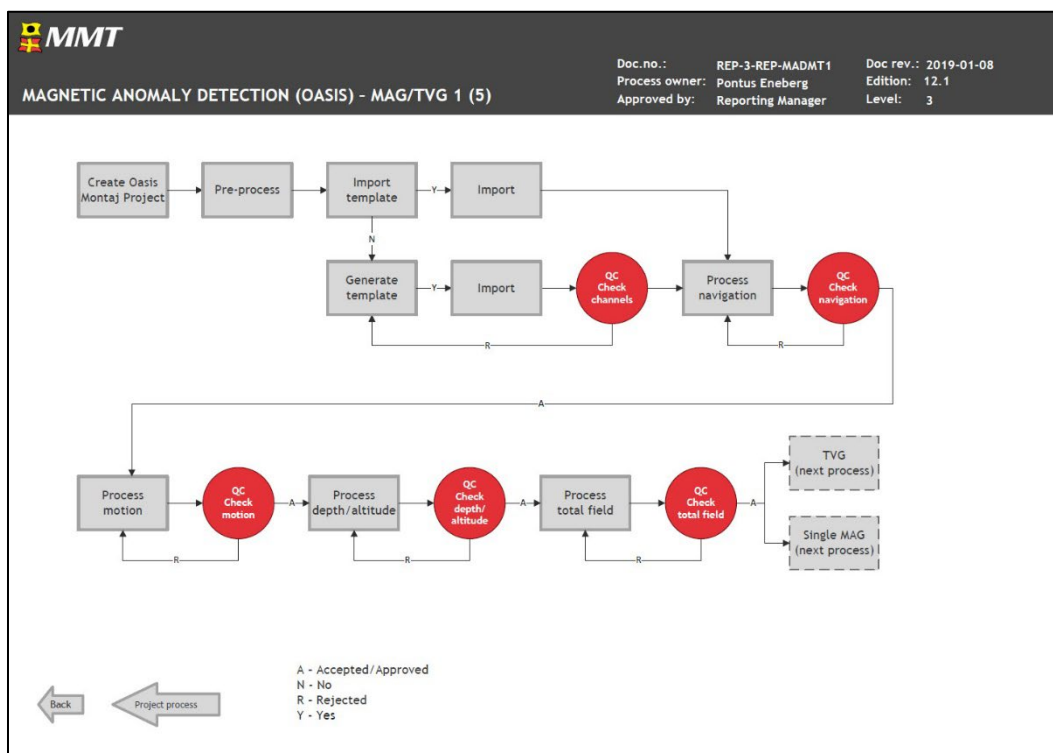


Figure 18 Workflow MAG processing (1 of 2).

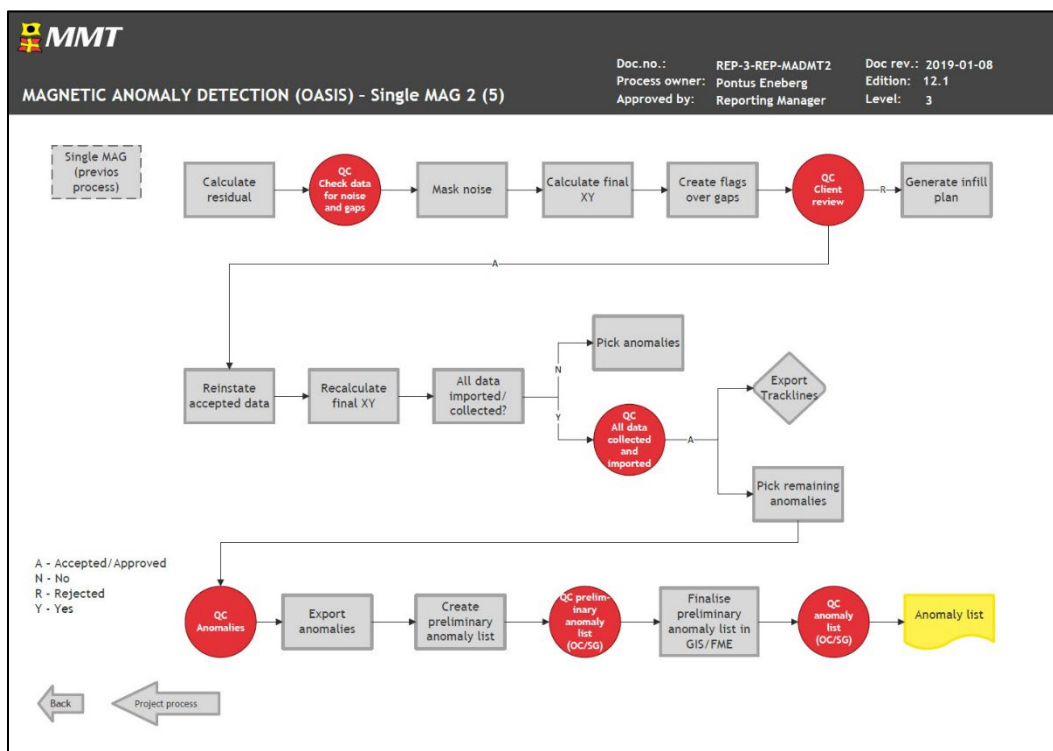


Figure 19 Workflow MAG processing (2 of 2).

4.5 | SEISMIC - 2D UHRS

The flow was divided into two main processing tracks: pre-stack TRIM track and FULL track.

- The main purposes of the TRIM track were to perform source signature deconvolution and to estimate a proper residual motion correction.
- The aim of the FULL track processing was to achieve the final seismic sections (MUL and MIG datasets) used for the final (refined) seismic interpretation.

Table 17 summarises the gridding parameters (used for all grids in the Kingdom Suite project). The selected settings were based on their ability to deliver optimal results (coverage between lines and minimising artefacts and edge effects).

Table 17 Gridding parameters.

Cell Size	5 m
Algorithm	Flex Gridding
Smoothness	6 (scale is 0 to 11)
Search radius	120 m

For full description of and details on the 2D UHRS processing see Appendix D|.

4.6 | SUB-BOTTOM PROFILER - INNOMAR

Prior to import, the SBP data files were converted from SES3 format to SGY format using an in-house software; MMT GeoTools. The conversion software corrects the navigation and applies vertical corrections to the data with the application of an SBET (Smoothed Best Estimate Trajectory) exported from PosPAC. The SGY files were then imported into RadExPro for signal processing. The seabed was auto tracked and then quality checked and manually adjusted, if required. Positional accuracy was verified during the MAC by using MBES data to locate features clearly distinguishable in both data sets and comparing the positions. Within RadExPro the processing flows were designed to improve the quality and resolution of the data by removing noise and enhancing the primary signal. In general, the signal processing flow applied to the data was:

- Burst noise removal
- TFD noise attenuation
- Source signature deconvolution
- Butterworth filtering
- Amplitude correction
- Amplitude recovery
- 2D spatial filter
- Export in standard SGY

Visual QC was performed before and after each processing step to check:

- The natural continuity of geological units was preserved
- Creations of artefacts which could mislead the interpretation process
- Suppression and/or removal of all kind of noise without compromising the true signal

Another in-house software, MMT PostProc GeoTools, was then used to write the final processed ASCII textual header to all SGYs. This program was also used to export corrected instrument tracklines, high resolution images of each SGY and conduct the depth conversion. The depth conversion is executed using water sound velocities acquired on the vessel. SVP data is loaded into the software to calculate the average sound speed in the water, and then a layer-cake velocity is used for the sediment. The velocity value for the sediment was 1600 m/s.

MMT PostProc GeoTools exports 3 final SGYs; time domain with corrected ASCII header, depth domain and an interval velocity SGY. All three of these SGYs are loaded into Kingdom Suite using Seismic Direct. Geological interpretation is then carried out on the data in the time domain, and later converted to the depth domain using the interval velocity SGY as a reference.

The general workflow of the SBP processing is outlined in Figure 20 and Figure 21.

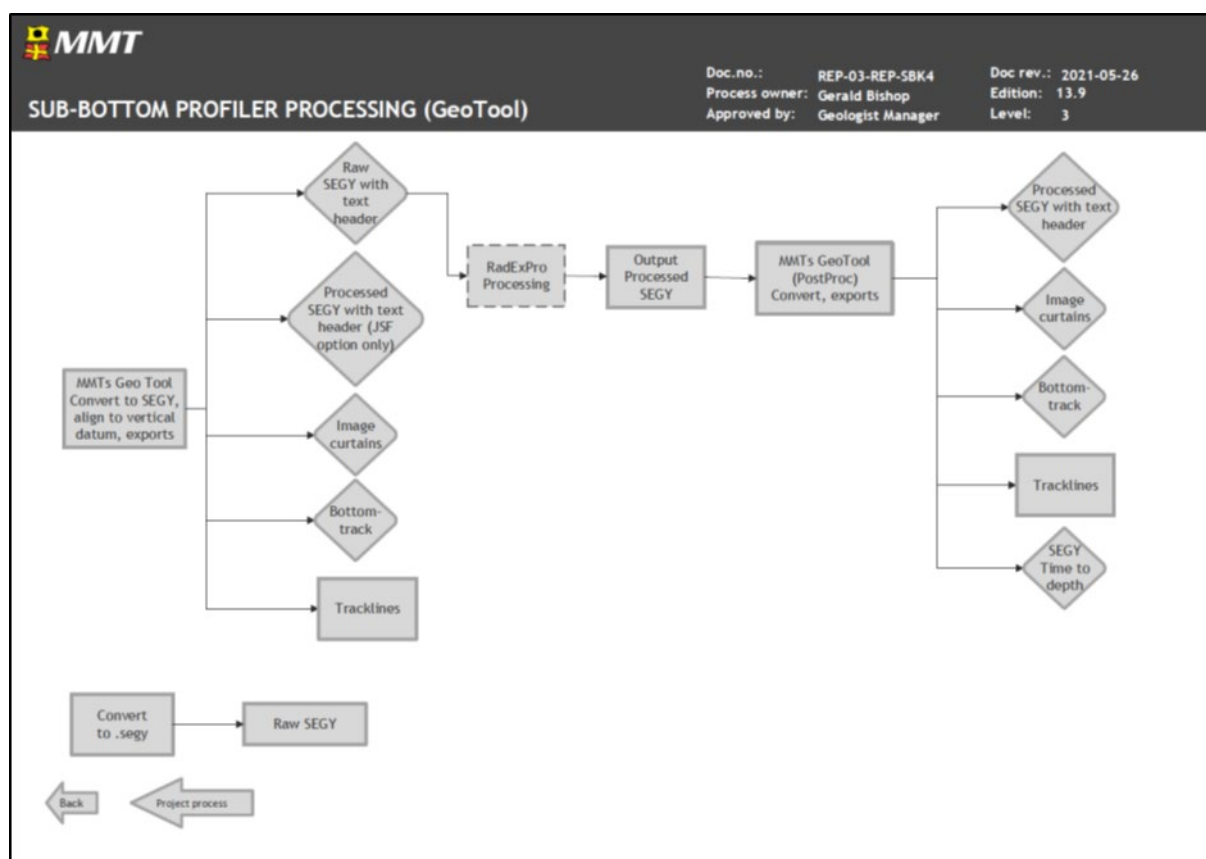


Figure 20 Workflow SBP processing (1 of 2).

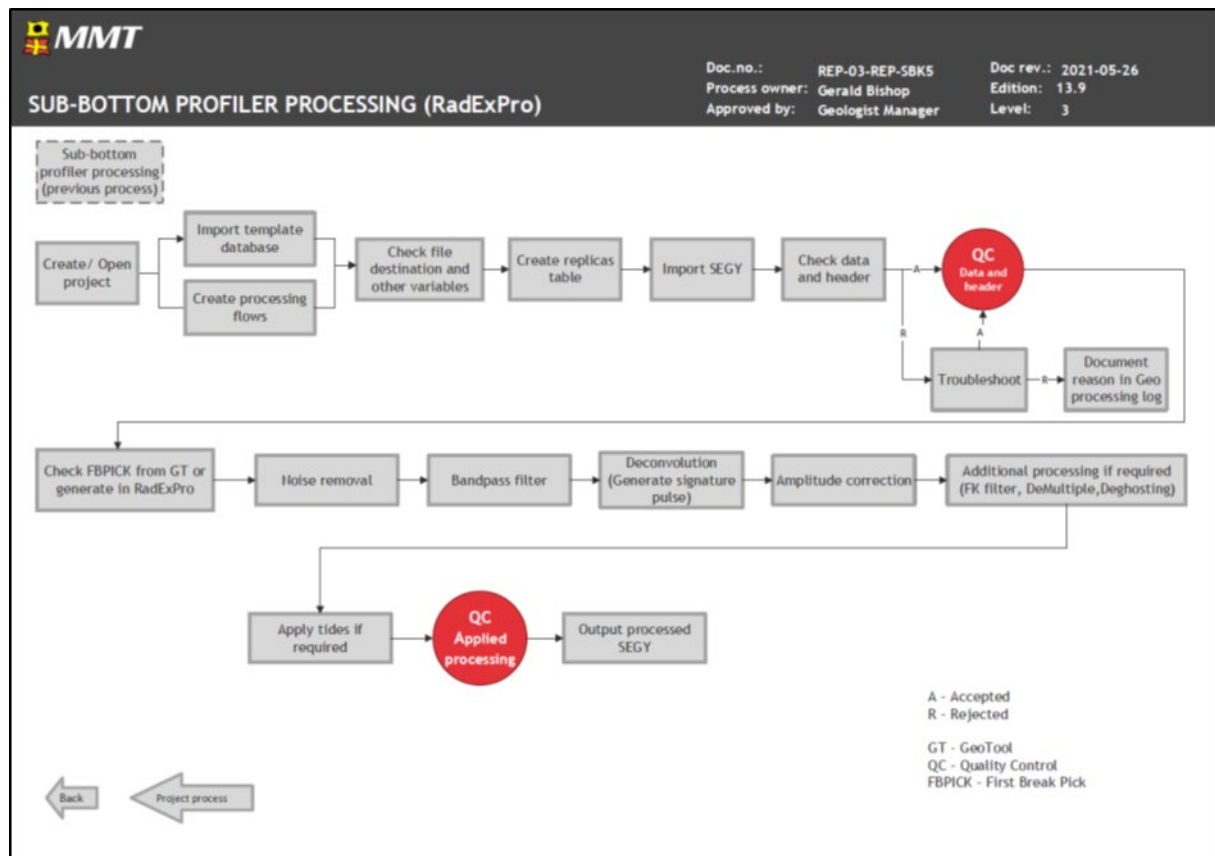


Figure 21 Workflow SBP processing (2 of 2).

5 | PROCESSED DATA QUALITY

5.1 | BATHYMETRY DATA

The processed MBES bathymetry data meets the required specifications. The horizontal and vertical uncertainty of the soundings data were, for the vast majority of the survey area, within acceptable tolerance. Checks were made during acquisition to ensure that sounding density conformed to the 16 soundings per 1 m cell criteria. Some low-density cells exist in the final dataset in Block 1, on the steep slopes on the western edge of the Artificial Island survey area. The low-density cells were evident during the survey, however they were discussed with the Client Representative and deemed acceptable.

The MBES data from Relume and Northern Franklin was combined in the office after survey operations were completed (Figure 22). The principal QC check that was required was to ensure that data from both vessels was vertically aligned. To do this the same methodology for checking vertical alignment within a single dataset was followed.

This is done by generating Caris HIPS QC surfaces from all MBES data within the survey area. A range of properties are computed for each surface and these are checked systematically to ensure the data falls within specification. The Standard Deviation at 95% confidence interval is checked in order to highlight areas where the vertical spread of soundings within a DTM grid node is high and checks can be made to determine the cause. If necessary, action can be taken to bring the soundings into closer alignment. Regions that have high standard deviations can occur where there are sound velocity errors, errors in the post-processed navigation, acquiring data in heavy weather and where there are steep slopes such as boulder fields.

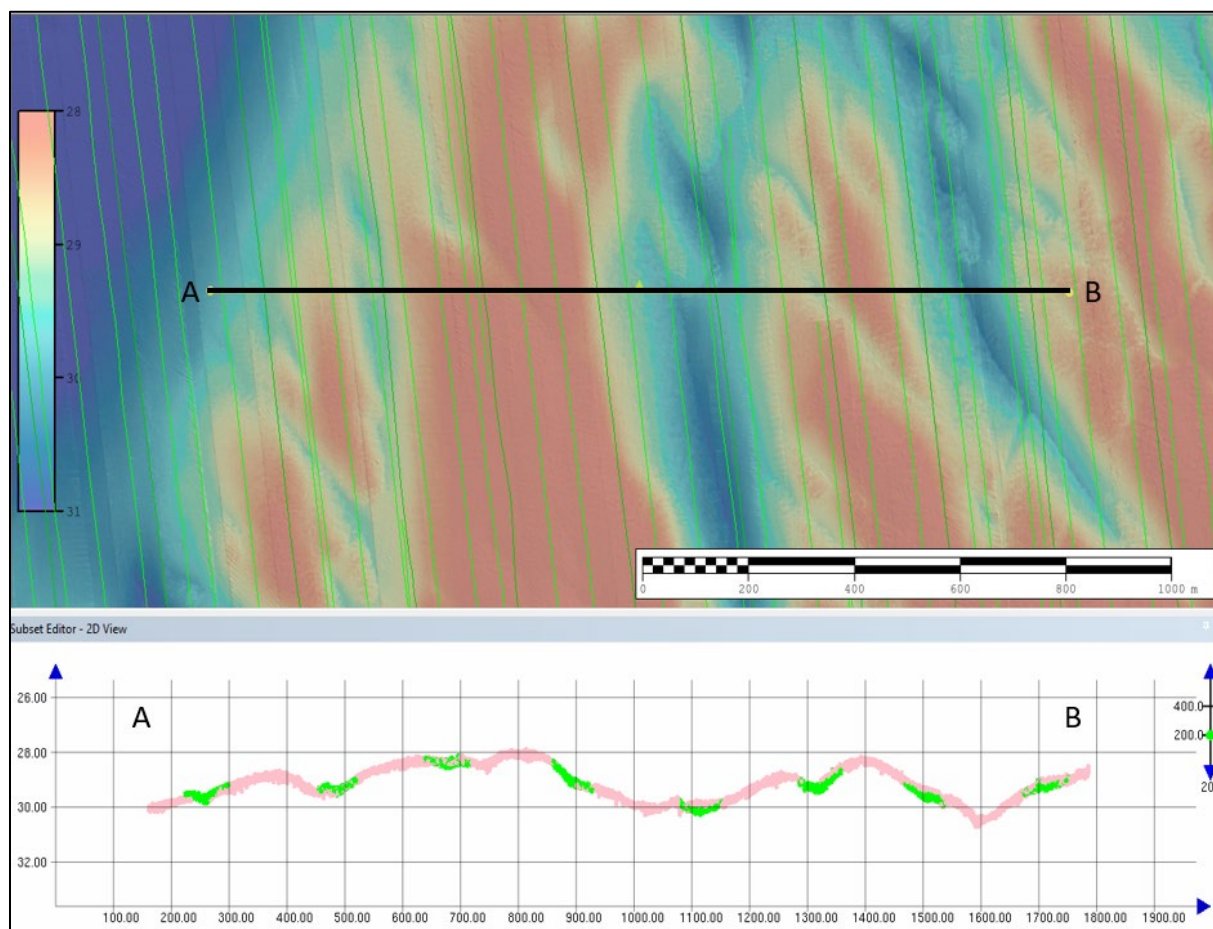


Figure 22 Cross section through the Artificial Island survey area. Image shows vertical alignment of Relume (green) and Northern Franklin (pink). View centred on 348598 E, 6266092 N. Caris HIPS depth convention is positive down. Vertical exaggeration of cross section is x200.

Figure 23 shows an overview of the Standard Deviation surface for the Artificial Island survey area, which presents regions as having low, medium and high standard deviations in green, orange and red, respectively. In the centre of the survey area there are long north-south trending strips of orange colour. These correspond to survey lines that were acquired during times with a high variability in the sound velocity through the water column causing the vertical spread of soundings to be higher than elsewhere.

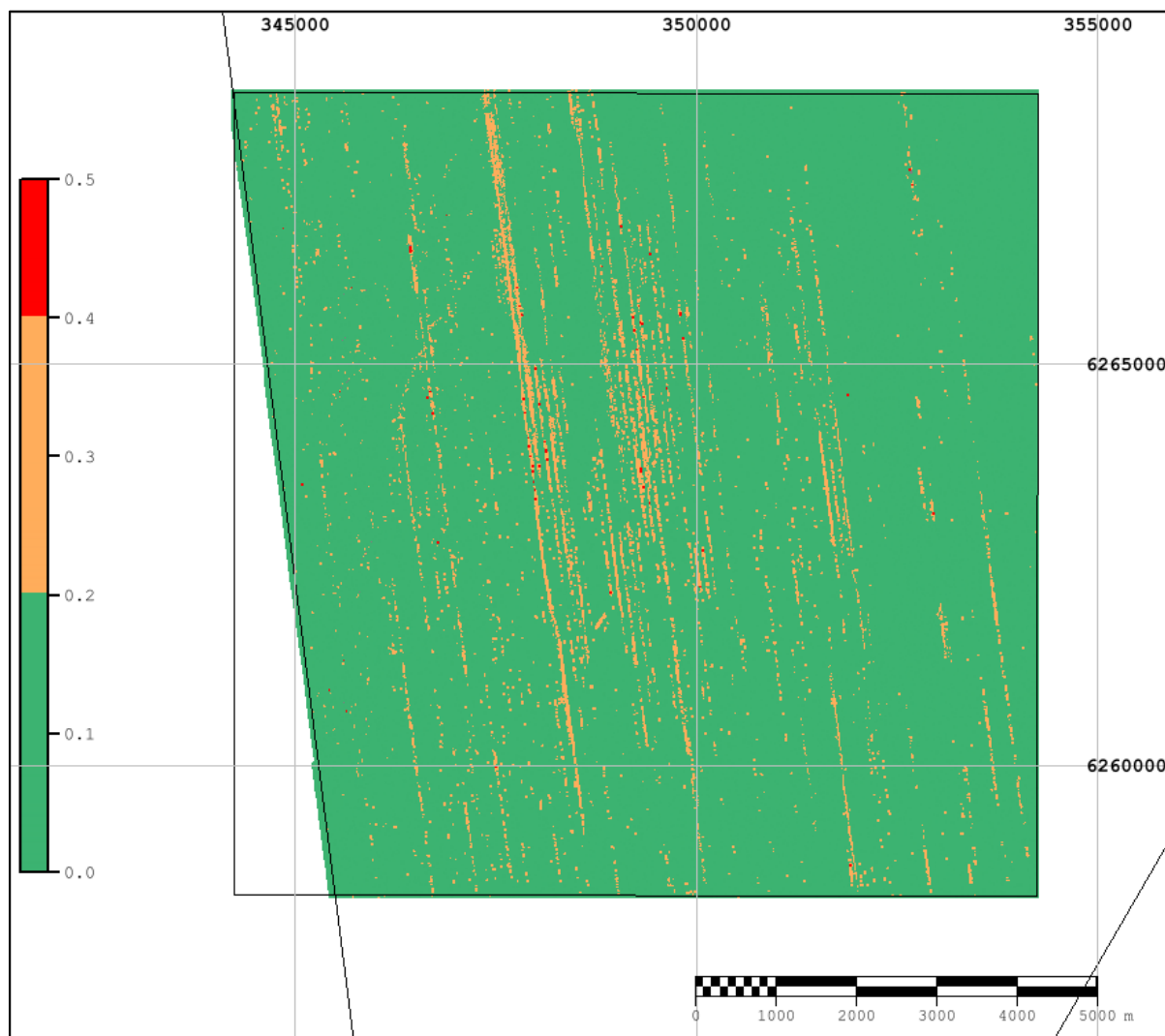


Figure 23 Standard deviation at 95% confidence interval for the Artificial Island survey area. Values are in metres.

Figure 24 and Figure 25 provide examples of the standard deviation surface and cross sections through the sounding data for areas where the sound velocity was stable and variable. Figure 24 shows a region with low standard deviation in the north east of the Artificial Island survey area. This highly exaggerated cross section shows that M/V Northern Franklin and M/V Relume produced data that was well aligned and displays a similar vertical spread of soundings with no sound velocity induced artefacts. Figure 25 shows a region towards the centre of the Artificial Island survey area which had variable sound velocity during the period of acquisition. In general, the sound velocity had higher degrees of variability in the centre of the survey area.

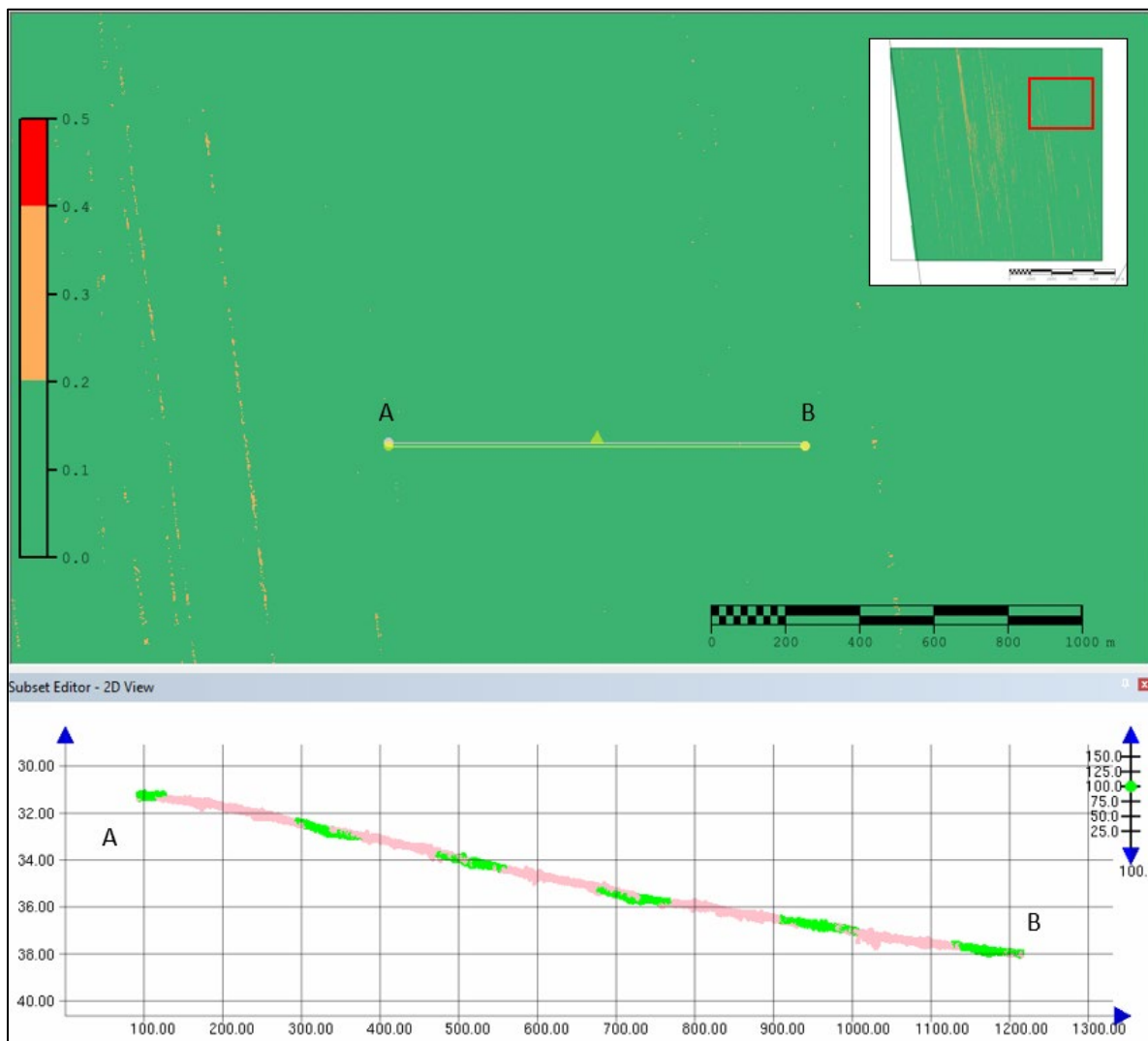


Figure 24 Example of MBES data acquired in good weather with a relatively stable sound velocity. The image shows a similar vertical spread of soundings for M/V Northern Franklin and M/V Relume. Soundings from M/V Northern Franklin shown in pink and M/V Relume in green. The yellow bar marks the location of the cross section in lower half of image. Caris HIPS depth convention is positive down, vertical exaggeration of cross section is x100.

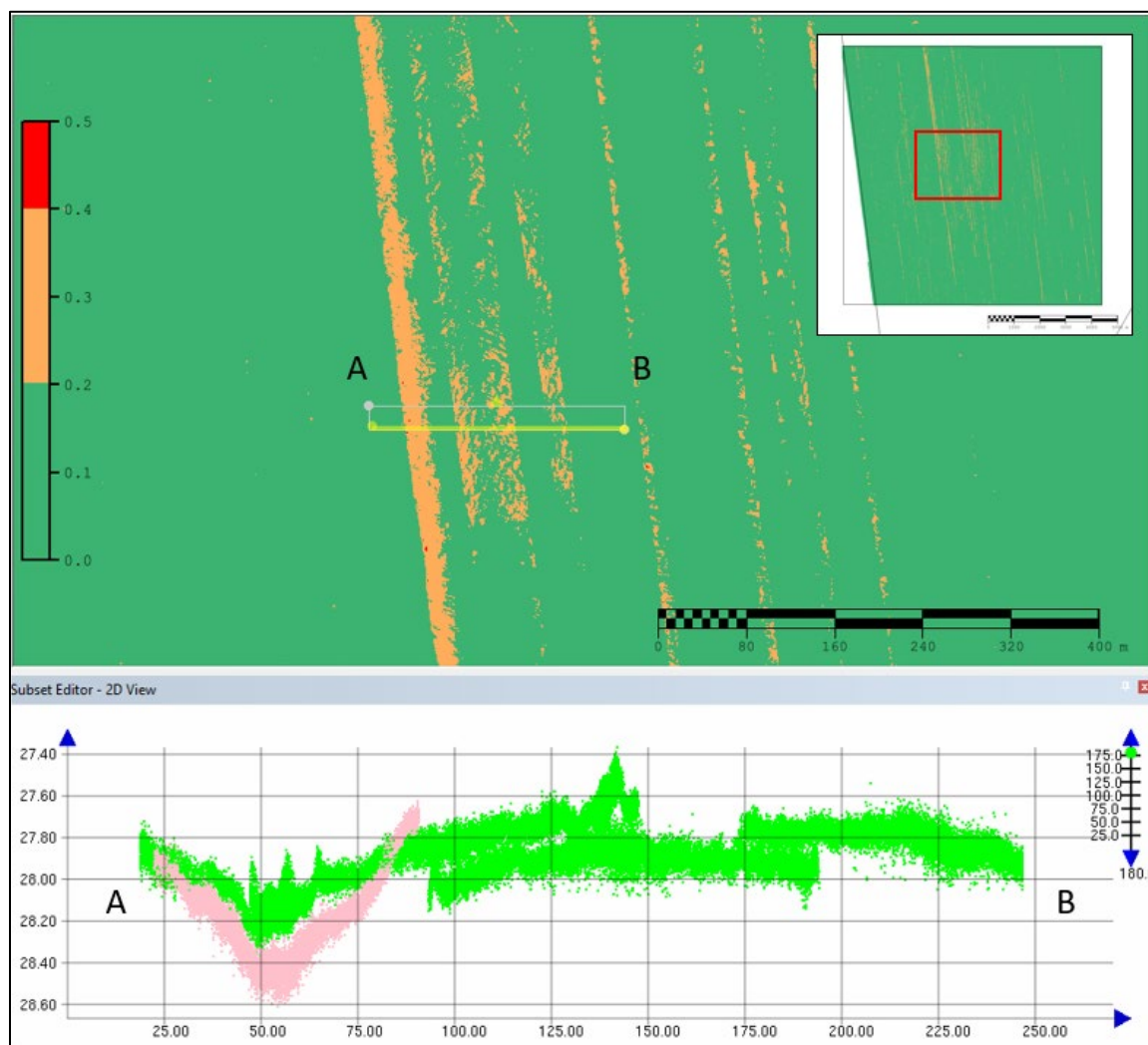


Figure 25 Example of MBES data acquired in area with variable sound velocity with sound velocity artefacts seen in the Relume data. Soundings from M/V Northern Franklin shown in pink and M/V Relume in green. The yellow bar marks the location of the cross section in lower half of image. Caris HIPS depth convention is positive down, vertical exaggeration of cross section is x180.

QC surfaces were computed to show the vertical separation between the mean seabed position and the positions of the shallowest and deepest soundings within a cell. The QC surfaces are used to target both systematic error correction and data cleaning. However, seabed features, such as boulders, as well as outlying soundings are highlighted by these surfaces, so careful assessment is made of all areas flagged as requiring data cleaning to ensure that real features are not removed from the dataset.

An example of these QC surfaces is shown in Figure 26. Steep slopes are highlighted in red and blue since the sounding data deviates from the mean surface by an amount greater than the threshold value for that depth. The surfaces are coloured to indicate the direction of the deviation. Cells where soundings are shallower than the mean surface are highlighted in red and cells where soundings are deeper than the mean surface are highlighted in blue.

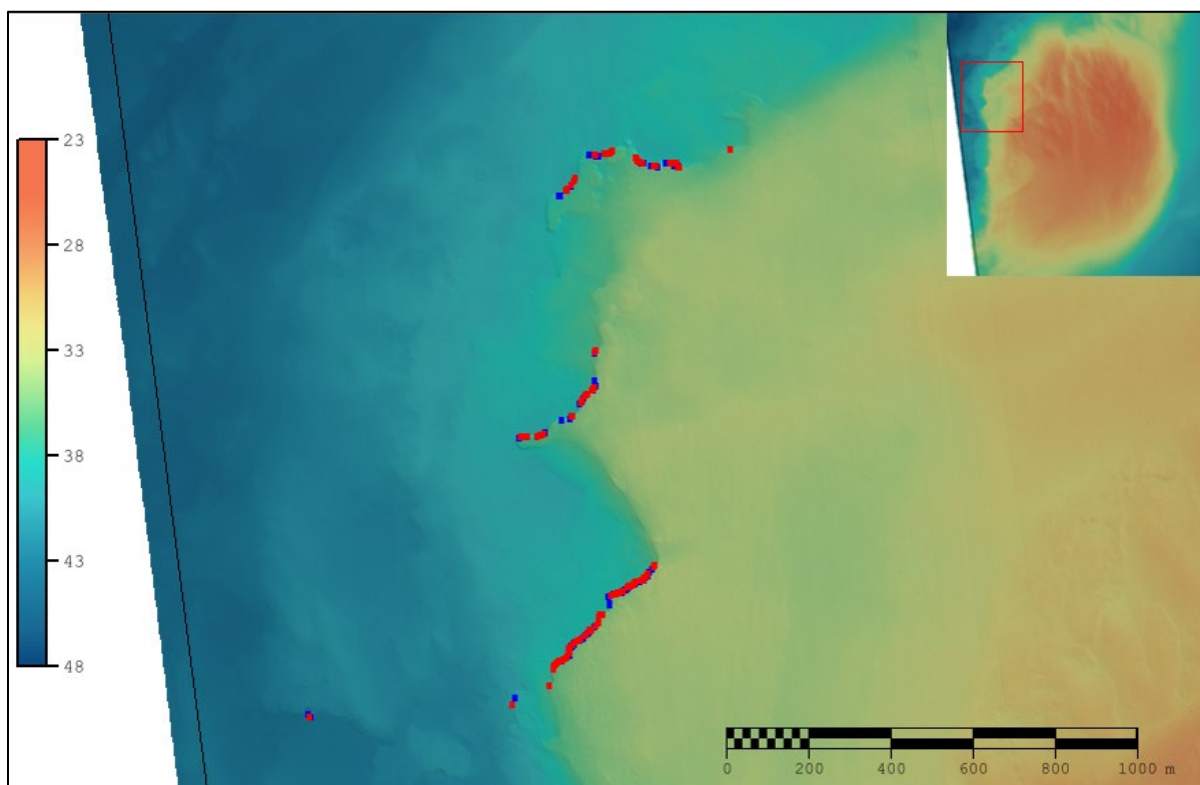


Figure 26 QC surfaces highlighting steep slopes in the Artificial Island survey area.
The QC surfaces are shown as dark blue and red cells.

Also, within Caris HIPS, surfaces were generated to show the Total Horizontal Uncertainty (THU) and Total Vertical Uncertainty (TVU) at 1 m resolution.

Figure 27 shows the combined TVU surface for the Artificial Island survey area. The colour scale represents areas where the TVU is low as green, medium as orange, and above 0.5 m as red. The results show that the survey area has TVU values within acceptable tolerance. The TVU values are calculated from all of the combined error sources associated with a sounding.

An overview of the THU results is shown in Figure 28. The range of values has been restricted to show areas with low THU as blue-green, medium THU as orange and higher THU as red. A few lines within the survey area have THU values between 0.25 m and 0.5 m. These moderately high THU values relate to survey lines that have higher than usual error associated with the post-processed navigation data, however cross sections through the soundings (not shown) indicate that the data is well aligned.

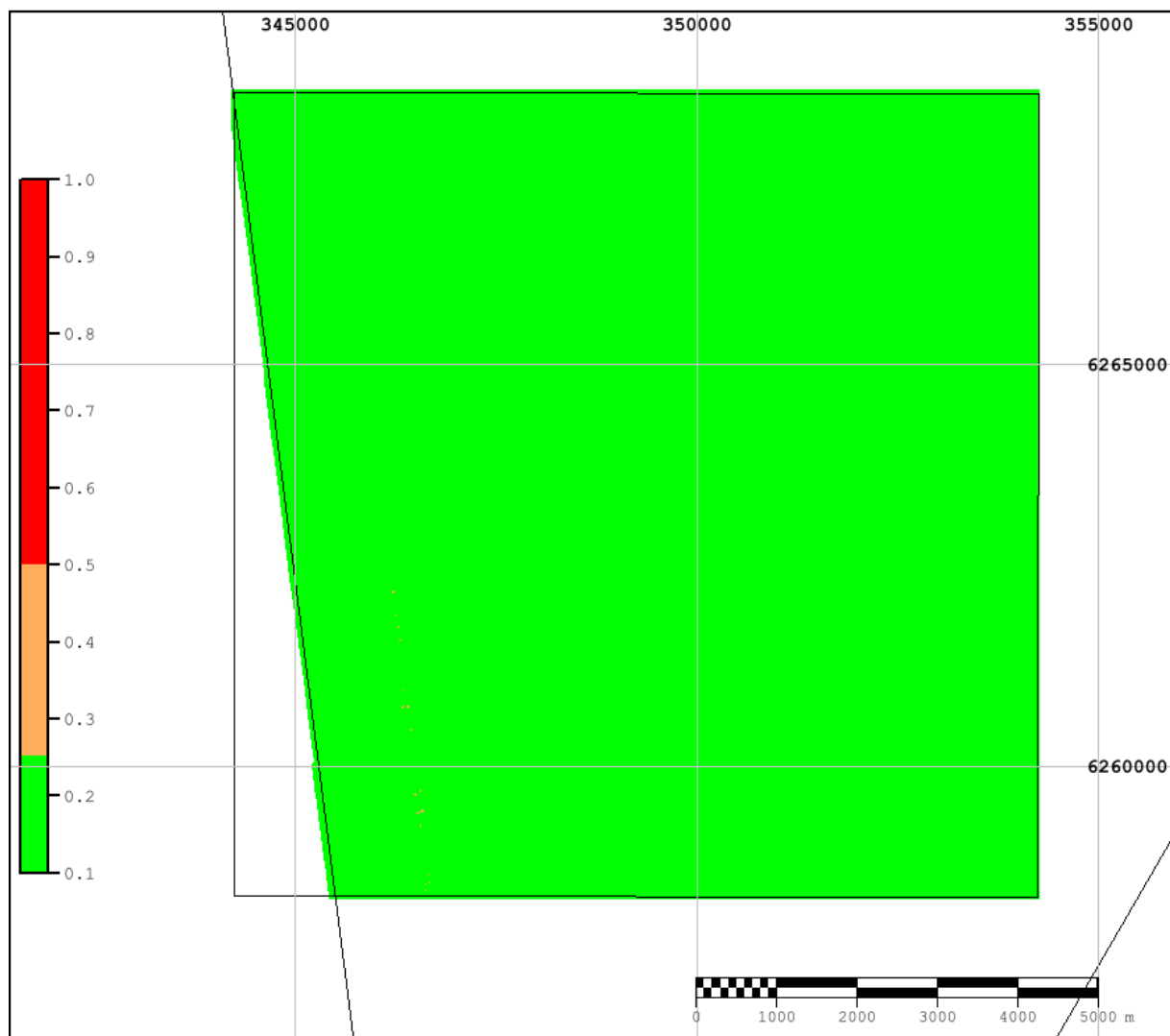


Figure 27 Total Vertical Uncertainty surface for the Artificial Island survey area.

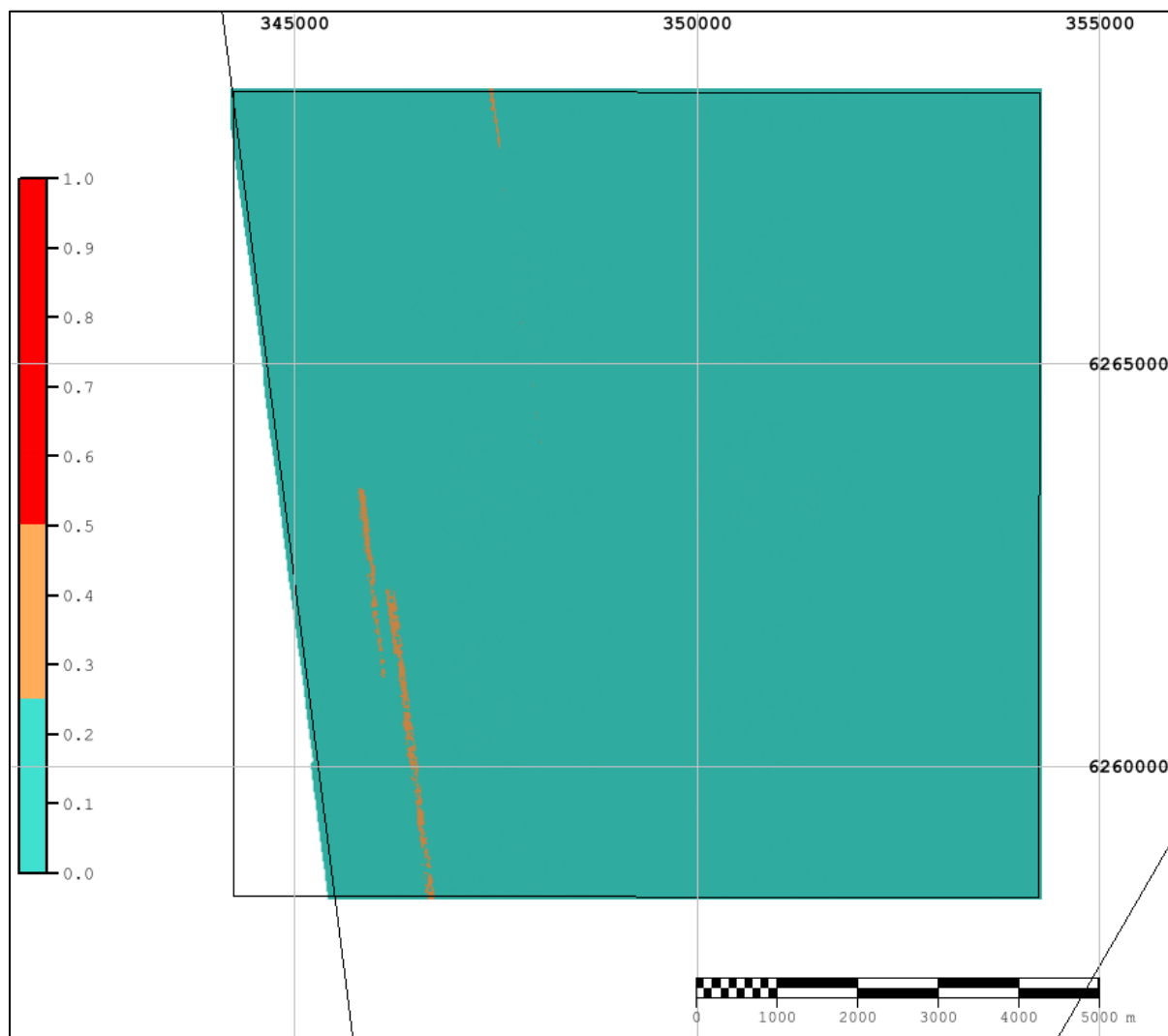


Figure 28 Total Horizontal Uncertainty surface for the Artificial Island survey area.

An artefact was seen in the data both on board the survey vessels and later in the office. The artefact appears as a ripple in the shoal surface when viewed from a 2D perspective and as a ripple on the outer beams of the swath when viewed as a point cloud from the side. This artefact is mainly seen in Blocks 1 and 2.

It is believed that the artefact is caused by a pycnocline in the area which affects the sound velocity. This in turn affects the position of the soundings as they are incorrectly calculated as being in a ripple formation. Unfortunately, standard refraction techniques aimed at minimising sound velocity-based errors are not effective in resolving the issue. Additional infill lines were run to replace lines that were affected, and soundings that were outside of the IHO Order 1a specifications were deleted, to minimise the effect of the anomaly on the final surface.

An image showing the typical appearance of these anomalies is shown in Figure 29.

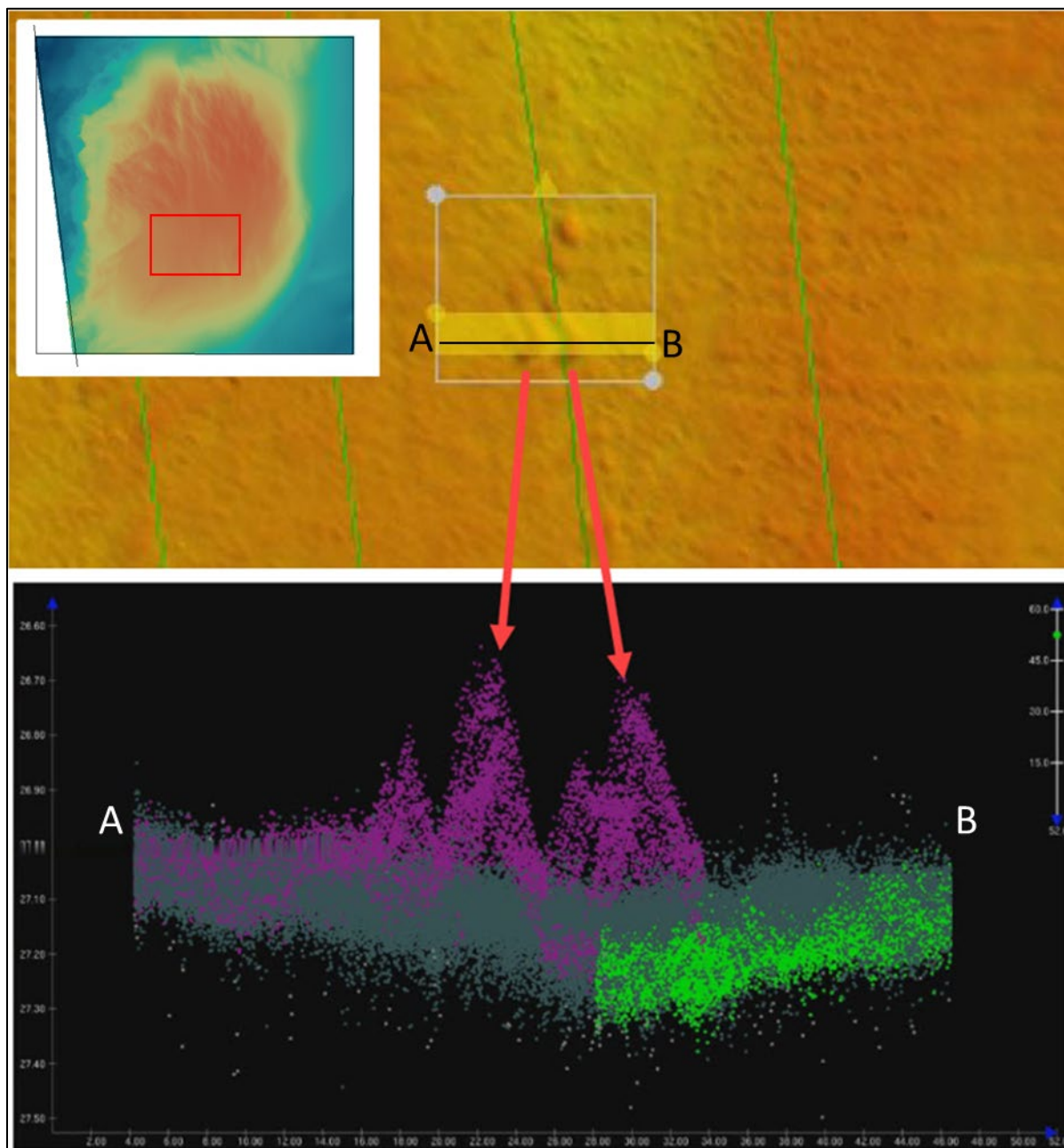


Figure 29 Example of anomaly in MBES caused by pycnocline.
Effect of anomaly seen in shoal surface on top and in soundings on the bottom.

5.2 | BACKSCATTER DATA

To assess the quality of the final processed backscatter data the XY+Intensity data for each block was imported to ArcGIS where they could be viewed as a single dataset (Figure 30). The colour scales for each block were adjusted so that they showed matching backscatter values in the same grey tone.

Assessment of the combined mosaic indicates that the boundaries between different sediment types were well delineated with good agreement between the relative intensities of the data acquired by Relume and Northern Franklin.

Since Relume and Northern Franklin were acquiring data on alternate survey lines there are some residual artefacts that arise from small differences in backscatter values detected by the two systems. As a result, some stripes that are aligned with the survey line direction are visible in the dataset (Figure 31).

Some outer beam noise that occurred with the Relume dataset has carried through to the final mosaics (Figure 32). However, these are also aligned with the survey line direction and can be accounted for during interpretation.

Beam-busts caused by excessive motion and bubble-entrainment (air-bubbles from white-water pass directly across the transducer face) are visible as dark lines that run perpendicular to the survey line direction and are restricted to a single MBES swath. An example of this is shown in Figure 33.

Despite the presence of these artefacts, the backscatter data is of sufficient quality to derive sediment boundaries and assist in the identification of contacts.

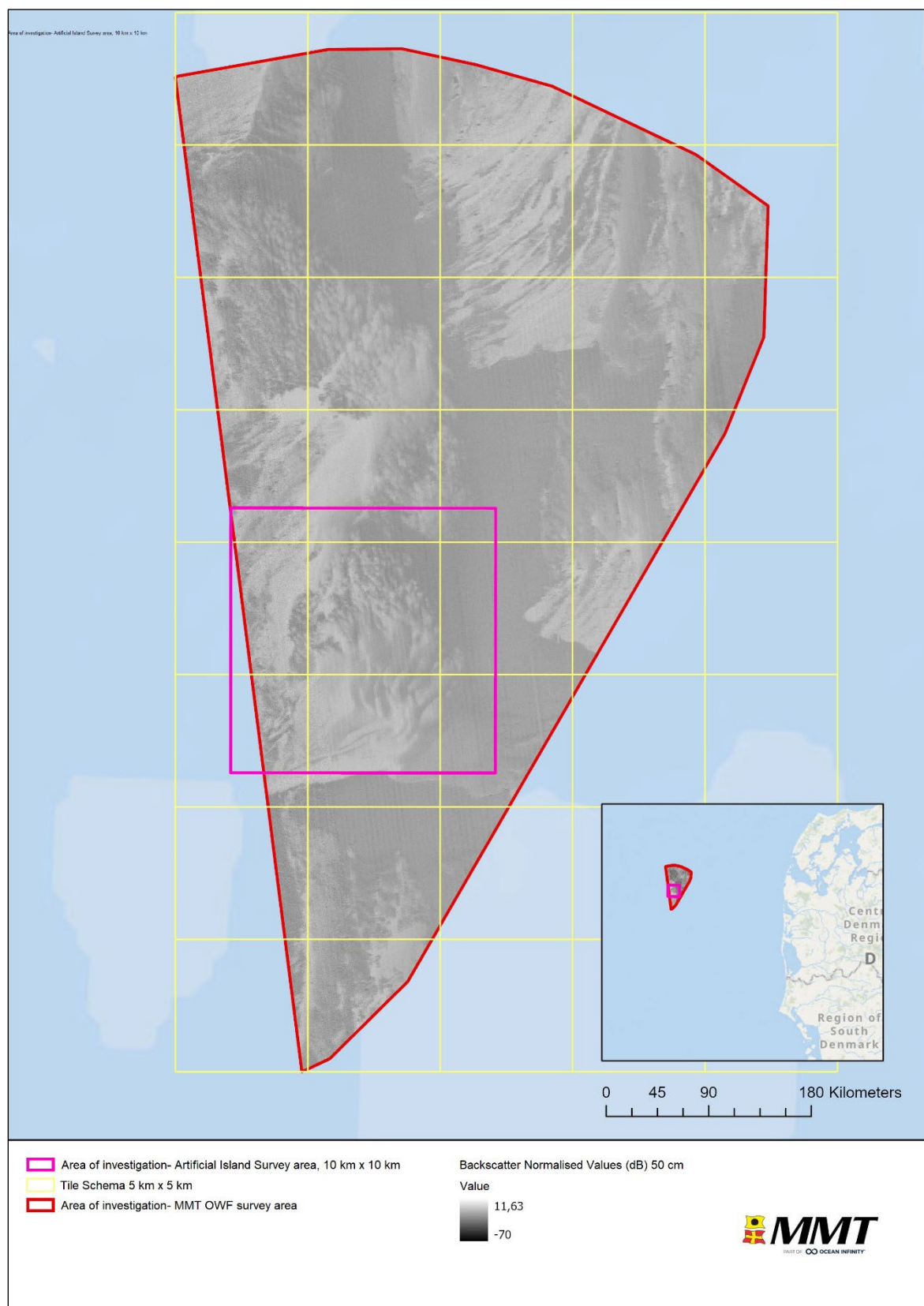


Figure 30 Overview of backscatter normalised values for the MMT OWF survey area.
 The Artificial Island survey area is marked with a magenta frame.

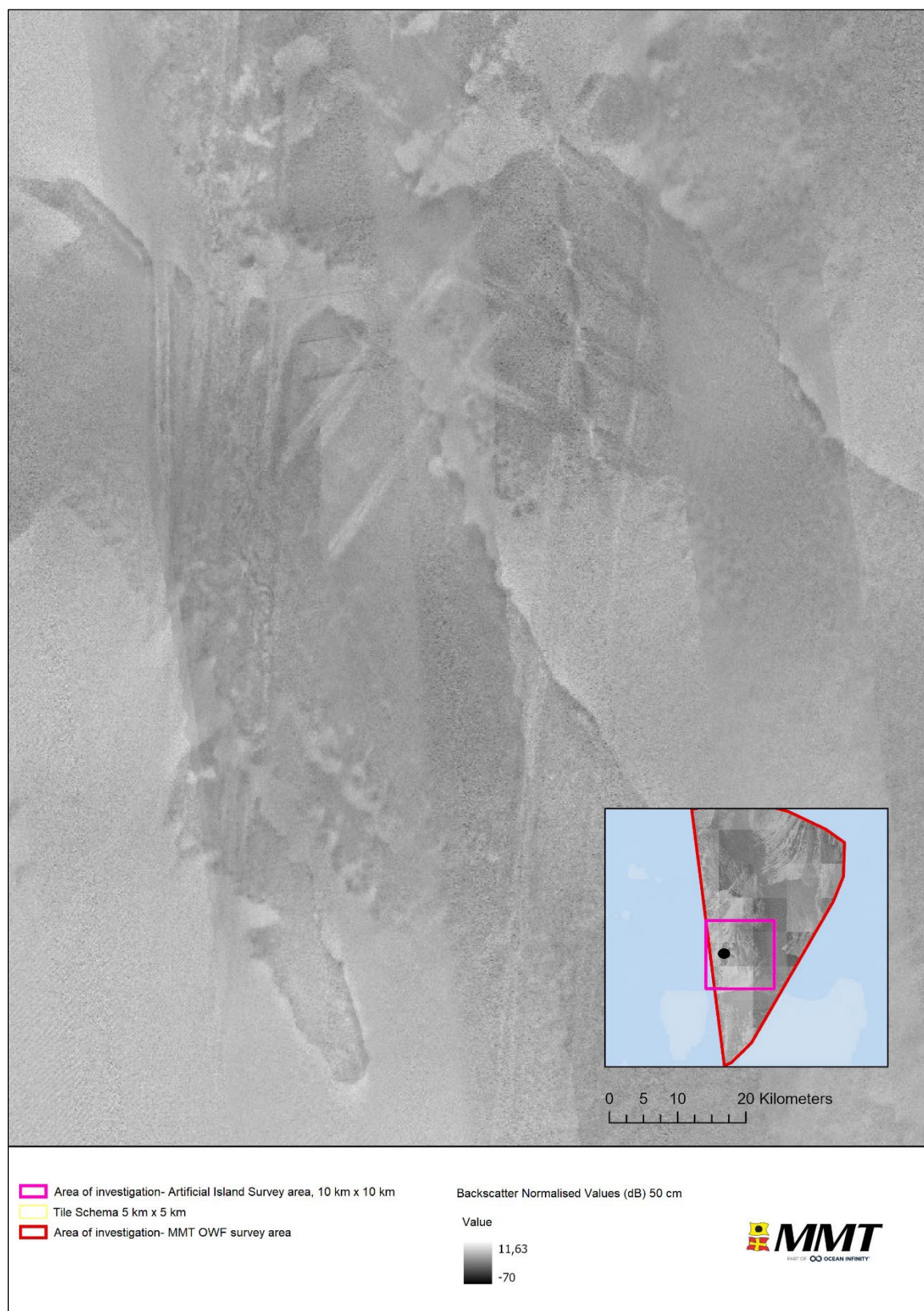


Figure 31 Backscatter mosaic with artefacts within the Artificial Island survey area. The artefacts are caused by smearing of data across sediment boundaries with large differences.



Figure 32 Outer beam busts visible in the Relume data, within the Artificial Island survey area.

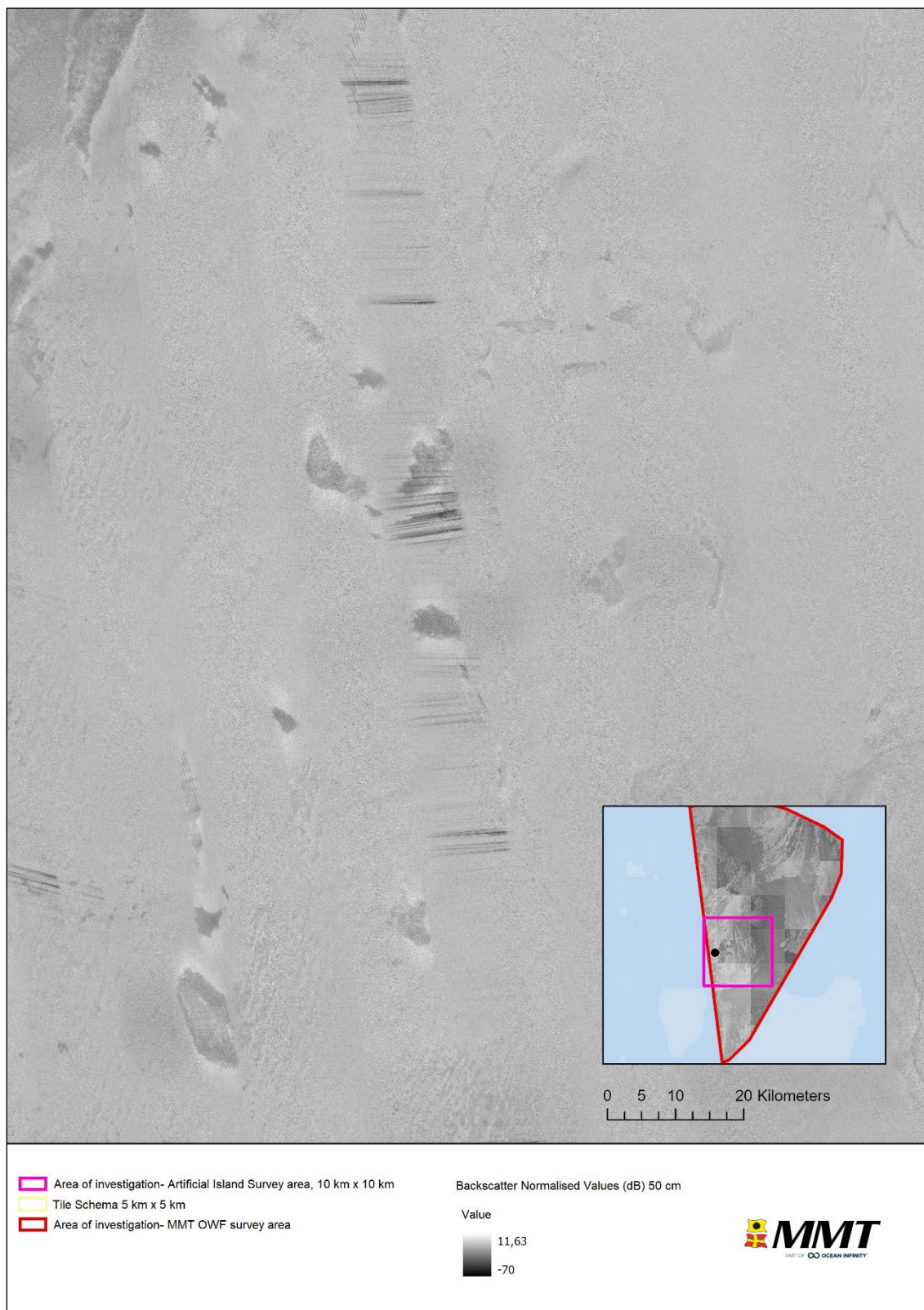
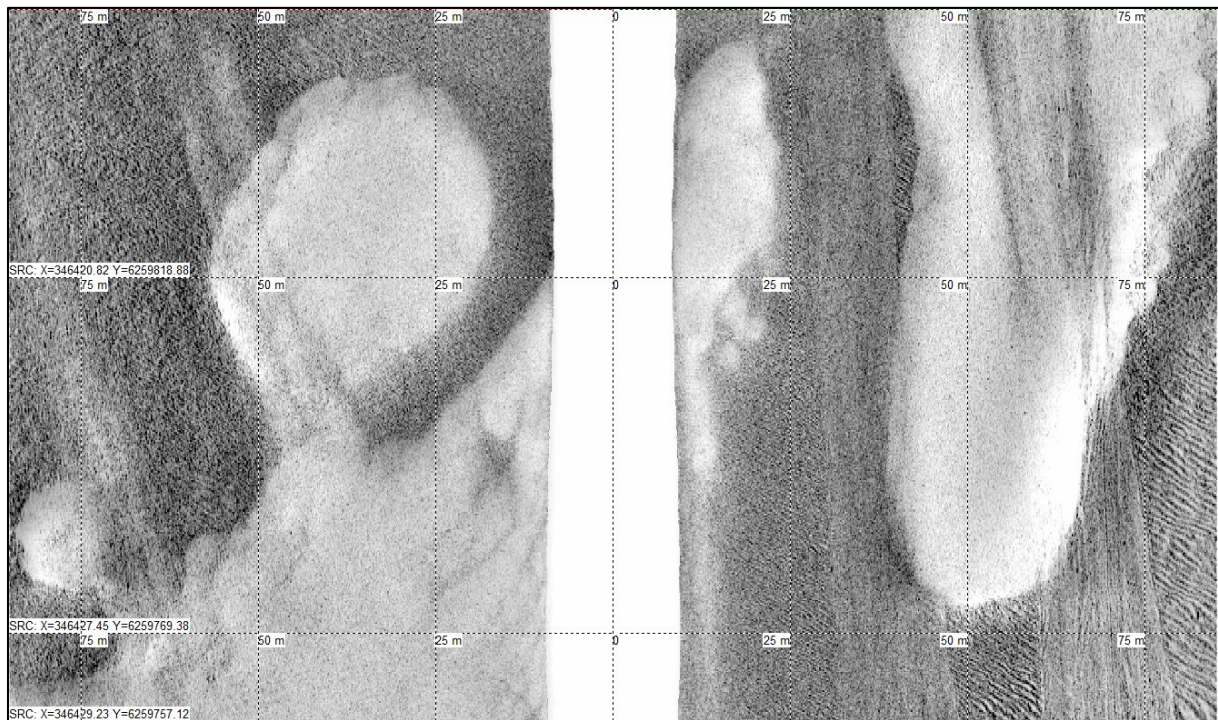


Figure 33 Beam busts caused by excessive vessel motion and/or bubble entrainment.
 Example is from within the Artificial Island survey area.

5.3 | SIDE SCAN SONAR DATA

The SSS data acquired at 80 m range with at 300/600 kHz frequency. The altitude of the SSS was kept at 10-12% of the range. 200% coverage was to be achieved, however in areas of pycnocline the specification was reduced to account for trimming out bad quality data caused by the pycnocline (see Section 1.4.1)). Coverage plots can be seen in Figure 40.



*Figure 34 Example of good high frequency SSS data from block BM01
The example is from within the Artificial Island survey area. Horizontal scale lines at 50 m intervals.*

The SSS data quality was generally good but there were areas of marginal data, due to environmental factors (detailed below). The multibeam and acquired backscatter were used in conjunction with the side scan data to ensure a comprehensive understanding of surficial sediments and interpretation of seabed contacts. This approach also mitigated any observed environmental factors on the sonar data.

A strong pycnocline was observed across the area particularly in shallower areas, such as the Artificial Island survey, mostly affecting the data in the outer ranges. The pycnocline effects obscure up to 35% of the data in some sections. An example from Relume is shown in Figure 37 and Figure 39. The noise varies along the lines and in most cases, it is possible to cover it with adjacent lines, achieving 100% coverage. The pycnocline artefacts are also visible in the SSS mosaics. Backscatter mosaics were delivered as per the scope of work.

Artefacts due to marginal weather were observed on some SSS records. These are due to roll and pitch motion on the towfish causing a 'striping' effect on the data, shown in Figure 35. The data had various amounts of gain applied to improve the overall appearance of the data and reduce the appearance of weather-related artefacts.

The high frequency data was generally more affected by environmental factors, such as weather and pycnocline, than the low frequency. An example showing the two frequency data sets from the same location is provided in Figure 37 and Figure 39.

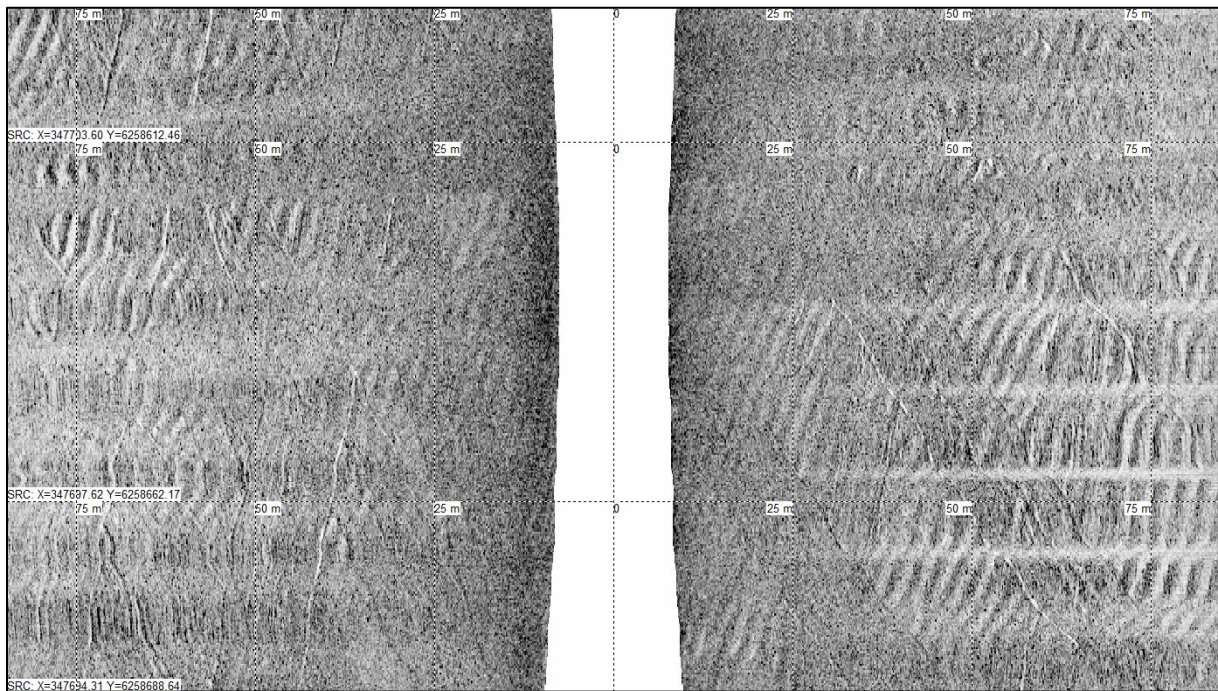


Figure 35 Example 1 high frequency SSS data from BM01 displaying a striping effect. Example is from within the Artificial Island survey area collected by the Northern Franklin. Horizontal scale lines at 50 m intervals.

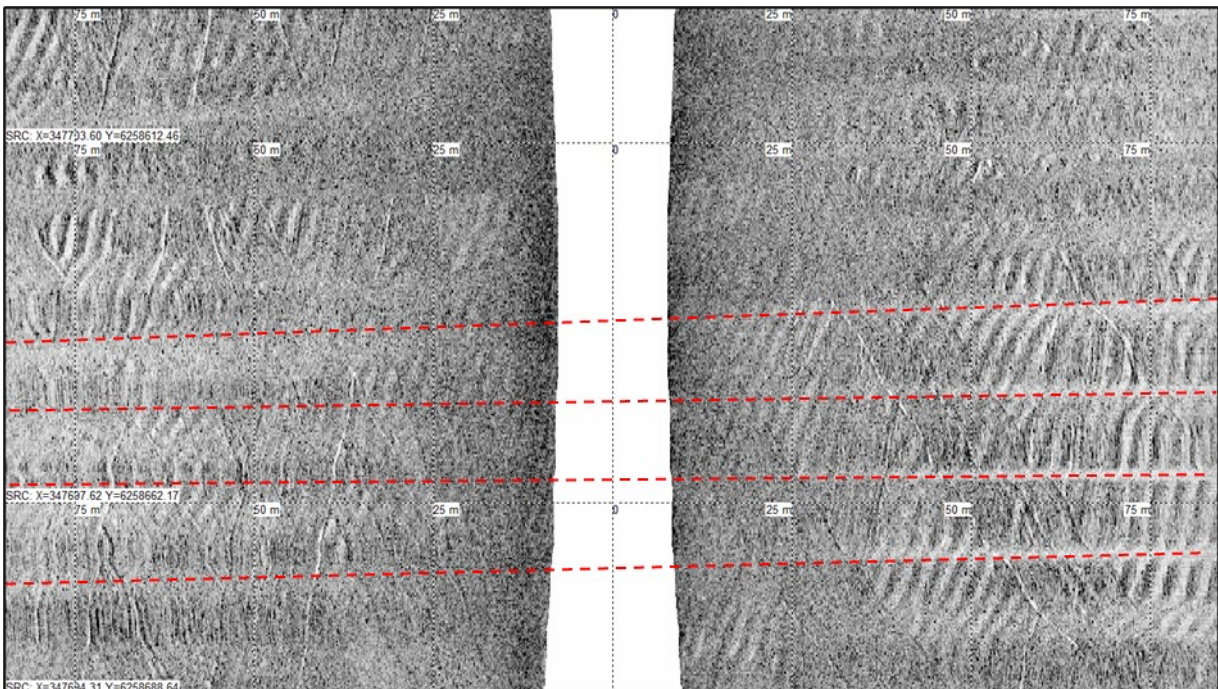


Figure 36 Example 2 high frequency SSS data from BM01 displaying a striping effect (highlighted) Example is from within the Artificial Island survey area collected by the Northern Franklin. Horizontal scale lines at 50 m intervals.

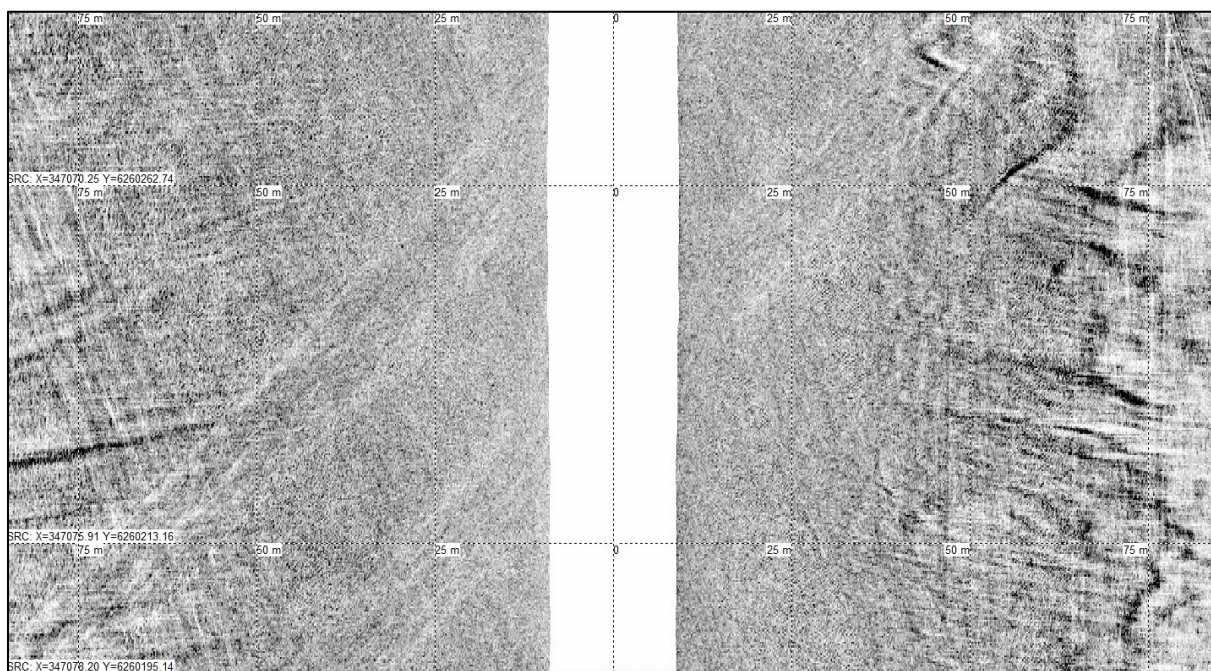


Figure 37 Example of high frequency SSS data from BM01 displaying a pycnocline
 Example is from within the Artificial Island survey area collected by the Northern Franklin. Horizontal scale lines at 50 m intervals.

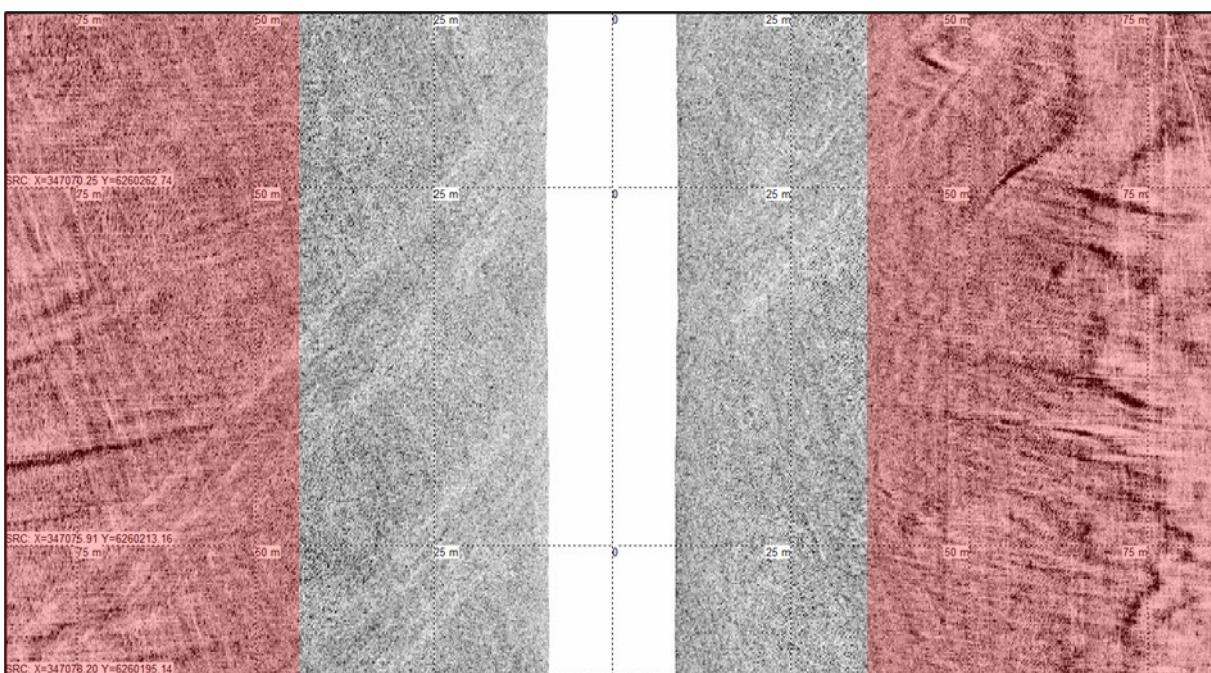


Figure 38 Example of high frequency SSS data from BM01 displaying a pycnocline (highlighted)
 Example is from within the Artificial Island survey area collected by the Northern Franklin. Horizontal scale lines at 50 m intervals.

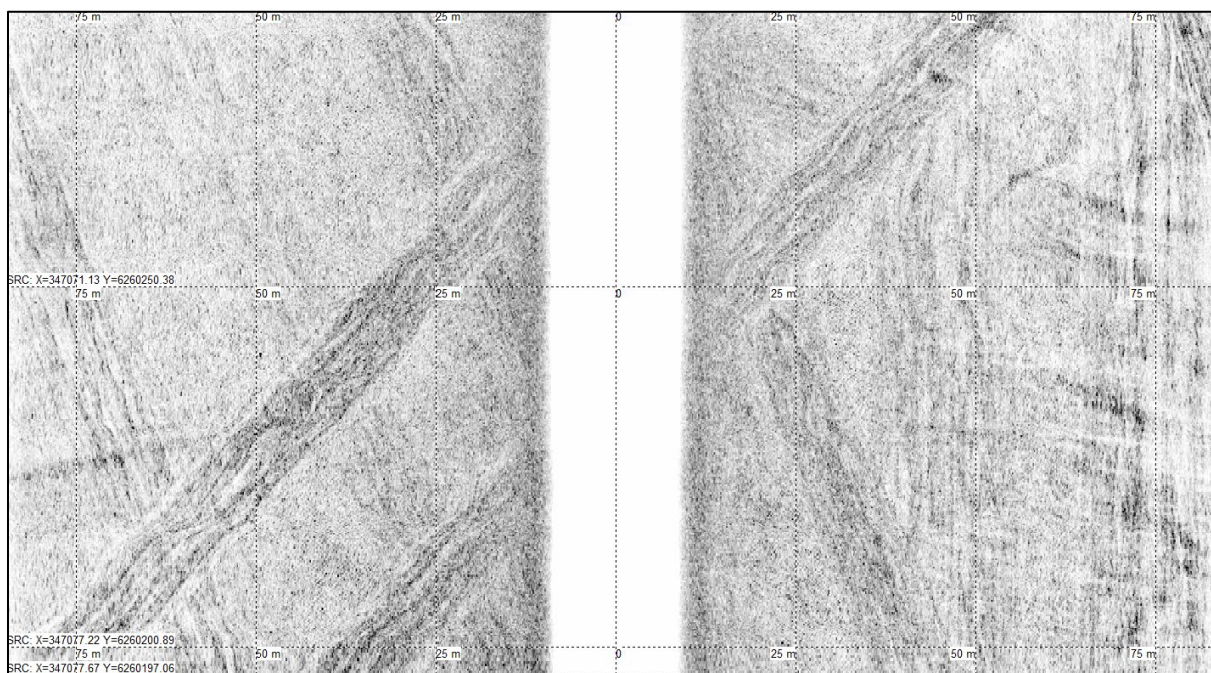


Figure 39 Example of low frequency SSS data from BM01 displaying less pycnocline
 The data is from within the Artificial Island survey area collected by the Northern Franklin. Horizontal scale lines at 50 m intervals.

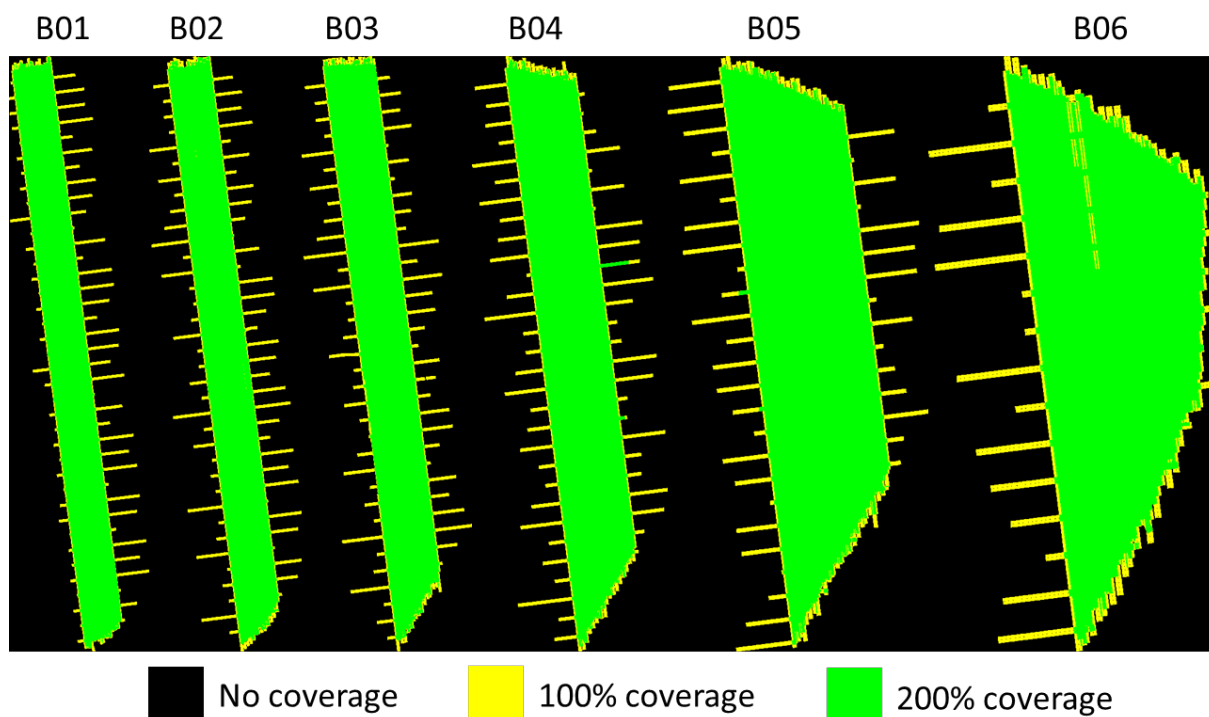


Figure 40 SSS coverage plots for each of the survey blocks.
 Accounted for adjusted range and 5 m nadir.

5.4 | MAGNETOMETER DATA

The MAG data was piggy backed behind the SSS tow fish. The intention was to keep the MAG altitude at less than 5 m. The aim was to be able to pick large anomalies as well as linear features such as cables and pipelines.

A statistical analysis for MAG altitude was conducted. In total, 2619 sections of lines were assessed, representing a total distance of 8530.42 km surveyed in the OWF area. While 95.29% of this distance was surveyed with an altitude of below 5.5 m. A total of 4807 km was surveyed at the target altitude below 5 m, representing 56.35% of the data. The Total Weighted Average Altitude for the whole survey was 4.91 m. Table 18 and Figure 41 outlines final figures for the OWF area.

Table 18 Summary of Average Altitudes, Percentages and Distances

Average Altitude (m)	Number of files / Line sections	Percentage (%)	Distance (km)
Alt ≤ 5m	1373	56.351	4807.00
Alt 5 – 5.5m	1113	38.942	3321.90
Alt 5.5 – 6m	130	4.647	396.37
Alt 6 – 6.5m	2	0.057	4.89
Alt 6.5 – 7m	1	0.003	0.26
Alt ≥ 7m	0	0.00	0.00
Totals	2619	100	8530.42

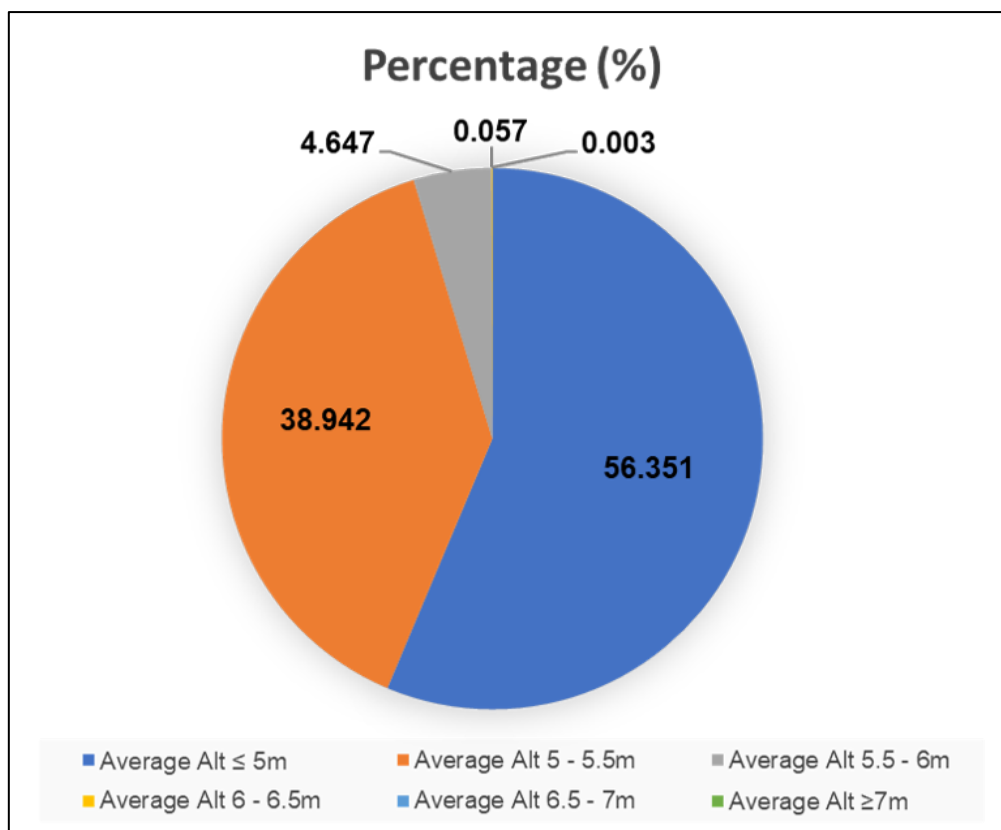


Figure 41 Pie chart illustration of Average Altitudes, Percentages and Distances

MAG data quality was generally good. Background noise levels were below ± 5 nT (Figure 42 and Figure 43). No data had to be rerun due to noise.

A number of reruns were required where the altitude was out of specifications or where the line was off track due to fishing gear. In general, navigation was good and minimal dropouts from the USBL system were observed. Where navigation was lost the total time of dropout had negligible impact on the overall positioning of the magnetometer.

The altitude averaged 5 m across the area and the signal strength was very good with a mean of approximately 1200.

The data was deemed fit to identify large hazards and cables as per the requirements of the work scope.

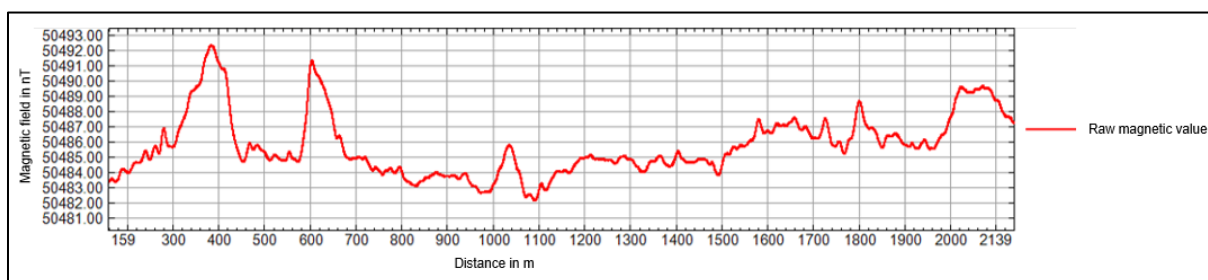


Figure 42 Magnetometer profile showing low background noise level for Northern Franklin.

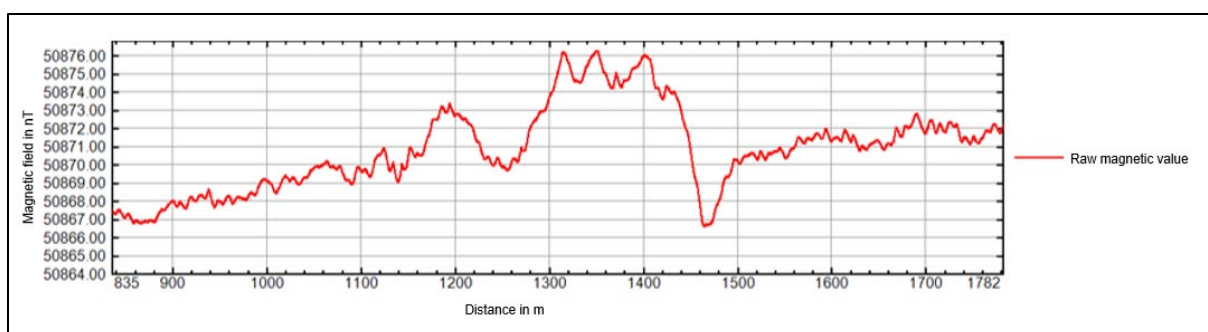


Figure 43 Magnetometer profile showing low background noise level for Relume.

5.5 | SEISMIC 2D UHRS DATA QUALITY ANALYSIS

In order to assess the data quality of every acquired line, the following Offline QC processing flow was applied to all lines, along with all external steps (Figure 44).

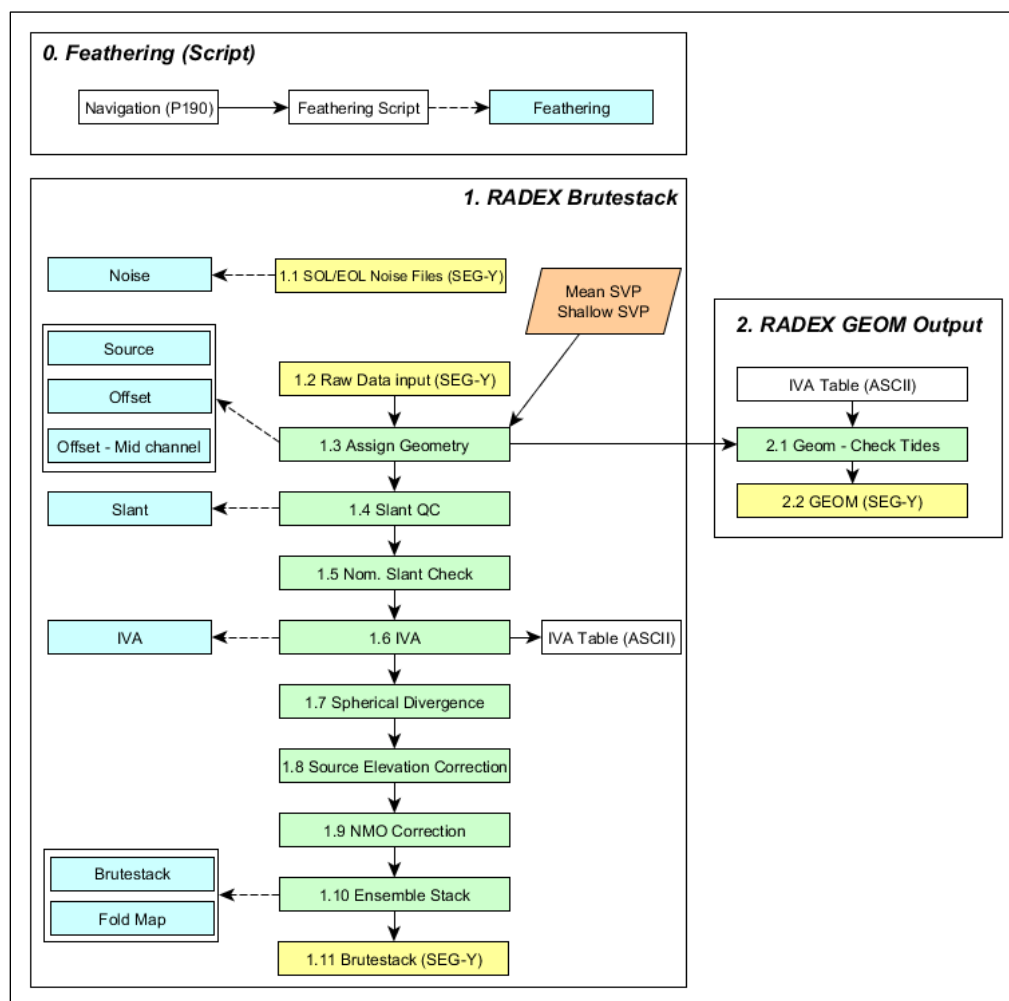


Figure 44 Processing workflow applied to the seismic lines. Green boxes represent the processing steps, blue boxes represent the QC plots, yellow boxes represent the imported and exported SEG-Y data, white boxes represent the intermediate data and the orange box the SVP data.

The UHRS QC & QA is a seismic processing service that ensures that the acquired UHRS data meets the contracted technical requirements:

- Throughout the survey the data was QC'd and made available for review within 24 hours of completion of survey operations;
- The agreed quality criteria were ensured during the QC/QA of the 2D seismic data in regards to:
 - Coverage;
 - Line keeping;
 - Data resolution;
 - Signal penetration;
 - Signal quality;
 - Feathering;
 - Data fold.

The offline QC was performed with key software and in house developed processing flows necessary to carry out the job to completion. The software used was RadEx Pro from Deco Geophysical.

5.5.1 | FEATHERING

The feathering angle was calculated along all the seismic profiles (see example in Figure 45). A maximum feathering angle of 8° was initially established for vessel steering and 15° for strong water currents. For the duration of the survey only the steering limit was surpassed on a few lines. On the other hand, the feathering values resulting from currents was always substantially below the established limit.

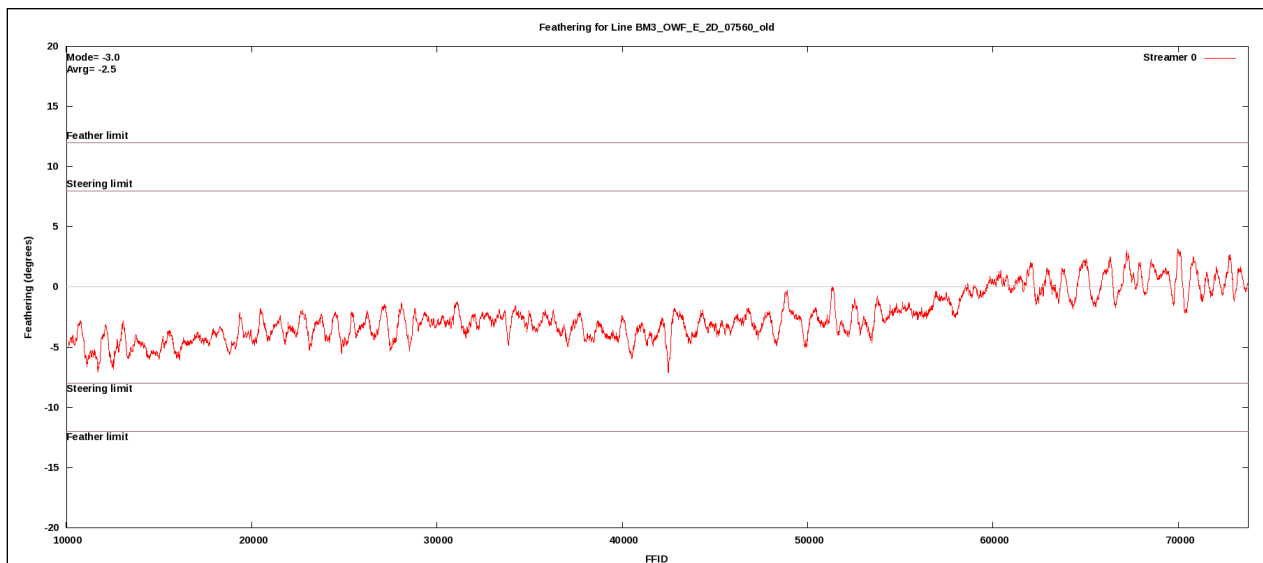


Figure 45 Feathering plot calculated for the line BM3_OWF_E_2D_07560.

5.5.2 | SIGNAL & NOISE ANALYSIS

The main sources of noise identified during the survey were (see Figure 46):

- Vessel noise – in red in Figure 46. This is a directional noise, that can be filtered using extended processing techniques without major negative impact on the signal.
- Front and tail cable tugging noise represented in blue and red, respectively, in Figure 46. The front/tail tugging occurs when the front/tail frame is pulled by waves and currents and that creates a low frequency vibration along the streamer. This is a directional noise that can be removed using an F-K filter.
- SIMOPS noise interference (Figure 47 and Figure 48) – Sporadic events when other vessels (Fugro Pioneer) came close to the Relume. In some cases, it was even possible to record a seismic pulse from their equipment (Figure 48).

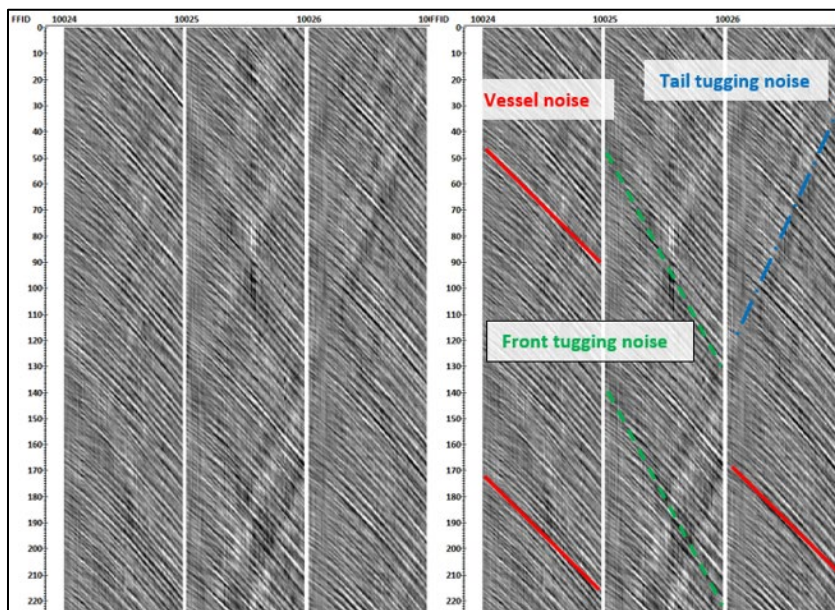


Figure 46 Main noise sources identified in the working limit noise test
 Vessel acoustic noise and cable tugging at the front and tail recorded by the M-UHRS streamer.

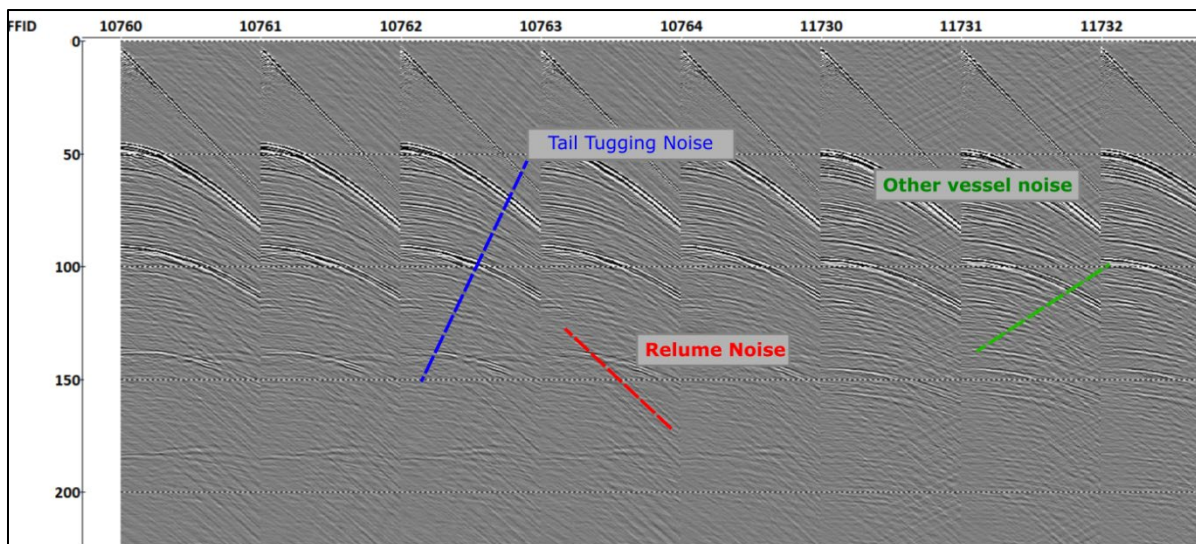


Figure 47 Main noise sources identified while in production, Relume.
 Acoustic noise (Red), cable tail tugging (Blue) and another vessel passing nearby (Green) recorded by the M-UHRS streamer.

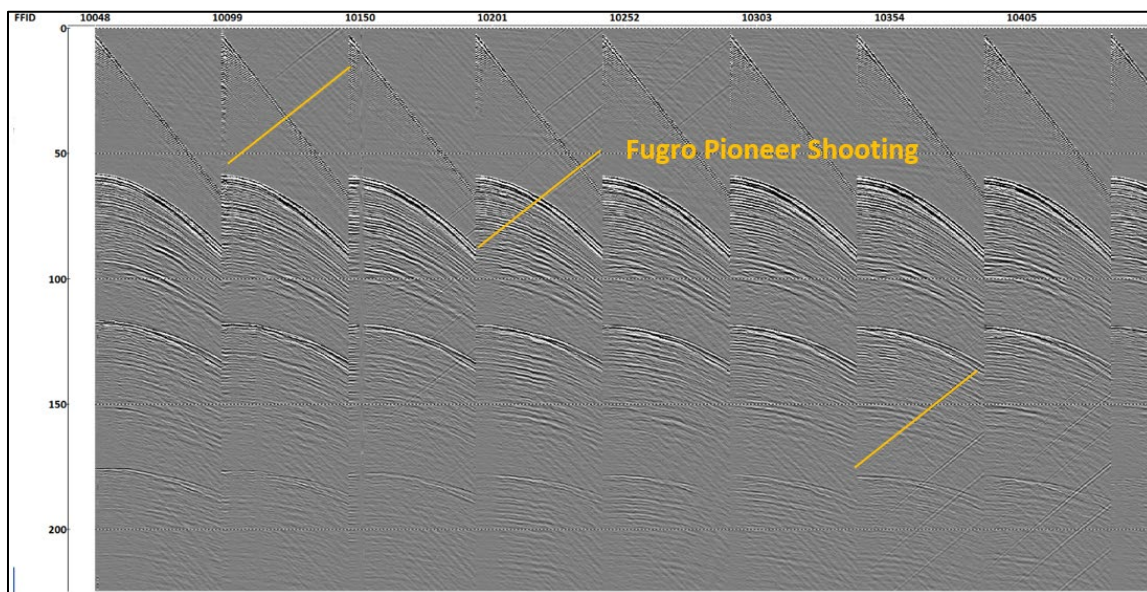


Figure 48 Fugro Pioneer shooting while in SIMOPS.

All the above-mentioned types of noise were thoroughly analysed. On a line-by-line basis, a noise check was performed before and after line acquisition, in order to assess the noise level variations. Generally, a difference of ± 20 dBs between sparker and the noise was achieved (Figure 49). The noise levels did not represent a major risk for the M-UHRS survey.

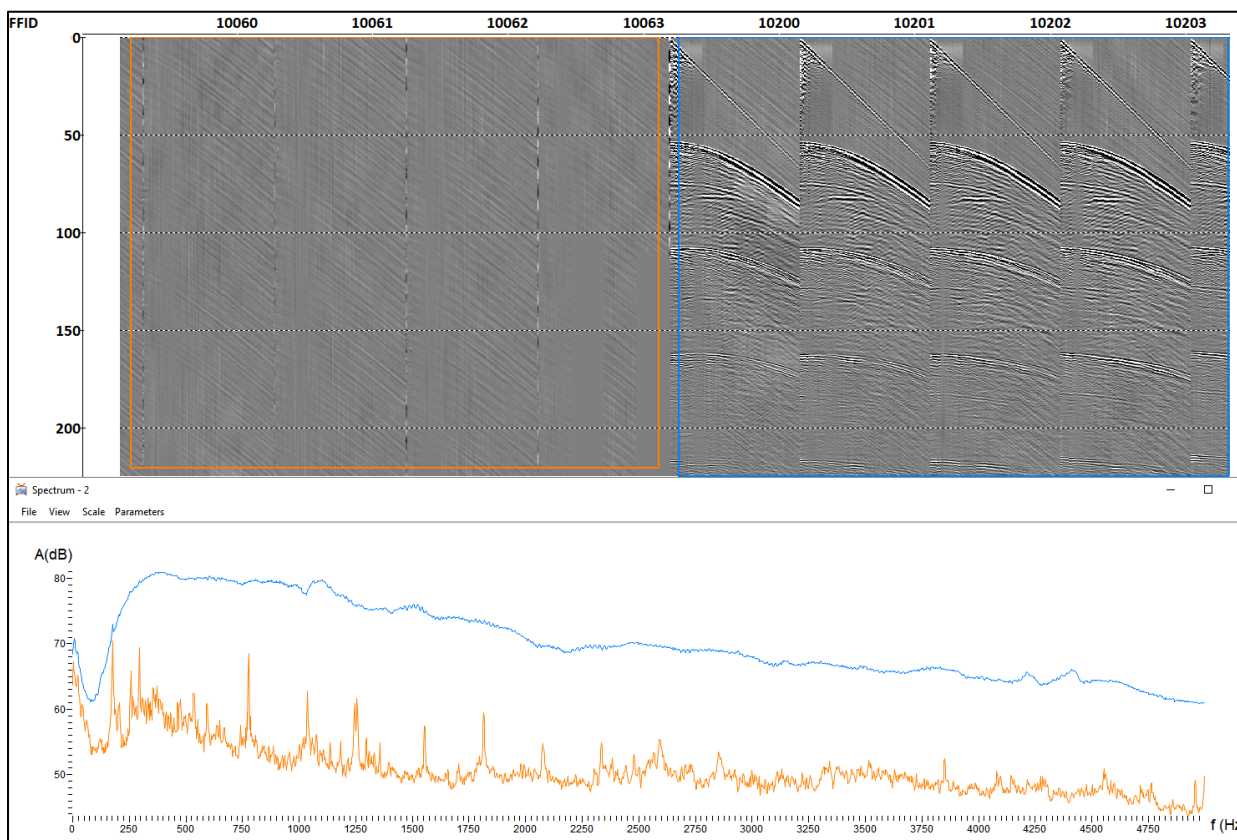


Figure 49 Frequency spectrum comparison between background noise and sparker signal . Background noise is shown in orange and sparker signal is shown in blue.

5.5.3 | SOURCE RECEIVER OFFSETS

Source and receiver positions and the relative offsets were initially calculated using the DGPS antennas located on top of the sources and on the streamer front and tail buoys. The accuracy of the source and receiver positioning was checked by comparing the offsets calculated from the source and receiver positions with direct arrival times (Equation 1). The offsets were estimated using the calculated distance between two points explained in Equation 1 and converted to time by dividing the obtained offset in metres by the measured water sound velocity (the sound velocity in the water was obtained from measured SVPs during the survey).

$$offset = \sqrt{(Sou_X - Rec_X)^2 + (Sou_Y - Rec_Y)^2}$$

Equation 1 – Equation used for calculating the offsets based on the positioning.

On average, the inline offset between the near channel of the streamer and the source was 1 m, and the crossline offset was 3 m. The source-receiver relative position did not change during the survey, although some variations could occur mainly due to surface currents.

In general, the offsets based on antenna position have a good match with the direct arrival (Figure 50 and Figure 51). Occasional mismatch was observed, mainly due to the loss of differential correction on the DGPS antenna (Figure 52), nevertheless the difference between the direct arrival and calculated offsets was reasonable and most of the time below 1 ms.

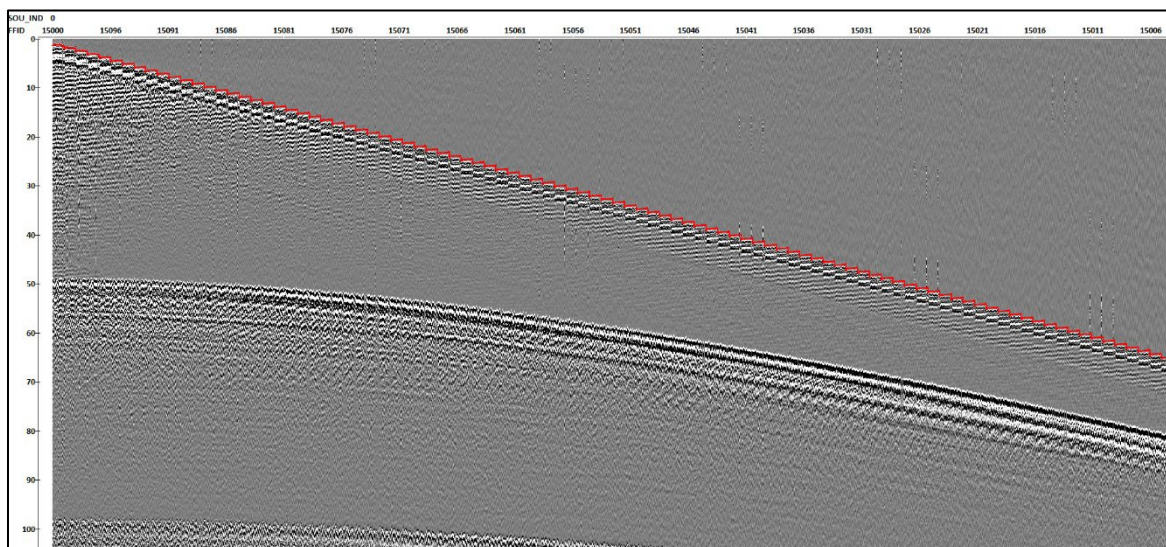


Figure 50 Channel domain showing the calculated offsets. The offsets are based on the DGPS positioning (red line) on top of the direct arrival, for all 96 channels, for line BM2_OWF_E_2D_02730. Vertical scale in TWT (ms).

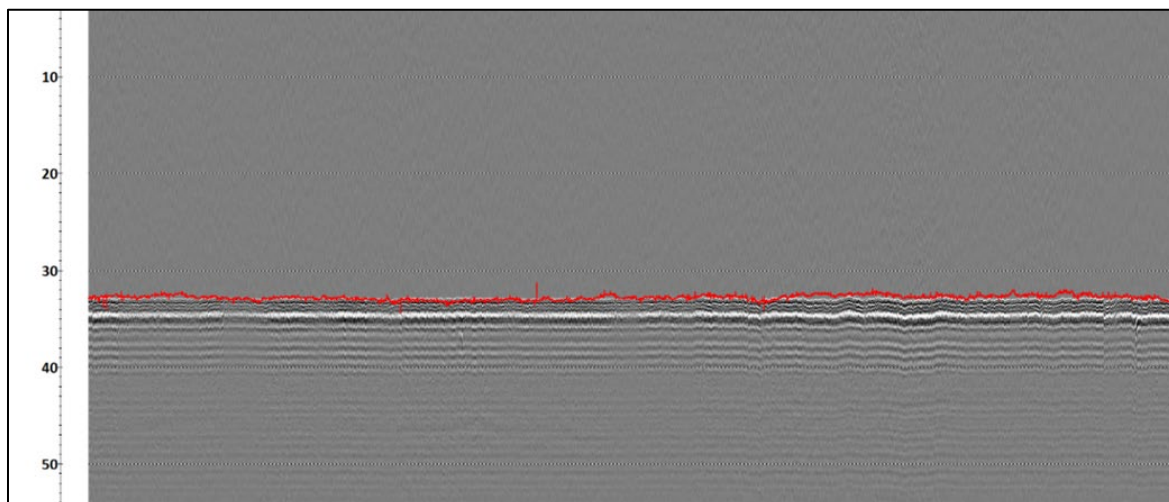


Figure 51 Profile BM4_OWF_E_2D_08820 in channel domain, showing the calculated offsets. The offsets are based on the DGPS positioning (red line) on top of the direct arrival for channel 48. Vertical scale in TWT (ms).

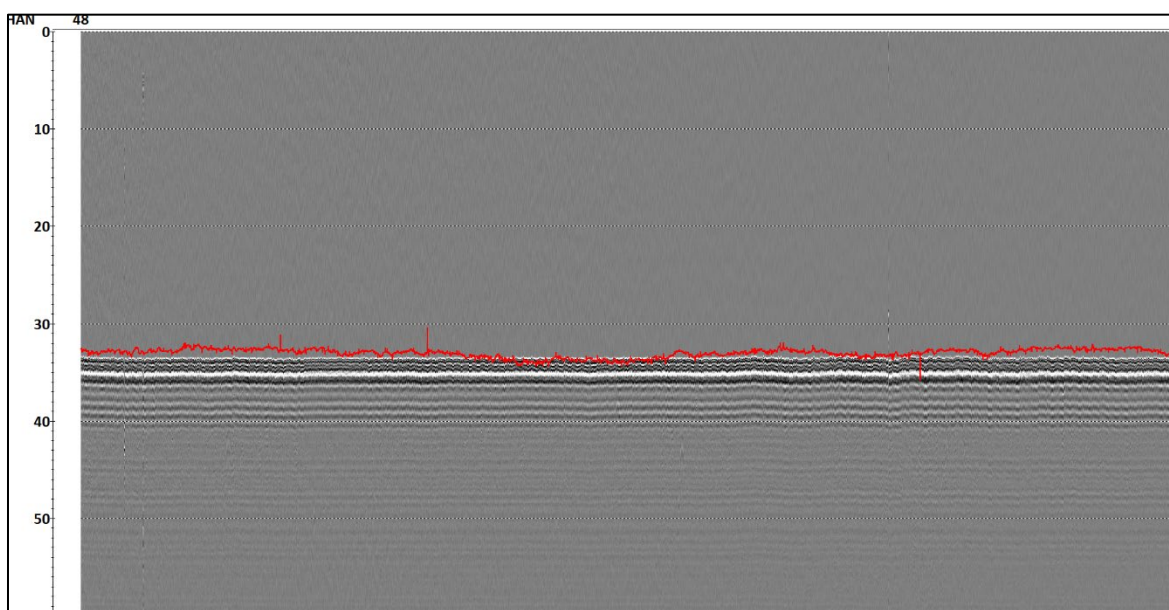


Figure 52 Profile BM5_OWF_E_2D_15540 in channel domain, showing the calculated offsets. The offsets are based on the DGPS positioning (red line) on top of the direct arrival for channel 48. Vertical scale in TWT (ms).

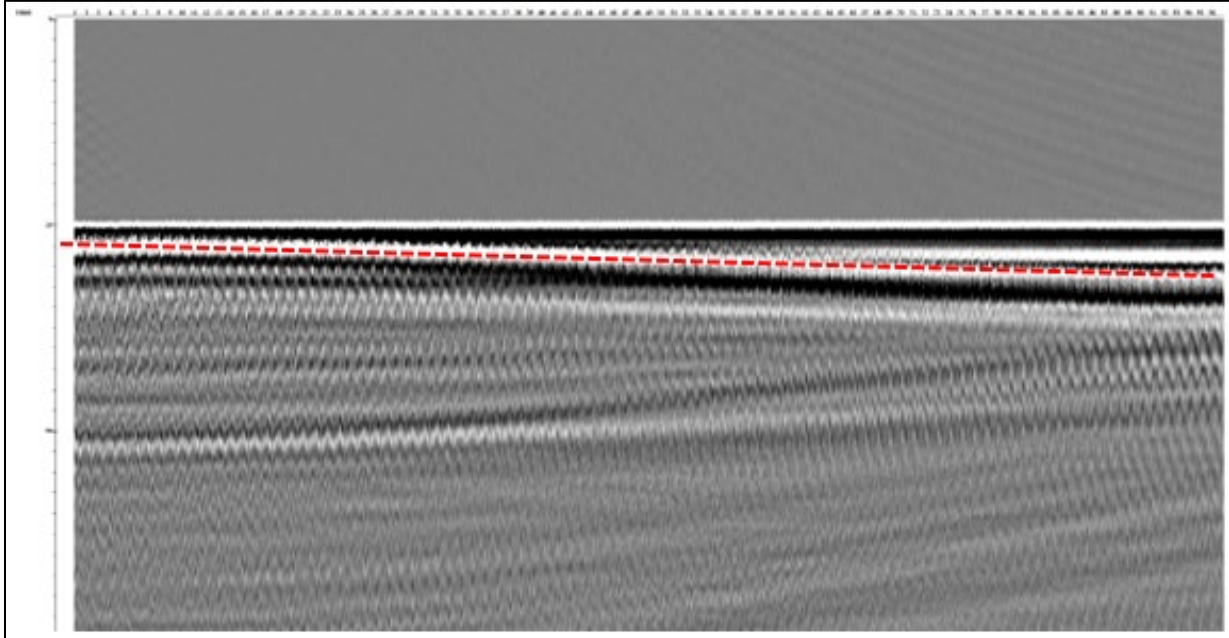
5.5.4 | STREAMER GROUP BALANCING

The streamer was balanced for the survey speed range of 3.5 - 3.8 knots STW. Along the streamer, several lead weights were placed in order to achieve the slant shape. To evaluate if the cable was properly slanted, a direct observation of the receiver ghost along all channels was done on a line-by-line basis (Figure 53).

Streamer balance integrity can vary depending on sea conditions, wave motion, vessel steering, surface currents, acquisition velocity, positioning precision and minor modifications of the system geometry

during equipment recovery and deployment operations. All these factors may have negative impact on the final UHRS data.

All the seismic profiles underwent to QC/QA in order to assess the streamer balancing and to ensure that the data could be successfully processed.



*Figure 53 Ghost reflection in channel domain with flatten seabed.
The image is showing the increasing ghost reflection depth along the channels (see the ghost reflection – red dashed line) for line BM3_OWF_E_2D_05880, vertical scale in TWT (ms).*

5.5.5 | INTERACTIVE VELOCITY ANALYSIS

Super gathers were generated every 1000 CDP comprising 3 CDP to build the dynamic stack. RMS velocity curves were generated through the interactive velocity analysis for all lines and were used for NMO corrections and stacking (Figure 54). Interactive velocity analysis was also used as a tool for data QC, mainly regarding penetration.

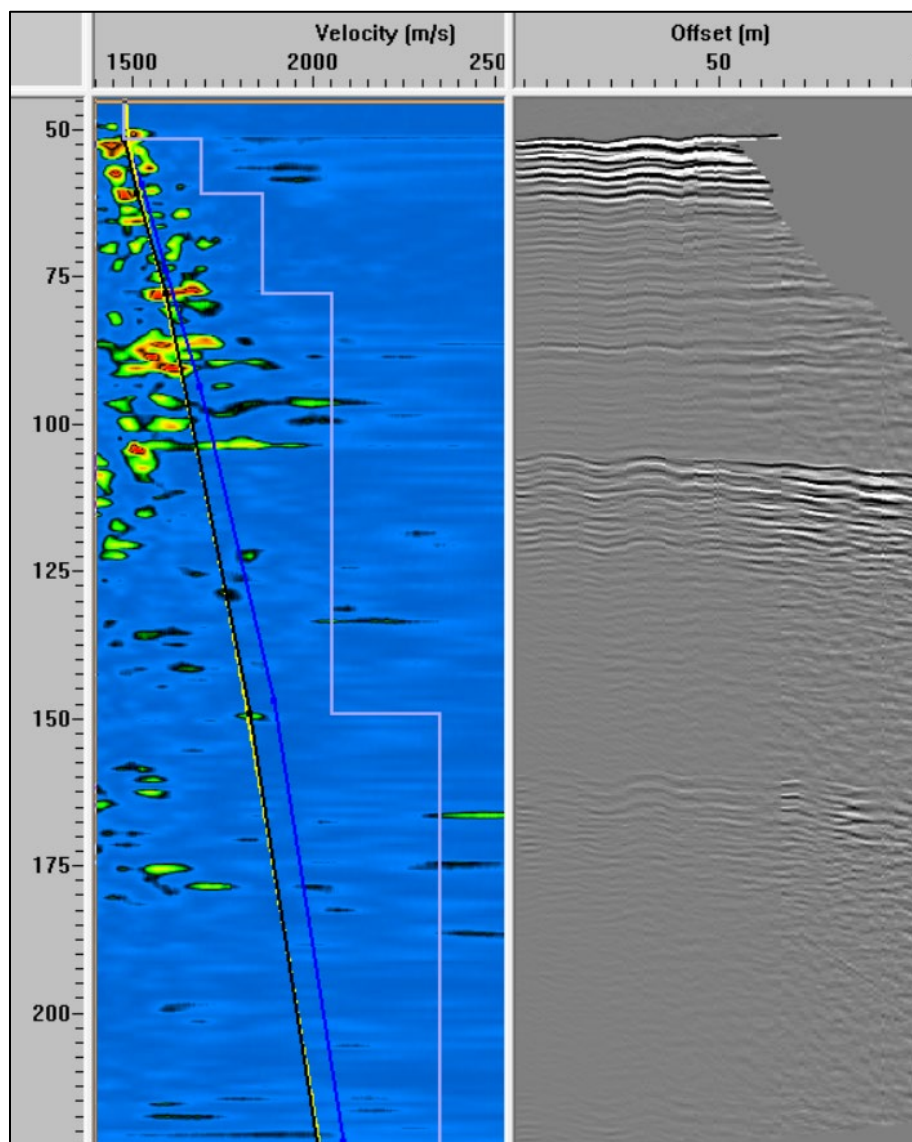


Figure 54 Velocity Analysis display for line BM3_OWF_E_2D_07770.
 The grey line represents the interval velocities and the black line shows the RMS velocity in the actual CDP gather; vertical scale in TWT (ms).

5.5.6 | CDP FOLD

The impact of the positioning solution, triggering, steering, feathering, navigation and the number of bad shots on the CDP bin fold regularity was assessed with CDP fold track plots (Figure 55). With minor deviations, all processed lines show a mean CDP fold around 192. Trace fold header recorded values were used to assess the cumulative impact of steering & feathering and bad shots on the seismic data.

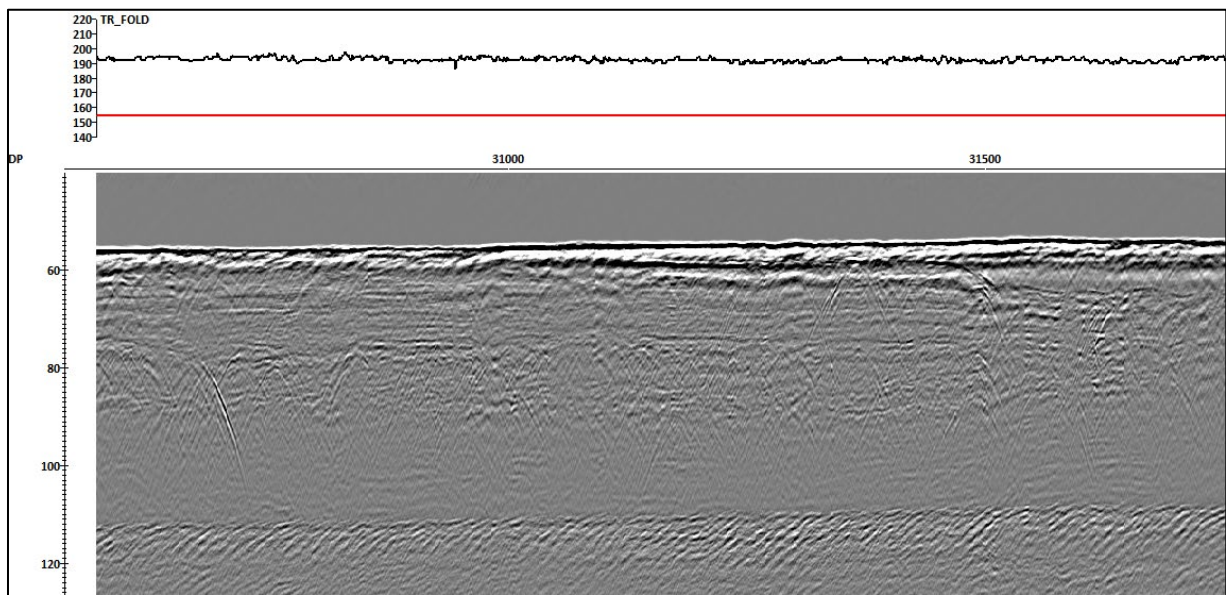
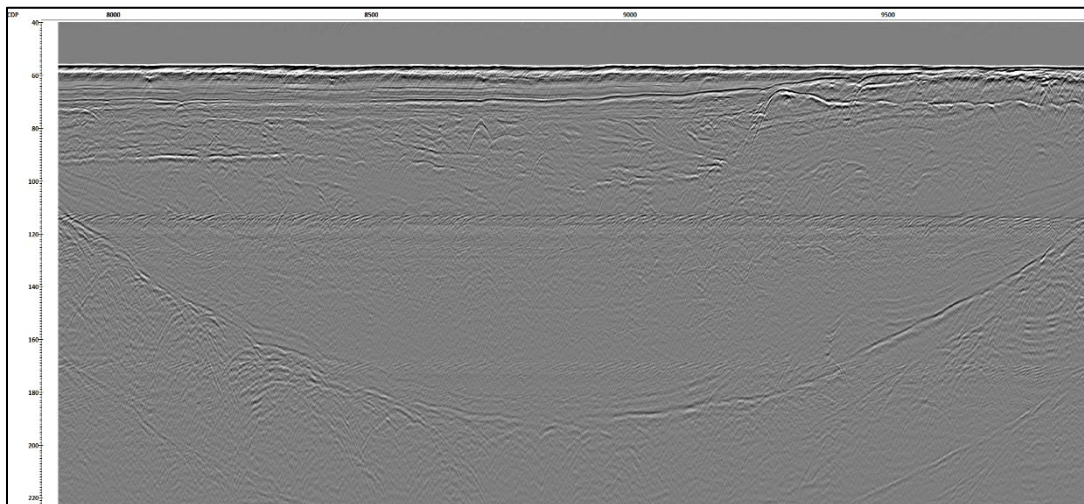


Figure 55 Trace fold values plotted on the top of stacked sections.
 The example shows line BM2_OWF_E_2D_05040 (black curve). Vertical scale in TWT (ms).

5.5.7 | BRUTESTACK

The offshore brutestack of every seismic profile provided a quick image of expected data quality and signal penetration (Figure 56). Several parameters were considered:

- Coverage – confirm by MMT if there were any gaps in the seismic data. Verified by MMT in QGIS project with the CDP Track Plots supplied by Geosurveys;
- Line keeping and coverage – verify if the steering of the vessel were along the line plan with a maximum error of 25 m – verified by MMT in QGIS project with the CDP Track Plots supplied by Geosurveys;
- Signal penetration – Identification of correlative reflections in the brutestack up to 225 ms below seabed, fulfilling the 100 m penetration requirement;
- Signal quality – verification of the existence of any artefacts in the seismic data.



*Figure 56 Brutestack for line BM4_OWF_E_2D_10080_01.
The image shows penetration until the end of the record and good signal to noise ratio. Vertical scale in TWT (s).*

5.5.8 | GEOM OUTPUT

The raw SEG-Y data acquired by GMSS had the following information on the headers:

- FFID number (Byte location 9);
- Channel number (Byte location 13);
- Source positions (SOU_X - Byte location 73, SOU_Y - Byte location 77);
- Receiver positions (REC_X - Byte location 81, REC_Y - Byte location 85).

The raw SEG-Y data was then imported into RadEx Pro (by GS personnel offshore) for data QC/QA, geometry assignment and tidal values import. Due to the more limited computational power on the offshore laptops, the geometry was assigned with a bin size of 1 m. This bin size was used for QC/QA purposes, with no impact on data quality assessment. Once the data arrived to GS office, the bin size was then recalculated to the agreed 0.5 m bin. Crooked-line geometry assignment gives a truer picture of the subsurface when compared with other geometry assignment methods because it considers the angular relationships between the shots and their receivers.

The GEOM SEG-Y dataset (raw data with filled headers - Linename_GEOM.sgy) was then exported with the additional headers filled:

- CDP number (CDP – Byte location 21);
- Source Receivers Offset (OFFSET – Byte location 37);
- CDP position (CDP_X – Byte location 181, CDP_Y – Byte location 185);
- Tide Height (TIDE_HGHT – Byte location 233).

5.6 | SEISMIC 2D UHRS DATA PROCESSING OFFICE

Quality control procedures were carried out throughout the processing scheme, as detailed within the present report and data control was registered along specifically designed logs. All processing steps were checked for the proper application of the seismic imaging enhancement. Several of these quality control plots were delivered to the client as part of this project submission, such as trace and offset QC; streamer slant check; source and receiver heave; image of the TRIM_STK (including trace fold) and image of final MIG (FULL).

Furthermore, at some stages, quality control supervision was carried out by the project's Principal Interpreter to ensure that the seismic processing was being properly applied and for troubleshooting purposes. Finally, and after all intermediate quality controls, lines were inspected by both geophysicists and geologists for acceptance.

Several challenges were encountered during the processing stage of the 2D UHRS seismic dataset received, mainly related to the following:

- Data processing on some profiles was negatively affected by sea conditions;
- Seismic amplitude balancing was corrected to all seismic profiles in order to achieve similar imaging of the subsurface;
- Fine tuning of the post-stack demultiple and post-stack migration in order to attain real geological features but also to attenuate the multiple energy and undesired diffraction effects, respectively;
- Seismic resolution improvement, both horizontal and vertical, was always the priority in all processing steps.

A full processing report detailing all quality control steps, is available in Appendix D].

5.7 | SUB-BOTTOM PROFILER DATA - INNOMAR

The Innomar data was collected in order to acquire good resolution data in the upper 10 m of the seabed. The settings of the Innomar were adjusted to achieve this.

SBP data quality was generally good (Figure 57). Some interference was introduced by the 2D UHRS Sparker (Figure 59) but was mostly removed by noise removal techniques using RadExPro (Figure 60). Penetration achieved up to 10 m (target depth), this was variable across the site due to changing ground conditions; achieved penetration was dependent on the distribution of channelling beneath an initial coarse unit and dependent on the presence of observable units below H10 (Figure 57). Average penetration was 5-8 m.

Data from Relume and Northern Franklin were signal processed to ensure consistent gains across datasets.

The Innomar SBP data was reviewed and compared to the 2D UHRS data specifically for shallow geology information. Interpretation was compared for consistency between SBP and UHRS datasets. SSS and MBES data was also used to confirm sediment boundaries on the surface.

In areas where horizons could not be tracked in the SBP data due to geological factors, the UHRS interpretation was used to interpolate the SBP interpretation for the purpose of producing more complete grids and isopachs. On some SBP lines, additional interpretation was added for the purpose of aligning with UHRS data. Some of these horizons appear below the area of interest on the SBP data.

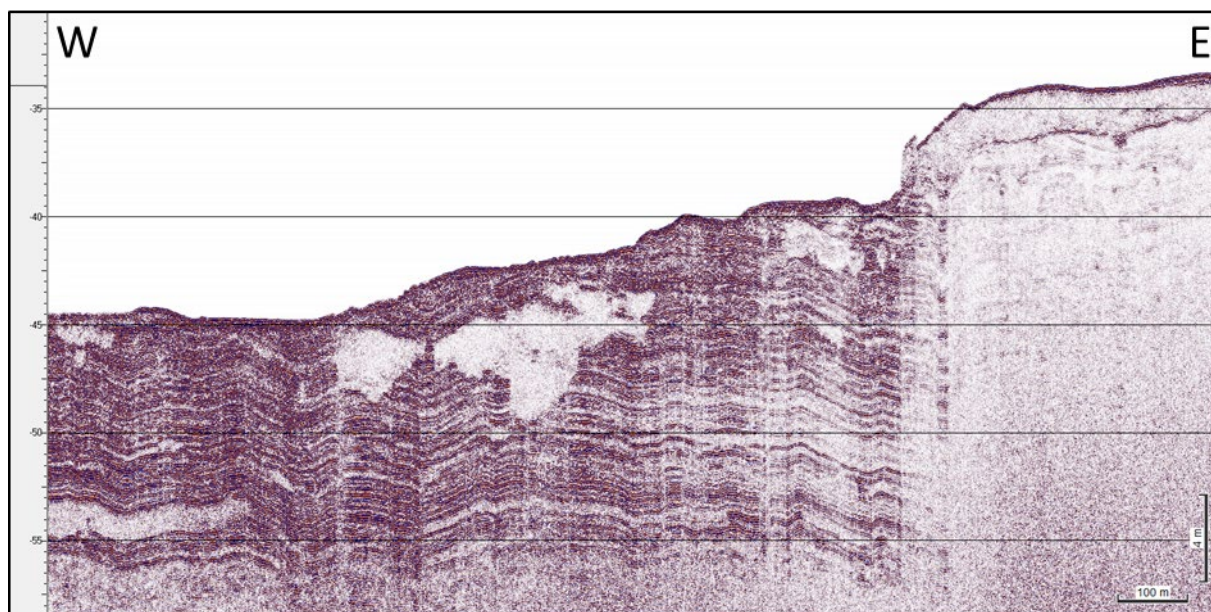


Figure 57 Innomar data showing achieved penetration of 10 m.

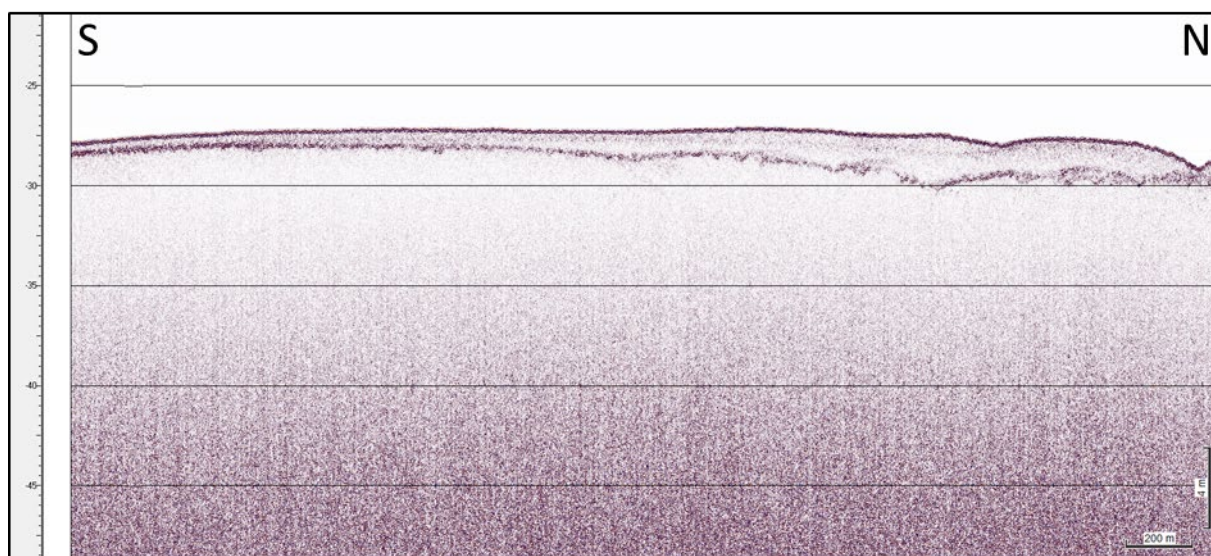


Figure 58 Innomar data showing limited penetration area where holocene unit exceeds 10 m. The example is from within the Artificial Island survey area.

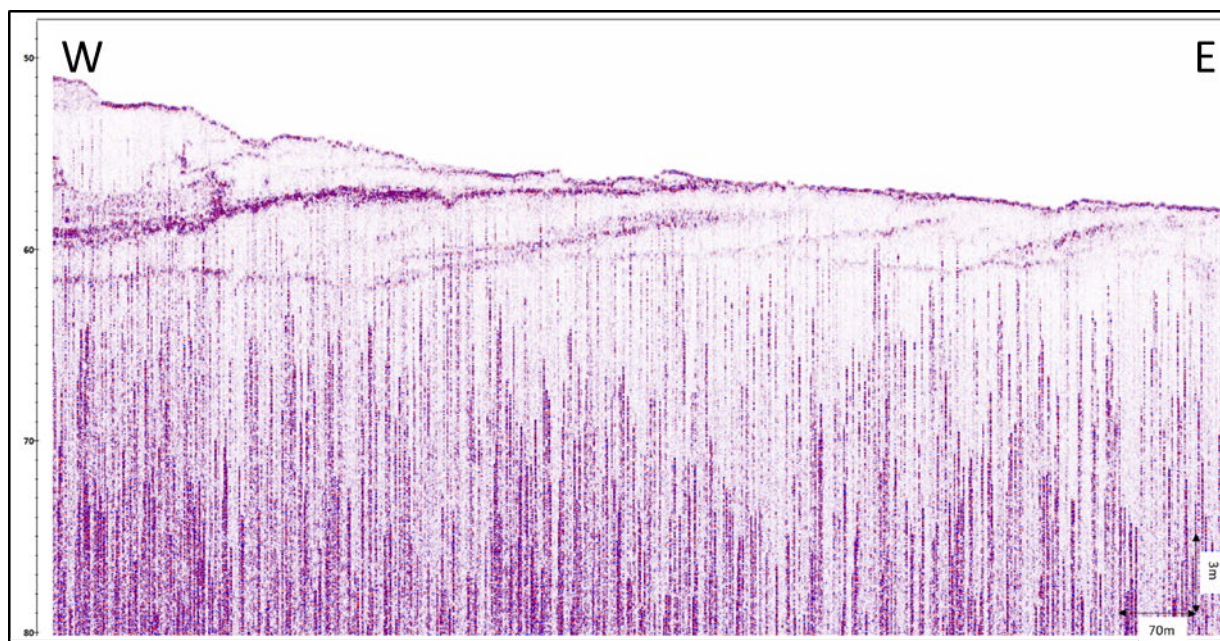


Figure 59 Raw Innomar data showing vertical striping Sparker interference.

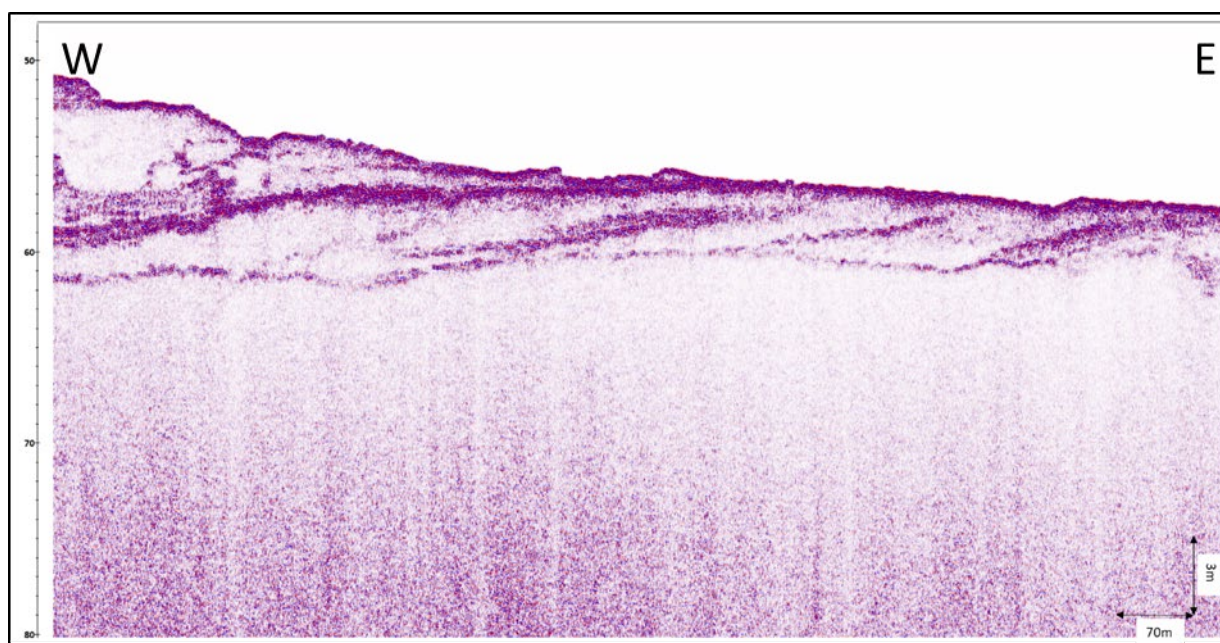


Figure 60 Processed Innomar data showing improved signal to noise ratio.

6 | BACKGROUND DATA AND CLASSIFICATIONS

Client provided background information and the GIS database were the main resources used during data interpretation. Additionally, academic literature resources were used to support interpretations and are listed within the references in Section 11|.

6.1 | SEABED GRADIENT CLASSIFICATION

The seabed gradient is classified according to Table 19.

Table 19 Seabed gradient classification.

CLASSIFICATION	GRADIENT
Very Gentle	< 1°
Gentle	1° - 4.9°
Moderate	5° - 9.9°
Steep	10° - 14.9°
Very Steep	> 15°

6.2 | SEABED SEDIMENT CLASSIFICATION


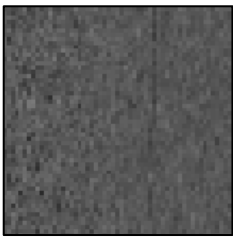
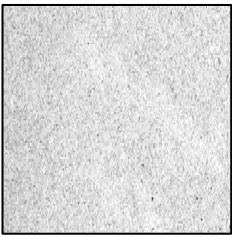
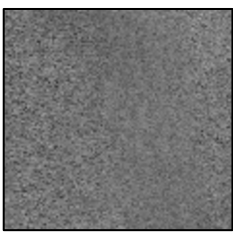
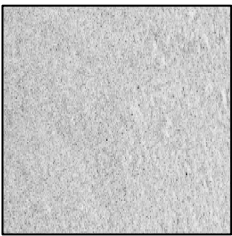
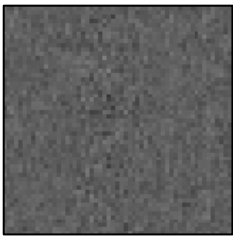

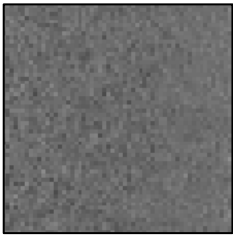
The interpretation of surficial sediment types was derived from the acoustic character of the high frequency side scan sonar (SSS) data, and the interpretations aided by multibeam echo sounder (MBES) bathymetric 3D surfaces, multibeam backscatter (MBBS) and sub-bottom profiler (SBP) data, along with the results from grab sampling. During the review of the SSS survey data, higher intensity sonar returns (darker grey to black colours) were interpreted as relatively coarser grained sediments, and lower intensity sonar returns (lighter grey colours) were interpreted as relatively finer grained sediments. Bathymetric data was used to assist in boulder field interpretation and to correct for the effects of seabed slope on sonar returns

The MBBS data shows the intensity of the reflected MBES signal and is used to assist interpretation of surficial sediment types (in conjunction with geotechnical data). In MBBS data high intensity sonar returns (lighter grey colours) were interpreted as relatively coarser grained sediments and low intensity sonar returns (darker grey colours) were interpreted as relatively finer grained sediments. Despite this representation being opposite to how SSS data is presented, MBES processing convention dictates this tonal relationship with MBBS data intensity.

The MBBS data is processed within QPS FMGT on a block-by-block basis and a single raster created using Safe Software FME. The resolution of the final MBBS raster is 0.5 m. The MBBS data was used to assist the surficial sediment interpretation.

The ID column in Table 20 defines the colour in the charts for the specific sediment type. All particle sizes refer to the soil classification in ISO 14688-1 (2002).

Table 20 Sediment classification.

ID	SSS Image	BS Image	Acoustic Description	Lithological Interpretation
			Low acoustic reflectivity. No texture. Texture indicates wave and stream working of the sediment.	MUD and sandy MUD Predominantly mud (silt & clay), may contain sand.
			Low to medium acoustic reflectivity. No texture.	Muddy SAND Predominantly sand with variable fractions of mud (silt & clay).
			Medium acoustic reflectivity, slightly grainy texture.	SAND Predominantly sand, may have minor fractions of clay, silt and/or gravel.
			Medium to high acoustic reflectivity. Slightly grainy to grainy texture, coarse texture in places.	GRAVEL and coarse SAND Predominantly gravelly sand, may contain silt. The ratio between sand and gravel can vary within this sediment type.

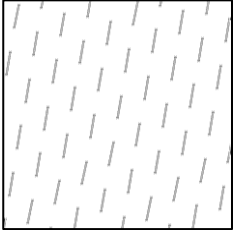
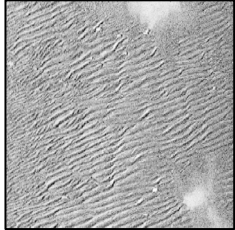
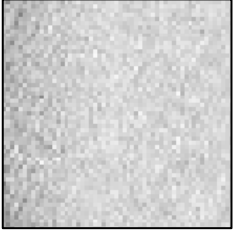
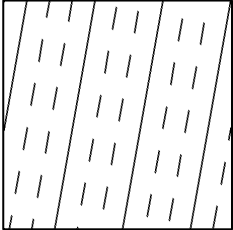
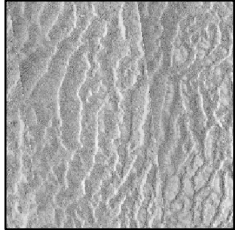
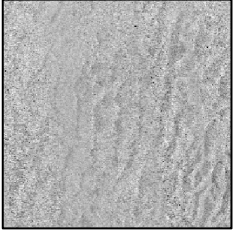
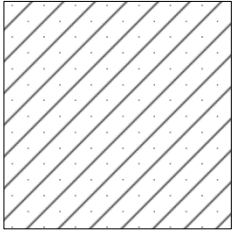
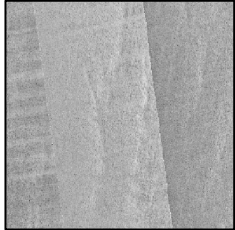
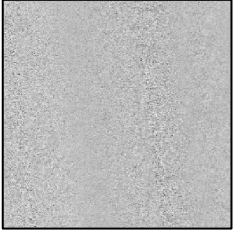
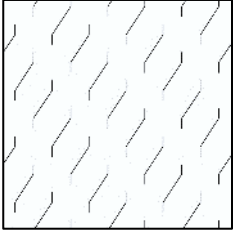
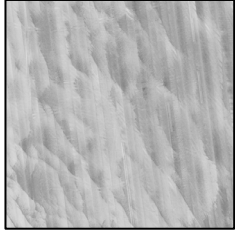
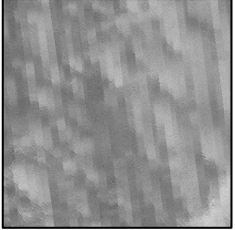
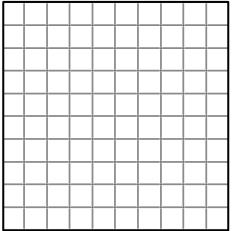
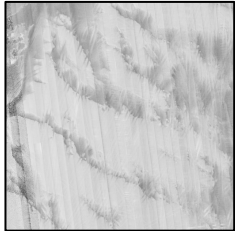
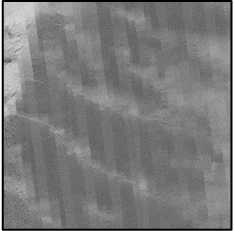
Note: the definition MUD has been used to keep in line with the TSG standards. MUD comprises of SILT and/or CLAY.

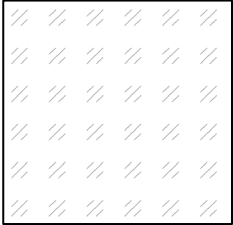
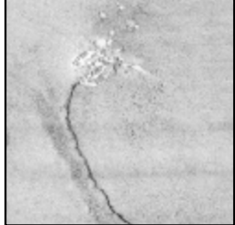
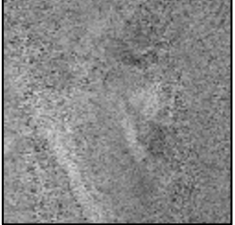
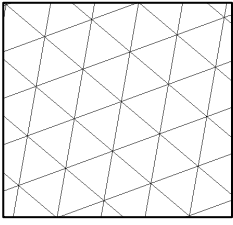
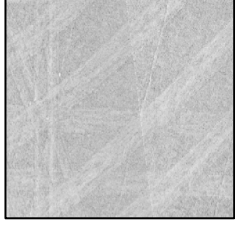
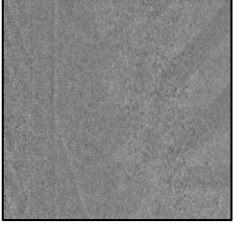
6.3 | SEABED FEATURE / BEDFORM CLASSIFICATION

The ID column in Table 21 defines the pattern in the charts for the specific feature type. Apart from the ones presented here, trawl marks were also digitized.

SSS, MBES and MBBS data have been used for interpretation of the seabed feature boundaries.

Table 21 Seabed features classification.

ID	SSS Image	BS Image	Seabed Feature	Criteria
			Ripples	Wavelength <5 m Height < 0.1 m Wavelength is the primary classifier.
			Large Ripples	Wavelength 5 – 15 m Height 0.1- 1 m Wavelength is the primary classifier.
			Megaripples	Wavelength 15 - 50 m Height 1 - 3 m Wavelength is the primary classifier.
			Sand Waves	Wavelength 50 - 200 m Height 3 - 5 m Wavelength is the primary classifier.
			Sandbars	Wavelength > 200 m Area of large-scale sediment transport/migration forming massive bedforms such as sandbars, sand ridges and sand dunes. This feature was added post scriptum to account for sediment formations which are larger than 200 m WL.

ID	SSS Image	BS Image	Seabed Feature	Criteria
			Other-Area of Interest	Unknown features – assessed for biogenic origins.
			Trawl Mark Area	Area with multiple trawl marks/seabed scars.

The SSS and MBES contacts were classified according to the following criteria:

- Boulder
- Man-made object (MMO) (Debris, fishing gear, man-made structures etc.)
- Other
- Wreck (none observed within the Artificial Island survey area)

Boulder density was not high enough to classify any boulder fields within the Artificial Island survey area (>40 boulders per 100 x 100 m). All boulders ≥ 1.0 m were interpreted.

Boulders were primarily interpreted in the MBES data. Subsequently, remaining boulders and all other contacts were interpreted in the SSS data.

In the GIS database all MAG anomalies are categorized as MMO, due to the inherent uncertainties of magnetic anomaly interpretation. Best efforts were made to avoid selecting anomalies that are likely to be geological in nature, but in the cases where differentiation between man-made or geologically derived anomalies were not possible, the anomaly was selected but with a comment of “Likely Geology”.

All MAG anomalies were compared to all MBES and SSS contacts. If a MAG anomaly was within 5 m of any contact detected in either MBES or SSS, it was automatically deemed a correlation and commented on in the contact listing, as well as in the GIS database.

MAG anomalies forming a linear pattern were commented as such as these could indicate the presence of fishing gear, cables, wire/chain or anything of a ferrous linear nature. Some linear anomalies were inferred to be of a geological nature and these were also commented as such.

6.4 | SUB-SEABED GEOLOGY CLASSIFICATION

The subsurface geological interpretation and description is based on the assessment of the 2D UHRS and Innomar SBP data acquired within the survey area.

The descriptions of the seismic units are provided according to the seismic facies, stratigraphic boundaries, and internal reflector terminations. The units used are presented in Table 22. Further details on the seismostratigraphic interpretation and the proposed Geological Ground Model can be found in section 8.6|Seismostratigraphic Interpretation.

SBP contacts are selected when diffraction hyperbolas are present and can be clearly related to a single object.

For further information on the processing steps and classification methods, see sections 4.5| and 4.6|.

Table 22 Summary of the seismic units.

SEISMIC UNITS	ACOUSTIC FACIES AND INTERNAL CONFIGURATION	LOWER BOUNDING SURFACE		EXPECTED COMPOSITION	KINGDOM REFLECTOR COLOUR	STRATIGRAPHY (TENTATIVE CORRESPONDENCE)	
		MORPHOLOGY	NATURE				
U05	Generally low amplitude. Transparent to chaotic facies with a discontinuous reflector.	Mostly flat	Erosive	Fine grained sands	Gold	Marine sand deposits	Holocene
U10	Generally low amplitude. At the base may be homogenously transparent or with small mound-channel patterns to chaotic; overlaid by oblique downlap reflectors and small lenses. Above, sub-horizontal parallel reflectors. Common discontinuous soft kicks.	Mostly flat, tabular	Wave cut ravinement surface; Erosive	Silty sands; gravels; gravelly sand lags	Light Green	Marine sand deposits	Holocene
U20	Two distinct facies: Channels: Micro-meso scale channels, chaotic to parallel infill, commonly mounded-chaotic at the base; Wide shallow basins: low amplitude to transparent homogeneous, faint micro-parallel reflectors and common negative high amplitude anomalies.	V-shape channels and tabular	Erosive	Basins: clays-silts-fine sands; channel infills: fine sands-sands (even gravelly lags/layers?). possible organic-rich.	Dark green	Infills of small basins and channels, likely in a restricted marine-tidal setting, partially associated to a subaerial fluvial system	
U25	Low amplitude micro-parallel reflectors, undulating; small-scale, scattered box-shaped channels with transparent infill negative amplitude at	Tabular	Erosive	Fine sediments: fine sands-silts (?)	Rosy Brown	Relatively low-energetic setting, possibly a transgressive estuary	

SEISMIC UNITS	ACOUSTIC FACIES AND INTERNAL CONFIGURATION	LOWER BOUNDING SURFACE		EXPECTED COMPOSITION	KINGDOM REFLECTOR COLOUR	STRATIGRAPHY (TENTATIVE CORRESPONDENCE)	
		MORPHOLOGY	NATURE				
	the base; channel frequency increase towards the top.						
U30	Composite facies; medium to high amplitude; upper section: sub-horizontal, parallel-wavy; centre: meso-micro channels-mounds-oblique; base: mounds, lenses, channel lateral migration, hummocky reflectors, and chaotic in parts.	Tabular	Erosive	Fining-upward, sandier at the base (?)	Orange	Higher energy than U25, fluvial	
U35	Base of three major basins. A composite facies, low to high amplitude; complex meso mounds-channels-lenses; internal erosion surfaces; base: large oblique lenses; the thickness of the internal packages decreases towards the top, becoming more sub-horizontal and sub-parallel, grading up.	Tabular	Erosive	Gravel and sands with enclaves of coarser-grained clasts, fining-upward (?)	Yellow	High energy fluvial bedforms (flash floods?)	
U40	Four types of channels and their lateral deposits: Type A: Base: mound-chaotic-composite, grading up meso-micro scale, chaotic in places; Top: channels, micro parallel wavy oblique	V and U-shaped channels	Erosive	Variable: sands, silts, clays	Dark Magenta	Drainage of glacial melt back from the north, and outwash plains	Glacial period (Weichselian?)

SEISMIC UNITS	ACOUSTIC FACIES AND INTERNAL CONFIGURATION	LOWER BOUNDING SURFACE		EXPECTED COMPOSITION	KINGDOM REFLECTOR COLOUR	STRATIGRAPHY (TENTATIVE CORRESPONDENCE)	
		MORPHOLOGY	NATURE				
	<p>reflectors; variable amplitudes from high to low.</p> <p>Type B: Generally chaotic-oblique-mound-channel to oblique above, common internal mounds-channels; variable amplitude.</p> <p>Type C; Base: chaotic-mound-channel, medium-high amplitude; Top: oblique-channel-mounds to meso-micro parallel wavy, chaotic, and homogenous.</p> <p>Type D: Composite with three facies associations; chaotic base with medium-high amplitude to composite mounds; middle facies sub-tabular with medium amplitude, meso-micro parallel obliques, wavy in places; top facies truncating the deposits below, mounds-channels.</p> <p>Channel lateral deposits/fringes: composite mound-channel facies.</p>						
H50	<p>Two distinct characters: NE region: uniform low to transparent amplitude; faint layering; scattered anomalies of positive amplitude. Elsewhere: low amplitude, parallel at base, chaotic</p>	Tabular	Erosive	Fine sediments, boulders (?)	Medium Orchid	Uncertain: glacial drift deposit (aqua till?) or glaciolacustrine deposition (?)	Glacial period (Weichselian?)

SEISMIC UNITS	ACOUSTIC FACIES AND INTERNAL CONFIGURATION	LOWER BOUNDING SURFACE		EXPECTED COMPOSITION	KINGDOM REFLECTOR COLOUR	STRATIGRAPHY (TENTATIVE CORRESPONDENCE)	
		MORPHOLOGY	NATURE				
	above, common oblique, local channels and transparent deposits.						
H60	Composite facies, low to high amplitude, complex internal features, meso mounds, channels, and lenses. Numerous oblique internal erosion surfaces. Large clinoform layers fill-in the larger incisions.	V-shape asymmetric channels and tabular	Erosive	Mainly sands with gravel and silt (?)	Red	High energy fluvial bedforms (flash floods?)	Glacial period (Weichselian?)
H70	Infilled channels/valleys. V-shaped: composite infill, two facies associations. U-shaped: Base:medium-high amplitude, meso mounds-channels-parallel, occasionally chaotic; Top: truncating base, lower amplitudes, meso-micro composite mounds-channels, parallel-obliques; common chaotic-homogeneous transparent.	V and U-shape channels	Erosive	Variable: sands, silts, clays	Blue	Glaci-fluvial deposition, in a proglacial, sub-aerial environment (reoccupation of tunnel valley depressions by fluvial systems?)	Glacial period (Weichselian?)
UKSA	Complex, wide range of internal structures affected by variable degrees of deformation, from better-preserved faulted blocks to completely disturbed/chaotic regions, to transparent and incoherent.	Variable	Deformation front	Variable: sands, silts, clays	Dark Red	Deformed deposits	Glacial period (Weichselian?)

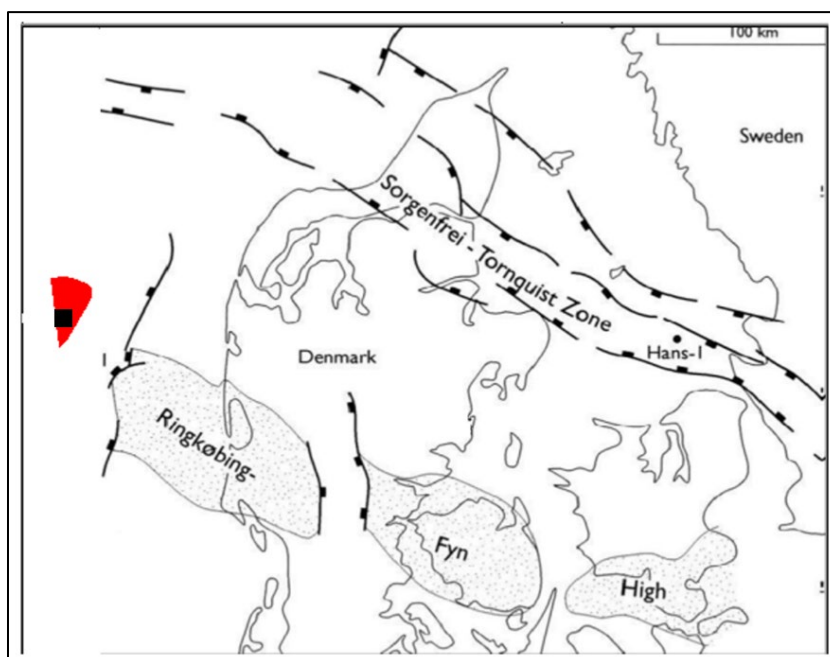
SEISMIC UNITS	ACOUSTIC FACIES AND INTERNAL CONFIGURATION	LOWER BOUNDING SURFACE		EXPECTED COMPOSITION	KINGDOM REFLECTOR COLOUR	STRATIGRAPHY (TENTATIVE CORRESPONDENCE)	
		MORPHOLOGY	NATURE				
H85	Composite facies, low-high amplitude, complex meso mounds, channels, and lenses, oblique reflectors, internal erosion surfaces. Strong negative amplitude near or at the base.	V-shape channels and tabular	Erosive	Mainly sands with gravel and silt (?). Organic-rich muds (?) at the base	Hot Pink	High energy fluvial (possibly outwash plain?)	
H90	Parallel-homogeneous facies at the base, association of parallel-mound-channel-shingled facies above, all prograding towards NW or W. Scattered small mounds.	Tabular	Erosive	Mainly sands-fine sediments	Cyan	Fan delta	
UKSB	Complex, wide range of internal structures affected by variable degrees of deformation, from better-preserved faulted blocks to completely disturbed/chaotic regions, to transparent and incoherent.	Variable	Deformation front	Variable: sands, silts, clays	Dark Red	Deformed deposits	Glacial period (Saalian?)
BSU	Layered sequence of parallel facies of variable amplitude, locally deformed.	-	-	Marine clays, silts to sands		Subparallel deposits, locally deformed	Pre-Quaternary

6.5 | GRAB SAMPLE CLASSIFICATION

For details on the grab sample classification, see section 8.10| and Appendix C|.

7 | GEOLOGICAL FRAMEWORK

The Danish sector of the North Sea basin is connected to the east by the Scandinavian Shield and by the WNW-ESE striking Sorgenfrei-Tornquist fault zone (Figure 61). The Ringkøbing-Fyn High, located further south, emerged during the Late Permian (Pre-Zechstein) as a result of tectonic subsidence (Vejbæk, 1997; Vejbæk et al., 2007). This structural feature divides the Danish sector of the North Sea basin into the North German Basin, located south of the Ringkøbing-Fyn High, and the Danish-Norwegian Basin, north of Ringkøbing-Fyn High. During the Zechstein (Late Permian), four to five cycles of evaporites were deposited, infilling the structural lows (Sorgenfrei and Buch, 1964; Vejbæk et al., 2007). Further deepening of the North Sea basin resulted in thousands of metres of Mesozoic sediment deposition over the evaporites. The thick Mesozoic deposits activated diapirism of the underlying evaporites. Subsequently, several cycles of glaciations resulted in further loading, inducing reactivation and upward migration of the salt diapirs (Nielsen et al., 2008). This halokinesis is likely to be ongoing in modern times, also indicated by a high level of earthquakes in the Danish Basin, measured in the period 1920 to 1995 (Gregersen et al. 1998)



*Figure 61 Major Danish structural elements
(After Stemmerik et al., 2000); MMT OWF survey area in red; Artificial Island area of investigation marked by black square.*

During the Late Cretaceous, a major tectonic inversion episode affected the North Sea region, associated with initiation of the Alpine Orogeny, (Clausen and Huuse, 1999; Japsen, 2000). Cretaceous tectonism was followed by sequential episodes of uplift and major sea level fluctuations during the Paleogene to Neogene (Japsen et al. 2008). These events resulted in variable rates and types of sediment deposition. A major regional unconformity occurs between the Upper Eocene and lower Upper Oligocene, Brejning Fm. (Mica Clay) (Rasmussen et al., 2010). The Neogene deltaic deposits show a general shift moving from east to west. The Miocene succession is hundreds of metres thick in the Danish sector of the North Sea. From the rim of the North Sea basin at the Sorgenfrei-Tornquist Zone towards the central basin, the Pre-Quaternary deposits are successively younger below the base of the Quaternary. The Quaternary base represents an unconformity east of the so-called the transition zone in the North Sea (Nielsen et al. 2008, Japsen 2003) (Figure 62). West of the transition, the Quaternary sequences rest conformably on Pliocene deltaic sediments (Nielsen et al. 2008). Often, the unconformity shows a significant relief due to Quaternary glacial processes, and occurs at depths of a few hundred metres within valley structures to just below the seabed along the Danish west coast (Andersen, 2004;

Huuse and Lykke-Andersen, 2000b; Leth et al., 2004, Novak and Duarte 2018). Across the wider region (e.g. central North Sea) this surface is characterized by strong undulation controlled by variable-scale structures in the Pre-Quaternary basement.

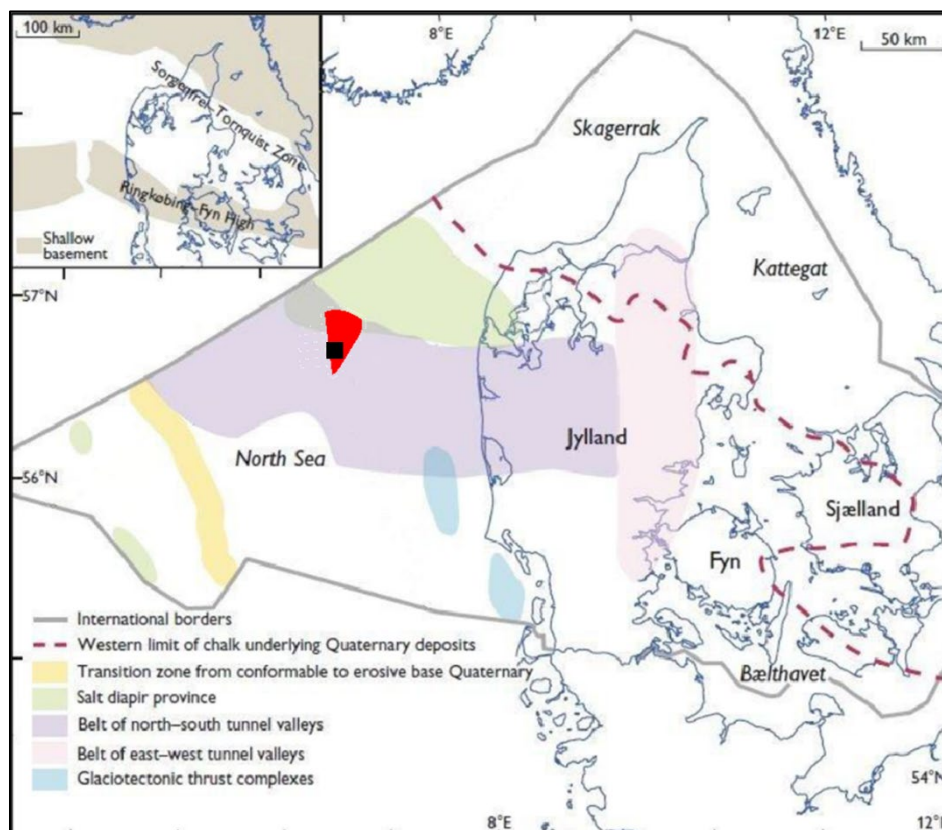


Figure 62 Regional geological map.

(After Nielsen et al., 2008); MMT OWF survey area in red; Artificial Island area of investigation marked by black square.

Only a few studies have been performed on the Quaternary deposits in the Danish North Sea. However, onshore studies provide a decent foundation for outlining the regional geology in the eastern North Sea (e.g., Sjørring and Frederiksen, 1980; Ehlers, 1990; Sandersen and Jørgensen, 2003; Pedersen, 2005; Jørgensen and Sandersen, 2006; Jacobsen, 2003; Høyer A-S et al., 2013; Houmark-Nielsen, 2007).

In general, the Quaternary sequence thins from the central North Sea towards the Danish mainland. The Elster and Saale ice sheets extended across the entire North Sea (Figure 63). Glaciation came from the northwest over northeast and from the Baltic region (Sjørring and Frederiksen, 1980; Ehlers, 1990). The Weichselian ice sheet extended north and east of the main stationary line at the Late Glacial Maximum (LGM), which was located from inland Jutland towards the northwest into the North Sea (Figure 63). Morphological elements such as moraine ridges and elongated boulder reefs, occurring perpendicular to the main stationary line, indicate the location of the ice boundary on the seabed west of the Thyborøn at the Danish west coast (Nicolaisen, 2010). Onshore, southwest of the LGM, the so called "hill islands" (Dalgas, 1867), which outline the Saalian landscape, are found to extend into the North Sea (Larsen, 2003; Larsen & Andersen, 2006; Leth et al., 2001; Anthony, 2001; Leth, 2003). Morphological remnants are absent on the seabed due to marine erosion. However, seismic profiles reveal horizons that have been interpreted to represent this same landscape. The northern part of the actual survey area is expected to cross over the LGM stationary line; however, central and southern survey area has only been overridden by Saaleian or older glaciations.

Large-scale glaciotectonic thrust complexes have been identified in the Danish North Sea, as well as onshore the Danish main land (e.g., Huuse and Andersen 2000a, 2000b, Larsen and Andersen 2005, Vaughan-Hirsch and Phillips 2017, Novak and Duarte 2018, Høyer et al. 2013, Shack Pedersen 2005, Jacobsen 2003). In the eastern North Sea, the décollement surfaces are located in the Miocene or in the Quaternary level, and the thrust blocks comprise these sediments. The formation of glacial tectonic complexes found to the west and south of the Weichselian LGM boundary are attributable to the Saalian or older ice cover (Andersen, 2004; Huuse and Lykke-Andersen, 2000b; Vaughan-Hirsch and Phillips, 2017).

Systems of buried shelf valleys, 100-300m deep and several tens of kilometres long, are present (Figure 63) (Andersen, 2004; Huuse and Lykke-Andersen, 2000b; Novak and Duarte 2018). The submarine valleys can be correlated to onshore valleys and are considered to be of the Elster and Saale ages. Younger, reactivated Saale valleys have been found north and east of the Weichselian main stationary line (Smed 1979, 1981a; Jørgensen et al., 2005).

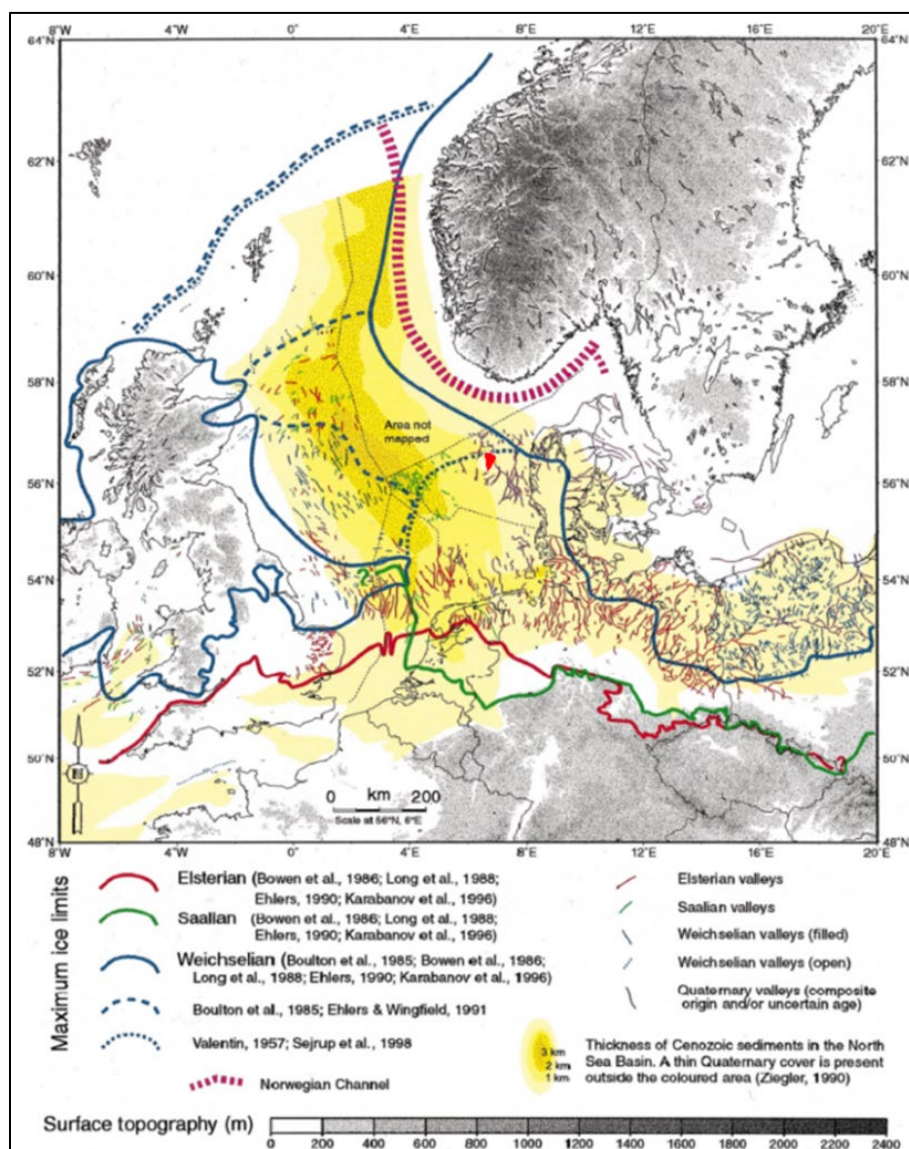


Figure 63 The Quaternary glaciations and overview of Quaternary valleys in northwest Europe. (Huuse, M., and Lykke-Andersen, H. 2000); site location in red.

The Paleo-North Sea extended across the region during the Eemian period. Eemian deposits are described both on and offshore in the south-westerly North Sea (Konradi et al., 2005), and Eem deposits representing valley infill were found in a borehole in the Vesterhav South MMT OWF survey area (Fugro 2014).

Deposits from the Weichselian glaciations (Figure 64) comprise tills alternating with glaciofluvial sand and gravel, glaciolacustrine clay, silt, and sand, toward the north and east of the main stationary line. Towards the west and south of the LGM, glaciofluvial sand and gravel were deposited in morphological lows above the older Saale landscape (Houmark-Nielsen, 2007). The LGM occurred in the region around 22ka BP. The glaciers' subsequent retreat generated accommodation space close to the ice front, where deposition of glaciolacustrine clay filled in, e.g. Younger Yoldia Clay around 16-15ka BP. As Weichselian ice melted back, the subglacial-generated valleys emerged and laminated clay, silt, and fine sand deposited in the valleys (Figure 64).

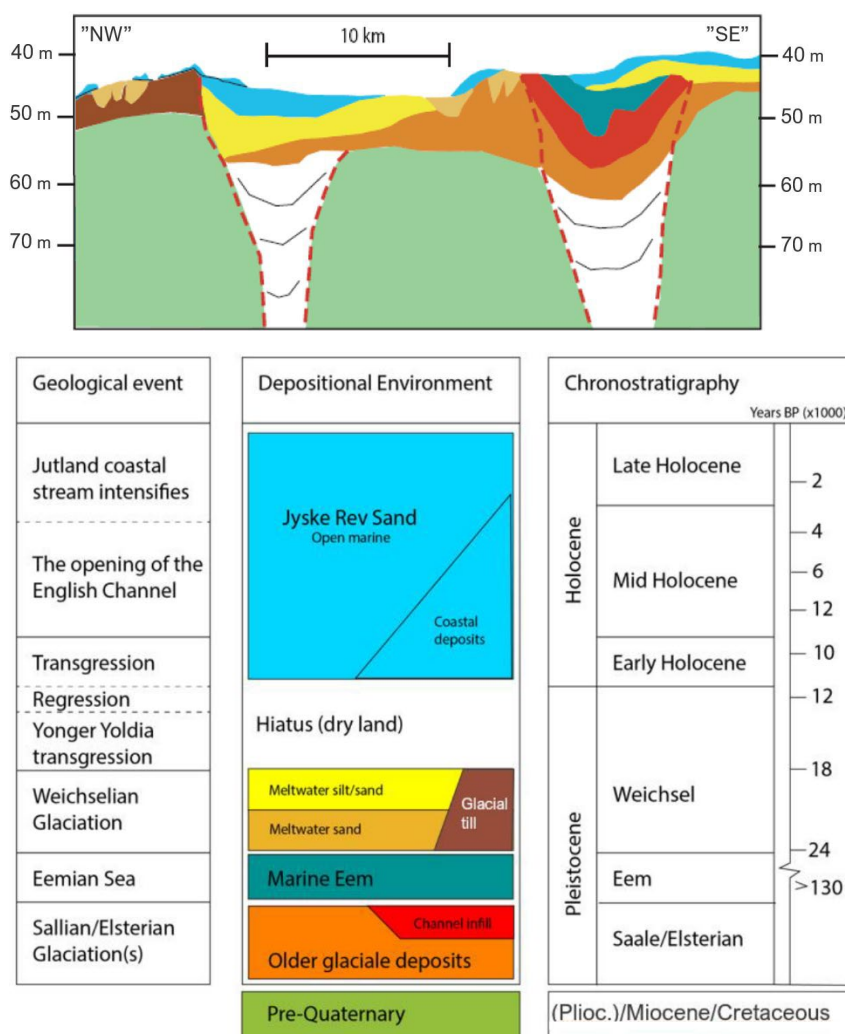


Figure 64 General stratigraphy model of the geology in the eastern Danish North Sea. A composite profile from NW towards SE representing approximately 50 km from Jyske Rev and towards the shore. Below: Stratigraphic unit names and their relative age. Same colour code used above and below. (After Nicolaisen, 2010).

The removal of the glacial load triggered isostatic rebound and a regression that took place until 11ka BP. During this timeframe, relative sea level was, at a minimum, 55 to 45 metres lower than present,

thus maintaining the eastern Danish shelf above sea level. Terrestrial conditions and rising temperatures increased organic material production, resulting in peat accumulations. This marker horizon has been found in many survey areas across Danish waters (Leth, 1996; Bennike et al., 1998, 2000; Novak and Björck, 2002; Novak and Pedersen, 2000). In the eastern Danish North Sea, fine-grained material was deposited in sheltered areas between till "islands", e.g. the Agger Clay unit (Leth, 1996). During the Holocene transgression, from 11ka BP to 6 ka BP, the Agger Clay depocenter shifted coastward and offshore low-lying islands were submerged. At the same time, coastal processes overtook the glaciogenic landscape where it was exposed to waves and currents. The result was the formation of spit/platform/lagoon deposits throughout the region (Nielsen and Johannesen, 2004; Johannesen et al., 2008; Novak and Pedersen, 2000).

In the eastern North Sea, metre-thick fossil sand waves were present at Jyske Rev (Leth 1996). These current- and wave-generated structures have often been formed around sandy-gravelly fossil beach ridges. Seismic data depict multiple generations of these events. After 6 ka BP, sea level was at its highest and the North Sea tidal system and coast-parallel Jylland current developed.

A recent mobile sediment unit is the latest deposit and is found to cover major areas of the eastern North Sea seabed. Coast-parallel strong currents and waves generate the active bedforms, i.e., mobile sandwaves and dunes. The Danish Coast Agency has documented bedform migrations of up to 20-50m per year; the dunes and waves are organized in kilometre-wide areas migrating across an apron of relict gravelly sand (Anthony and Møller, 2003; Anthony and Leth, 2001; Leth et al., 2004).

8 | RESULTS

8.1 | GENERAL

The results from the Artificial Island area of investigation geophysical survey are presented in this report together with associated north-up charts. The charts are presented in Appendix A]. The results of the grab sample campaign are presented in Appendix C].

To facilitate survey data management and survey planning, and to allow the fishing community to plan around the survey work, the MMT OWF survey area was divided into 22 smaller areas. These included six blocks for the main lines (BM1 to BM6) and four areas for the cross lines (BX1 to BX4).

The Artificial Island area of investigation is located within B1 to B4, and cross blocks BX3 to BX4 as shown in Figure 5. All data from the MMT OWF survey area has been trimmed to the 10 km x 10 km Artificial Island survey area boundary.

To assist with organisation in reporting, the survey area was separated into a reporting tile schema. The Artificial Island survey area is within Tiles T13, T14, T15, T16, T19, T20, T21 and T22. The layout of the tiles and the survey area are shown in Figure 6.

8.2 | BATHYMETRY

Overall, the bathymetric depth changes moderately across the Artificial Island survey area. The minimum surveyed depth is 25.75 m at 350742.0 m E, 6264515.0 m N on the Artificial Island survey area (Tile 15). The maximum surveyed depth is 48.17 m at 344391.0 m E, 6267808.0 m N in the north western part of the Artificial Island survey area (Tile 13). The depth range across the area is 22.42 m. Figure 65 shows an overview of the bathymetry within the Artificial Island survey area. Two profile lines are shown running from west to east across the site.

Profile data derived from these lines is shown in Figure 66. The horizontal scale of both profiles starts with 0 km at the western boundary of the 10 km x 10 km area. This has been done so the relative positions of the profiles are normalised and permits any features that may extend between the profiles to be visually aligned. The profiles have a strong vertical exaggeration so that features can be identified along the profiles.

The profiles show that the water depth generally increases on either side of the Artificial Island survey area.

The profiles are used to manage the presentation of the bathymetry results over the Artificial Island survey area, with a sub-section of the report for each profile and regionally related features of interest.

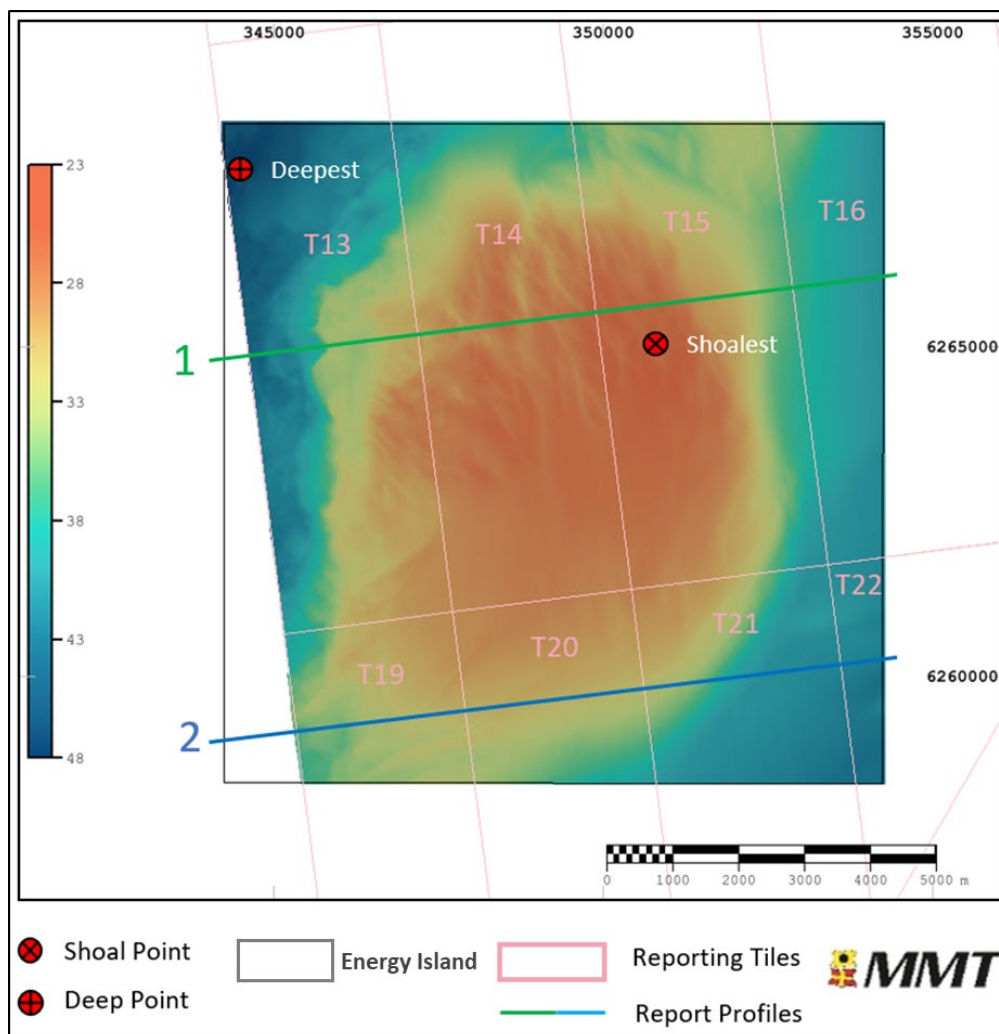


Figure 65 Overview of the bathymetry data.
 Bathymetry and positions of profile lines in Figure 66.

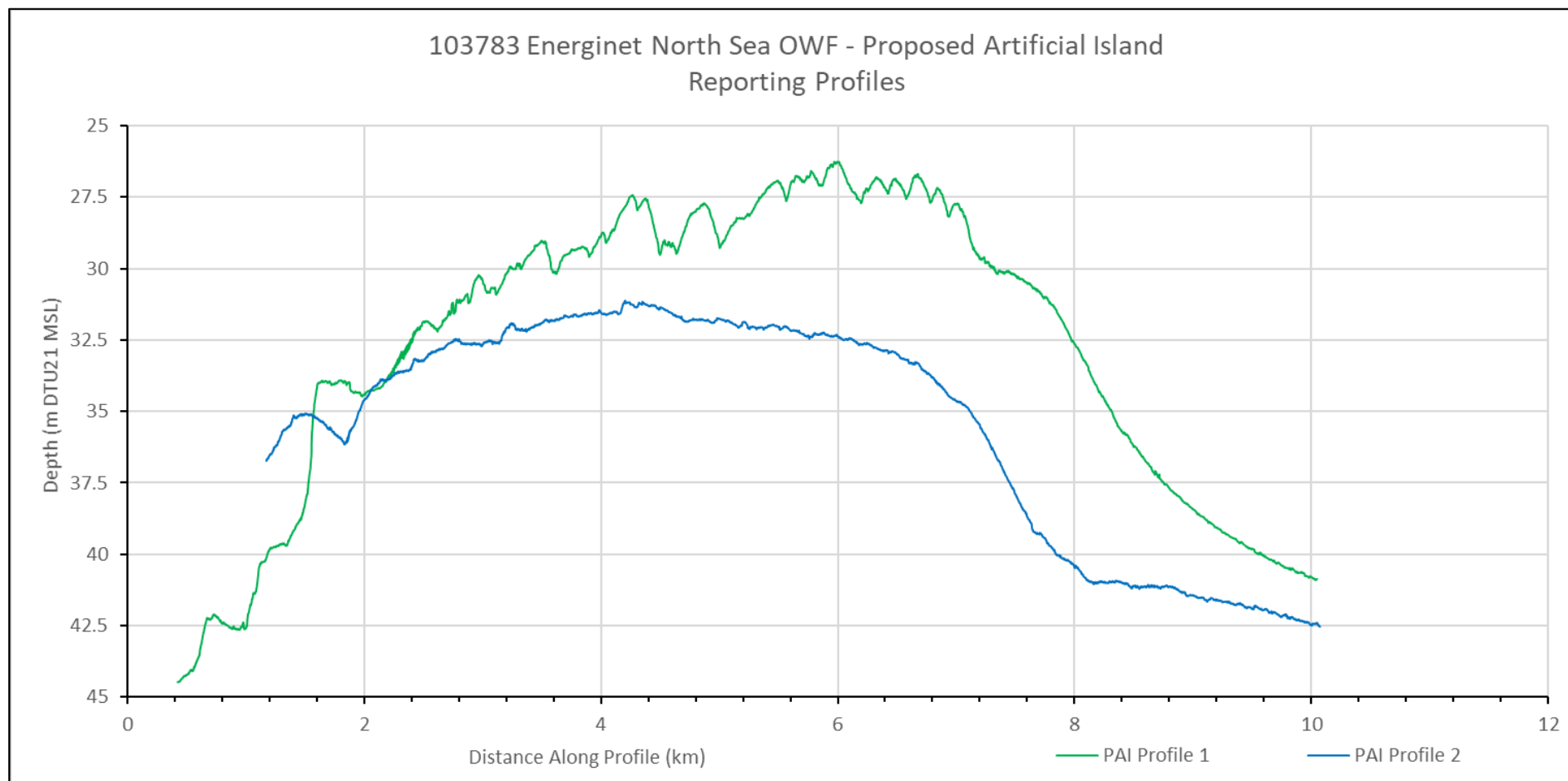


Figure 66 Profiles across the Artificial Island survey area showing depth relative to DTU21 MSL. Profiles have been shifted so that the KP values start on the western boundary of the 10 km x 10 km Artificial Island survey area. Profiles exported from Navimodel with depth convention positive down.

8.2.1 | PROFILE 1

Profile 1 (Figure 66) crosses the north of the Artificial Island survey area and spans 9.7 km. This profile shows the most dramatic change in depth with steep sides on either side of the Artificial Island survey area. The profile shows that the water depth generally increases on either side of the Artificial Island area of Investigation. Over the Artificial Island survey area, the profile shows high frequency variations in depth which relate to ripples and sand waves composed of GRAVEL and coarse SAND.

The depth variation along this profile is 18.40 m from a minimum depth of 26.25 m at 350185.0 m E, 6265450.0 m N to a maximum depth of 44.63 m at 344612.0 m E, 6264897.0 m N. Reporting Tiles T13 to T16 cover Profile 1.

The steepest bedform slopes observed in the Artificial Island survey area are on the western side of the area in Tile T13, with the steepest slope observed at the north west of the Artificial Island survey area (Figure 67).

The deepest part of the Artificial Island survey area is found within Tile T13 with a depth of 48.12 m at 344382.0 m E, 6267798.0 m N (Figure 68).

The shallowest part of the Artificial Island survey area is found within Tile T15 with a depth of 25.79 m at 350767.0 m E, 6264547.0 m N (Figure 69). This area is characterised by large sand wave and sandbar formations with a wavelength of 100 to 300 m and heights between 1.0 to 2.0 m.

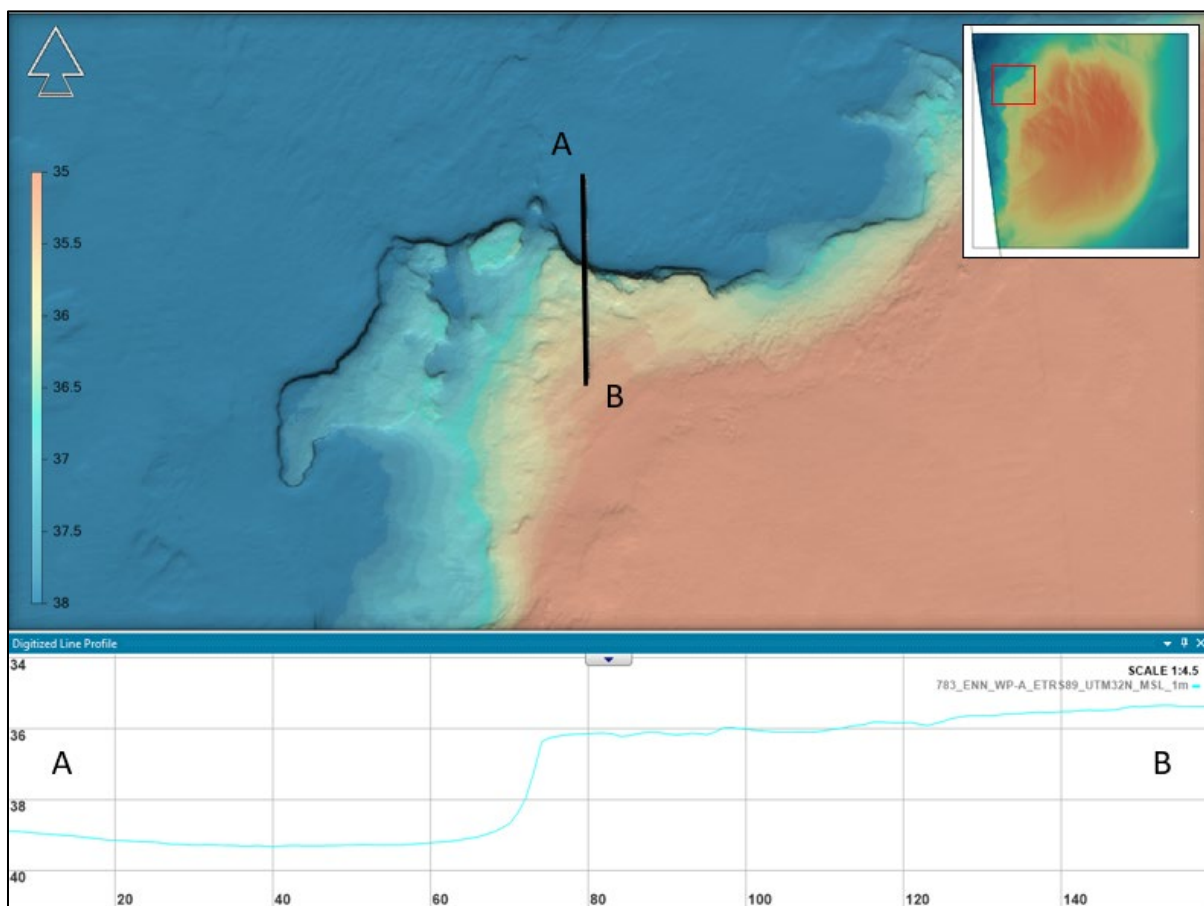


Figure 67 MBES data with profile showing steepest slope of the Artificial Island survey area.

The data is from reporting Tile 13.

NaviModel depth convention is positive down, vertical exaggeration of profile x4.5. Red box in inset map highlights figure location.

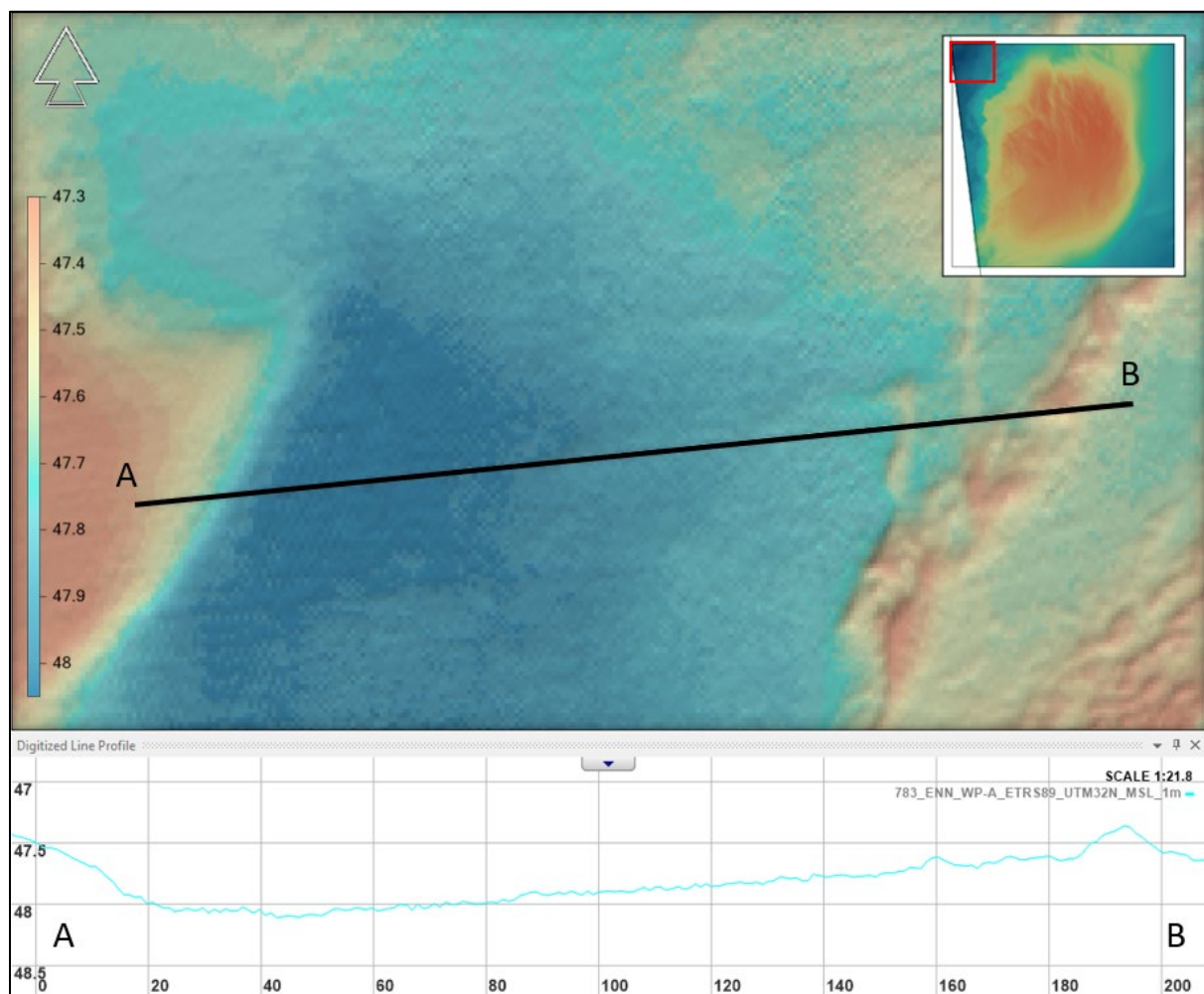


Figure 68 MBES data with profile showing deepest depth of the Artificial Island survey area. The data is from reporting Tile T13. NaviModel depth convention is positive down, vertical exaggeration of profile x21. Red box in inset map highlights figure location.

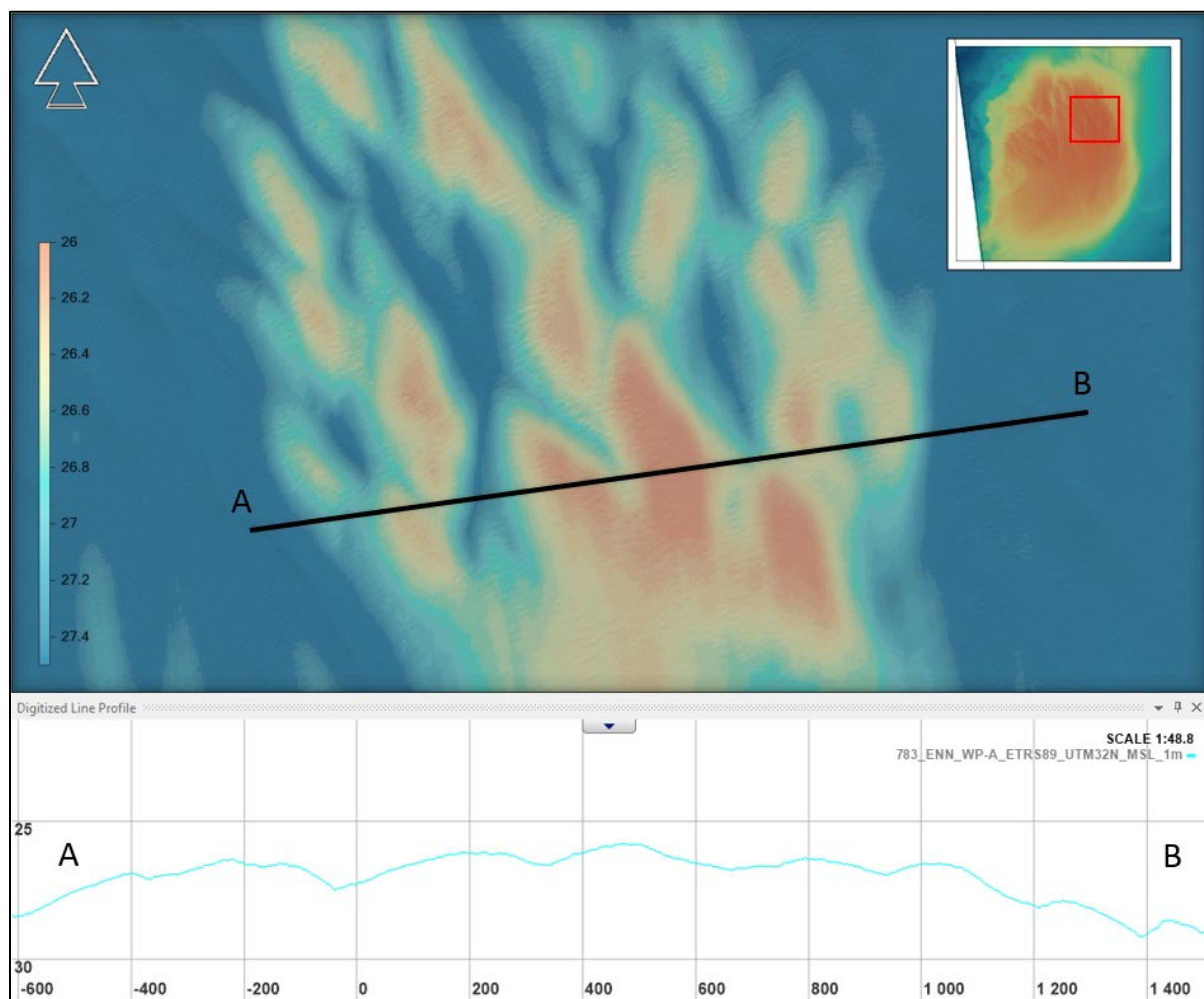


Figure 69 MBES data with profile showing shallowest depth of the Artificial Island survey area
 The data is from reporting Tile T15.
 NaviModel depth convention is positive down, vertical exaggeration of profile x48. Red box in inset
 map highlights figure location.

8.2.2 | PROFILE 2

Profile 2 (Figure 66) crosses the south of the Artificial Island survey area and spans 9 km of the survey area. The profile shows that the shallow waters over the Artificial Island area of investigation extend further to the west than in Profile 1. However, towards the east there is still the steeper drop off towards deeper waters. Over the Artificial Island survey area, the profile is smoother indicating less of the depth variations associated with sand waves.

The depth variation along this profile is 11.42 m from a minimum depth of 31.13 m at 348412.0 m E, 6259460.0 m N to a maximum depth of 42.55 m at 354250.0 m E, 6260158.0 m N.

Reporting Tiles T19 to T22 cover Profile 2. The northern areas of Tiles 19 – 21 contain the southern part of the Artificial Island survey area. This side of the Artificial Island survey area has a gentle slope (Figure 70) that gradually drops in a south easterly direction to the flat and featureless seabed extending further to the east.

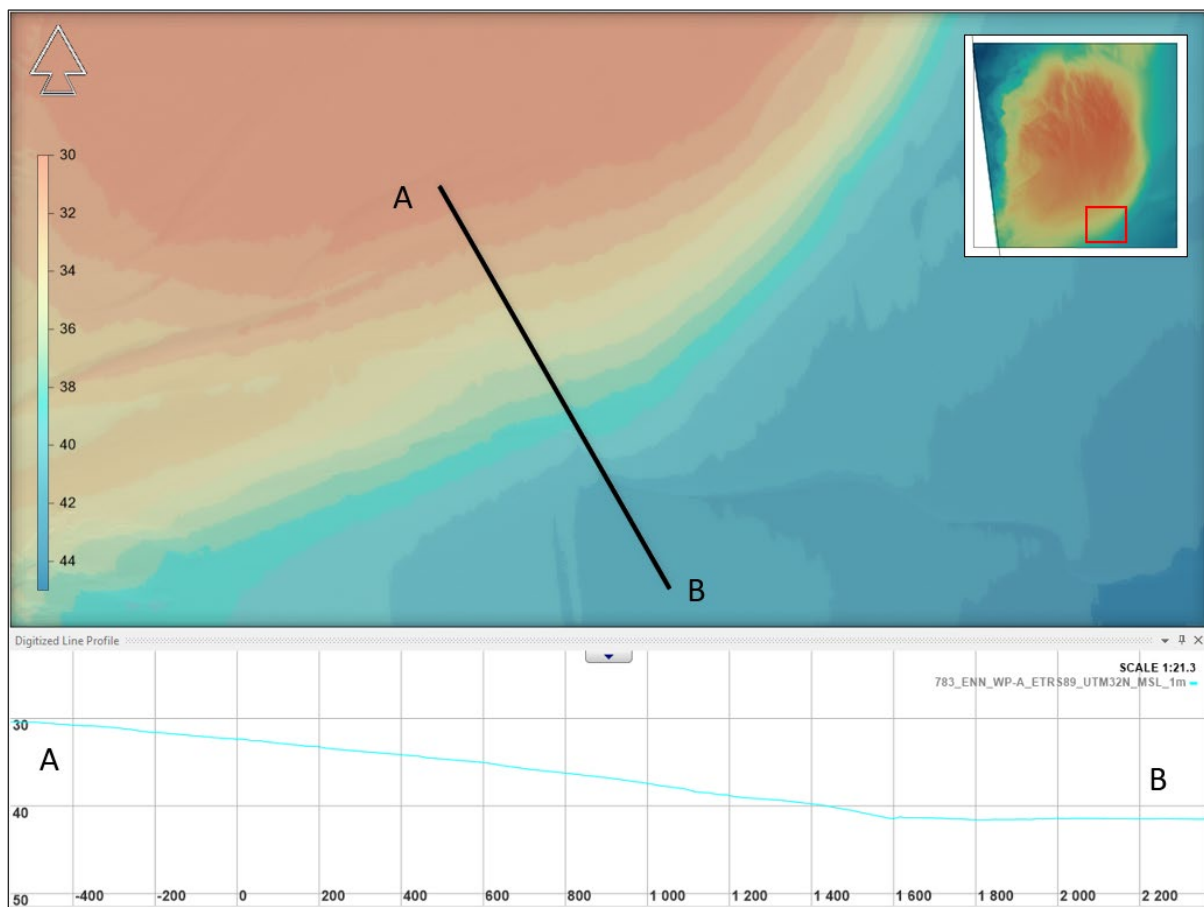


Figure 70 MBES image depicting gentle slope from the Artificial Island survey area
 The example is taken from reporting tile T20.
 NaviModel depth convention is positive down, vertical exaggeration of profile x21. Red box in inset map highlights figure location.

8.2.3 | SLOPE ANALYSIS

Slope angles were derived from the 1 m resolution bathymetry data in Caris HIPS. This data has been used as the basis for examining gradients across the site as it is less susceptible to picking up system noise as areas with high angles of slope.

The slope surface was coloured according to MMT's Slope Classification scheme (Figure 71) and showed that gradients across the site are typically very gentle ($<1^\circ$) and gentle (1° to 5°). However, the overview image masks the presence of higher slope angles found within the survey area.

Figure 73 highlights the zones where slopes are greater than 15° and divides these into groups of 15° - 20° , 20° - 30° , 30° - 45° and $>45^\circ$ (of which there are none in the Artificial Island survey area). The map shows that the high slope areas define the western edge of the sandwave/sandbar field. Along these scarps maximum values regularly exceed 30° towards the northern half of their extent. Towards the south the maximum gradients are between 20° and 30° .

The highest slope angle within the Artificial Island survey area is 44° and this is located on the side of a steep bank at 345825.0 m E, 6265890.0 m N (Figure 72). This steep bank is classified as Other-Area of Interest and is located on the north western edge of the area.

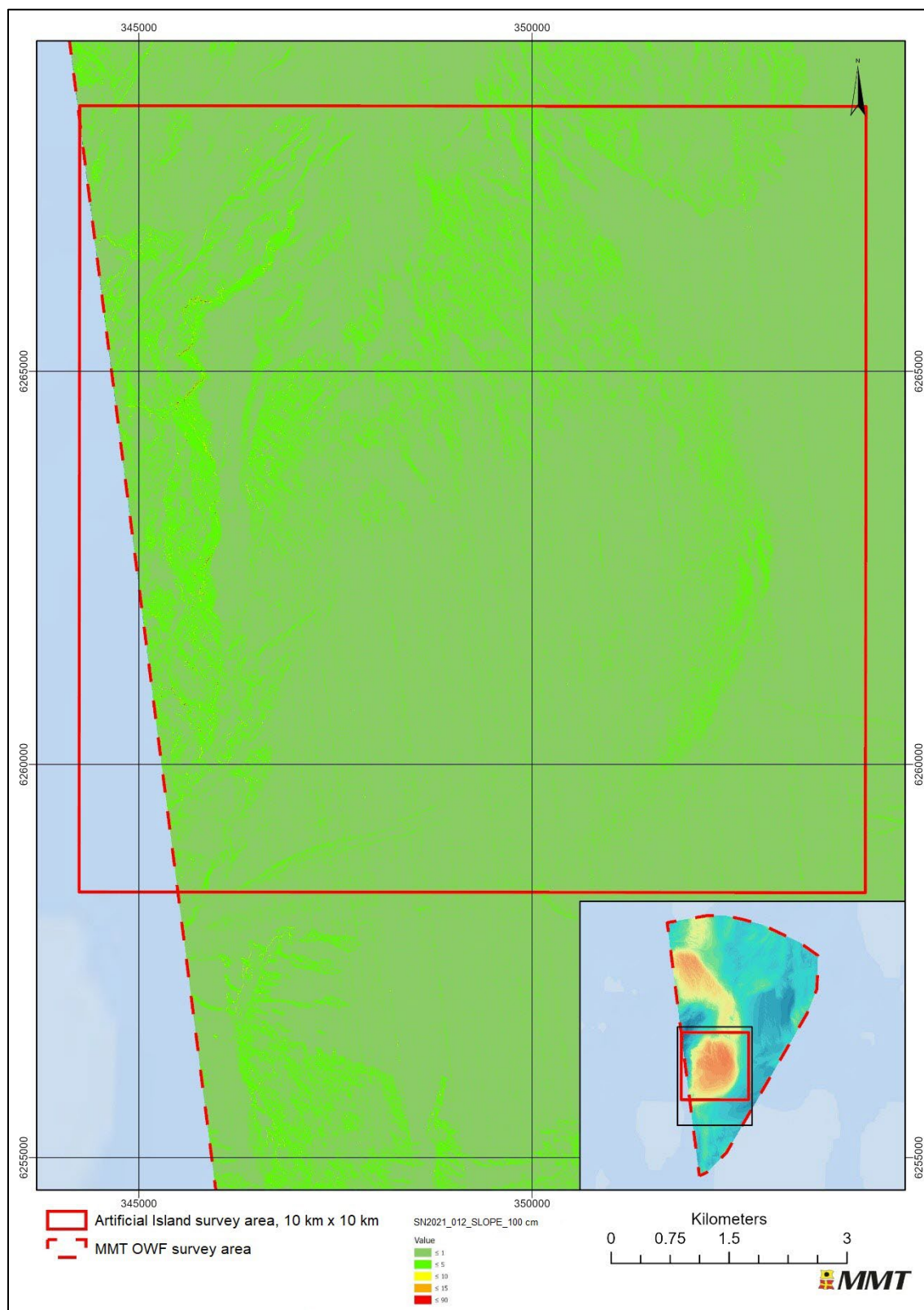


Figure 71 Overview of slope gradients across the Artificial Island survey area.

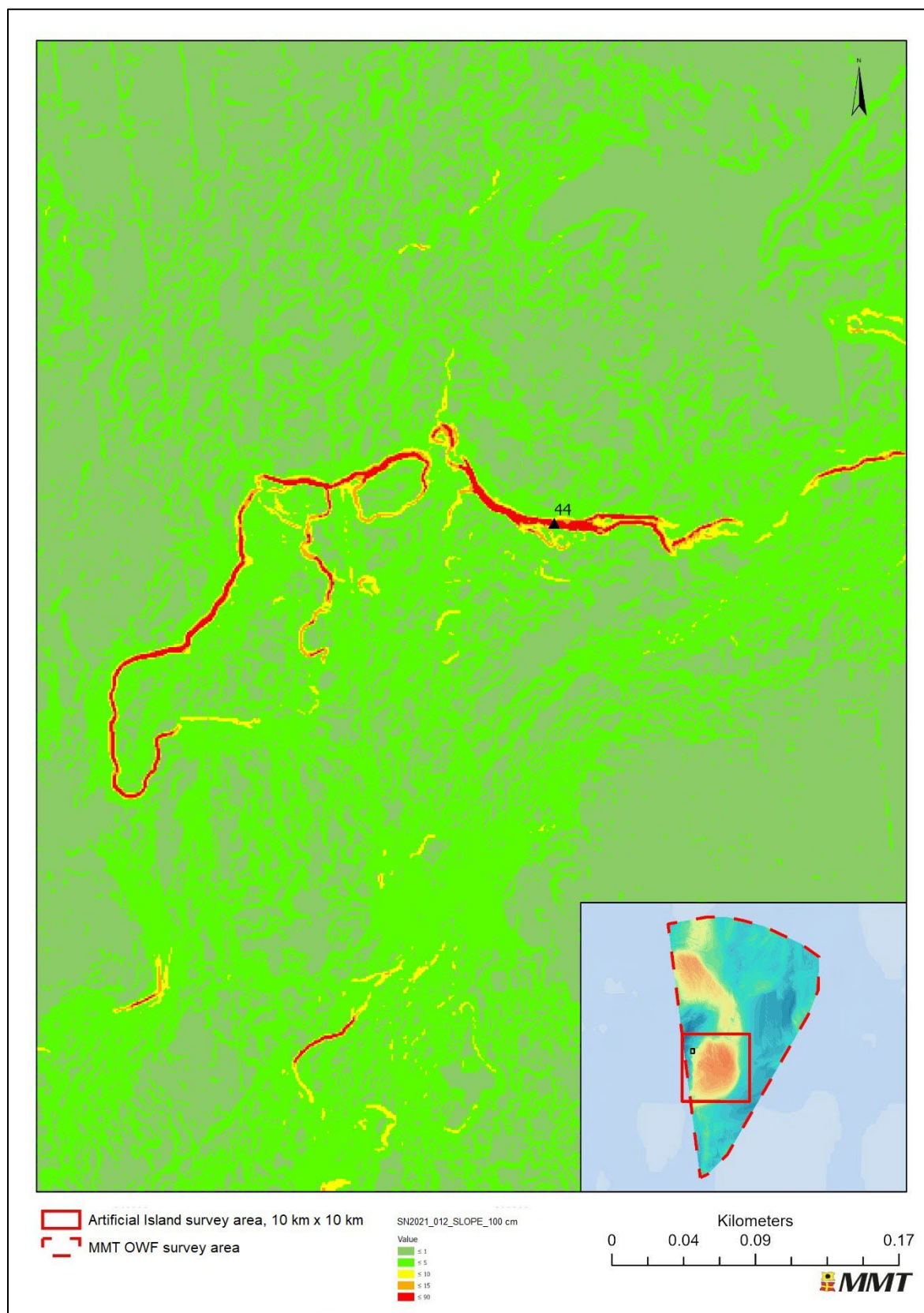


Figure 72 Bedform feature (Other-Area of Interest) with slope angles up to 44°. The feature is located in the northwest of the Artificial Island survey area.

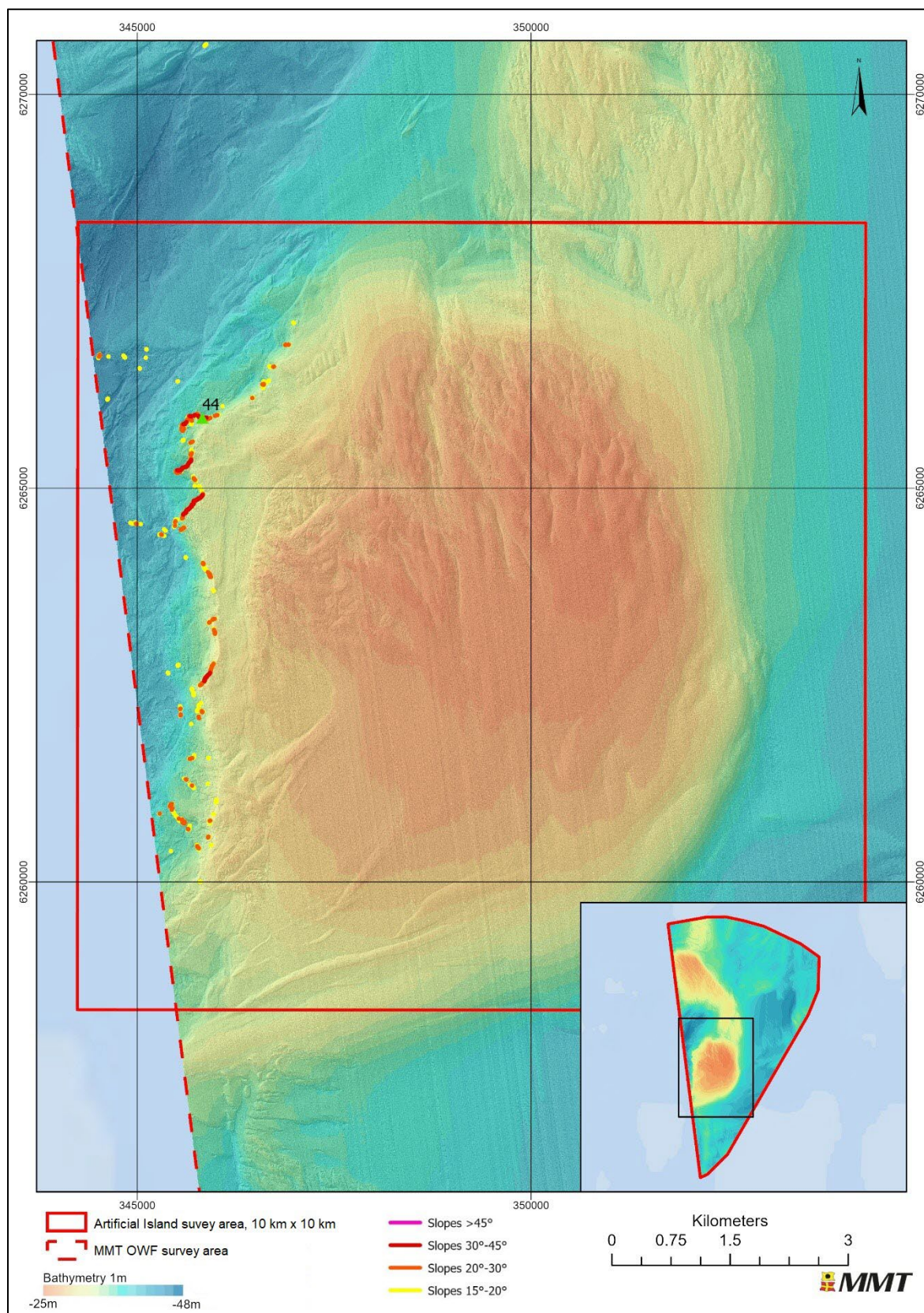


Figure 73 High slope areas within the Artificial Island survey area.

8.3 | SURFICIAL GEOLOGY AND SEABED FEATURES

8.3.1 | SEABED SEDIMENTS

The surficial geology is interpreted from the SSS data based on the relative SSS reflectivity, where lighter reflectivity is interpreted as relatively finer grained sediments and darker reflectivity is interpreted as relatively coarser grained sediments. The SSS imagery has low to medium acoustic reflectivity overall. Backscatter data was used to confirm sediment boundaries. MBES bathymetric data was used to correct the interpretation for the effects of seabed slope on sonar returns. MBBS data was also used to confirm the interpretation of SSS data and to assist with boulder picking.

A total of 21 Grab Sample locations were sampled in the Artificial Island survey area and were used to aid interpretation (section 8.10| and Appendix C|).

The seabed sediments in the Artificial Island area of investigation are dominated by GRAVEL and coarse SAND (medium to high acoustic reflectivity) and SAND (medium acoustic reflectivity). Less frequently observed is muddy (silty) SAND (low to medium acoustic reflectivity) and very occasional areas of MUD and sandy MUD (low acoustic reflectivity) are present.

The GRAVEL and coarse SAND is more prominent in the western and central parts of the Artificial Island survey area (Reporting Tiles T13, T14, T15, T19, T20, T21). The GRAVEL and coarse SAND is often observed alternating with bands of SAND which is also more prominent in the western and central parts of the Artificial Island survey area (Reporting Tiles T13, T14, T15, T16, T19, T20, T21, T22).

The less frequent MUD and SANDY mud is more prominent in the north east of the Artificial Island survey area (Reporting Tiles T14, T15, T16, T21 and T22) as well as some small scattered areas of muddy SAND observed on the western edge of the Artificial Island survey area (Reporting Tiles T13 and T19).

Small, isolated patches of MUD and sandy MUD are observed in the north west of the Artificial Island area of investigation (Reporting Tile T13).

In the areas of fine sediment (muddy SAND, MUD and sandy MUD), the seabed is usually featureless with ripples occurring mostly in areas of GRAVEL and coarse SAND or SAND, see section 8.3.2| and Figure 77 for details.

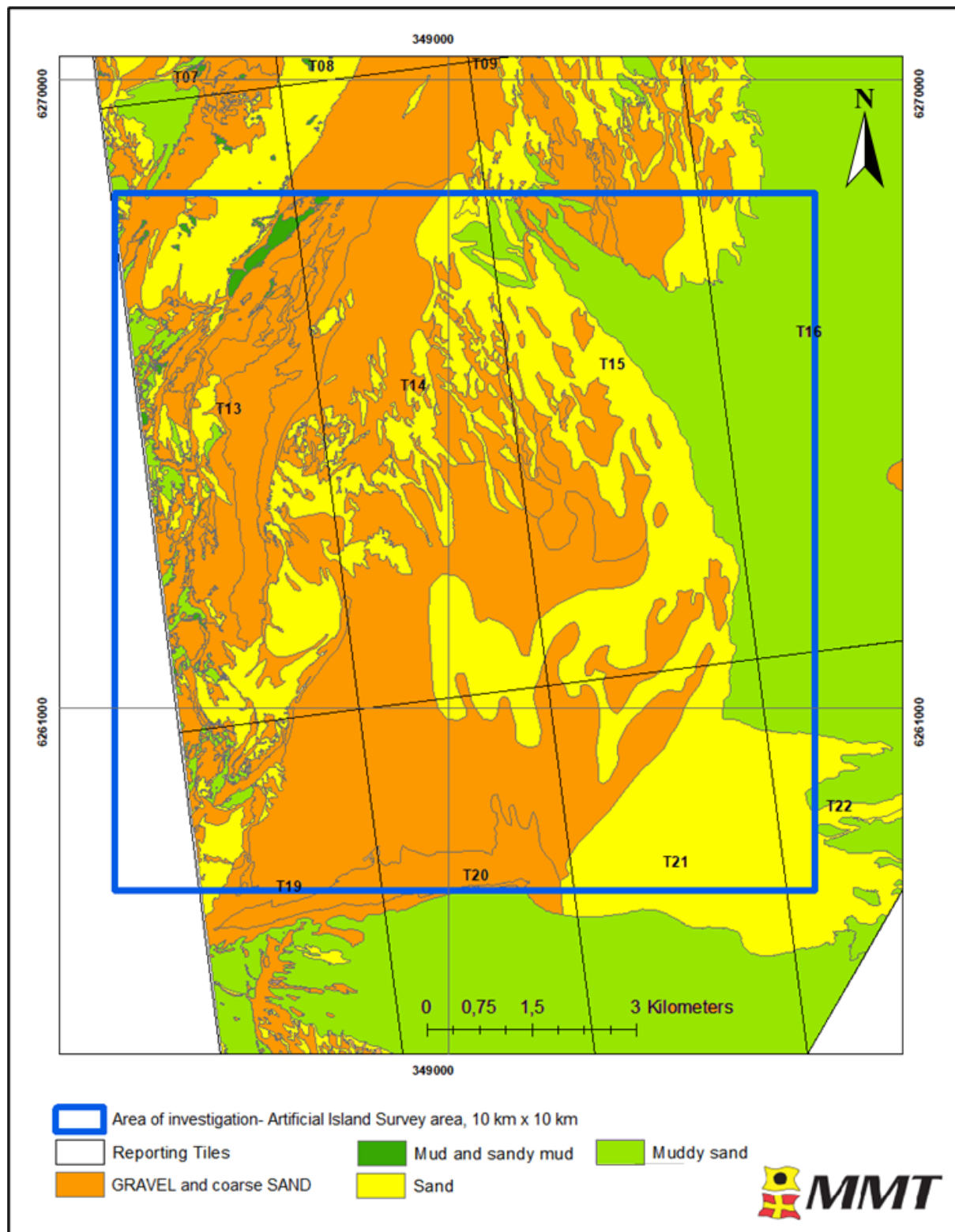


Figure 74 Seabed sediments within the Artificial Island survey area

SSS data examples showing different sediments is presented in Figure 75 and Figure 76.

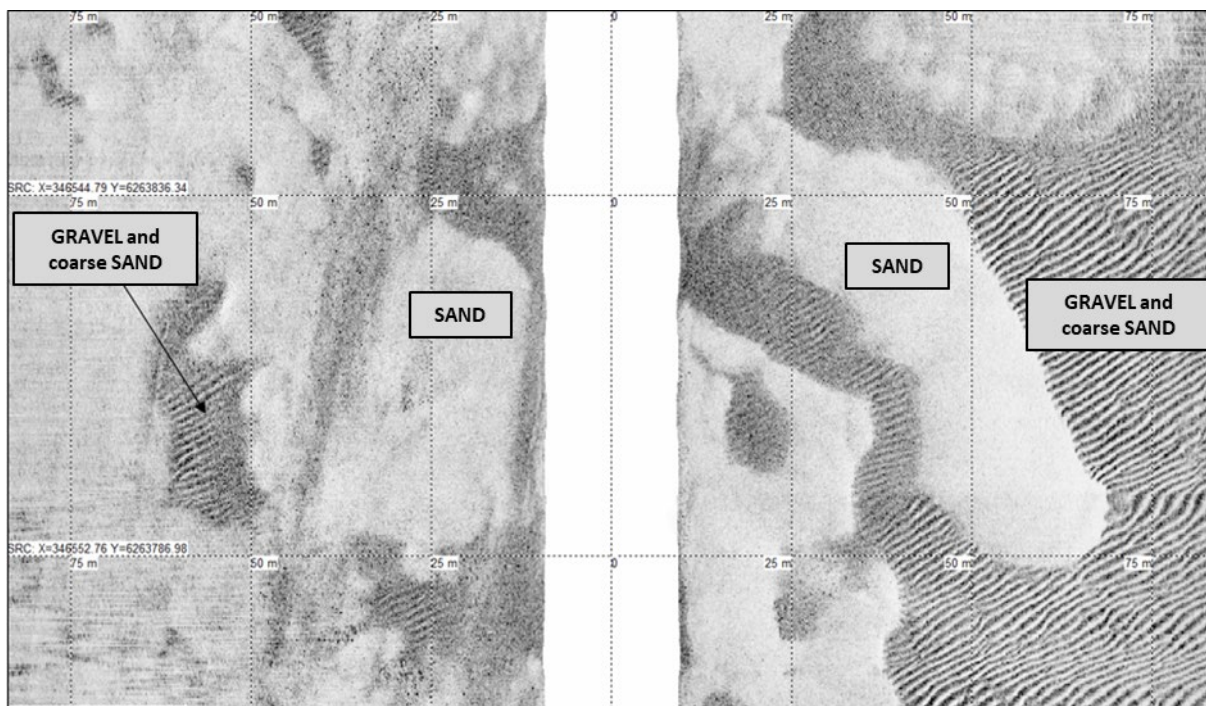


Figure 75 SSS data showing sediments of GRAVEL and coarse SAND and SAND. The data is high frequency SSS and is retrieved from within the Artificial Island survey area, reporting Tile 13. Horizontal scale lines at 50 m intervals.

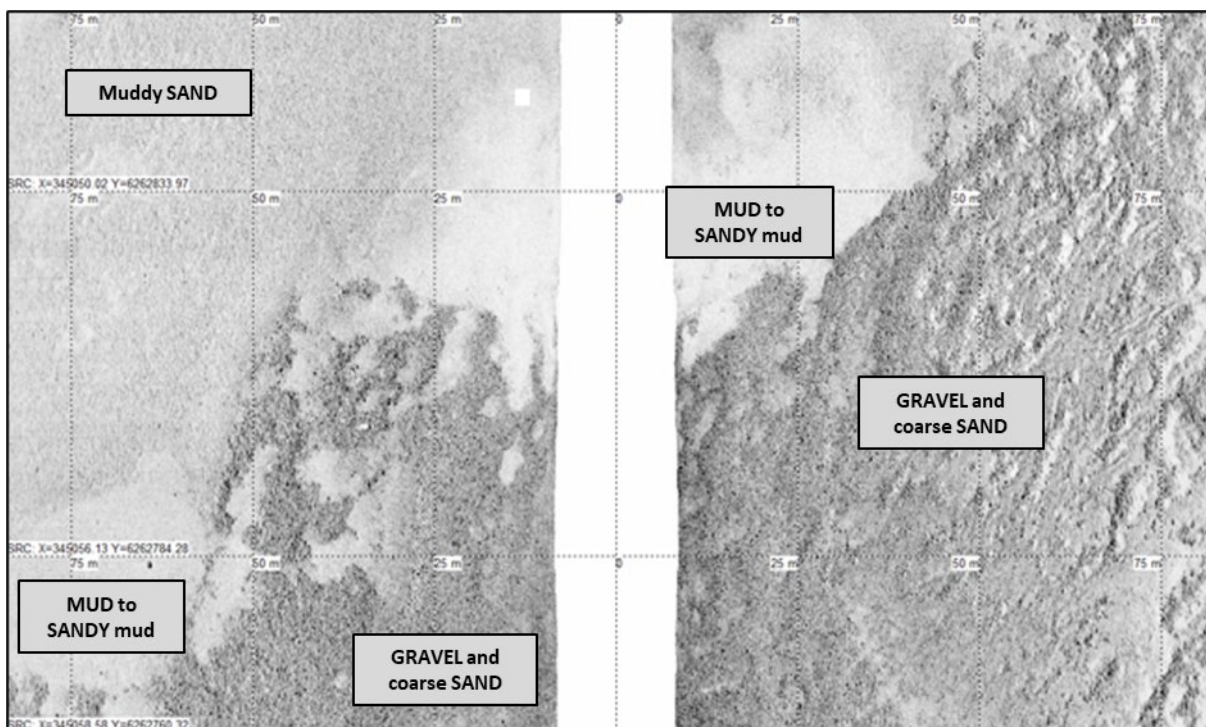


Figure 76 SSS data showing varying sediments within the Artificial Island survey area. The sediments shown are interpreted as GRAVEL and coarse SAND (medium to high acoustic return), Muddy SAND (low to medium acoustic return) and MUD and sandy MUD (low acoustic return). The data is high frequency SSS retrieved in reporting Tile 13. Horizontal scale lines at 50 m intervals.

8.3.2 | MOBILE SEDIMENTS

Areas of ripples, large ripples and megaripples, indicative of mobile sediments, are frequently present across the western part of the Artificial Island survey area, whilst larger scale sand waves and sandbars are frequently present across the central and western part of the Artificial Island survey area. Figure 77 shows an overview of mobile sediments observed in the Artificial Island area of investigation.

Area of ripples are commonly seen in the west of the Artificial Island survey area (Reporting Tiles T13, T14, T15, T19 and T20). The ripples typically exhibit wavelengths of less than 2 m, are approximately 0.1 to 0.2 m in height and appear in elongated bands of variable width. A few scattered areas of large ripples are seen in the west of the Artificial Island area of investigation (Reporting Tile T13) and typically exhibit wave lengths of 5-7 m. One area of megaripples is visible in the west of the survey area (Reporting Tile T13), with wavelength of ~30 m.

The ripples, large ripples and megaripples are all in areas of GRAVEL and coarse SAND (Figure 78) and exhibit a northeast-southwest orientation (Figure 79), with the dominating current regime (and hence direction of sediment transport) from northwest to southeast.

Some sand wave areas are observed in the central and northern part of the Artificial Island survey area (Reporting Tiles T14, T15 and T16), with wavelengths ranging between 50 m - 200 m and orientated north-south. The sand waves typically comprise of SAND or GRAVEL and coarse SAND (Figure 80).

Some larger scale mobile sediment bedforms are observed in the west of the Artificial Island survey area (Reporting Tiles T13, T14, T19 and T20), upon which the smaller scale, more mobile and more recent bedforms, mentioned above are often superimposed. These areas of sediment migration form sandbars, sand ridges and sand dunes; they have all been defined under the same seabed feature category of sandbars but have various wavelengths (>200 m) and various orientations.

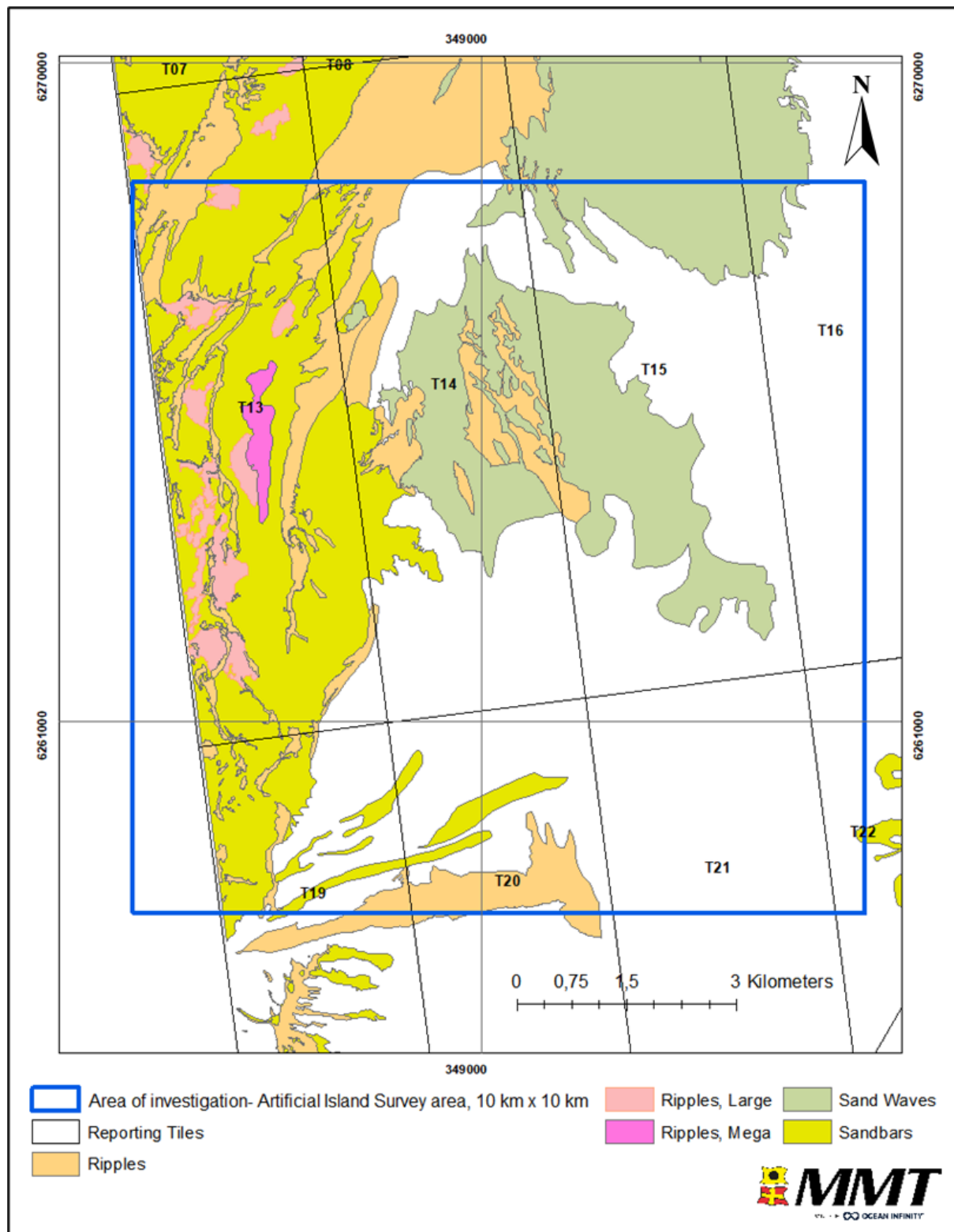


Figure 77 Distribution of mobile bedforms in the Artificial Island survey area.
 The image shows the distribution of Ripples, Large Ripples, Megaripples, Sand Waves and Sandbars

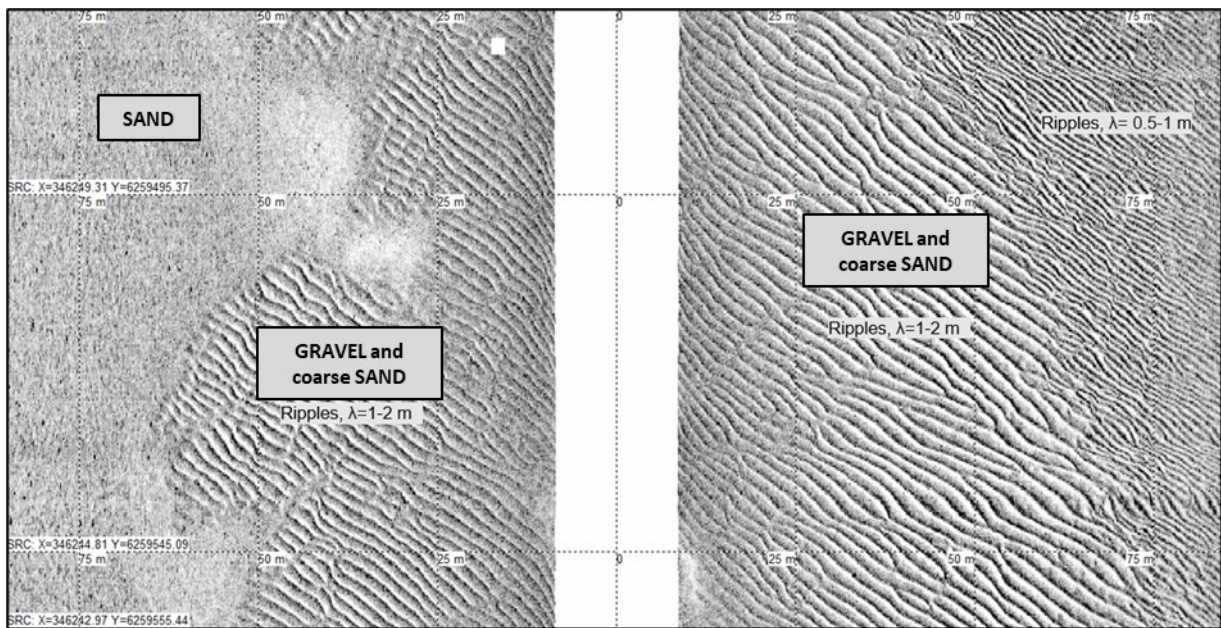


Figure 78 High frequency SSS example of ripples 0.5 -2 m wavelength. The ripples are located in sediment of GRAVEL and coarse SAND (medium to high acoustic return), in reporting Tile 19 within the Artificial Island survey area. Horizontal scale lines at 50 m intervals.

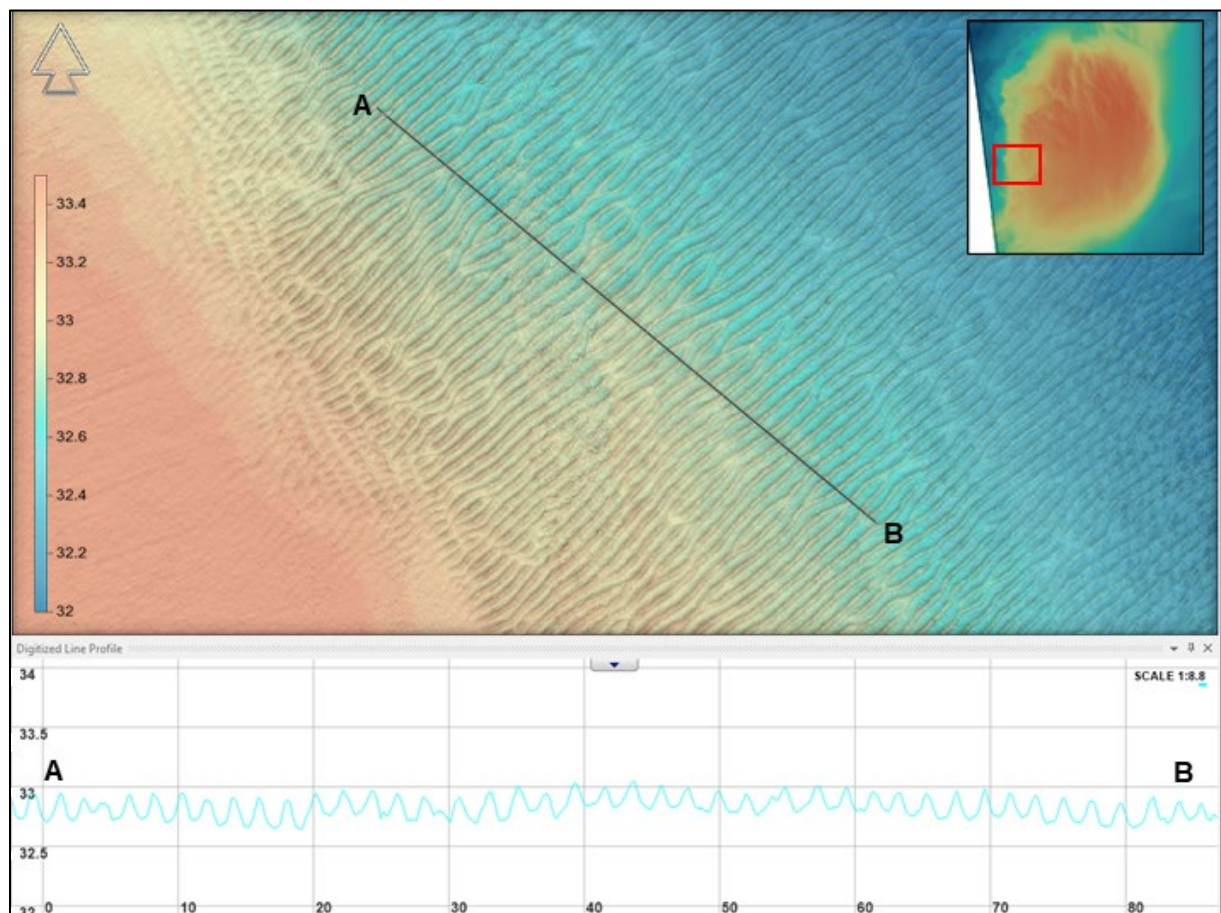


Figure 79 MBES DTM image in T13, within the Artificial Island survey area, showing ripples.

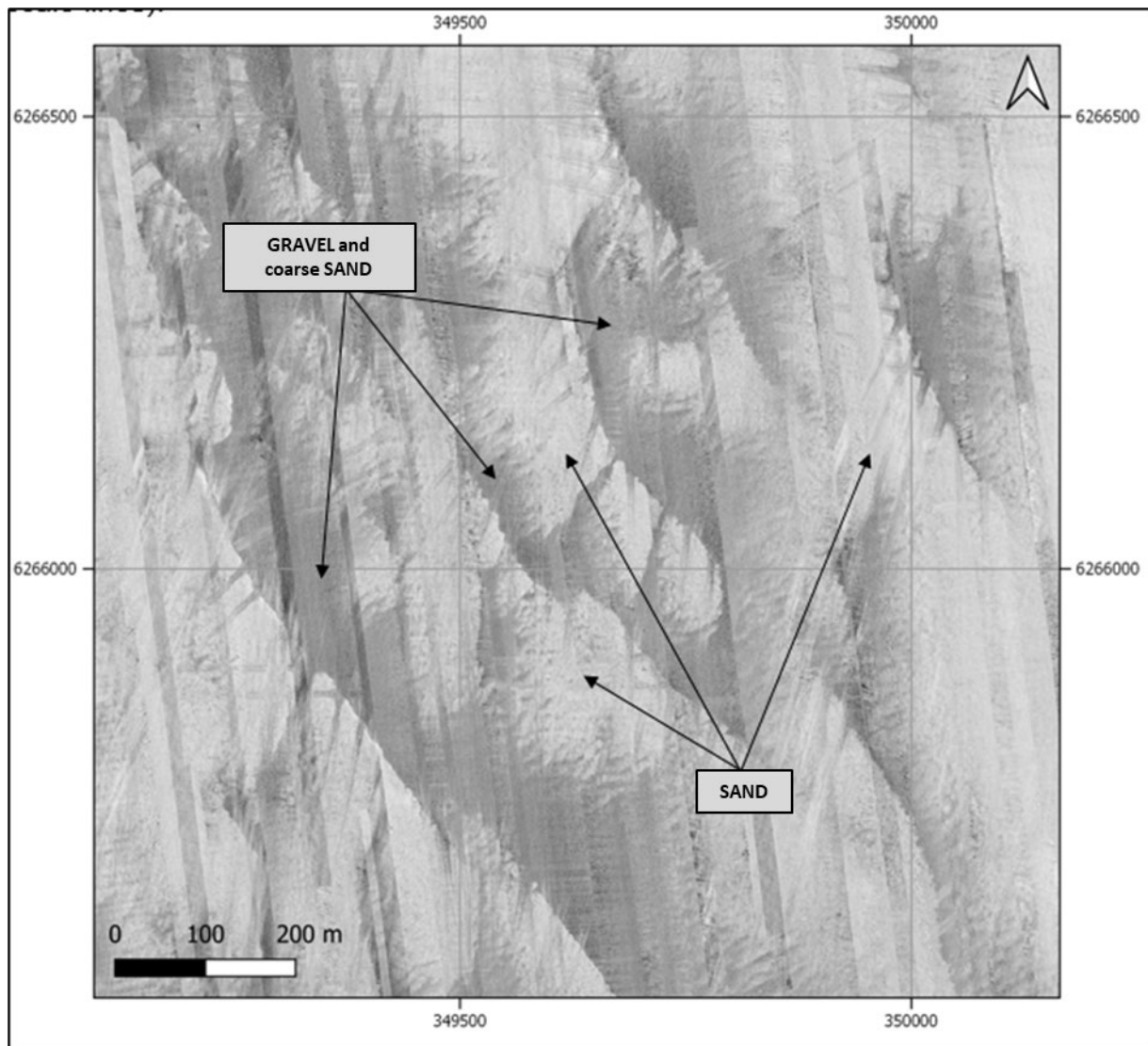


Figure 80 High frequency SSS mosaic showing sand waves.
The sand waves are 100-200 m wavelength and are located in reporting Tile 14 within the Artificial Island survey area, in sediments consisting of SAND alternating with GRAVEL and coarse SAND.

8.3.3 | BOULDERS

Within the Artificial Island survey area, 221 individual boulders >1.0m have been identified. No boulder fields were observed within the Artificial Island survey area, but boulders are of a higher concentration to the west of the Artificial Island area of investigation (Reporting Tiles T13 and T19).

Figure 81 shows an overview of the boulders observed in the Artificial Island survey area.

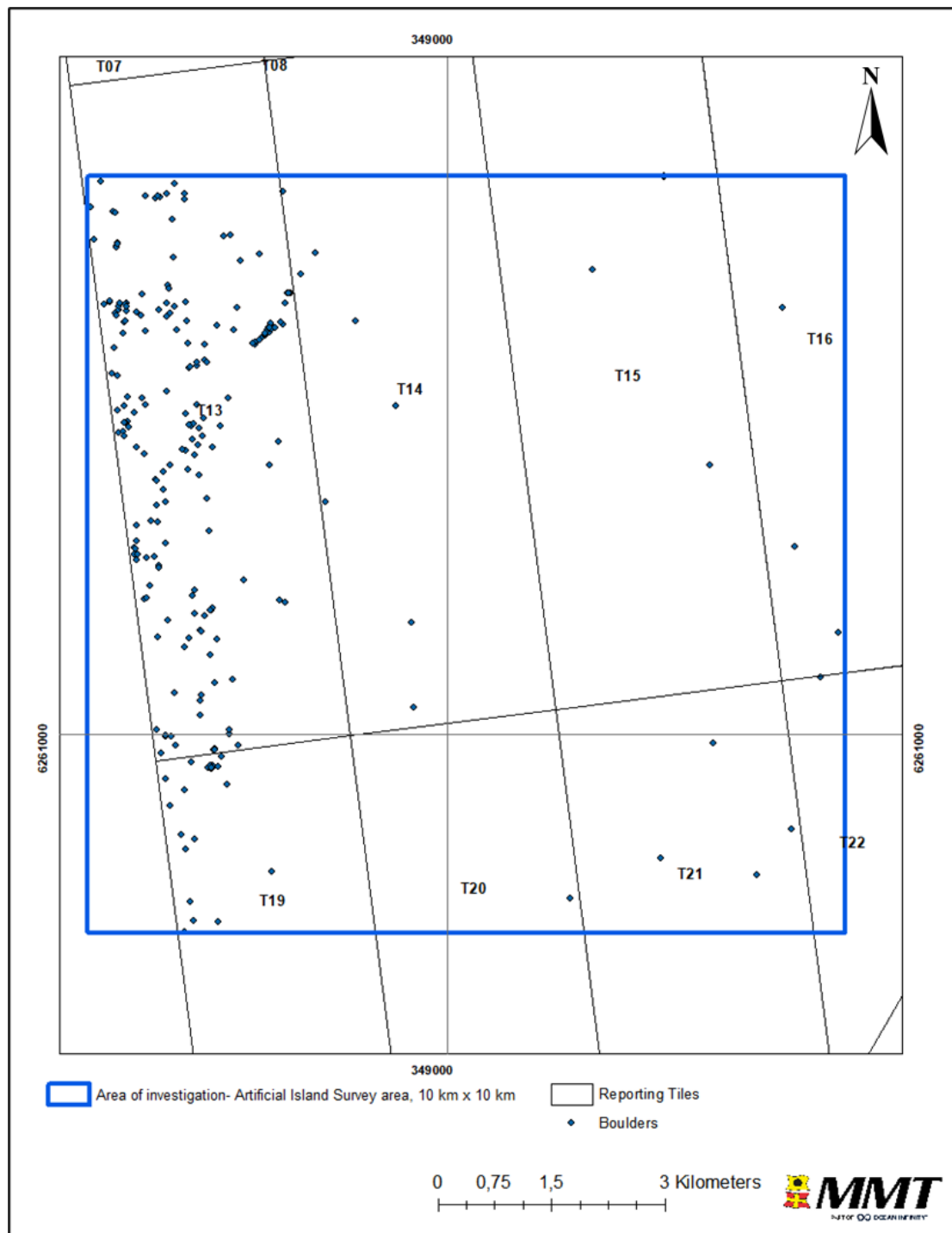


Figure 81 Distribution of individual boulders in the Artificial Island survey area.
 No boulder fields are present in the area.

8.3.4 | TRAWL MARKS

Evidence of trawling is found across the majority of the Artificial Island survey area (Reporting Tiles T13, T14, T15, T16, T19, T20, T21 and T22), see Figure 82 and Figure 83. Evidence of both older and more recent activity can be observed through areas of fainter scars overlaid by more prominent scars displaying greater seabed interference and suggesting a highly active area. The observed trawl scars show no predominant orientation and mostly consist of two parallel scars, each ~10-15 m wide, spaced approximately 30 m apart.

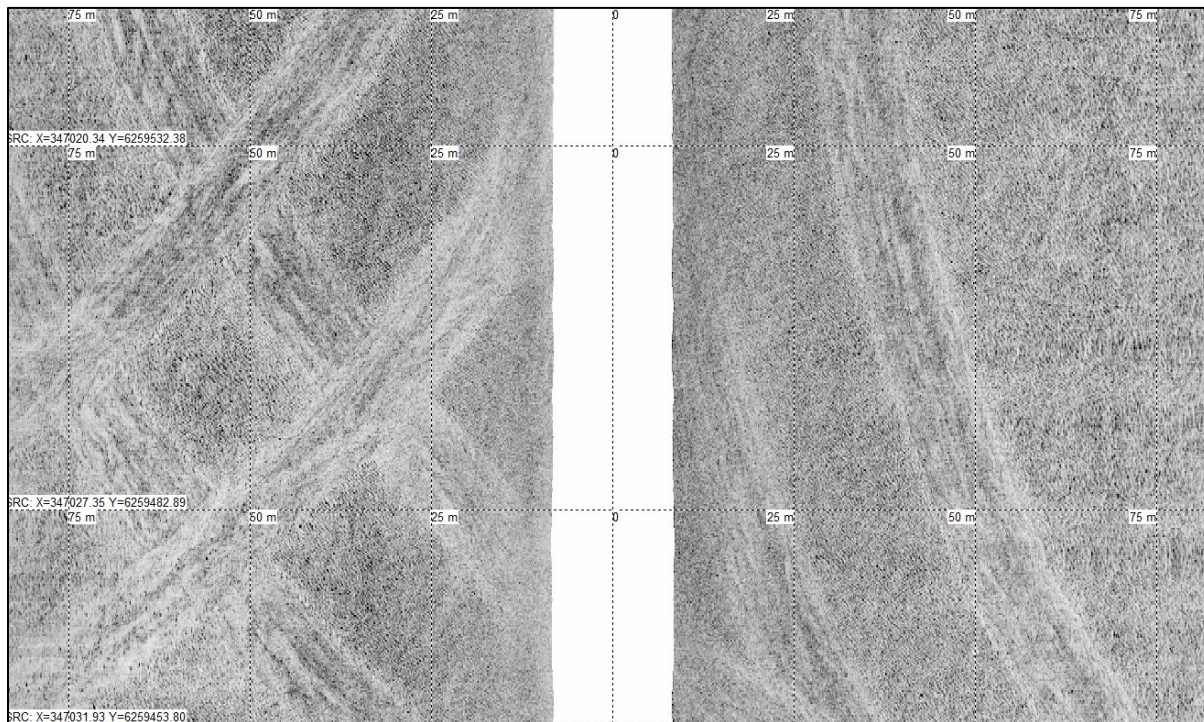


Figure 82 High frequency SSS data showing trawl marks in GRAVEL and coarse SAND. The area is located in reporting Tile19 within the Artificial Island survey area. Horizontal scale lines at 50 m intervals.

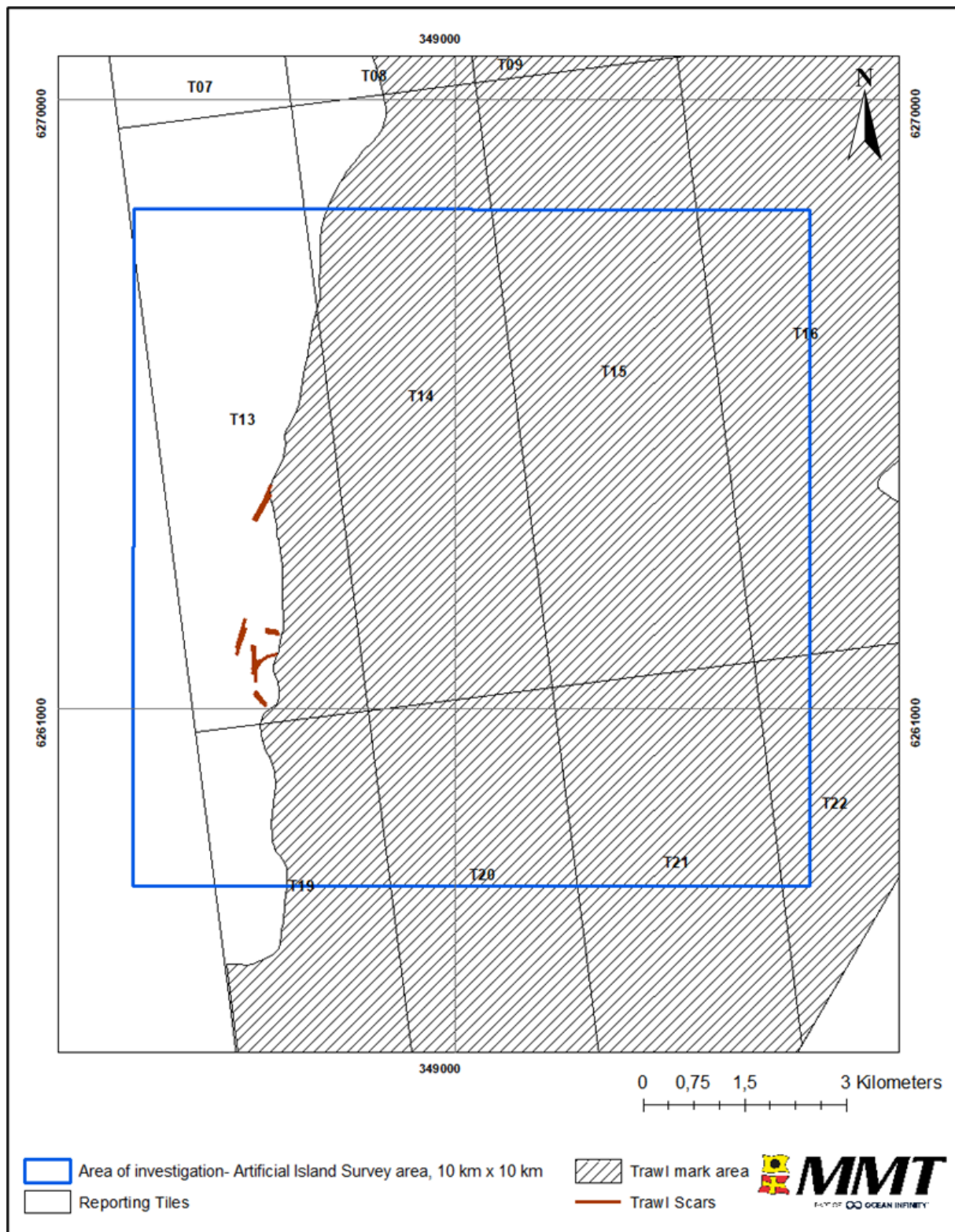
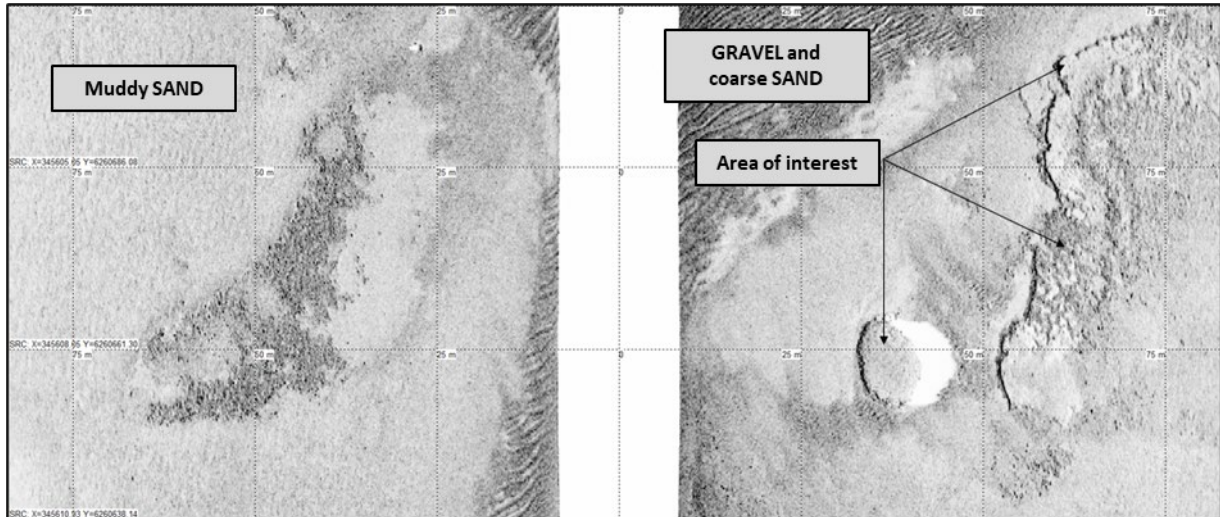


Figure 83 Distribution of trawl marks in the Artificial Island survey area.

8.3.5 | OTHER - AREAS OF INTEREST

Some occasional areas have been defined as features of interest on the western edge and the southeast corner of the Artificial Island survey area (Reporting Tiles T13, T19, T21, T22), see Figure 84. These areas comprise of mounds that were assessed to determine whether they could be biogenic in origin. Assessment by a senior biologist determined they are unlikely to be of a biogenic nature. They have been retained as a feature for future consideration.



*Figure 84 SSS data example of an area of interest
The area is located in reporting Tile19 within the Artificial Island survey area. Horizontal scale lines at 25 m intervals.*

8.4 | CONTACTS AND ANOMALIES

In total, 408 individual seabed contacts and magnetic anomalies were detected in the Artificial Island survey area. These were detected with SSS, MBES and/or MAG. All seabed objects are detected with either SSS or MBES. Boulders were primarily interpreted in the MBES data. Subsequently, remaining boulders and all other contacts were interpreted in the SSS data. All duplicates have been removed. Positional accuracy between contacts visible in the MBES and SSS data is good, less than 2 m.

A total of 280 contacts - 181 MBES and 99 SSS contacts - were detected within the Artificial Island area of investigation. They were classified as: boulders >1.0m (221), debris (51), other (6), wire (1) and fishing equipment (1). All MBES contacts have been classified as boulders.

No boulder fields were observed within the Artificial Island survey area, but boulders are of a higher concentration to the west of the area (Reporting Tiles T13 and T19).

No wrecks were observed within the Artificial Island area of investigation.

SSS and MBES contacts are summarised in Table 23.

A total of 128 magnetic anomalies were detected within the Artificial Island survey area. 70 of these were individual discrete anomalies, whilst 58 anomalies were interpreted to form 8 linear anomalies. One of these linear anomalies corresponded to the database position of the buried TAT-14 cable and was associated with 27 discrete anomalies (see Section 8.5j).

If a SSS or MBES contact were located within 5 m of a MAG anomaly, correlation information was added in the contact listings – only 1 SSS anomaly correlated with a MAG anomaly.

Magnetic anomalies are summarised in Table 24.

Full details of all contacts and anomalies are presented in Appendix Bj.

Table 23 Summary of SSS and MBES contacts.

CLASSIFICATION	NUMBER OF CONTACTS
Boulder	221
Wire	1
Debris	51
Fishing equipment	1
Other	6
Total	280

Table 24 Summary of magnetic anomalies.

CLASSIFICATION	NUMBER OF ANOMALIES
Discrete	58
Discrete forming linear	70 (8 magnetic linear features)
Total	128

Sub-seabed contacts were identified in the SBP data, with contacts selected when diffraction hyperbolas were visible, summarised in Table 25.

Table 25 Summary of SBP Contacts.

CLASSIFICATION	NUMBER OF CONTACTS
SBP Point Contacts (hyperbola)	2
Total	2

8.5 | EXISTING INFRASTRUCTURE (CABLES AND PIPELINES)

A cable presented in the background data (TAT-14) and confirmed with linear Mag in the south-west of the Artificial Island survey area in Reporting Tile T19, trending northwest to southeast. The cable is mostly buried but one possible exposure is found in the very far west of the Artificial Island survey area where it might be exposed for 39.2 m, see Figure 85. Figure 86 shows the client supplied cable crossing the south west corner of the Artificial Island area of investigation. This exposure is between 345275.33 N, 6259616.20 E, and 345310.08 N, 6259594.56 E. This exposure is approximately 57 m outside of the OWF East area.

A total of 27 discrete Magnetic anomalies correlates with the client-supplied database position of the cable.

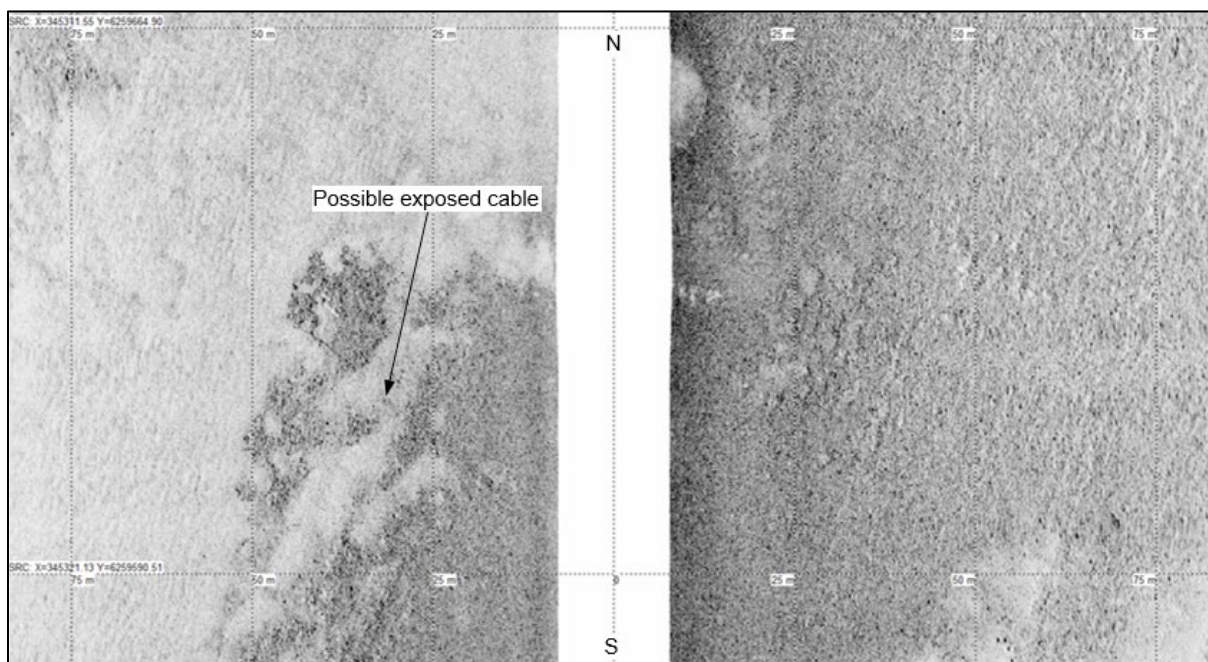


Figure 85 SSS data showing possible exposed TAT-14 cable.
 The cable is located in reporting Tile 19 within the Artificial Island survey area. Horizontal scale lines at 75m intervals.

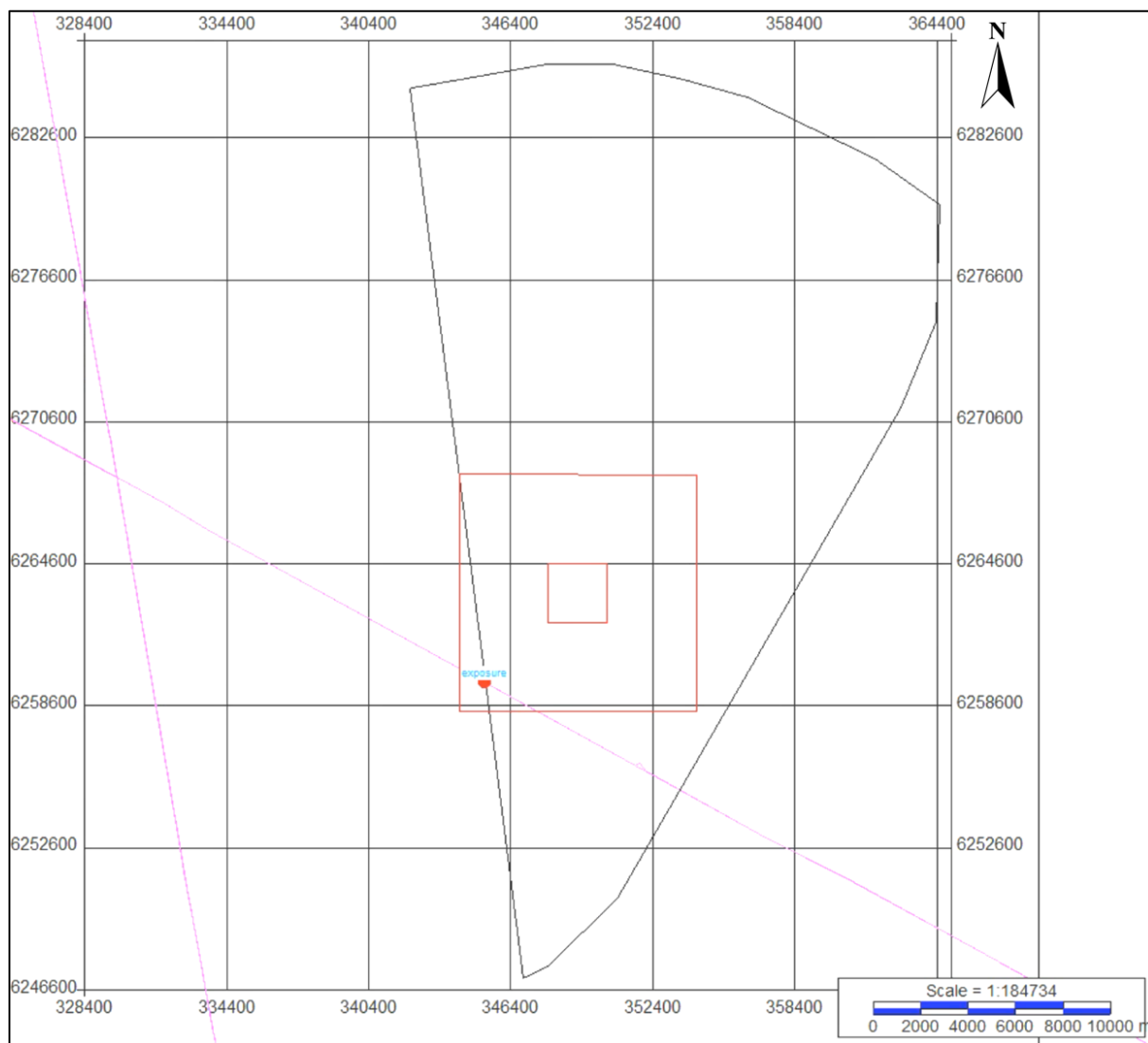


Figure 86 Map overview of possible cable exposure

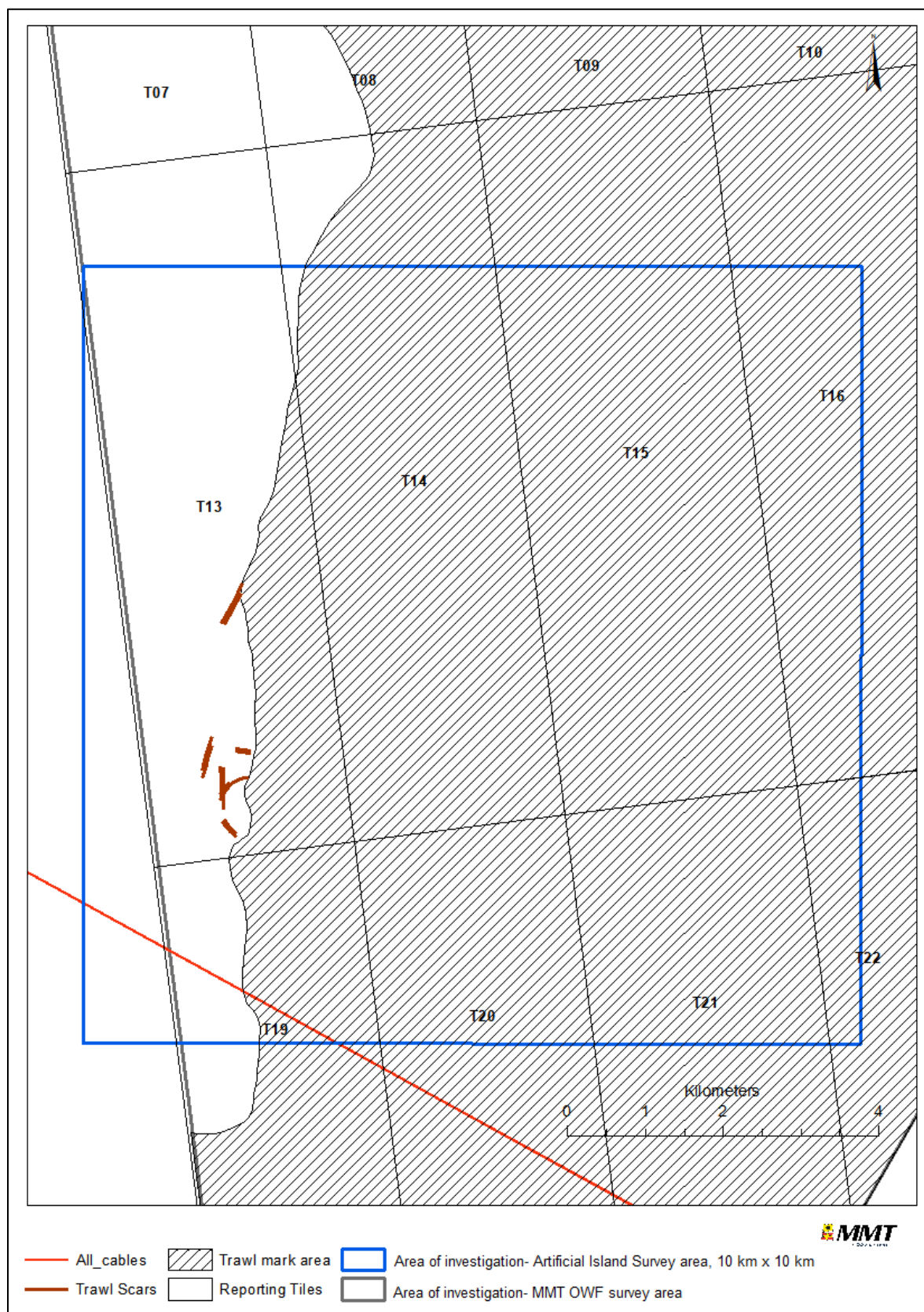


Figure 87 Existing cable (from client) crossing the Artificial Island survey area.

8.6 | SEISMOSTRATIGRAPHIC INTERPRETATION

The subsurface geological interpretation and description is based on the assessment of the 2D UHRS data acquired within the full MMT OWF survey area. This report summarises the findings and interpretations within the Artificial Island survey area.

The original contract regarding the geomodel for this project was based on mapping eight horizons, however twelve horizons were mapped in order to capture the subsurface complexity of the geological framework in this site.

8.6.1 | SUB-SEABED GEOLOGY - GEOMODEL

The Geological Ground Model was defined from the integration of geophysical survey and grab sample results acquired within the MMT OWF survey area. Geotechnical information, provided by Energinet in the form of borehole data, was scarce. The data comprise six vibrocores from the Jupiter Well Database (GEUS), limited to the upper 5.8 m of sediments below the seabed and away from any 2D UHRS line. Given the paucity of geotechnical sampling across the site, extrapolations of sediment type and characteristics away from the coring locations was reliant on seismic facies analysis. A thorough revision of the available scientific literature was carried out to steer the seismic interpretation and ensure the formulation of a Geological Ground Model that is consistent with the known geologic evolution of the region.

Seismostratigraphic interpretation of the 2D UHRS data and the single-channel SBP data was the basis for the geological ground model presented here. The interpretation approach employed included aspects of sequence stratigraphy, kinetostratigraphy, lithostratigraphy, and seismic facies analysis.

The geological ground model comprises 12 horizons that correspond to seismic reflectors and/or boundaries deemed significant to build the main sub-surface geological framework, distinct depositional and erosion events, marking relevant environmental changes, and shifts in sediment types. The criteria for horizon selection were structure significance in the site's stratigraphic framework, spatial reflector continuity, and delimitation of seismic facies interfaces. The mapped horizons represent the bounding surfaces of the 12 seismic units described here. An additional seismic unit, referred to as the Base Unit, is also included in the model, the details of which are discussed later in this section. The lateral assemblage and vertical stacking of these units represent the structural aspect of the geological ground model. The associations and relationships amongst the structural elements represent the geologic evolution of the depositional environments at the site. Alongside the model, a careful and detailed analysis of direct seismic indicators (e.g., diffractions, amplitude anomalies, acoustic blanking, etc.) was carried out as part of the assessment of potential geohazards within the sub-surface.

An analytical interpretation of the Geological Ground Model is provided in the Discussion section. However, a short introduction to the site's seismostratigraphic character is provided here to assist the descriptions of the individual seismic units comprising the model.

Due to the complex geological architecture of the area and to facilitate the description of the model, the main site was divided in three sectors, believed to represent distinct domains of sediment deposition and deformation: North sector; Central sector; and South sector (Figure 88). The spatial distribution of the interpreted seismic units across these sectors is discontinuous, and not all units occur within each sector.

The Artificial Island survey area is located in the western limit of the main site, partially encompassing the sectors Central and South (Figure 88 and Figure 89). The seismic units occurring within the Artificial Island survey area are shown in Table 26. Seismic unit U50 is present only in the North sector; as such, it is not featured in this report.

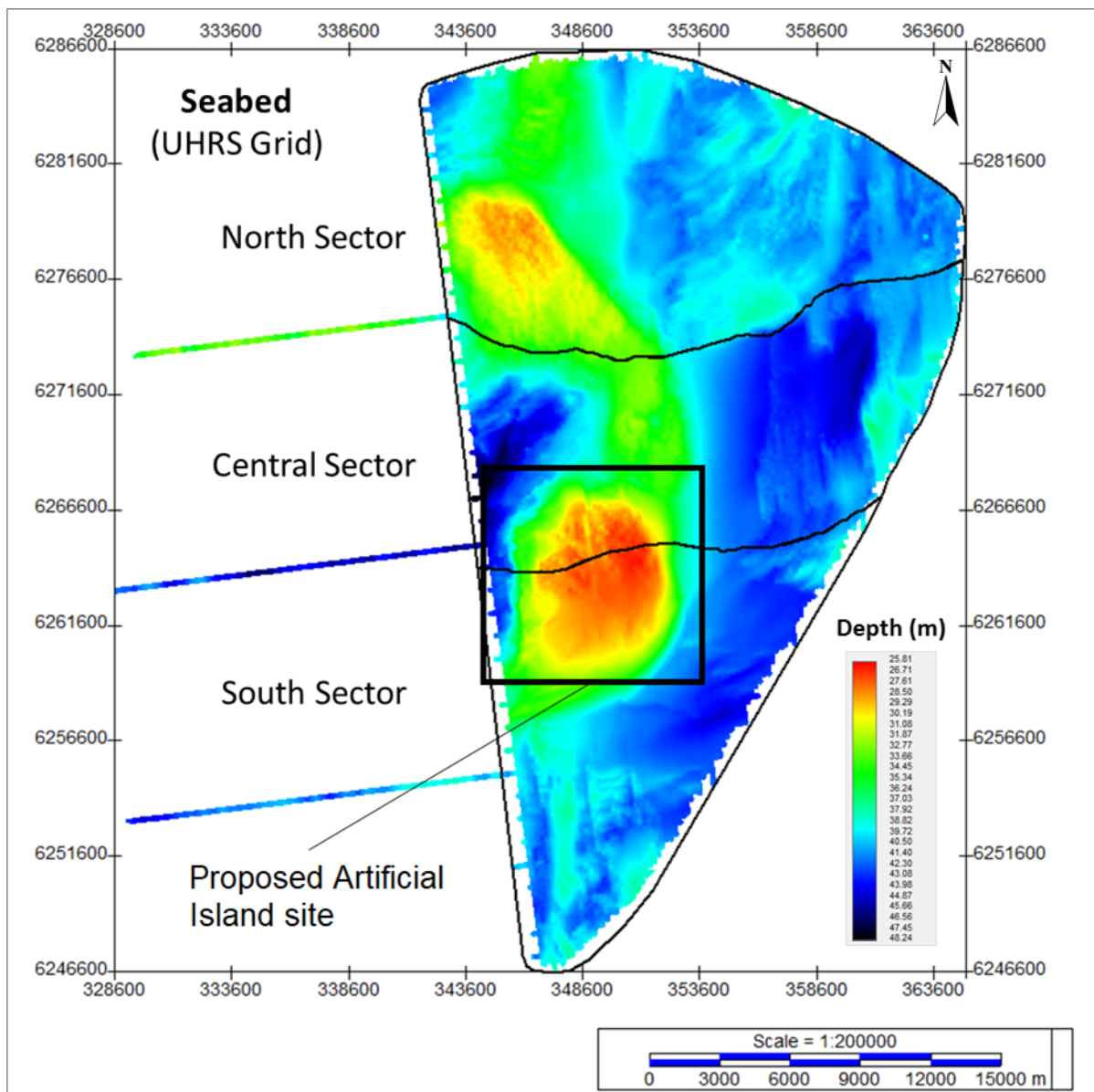


Figure 38 Seabed of the MMT OWF survey area.
 The image also shows the location of the Artificial Island survey area – UHRS grid. Units in metres MSL.

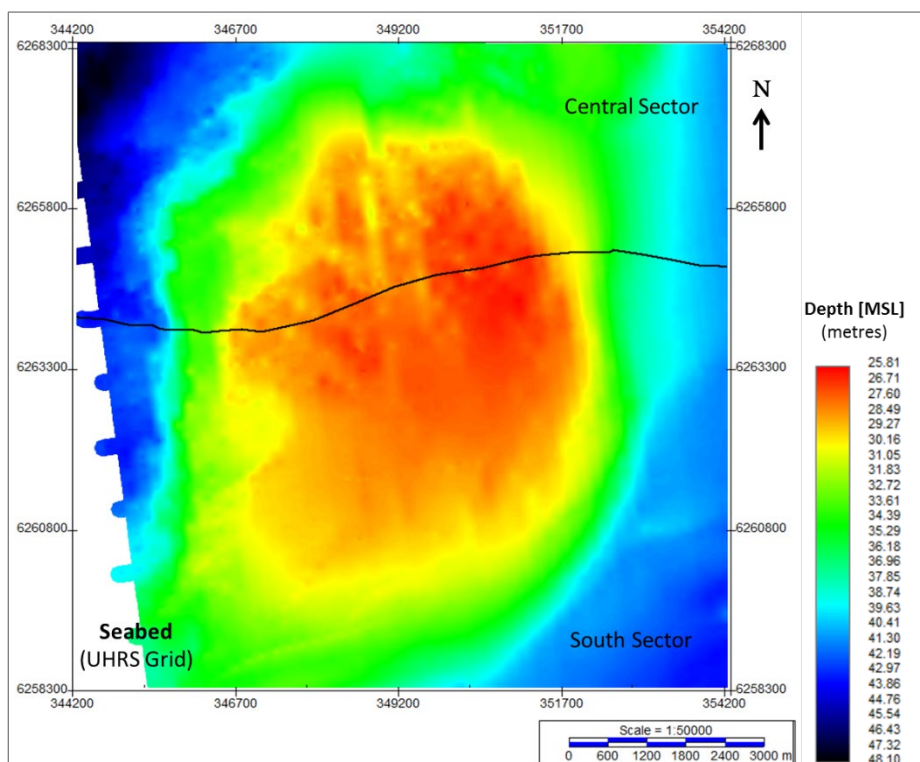


Figure 89 Seabed of the Artificial Island survey area UHRs grid. Units in metres MSL.

Table 26 Distribution of interpreted seismic units present in the Artificial Island survey area (2DUHRs), and their distribution according to the Central and South sectors.

	Sectors		
	Sector_N	Sector_Central	Sector_S
H05	U05		
H10i	H10 internal		
H10	U10		
H20	U20		
H25	U25		
H30	U30		
H35	U35		
H40	U40		
H50	U50		
H60	U60		U60
H70	U70		
KSA	KSA		
H85			U85
H90	U90		U90
KSB			KSB
	BSU		

Figure 90 below shows a north-south profile with seismostratigraphic interpretation, displaying the mapped horizons and the interpreted seismic units. The horizons that bound the seismic units represent seismostratigraphic boundaries and mark the base of the deposits they define. As such, these boundaries have chronostratigraphic and kinetostratigraphic meaning, and should not be interpreted in

lithostratigraphic terms. The bases and units are numbered sequentially based on their stratigraphic position, and have an alphanumeric naming convention (e.g., H10 corresponds to the base of seismic unit U10 (Figure 90). The deepest and oldest seismic unit is referred to Base Seismic Unit (BSU). The top of the Base Seismic Unit is defined by a composite surface produced from the amalgamation of the deepest mapped horizons. The bottom of the Base Seismic Unit corresponds to the processing “last knee” that is an artificial, linear boundary near the terminus of the seismic record. The labelling scheme in Figure 90 was applied to all seismic examples in this report.

The fundamental stratigraphic controls on the site’s geology, as inferred from the seismic data, are eustasy, isostasy, autogenic processes, and glaciogenic deposition and deformation. The deeper deposits exhibit a strong glacial signal, and the upper deposits carry a eustatic-isostatic and autogenic signal. The separation of the two structural regimes is approximated by H70 and H35. Most of the seismic units beneath this boundary are characterized by glaciogenic deposition and deformation.

The deepest seismic units BSU, U90, and U85 have origins ascribed to non-glacial processes. However, their physical contact with the grounded shelf ice has rendered them tectonized and possibly otherwise modified by glacial processes. These strongly-deformed strata were individualised from the better-preserved sequences with horizon KS. Horizon KS represents a deformation front boundary and, although part of the geological model, should not be interpreted with a chronostratigraphic meaning. Horizon KS defines the base of Unit UKS, which encompasses sediments belonging to seismic units BSU, U90, and U85 that were deformed to a degree in which their physical properties may be significantly different than their stratigraphically-equivalent strata.

The upper assemblage of seismic units, those occurring above UKS and H70, demonstrate characteristics of high frequency sedimentary sequences. These deposits are interpreted to represent cycles of deposition and erosion associated with sea-level fluctuations (transgressions and regressions). Superimposed on the eustatic-isostatic signal is the complex sedimentological arrangement produced by autogenic processes, including channel migration and avulsion, shallow basin, and coastal sediment dynamics.

Both systems of eustasy-isostasy and glacial dynamics taken in isolation are complex. The combination of the two, in conjunction with a strong overprinting of autogenic signal, has produced a highly fragmented and heterogeneous geologic structure. Furthermore, despite not being directly imaged in the UHRS record, some deeper structures indicate the occurrence of salt tectonics, which may have partially influenced the overall distribution of all the sedimentary sequences observed. Thus, the preservation of the geological sequences is limited due to the complex geological evolution of the area; variable sedimentary cycles; distinct erosional events; various stages of glaciers emplacement, erosion, and deformation. Attribution of seismic units to time specific regions of the quaternary sea-level curve was not possible with the available data.

In summary, despite the complex nature of the of site’s stratal architecture, a reasonable approximation of the prevailing geologic conditions was captured in the 12 seismic units that were mapped. These units represent the structural elements of the Geological Ground Model and relate to two general different processes. The upper process is represented by the high frequency shelf sequences, and the lower represents the deposits directly impacted by shelf glaciation. The principal characteristics of the model’s individual seismic units are detailed below.

All figures and seismic interpretation work that are included in this report are part of the Kingdom Suite project associated to this report. All seismic profiles are FULL-processed, migrated and in depth (metres). Numbers on the horizontal and vertical axis refer to distance in metres. The colourbar for the seismic display is identical for all profiles (‘Black to White 200’ in Kingdom Suite). The colourbar used to show the lateral extension for each basemap is the 3D Effects: warm colours (red) indicate shallower depths, and cool colours (blue) indicate greater depths (unless stated otherwise). For every seismic unit, three basemaps are presented: (1) spatial extent of the mapped horizon, (2) grid of the depth below seabed of the base of the unit, (3) grid of the thickness of the unit. Vertical exaggeration on seismic section figures is variable: horizontal and vertical scales were adjusted to best illustrate the features of interest.

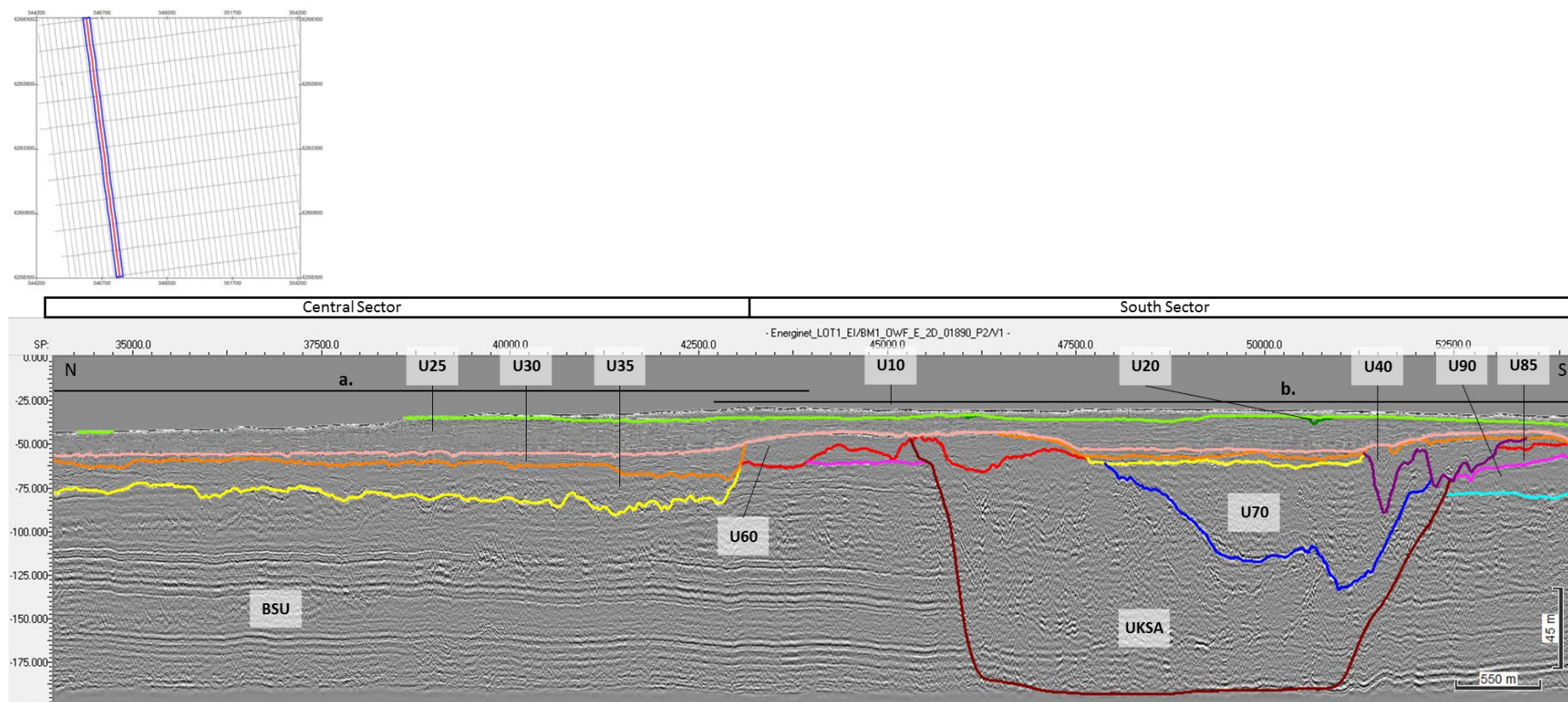


Figure 90 General sub-surface architecture of survey.
 Interpreted seismic units and nomenclature used for the geological Ground Model, and site sub-division into sectors Central and South. Subsequent Figure 91 and Figure 92 show in more detail the different sectors. Seismic Profile BM4_01890_P2

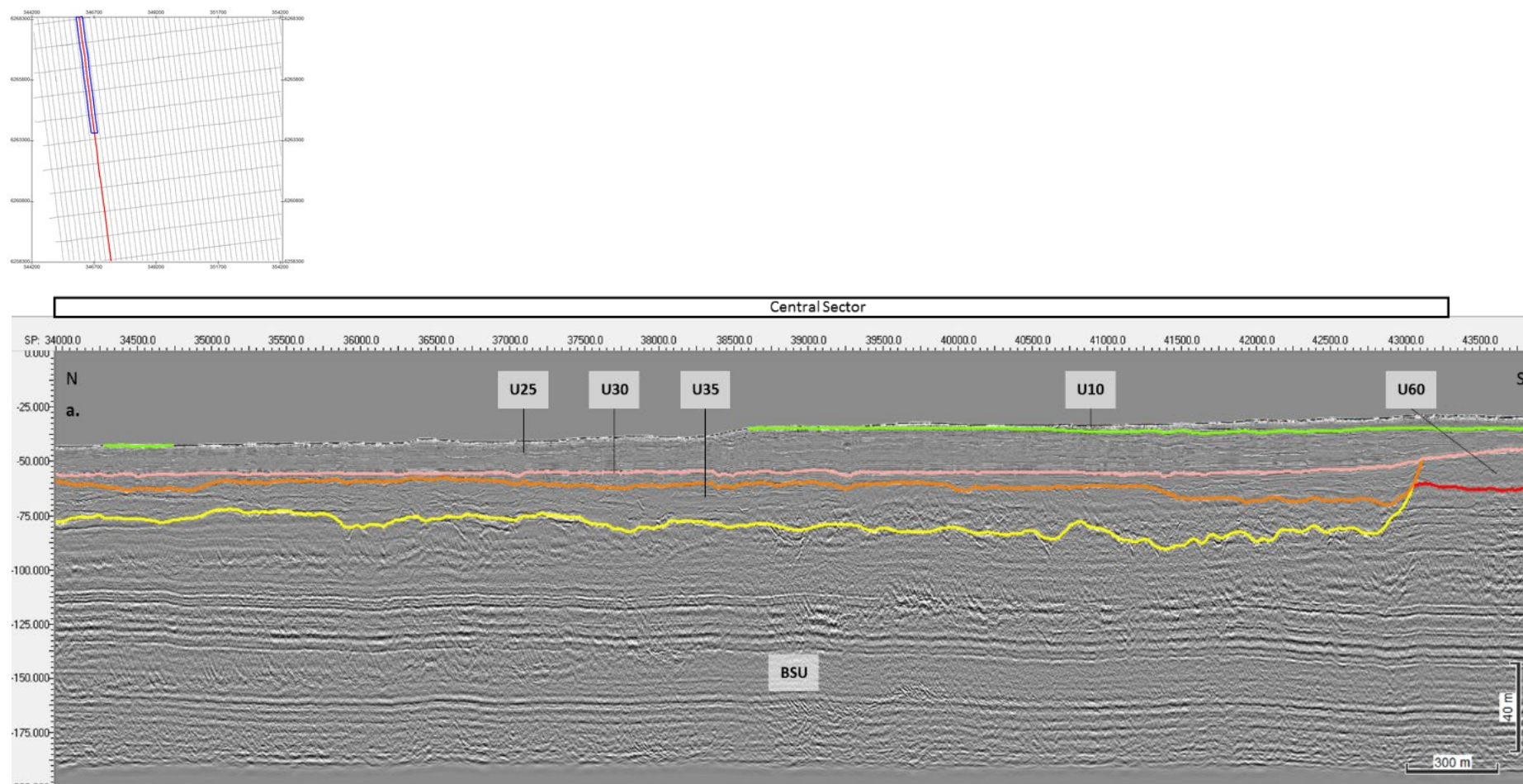


Figure 91 General sub-surface architecture of the Central sector.
 The image shows interpreted seismic units and nomenclature used.
 Seismic Profile BM4_01890_P2

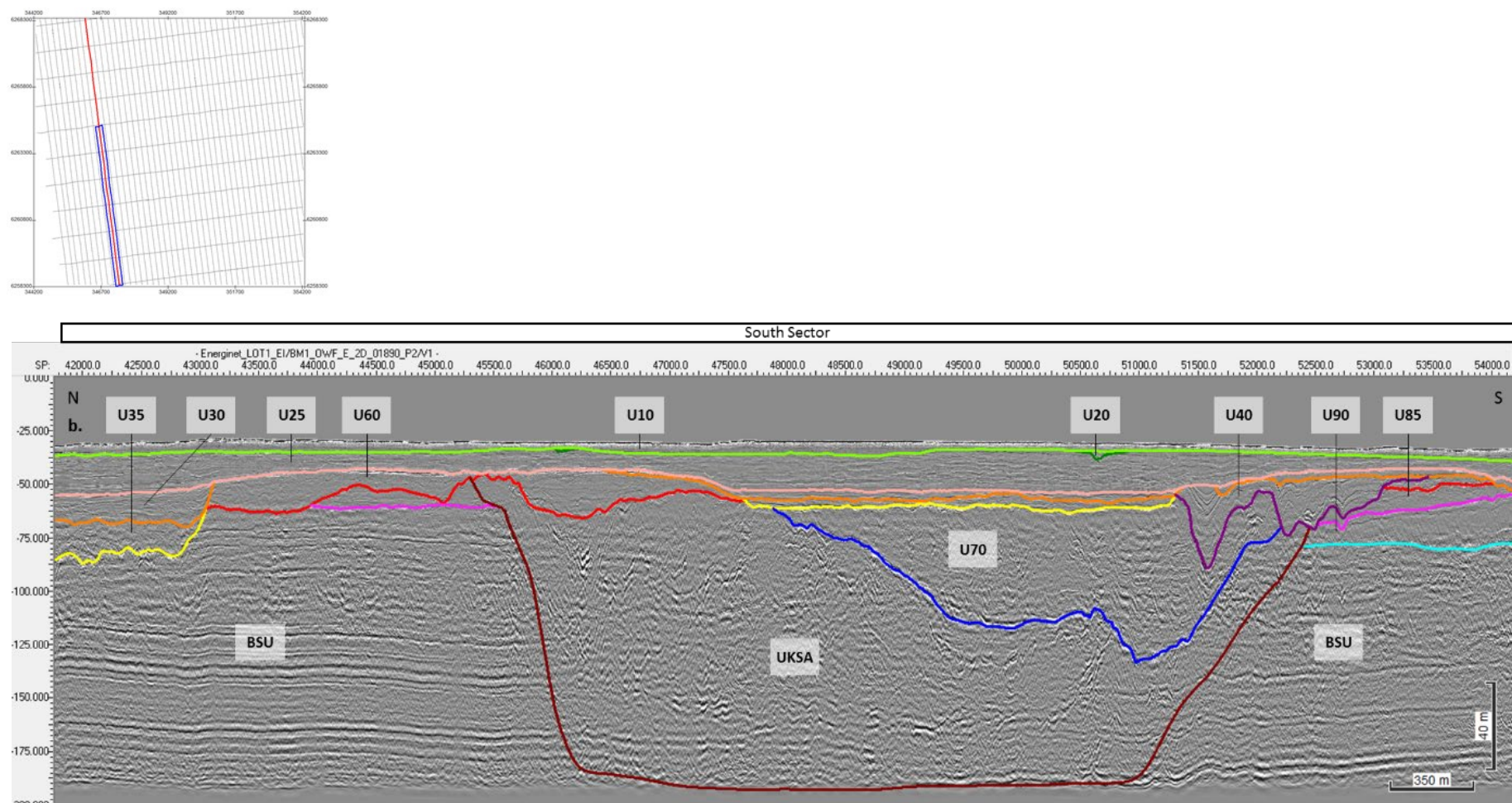


Figure 92 General sub-surface architecture of the South sector.
 The image shows interpreted seismic units and nomenclature used.
 Seismic Profile BM4_01890_P2

8.6.2 | SEISMIC UNIT U05

Seismic unit U05 is mostly presented in the northern half of the entire survey area, where unit U10 is relatively thick. The base of unit U05 is defined by horizon H05. Seismic unit U05 comprises of recent marine sediments. The spatial distribution, vertically referenced to MSL and thickness, are presented in Figure 93 and Figure 94.

Horizon H05 ranges in depths between 26.4 m and 37.9 m below MSL (Figure 93) and between 0 m and 2.7 m depth below seabed (Figure 94). It follows a flat, low to medium amplitude reflector. Unit U05 only exists on top of U10, especially where thicker, such as mounded structures and sand waves, and is likely made up of silty-sands. U05 is interpreted to be of Holocene in age.

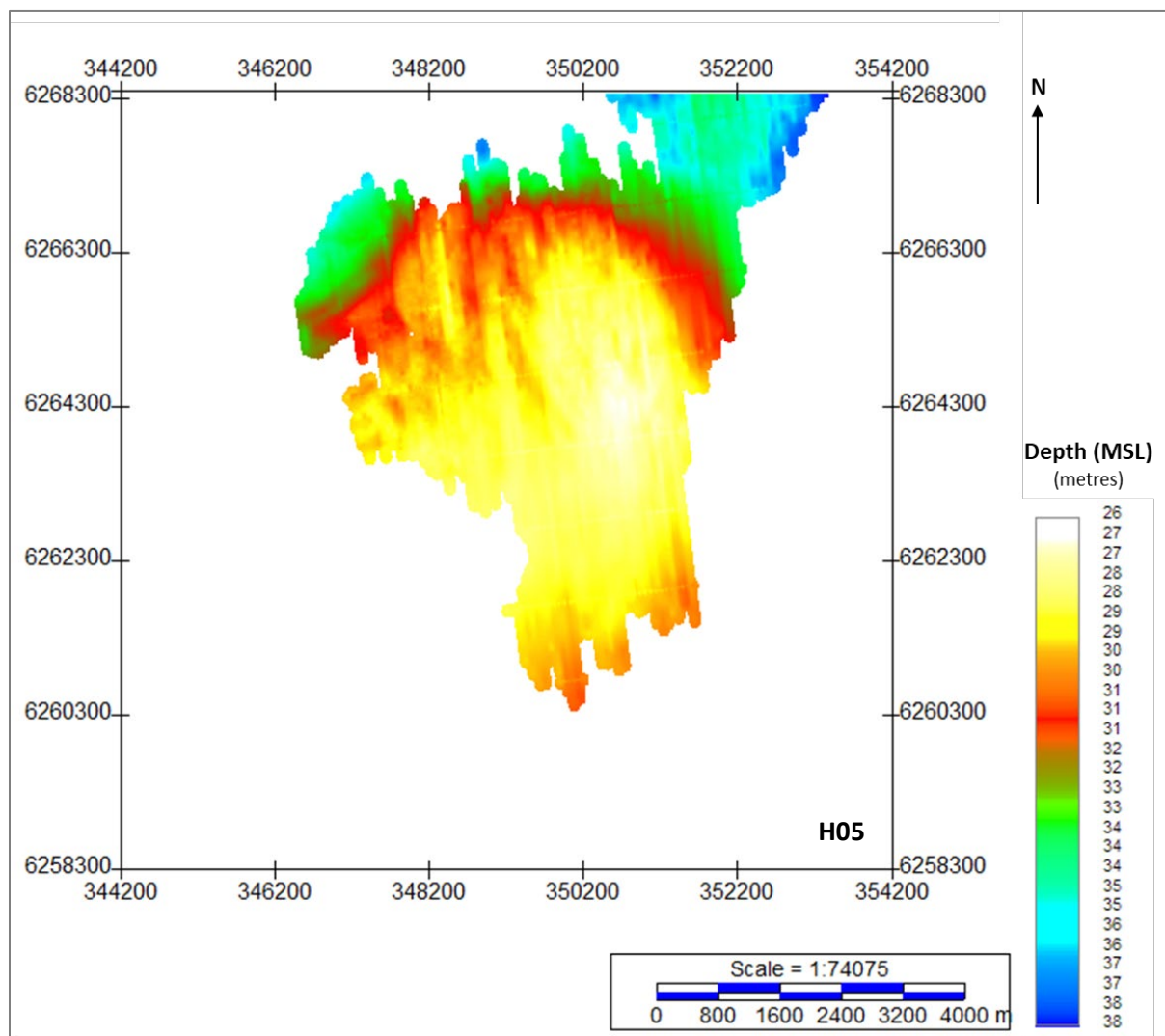


Figure 93 Map showing the lateral extent of U05.
 Units in metres below MSL.

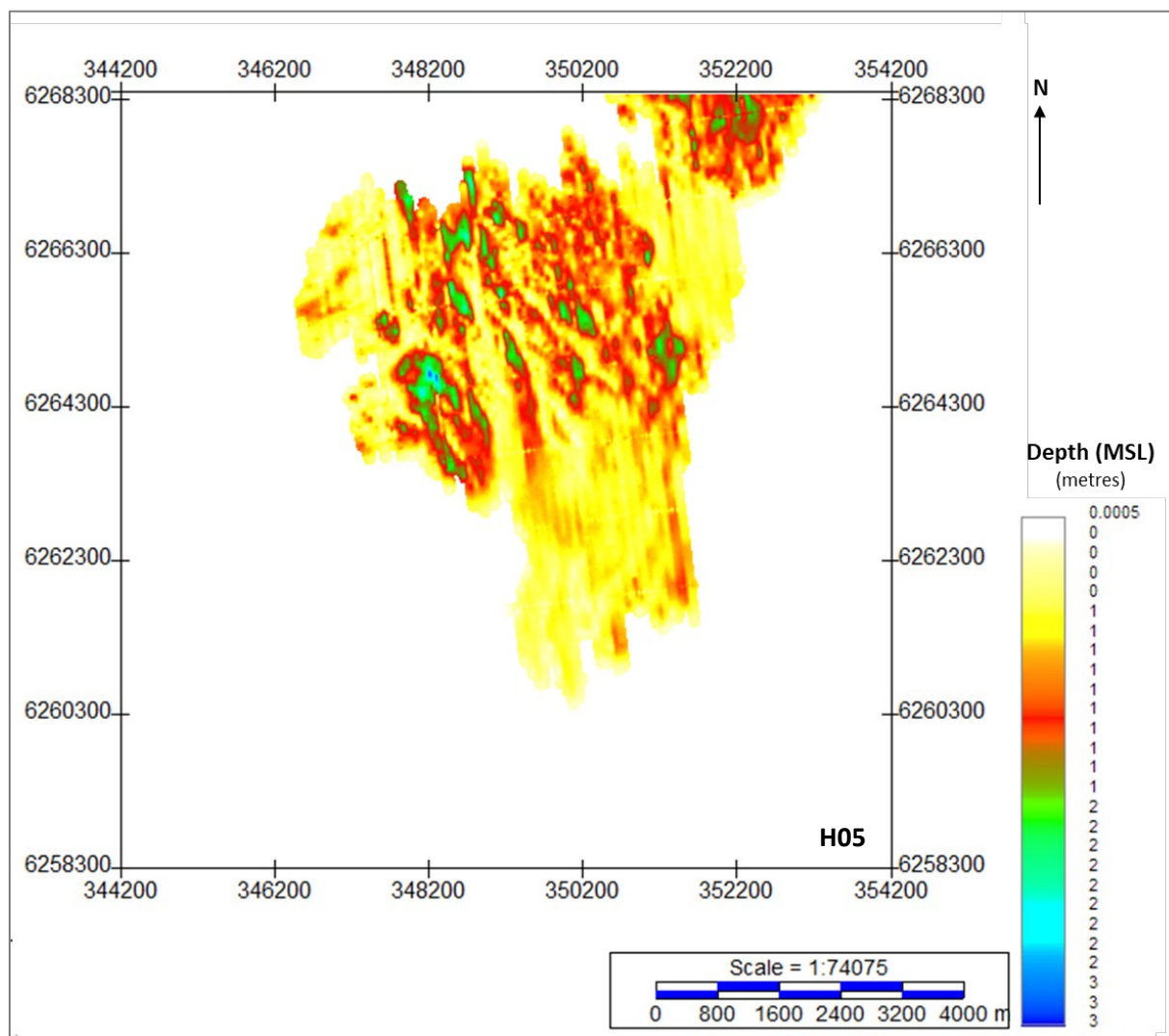


Figure 94 Depth below seabed of H05.
 Units in metres below seabed.

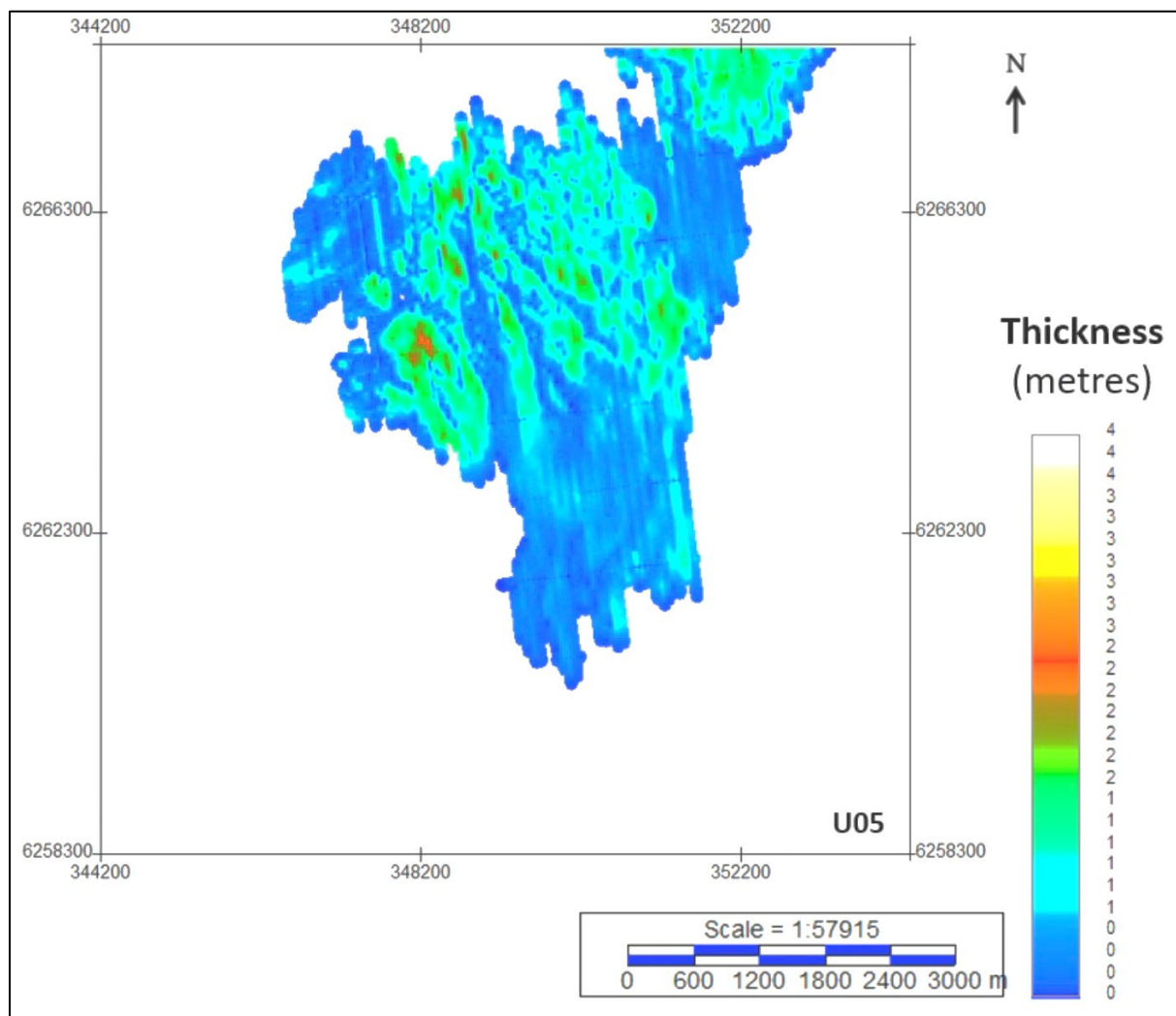


Figure 95 Thickness of unit U05.
 Units in metres.

8.6.3 | SEISMIC UNIT U10

Seismic unit U10 is a major element of the ground model, and extends spatially across the majority of the Artificial Island survey area. The base of Seismic Unit U10 is defined by horizon H10. Seismic unit U10 comprises the recent marine sediments that make up the seabed bedforms where present. The spatial distribution, vertical reference to MSL and the seabed, and thickness of the unit are presented in, Figure 96 and Figure 97.

Horizon H10 ranges in depth between 31.7 m and 46.2 m below MSL (Figure 96) and between 0 m and 16.3 m depth below the seabed (Figure 97). It follows a flat, planar, and even reflector of medium to high amplitude (Figure 98); or it is observed as a micro-undulating (hyperbolic) reflector with stippled high amplitudes. On localised facies shift, H10 follows a faint low amplitude reflector, and rarely displays reversed polarity.

Seismic unit U10 has a tabular external morphology in regions where it is thinner (from 0 m to 4 m thick); or it forms wide mounds of thicker sediment accumulation (up to 16.3 m thick).

The seismic facies of U10 have a generally low to medium amplitude response. Where thicker, within the mounded structures, its internal facies varies both vertically and laterally: at the base it may be

homogenously transparent or with small mound-channel patterns to chaotic; overlaid by oblique downlap reflectors and small lenses (Figure 100). Above these, sits a thinner deposit of sub-horizontal and parallel reflectors. The latter is also observed in areas where U10 is thinner. Stippled high amplitude facies are locally observed at the base. Common discontinuous high amplitude reflectors and negative high impedance contrasts occur across the unit's extent.

Horizon H10 is interpreted as a transgressive ravinement surface. The deposits of U10 are interpreted to be related to a marine transgressive setting (possibly high stand). Seismic unit U10 is likely made up of silty-sands and a gravelly sand lag that rest above the H10 ravinement surface. U10 is interpreted to be of Holocene in age. Stippled high amplitude facies may indicate coarser-grained material, such as gravel.

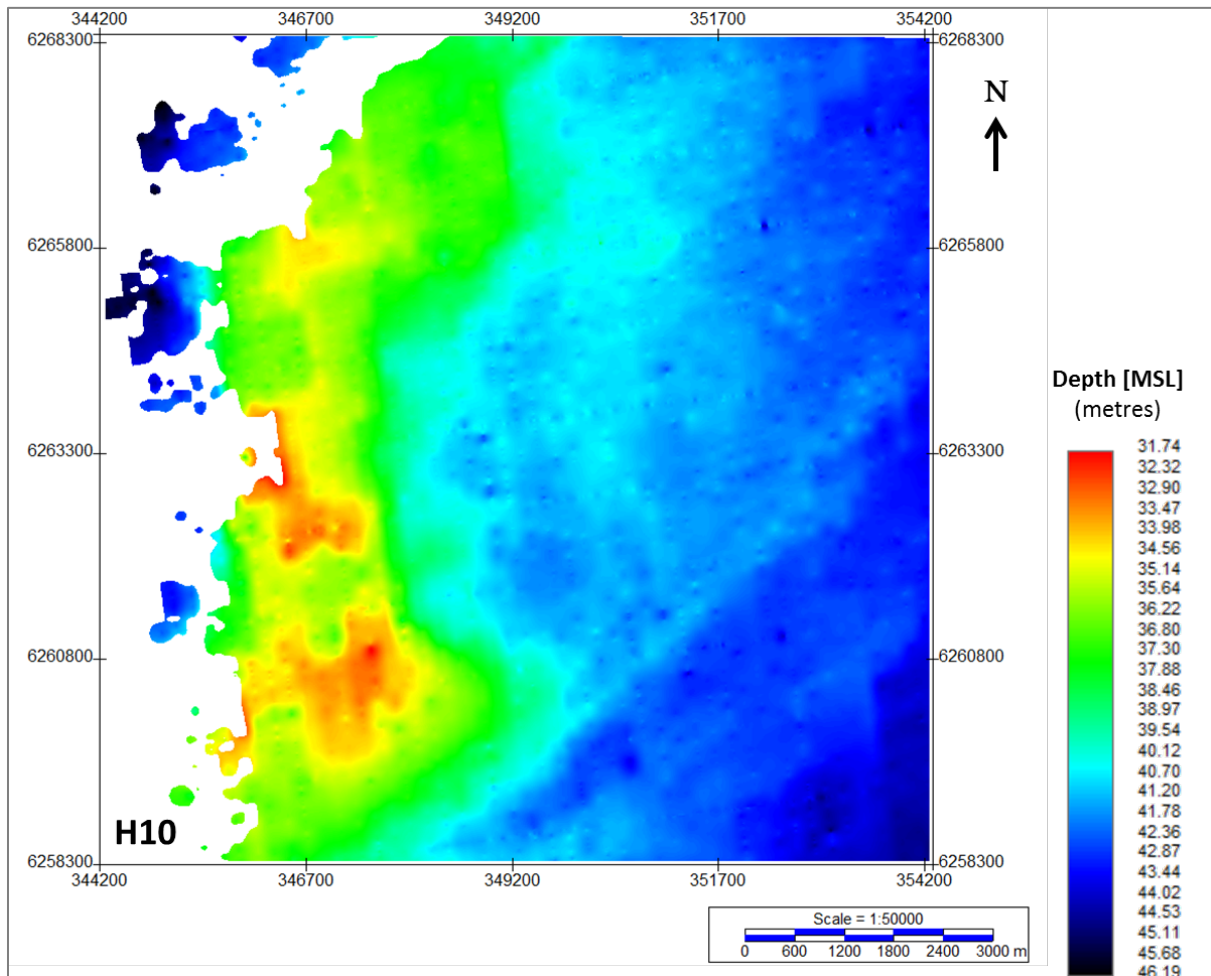


Figure 96 Map showing the lateral extent of U10.
 Units in metres below MSL.

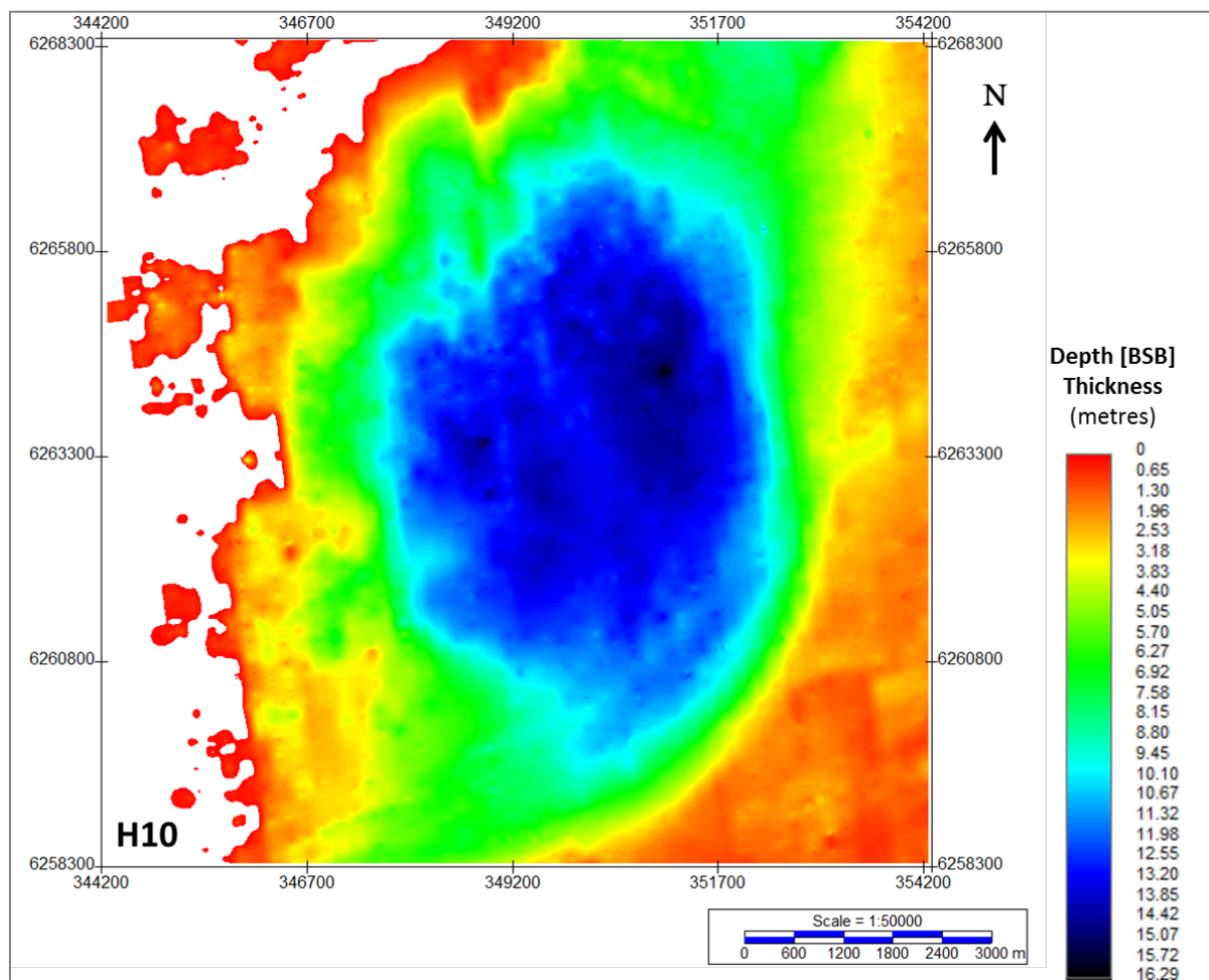


Figure 97 Depth below seabed of H10, corresponding to the thickness of unit U10.
 Units in metres below seabed.

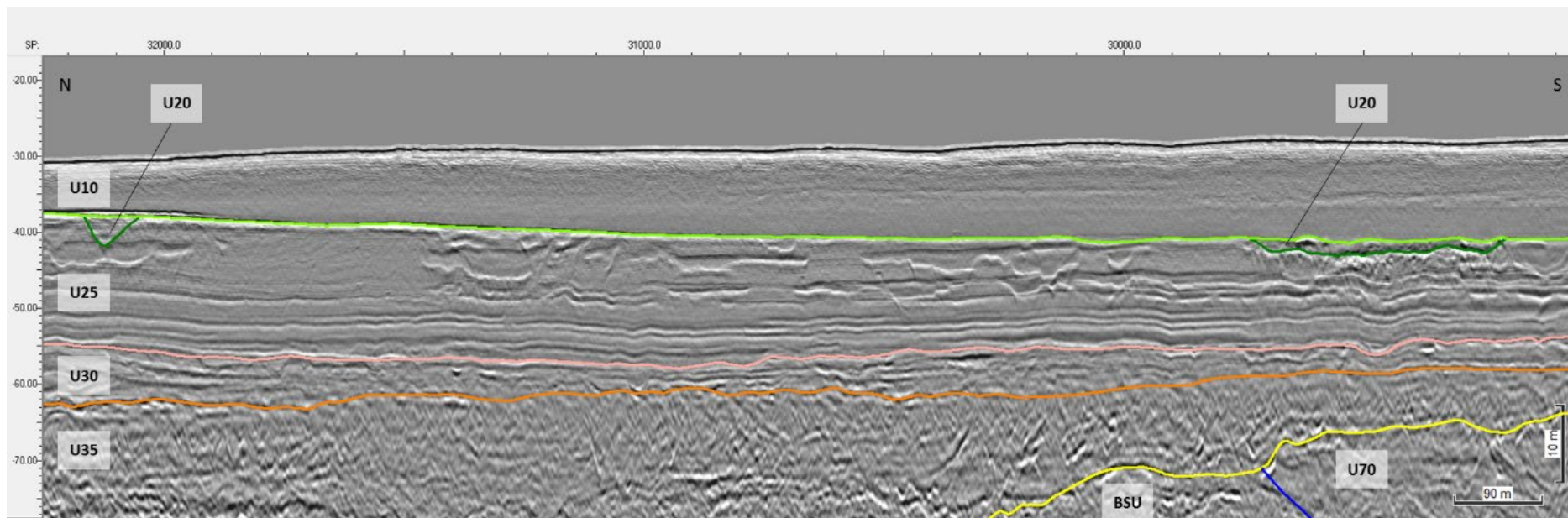
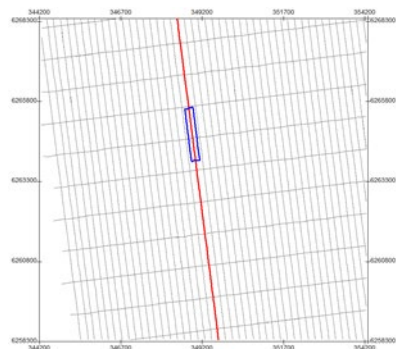


Figure 98 General facies of Seismic Unit U10, and the character of horizon H10 (light green).
 Seismic profile BM2_OWF_E_2D_04200

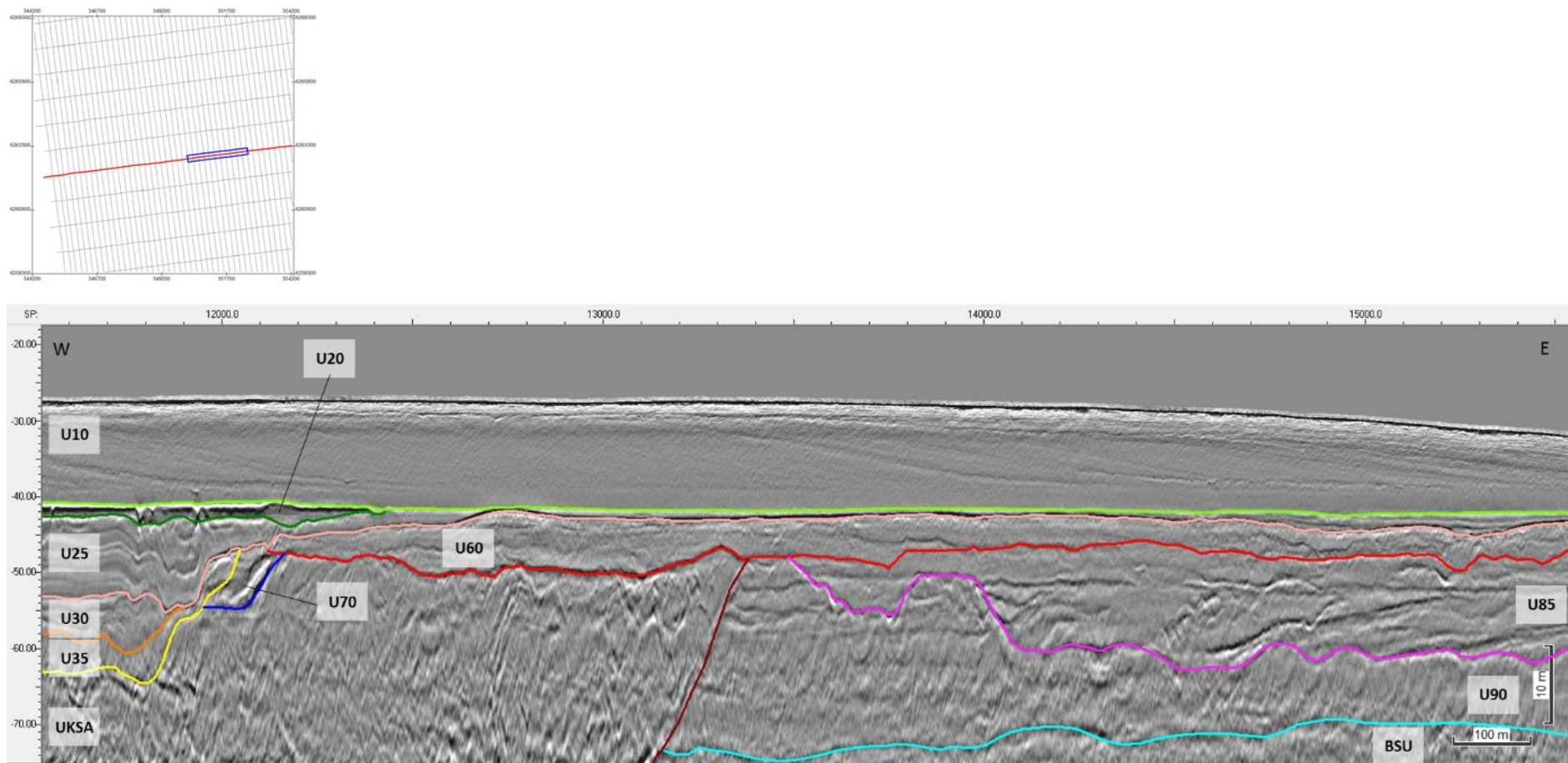


Figure 99 Oblique facies of U10, overlaid by a package of sub-horizontal parallel reflectors.
 Seismic profile BX3_OWF_E_XL_23000

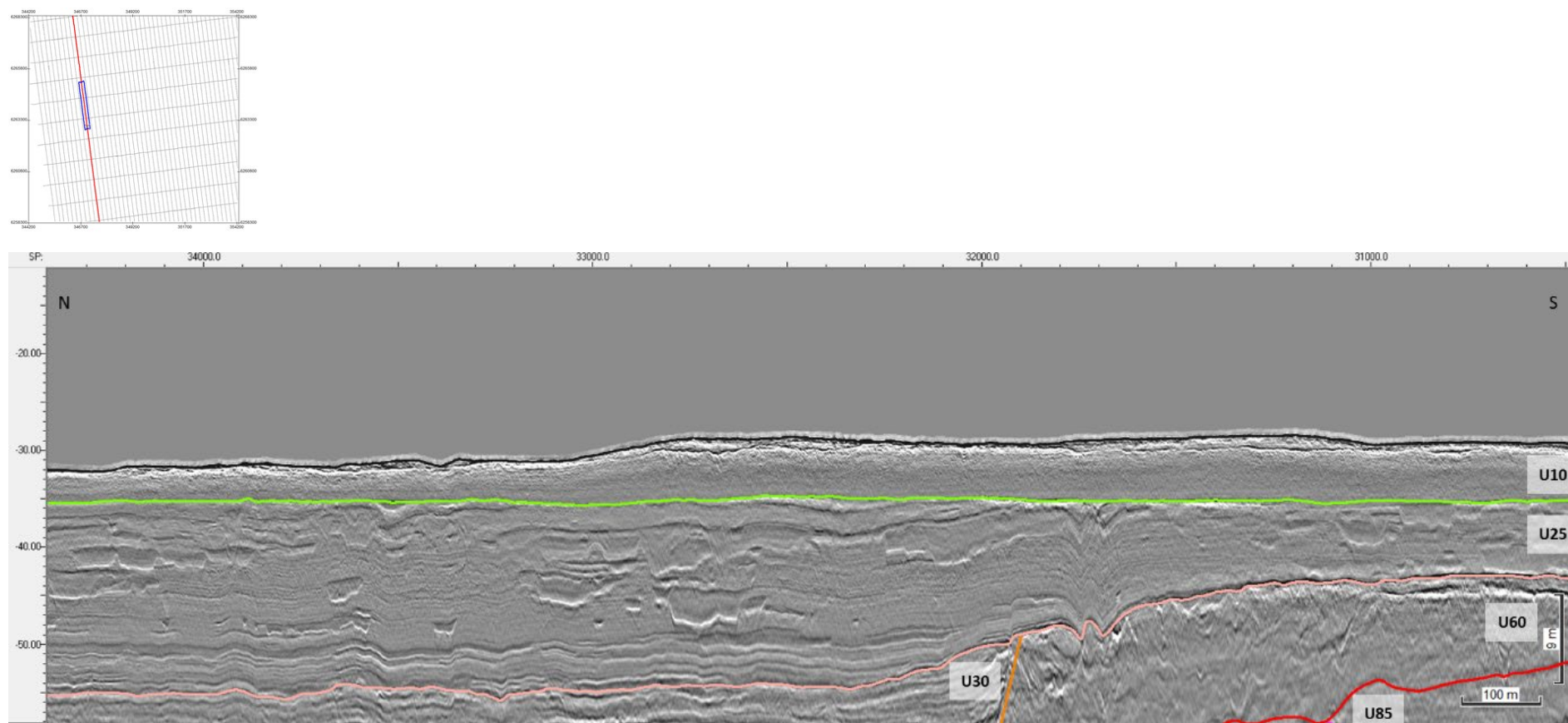


Figure 100 Internal facies of Seismic Unit U10, and horizon H10 (light green).
Seismic profile BM1_OWF_E_2D_02100

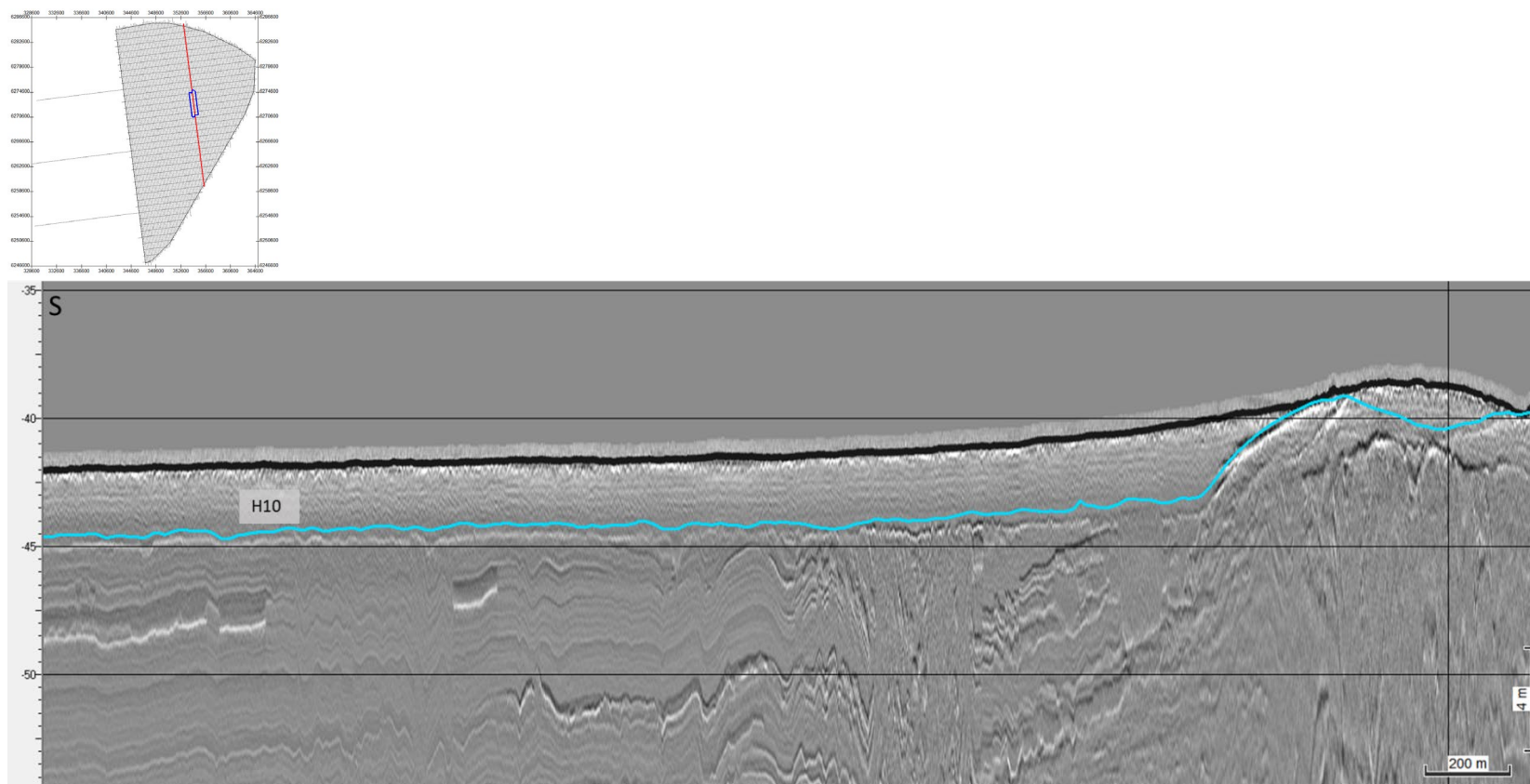


Figure 101 Grid overlay from interpretation of H10 as interpreted on the Innomar SBP.
 Seismic profile BM4_OWF_E_2D_10920

8.6.4 | SEISMIC UNIT U20

The base of Seismic Unit U20 is delineated by H20 and is found discontinuously across the Artificial Island survey area. The spatial distribution, vertical reference to MSL and the seabed, and thickness of the unit are presented in Figure 102, Figure 103 and Figure 104.

Horizon H20 ranges in depth between 32.6 m and 60.8 m below MSL (Figure 102), and between 0 m and 23.8 m depth below the seabed (Figure 103). It delineates the base of channelised incisions (Figure 105 to Figure 107), following a reflector of varying amplitude (from medium-high to low-medium), and marking an erosion surface (with reliefs of 3 to 15 m) and a significant facies shift.

Seismic unit U20 has a thickness range between 0 m to 19.5 m. V-shaped channels are incised up to 60 m depth MSL (23.5 m BSB), corresponding to the areas where U20 is thicker, especially towards the south.

Seismic unit U20 comprises two distinct facies:

- 1) **Channels:** Micro to meso-scale channels with chaotic to parallel infill, commonly mounded-chaotic at the base (Figure 105 to Figure 107).
- 2) **Wide shallow basins:** Low amplitude to transparent homogeneous, with faint micro-parallel reflectors and common negative high amplitude anomalies at the base and internally (Figure 105 and Figure 107).

Where these two facies are associated, the channel facies occur at the base of U20, with the wide basin facies above it (Figure 107). Separating these facies is usually a strong reflector of negative high amplitude.

Horizon H20 is interpreted as a truncating erosional surface, and the general spatial arrangement of U20 is indicative of a drainage network. U20 is interpreted to have been deposited in restricted marine-tidal setting, partially associated to a subaerial fluvial system.

Within the wide basins, the deposits of U20 are expected to comprise fine sediments, from clays-silts-fine sands; whereas channel infills are likely to contain slightly coarser sediments such as fine sands-sands (even gravelly lags/layers?). The large amount of observed negative high amplitude reflectors may be related to the occurrence of organic matter within this unit.

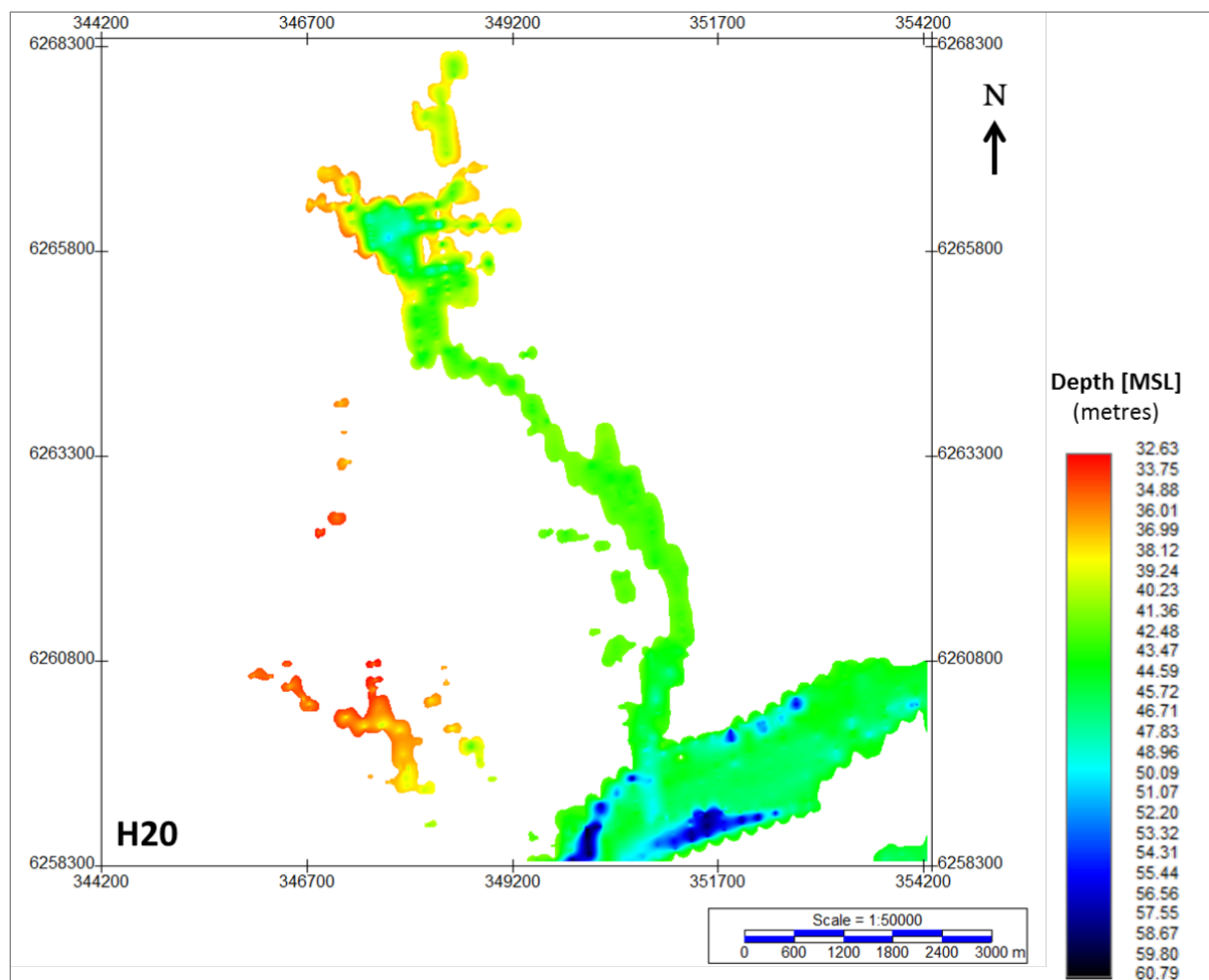


Figure 102 Map showing the lateral extent of H20.
 Depth below MSL. Units in metres.

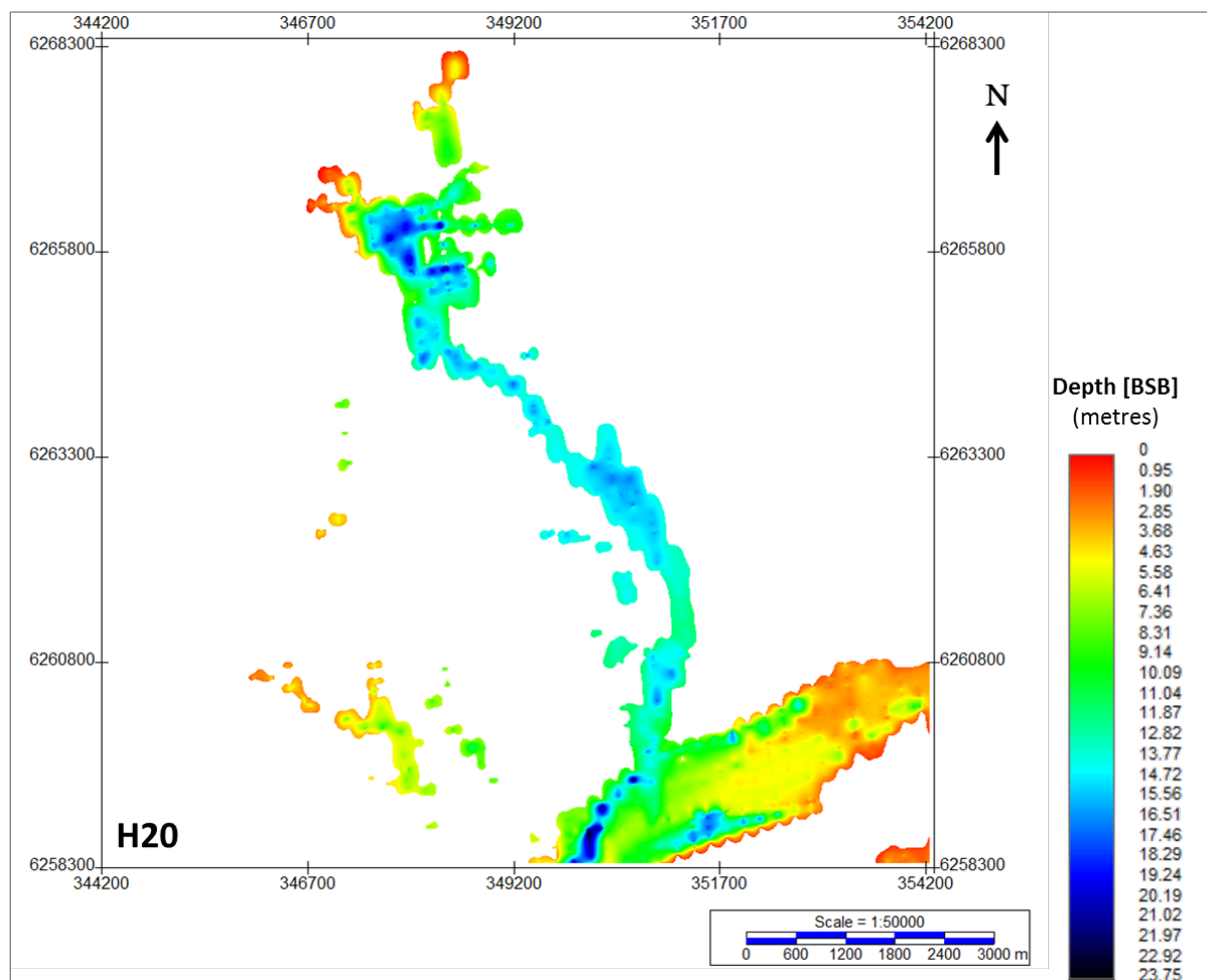


Figure 103 Depth below seabed of H20.
 Units in metres below seabed.

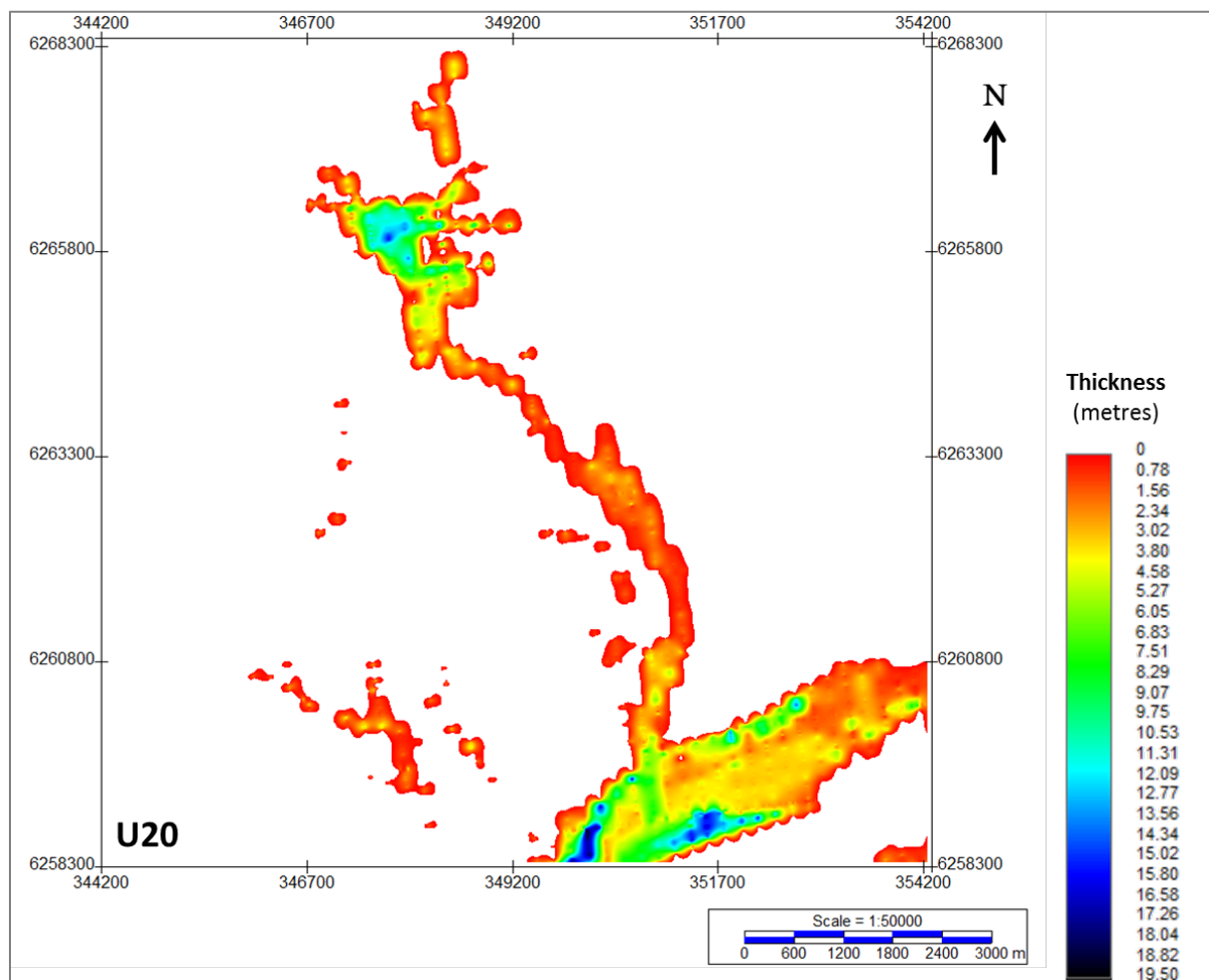


Figure 104 Thickness of unit U20.
 Units in metres.

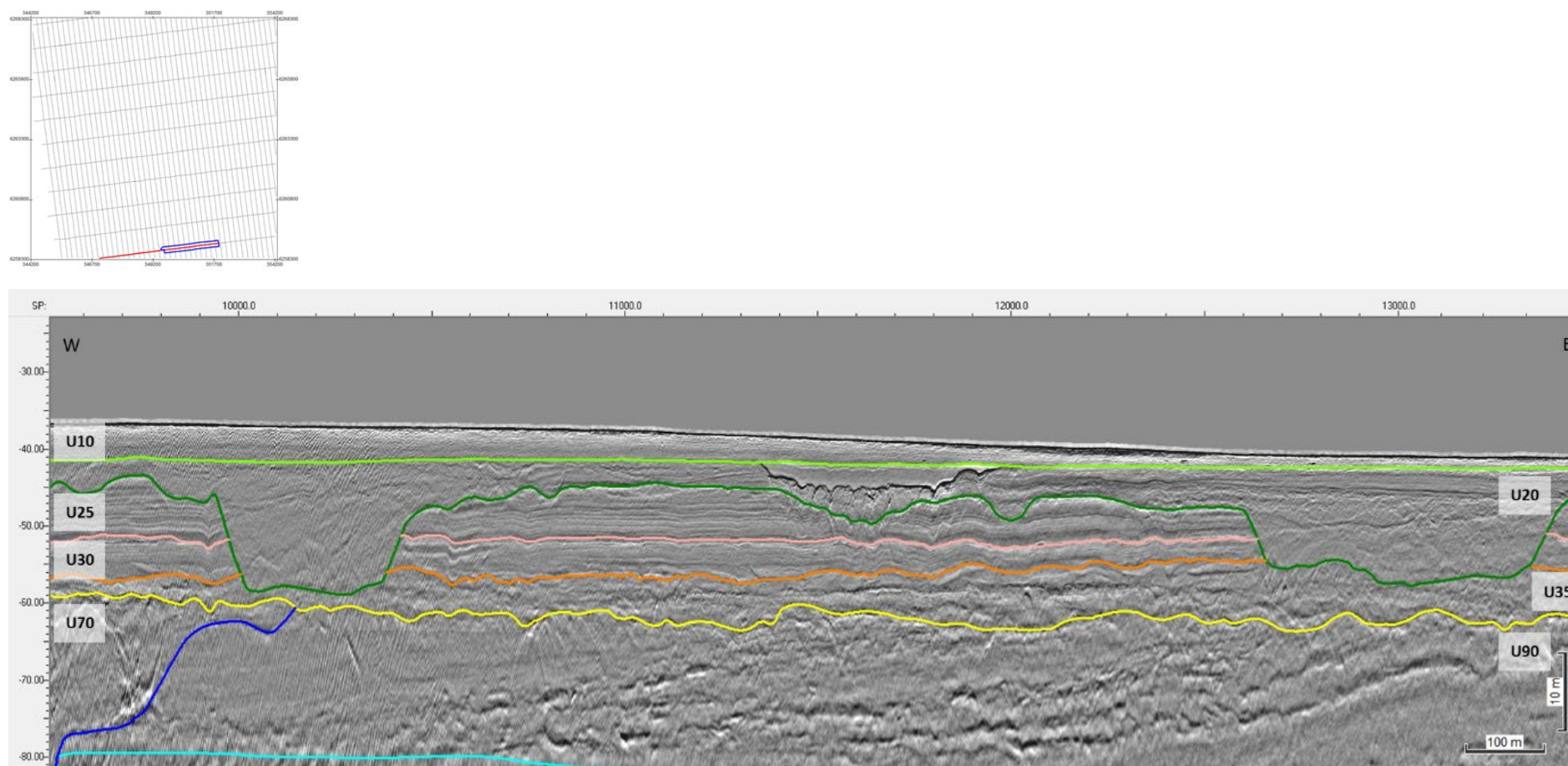


Figure 105 Seismic facies of seismic Unit U20, and the character of horizon H20 (dark green).
 Seismic profile BX4_OWF_E_XL_27000

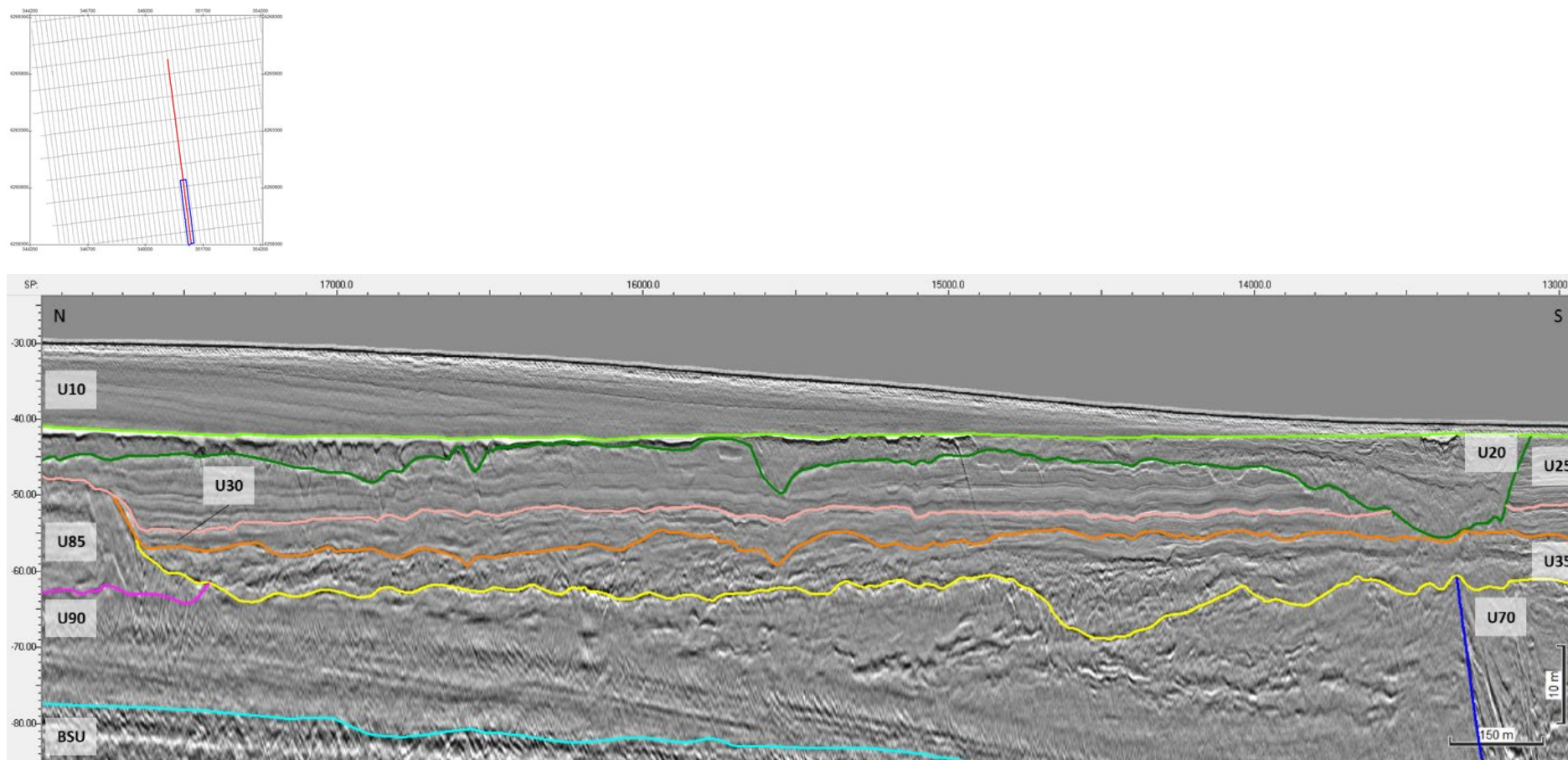


Figure 106 Channel facies of Seismic Unit U20, with a high negative amplitude reflector at the top.
 Seismic profile BM3_OWF_E_2D_05670

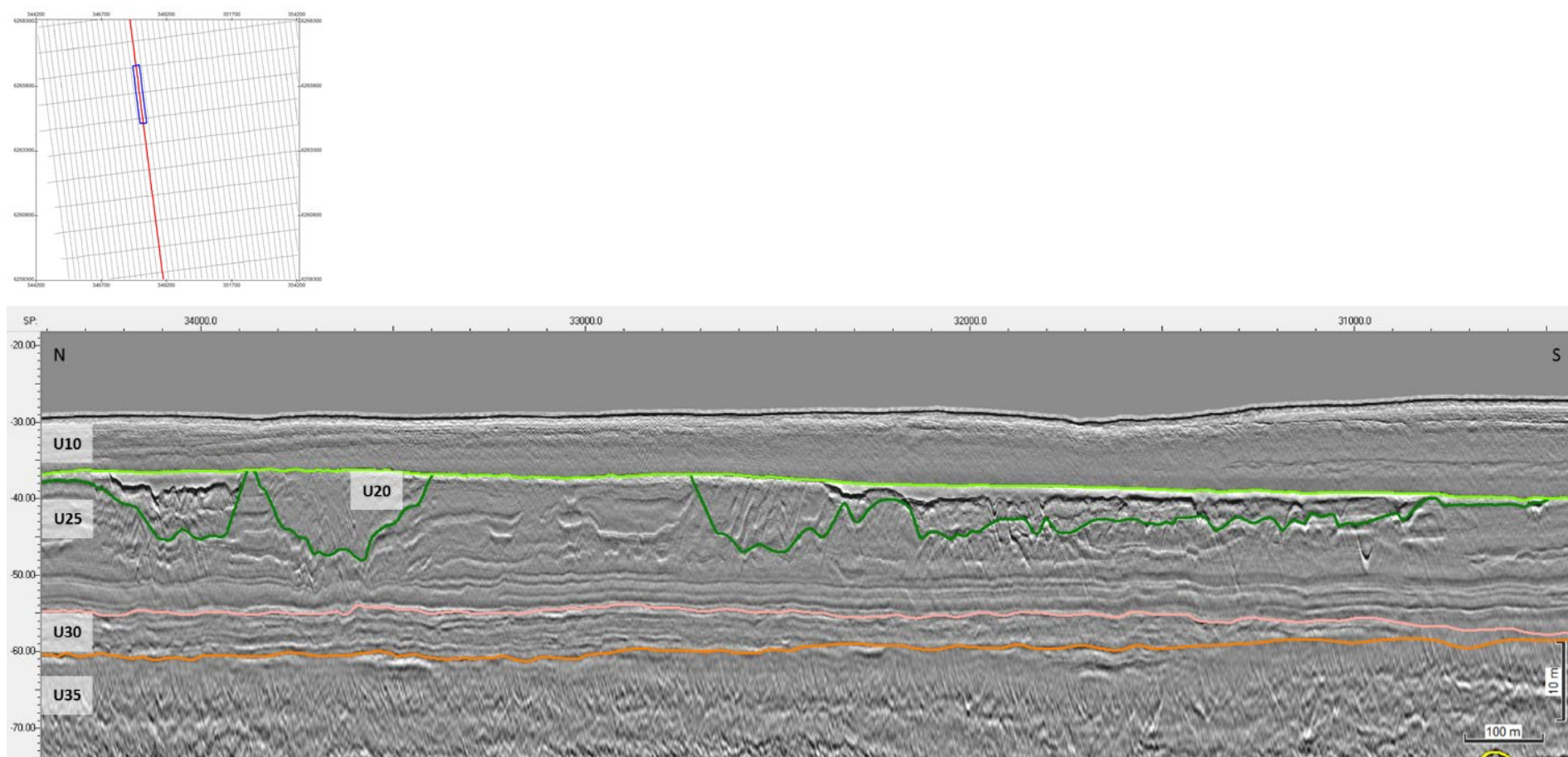


Figure 107 Two distinct facies of Unit U20: channel facies at the base; basin facies at the top.
Seismic profile BM2_OWF_E_2D_03570

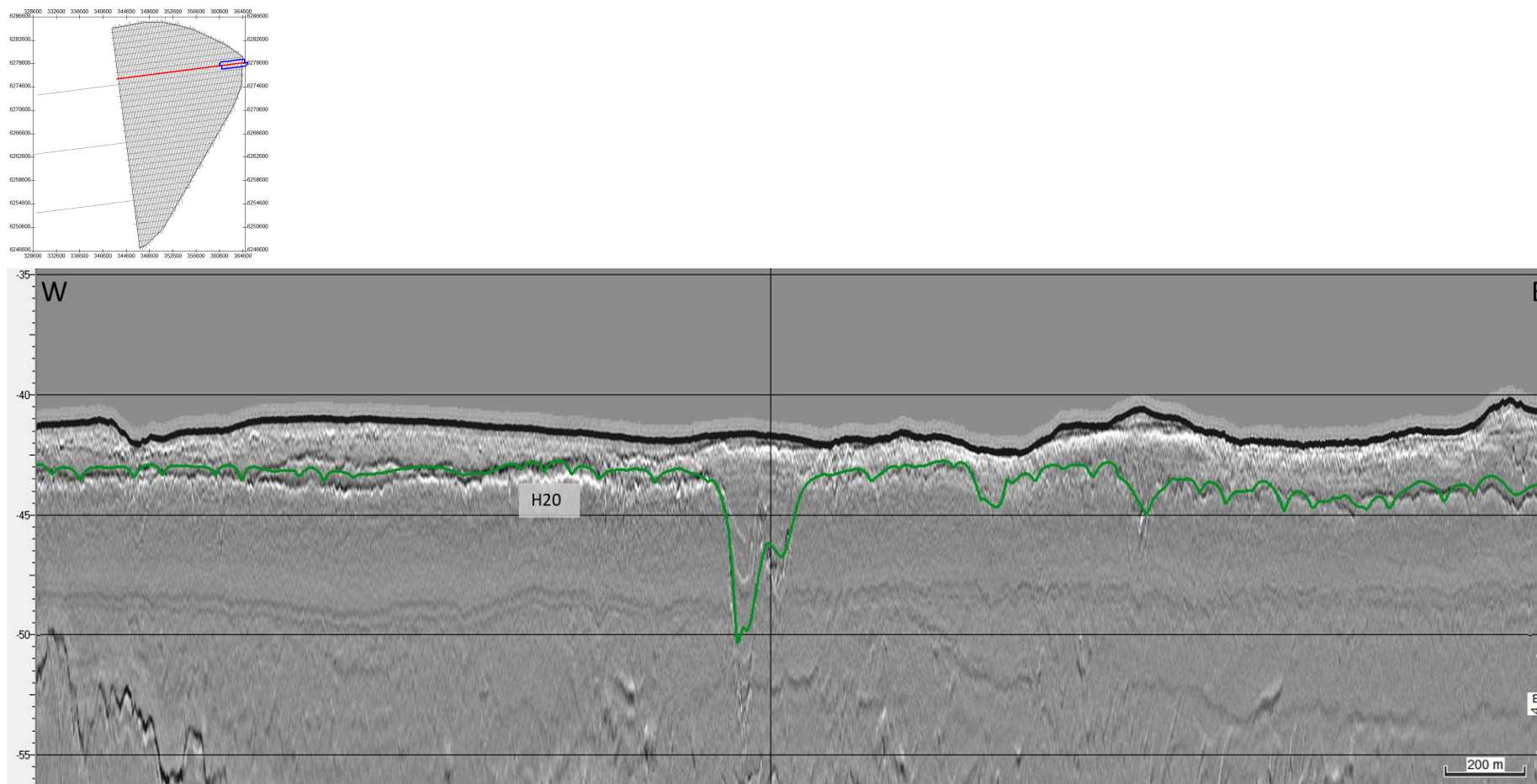


Figure 108 Grid overlay from interpretation of H20 as interpreted on the Innomar SBP.
 Seismic profile BM2_OWF_E_XL_09000

8.6.5 | SEISMIC UNIT U25

Seismic unit U25 is a major component of the ground model, and extends spatially across the entire Artificial Island survey area. The spatial distribution, vertical reference to MSL and the seabed, and thickness of the unit are presented in Figure 109, Figure 110 and Figure 111).

The base of U25 is defined by horizon H25, between 41.2 m and 59.7 m depth below MSL (Figure 109), and between 0 m and 30.7 m depth below the seabed (Figure 110). H25 is a continuous and slightly undulating reflector of variable amplitude (low-high). Locally this horizon defines a vertical facies shift from U30 below and the deposits of U25, commonly marking variations of acoustic impedance.

Seismic unit U25 has different expressions across the survey sectors. In areas of the south sectors, where it is thinner (1-5 m thick), U25 has a tabular morphology. In the central sector and parts of the south sector, U25 infills wide basins, reaching its maximum thickness of up to 22.7 m (Figure 111). It is often truncated by H20.

In general, the seismic facies of U25 is characterized by low amplitude micro-parallel reflectors, gently undulating in places (Figure 112 to Figure 115). In the south sector, where the unit is thinner, its facies is usually transparent and homogeneous at the base (Figure 114), and above may exhibit faint small channels and mounds.

The central sector delineates the margins of a wide basin inside the full MMT OWF survey area. This basin is only partially imaged within the Artificial Island survey area, present across the whole central sector, covering an area of 3.5-4.5 km width (N-S direction) and 10 km long (E-W direction) (Figure 109). Connected to this central basin at its southern limit are two other elongated depressions (south sector). The largest of the two (towards W), with a general orientation N-S, is 6.5 km long and 4.2 km at its widest part. The smaller basin (towards E) is oriented NW-SE and is 1.8 km x 3.6 km in size.

Within these basins, seismic unit U25 is thicker, comprising mostly low amplitude parallel facies, gently undulating in places (Figure 112 to Figure 115). The thickness and acoustic amplitude decrease towards the top. Small-scale, box-shaped channels with transparent infill are scattered at several levels within U25, truncating the thinly-layered sequence (Figure 112). The base of these channels is generally marked by a negative amplitude reflector. The occurrence and size of these channels increase towards the top of the unit, with common vertical stacking.

The sediments constituting seismic unit U25 are interpreted to have been deposited in a relatively low-energetic setting, possibly related to a flood plain/transgressive estuary. However, the increase of small channel-incisions within the upper deposits of U25 suggests the onset of a regressive event/fluctuation. From the seismic character of U25 and its interpreted depositional system, it is estimated that the thinly-layered deposits comprise fine sediments, such as fine sands-silts (?), and that the transparent channel infill may correspond to unstructured fine sediments (?).

Outside the Artificial Island survey area, in localised regions near the N margin of the central basin, seismic unit U25 exhibits variable degrees of internal deformation, most likely the result of dewatering/compaction and gravitational stresses.

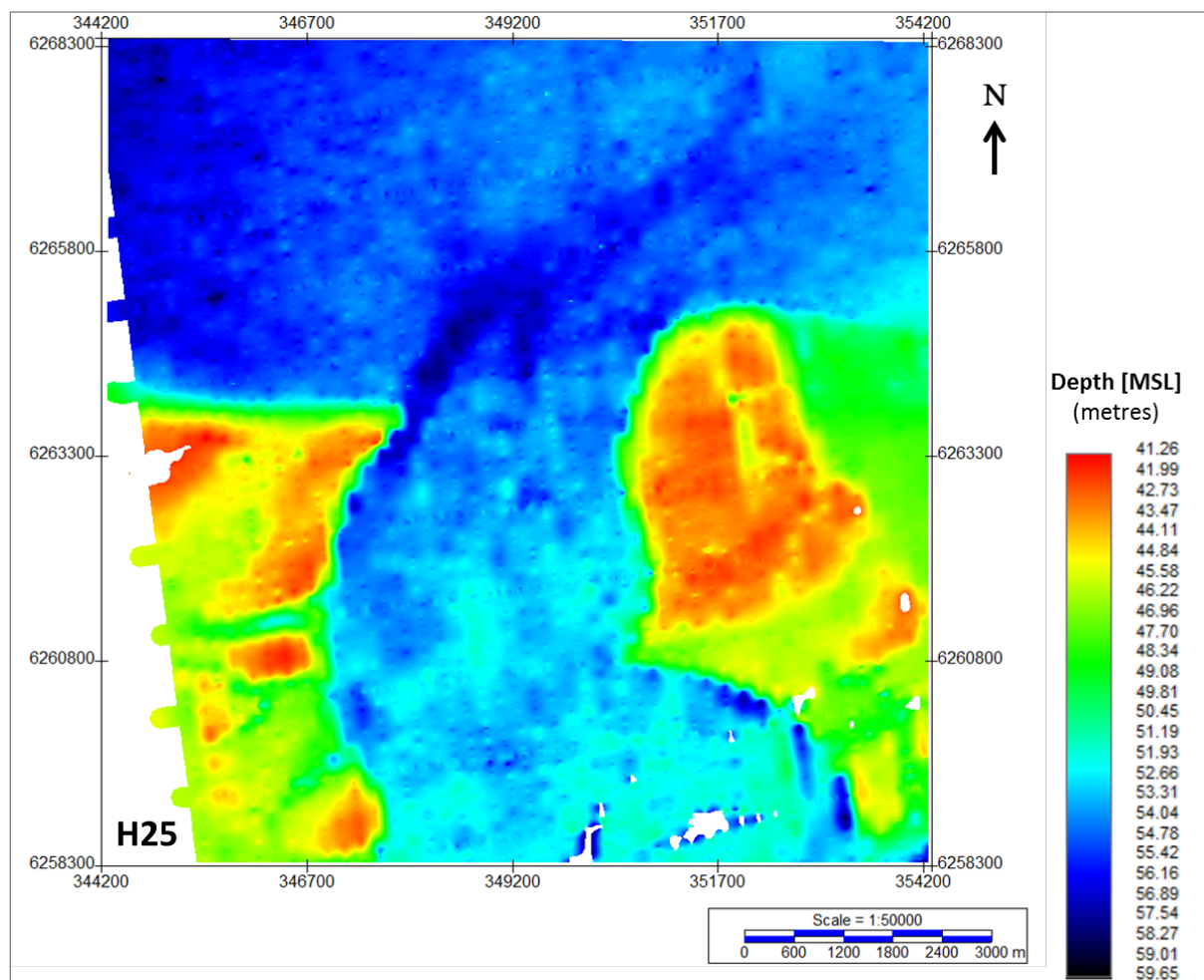


Figure 109 Map showing the lateral extent of U25.
 Units in metres below MSL.

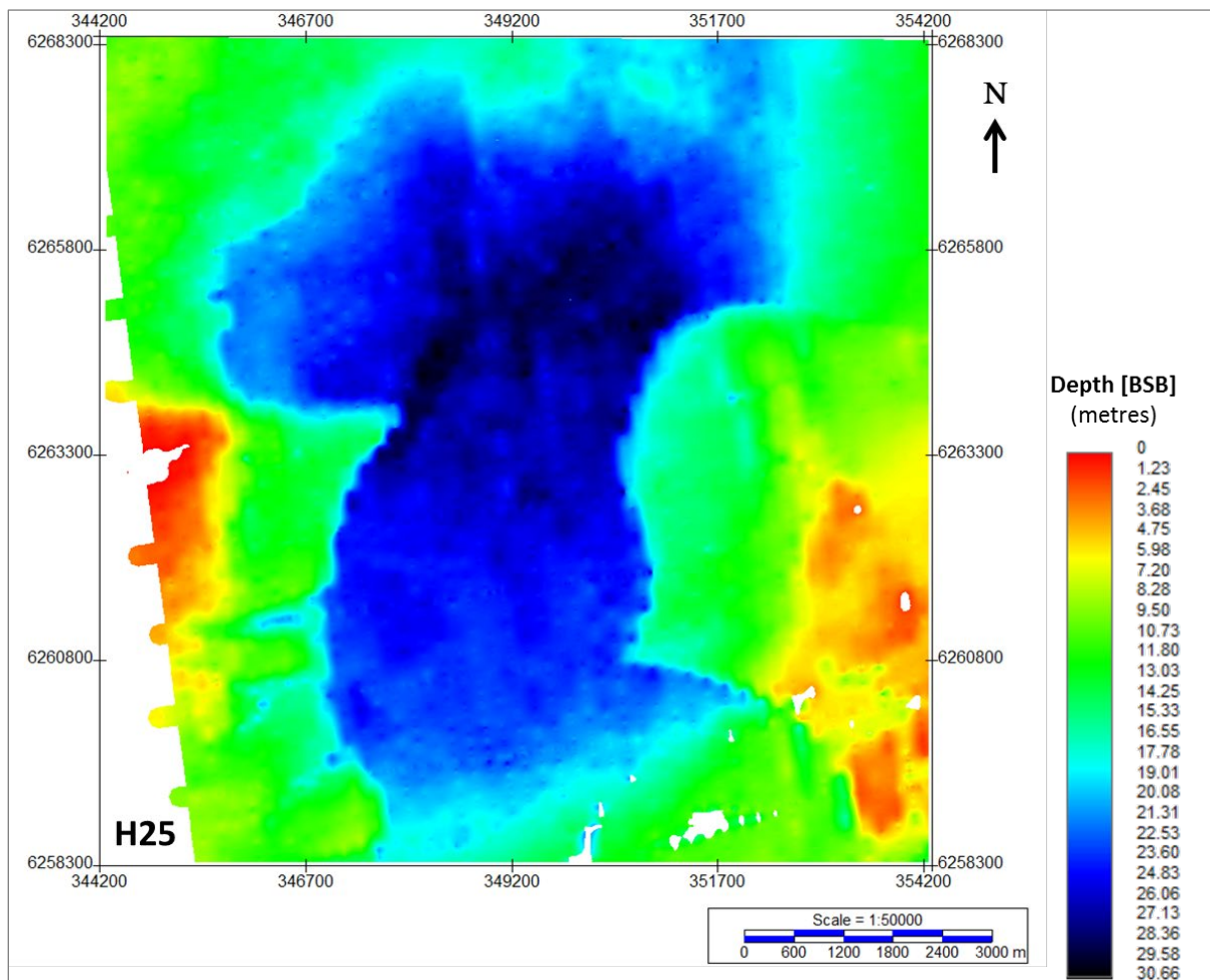


Figure 110 Depth below seabed of H25.
 Units in metres below seabed.

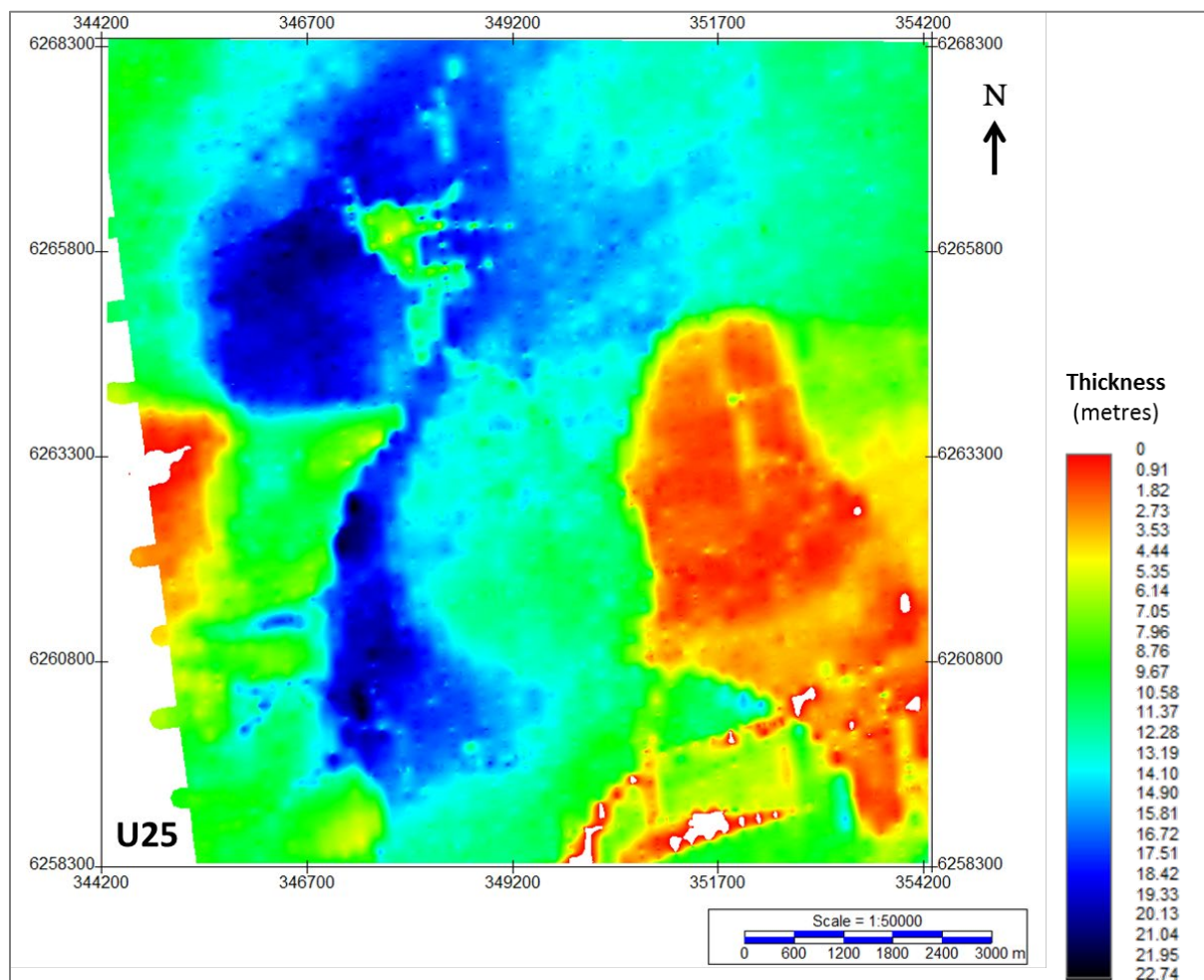


Figure 111 Thickness of unit U25.
 Units in metres.

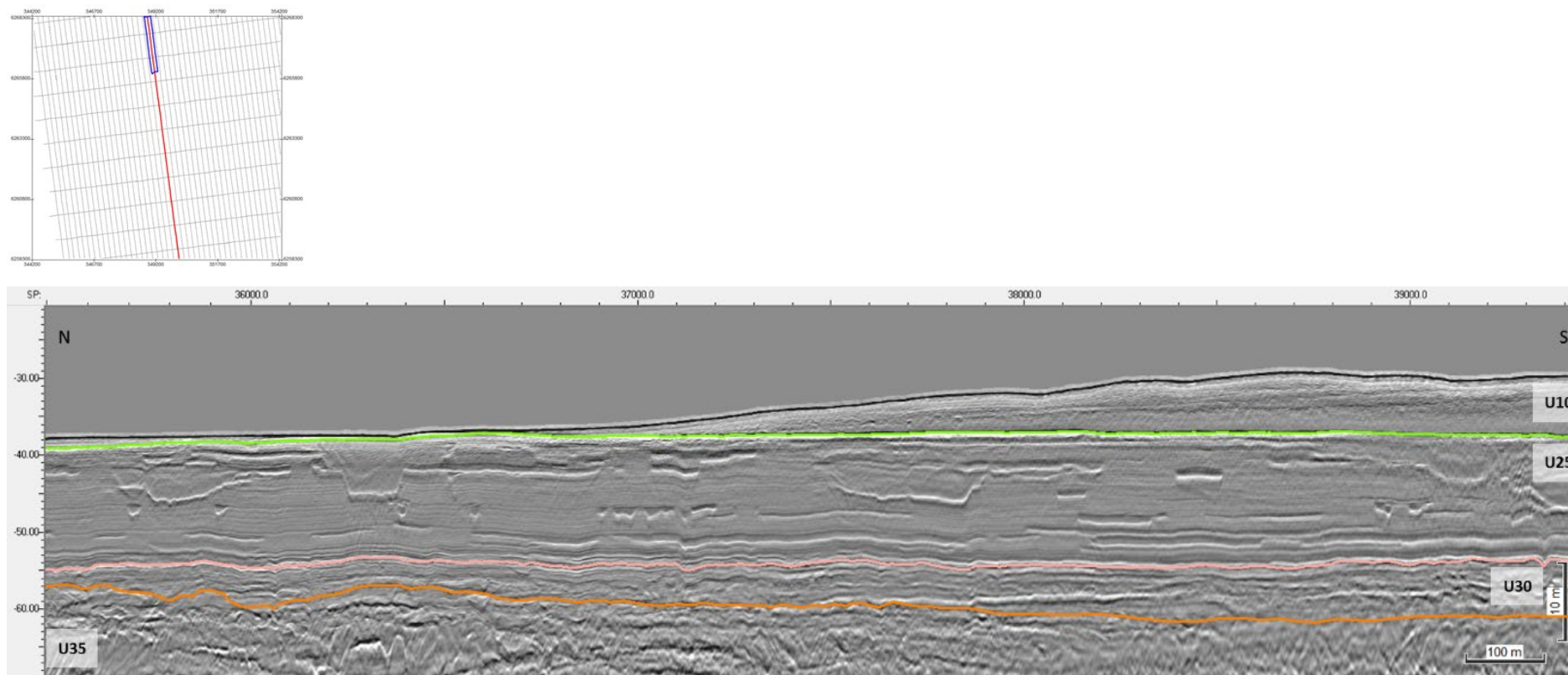


Figure 112 General facies of Seismic Unit U25 within the central basin.
 In this area, the unit is thicker, with channel frequency increasing towards the top. The image also shows the character of horizon H25 (rosy brown).
 Seismic profile BM2_OWF_E_2D_04620

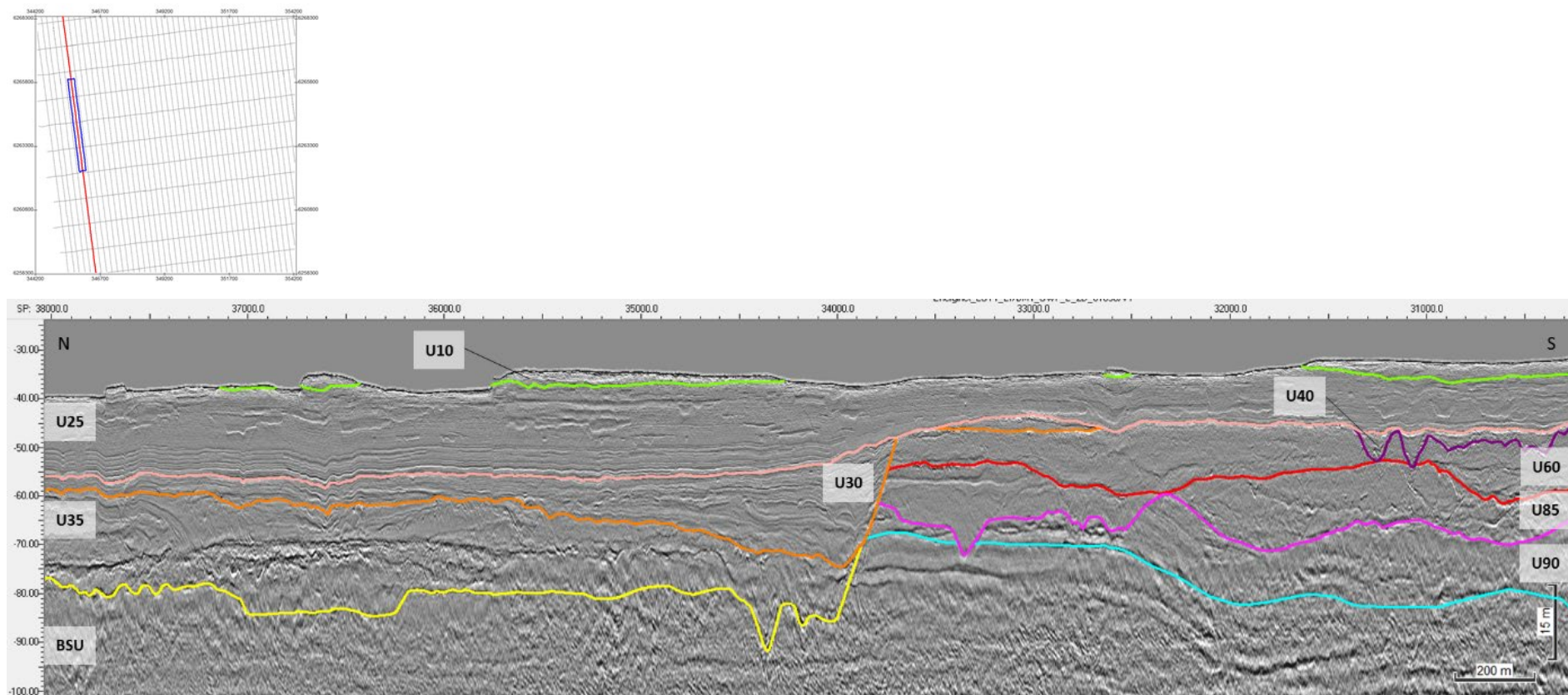


Figure 113 Facies of Seismic Unit U25 and the SW limit of the central basin
 The image shows the transition of U25 from the central to the south sectors.
 Seismic profile BM1_OWF_E_2D_01050

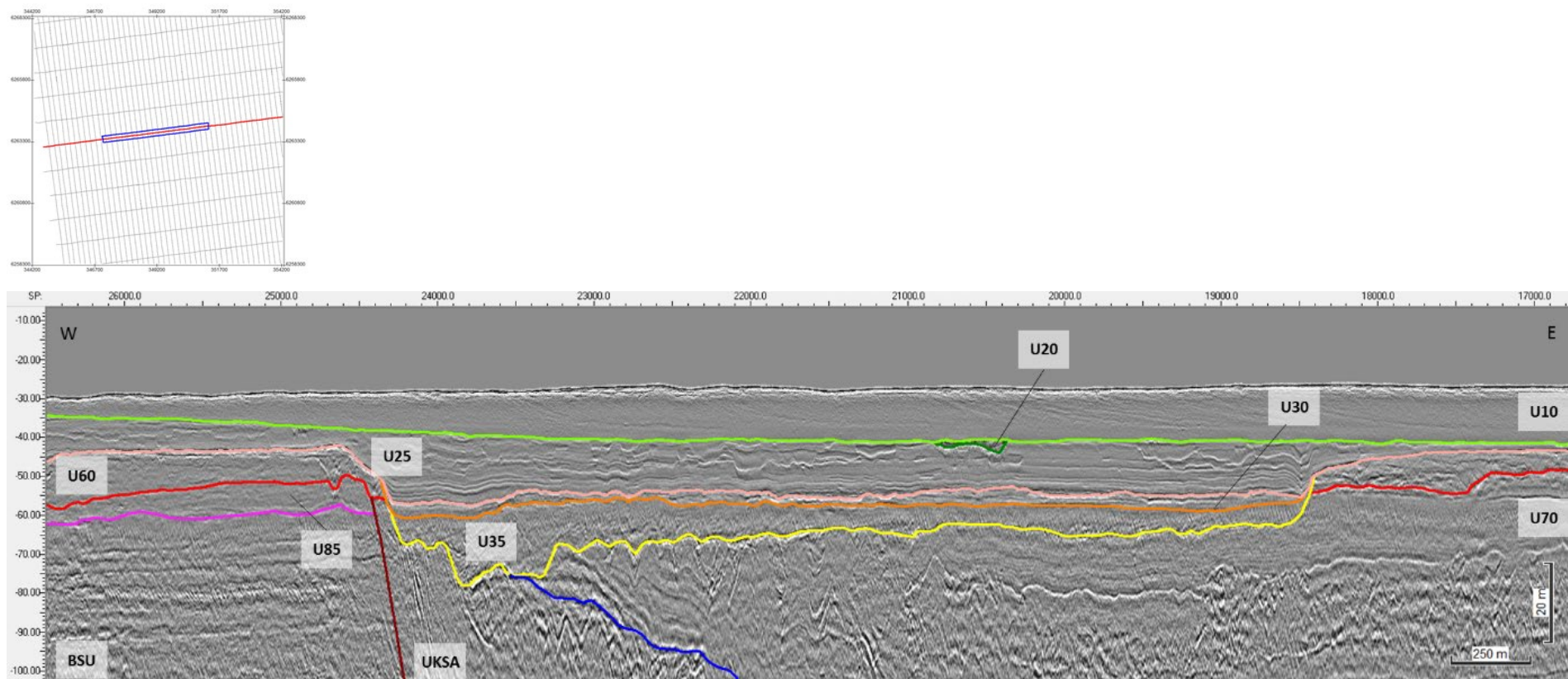
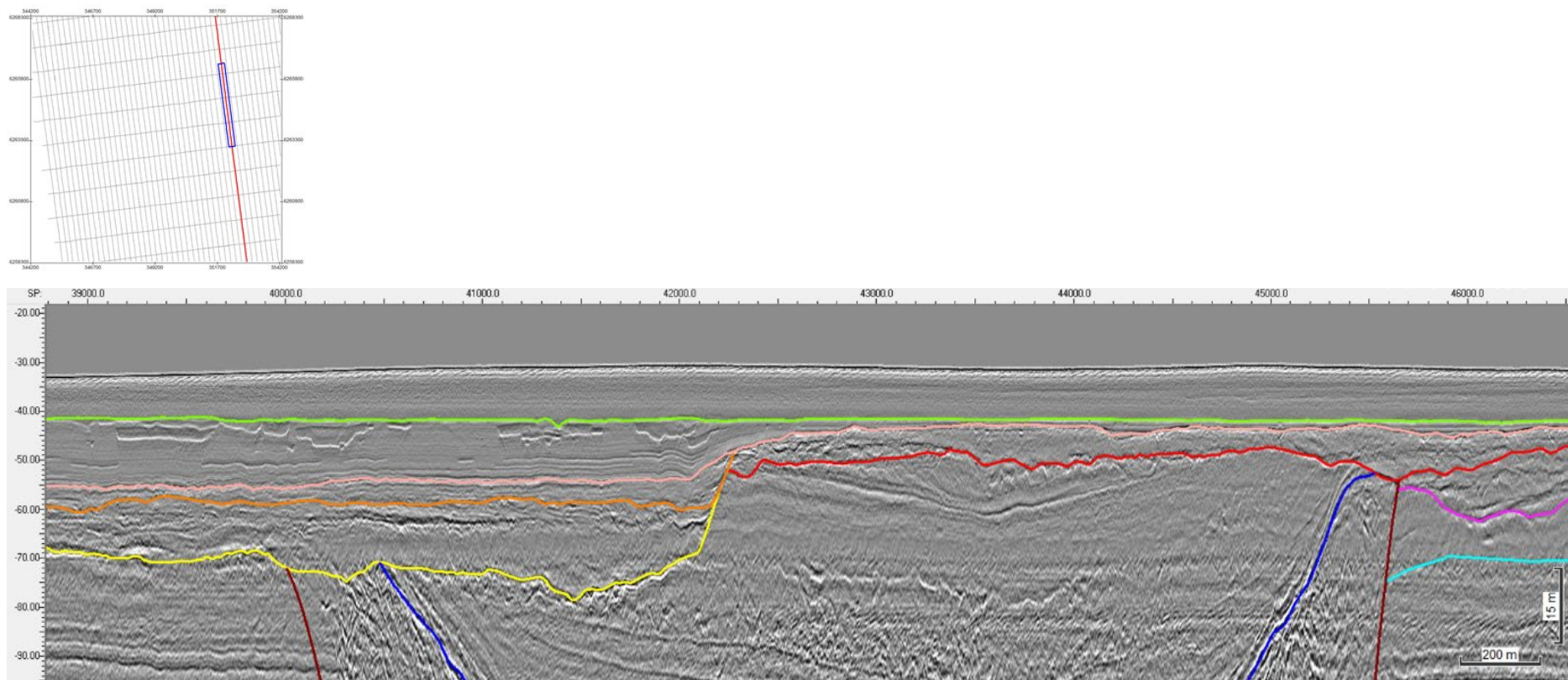


Figure 114 U25 facies at transition from the central basin to the narrower N-S basin in the south.
 Seismic profile BX3_OWF_E_XL_22000



*Figure 115 Facies of Seismic Unit U25 and the SE limit of the central basin.
 The image shows the transition of U25 from the central to the south sectors.
 Seismic profile BM3_OWF_E_2D_07350*

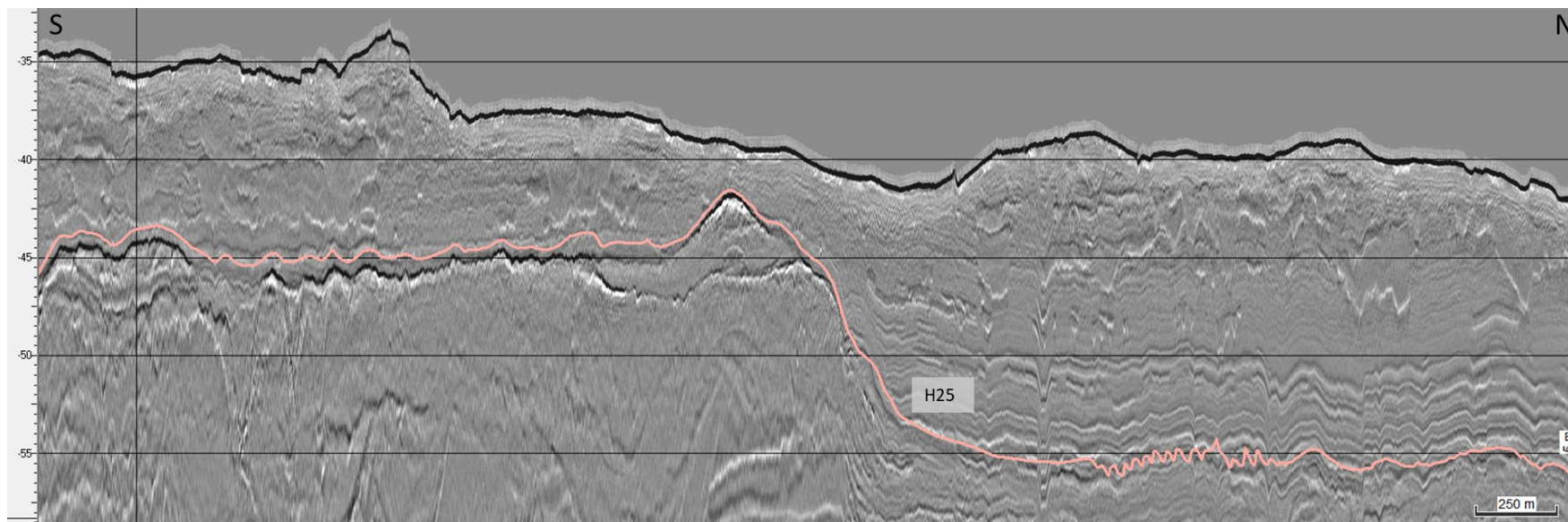
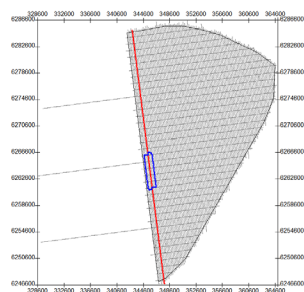


Figure 116 Grid overlay from interpretation of H25 as interpreted on the Innomar SBP.
 Seismic profile BM1_OWF_E_2D_00

8.6.6 | SEISMIC UNIT U30

Seismic unit U30 is a major element of the ground model, and has a similar spatial distribution to U25, albeit discontinuous in the south sector. The base of Seismic Unit U30 is defined by horizon H30 and is present discontinuously within the survey area. The spatial distribution, vertical reference to MLS and the seabed, and thickness of the unit are presented in Figure 117, Figure 118 and Figure 119.

Horizon H30 ranges in depth between 42.3 m and 77.6 m below MSL (Figure 117), and between 0.3 m and 42.16 m depth below the seabed (Figure 118). Horizon H30 represents an uneven, undulating surface, occasionally defined by a significant vertical facies shift (Figure 120). When present and continuous, H30 was mapped along a reflector of variable amplitude (low to high). This uneven base marks an erosional surface that truncates the deposits below it (Figure 121).

Seismic unit U30 has a tabular or tabular wavy morphology, usually 2 m to 10 m thick. The thickest deposits of U30 are located along the margins of the central basin, reaching a maximum of 26.3 m (Figure 119). U30 is locally truncated by H20 incisions.

Within the central basin and the two minor ones, unit U30 is characterized by composite facies of medium to high amplitude configurations (Figure 121). Towards the top, reflectors are sub-horizontal, parallel and wavy. Below the latter, meso- to micro-scale channels and mounds are observed, with internal oblique, parallel, down lapping reflectors. Towards the base, the complexity of the seismic facies increases, with common mounds, lenses, patterns of channel lateral migration, hummocky reflectors, and chaotic in parts.

The sediments constituting seismic unit U30 are interpreted to have been deposited in setting of slightly higher energy than the overlying U25, as evidenced by the occurrence of channel and chaotic deposits at the base. The sequence of seismic facies within U30 is indicative of decrease of energy from the base towards the top, possibly associated to a transgressive event. From the seismic character of U30 and its interpreted depositional system, it is estimated that, in general, there is a decrease in grain size towards the top, with probable sandier sediments at the base, getting progressively finer upwards (?).

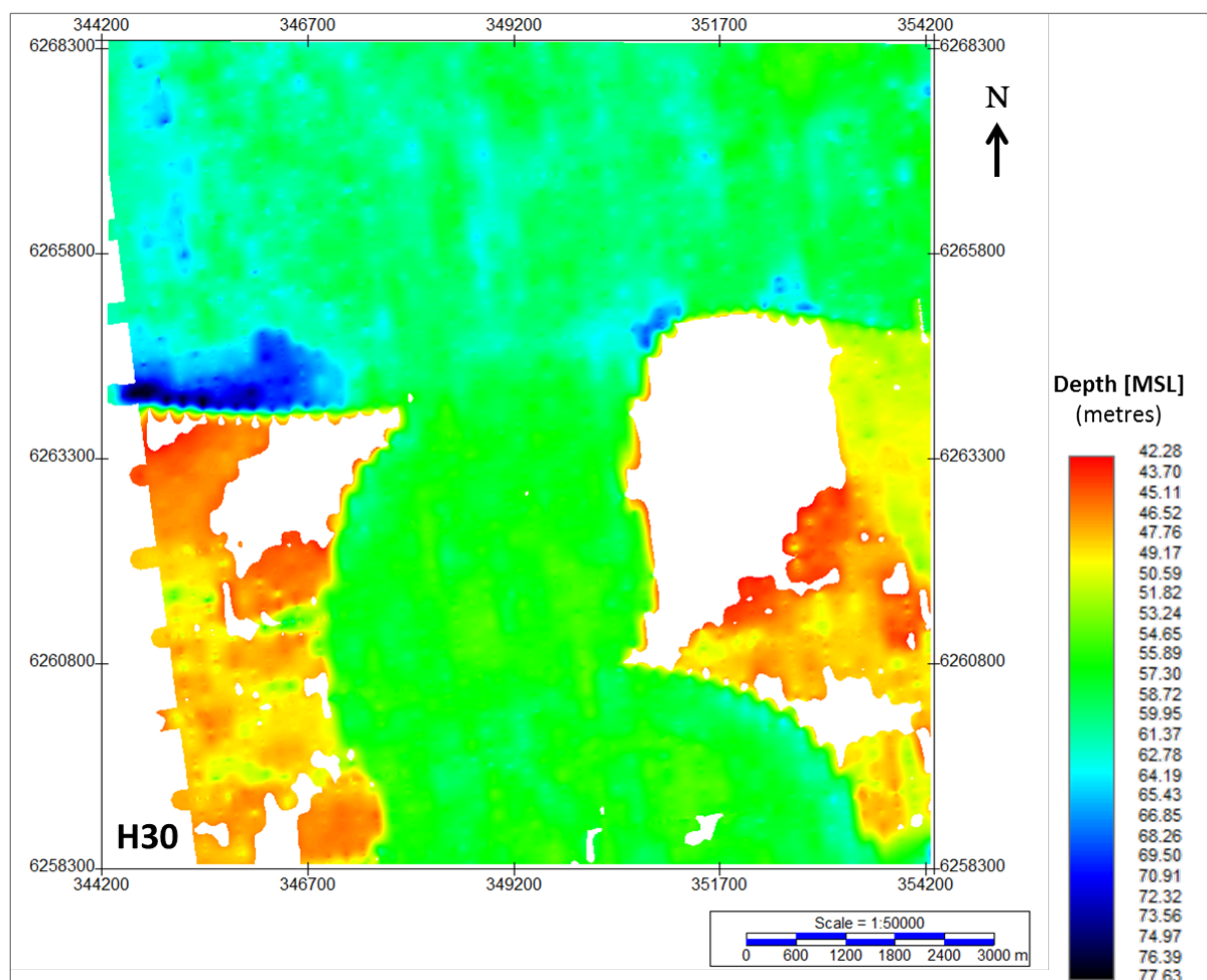


Figure 117 Map showing the lateral extent of U30.
 Units in metres below MSL.

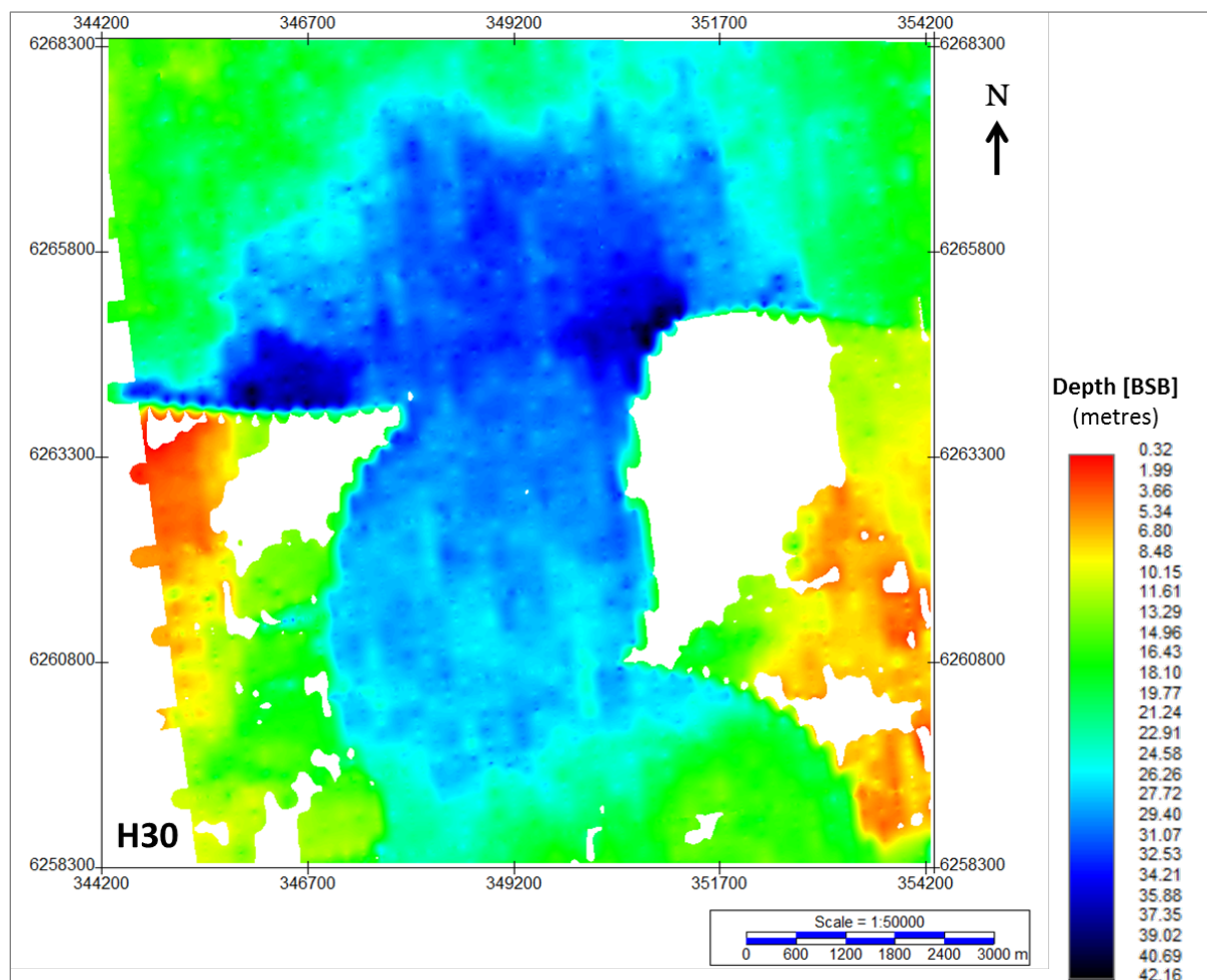


Figure 118 Depth below seabed of H30.
 Units in metres below seabed.

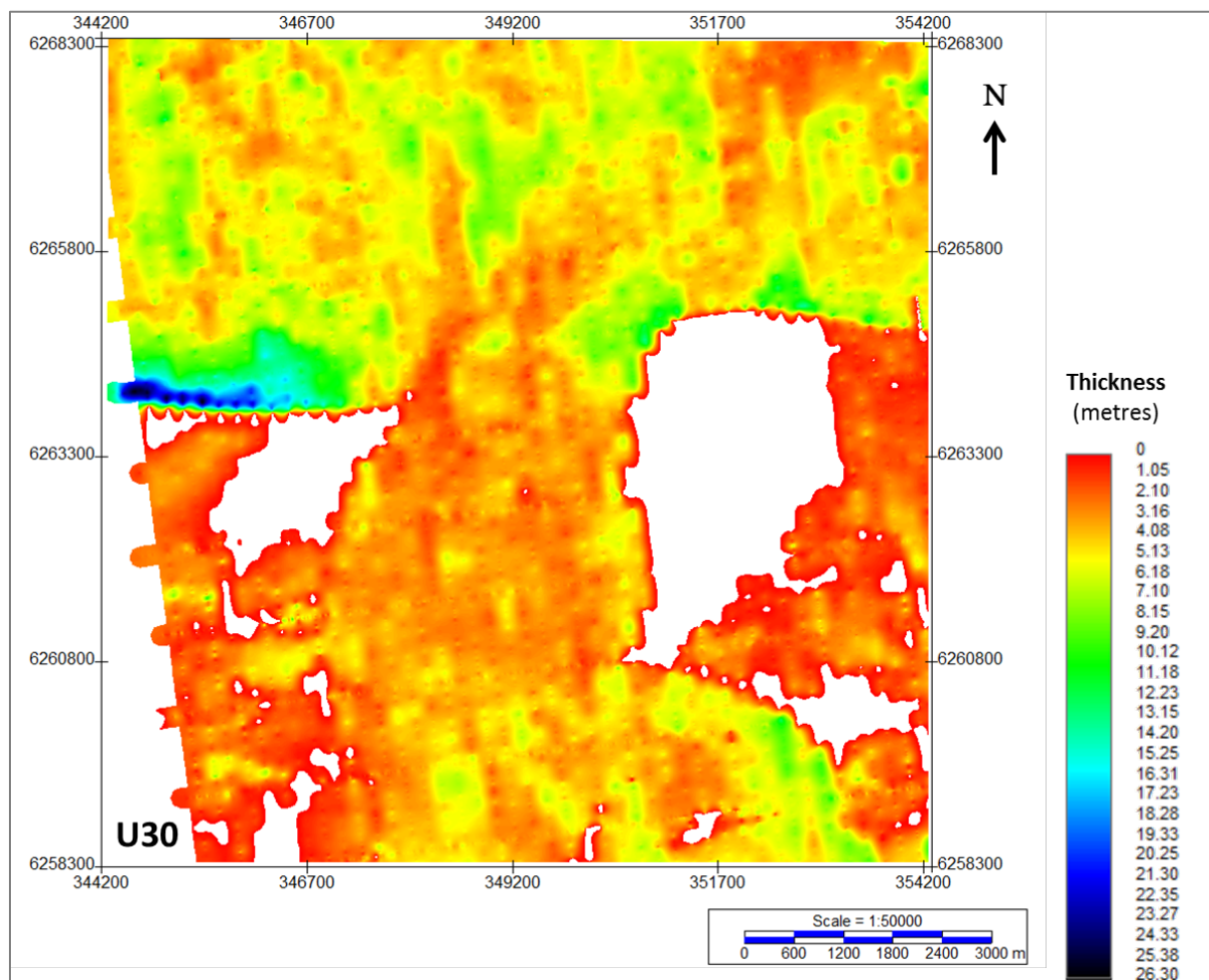


Figure 119 Thickness of unit U30.
 Units in metres.

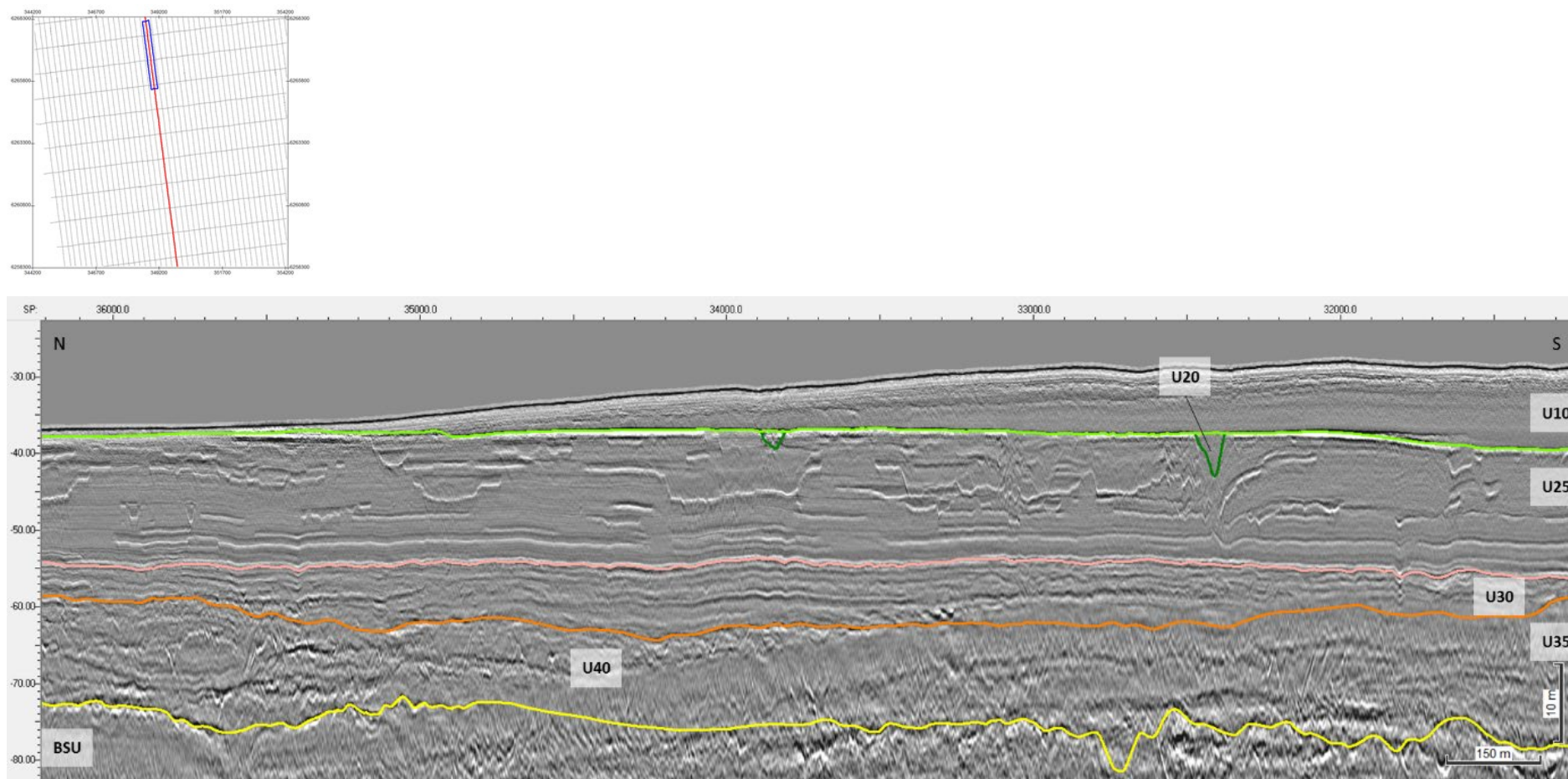


Figure 120 General facies of Unit U30, and the character of horizon H30 (orange).
 Seismic profile BM2_OWF_E_2D_04410

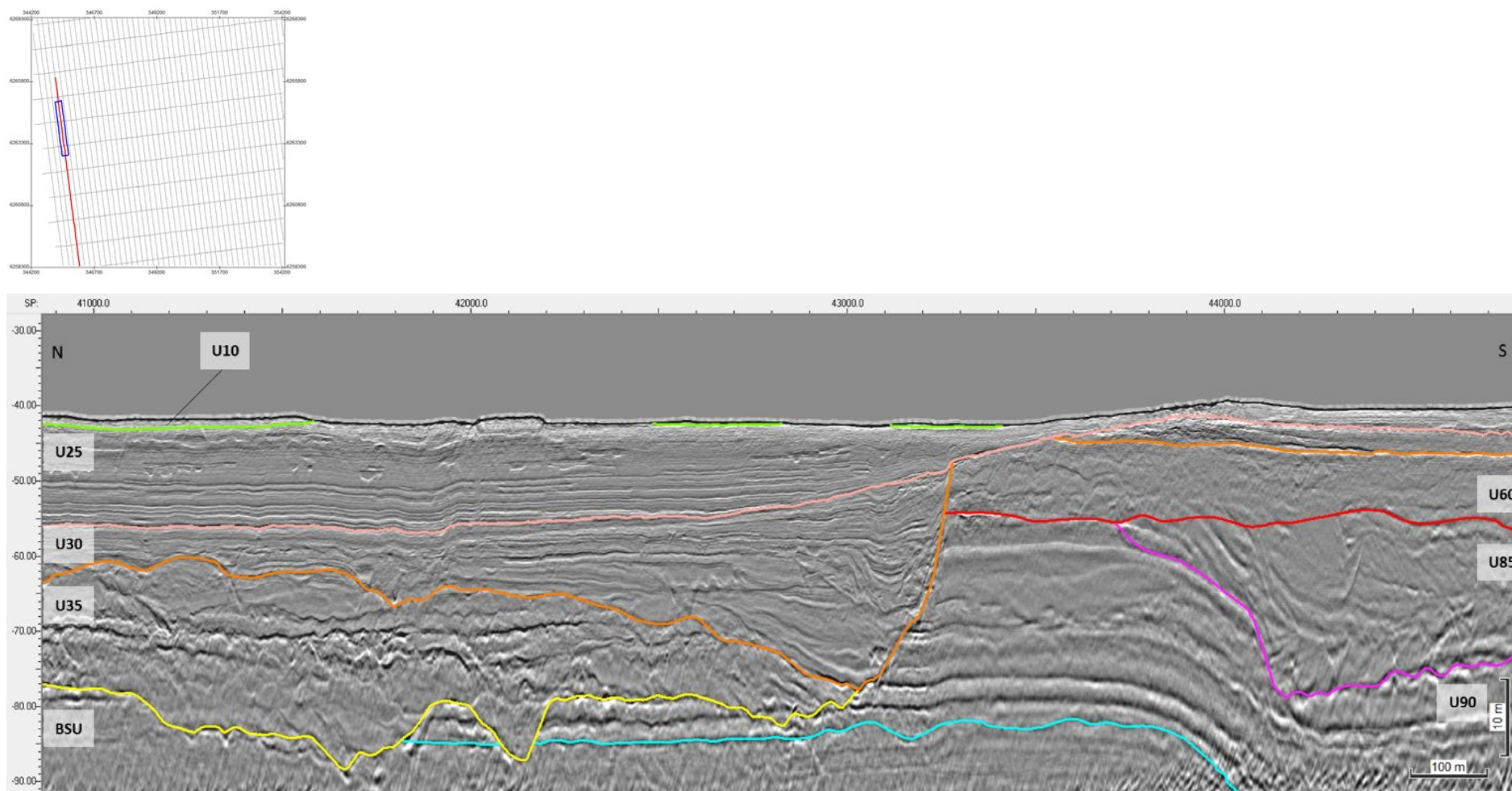


Figure 121 H30 truncating the underlying deposits.
 The image shows the thicker facies of U30 near the SW margin of the central basin.
 Seismic profile BM1_OWF_E_2D_00630

8.6.7 | SEISMIC UNIT U35

Seismic unit U35 is found exclusively within the three major basins of the site. The base of Seismic Unit U35 is defined by horizon H35. The spatial distribution, vertical reference to MLS and the seabed, and thickness of the unit are presented in Figure 122, Figure 123 and Figure 124

Horizon H35 ranges in depth between 42.4 m and 96.1 m below MSL (Figure 122), and between 5.3 m and 60.7 m depth below the seabed (Figure 123). Horizon H35 represents an uneven, rugose, undulating surface (<5 m relief) marking an additional, vertical facies shift within the basins' deposits (Figure 125). This uneven base marks an erosional (Figure 125). When present and continuous, H35 was mapped along a reflector of variable amplitude (low to high).

Seismic unit U35 has a tabular to a mega lens-shaped morphology, usually 2 m to 20-25 m thick. The thickest deposits of U35 are located near the southern margin of the central basin, reaching up to 36.3 m thick (Figure 124). The thinner packages occur within the two basins in the south sector of the site.

U35 comprises the basal deposits of the three major basins. This unit is characterized by composite facies of low to high amplitude reflectors (Figure 125 and Figure 127). Compared to U30 above, U35 comprises larger proportioned and more complex seismic facies associations, such as meso-scale mounds, channels, and lenses. There are numerous internal erosional surfaces separating these features. Large oblique lenses with internal downlaps forming clinoform structures occur at the base. In general, the thickness of the internal packages decreases towards the top, becoming more sub-horizontal and sub-parallel, grading up.

Seismic unit U35 sediments are interpreted to have been deposited in a high energy setting, as evidenced by the meso-scale facies association, the numerous internal erosional surfaces, and more complex geometries. Horizon H35 is an unconformity surface that shaped the base of all three major basins. The ridges and trenches observed at the base elsewhere in the central basin are associated to a major erosional event, filled-in with high energy, fluvial, mega-bedform deposits (flash floods?). The combined sequence of seismic facies U35-U30-U25 present within these is indicative of an overall decrease of energy from the base towards the top. From the seismic character of U35 and its interpreted depositional system, it is estimated that the sediments are likely gravel and sands with enclaves of coarser-grained clasts, possibly decreasing in grain size towards the top of the unit (fining-upward sequence?).

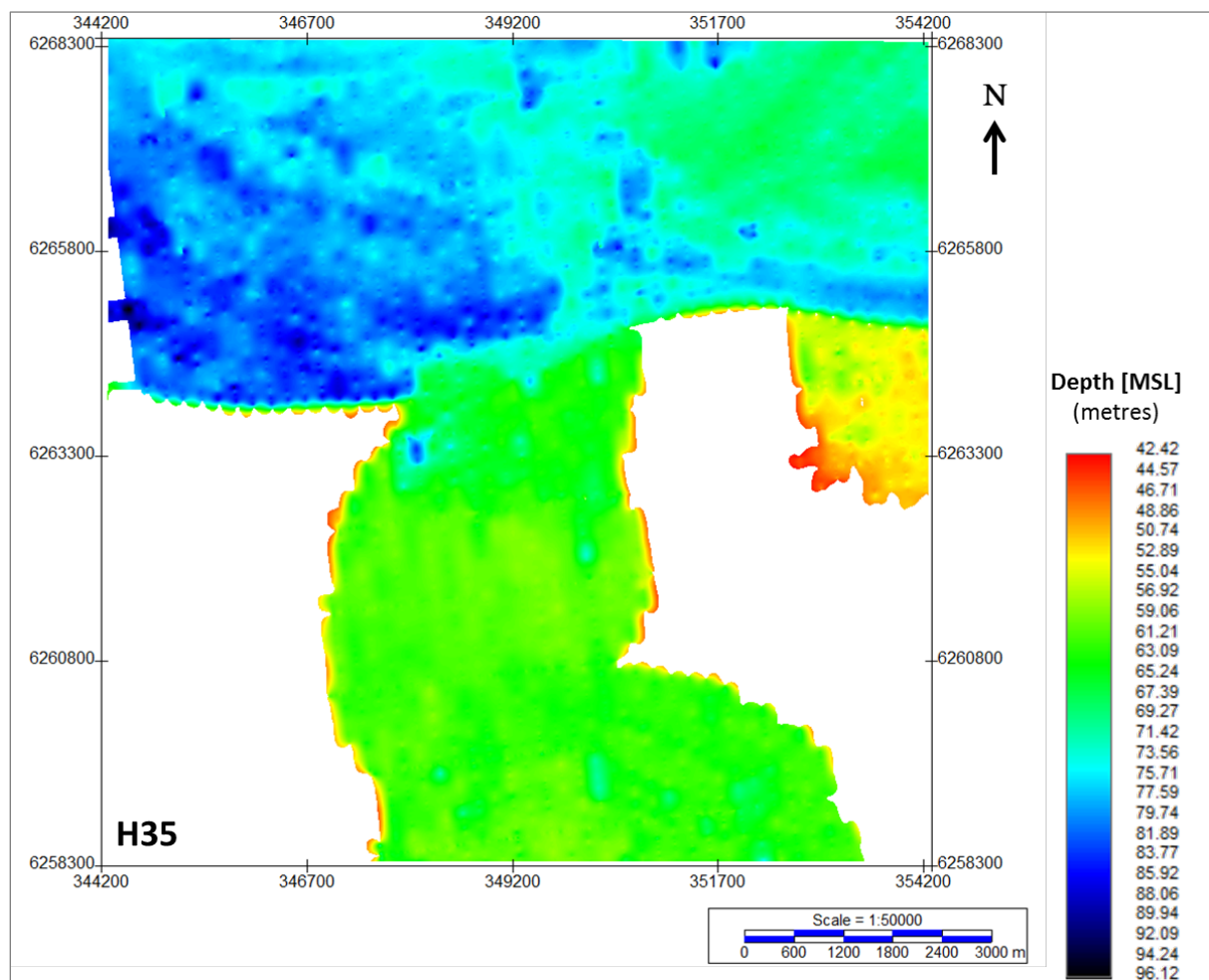


Figure 122 Map showing the lateral extent of U35.
 Units in metres below MSL.

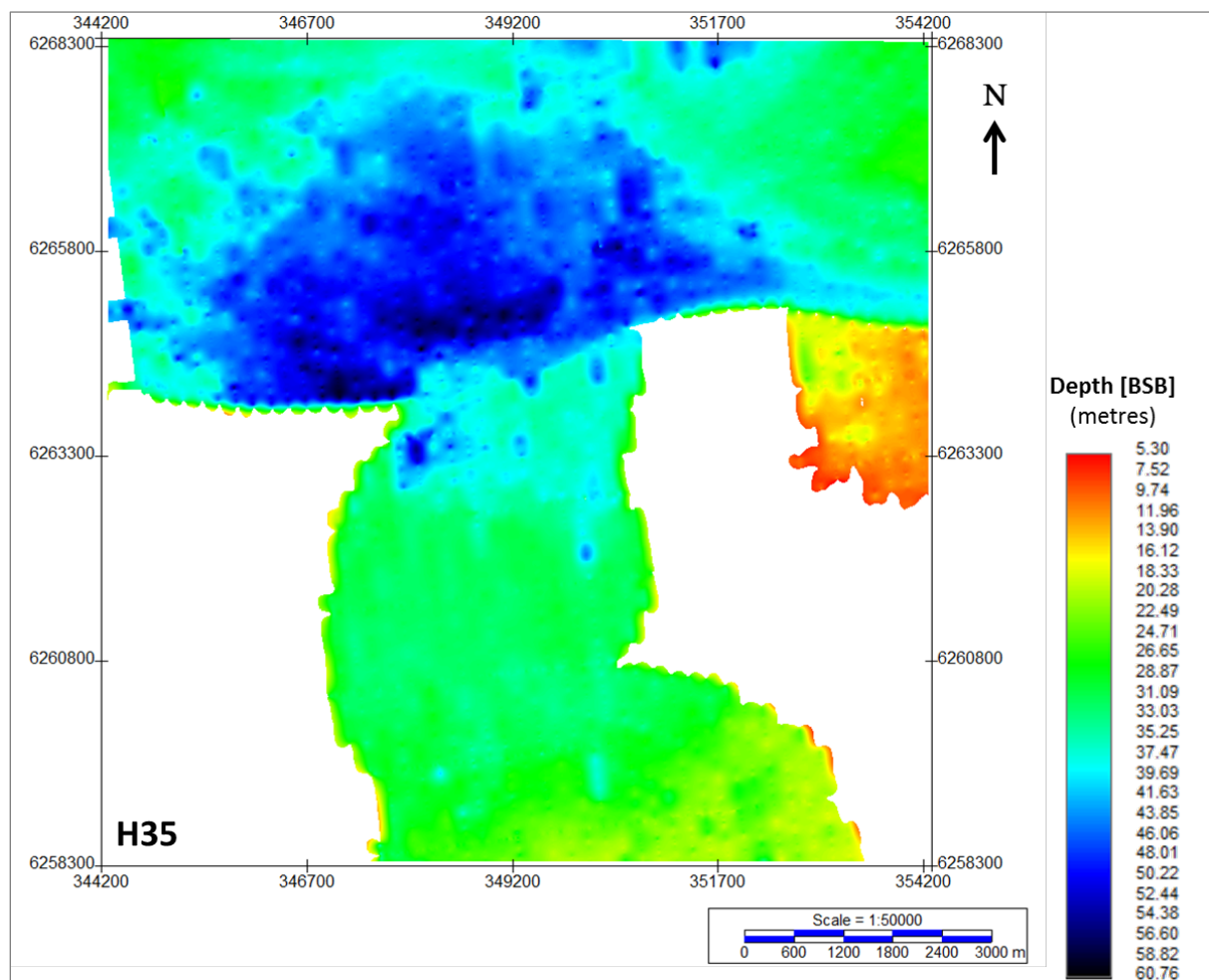


Figure 123 Depth below seabed of H35.
 Units in metres below seabed.

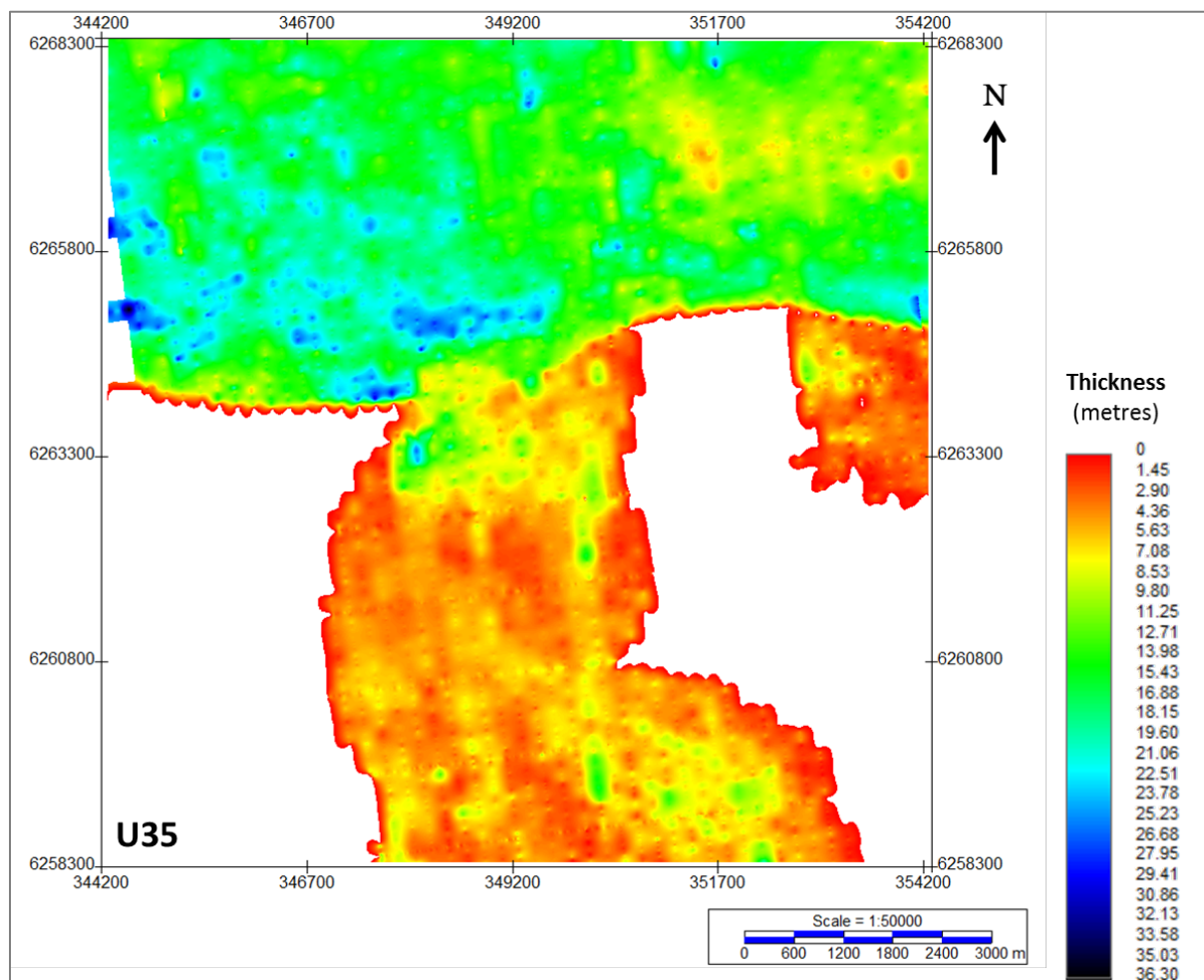


Figure 124 Thickness of unit U35.
 Units in metres.

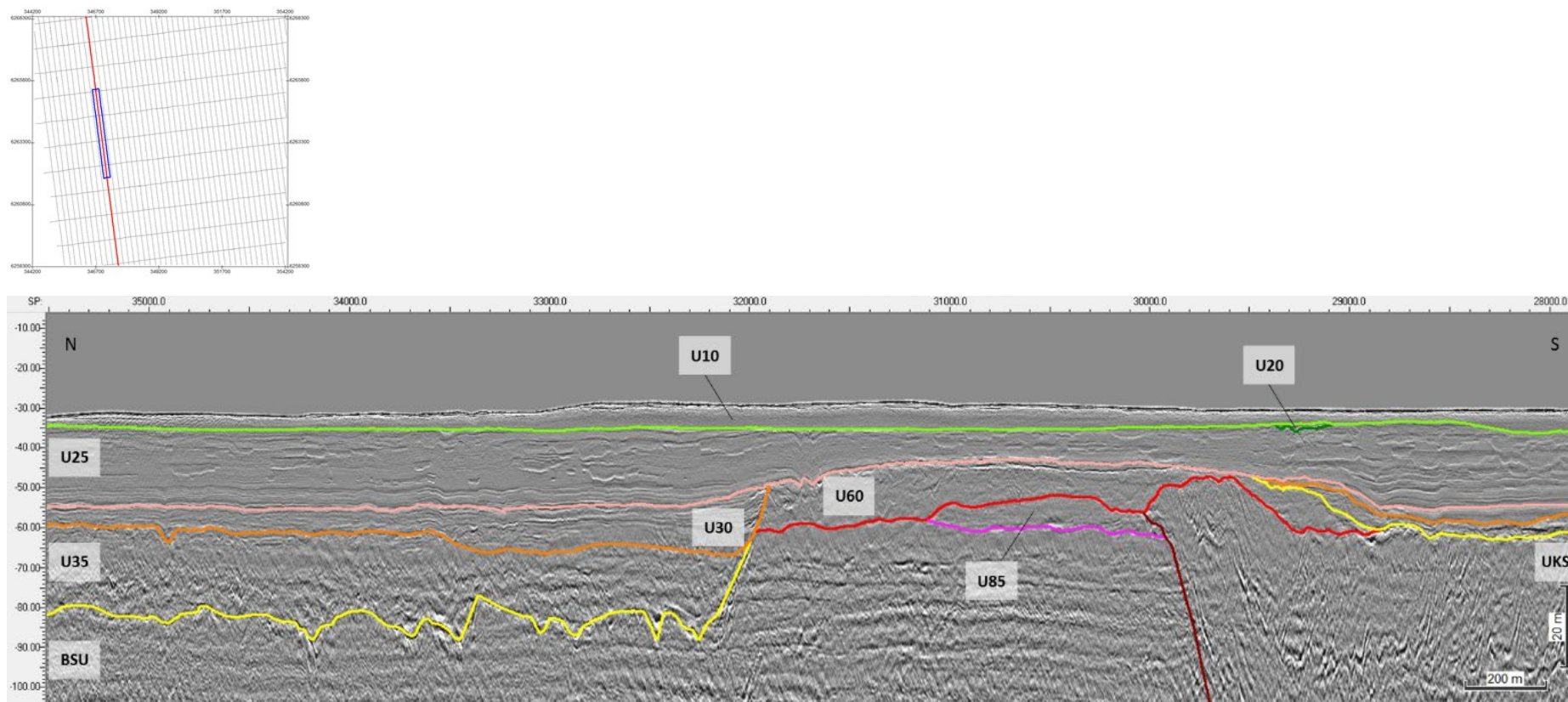


Figure 125 General facies of Seismic Unit U35, and the character of horizon H35 (yellow).
 Seismic profile BM1_OWF_E_2D_02100

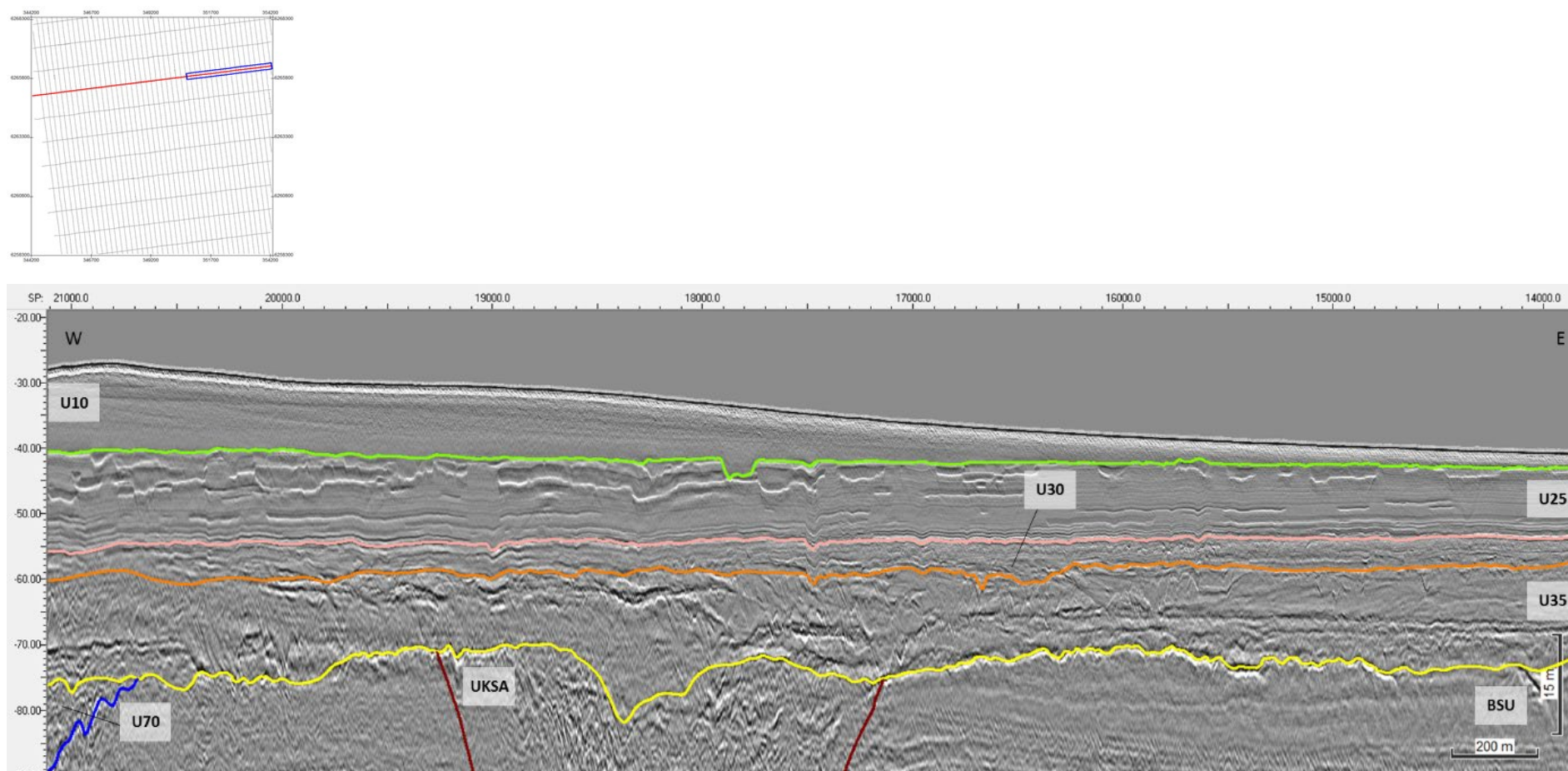


Figure 126 General facies of Seismic Unit U35, truncating the units below.
 Seismic profile BX3_OWF_E_2D_Baseline_2

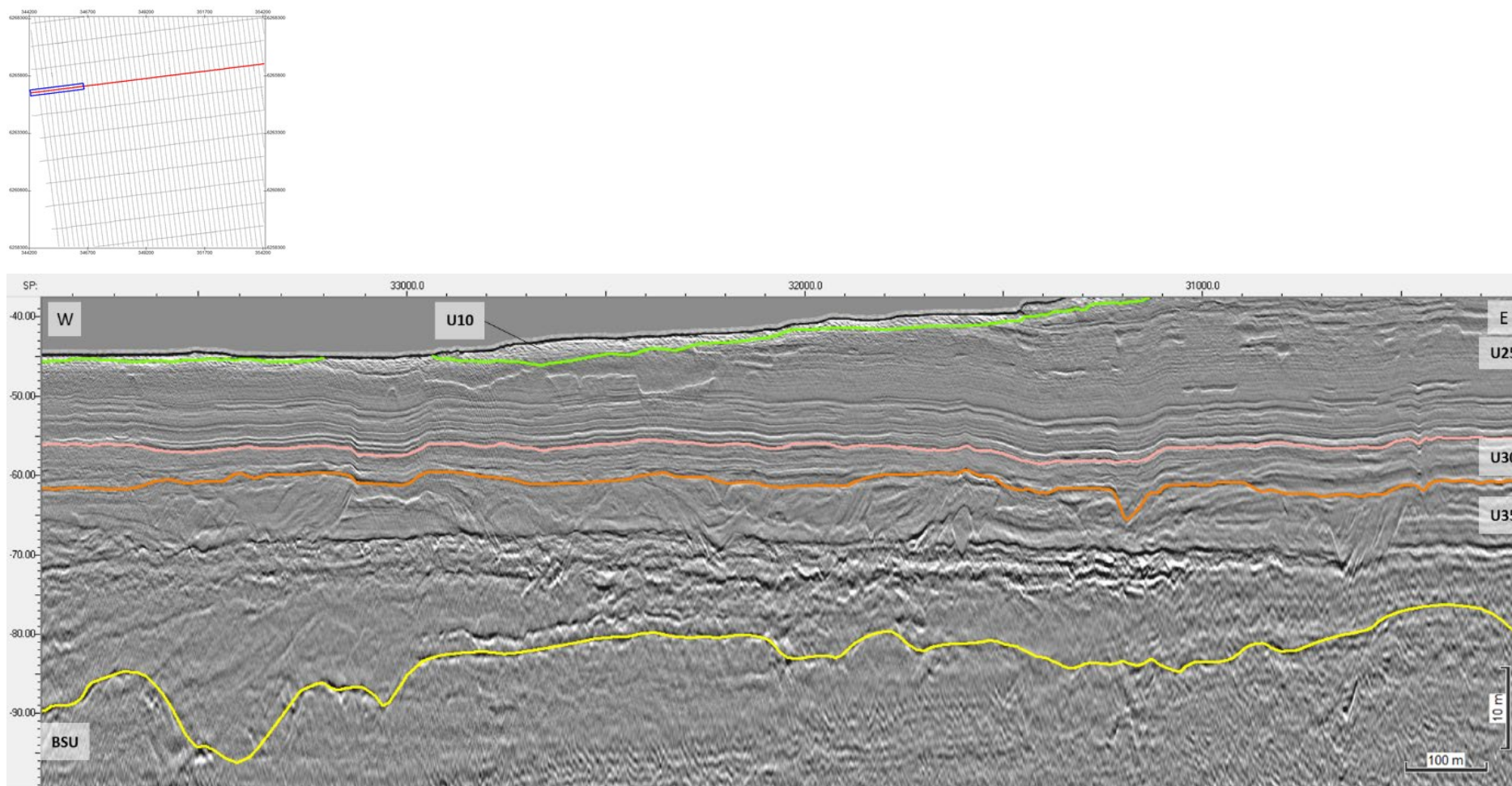


Figure 127 The complex composite facies of Seismic Unit U35.
 Seismic profile BX3_OWF_E_2D_Baseline_2

8.6.8 | SEISMIC UNIT U40

Seismic unit U40 is a key element of the ground model, and extends spatially across the three sectors of the site. The base of Seismic Unit U40 is defined by horizon H40 and is present discontinuously within the survey area. The spatial distribution, vertical reference to MLS and the seabed, and thickness of the unit are presented in Figure 128, Figure 129 and Figure 130.

The main features of seismic unit U40 are large channel incisions delineated at the base by horizon H40, often defined by a vertical facies shift and truncation of the underlying unit. H40 also traces the undulating base of the channel lateral deposits, following a discontinuous reflector of low to medium amplitude. Horizon H40 ranges in depth between 43.7 m and 89.2 m below MSL (Figure 128) and between 2.6 m and 57.8 m depth below the seabed (Figure 129).

The channel incisions of U40 exhibit a wide range of sizes and depositional characteristics, but typically display a V-shape morphology, or U-shape. The larger incisions (total = 5 channels) have been classified into channels of type A or D, in order to best describe their wide variability in size, orientation, and seismic facies (described below; Figure 131). Within the Artificial Island survey area, only a small portion of a large incision is captured (part of CH_11), in the SE corner of the site. Smaller incisions have not been included in this assessment, although they may have been mapped by H40.

Type A channels (polygons H40 CH_05, CH_07, CH_12, CH_14)

Shape: V or U; Orientation: E-W; Max Depth BSL: 60-80 m; Relief: 25-30 m; Width: 800-2200 m; Length: 3000-4000 m.

Example: H40_CH_05, CH_07, CH_14 (Figure 132 and Figure 133).

Seismic facies: Base deposits characterised by mound-chaotic facies with composite mounds above, grading up from meso to micro scale, chaotic in places; upper sections usually with channel facies, with micro parallel wavy and oblique reflectors; variable amplitudes from high to low.

Type D channels (polygon H40 CH_11)

Shape: U; Orientation: ENE-WSW; Max Depth BSL: 90 m; Relief: 40 m; Width: 445 m; Length: 670 m.

Example: H40_CH_11 (Figure 134).

Seismic facies: Composite facies usually comprising three associations; chaotic base with medium-high amplitude to composite mounds; middle facies characterised by sub-tabular deposits with medium amplitude, meso-micro parallel obliques, wavy in places; top facies truncating the deposits below, comprising mounds-channels.

Some U40 channels are positioned (at least partially) directly above older incisions (commonly of U70), exploiting pre-existing incisions. The U40 channel system is interpreted to be associated with drainage of glacier melt back from the north, and outwash plains. The seismic facies pattern in U40 is interpreted to represent channel deposition with variable infill history – i.e. periods with high energy and coarser material deposition, and periods of lower energy with deposits of (clay) silt and sand, which may be related to glaciolacustrine deposition.

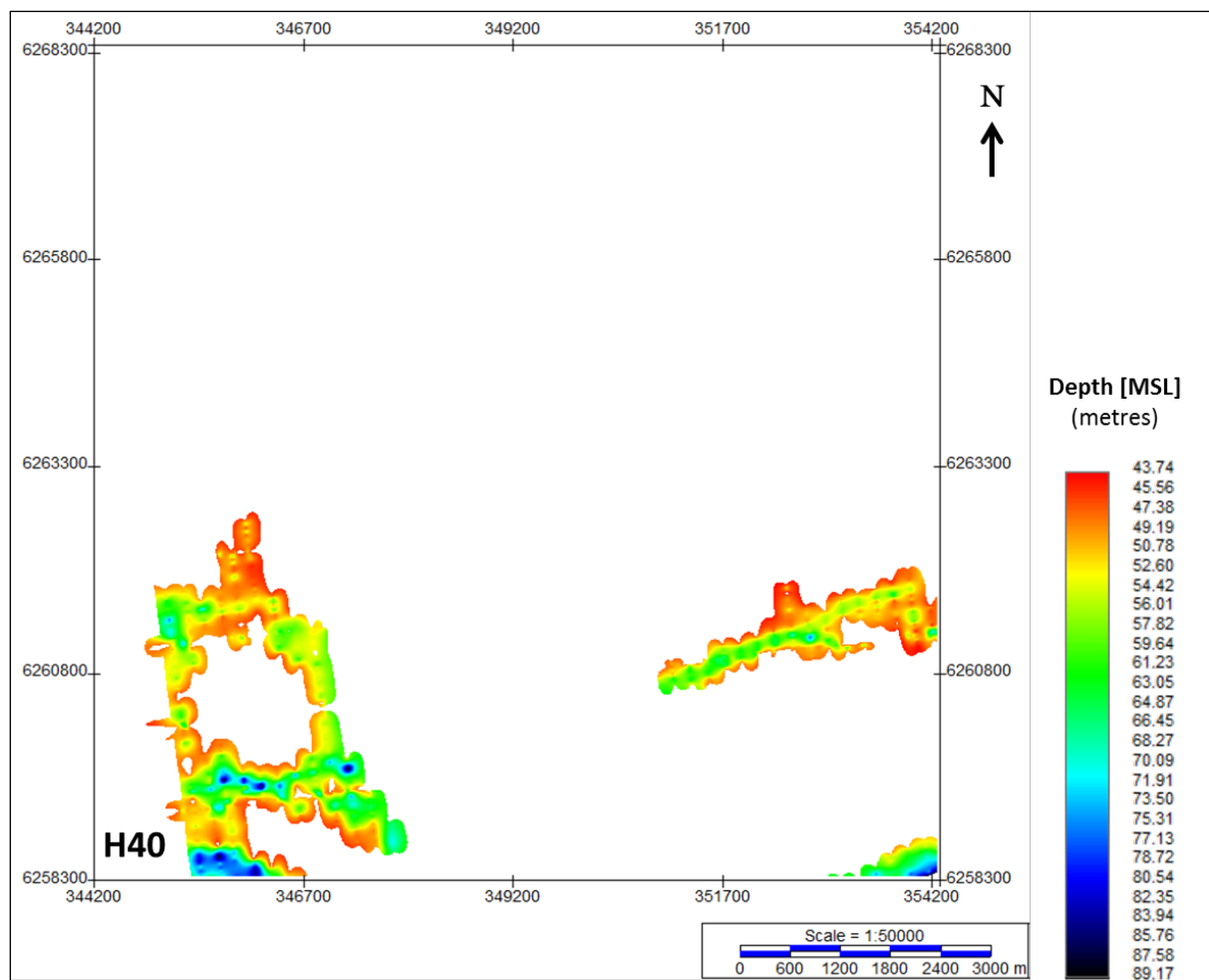


Figure 128 Map showing the lateral extent of U40.
 Units in metres below MSL.

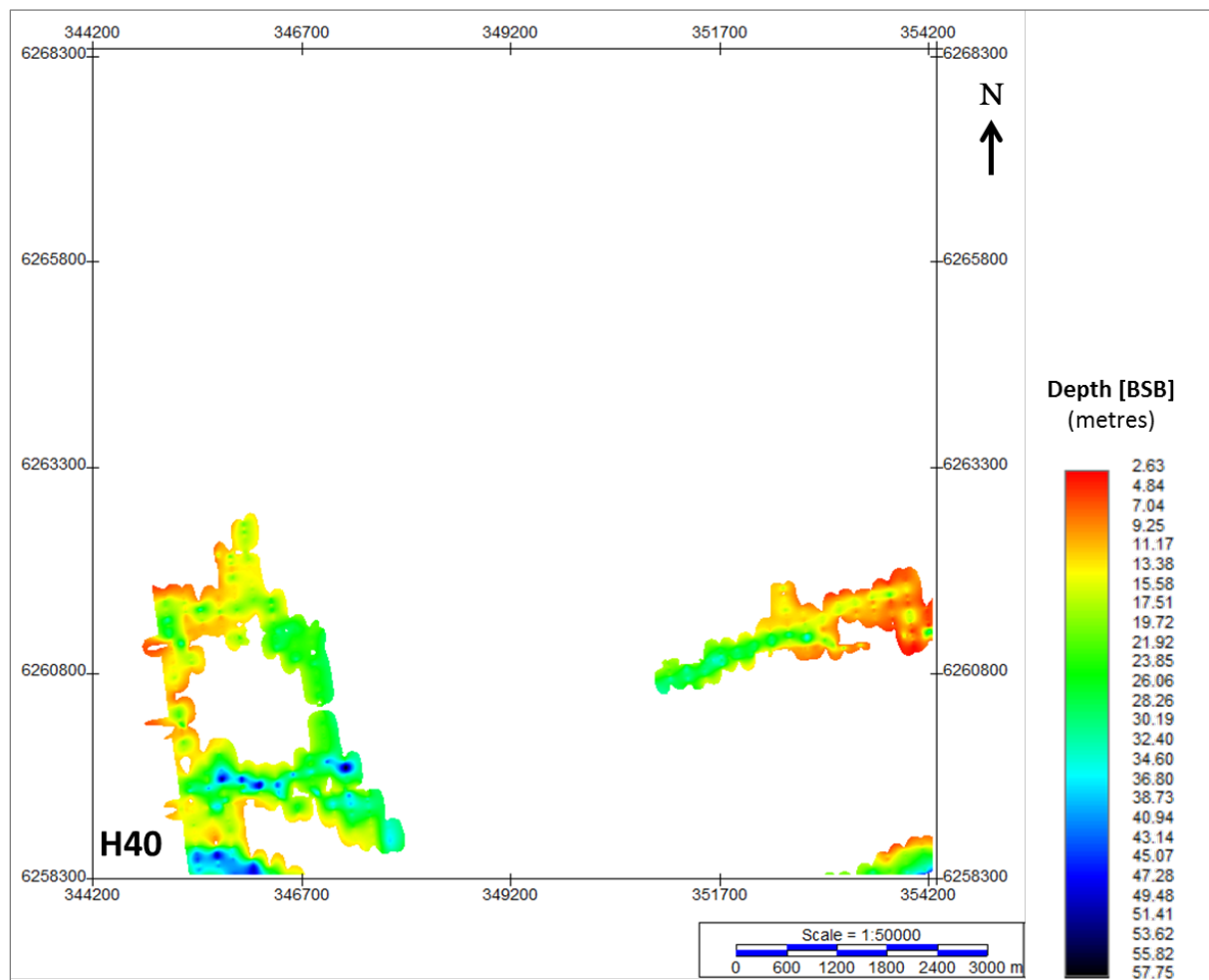


Figure 129 Depth below seabed of H40.
 Units in metres below seabed.

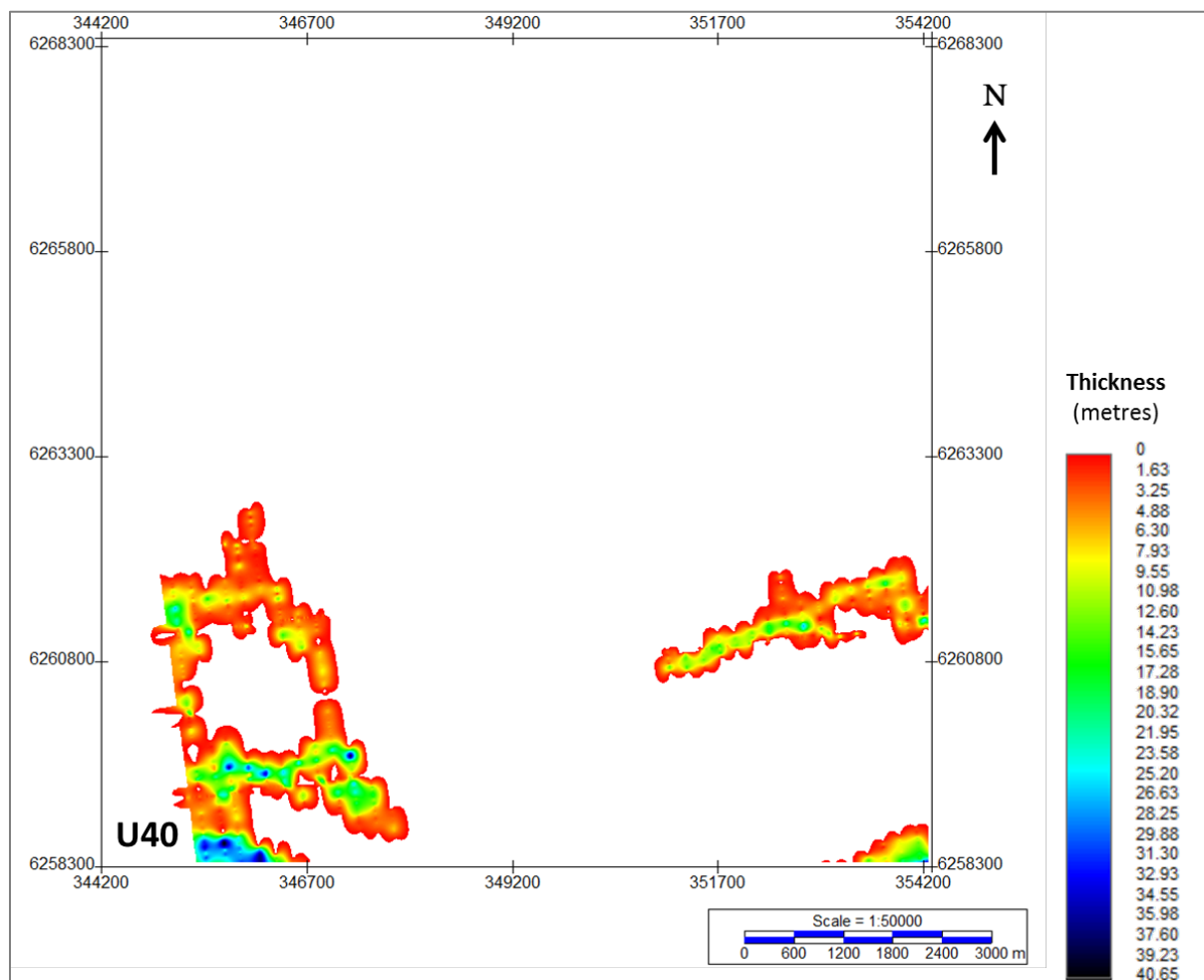


Figure 130 Thickness of unit U40.
 Units in metres.

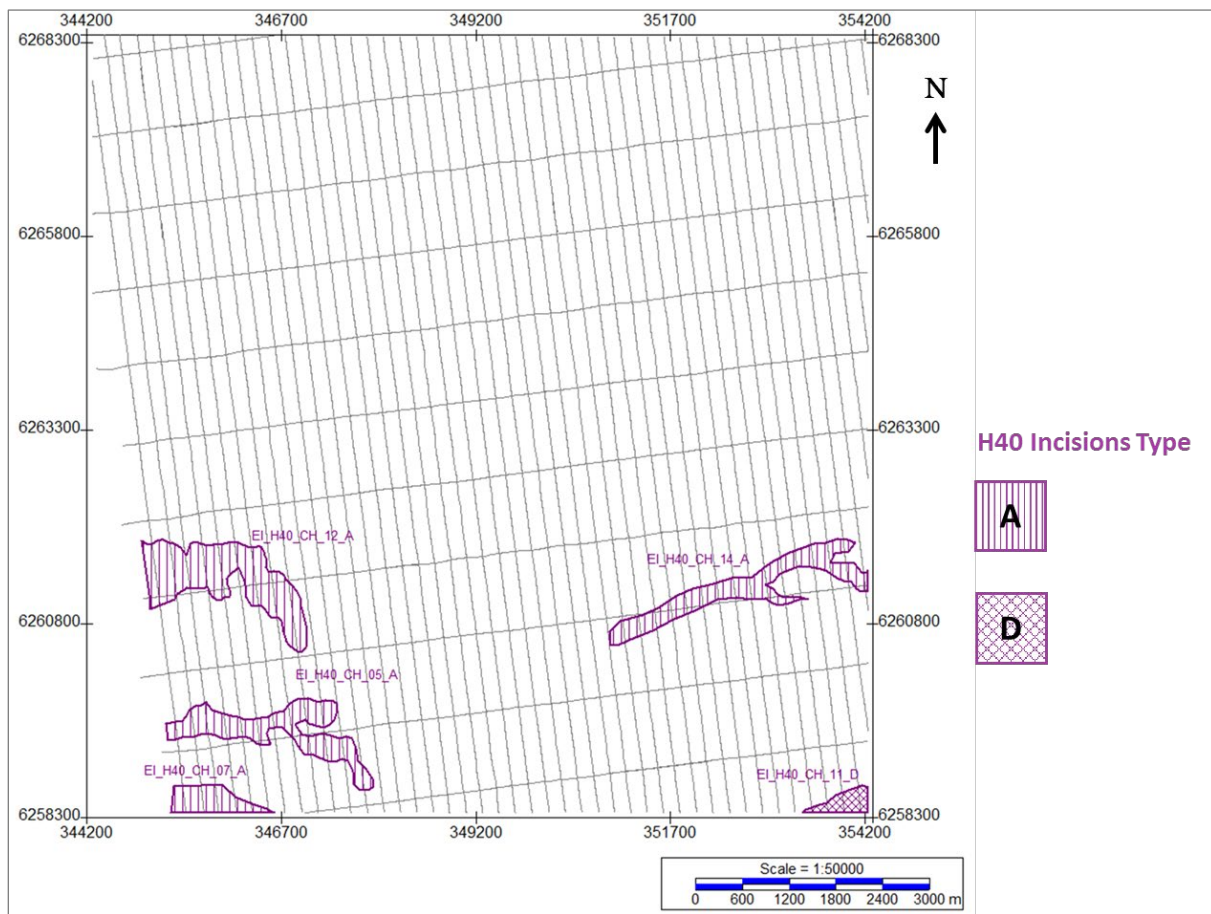


Figure 131 Spatial distribution of the different types of channels identified for Seismic Unit U40.

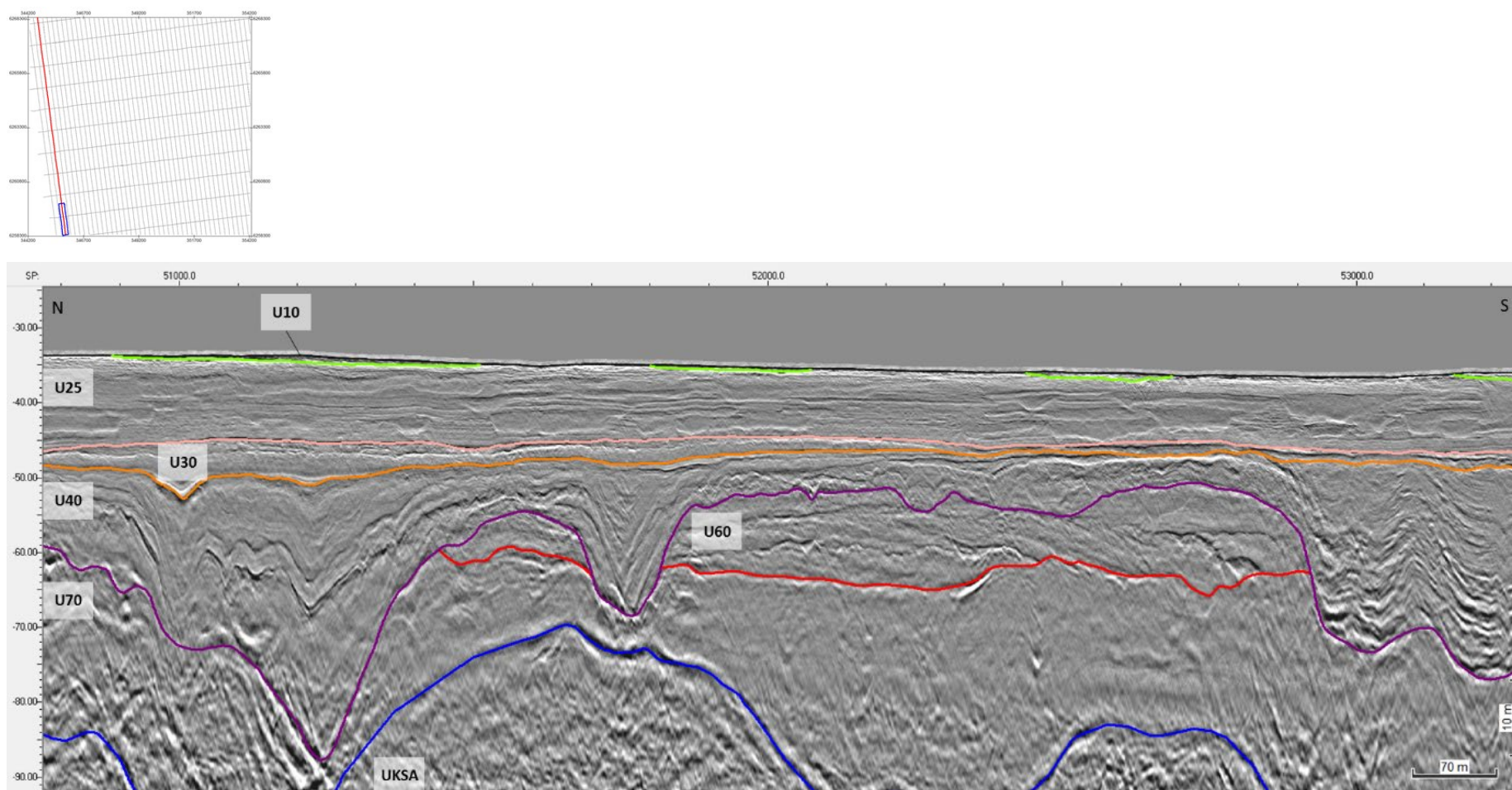


Figure 132 General facies of Type A channels of Seismic Unit U40.
 The image also shows the character of horizon H40 (deep magenta).
 Example shown: H40_CH_05 (northern channel) and H40_CH_07 (southern channel). Seismic profile BM1_OWF_E_2D_02100.

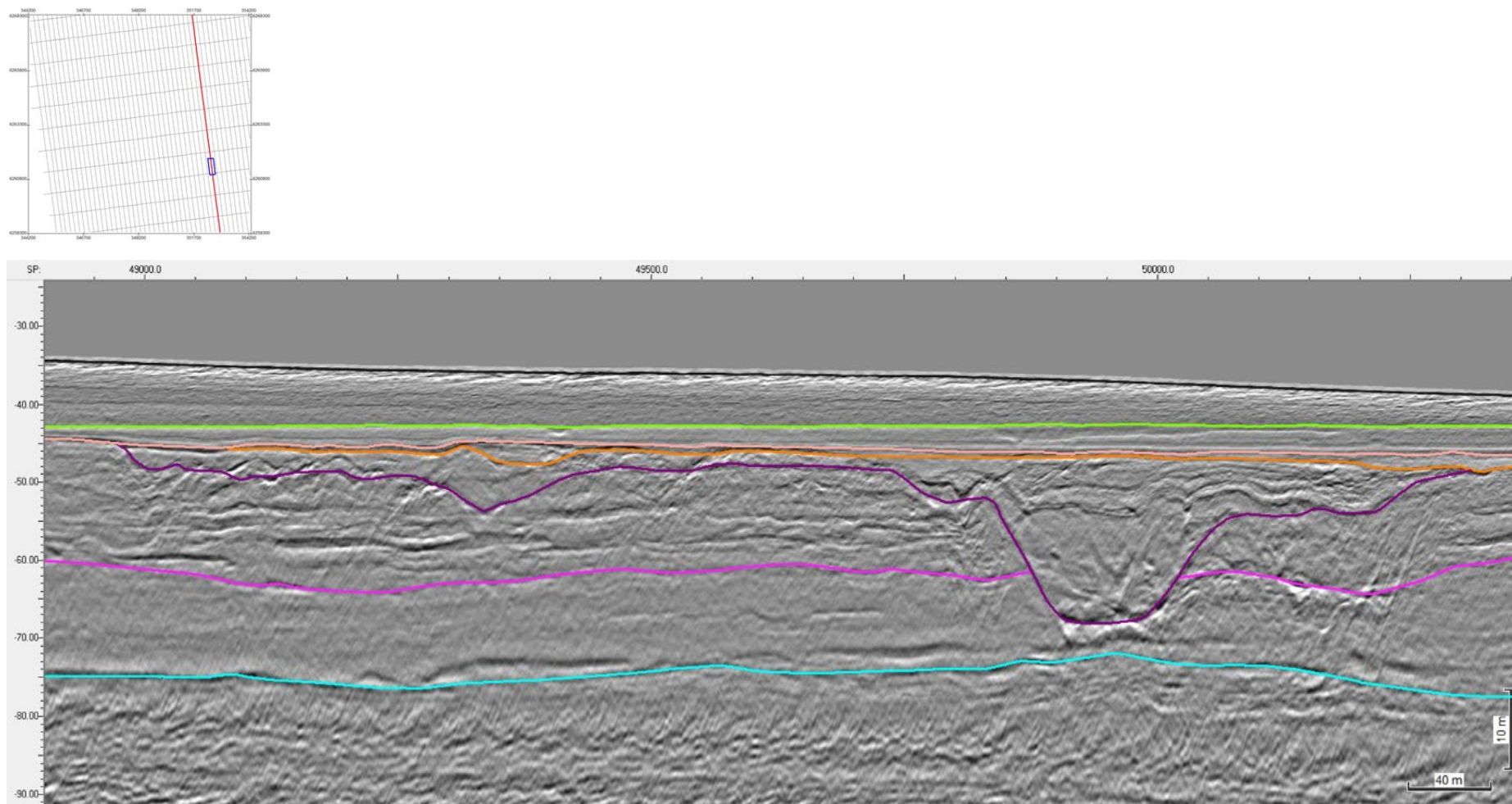


Figure 133 General facies of Type A channels of Seismic Unit U40.
 The image also shows the character of horizon H40 (deep magenta).
 Example shown: H40_CH_14. Seismic profile BM3_OWF_E_2D_07350

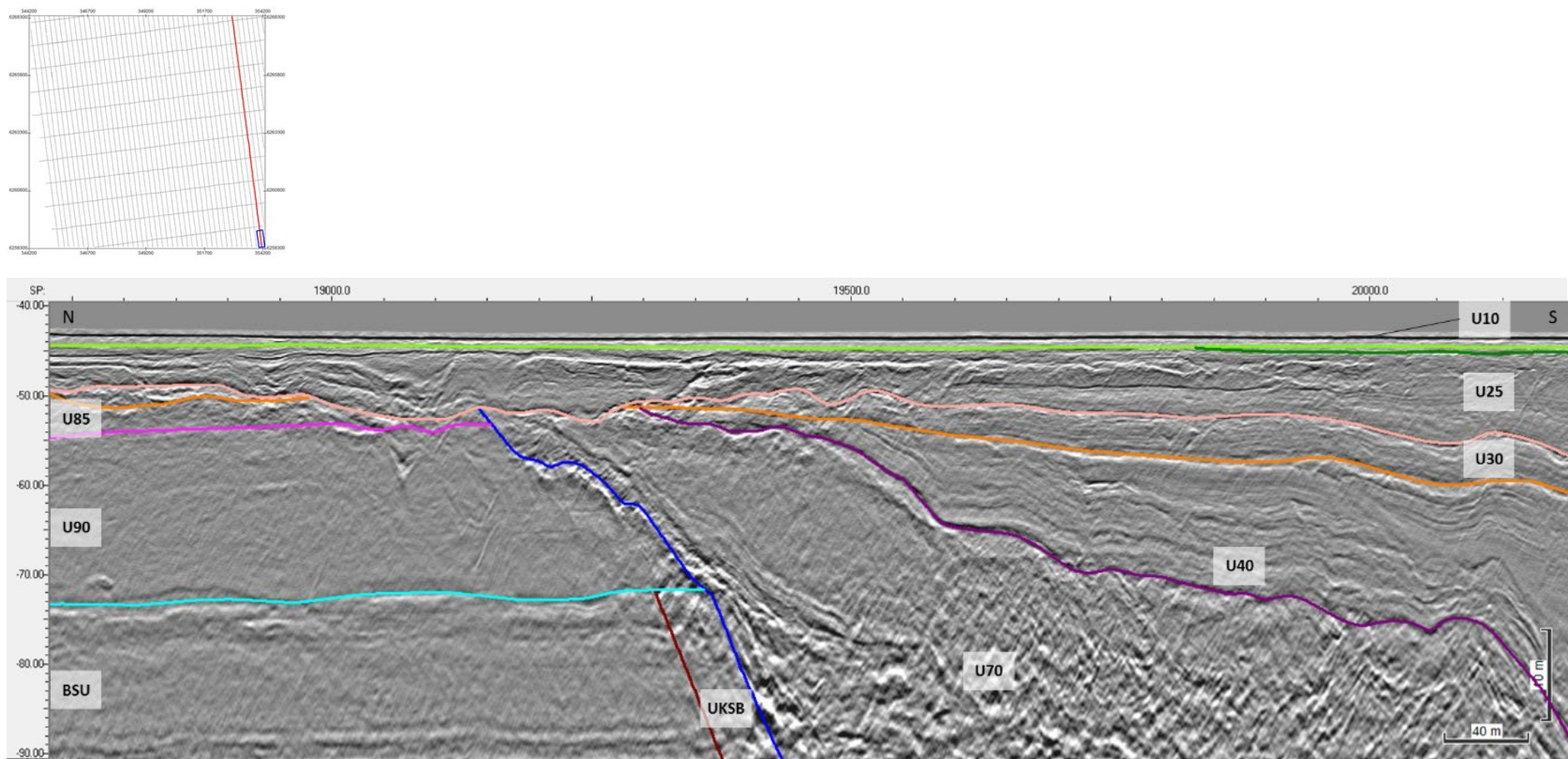


Figure 134 General facies of Type D channels of Seismic Unit U40.
 The image also shows the character of horizon H40 (deep magenta).
 Example shown: H40_CH_11. Seismic profile BM4_OWF_E_2D_08610

8.6.9 | SEISMIC UNIT U50

Seismic unit U50 only occurs within the north sector of the full MMT OWF survey area, not present with the Artificial Island survey area.

Seismic unit U50 deposits are interpreted to comprise fine sediments. Scattered point diffractors within U50 may be related to the presence of boulders. The origin of seismic unit U50 is uncertain, as it may correspond to a glacial drift deposit (aqua till?) or be associated to glaciolacustrine deposition (?).

8.6.10 | SEISMIC UNIT U60

Seismic unit U60 occurs within the north and south sectors of the survey area. The base of Seismic Unit U60 is defined by horizon H60 and is present discontinuously within the survey area. The spatial distribution, vertical reference to MSL and the seabed, and thickness of the unit are presented in Figure 135, Figure 136 and Figure 137

Horizon H60 ranges in depth between 42.3 m and 68.3 m below MSL (Figure 135) and between 6 m and 43.6 m depth below the seabed (Figure 136) Horizon H60 traces an uneven, rugose, undulating surface of pronounced relief (up to 20 m vertical range), truncating the units below it (Figure 138). H60 follows a positive reflector of high amplitude.

Seismic unit U60 is generally a thick (4-10 m) unit of sub-horizontal tabular to mega-lens shape, thickening at localized incisions of variable size (up to 22.6 m thick) (Figure 137). These incisions form channelized areas with a symmetrical to asymmetrical V-shape, with heights ranging from <5 m to ~22 m depth (Figure 138).

Seismic unit U60 is recognizable in the UHRS dataset by its composite facies of low to high amplitude reflectors (Figure 138 and Figure 139). U60 comprises complex internal features of meso-scale proportions, such as mounds, channels, and lenses. There are numerous oblique internal erosional surfaces separating these features, marked by high amplitude reflectors. Large clinoform layers fill-in the larger incisions. In general, the thickness of the internal packages decreases towards the top, becoming more sub-horizontal and sub-parallel.

Seismic unit U60 sediments are interpreted to have been deposited in a high energy setting. The infill within the wide valleys are mega-bedforms, interpreted to be high energy fluvial bedforms (related to flash floods?), evidenced by the meso-scale seismic facies association, the numerous internal erosional surfaces, and more complex geometries. Horizon H60 is an unconformity that shaped a pronounced paleo-relief. From the seismic character of U60 and its interpreted depositional system, it is estimated that the sediments are mainly sands with gravel and silt (?).

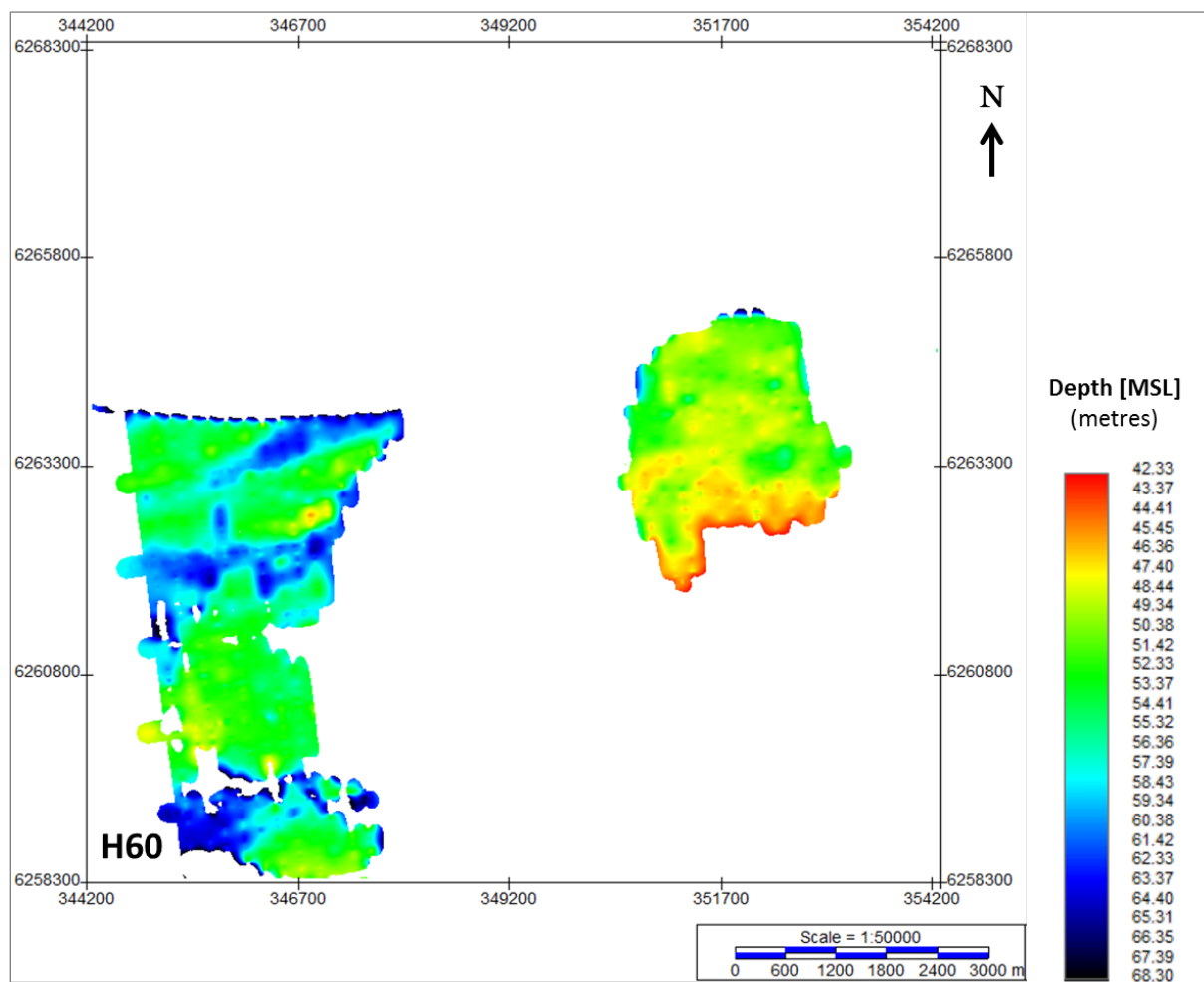


Figure 135 Map showing the lateral extent of U60.
 Units in metres below MSL.

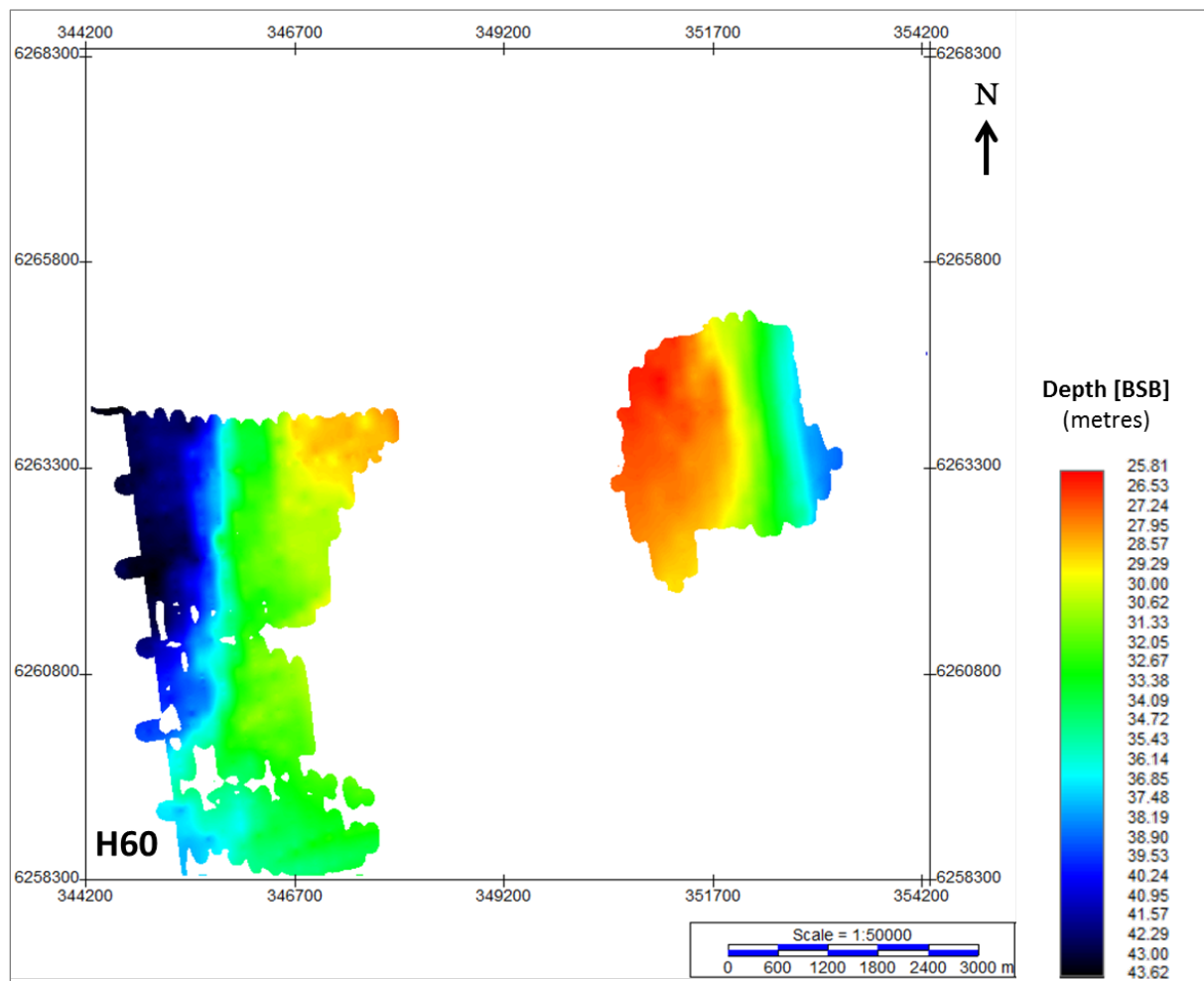


Figure 136 Depth below seabed of H60.
 Units in metres below seabed.

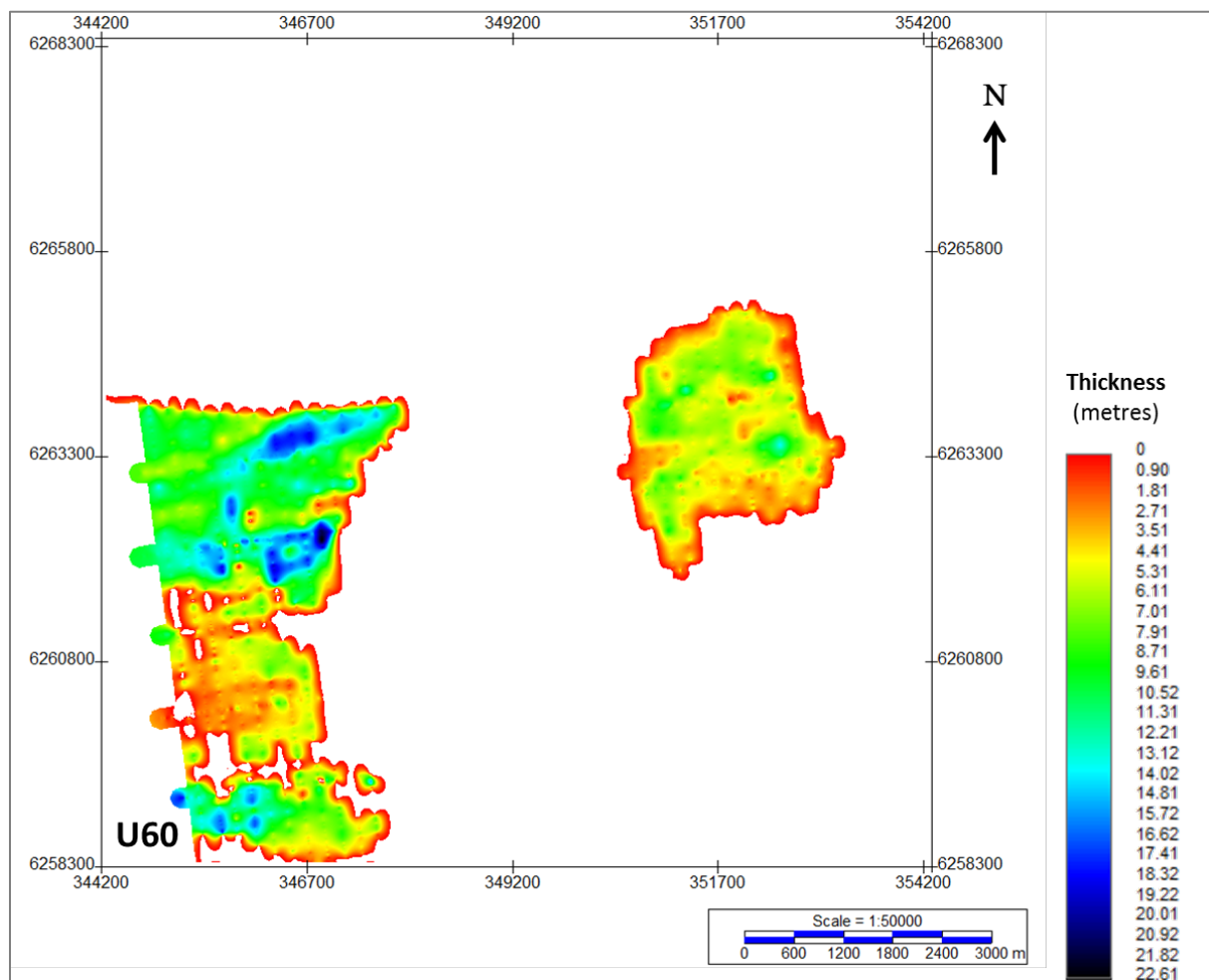


Figure 137 Thickness of unit U60.
 Units in metres.

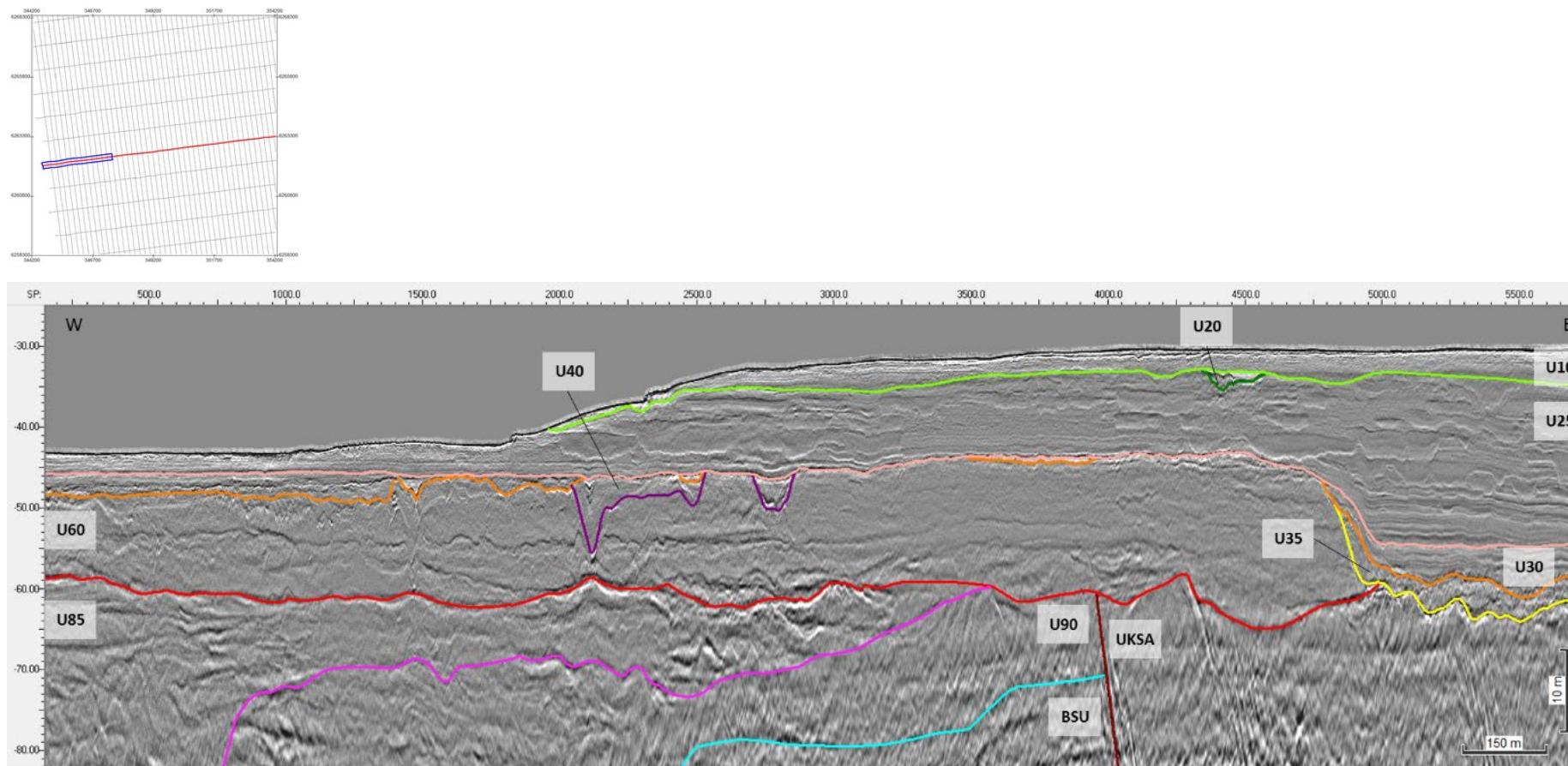


Figure 138 General facies of Seismic Unit U60, and the character of horizon H60 (red).
 Seismic profile BX3_OWF_E_XL_23000

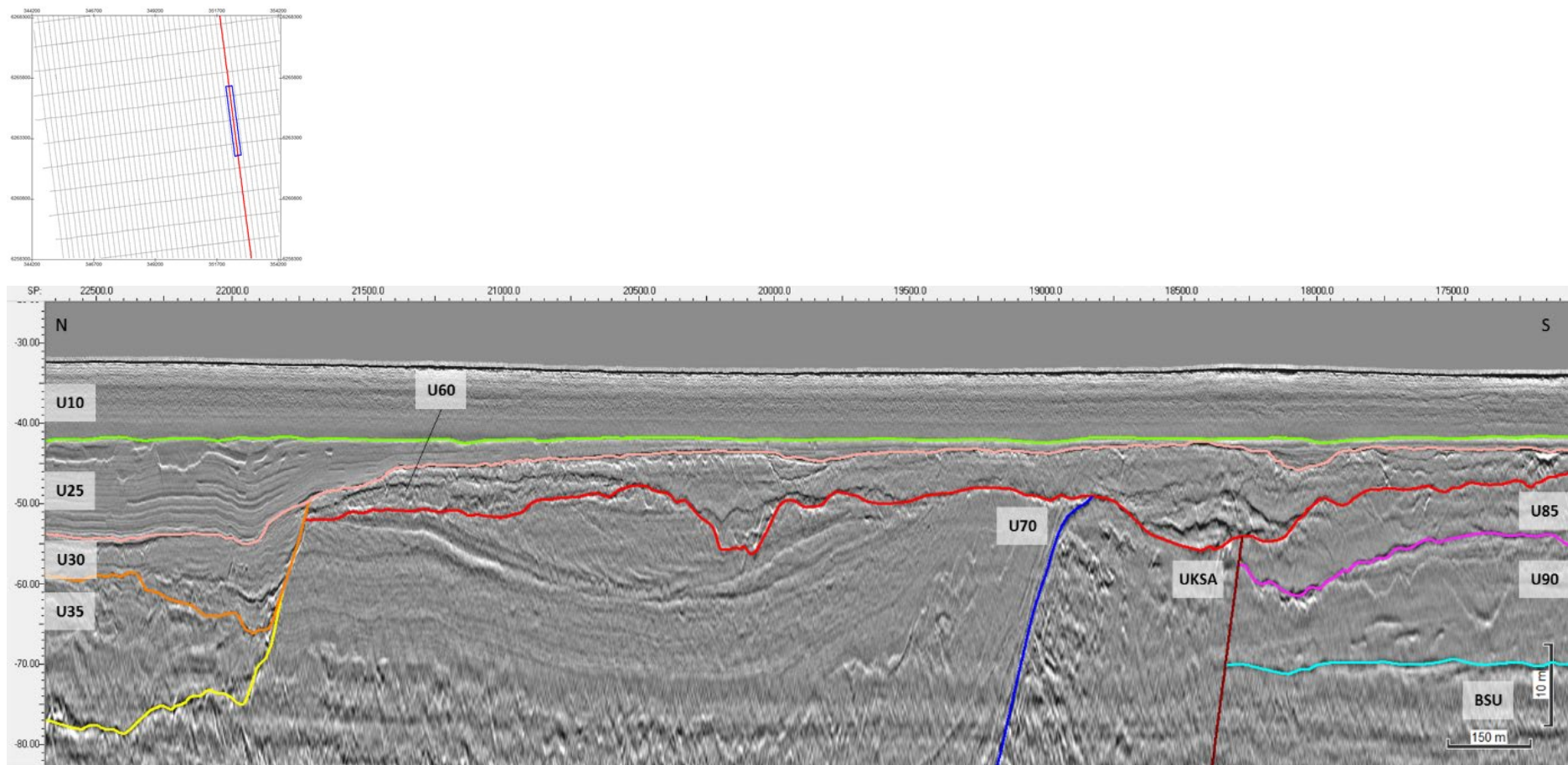


Figure 139 General facies of Seismic Unit U60, and the character of horizon H60 (red).
 Seismic profile BM3_OWF_E_2D_07560

8.6.11 | SEISMIC UNIT U70

Seismic unit U70 is a major element of the ground model, and extends spatially across the two sectors of the Artificial Island survey area. The base of Seismic Unit U70 is defined by horizon H70 and is present discontinuously within the site. The spatial distribution, vertical reference to MSL and the seabed, and thickness of the unit are presented in Figure 140, Figure 141 and Figure 142.

The main features of seismic unit U70 are large channel incisions delineated at the base by horizon H70. H70 is mapped either along medium-high amplitude reflector or tracing a vertical facies shift, truncating the units below it. H70 is locally undulating. Horizon H70 ranges in depth between 46.87 m and 164.5 m below MSL (Figure 140) and between 3.9 m and 133.1 m depth below the seabed (Figure 141).

The channel incisions of U70 exhibit a wide range of sizes, orientations, and internal facies. Three major incisions were identified and delineated by polygons H70 CH_06, CH_08, and CH_09 (Figure 143). Their general characteristics are summarised in Table 27.

Table 27 General characteristics of the large incisions within seismic unit U70. Polygons displayed in Figure 143.

Polygon ID	Shape	Orientation	Max Depth (m BSL)	Relief (m)	Width (m)	Length (m)
H70_CH_06	U open	NE-SW	140	<60	1200	23000
H70_CH_08	U open	N-S to NE-SW	160	<100	800	12000
H70_CH_09	U	WNW-ESE	170	<100	1200	6000

The infill deposits of these incisions exhibit a basal facies of medium to high amplitude, with meso-scale mounds-channels-parallel, occasionally chaotic (Figure 144 to Figure 147). The upper facies have a truncating base, generally lower amplitudes, and comprises meso-micro composite mounds-channels, parallel-obliques. Chaotic-homogeneous transparent facies are also common in these upper sections.

For the most part, these incisions rest above older deformed sediments which may be related to glaciotectonism and to the formation of the valley itself (evidenced by collapse structures directly below H70) (Figure 144). The deposits that infill these incisions have a composite facies that is generally organised and layered (albeit chaotic in places), which may be associated to glaci-fluvial deposition, in a proglacial, sub-aerial environment (e.g. reoccupation of tunnel valley depressions by fluvial systems).

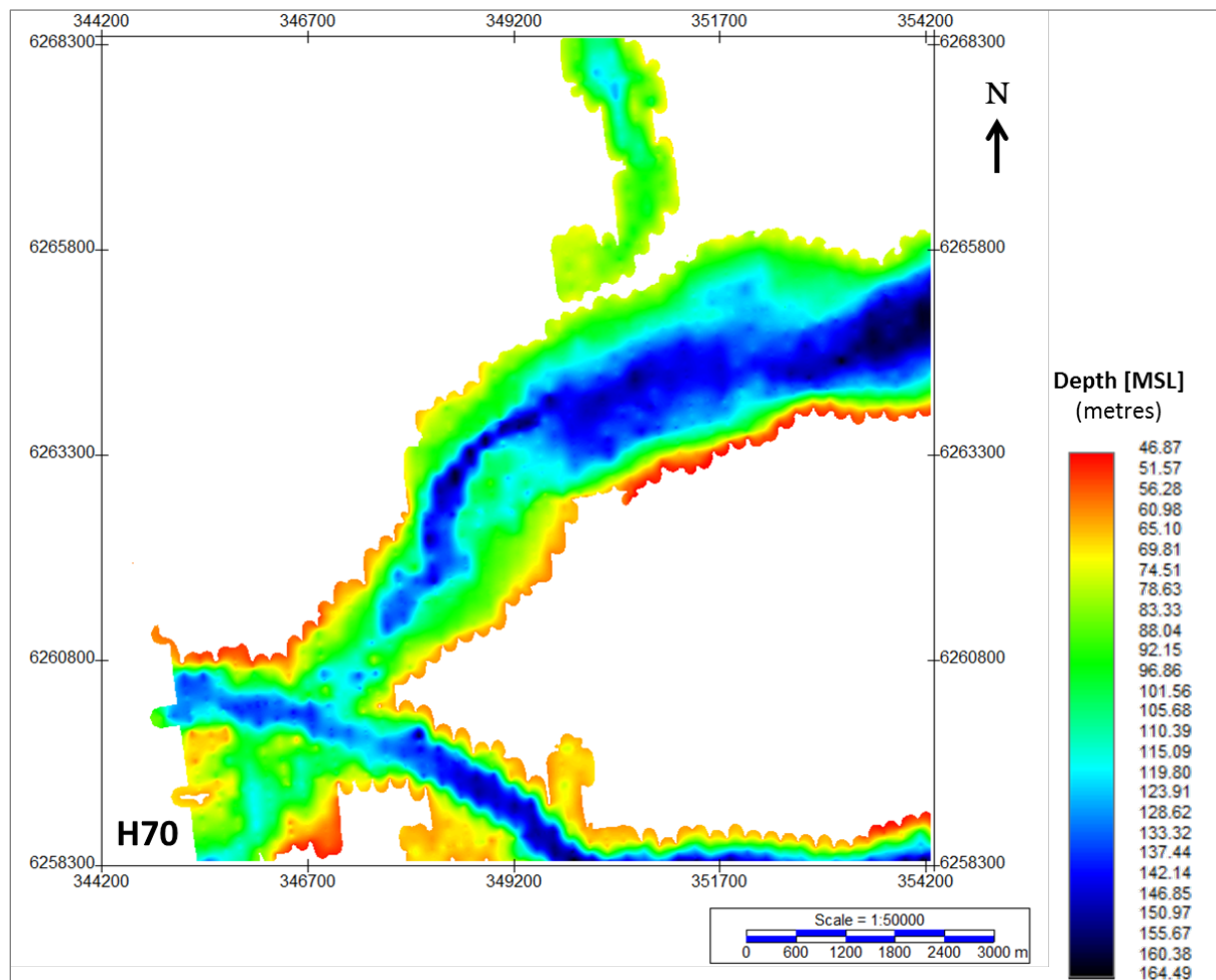


Figure 140 Map showing the lateral extent of U70.
 Units in metres below MSL.

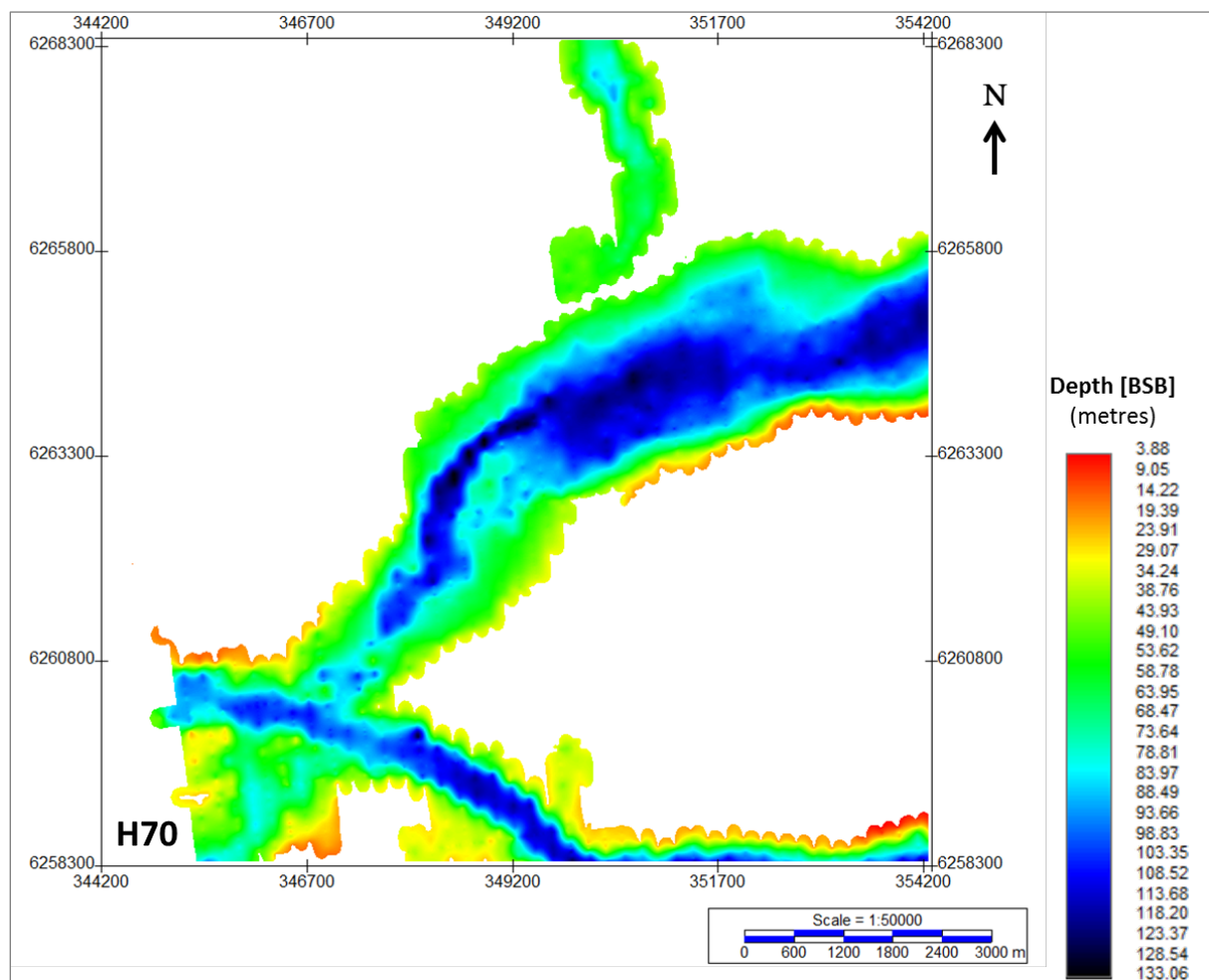


Figure 141 Depth below seabed of H70.
 Units in metres below seabed.

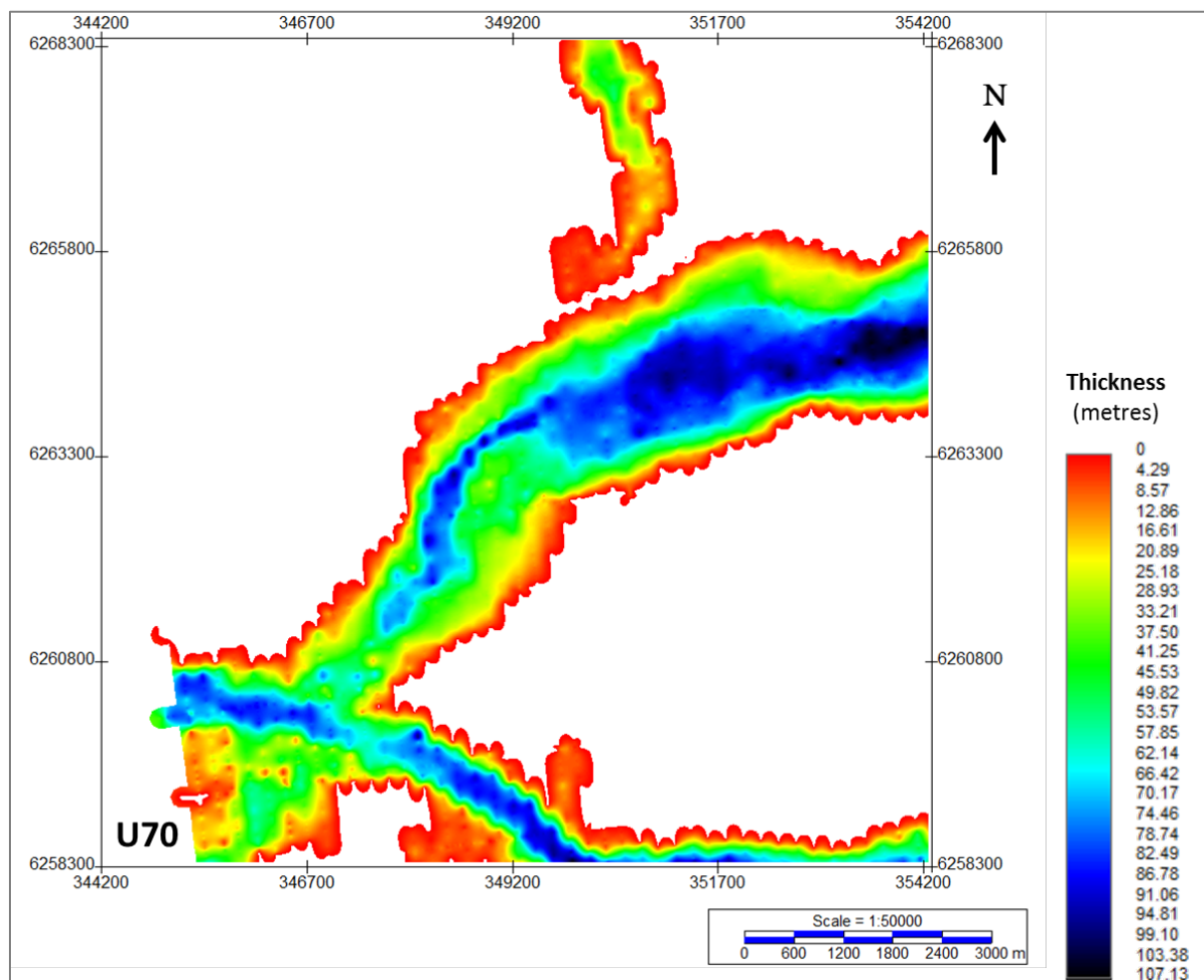


Figure 142 Thickness of unit U70.
 Units in metres.

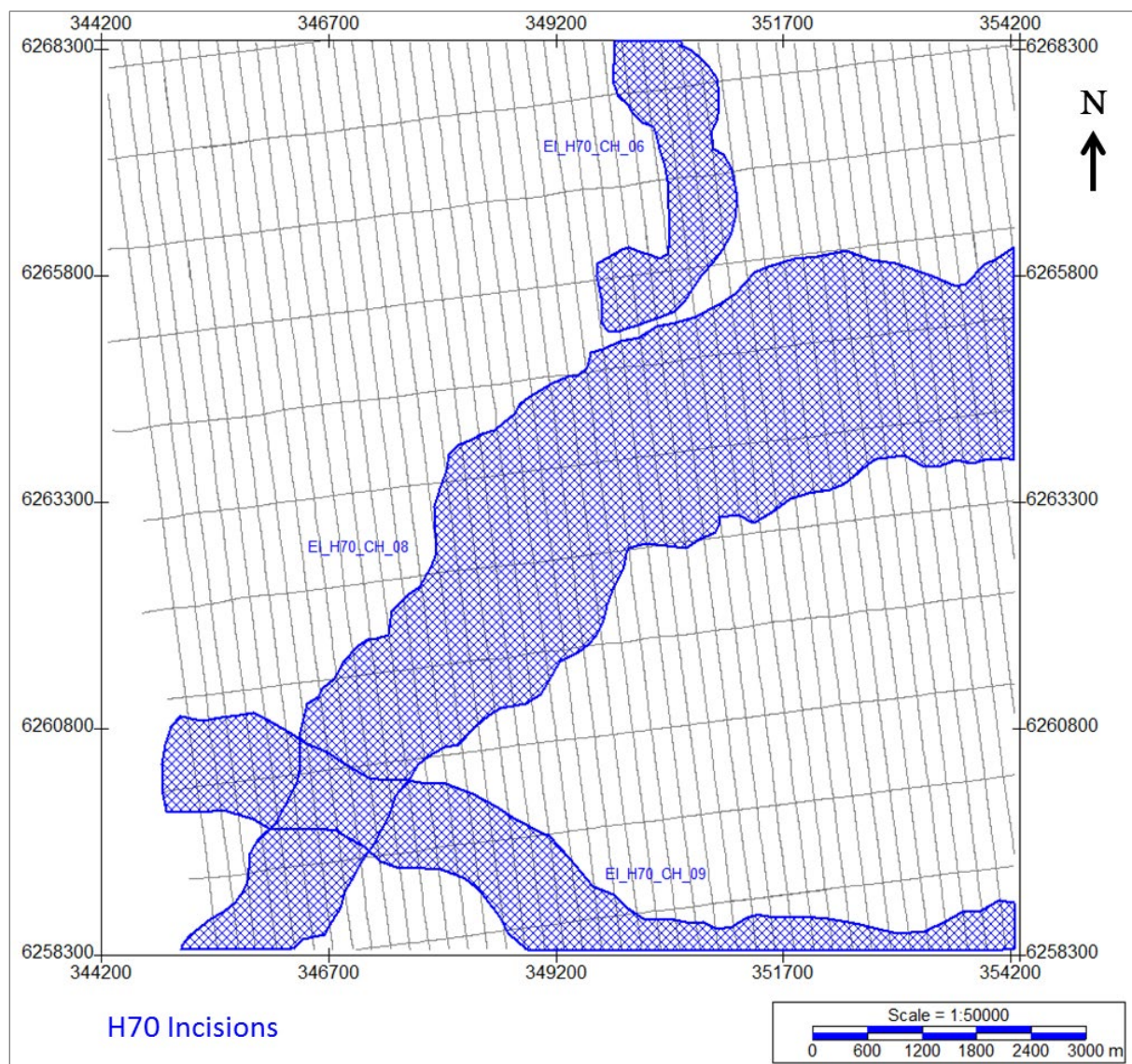


Figure 143 Spatial distribution of the major incisions identified for Seismic Unit U70.

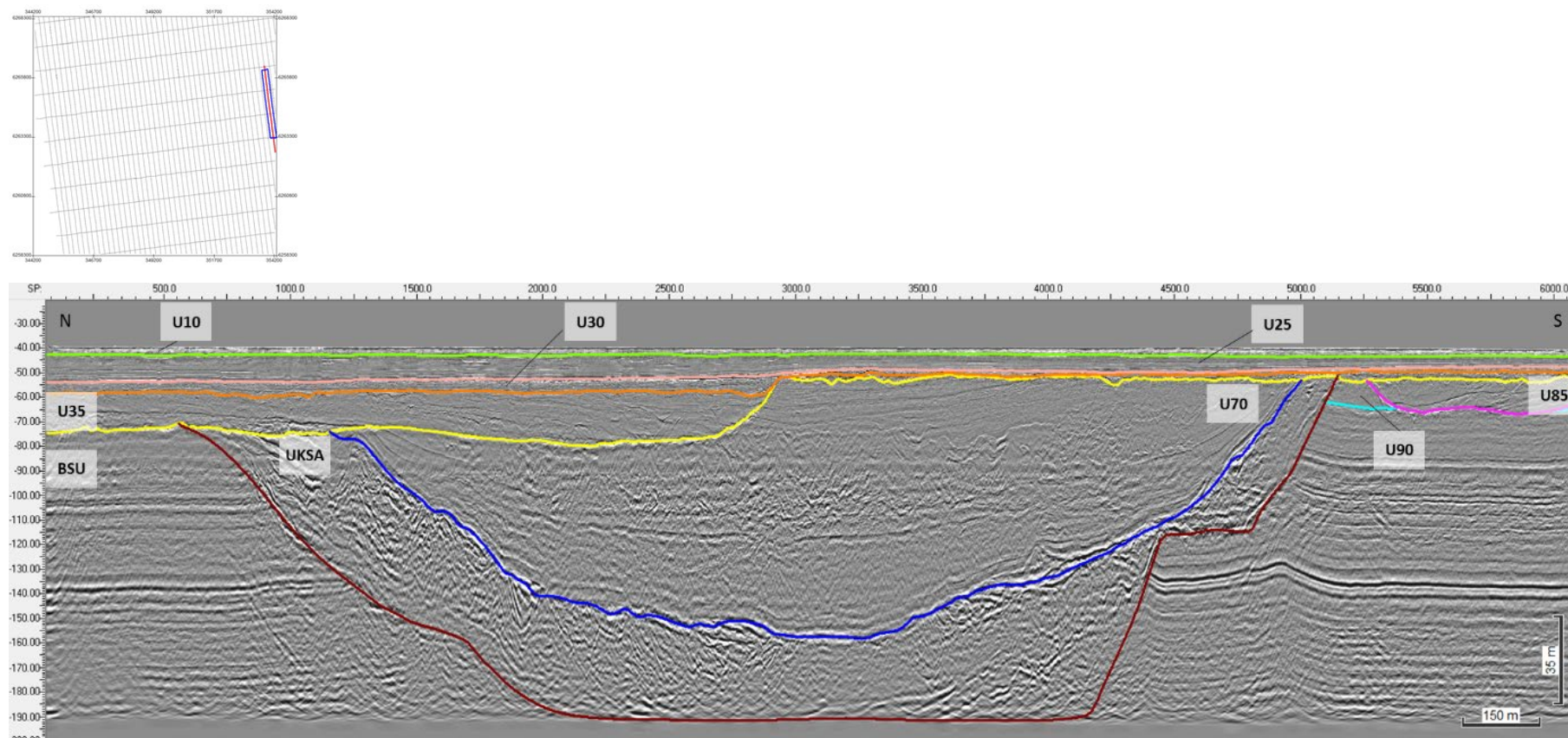


Figure 144 General facies of a U-shaped channel of Unit U70.
 The image also shows the extensional features below H70 which are interpreted to result from collapse of the valley flanks.
 Example shown: H70_CH_08. Seismic profile BM4_OWF_E_2D_09240

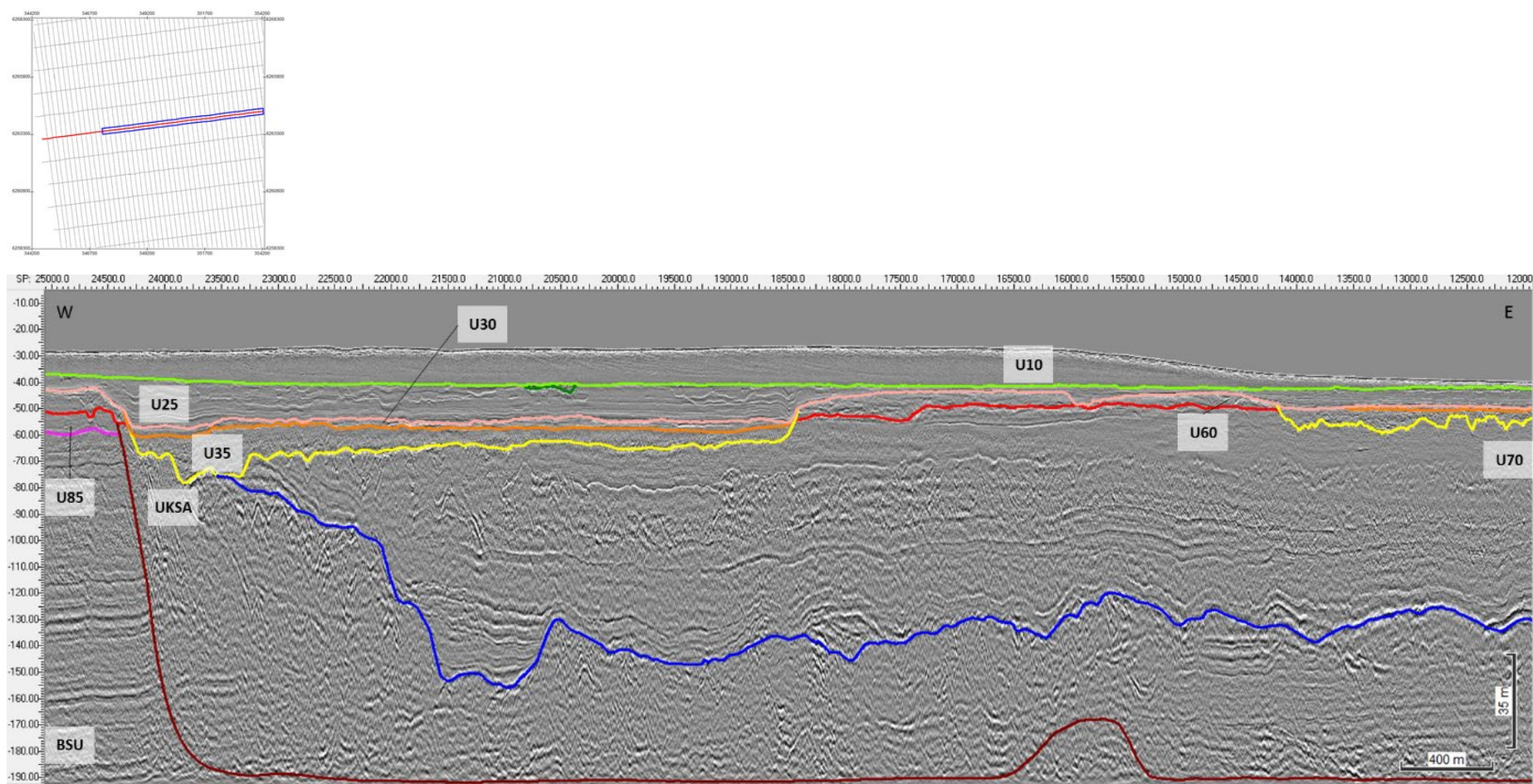


Figure 145 General facies along the length of a channel of Seismic Unit U70.
 Example shown: H70_CH_08. Seismic profile BX3_OWF_E_XL_22000

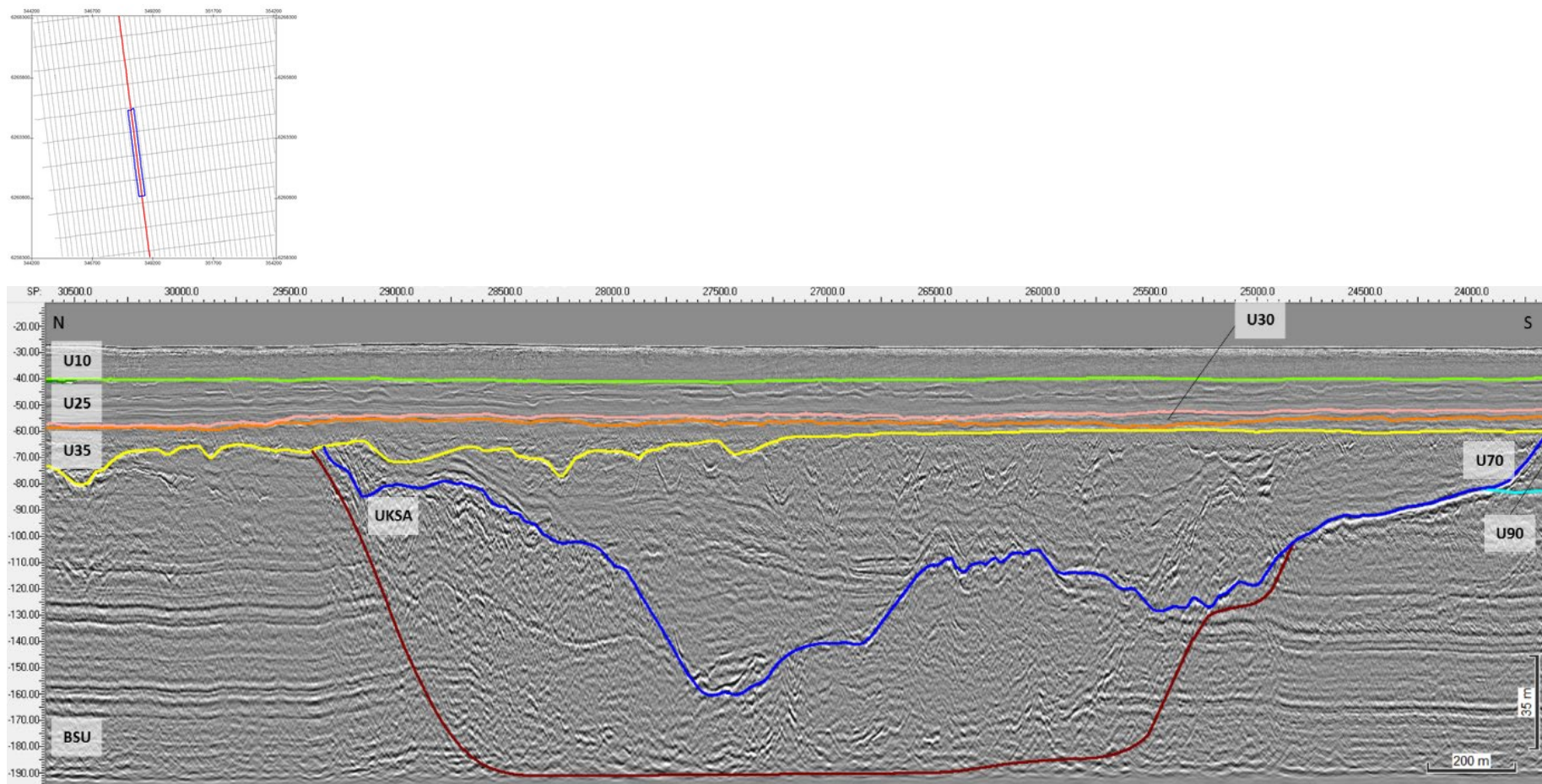


Figure 146 Composite facies of a U70 channel.
 Seismic profile BM2_OWF_E_2D_03570

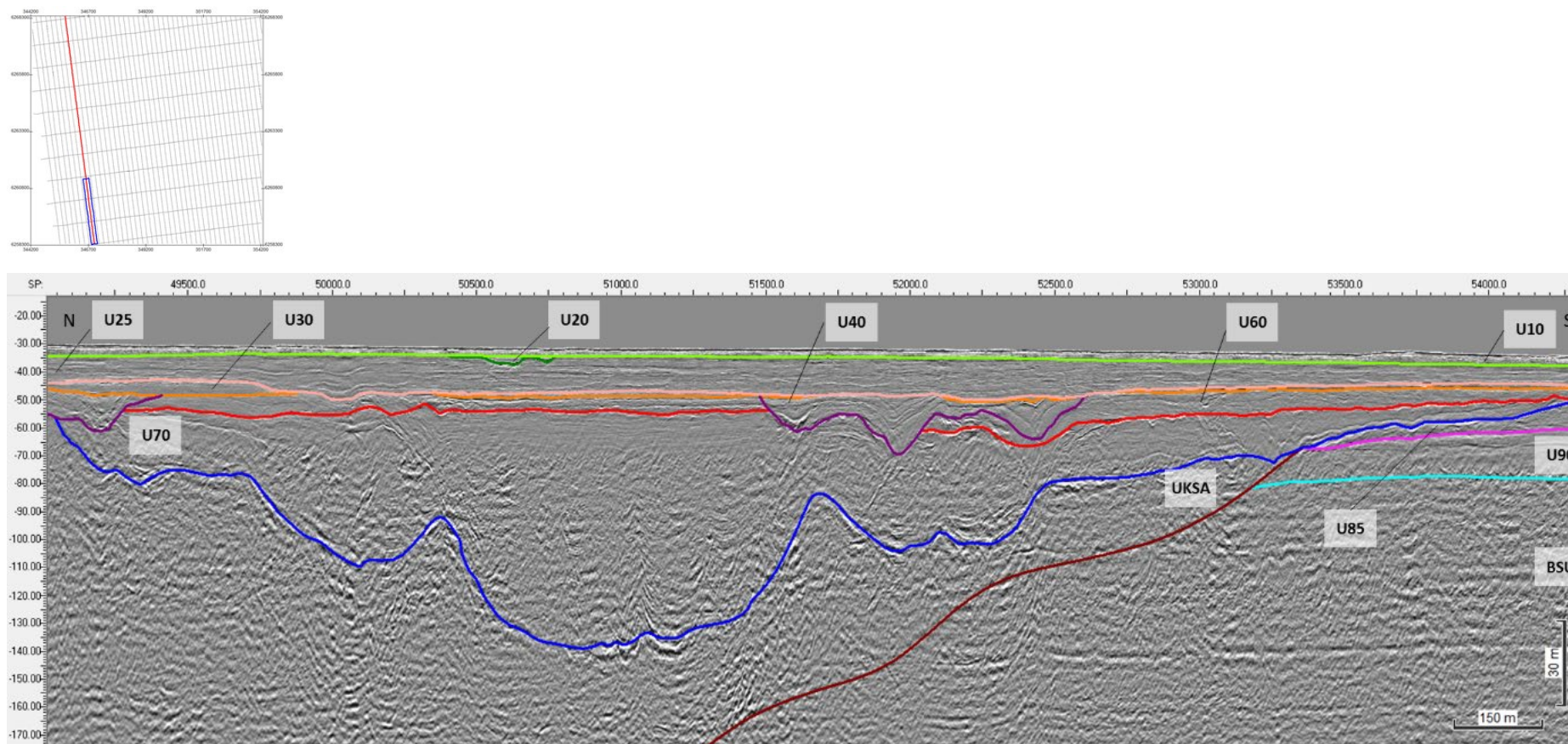


Figure 147 Composite facies of the intersection area of U70 channels.
 The channels shown are H70_CH_08 and H70_CH_09. Seismic profile BM1_OWF_E_2D_01470

8.6.12 | SEISMIC UNIT U85

Seismic unit U85 occurs solely in the south sector of the area. The base of Seismic Unit U85 is defined by horizon H85 and is present discontinuously within the survey area. The spatial distribution, vertical reference to MSL and the seabed, and thickness of the unit are presented in Figure 148, Figure 149 and Figure 150.

Horizon H85 ranges in depth between 47.5 m and 90.5 m below MSL (Figure 148), and between 7.8 m and 64.0 m depth below the seabed (Figure 149). Horizon H85 traces an uneven, rugose, undulating surface, truncating the units below it (unconformity; Figure 151). Where present, H85 follows a positive reflector of high amplitude. However, H85 is mostly defined by a vertical facies shift.

Seismic unit U85 has generally sub-horizontal tabular morphology, with thicknesses ranging from <0.5 m to 38.1 m (Figure 150). Within the south sector, it is only present outside the limits of the two major basins.

Seismic unit U85 exhibits a composite facies of low to high amplitude reflectors (Figure 151 and Figure 152). Similar to U30 and U60, unit U85 comprises complex internal features of meso-scale proportions, such as mounds, channels, and lenses, with oblique reflectors. Internal surfaces separate these features, marked by medium-high amplitude.

Seismic unit U85 sediments are interpreted to have been deposited in a high energy setting, likely of fluvial nature (possibly outwash plain?), as evidenced by the meso-scale seismic facies association, the numerous stacked subunits, internal surfaces, and channel incisions. Horizon H85 appears as an unconformity that shaped a pronounced paleo-relief. From the seismic character of U85 and its interpreted depositional system, it is estimated that the sediments are mainly sands with gravel and silt (?). Soft sediment deposits (such as muds, possibly organic-rich) are likely found near the base of U85, as indicated by the high amplitude negative reflectors.

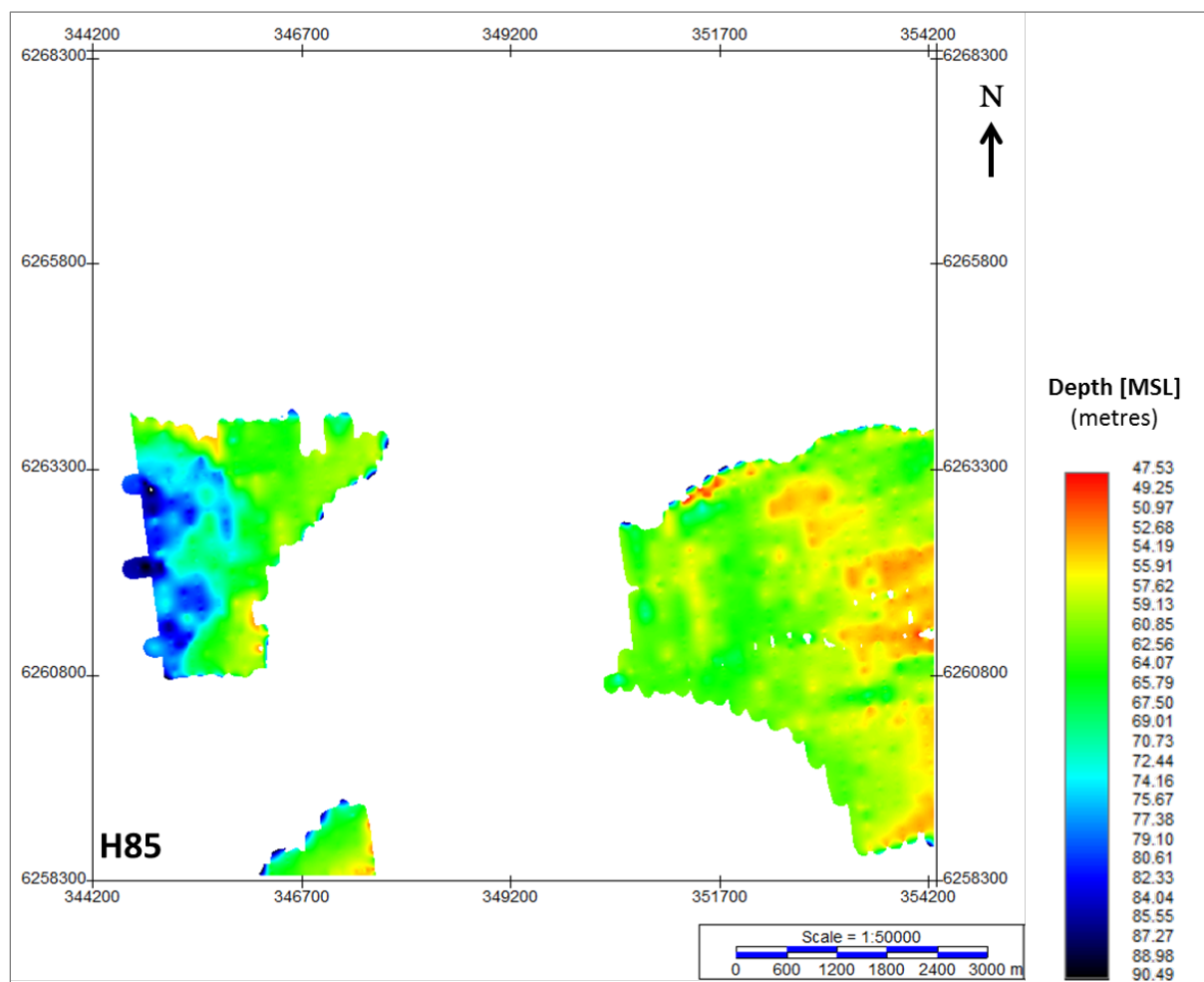


Figure 148 Map showing the lateral extent of U85.
 Units in metres below MSL.

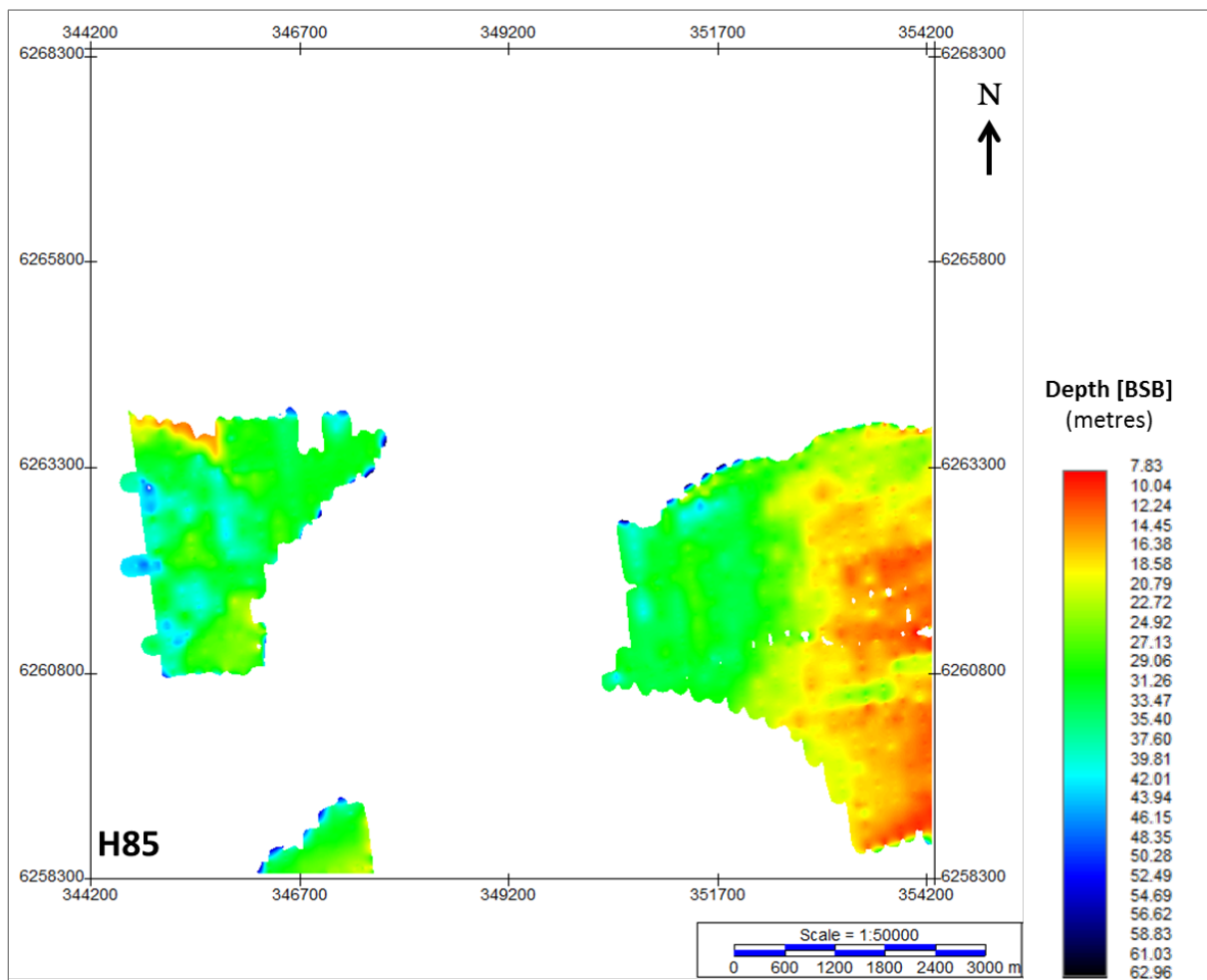


Figure 149 Depth below seabed of H85.
 Units in metres below seabed.

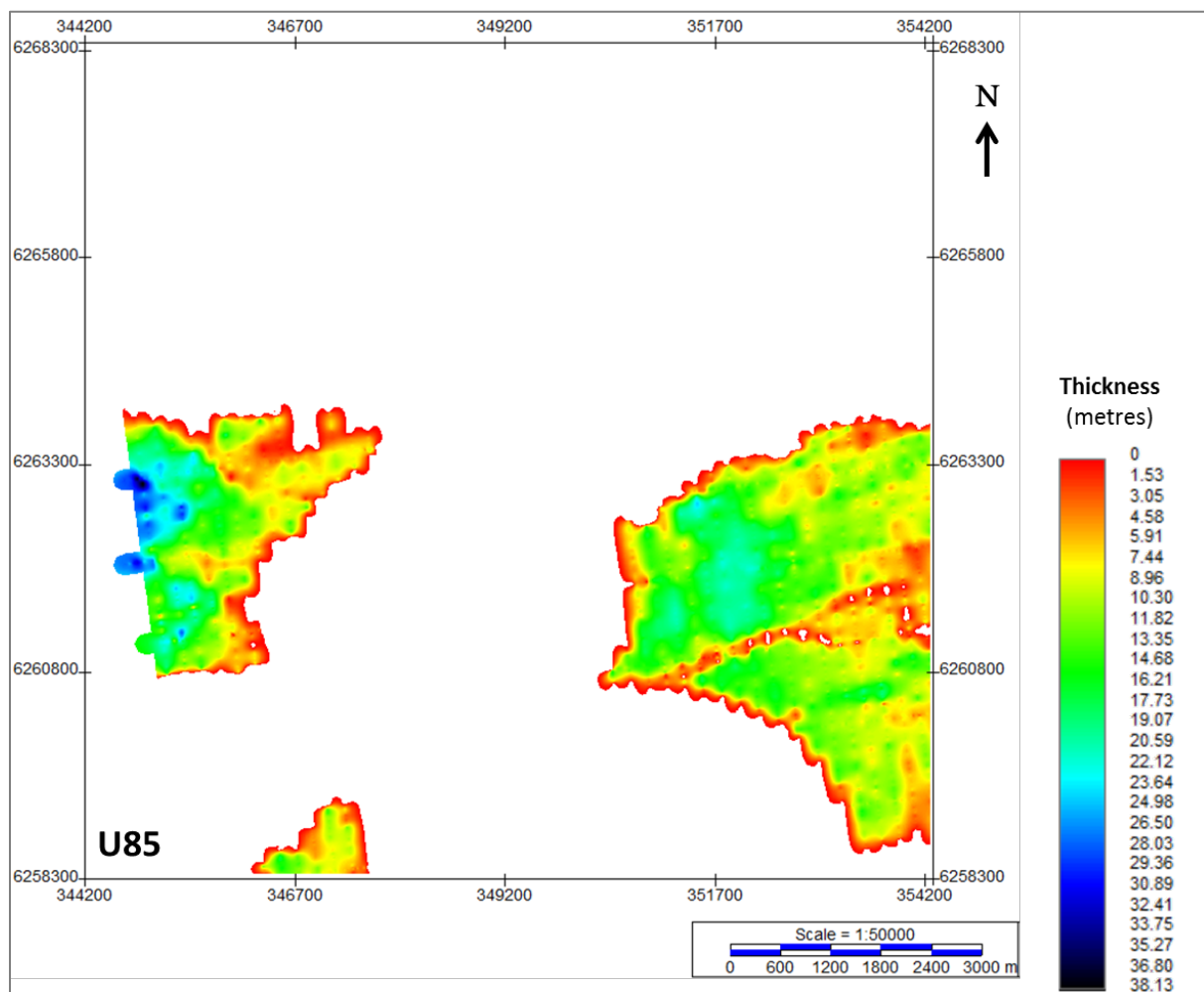


Figure 150 Thickness of unit U85.
 Units in metres.

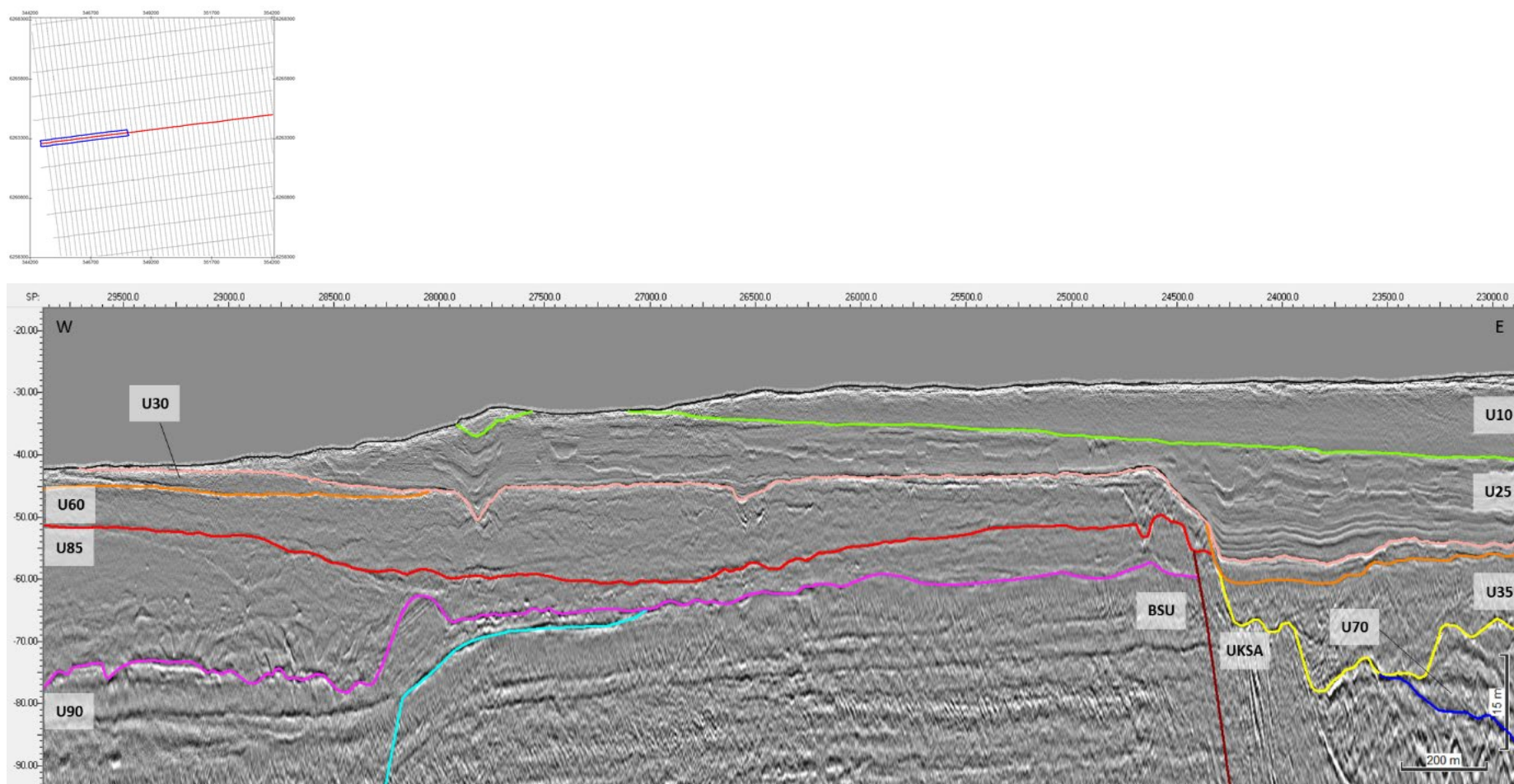


Figure 151 General facies of Seismic Unit U85, and the character of horizon H85 (hot pink).
 Seismic profile BX3_OWF_E_XL_22000

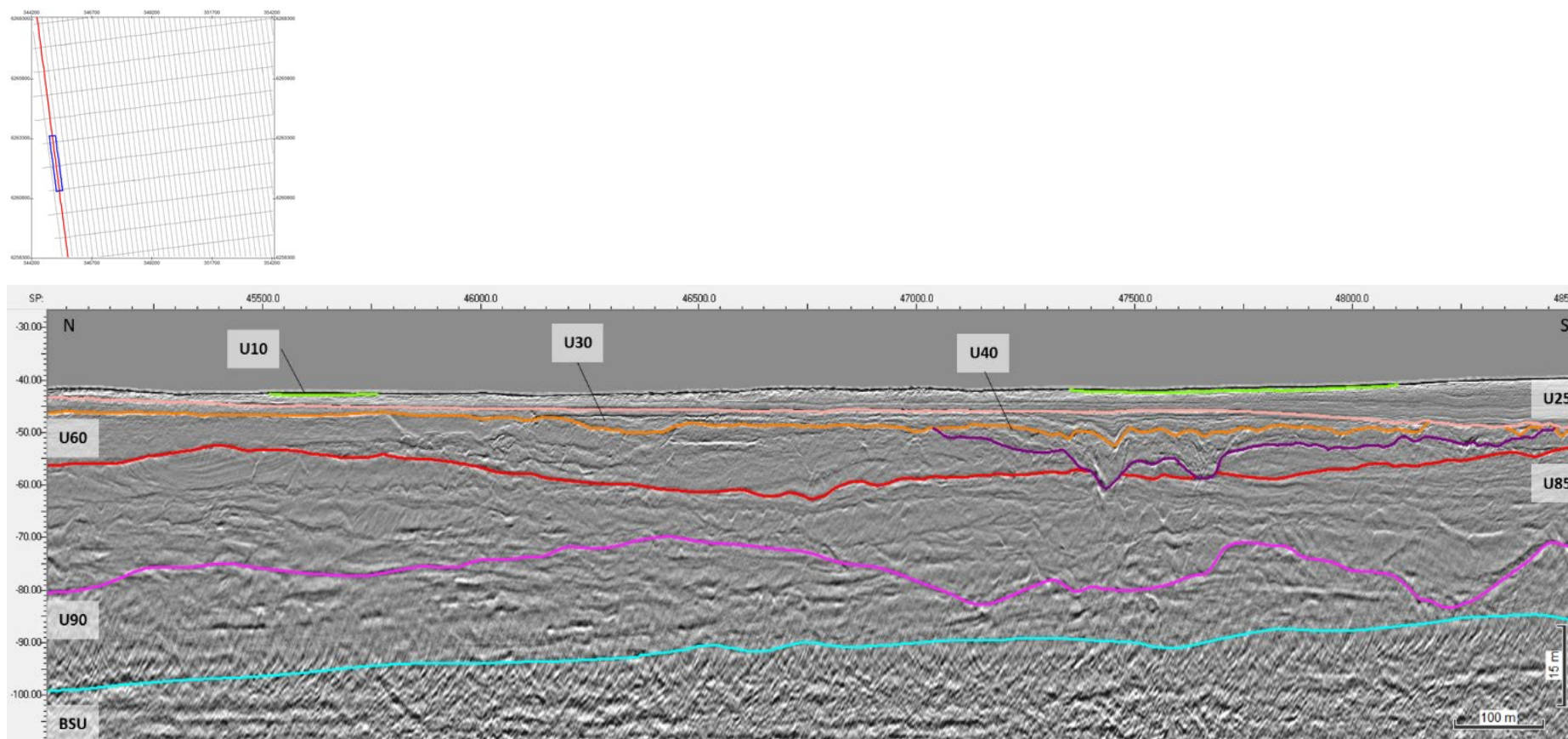


Figure 152 General facies of Seismic Unit U85, and the character of horizon H85 (hot pink).
 Seismic profile BM1_OWF_E_2D_00210

8.6.13 | SEISMIC UNIT U90

Seismic unit U90 occurs mostly in the south sector and within a restricted area of the north sector. The base of Seismic Unit U90 is defined by horizon H90 and is present discontinuously within the site. The spatial distribution, vertical reference to MSL and the seabed, and thickness of the unit are presented in Figure 153, Figure 154 and Figure 155.

Horizon H90 ranges in depth between 60.0 m and 100.79 m below MSL (Figure 153) and between 21.5 m and 73.19 m depth below the seabed (Figure 154). Horizon H90 is mostly defined by a vertical facies shift, corresponding to a planar, slightly undulating surface, generally gently dipping towards SW/SSW in the south sector and dipping NW/NNW in the north sector. Where present, H90 follows a positive reflector of medium amplitude, truncating the units below it (Figure 165).

Seismic unit U90 has generally tabular shape, with thicknesses ranging from <7 m to 37.4 m (Figure 155). Thickness variations are mostly the result of truncation of U90 by the units U85, U70, U40, U35, and U25 above it.

Seismic unit U90 is characterized by its parallel-homogeneous facies at the base and an association of parallel-mound-channel-shingled facies above, all prograding towards NW or W (Figure 156 and Figure 157). Scattered along the internal surfaces are small-scale mounds-lenses, with a uniform positive amplitude character, and a negative reflector at the base. These features are most commonly seen at the base of the unit.

Seismic unit U90 sediments are interpreted to have been deposited in a delta setting, as evidenced by its internal progradational nature, dipping towards the deeper sections to the NW-W. From the seismic character of U90 and its interpreted depositional system, it is estimated that the sediments are mainly sands-fine sediments (?). The scattered internal mounds-lenses may correspond to sandbars (?).

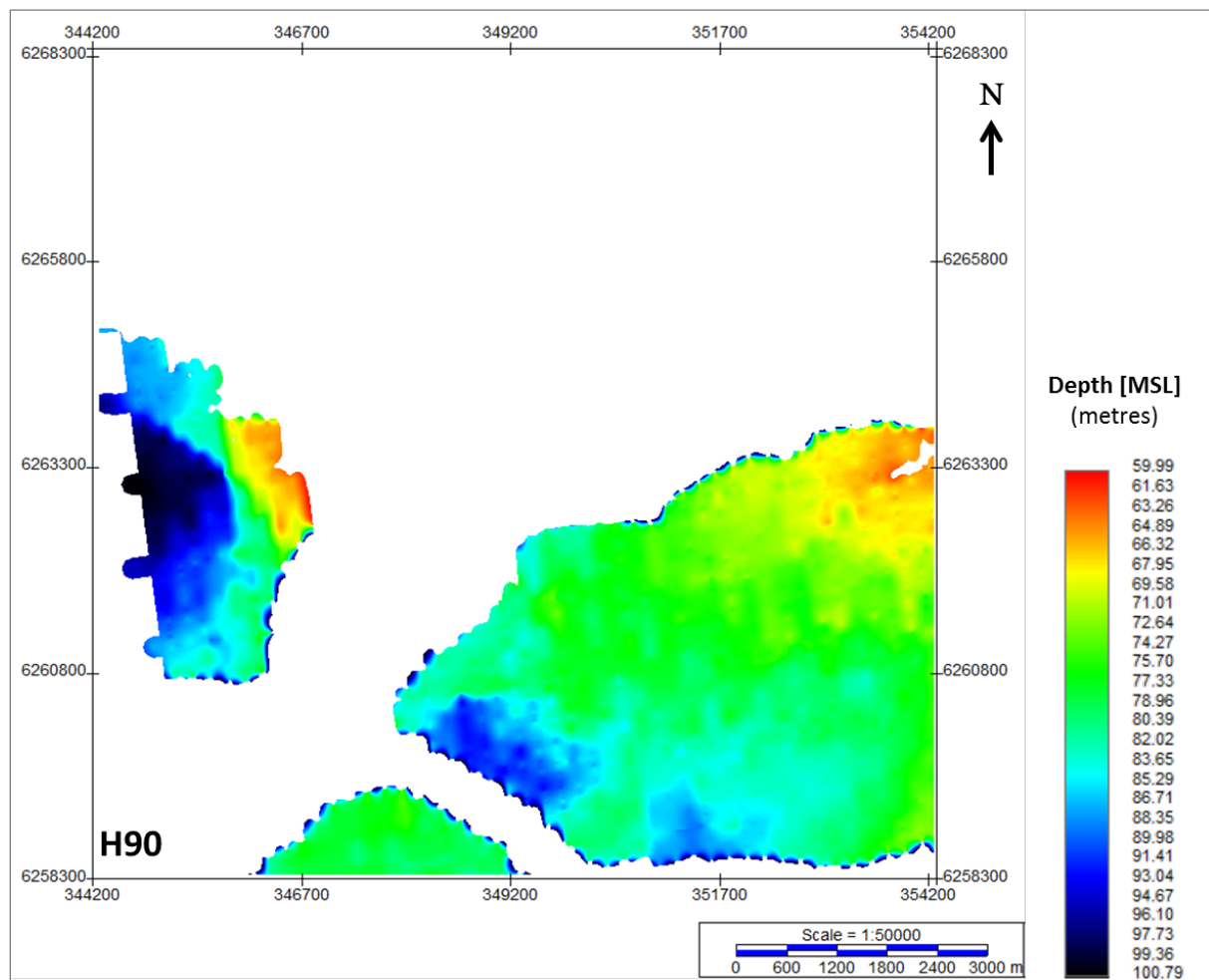


Figure 153 Map showing the lateral extent of U90.
 Units in metres below MSL.

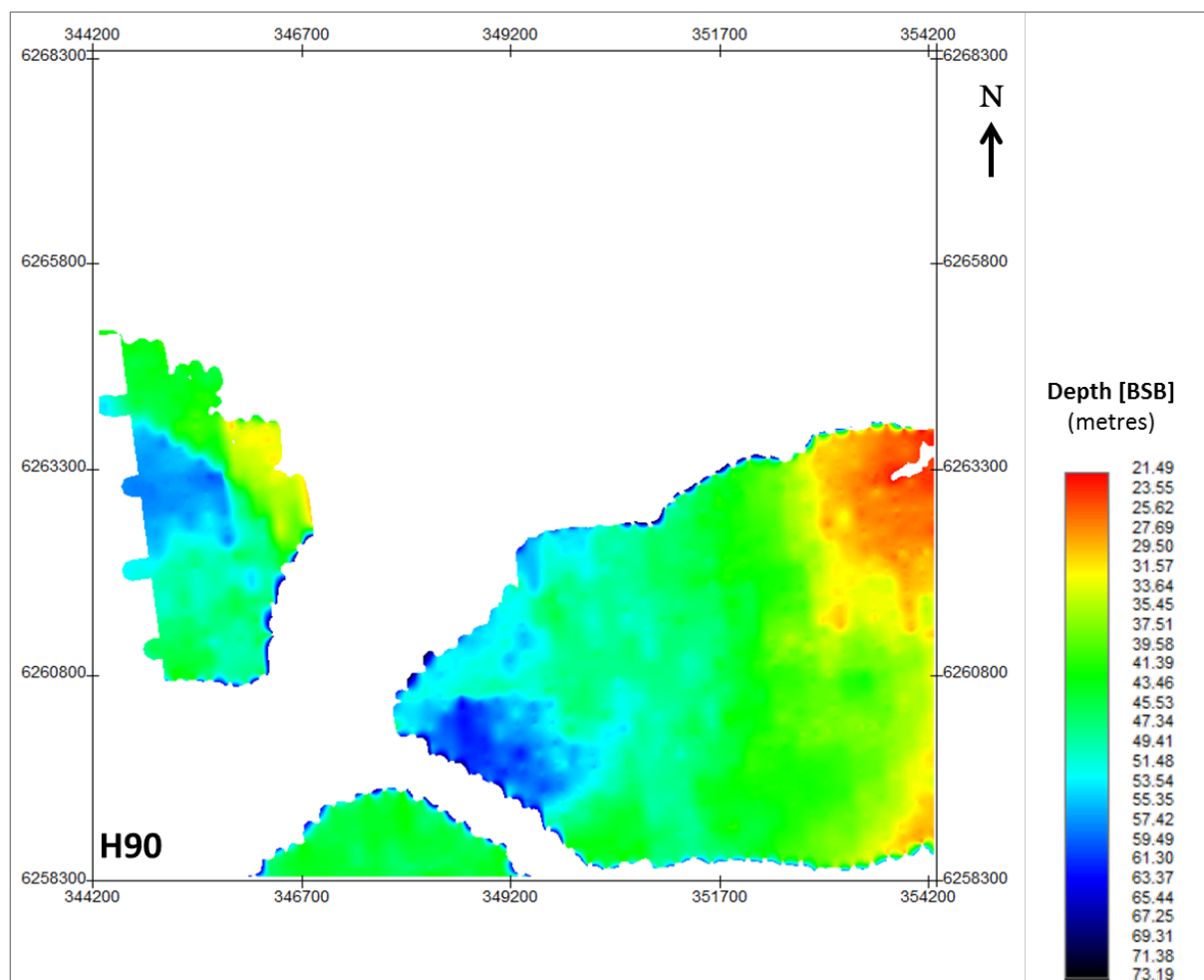


Figure 154 Depth below seabed of H90.
 Units in metres below seabed.

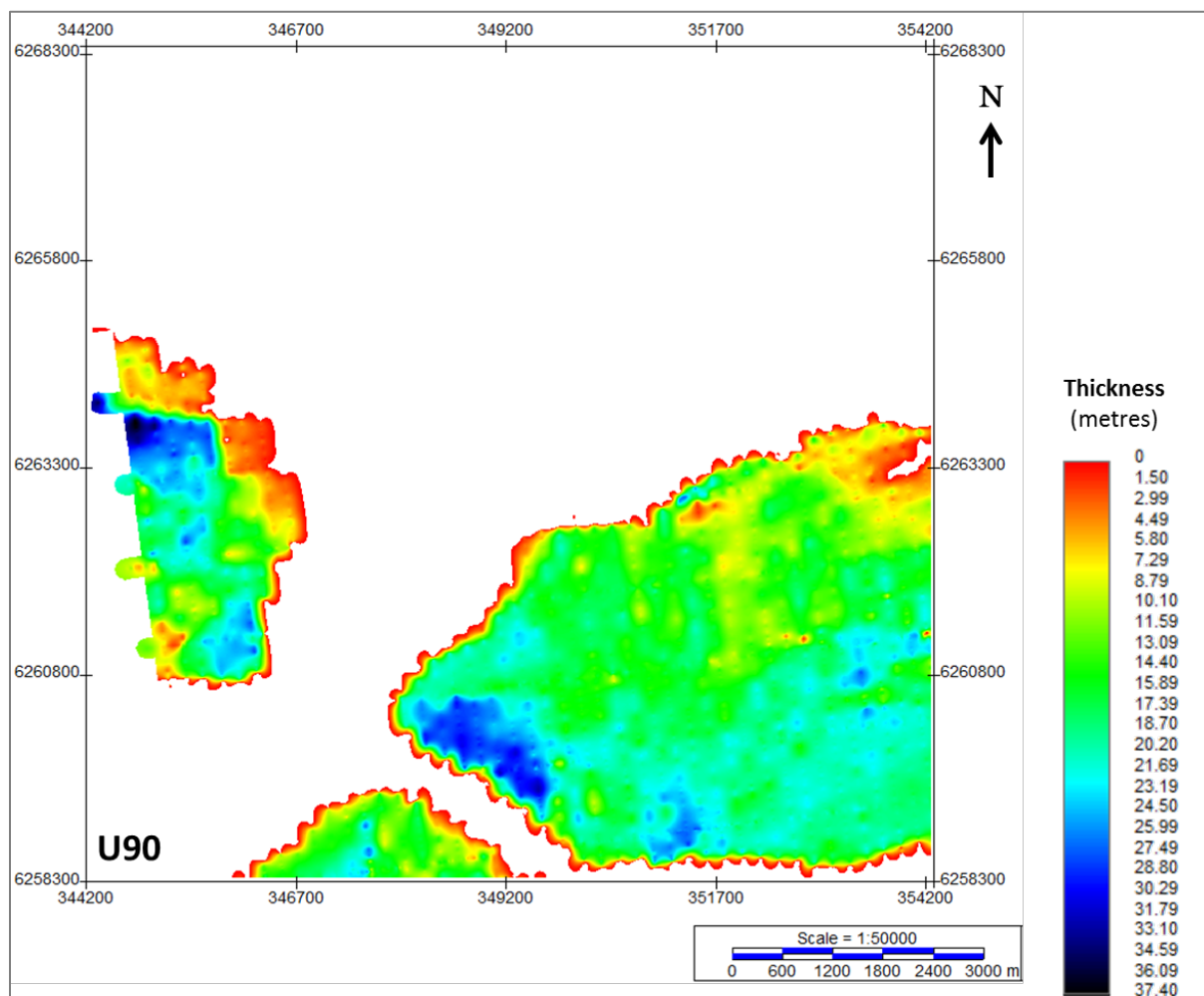


Figure 155 Thickness of unit U90.
 Units in metres.

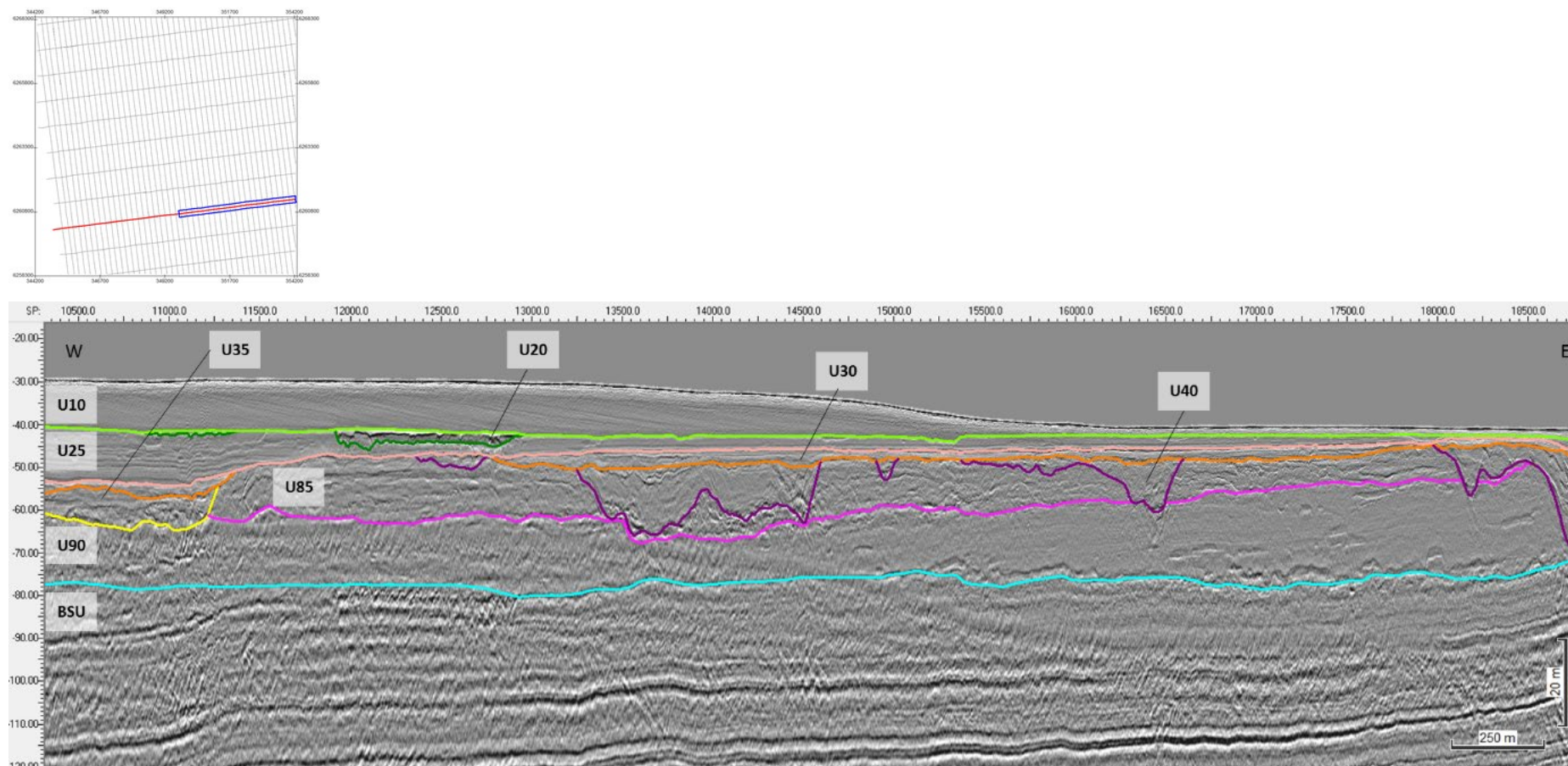


Figure 156 General facies of Seismic Unit U90, and the character of horizon H90 (cyan).
 Seismic profile BX4_OWF_E_XL_25000

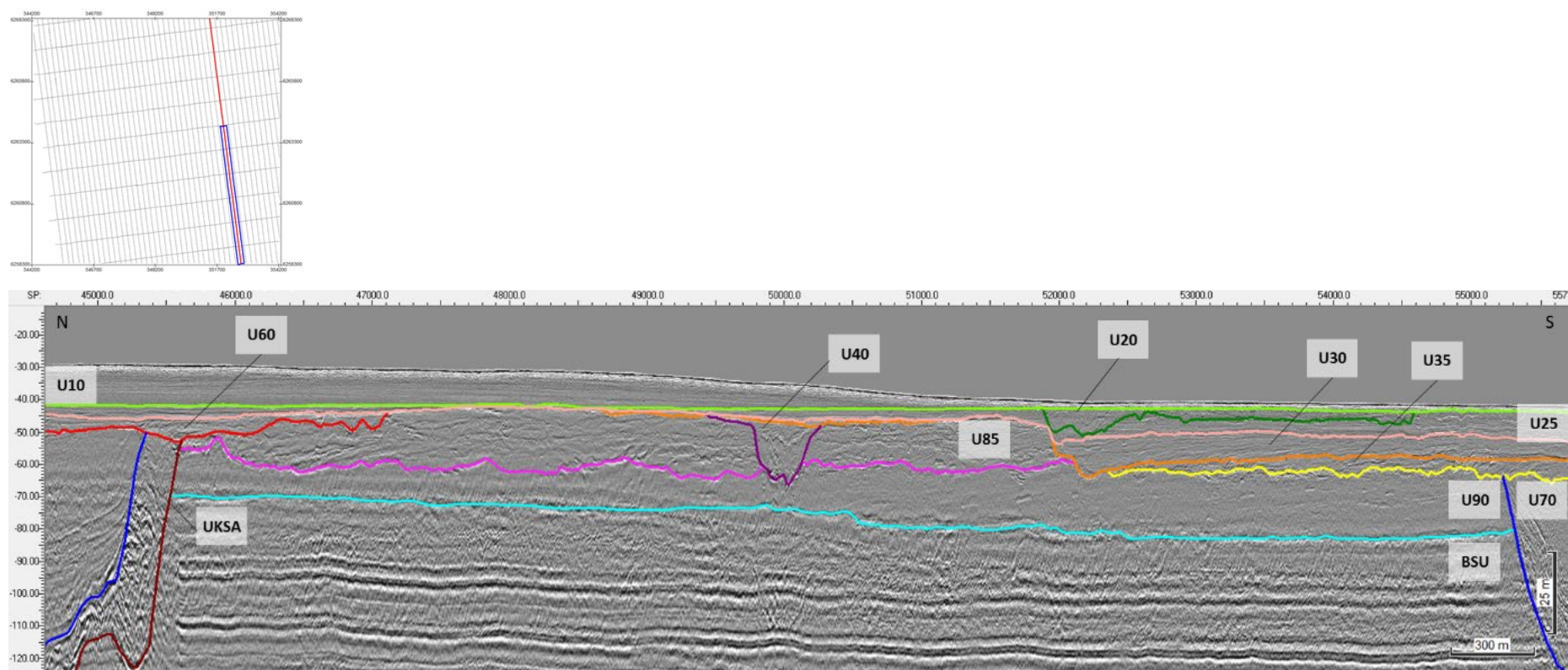


Figure 157 General facies of Seismic Unit U90, and the character of horizon H90 (cyan).
 Seismic profile BM3_OWF_E_2D_07140

8.6.14 | SEISMIC UNIT UKS

Seismic unit UKS is a major structural element of the ground model and occurs discontinuously in the Artificial Island survey area. The base of this unit is horizon KS. The spatial distribution, vertical reference to MSL and the seabed, and thickness of the unit are presented in Figure 158 to Figure 163.

Horizon KS defines a significant vertical and lateral facies shift, separating deformed sediments from preserved deposits older than H70. Horizon KS ranges in depth between 46.7 m and 193.7 m below MSL (Figure 158 and Figure 161) between 11.15 m and 165.2 m depth below the seabed (Figure 159 and Figure 162).

Horizon KS represents a deformation front boundary and, although part of the geological model, should not be interpreted with a chronostratigraphic meaning. It is an amalgamation of surfaces of glacial erosion, decollements, fault planes, and shear/fracture zone boundaries (Figure 164 to Figure 166).

Seismic unit UKS encompasses strongly deformed sediments of units U85, U90 (?), and the Base Seismic Unit (described below). The seismic facies of this unit is very complex, in a wide range of internal structures affected by variable degrees of deformation, from better-preserved faulted blocks to completely disturbed/chaotic regions. Where deformation has entirely erased primary depositional structure, seismic facies may be near transparent and incoherent.

Horizon KS was sub-divided into the two sub-horizons – KSA (Figure 158 to Figure 160) and KSB (Figure 161 to Figure 163) – each delineating distinct regions of deformation:

- Sub-horizon KSA extends across parts of the central and south sector; it truncates all seismic units below H70 (Figure 164 and Figure 165)
- Sub-horizon KSB is present in the SE corner of the Artificial Island survey area, in a very limited area; from its occurrence elsewhere in the full MMT OWF survey area, it appears to be older than U85-U90, as these units truncate deformed deposits in this area.

Compressional thrusting and folding are the main types of deformation observed. It is interpreted that these structures are the result of glaciotectionics. However, extensional faults are also recognized in the UHRS. Details on the several types of deformation identified are discussed in section 8.8.1].

Due to the limitation in the contracted number of horizons but specially because of the difficulty in recognizing the complex old tunnel valleys that may be present within this unit, these features were not mapped.

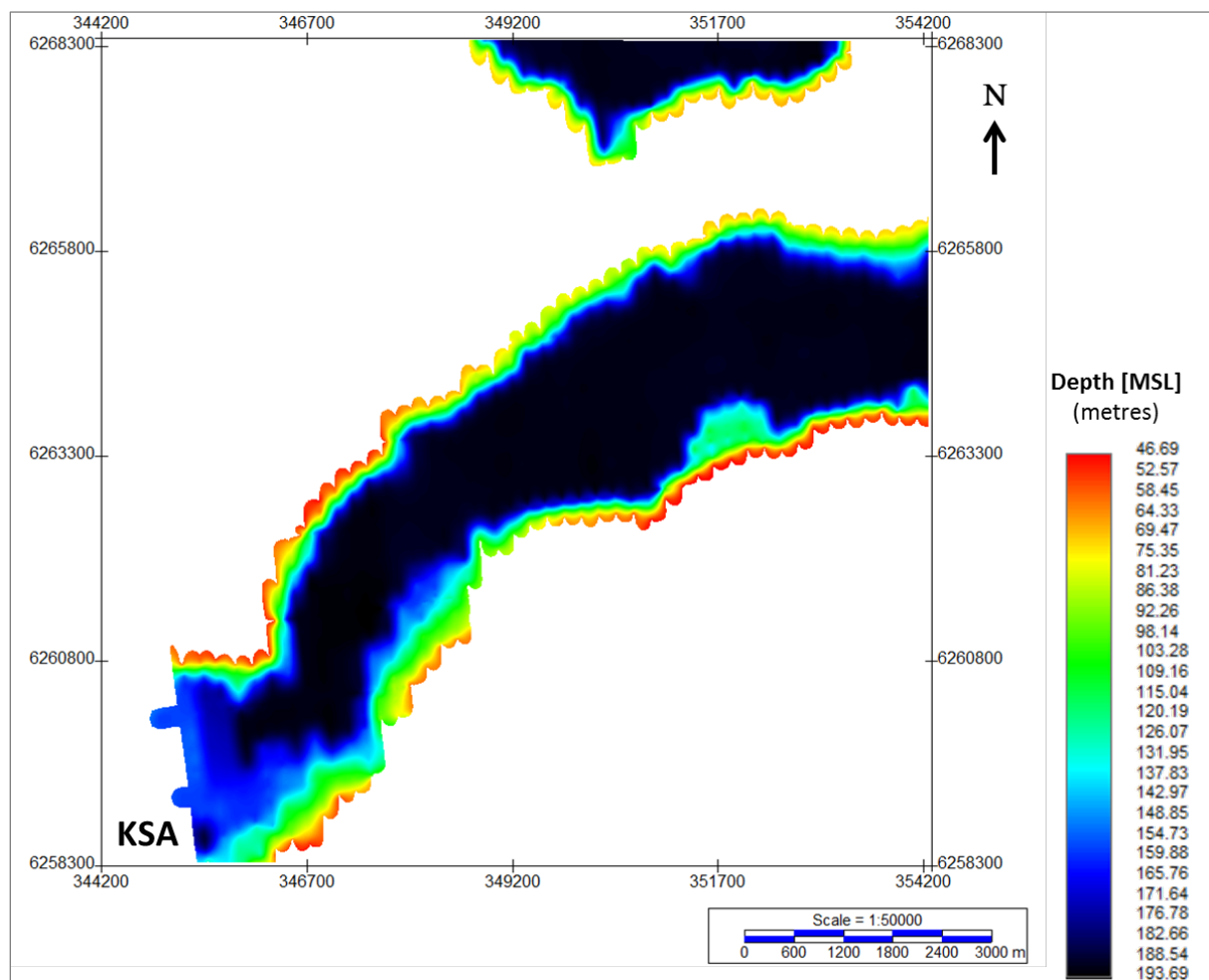


Figure 158 Map showing the lateral extent of horizon KSA.
 Units in metres below MSL.

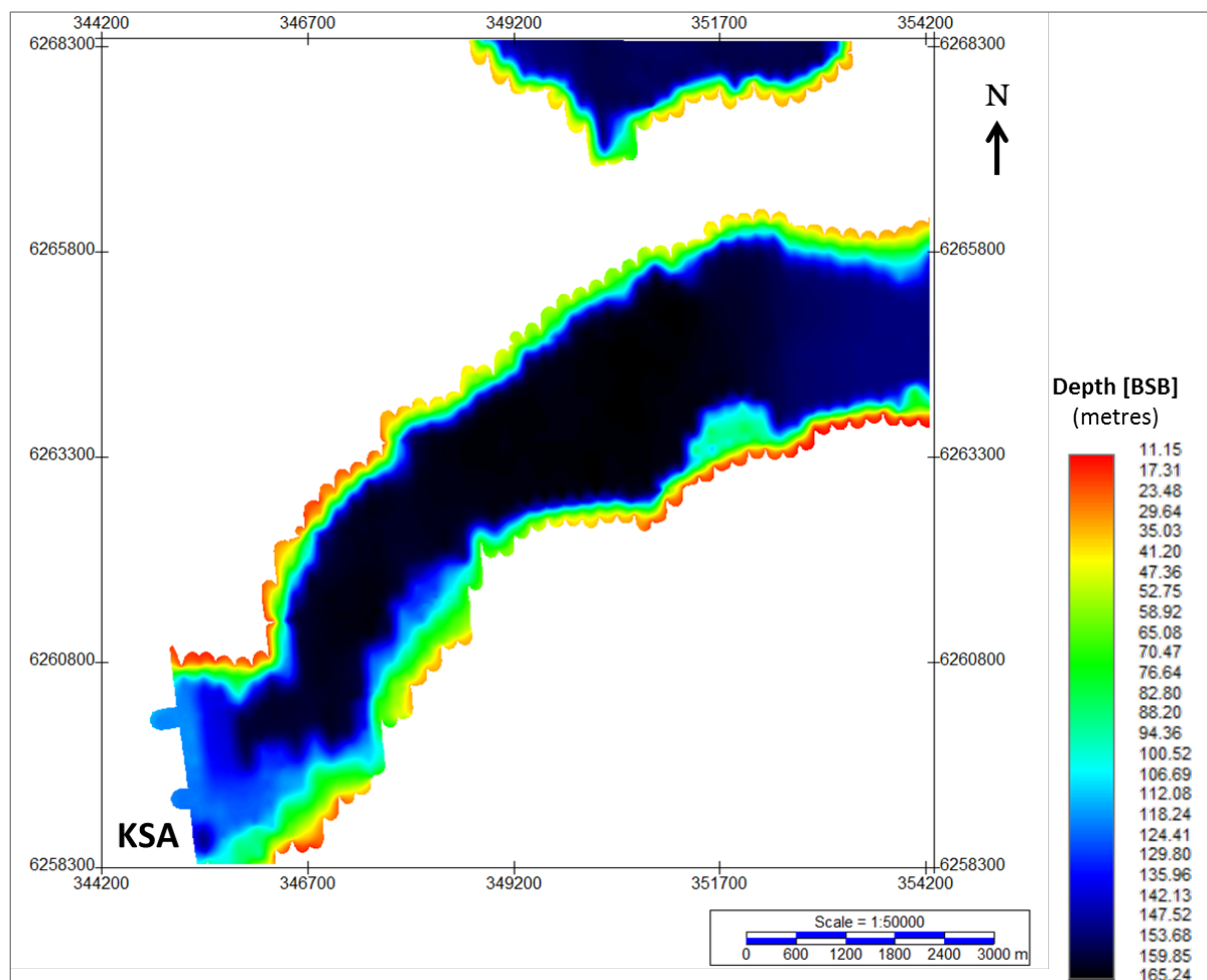


Figure 159 Depth below seabed of horizon KSA.
 Units in metres below seabed.

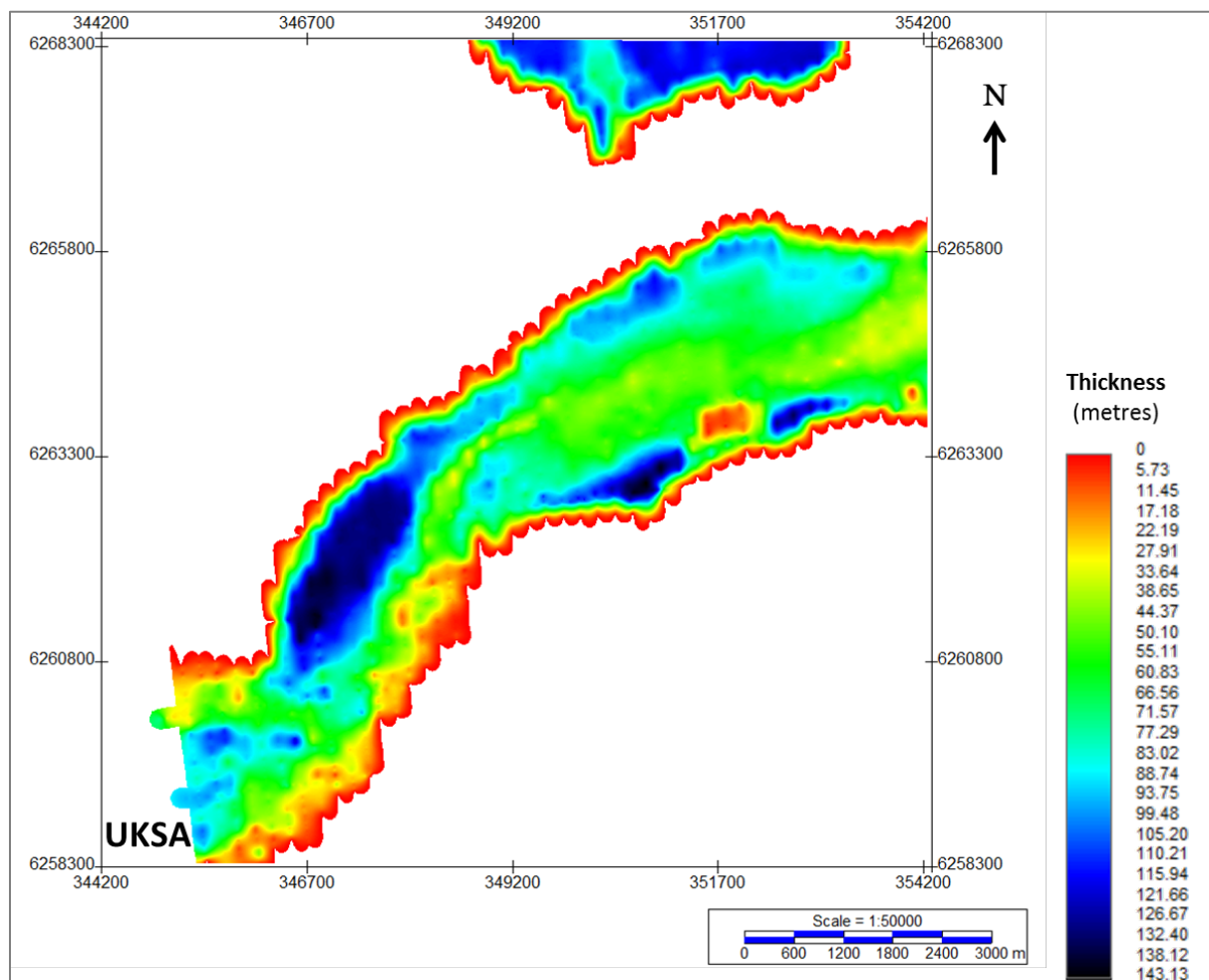


Figure 160 Thickness of unit UKSA.
 Units in metres.

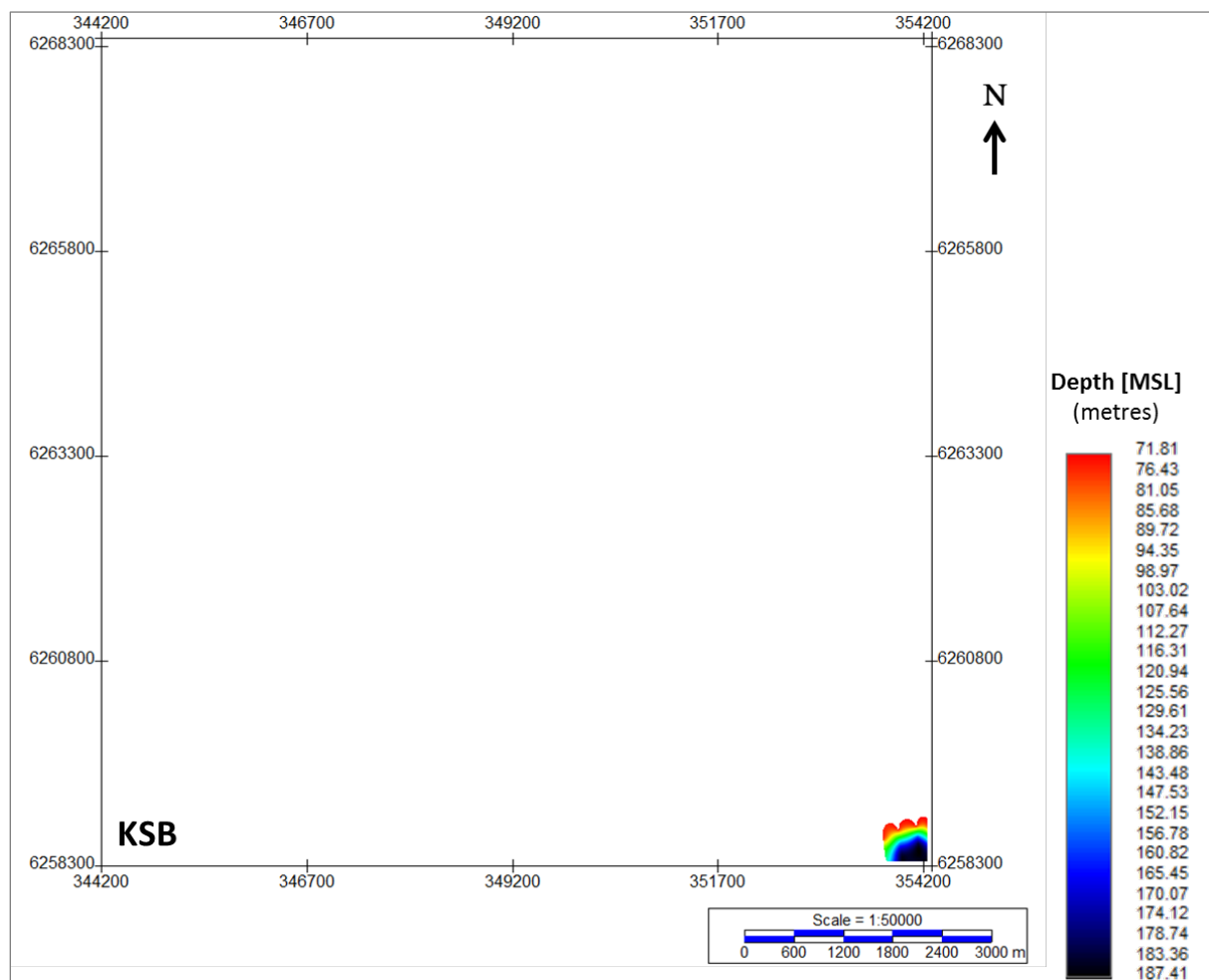


Figure 161 Map showing the lateral extent of horizon KSB.
 Units in metres below MSL.

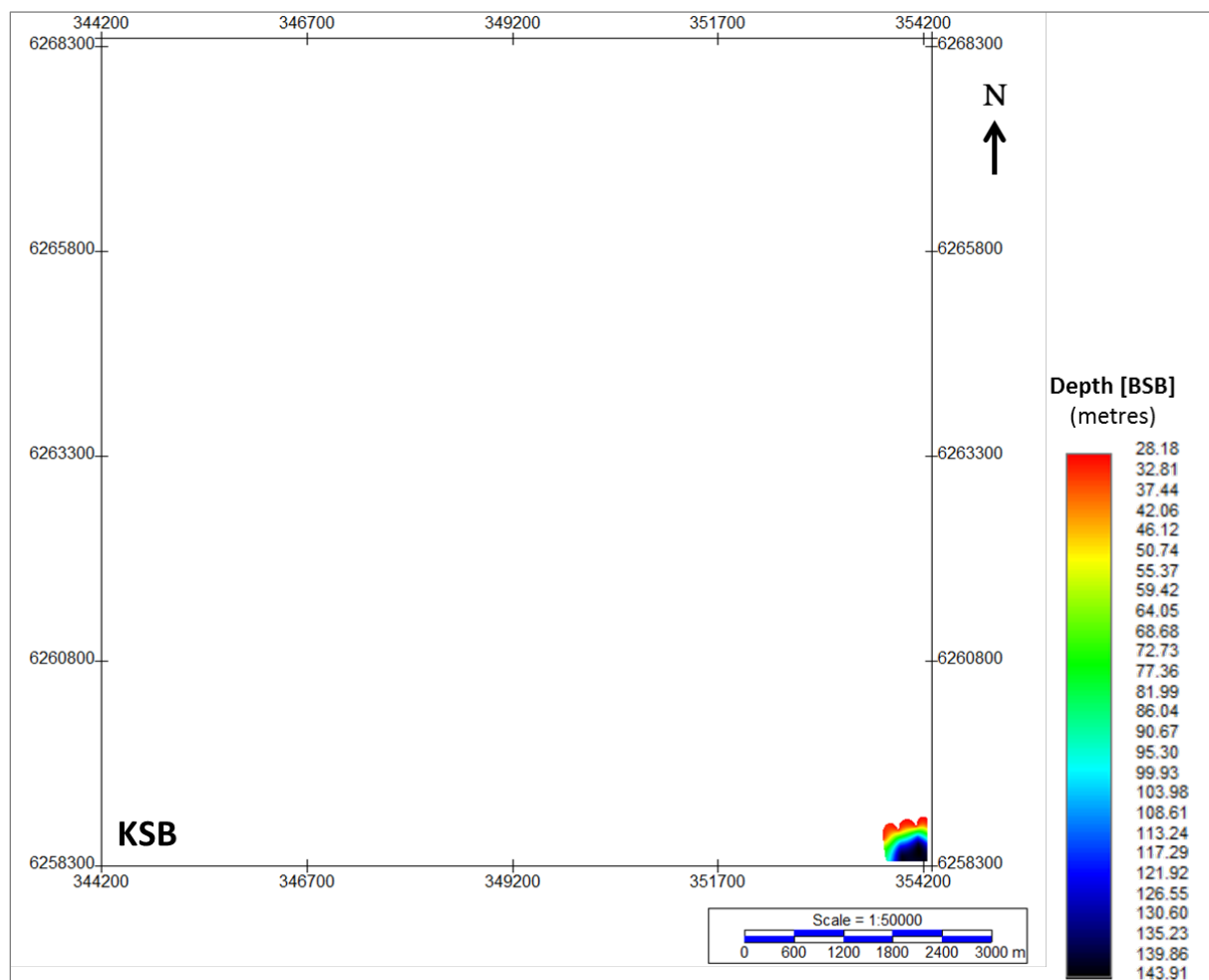


Figure 162 Depth below seabed of horizon KSB.
 Units in metres below seabed.

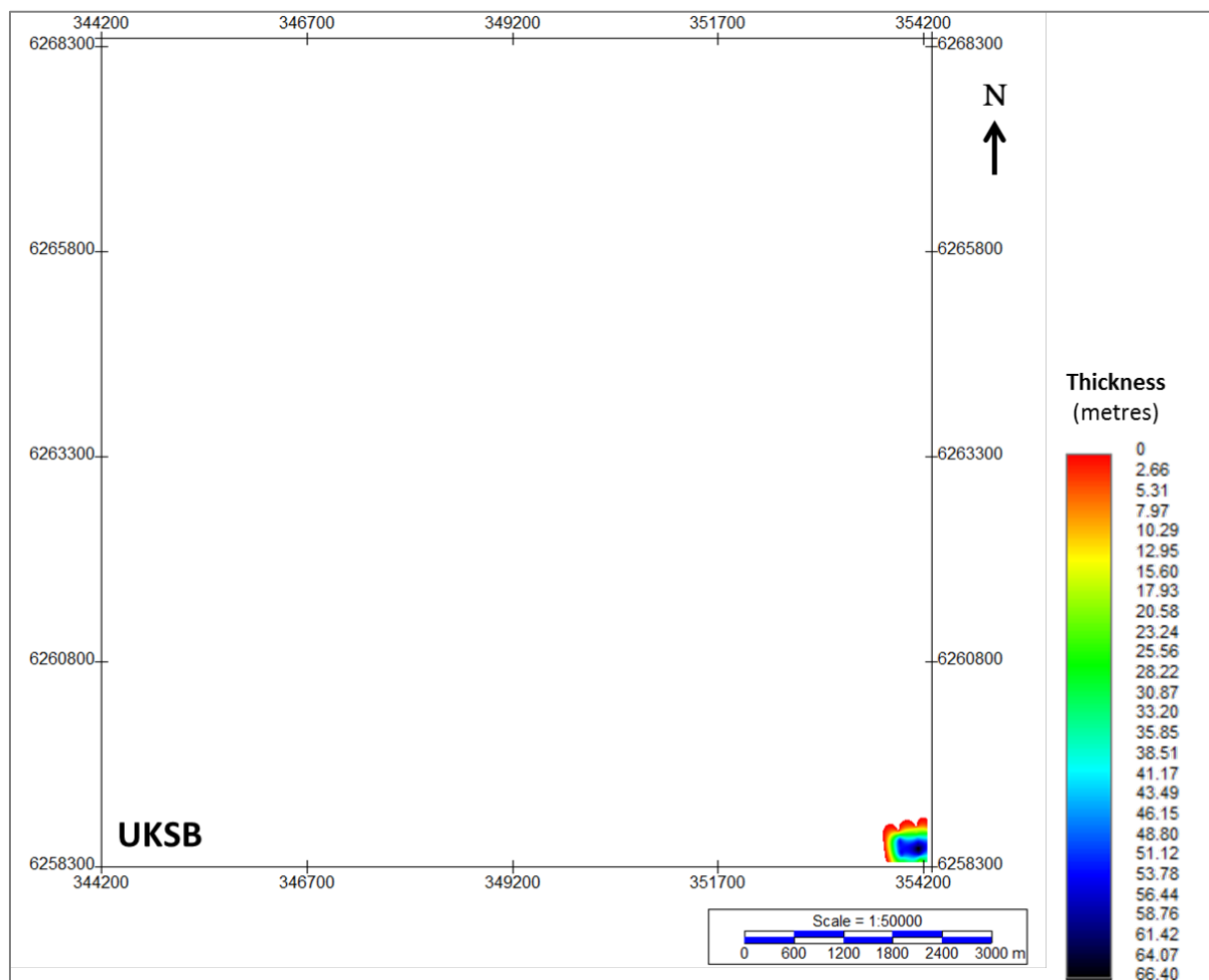


Figure 163 Thickness of unit UKSB.
 Units in metres.

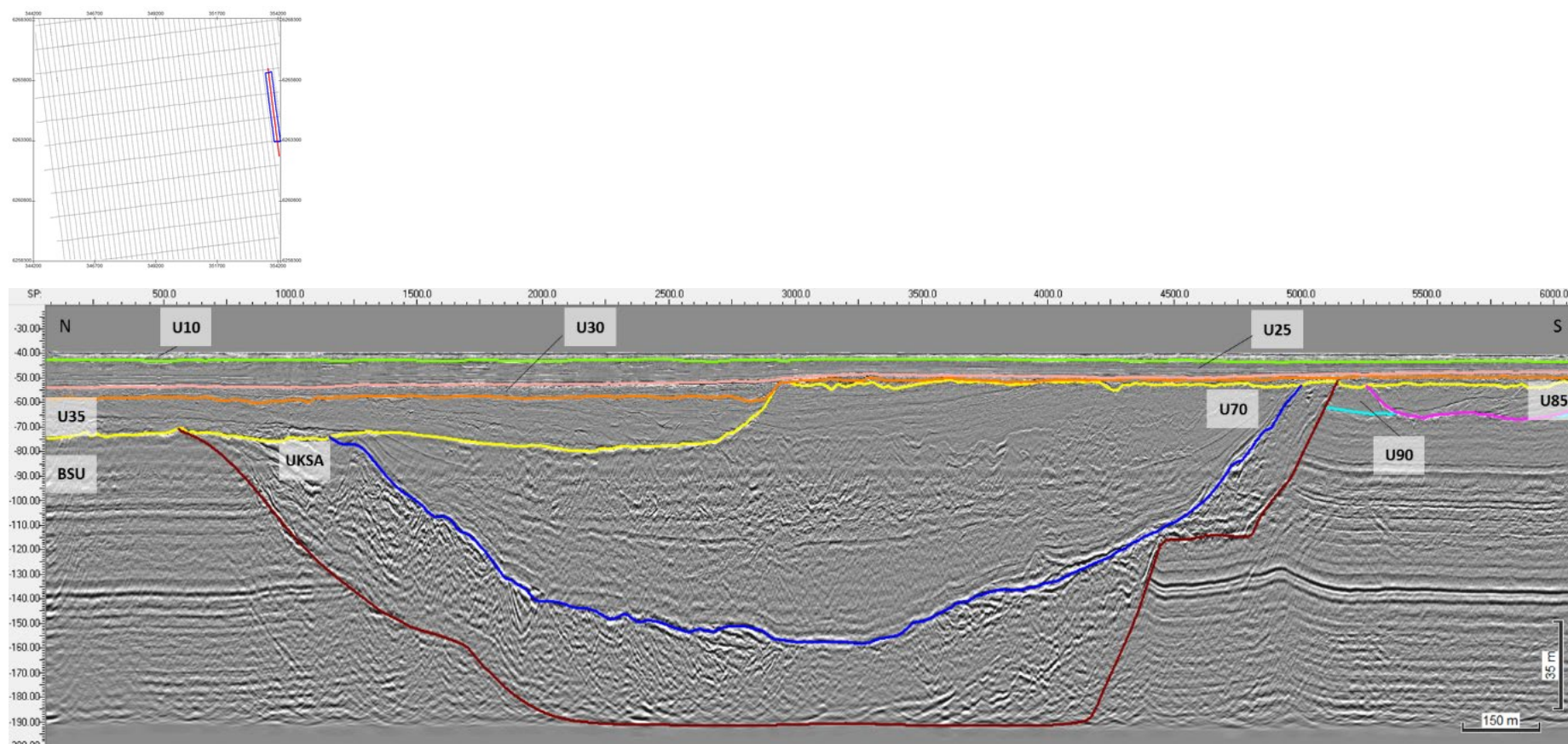


Figure 164 Seismic Unit UKSA deformation below H70_CH_08 incision.
 The image shows the complex and chaotic facies within the incision. Some extensional features can be discerned below H70, which are interpreted to result from collapse of the valley flanks. Seismic profile BM4_OWF_E_2D_09240

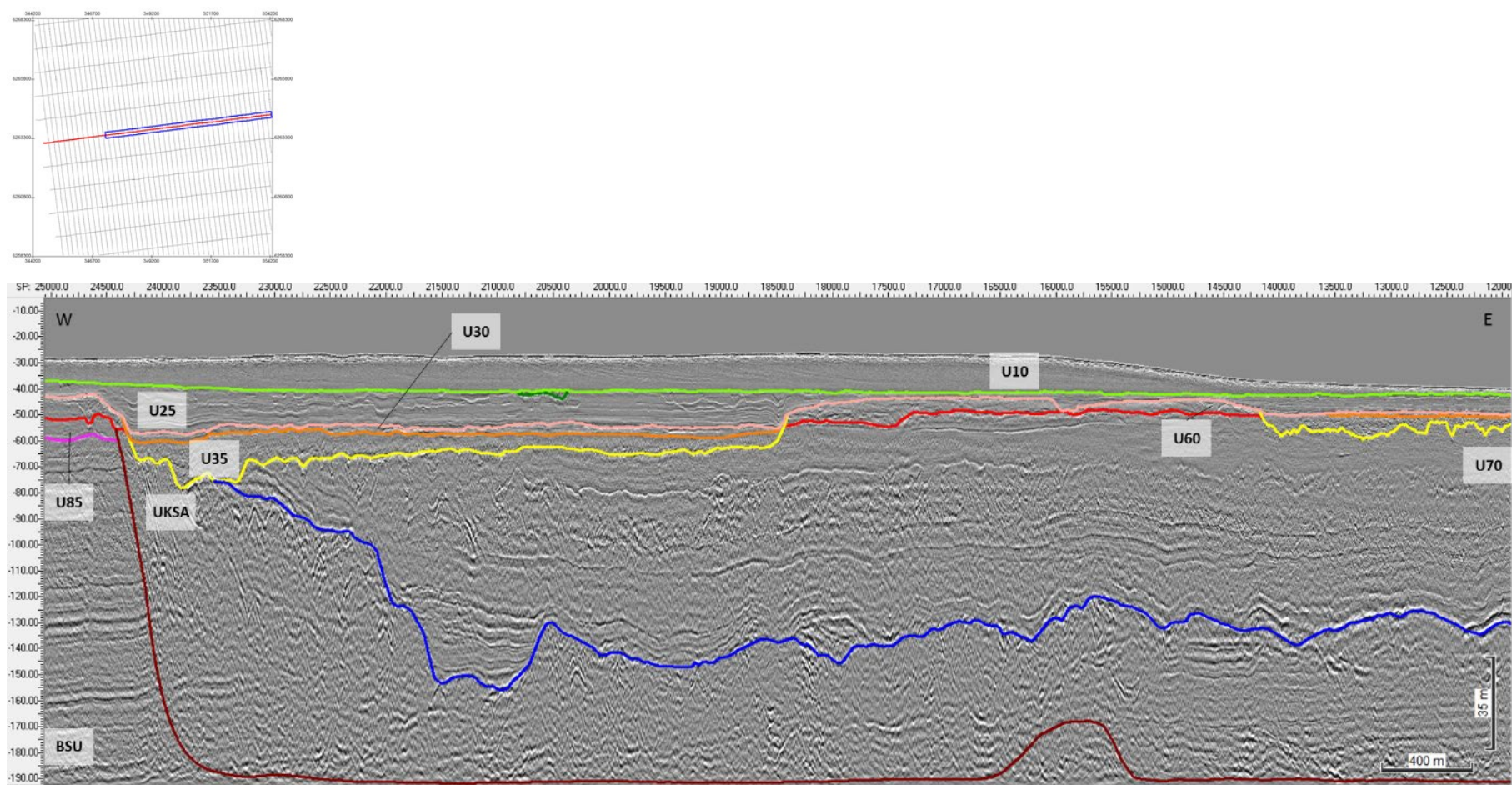


Figure 165 Complex and chaotic facies of Seismic Unit UKSA.
 The image shows horizon KSB delineating a decollement surface, and the deformation front plane. Seismic profile BX3_OWF_E_XL_22000

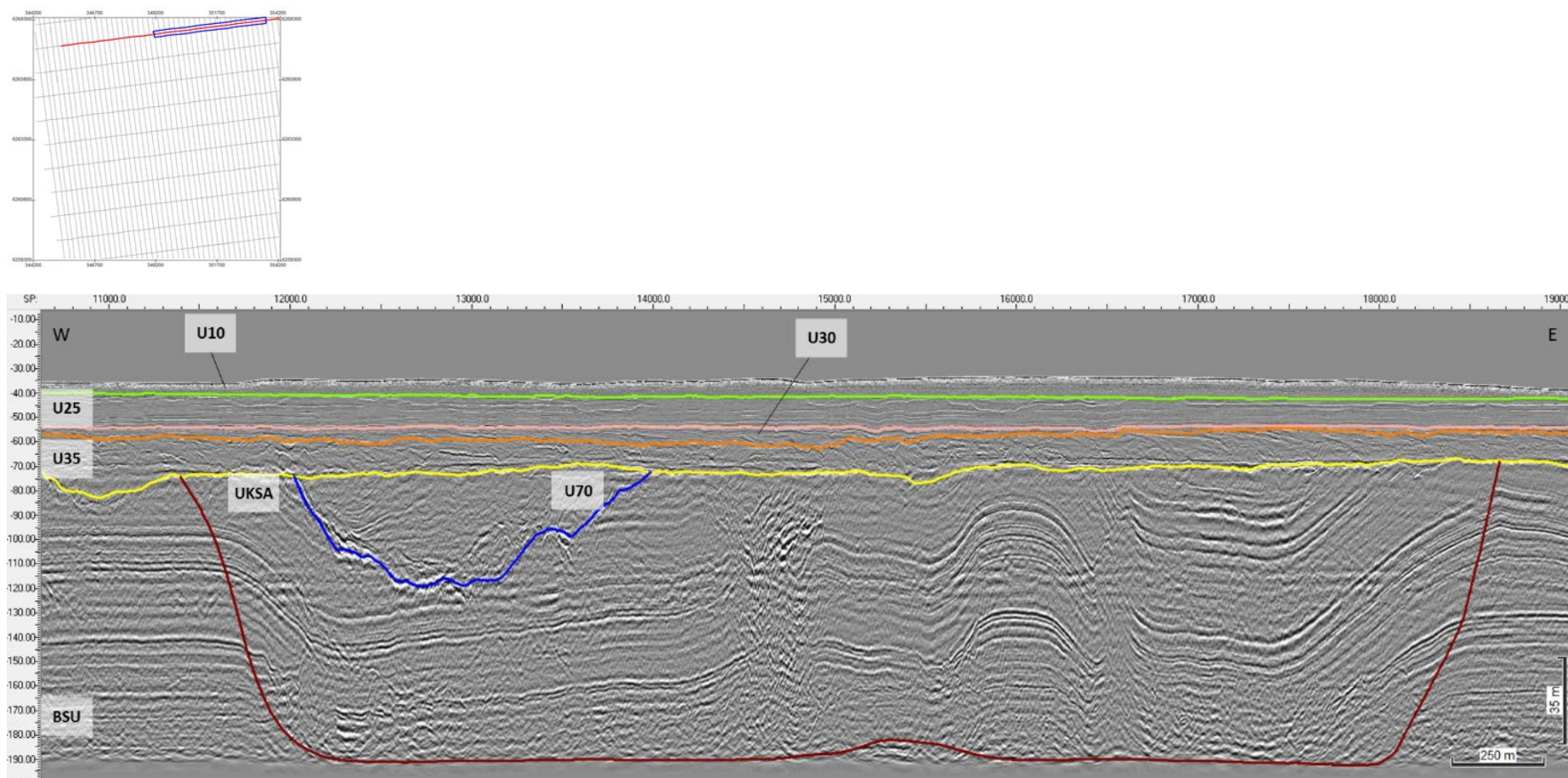


Figure 166 Less intensely deformed sediments, delineated by horizon. Deformed sediments are interpreted to be Pre-Quaternary, constituting the Base Seismic Unit. Note the better preserved strata within the faulted block. The deformation along the rims of this region is extensional in nature, suggesting an area of subsidence, marked by polygon KSA_Subside (see section 8.8.1). Seismic profile BX3_OWF_E_XL_18000

8.6.15 | BASE SEISMIC UNIT BSU

The Base Seismic Unit BSU is a major element of the ground model, and extends spatially across the Artificial Island survey area, except where UKS extends to the base of the seismic record. The base of the unit is at the processing “last knee”, near the terminus of the record. The upper boundary is delineated by a contiguous union of all the deepest mapped horizons. The spatial distribution and (apparent) thickness of the unit are presented in Figure 167.

The seismic facies of BSU comprises a layered sequence of parallel facies of variable amplitude (Figure 168). Faults, fractures and gentle folding of the whole succession are locally observed, but the original configuration of the strata remain well-preserved (otherwise it would be included within the unit UKS). In the vicinity of the deformed deposits of UKS, the deformation of the Base Seismic unit intensifies (Figure 168).

From the characteristics of the Base Seismic Unit, it is interpreted that it corresponds to marine Pre-Quaternary strata.

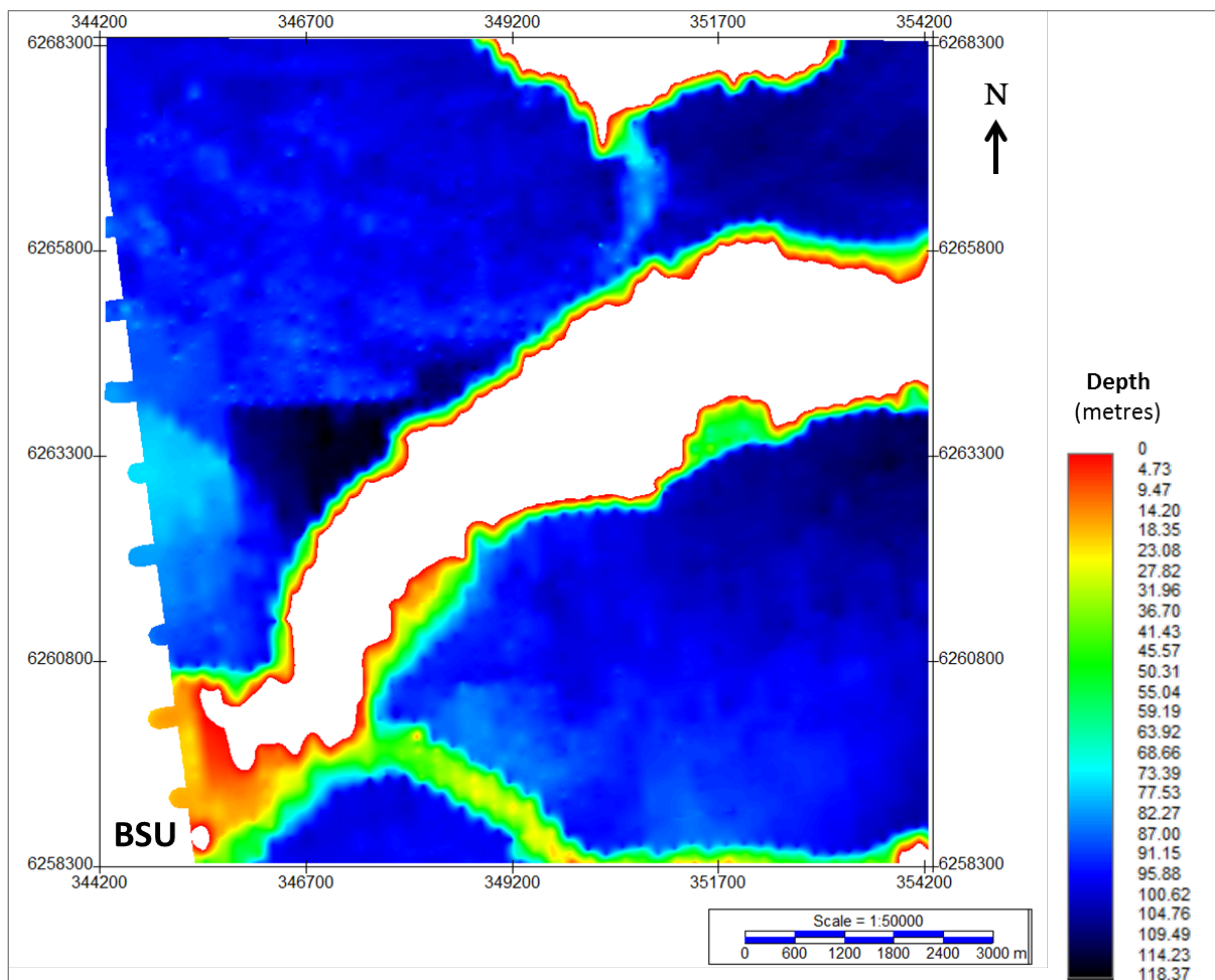


Figure 167 Thickness of Base Seismic Unit BSU.
Units in metres.

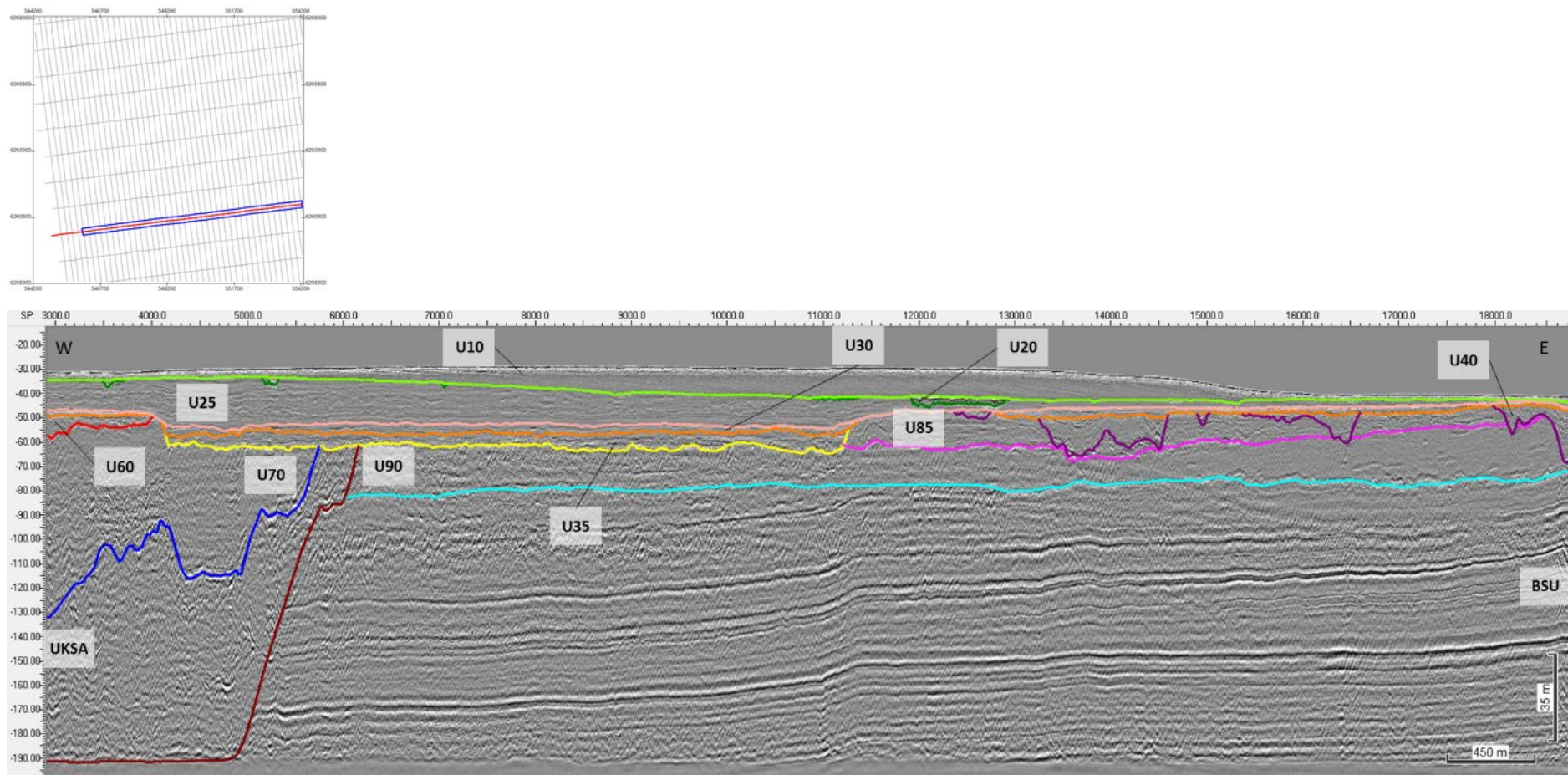


Figure 168 General facies of the Base Seismic Unit.
 Seismic profile BX4_OWF_E_XL_25000

8.6.16 | SUMMARY AND DISCUSSION

The subsurface geological interpretation and description presented here is based on the assessment of the 2D UHRS data acquired within the full MMT OWF survey area. This report summarises the findings and interpretations within the Artificial Island survey area.

The Ground Model presented in this report comprises 12 horizons, defining 13 seismic units that make up its geological framework. The geotechnical information available within the survey area was scarce and superficial. As such, the inferred depositional environments and sediment composition descriptions contained in this report are based largely on seismic interpretation techniques. Seismic facies analysis, reflector terminations, and stratigraphic architecture provided the foundation for the 2D UHR seismic interpretation. A review of the relevant scientific literature guided the interpretation process and placed the results within the known geologic context. However, it is important to understand that there are limitations associated to the interpretation provided, especially taking into account the lack of direct sampling of the deeper sub-surface (>5m BSB) deposits, that would provide ground-truthing information to complement our findings.

Also relevant is the complex geological architecture of the area. The degree of complexity, and by extension, heterogeneity and spatial and vertical variations, posed challenges to the interpretation of the UHRS data.

To facilitate the description of the model, the full MMT OWF survey area was divided in three sectors (North, Central, and South), believed to represent distinct domains of sediment deposition and deformation. The Artificial Island survey area is located in the western limit of the main site, partially encompassing the sectors Central and South.

The large-scale depositional systems identified can be described as dominated by: 1) the direct and proximal influence of glacial processes; or 2) high frequency, variable amplitude, sea-level fluctuations and related depositional environments and shoreline migration. The separation of the two regimes is approximated by horizon H70 and H35. Most of the older seismic units beneath this boundary are characterized by glaciogenic deposition and deformation. The more recent units above this boundary exhibit characteristics of high frequency sequences. These are interpreted to represent cycles of deposition and erosion associated with sea-level fluctuations (transgressions and regressions).

Precise dating of seismic units to the Quaternary and its sea-level curve is not possible with the available data. One exception might be the last and most recent Holocene transgression. However, despite absolute chronological uncertainty, reasonable inferences can be made about the sea-level variations. Based on diagnostic characteristics of the seismic units' surfaces, stratal terminations and facies patterns, we have estimated sea-level behaviour for many of the seismic units. Alongside the model, the assessment of potential geohazards within the sub-surface provided important clues regarding the timing of the different deformation events that took place in the area, complementing our interpretations. These are described in section 8.8.1|Sediment Deformation.

The deposition of the deepest strata imaged in the UHRS data – Base Seismic Unit BSU – marks the beginning of the geological evolution of the survey area as defined by the Ground Model. These deposits correspond to the marine-deltaic Pre-Quaternary sequence. These sediments were likely affected by salt-tectonics (associated to the Zechstein salt diapirism; see section C), as evidenced by the occurrence of extensional faulting and subsidence in the North and Central sectors. The Pre-Quaternary sequence exhibits evidence for deformation near the east limit of the site (deformed seismic unit UKS_B). There, fault pattern analysis suggest deformation towards the NW, possibly associated with Saalian glaciotectonism (maybe older) (see section B). Following, a large sub-aerial exposure and associated erosion event took place. This is captured by H90, displaying truncation the locally deformed Pre-Quaternary deposits. Above this surface, a delta system is present in unit U90, followed by the fluvial deposits of U85.

A more recent and new episode of glaciotectionism ensued, with thrust deformation advancing from NE (NE-SW oriented), forming the large thrust complexes. These are present in the North sector (unit UKS_A), evidenced by the intense deformation of units BSU, U90, and U85. This deformation is likely related to the Weichselian glaciation, synchronous to the generation of the large tunnel valleys (or re-use of older) in which the U70 glacio-fluvial system is present. High energy fluvial bedforms corresponding to unit U60 were deposited, possibly also associated to outwash plains, and flash flood events. Above U60 deposits, fine sediments of unit U50 accumulated in a lower energy setting, outside the Artificial Island survey area (north sector). The origin of U50 is uncertain, as it may correspond to a glacial drift deposit (aqua till?), or comprised of glaciolacustrine sediments. Scattered point diffractors within U50 may be related to the presence of boulders. Glacial meltdown and ice retreat may be associated with the establishment of the drainage network and subsequent sediment infilling of U40, alongside local glaciolacustrine deposition. This Weichselian (?) glaciogenic deposition and deformation is capped by the erosional event of H35, which carved the three major basins located in the Central and South sectors.

Sediment deposition above H35 appears to be dominated by high frequency sea-level fluctuations, related to eustatic-isostatic and autogenic processes, away from any glacial influence. An overall transgressive sequence infilled the basins, starting with the deposition of U35 fluvial bedforms at the base, followed by the finer deposits of U30. As the sea level rose, flooding of the basins led to the deposition of the lower section of unit U25, likely within a transgressive estuary setting, no longer constrained by the basins' margins. The increase of small channel-incisions within the upper deposits of U25 suggests the occurrence of a regressive event/fluctuation (at least in relative terms). The deposits of U20 consist of infills of small basins and/or channels, which could be related to a restricted marine-tidal deposition and partially to a subaerial fluvial infill. Above the ravinement surface of H10 (likely a wave cut) rests the last and most recent U10 deposits. This unit is made up of the recent transgressive deposits (possibly some high-stand) and includes the modern seabed marine sandy deposits

8.7 | SEABED HAZARDS

Below are summaries of various seabed hazards in the Artificial Island area of investigation.

8.7.1 | GRADIENTS

Slope angles across the site are typically very gentle ($<1^\circ$) and gentle (1° to 5°).

Very steep slope angles (15° to a maximum of 44°) were observed within the survey area but these were restricted to steep banks on the western side of the Artificial Island survey area.

For complete details refer to section 8.2.3| Slope Analysis.

8.7.2 | MOBILE SEDIMENT AND BEDFORMS

Extensive areas of mobile sediments are present across approximately half of the Artificial Island survey area. The mobile sediments range from smaller wavelength bedforms such as ripples, large ripples, megaripples to larger scale sediment bedforms such as sand waves and sandbars.

For complete details refer to section 8.3.2| Mobile Sediments.

8.7.3 | BOULDERS

No boulder fields are observed within the Artificial Island survey area but scattered boulders are present throughout. Boulders are of a higher concentration to the west of the Artificial Island survey area (Reporting Tiles T13 and T19).

For complete details refer to section 8.3.3| Boulders.

8.7.4 | EXISTING INFRASTRUCTURE AND WRECKS

The client supplied background data indicates the TAT-14 cable crosses the south-west corner of the Artificial Island survey area, trending northwest to southeast. The cable is buried and observed on MAG data, with a possible seabed exposure observed in the SSS data for 39.2 m on the very western extent of the Artificial Island survey area.

No wrecks were observed in the survey area.

For complete details refer to section 8.5| Existing Infrastructure (Cables and Pipelines).

8.8 | SUB-SEABED HAZARDS

The 2D UHRS datasets were inspected in order to identify any potential constraints on future developments of the site; it does not directly correlate with a risk. This careful assessment revealed the presence of potential geohazards within the sub-surface of the survey area. The most relevant geohazards identified are:

- Sediment deformation:
 - Faulting;
 - Glaciotectonics;
 - Gravitational deformation;
 - Salt dome related tectonics;
- Buried channels and tunnel valleys;
- Soft sediments and organic-rich deposits;
- Coarse sediments, gravel beds, and boulders;
- Fluid flow and gas features;
- Lacustrine deposits.

The interpretation and mapping of all geohazards described in this section were performed using manual picking as seismic data resolution and human precision allowed.

A more detailed description of the aforementioned geological hazards is presented within the sections below.

8.8.1 | SEDIMENT DEFORMATION

Areas of tectonization/deformation were identified throughout the full MMT OWF survey area and within the Artificial Island survey area. Distinct patterns and degrees of deformation are observed, depending on which deformation process took place. Deformation levels range within a large spectrum, from low (minor) to high (strong). In areas of low deformation, minor folding (wavy reflectors) and small-displacement faulting is observed within well-preserved strata, with the original stratigraphy of the unit mostly intact (Figure 169 A). With intensifying sediment deformation, large-scale/displacement faults, shear/fracture zones, decollements, and high amplitude folding occur (Figure 169 C). On the extreme end, strongly deformed sediments present themselves as seismically chaotic and incoherent, with no discernible internal seismic reflectors (Figure 169 D). The materials within these units are likely to have experienced variable and complex stress, i.e., compressional, tensional, and shear. These units should have geotechnical significance given their complex stress/load histories.

In the survey area, the process in which the sediments became deformed are interpreted to have different origins: glacio-tectonics; salt tectonics; and gravitational deformation. These processes may work independently or simultaneously, increasing even further the complexity of the units' seismic facies.

Regardless of the process, fault surfaces/zones are always observed. Fault mapping in the survey area is described below, followed by the different modes of deformation identified

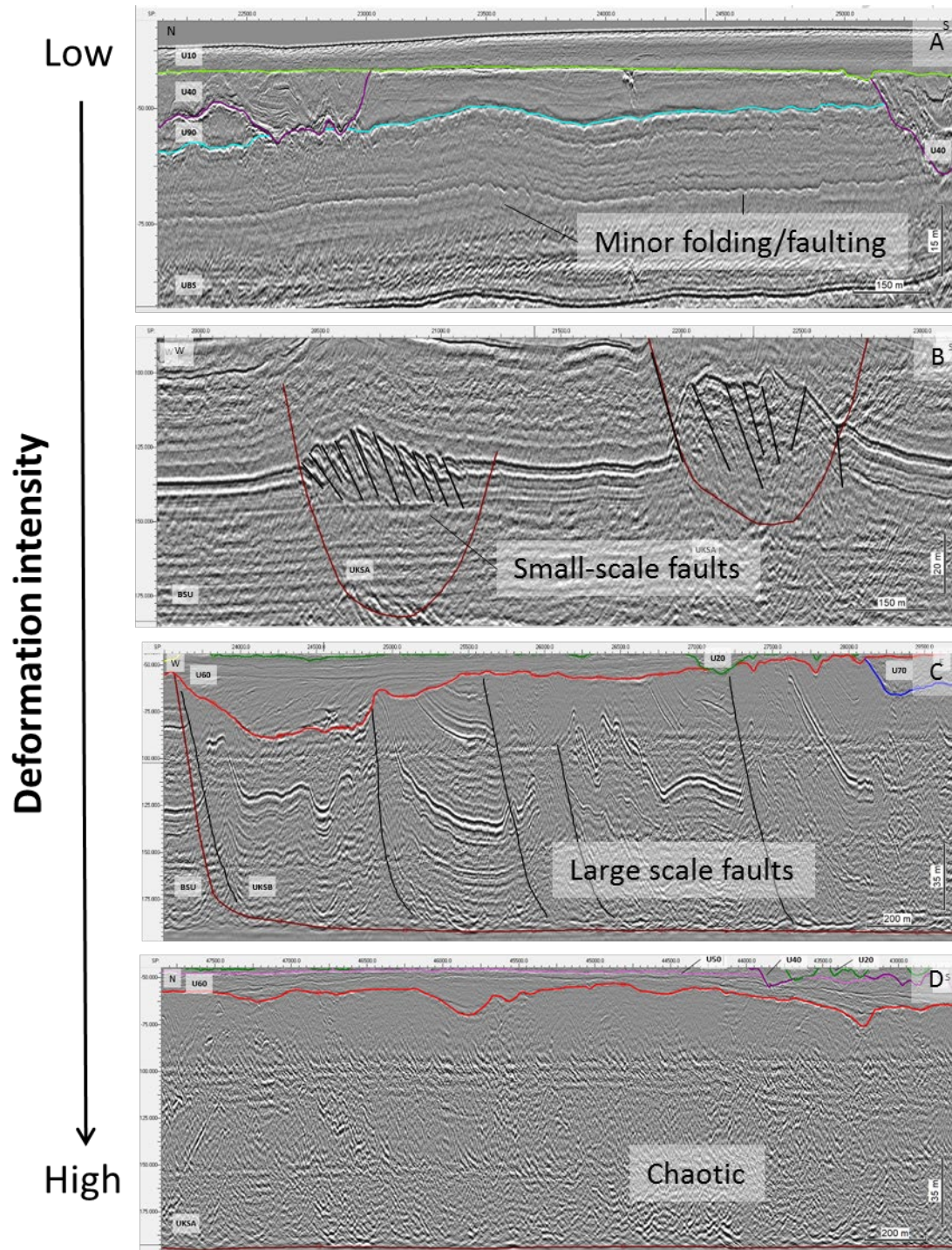


Figure 169 Different levels of deformation observed within the site. Deformation intensity ranges from (A) low (minor folding and small-displacement faulting) to (C) major (large-scale/displacement faults, shear/fracture zones, decollements, and high amplitude folding). Extreme deformation (D) is observed as seismically chaotic and incoherent. Images (A), (B), (C), and (D) are sections of lines BM3_OWF_E_2D_07350, BX4_OWF_E_XL_23000 (B and C), BM4_OWF_E_2D_10710, respectively

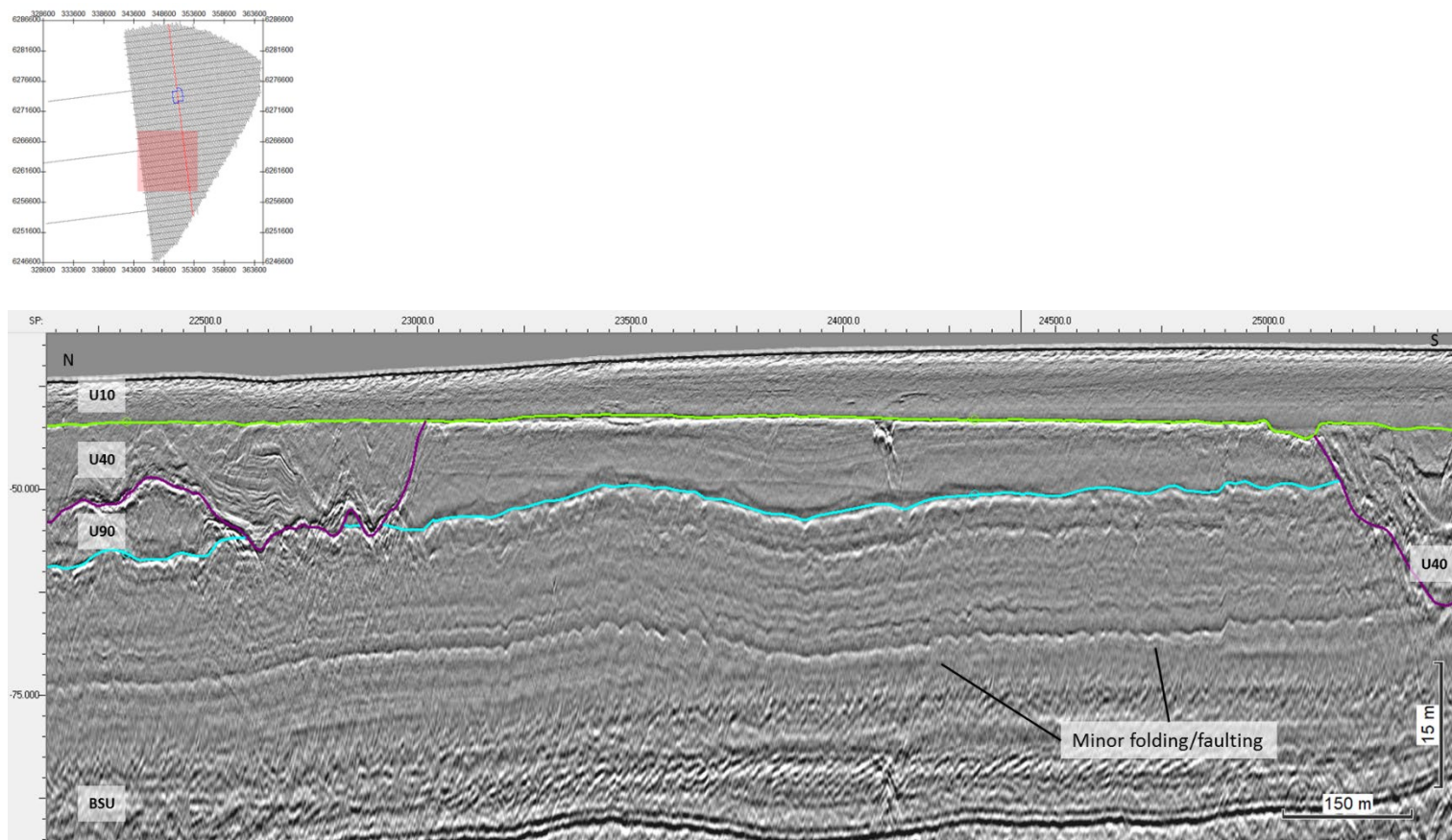


Figure 170 Seismic profile displaying minor folding and faulting affecting the BSU sequence.
 Section outside the Energy Island site (red square).
 Line BM3_OWF_E_2D_07350

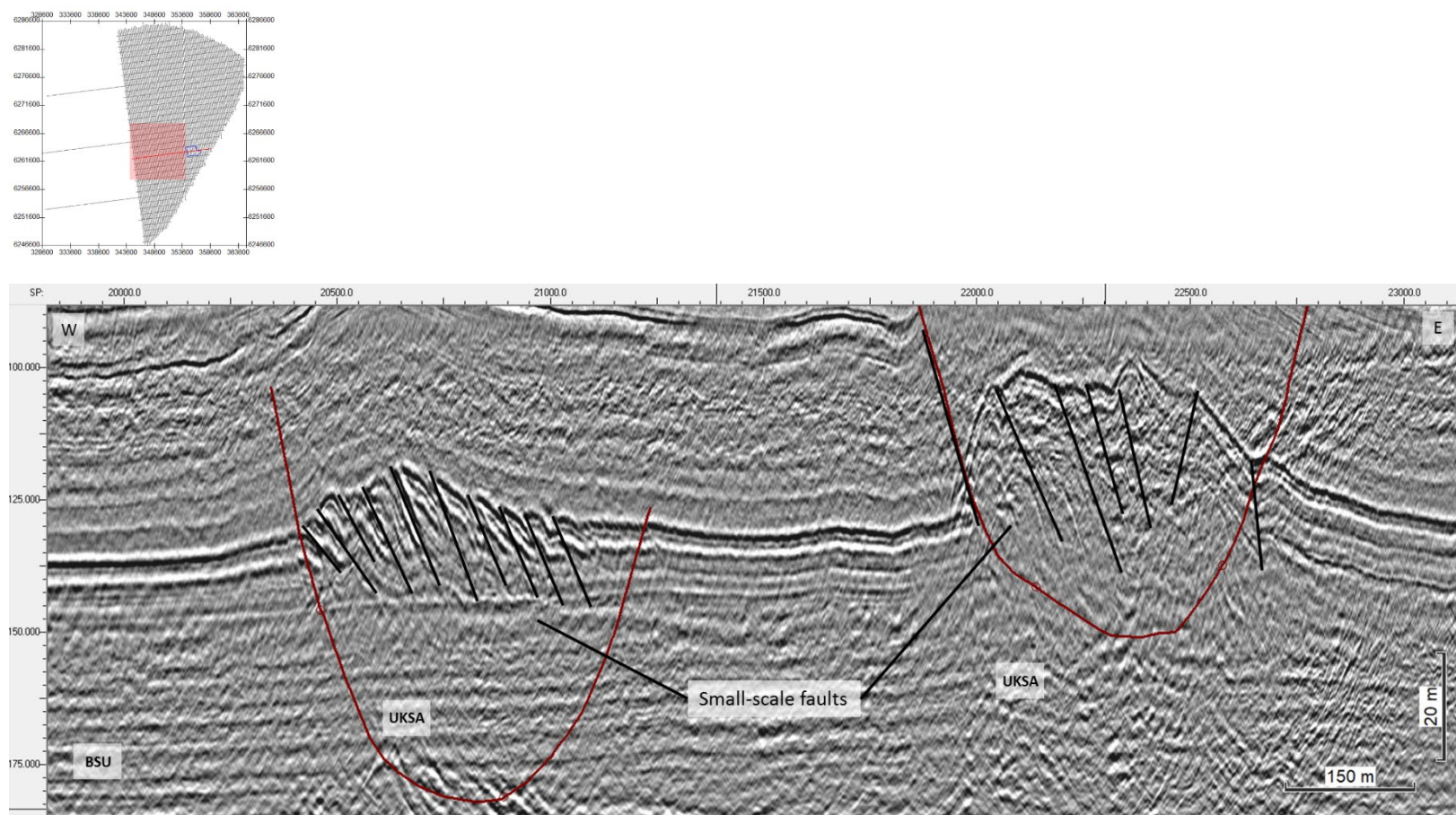


Figure 171 Seismic profile displaying small scale faults within a thrust complex.
 Section outside the Energy Island site (red square).
 Line BX4_OWF_E_XL_23000

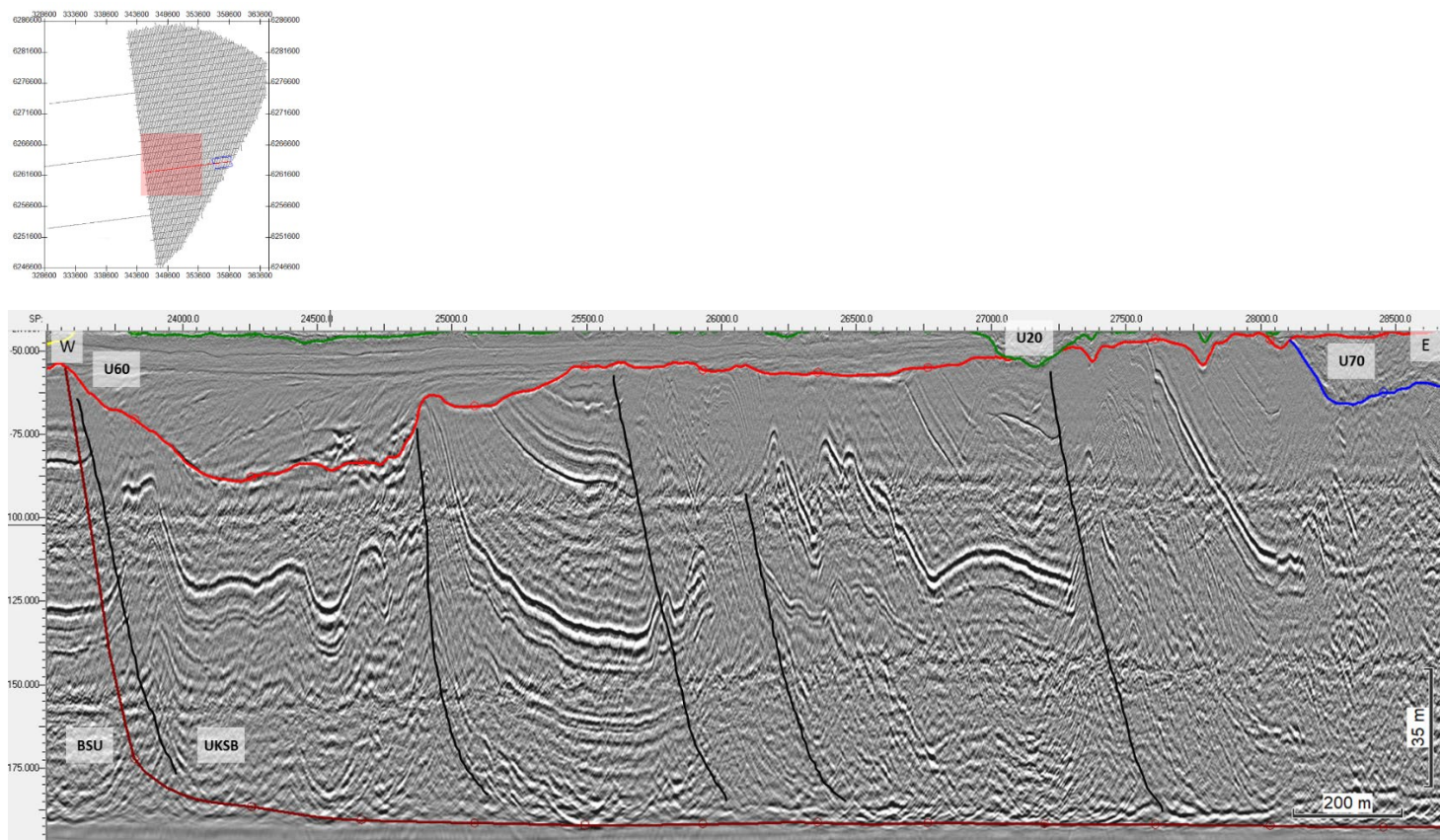


Figure 172 Seismic profile displaying large scale faults within a thrust complex.
 Section outside the Energy Island site (red square).
 Line BX4_OWF_E_XL_23000

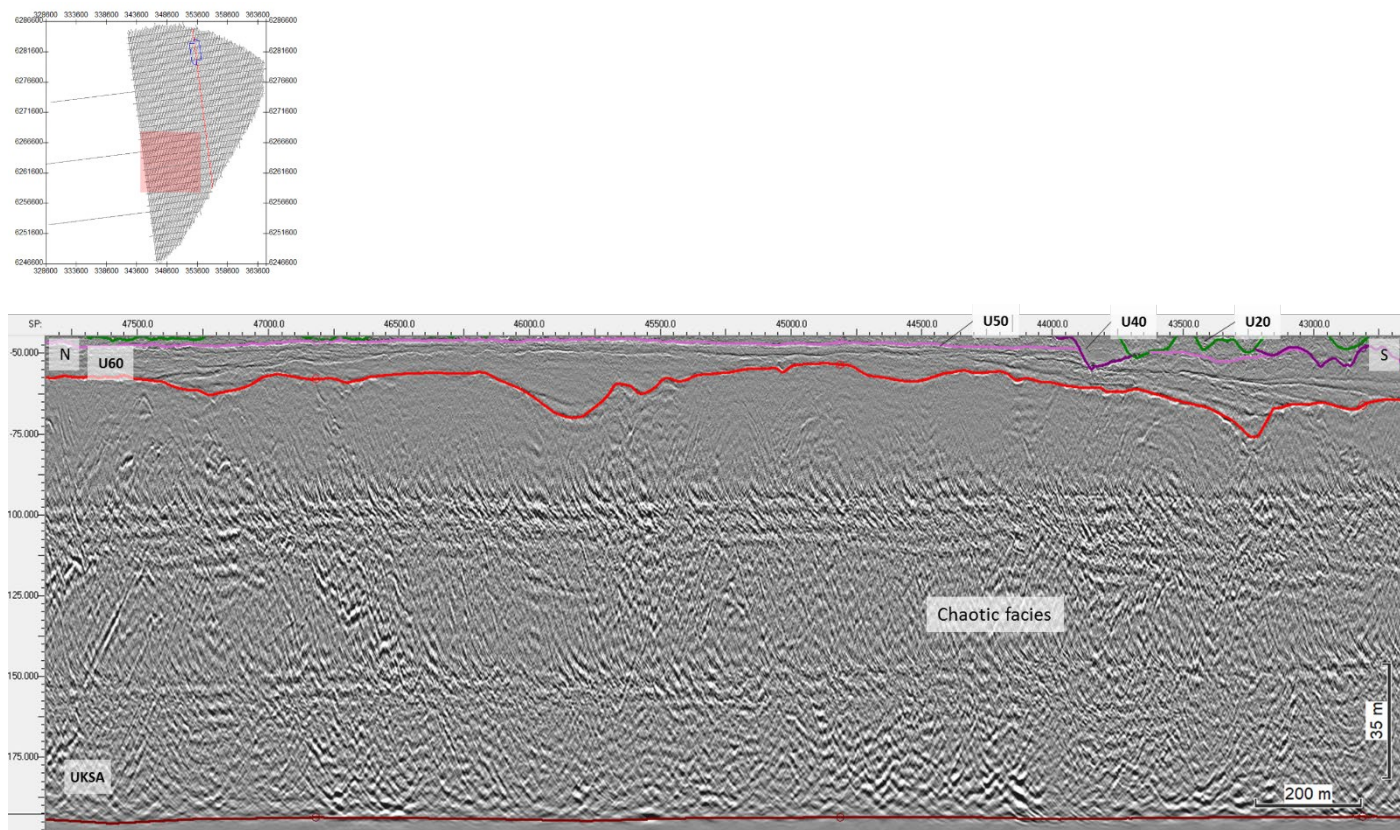


Figure 173 Seismic profile displaying intense deformation within a thrust complex, obliterating reflector's continuity and organization – chaotic facies. Section outside the Energy Island site (red square). Line BM4_OWF_E_2D_10710

A. Faulting

Evidence of faulting has been identified across the site. Faults were picked manually where relevant planar discontinuities, displacement of seismic reflectors, and major reflector-fault drags were recognised on the seismic data. Depending on the angle between the faults and the seismic sections, some features may appear more noticeable than others. A way to mitigate this was by inspecting the fault basemap to ensure that features were digitized on a coherent and continuous manner; i.e., tracing was done from profiles where the faults were more evident to profiles with reduced expression. Figure 174 displays the final fault basemap produced. Minor, isolated, and dubious features may have been left out due to the complexity of the subsurface framework and difficulty in recognizing all features and faults, as line spacing dictates the resolution in which subsurface features can be traced laterally (ex., tectonic structures).

Faults are observed affecting all units, but do not greatly affect sediments of U20 and younger (Figure 175 to Figure 186). Their type and size are highly variable. The majority of faulting is captured within UKS, as this unit represents the extent of sediment deformation. Horizon KS, the surface that delineates the deformation front, may itself be a fault plane (Figure 175).

The majority of the faulting in the site is related to glaciotectonics (see section below). However, salt tectonics and gravitational deformation are also interpreted as fault-producing processes in the area (see sections below).

Lack of fault identification should not be taken as an assumption of total absence.

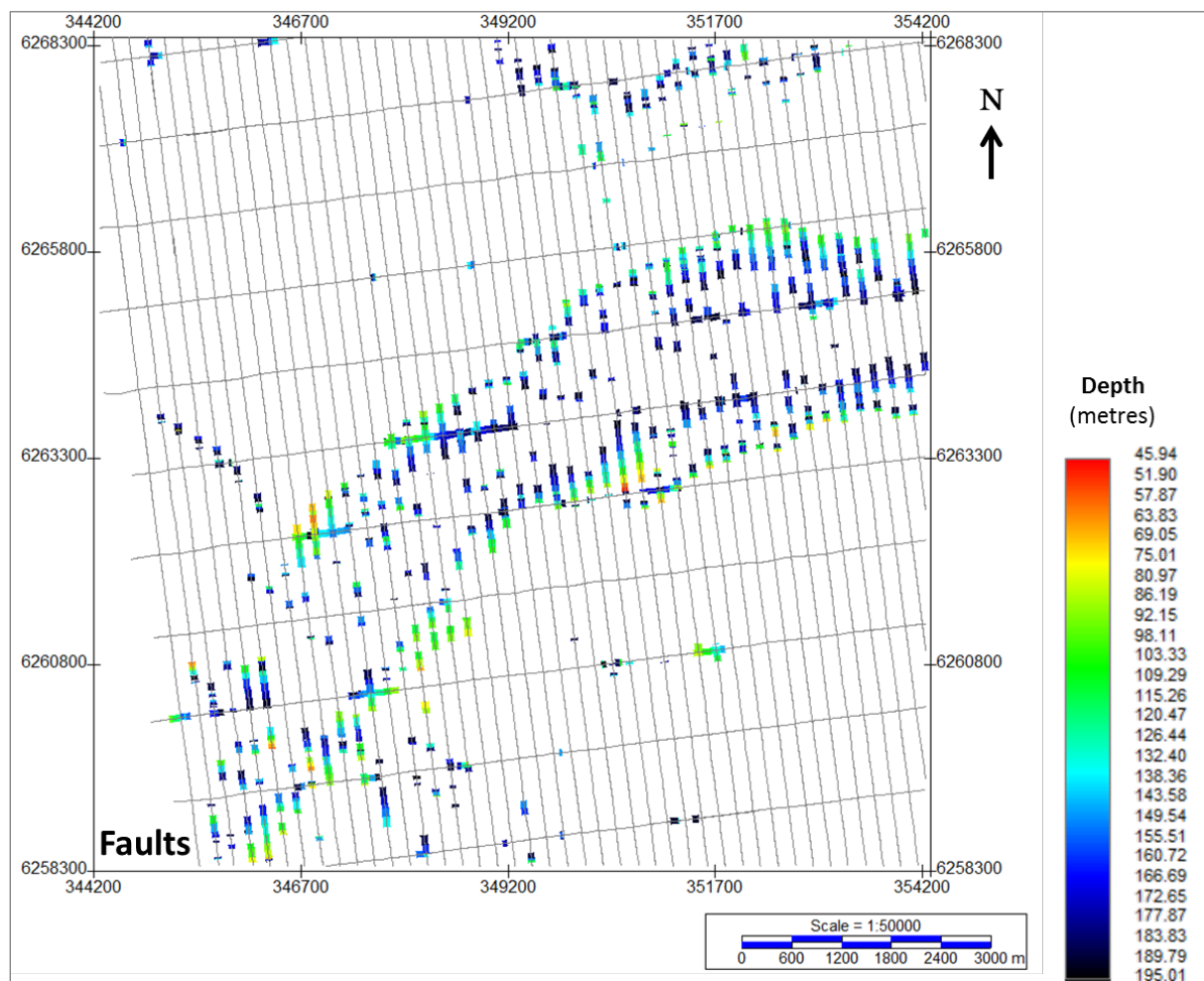


Figure 174 Map displaying all the interpreted faults in the site.
 Units in metres below BSB.

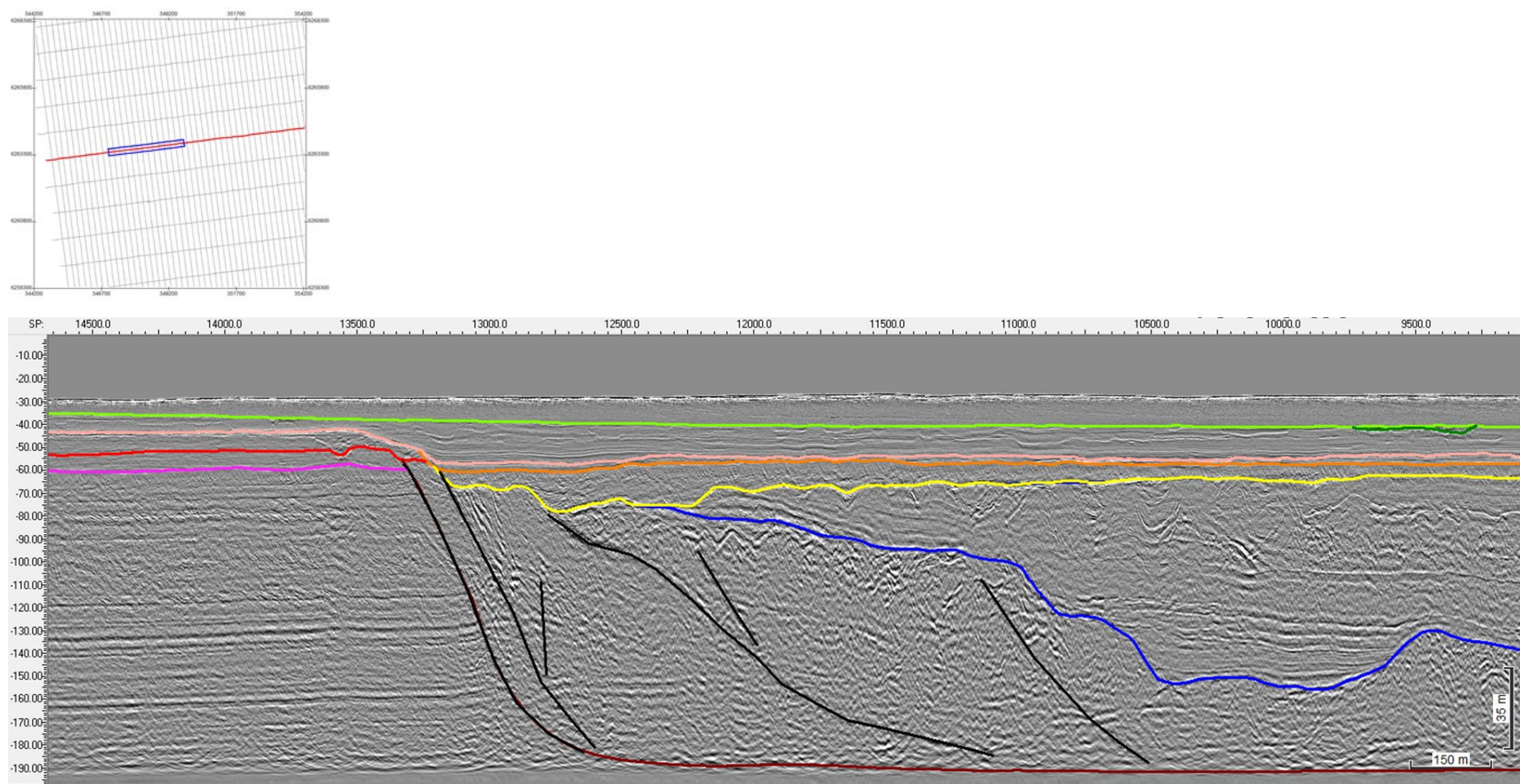


Figure 175 Thrust complex of Seismic Unit UKSA
 Horizon KSA delineating a decollement surface, flats and ramps, and the deformation front plane. Seismic profile BX3_OWF_E_XL_22000

B. Glaciotectonics

Seismic unit UKS captures the vast majority of the tectonized deposits and the distribution of the different patterns of deformation identified (see section 8.6.14)) The UHRS data clearly depicts the distribution and extent of glaciotectonism within unit UKS.

In the survey area, deformation is mostly interpreted as large-scale thrust structures (including imbricated faults, fault ramps, fault-drags, and folds; Figure 175), typical of glaciotectonic thrust complexes formed ahead of an ice sheet as it moves forward.

Two distinct areas of thrust deformation were identified within the survey area, delineated by the polygons KSA_Tunnel Valley and KSB_Thrusting (Figure 176).

Horizon KSA truncates seismic units below H70, i.e., this glacial deformation affects units U85, U90, and BSU (Figure 175). However, deformation within the SE corner of the site (KSB_Thrusting) appears to be older than U85-U90, as these units truncate deformed deposits in this area, affecting mostly a region outside the Artificial Island survey area. As such, the glaciotectonic deformation towards north (KSA) is interpreted to be relatively younger than the deformation in the SE corner (KSB). In order to better understand these two different stages of glaciotectonism in the area, a small sample of the largest thrust faults from the full MMT OWF survey area were analysed according to their general orientation, to provide clues on the main directions of ice push acting on the site. This assessment is presented and discussed in the MMT OWF survey area report. The two distinct thrust directions given by the fault analysis further support the occurrence of at least two different stages of glaciotectonism.

Within the Artificial Island survey area, the effects of these two stages of glaciotectonism are less intense than the deformation observed elsewhere. Most glaciotectonic deformation within the area is associated to the development of the large tunnel valley H70_CH_08, occurring below Seismic Unit H70 (Figure 175).

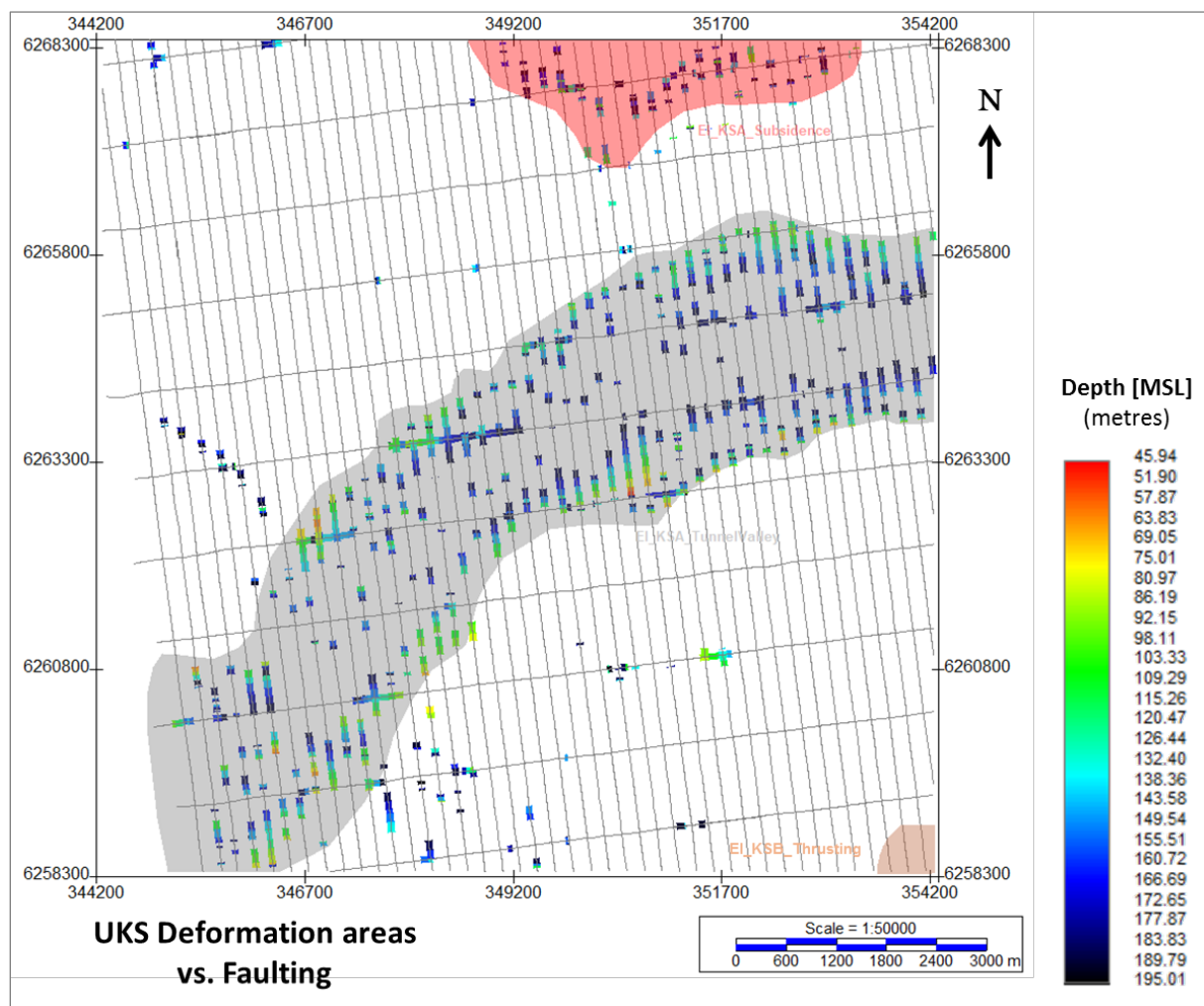


Figure 176 Deformation and faults within the Seismic Unit UKS
 The image shows deformation domains within the Seismic Unit UKS (composite of UKSA and UKSB) and sampled faults used for fault pattern analysis.

C. Salt tectonics

Large faults with extensional displacement are locally observed affecting the deeper Pre-Quaternary deposits, within unit UKS. The occurrence of these normal faults is limited to a region at the northern limit of the Artificial Island survey area. Large normal faults laterally bound this region, resulting in the subsidence of a Pre-Quaternary block delineated by the polygon KSA_Subside (Figure 177).

All the normal faults observed in the survey area extend deeper than the UHR seismic record. As such, and due to their extensional character, these areas were compared with the known basement structure of the region to assess the possibility of salt tectonics as their origin. Figure 178 displays the polygon KSA_Extension overlaid on the Base of Chalk Structure Map (GEUS). The highlighted areas of extension/subsidence occur vertically above previously identified major extensional faults associated to the Zechstein salt tectonism (Michelsen, 1993). Thus, it is interpreted that the deformation observed within these areas is most likely related to deep salt diapirism (ex., salt movement related to glacial load and melt back).

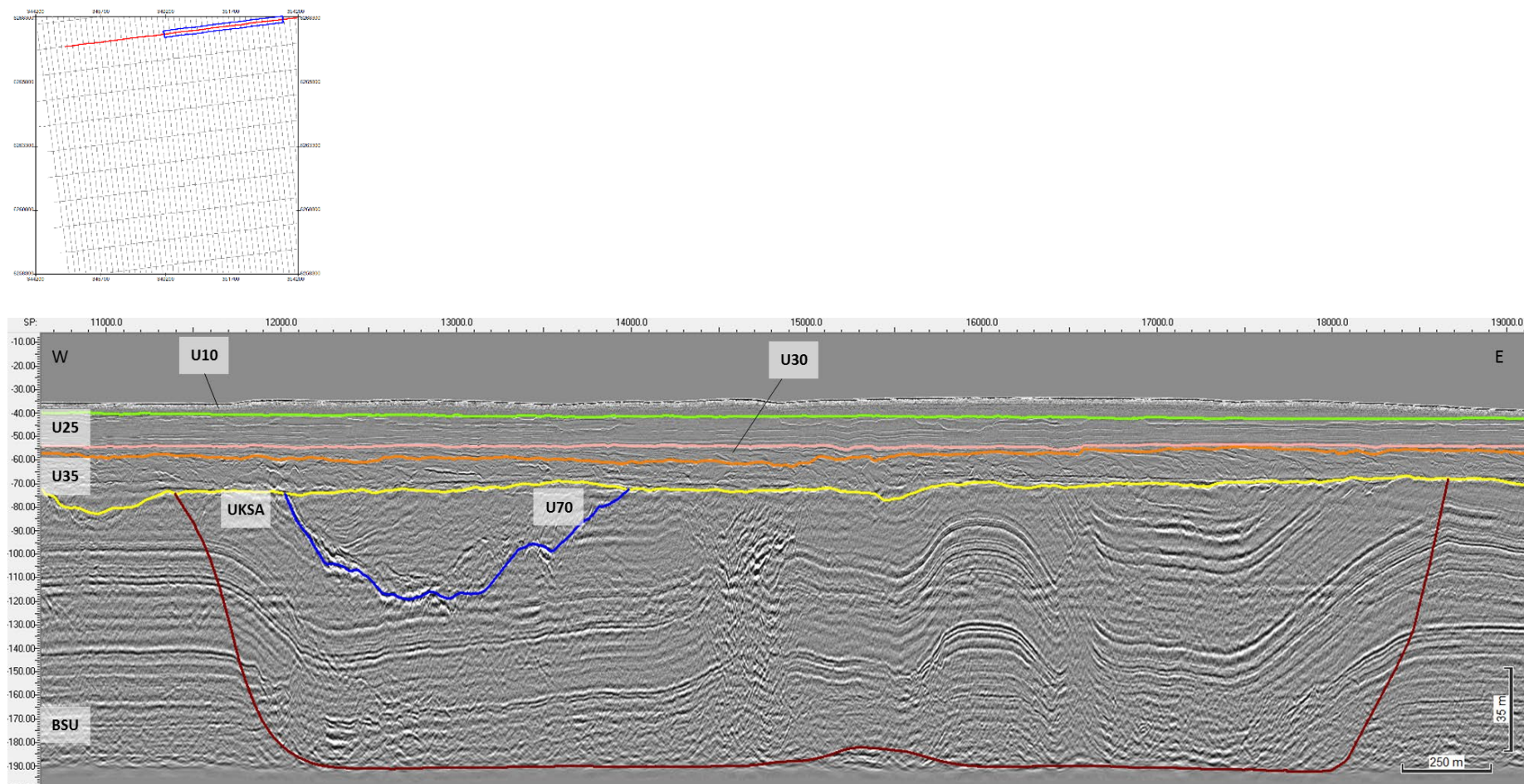


Figure 177 Subsidence area bounded by large normal faults in the northern limit of the area.
 The area is delimited by the polygon KSA_subsidence. Seismic profile BX3_OWF_E_XL_18000

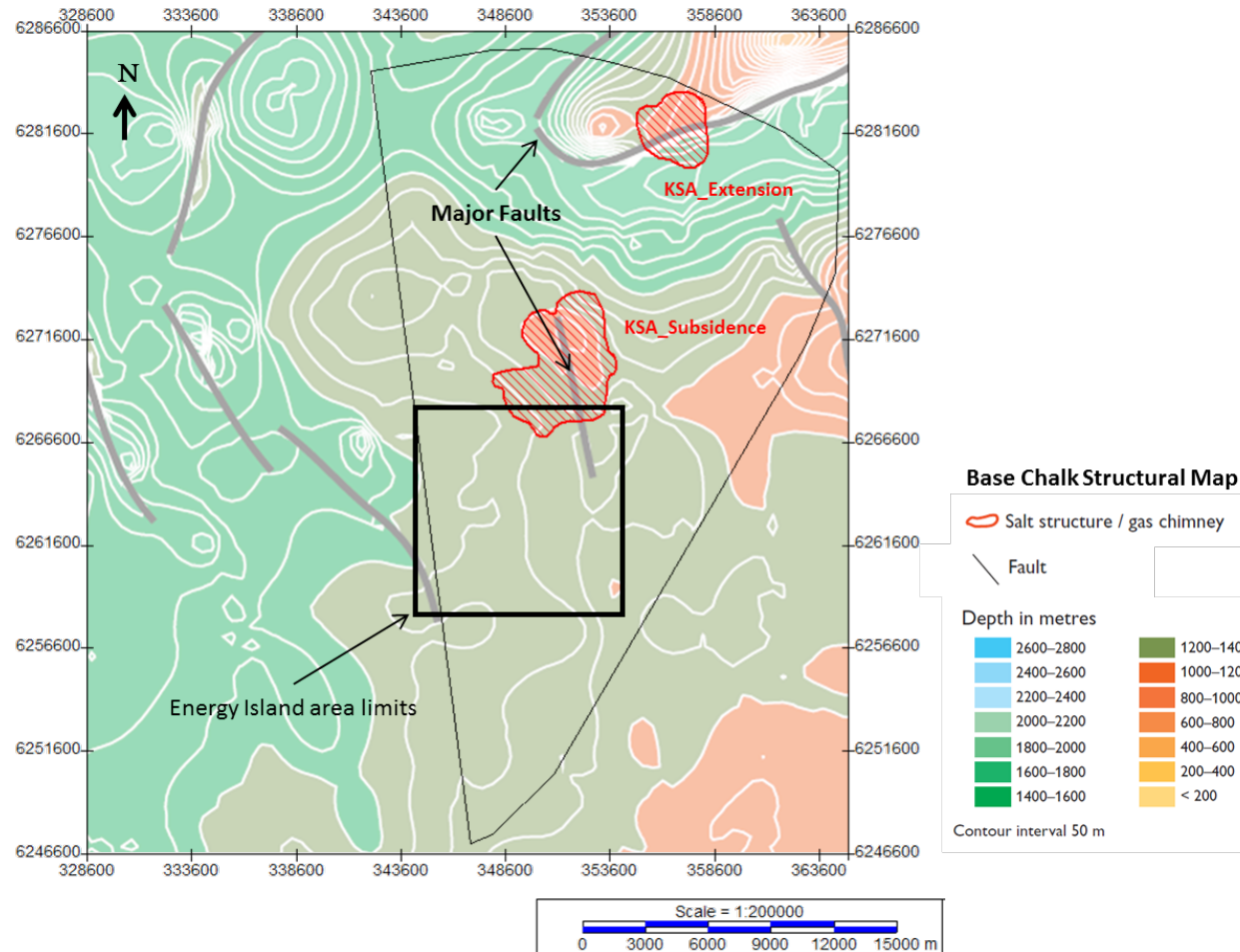


Figure 178 Structural map of the base of the Chalk deposits (GEUS), showing the main structural features related to salt tectonics in the area. Polygons KSA_Subsidence and KSA_Extension occur vertically above major deep fault structures. As such, it is likely that extensional deformation observed in the area is related to salt movement.

D. Gravitational deformation

Slope failure, collapse along the flanks of tunnel valleys and major incisions (upslope extensional faulting with chaotic facies at the base) are some of the structures observed in the survey area that may be related to gravitational deformation.

Polygon KSA_TunnelValley delineates deformation that occurs directly below the large NE-SW valley of U70 (delineated by the polygon H70_CH_08), along its full length (Figure 179). This deformation has mostly a disorganized character.

The base of the valley flanks is uneven (along H70), with numerous steps resembling small extensional displacements. In the upper sections of the deformed sediments, immediately below H70, better-preserved strata dip inwards towards the centre of the valley, showing disturbed/chaotic facies (stacked chaotic-mound facies association) towards the base. Such deposits could result from slope failure or collapse along the flanks, as a result of gravitational failure.

It is interpreted that the U70 valley was emplaced along the pre-existent deformation “corridor”, exploiting this weakened area.

These collapse features and small slump deposits are observed associated to the flanks of other large incisions in the survey area.

Local areas of seismic unit U25 that occur outside the Artificial Island survey area exhibit variable degrees of internal deformation. This deformation is typically observed as minor folding in less-deformed areas and as intra-U25 faulting (with minor displacements, both extensional and compressional) in more intensely-deformed strata, typically occurring near the steep margins of the central basin. These deformation patterns are intrinsic to U25, not affecting the units above and below. As such, it is interpreted that this deformation is most likely related to thin-skinned gravitational tectonics, possibly also associated to sediment dewatering.

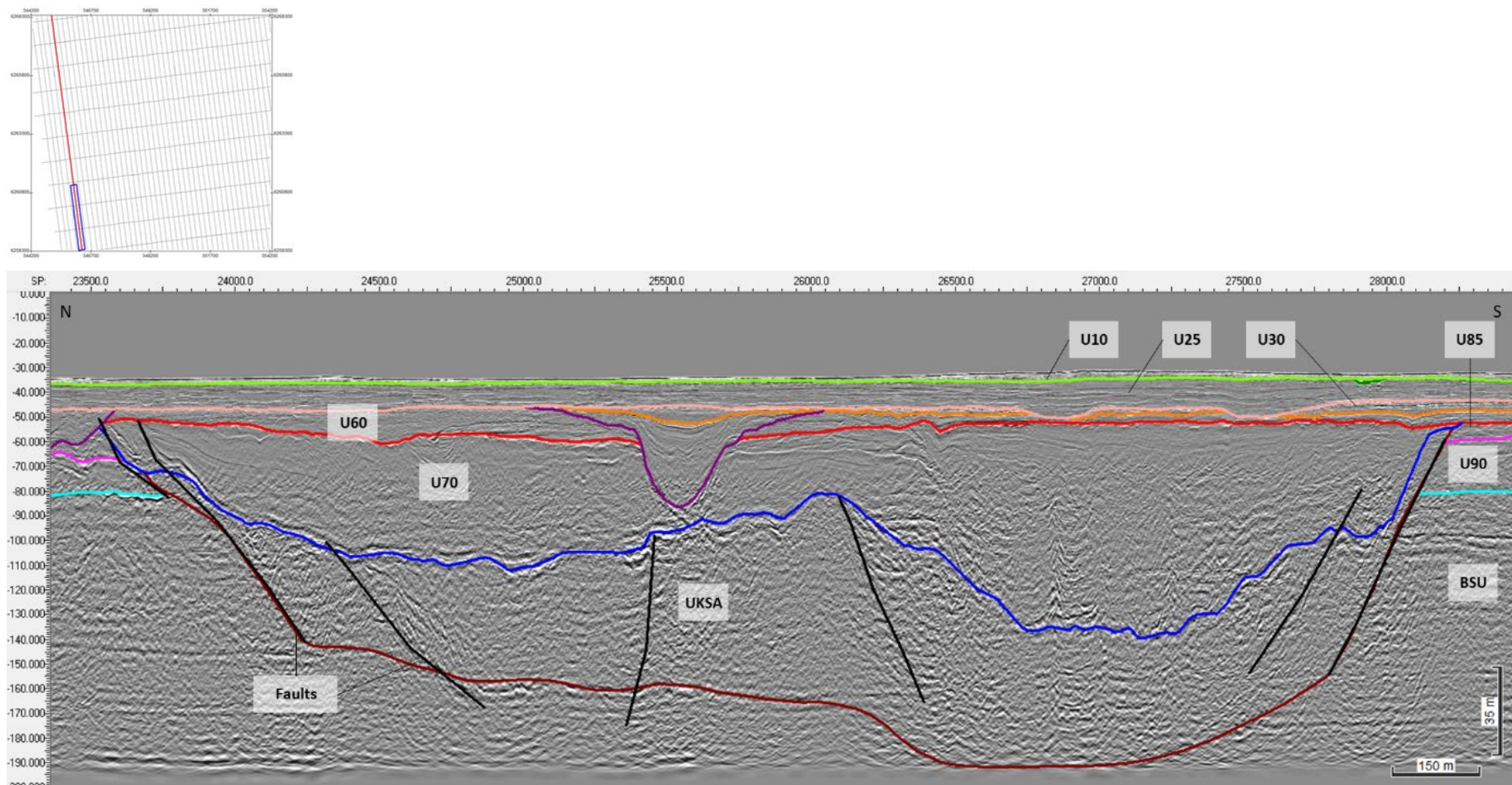


Figure 179 Extensional features below a U70 valley (H70_CH_08).
 The features are interpreted to result from collapse of the valley flanks.
 Seismic profile BM1_OWF_E_2D_00840_01

8.8.2 | BURIED CHANNELS AND TUNNEL VALLEYS

Multiple paleo-valley, basins, and channel systems are widespread throughout the site, displaying a range of sizes and depositional characteristics. Often, the channels are interpreted as multi-generational, appearing as a vertical succession of channels/valleys nested one within another. The most significant erosional surfaces were identified and mapped; these major events correspond to the bases of the units described above. The channels can be easily identified in the various horizon basemaps presented in the previous chapter.

Figure 180 display a composite surface resulting from the addition of all base horizons of units U10 to U70. In this composite surface, all major channel and valley incisions may be observed, highlighting the diversity in size and drainage pathways, and vertical succession. The major incisions are identified by the polygons marked in Figure 181, showing their associated seismic unit.

Due to the large number of paleo-incisions in this area, the mapping of these as geohazards was focused on the major features that are not already delineated by the unit's basal horizons. Therefore, all minor paleo-valleys have not been included in this mapping. Within the Artificial Island survey area, all the major channel features have been mapped by a unit's basal horizon. As such, no major channels were mapped as a geohazard horizon.

Details on the seismic character of major incisions marked by unit bases can be found in the respective unit's description (see section 8.6.1|).

Channel morphology is diverse and ranges from V-shaped, U-shaped, to box-shaped. Similarly, there exists a broad distribution of channel widths and depths observable in the UHRS data. The sediment infill of the channel features varies laterally and vertically. This degree of sediment heterogeneity may result in significant variability of geotechnical parameters within the channels.

From a hazard standpoint, the infill of tunnel valleys may be problematic for a variety of reasons. Tunnel valley infill is nearly always complex, with a heterogenous sediment composition, where lithological and mechanical properties may change rapidly over small spatial scales. Also, faulting and fracturing, from direct ice incision and pressurized hydraulic action, are common in tunnel valleys. Tills are commonly deposited near the base of tunnel valleys. Lastly, the complex load, and stress histories of tunnel valleys and their marginal deposits translates into abrupt differences in mechanical properties.

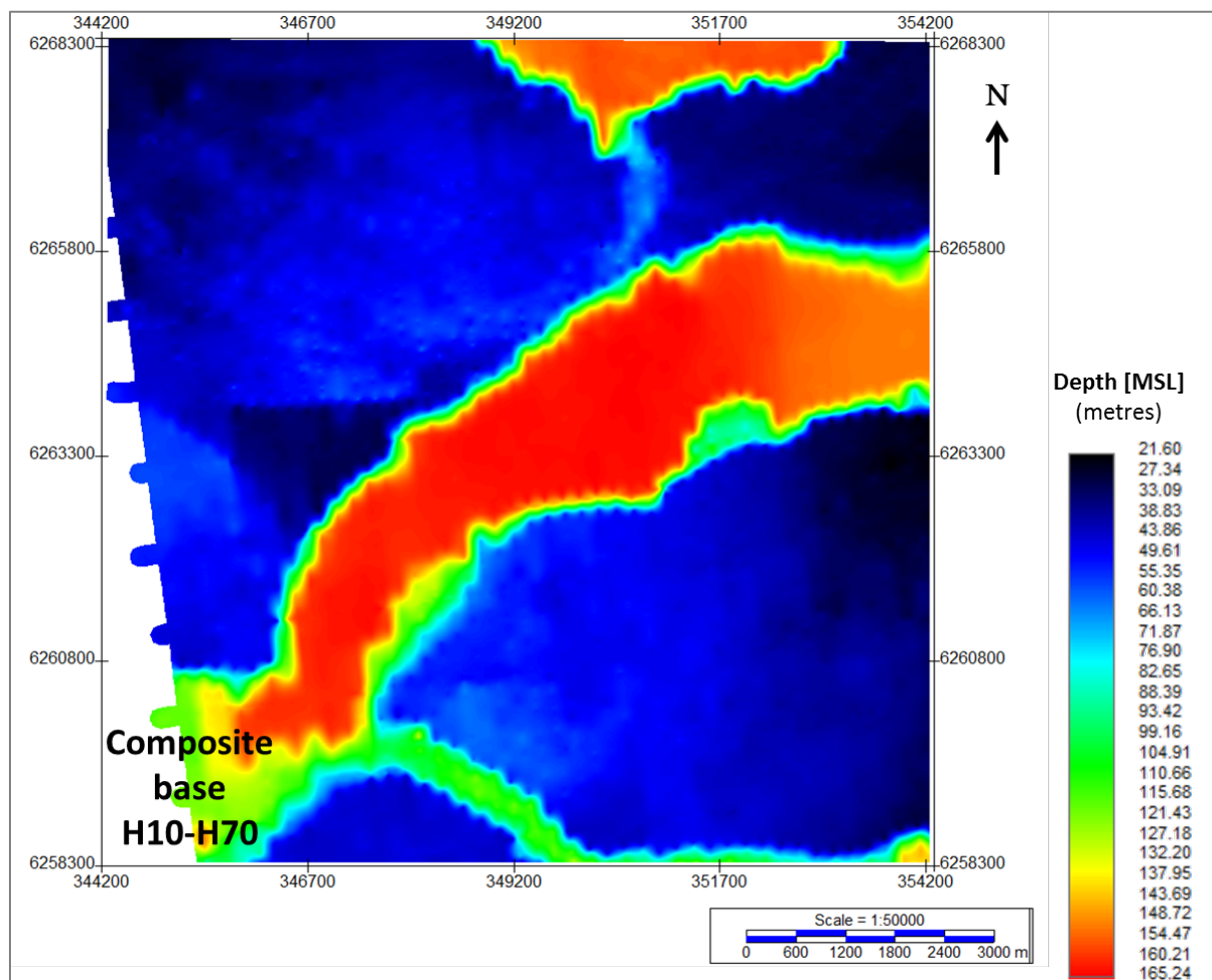
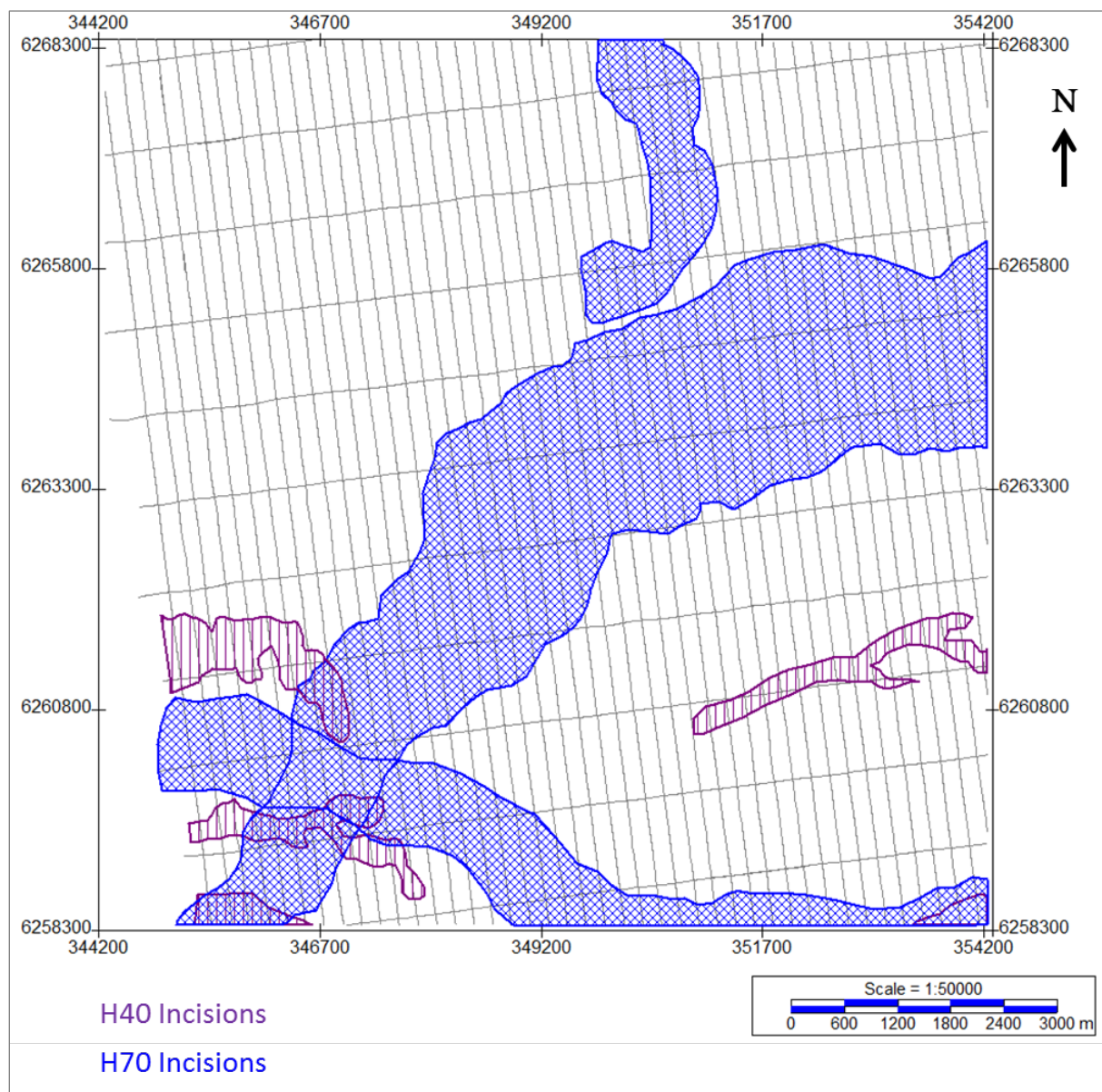


Figure 180 Composite surface from the addition of all base horizons of units U10 to U70. All major channel and valley incisions are observed, highlighting the diversity in size and drainage pathways.



*Figure 181 Map of the composite surface.
 The surface is derived from the addition of all base horizons of units U10 to U70, against all the interpreted major incisions of U40, U60, and U70.*

8.8.3 | SOFT SEDIMENTS AND ORGANIC-RICH DEPOSITS

Where a high-amplitude, negative impedance (soft kick) is present, a transition to less dense, lower velocity sediments may be inferred. The combination of the reflector's physical attributes and their geologic context, provides a means to delineate soft sediment deposits.

Soft kick features are common throughout the site and were mapped according to the unit where they are found. These are distributed as follows:

Table 28 Distribution of soft kick features within the survey area.

GHz_SK Horizon	Associated Seismic Unit	Depth MSL min	Depth MSL max	Depth BSB min	Depth BSB max	Figures
GHz SK 10	U10	28.25m	47.11m	<0.50m	9.37m	Figure 182 Figure 183
GHz SK 20	U20	32.67m	58.85m	<0.50m	26.14m	Figure 184 Figure 185
GHz SK 25	U25	33.85m	57.59m	<0.50m	27.73m	Figure 186 Figure 187
GHz SK 30	U30	54.09m	72.18m	15.15m	28.96m	Figure 188 Figure 189
GHz SK 35	U35	56.65m	79.88m	13.77m	39.11m	Figure 190 Figure 191
GHz SK 60	U60	43.72m	83.85m	0.84m	43.99m	Figure 192 Figure 193

The highest concentrations of soft kicks are found within U10 and U20 (Figure 194). These features are interpreted to be mud deposits, possibly organic-rich.

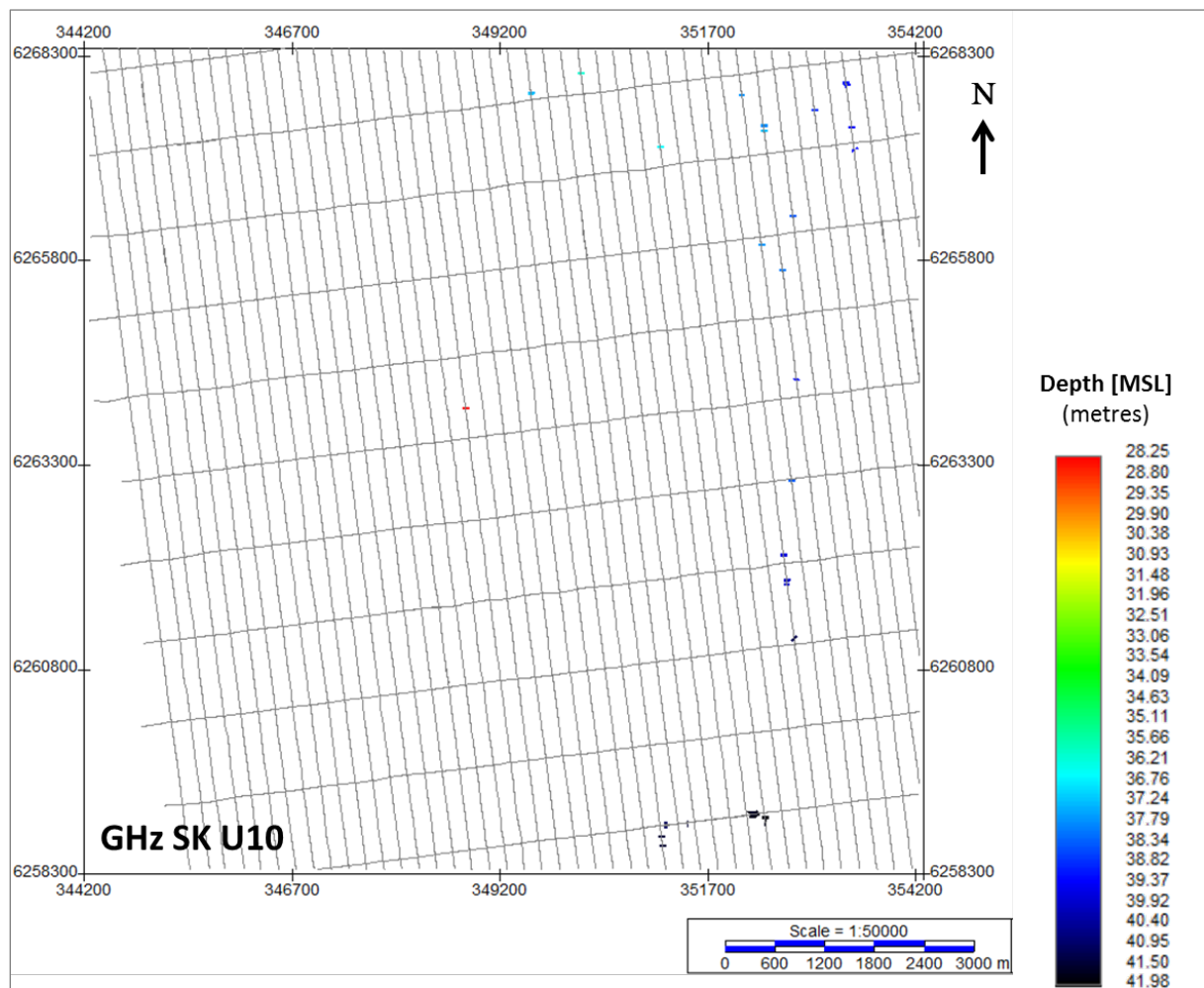


Figure 182 Lateral extent of the negative impedance contrasts deposits within U10.
 Units in metres below MSL.

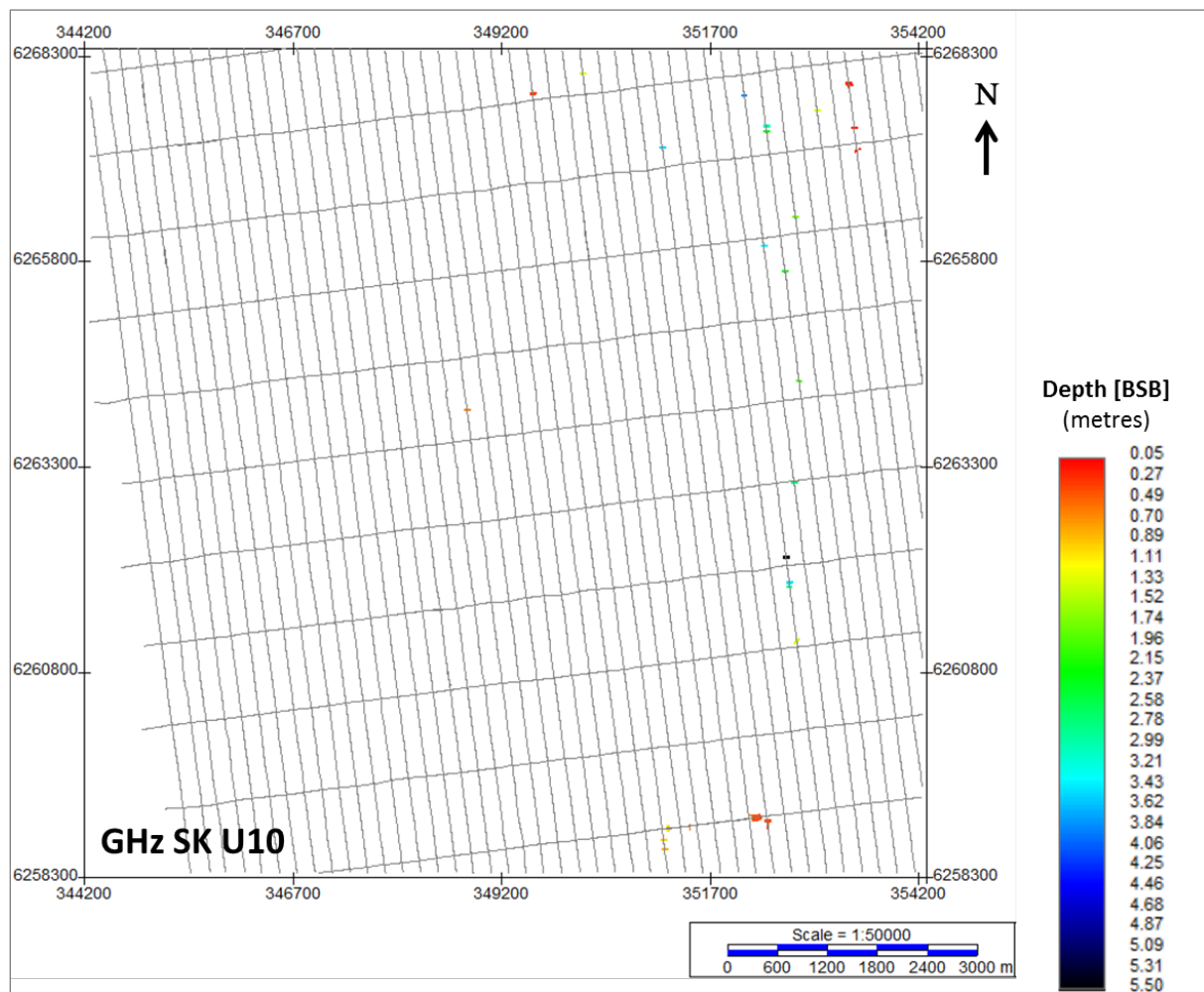


Figure 183 Depth below seabed of GHz_SK_U10.
 Units in metres below seabed.

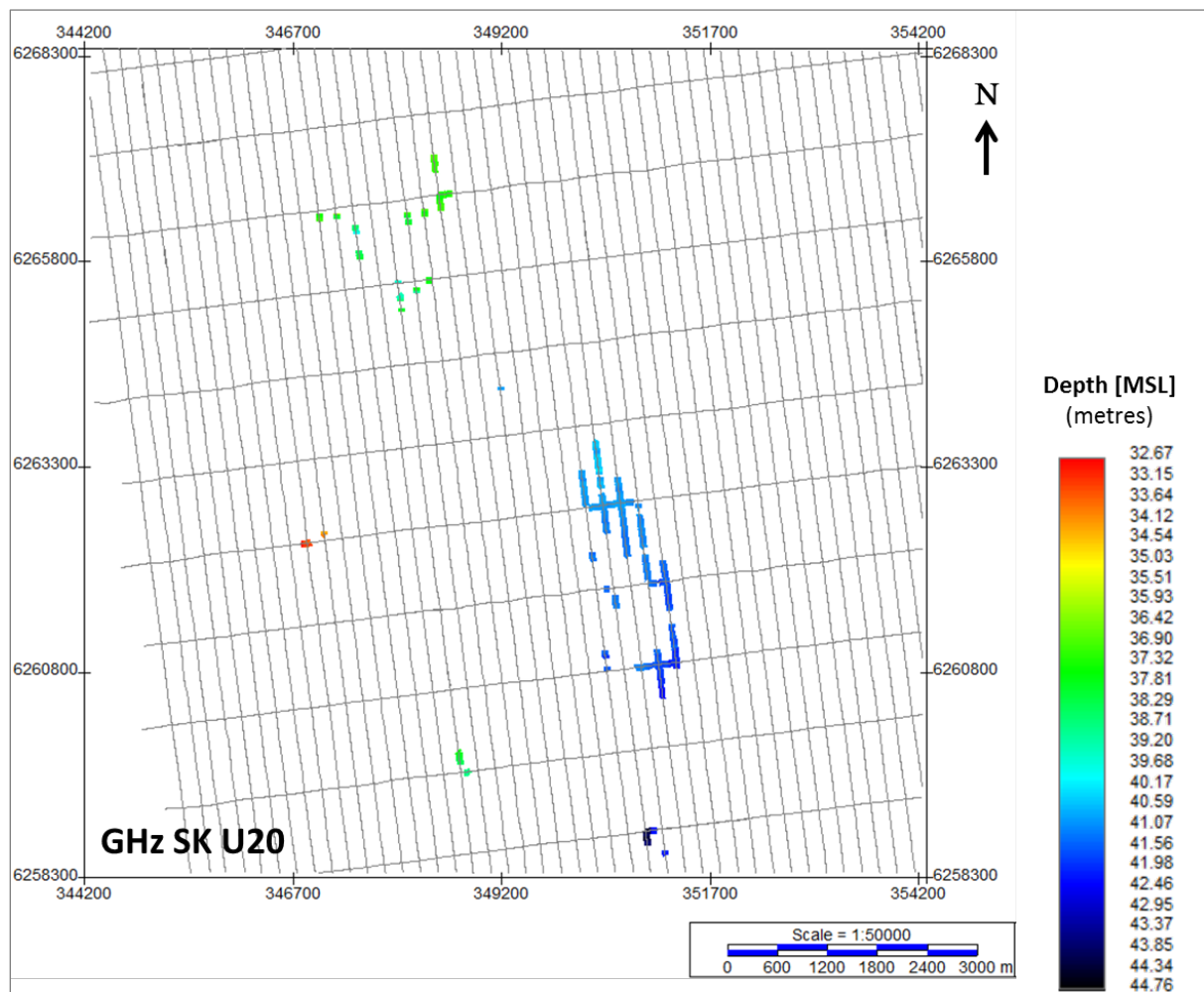


Figure 184 Lateral extent of the negative impedance contrasts deposits within U20.
 Units in metres below MSL.

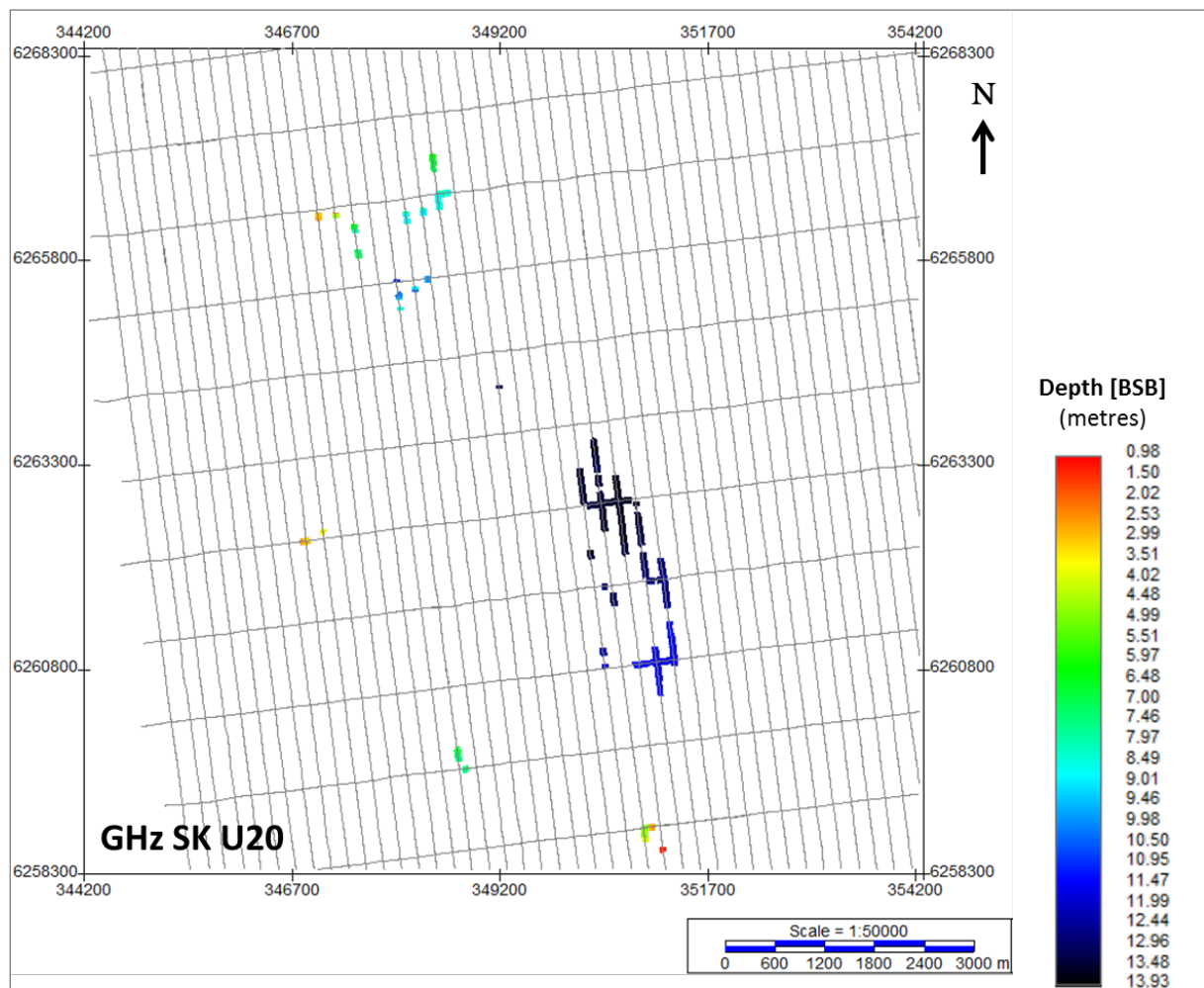


Figure 185 Depth below seabed of GHz_SK_U20.
 Units in metres below seabed.

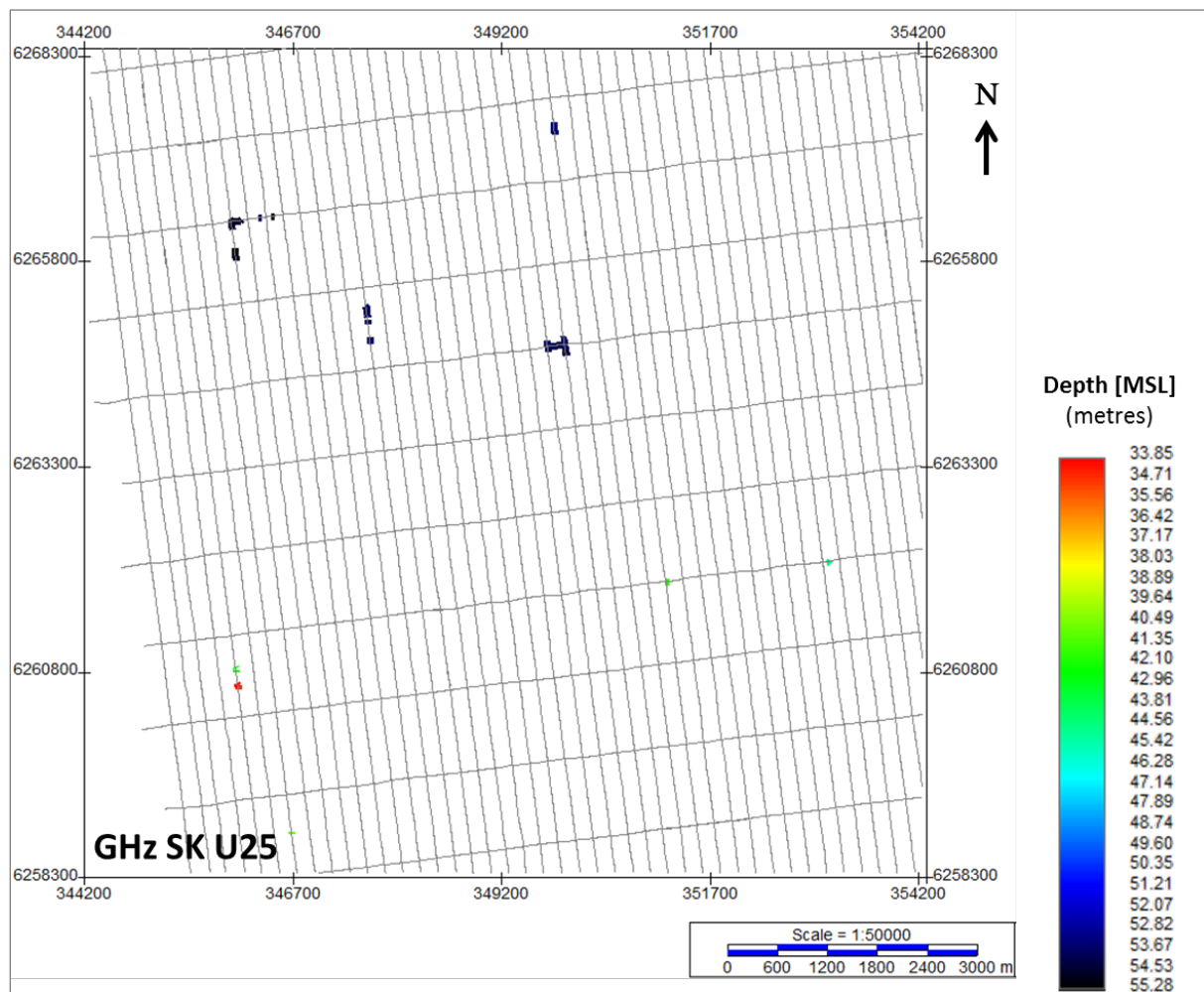


Figure 186 Lateral extent of the negative impedance contrasts deposits within U25.
 Units in metres below MSL.

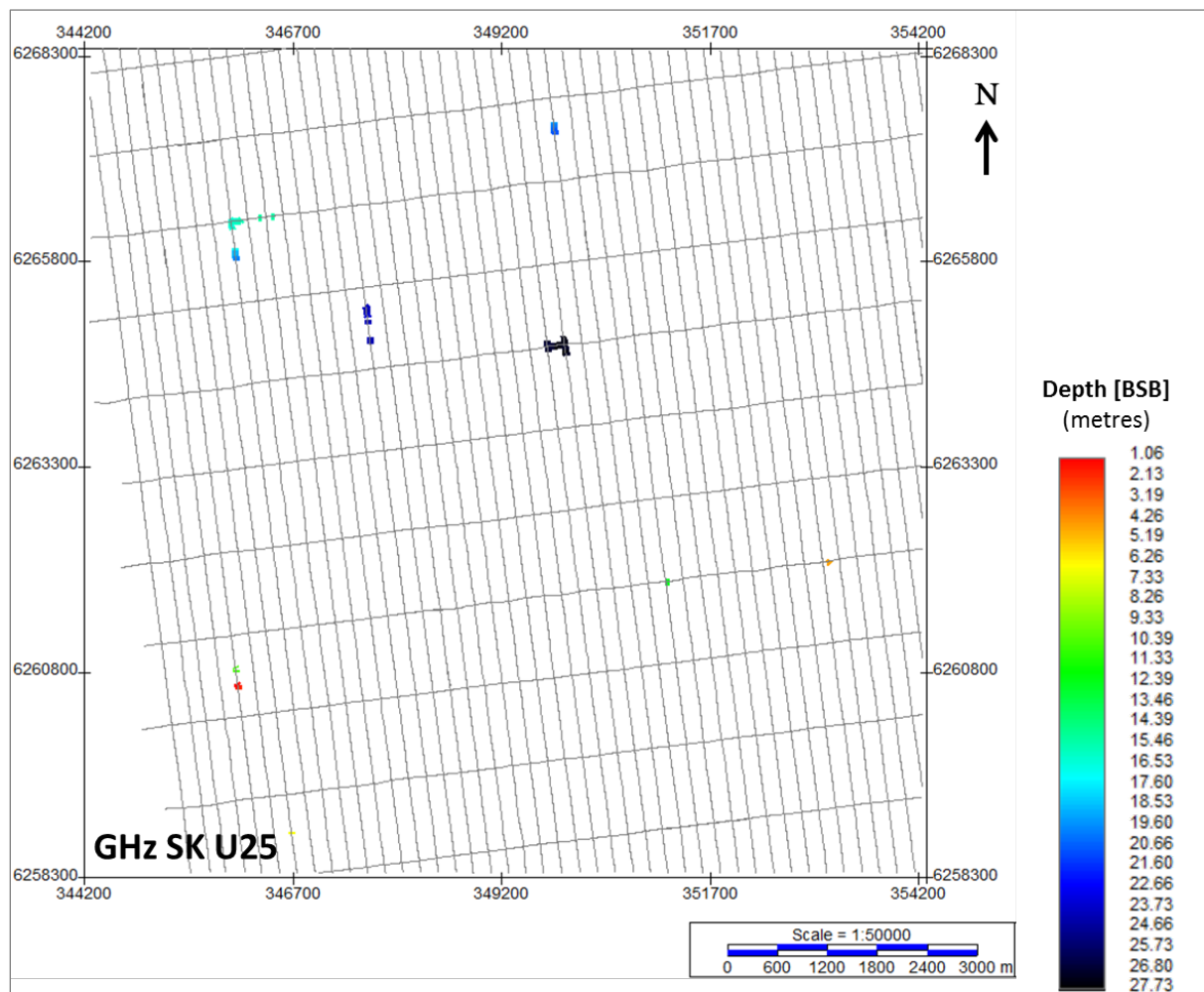


Figure 187 Depth below seabed of GHz_SK_U25.
 Units in metres below seabed.

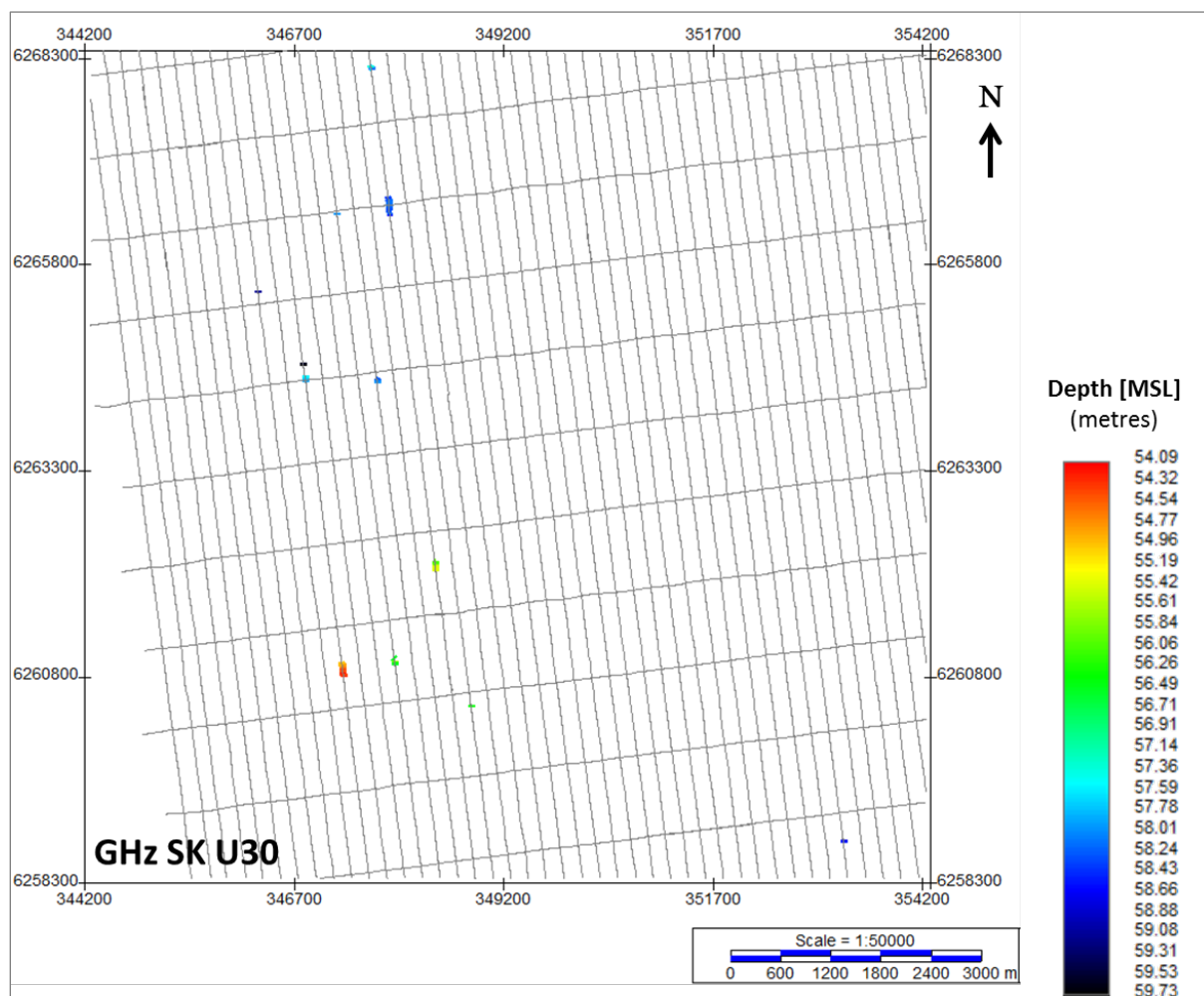


Figure 188 Lateral extent of the negative impedance contrasts deposits within U30.
 Units in metres below MSL.

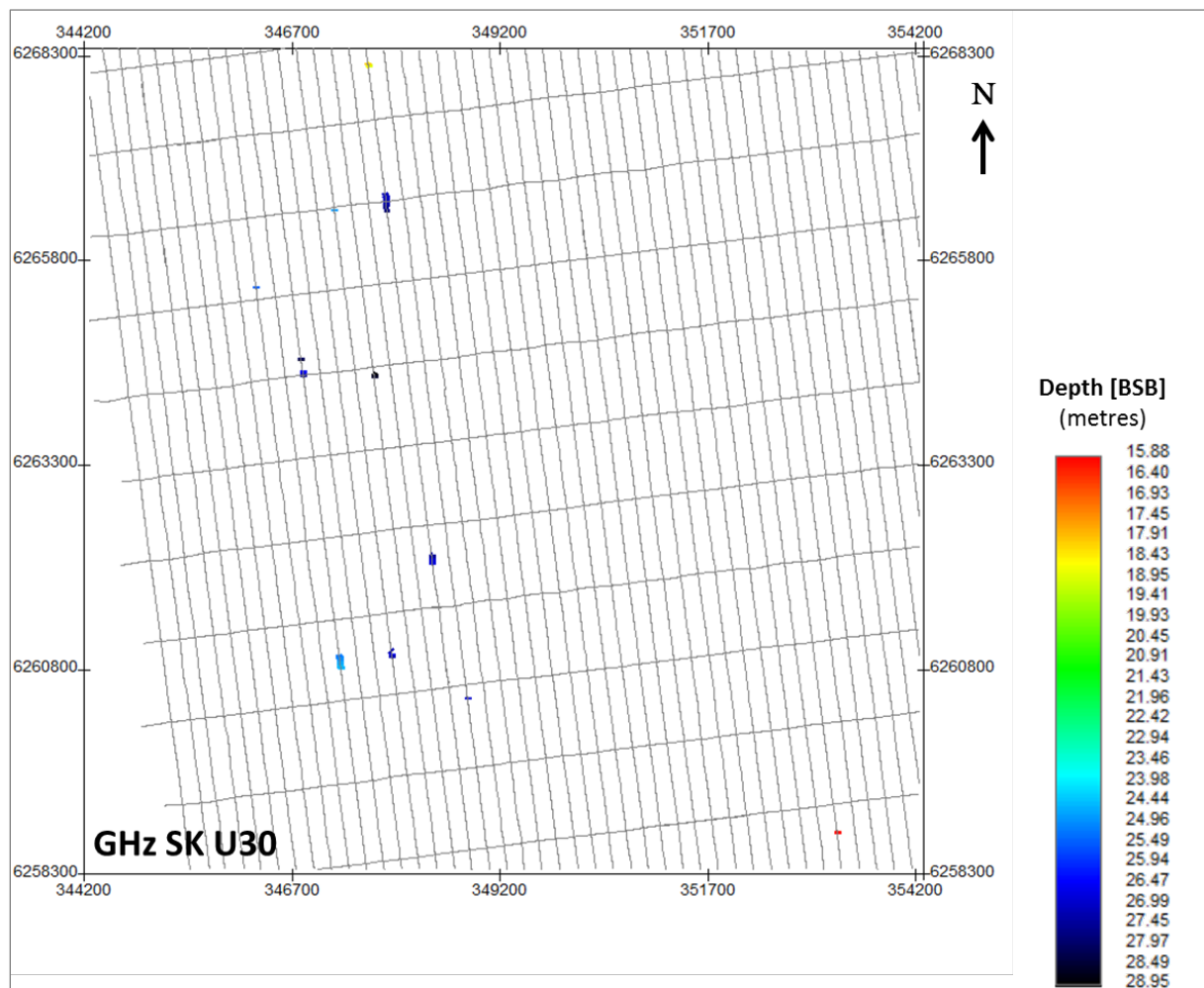


Figure 189 Depth below seabed of GHz_SK_U30.
 Units in metres below seabed.

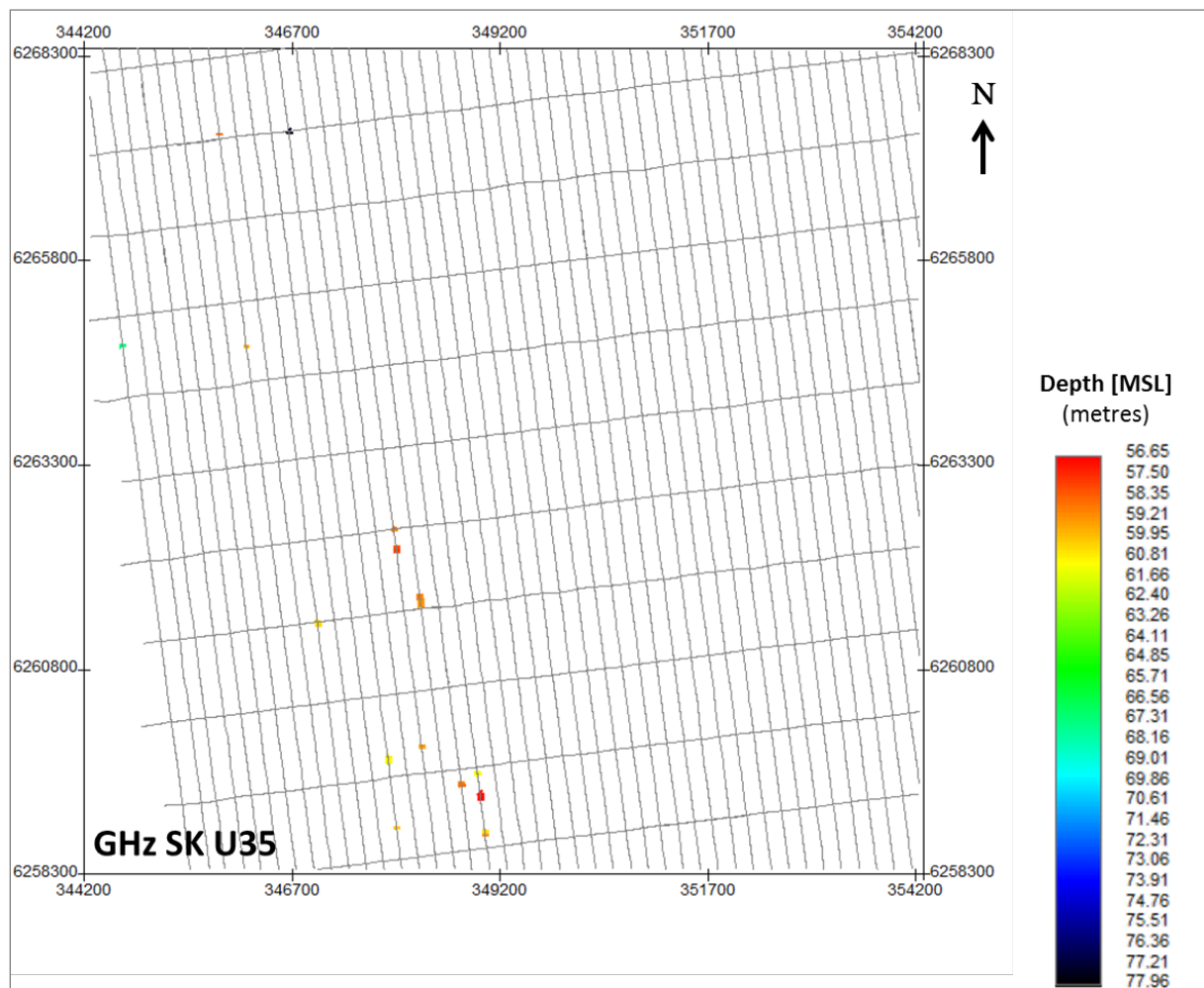


Figure 190 Lateral extent of the negative impedance contrasts deposits within U35.
 Units in metres below MSL.

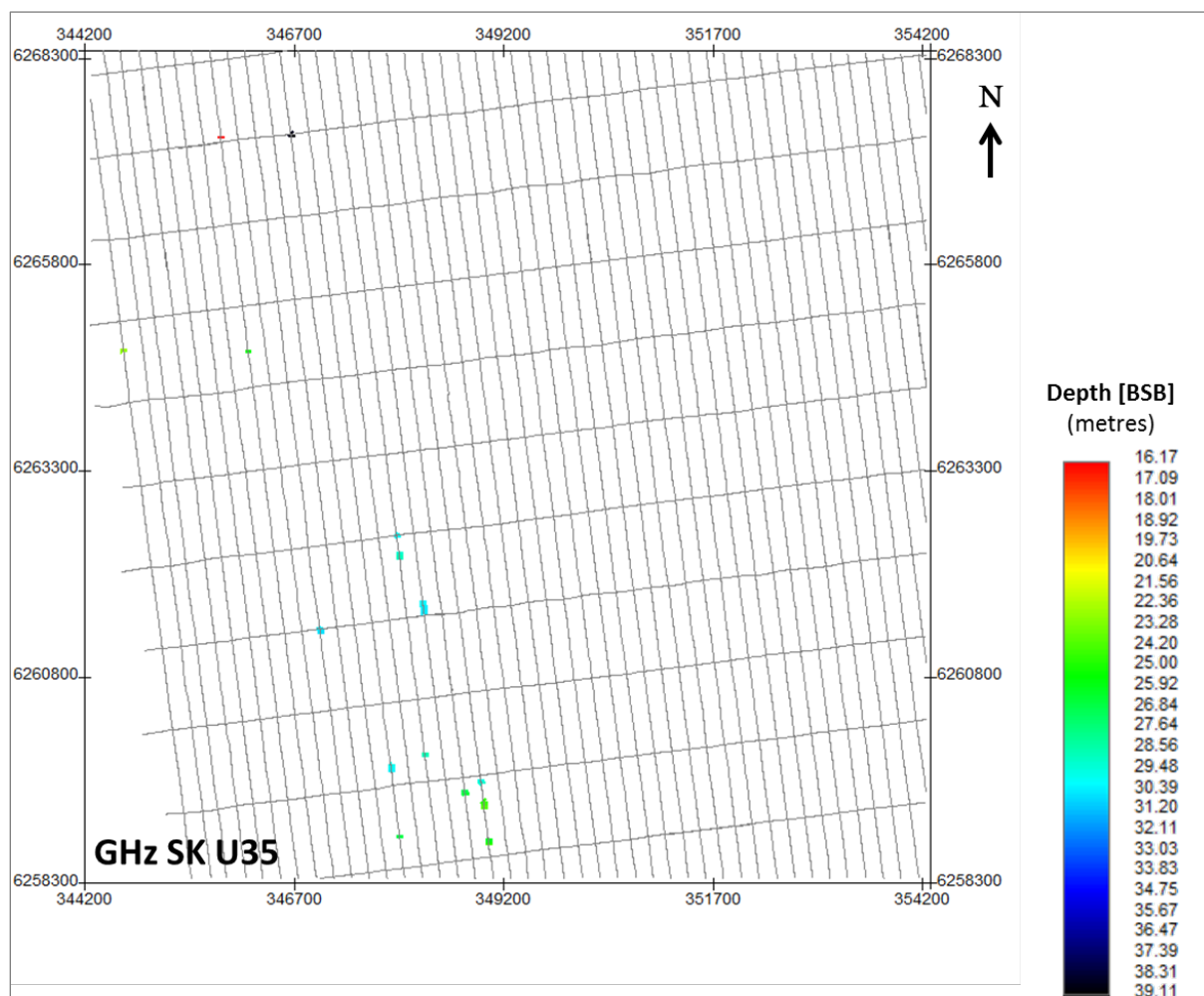


Figure 191 Depth below seabed of GHz_SK_U35.
 Units in metres below seabed.

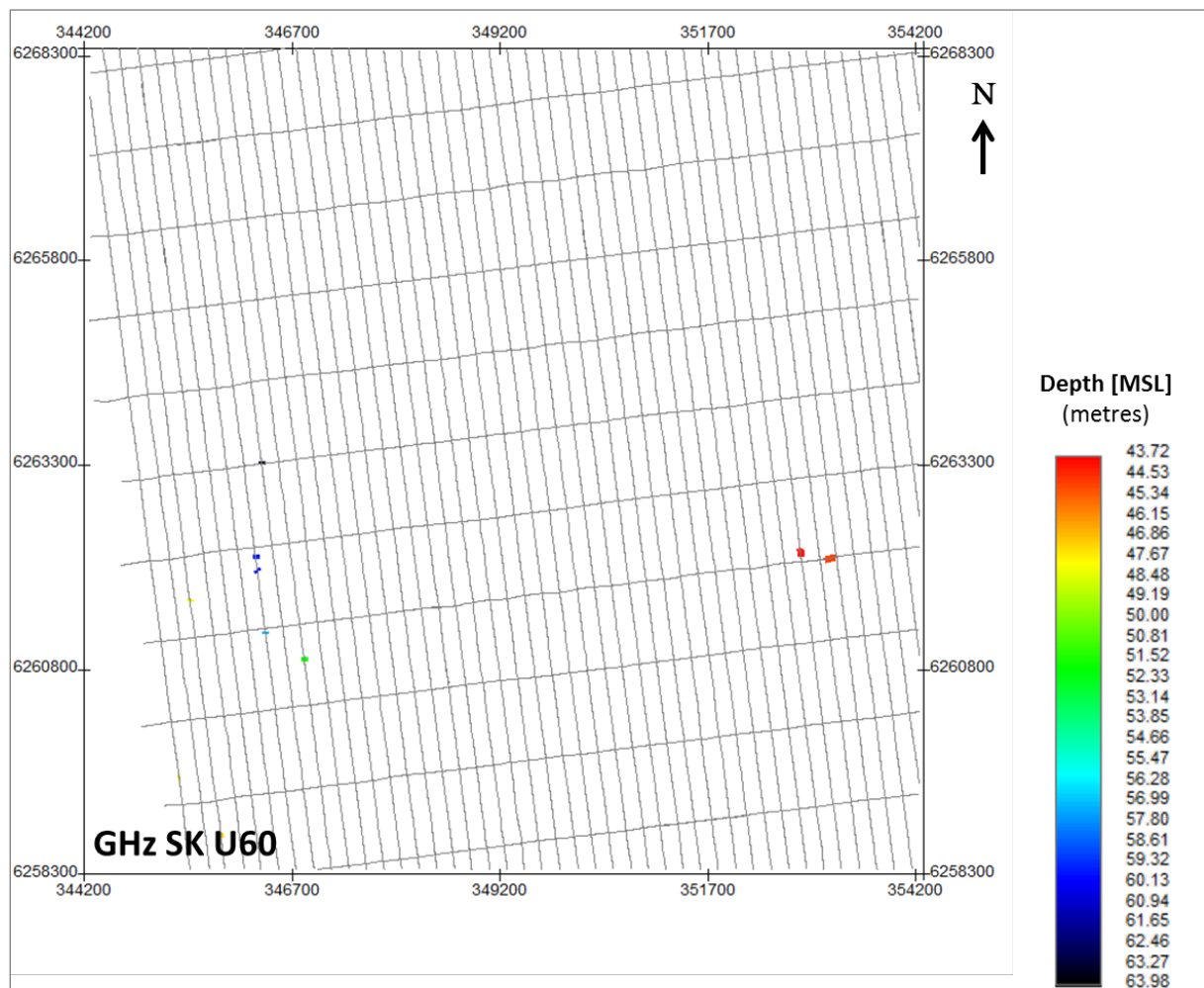


Figure 192 Lateral extent of the negative impedance contrasts deposits within U60.
 Units in metres below MSL.

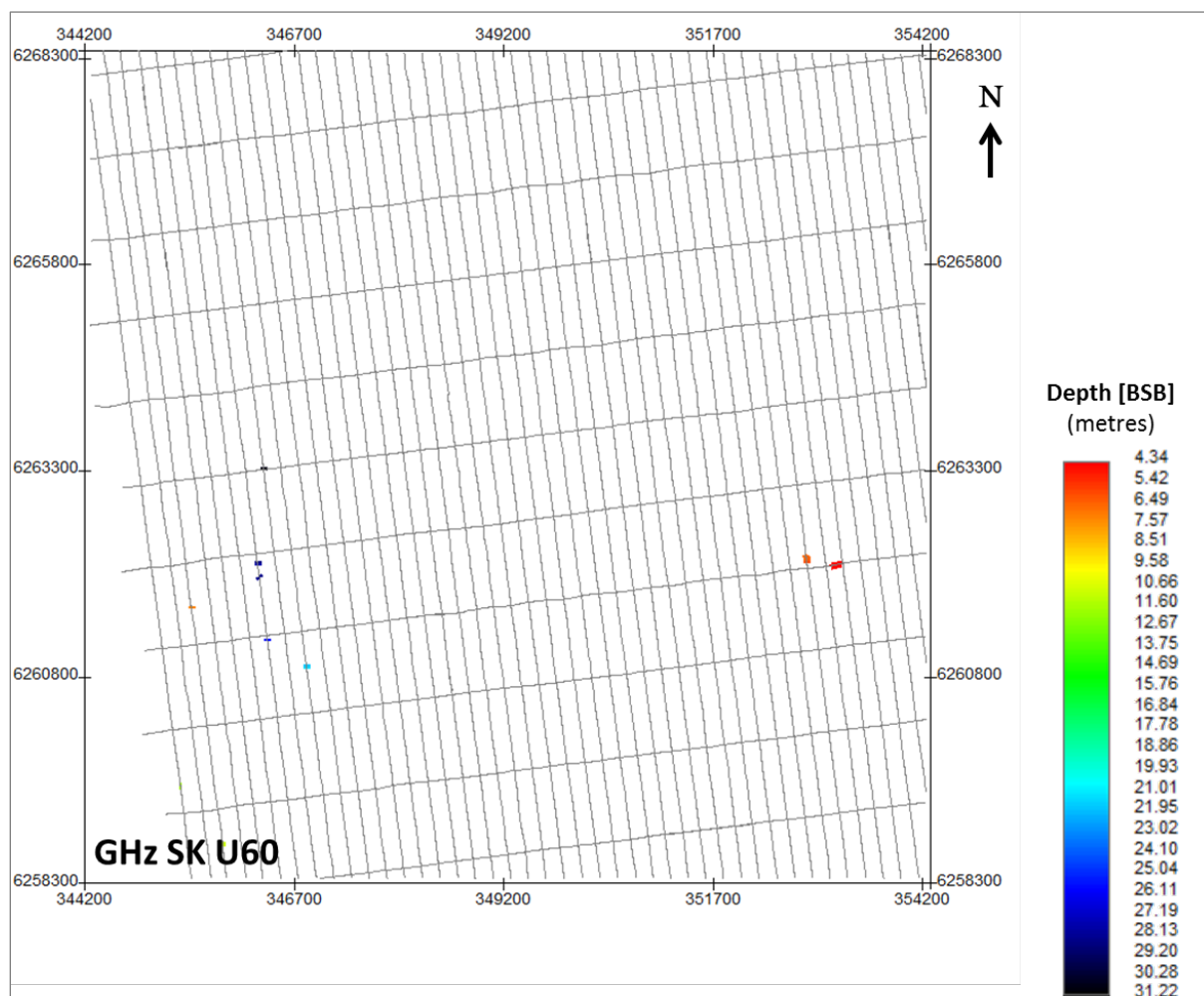


Figure 193 Depth below seabed of GHz_SK_U60.
 Units in metres below seabed.

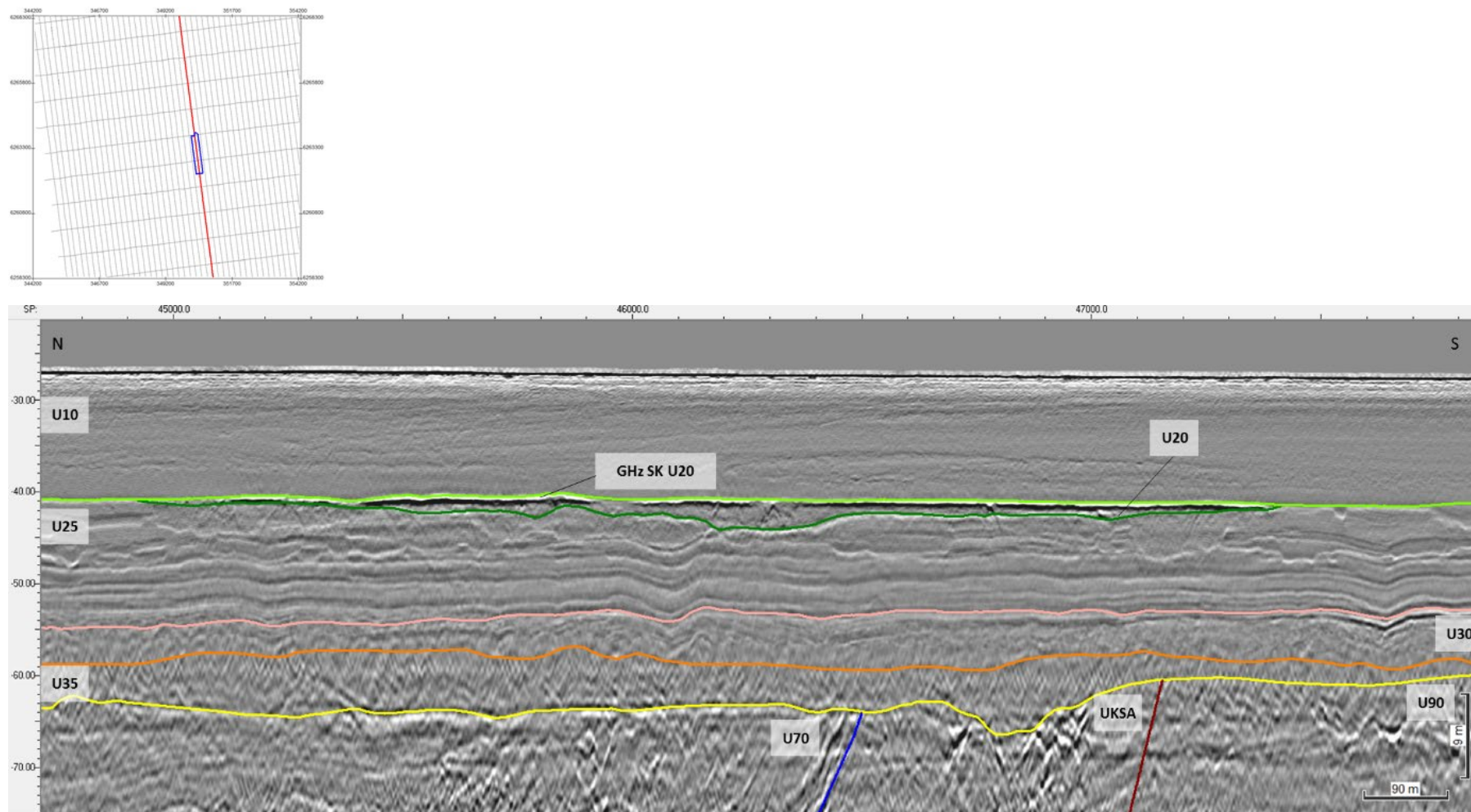


Figure 194 Negative impedance contrasts at the top of U20.
 Seismic profile BM3_OWF_E_2D_05460

8.8.4 | COARSE SEDIMENTS / GRAVEL BEDS / BOULDERS

Coarser material, such as boulder accumulations, cobbles, and gravel lags are present in glacial environments. These are potential hazards and may constitute a constraint on drilling and other operations.

Seismic diffractions, characterized by a parabolic or hyperbolic geometry in UHRS data, may be produced from the contact of the acoustic wave front and a boulder. However, in order to interpret such reflection patterns as boulders, the acoustic signature and geological/seismostratigraphic context have to be taken into consideration, since identical diffractions may originate from rugose surfaces, faulted layering, channelized acoustic interfaces, and out-of-plane echoes.

Interpreted areas of potential gravel/boulders were traced by horizon GHZ_Gravel. These areas were identified between 37.9 m and 84.4 m below MSL (Figure 195), and 1.6 m and 48.9 m BSB (Figure 196).

Mappable concentrations of interpreted gravel were delineated at the base of seismic units U35 (Figure 197) and U40. The gravel concentrations in U35 appear to be along the margins of the basin within the central sector (Figure 195 and Figure 196).

The highest probability for the occurrence of cobbles and boulders is estimated to be within seismic units related outwash products from tills. These units are U40, U70, and UKS.

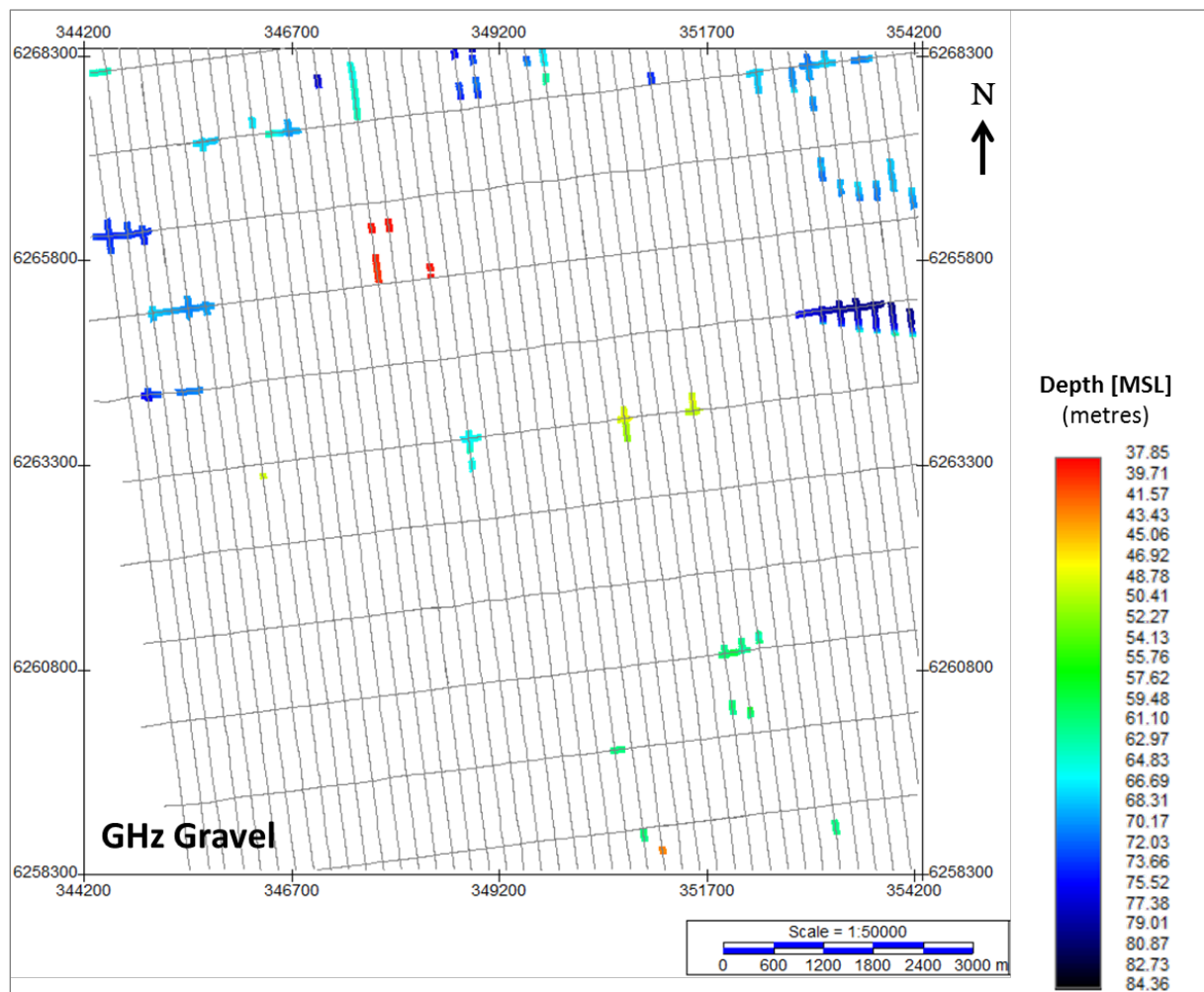


Figure 195 Map showing the lateral extent of GHZ_Gravel.
 Units in metres below MSL.

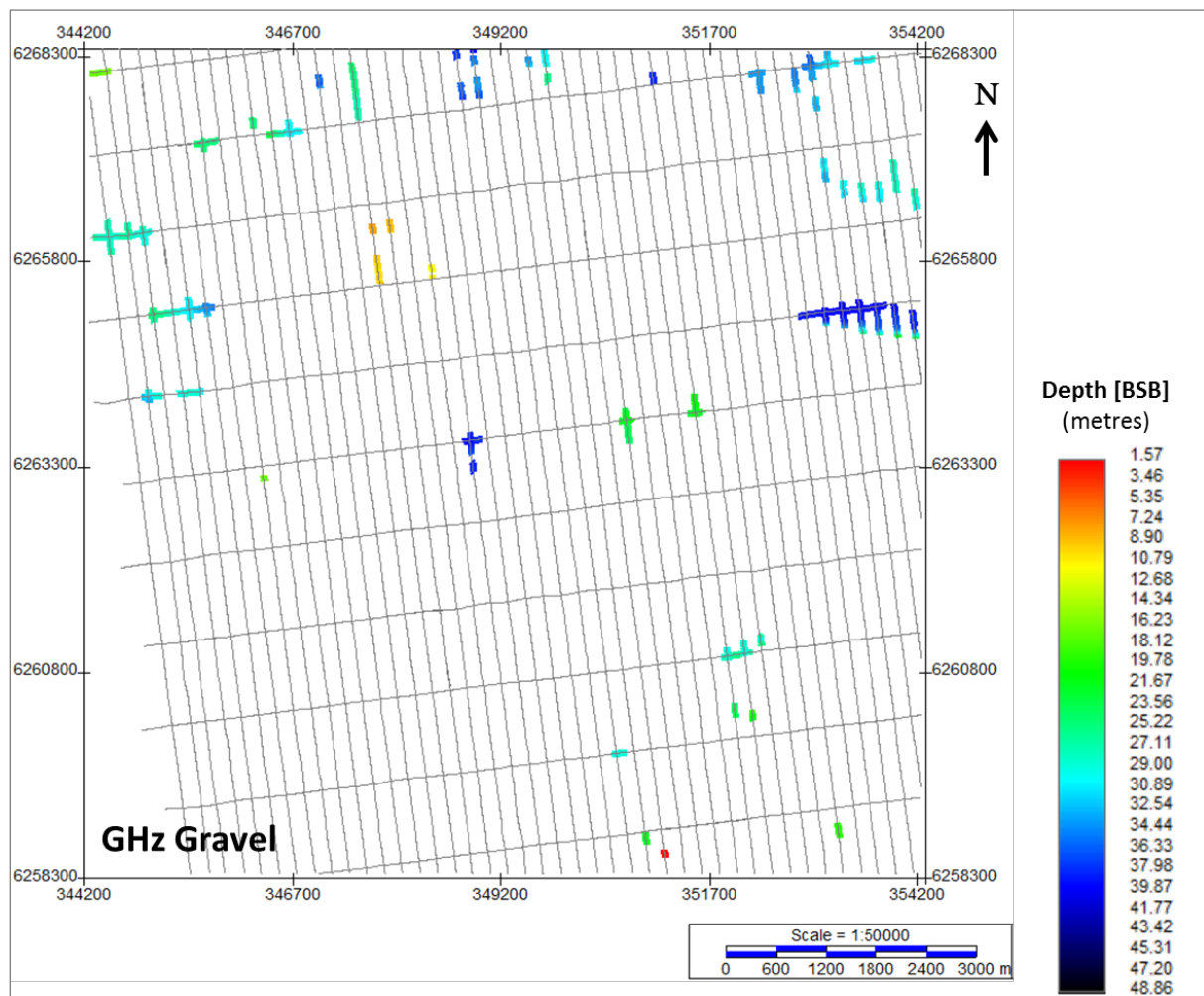


Figure 196 Depth below seabed of GHz_Gravel.
 Units in metres below seabed.

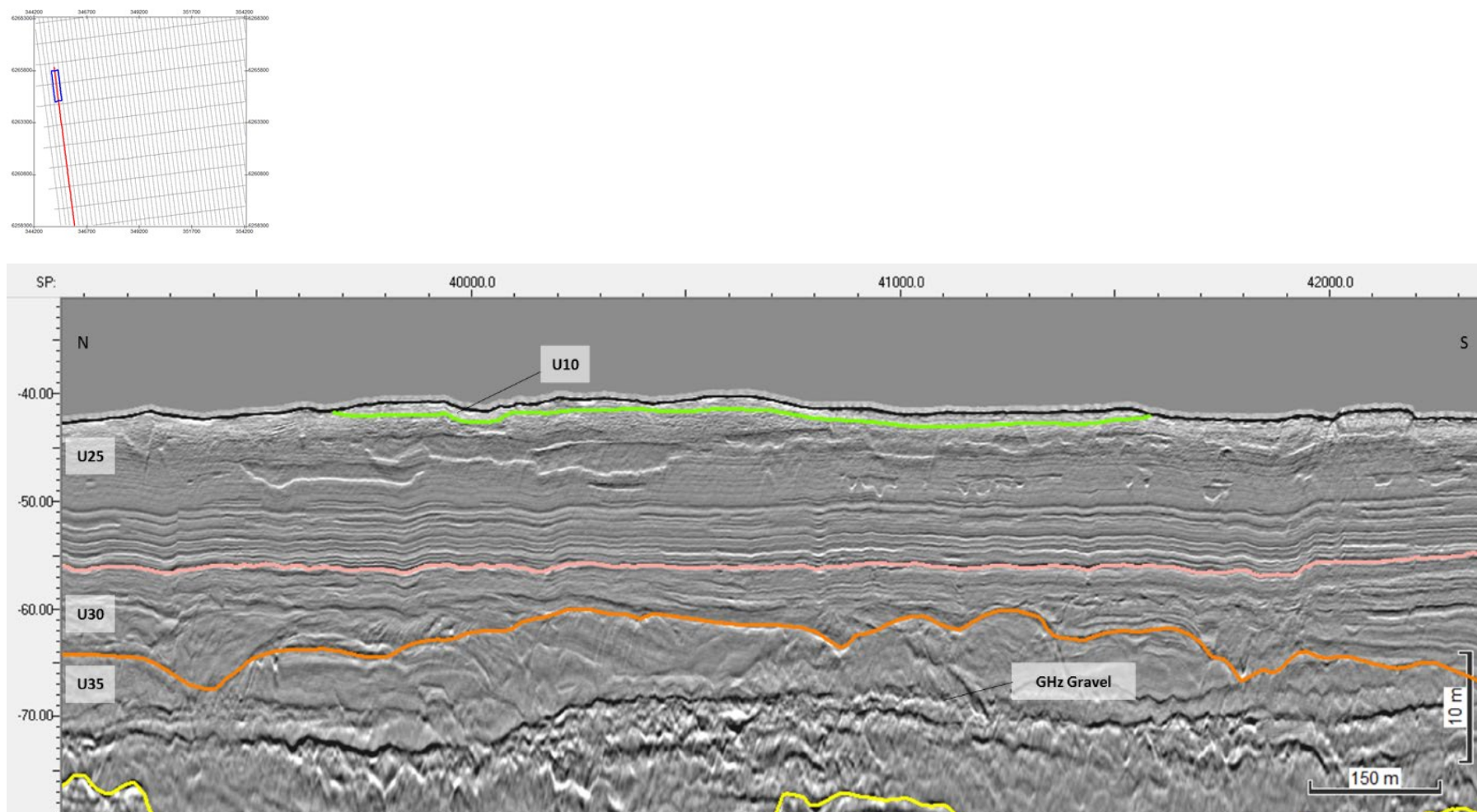


Figure 197 Possible coarse layer within U35.
 Seismic profile BM1_OWF_E_2D_00630_01_P2

8.8.5 | TILL DEPOSITS

Interpreting till deposits in UHRS data with high confidence can be difficult. Given its broad classification, and that it may contain sediment of any grain size, predicting its seismic characteristics is uncertain. However, taking into account the geological setting of the area, there should be a reasonable expectation of till in the units directly associated with glaciation. Tills are commonly associated with and located in conjunction with glaciotectonism. Given this relationship, tills may be present within U40, U70, and UKS. Till may preferentially occur at the basal margins of the tectonized deposits, and associated to glacial surfaces of erosion or retreat.

8.8.6 | FLUID FLOW AND GAS FEATURES

Acoustic blanking, amplitude anomalies, phase reversals, and hyperbolas in the MUL (non-migrated) datasets may indicate the presence of gas in UHRS data. These indicators typically appear quite prominently when concentrations of free gas are present in sediments. However, the presence of a single marker of the mentioned items was never taken as evidence for the presence of shallow gas as there are a number of geological features that can be responsible for each of them individually. Instead, it was the combined presence of the mentioned evidences that was taken as indicator of the likely presence of shallow gas. Furthermore, signal masking, or acoustic turbidity, or decreased amplitudes were inspected either directly on the migrated and un-migrated seismic sections or on other amplitude-derived attributes, like envelope and reflectance datasets.

No unambiguous seismic anomalies suggesting the presence of detectable gas in the subsurface were identified in the UHRS data. This statement is not an assertion that no gas exists within the survey area.

8.8.7 | LACUSTRINE SEDIMENTS

Lake systems are typically low energy settings where fine sediment deposition prevails (silts, fine sands, and clays), and are commonly associated to glacial environments. On seismic data, lacustrine sediments are characterised by draping successions of micro-parallel, continuous reflectors. The materials within these deposits may differ significantly from adjacent units, constituting a hazard from a geotechnical point of view.

Such deposits were identified in the survey area. The base of these deposits was mapped as horizon GHZ_Lacustrine (Figure 198 and Figure 199). Their occurrence is exclusively associated to U40 (Figure 200), and can be found between 45.4 m and 67.1 m depth MSL, or 8.6 m to 35.8 m depth BSB.

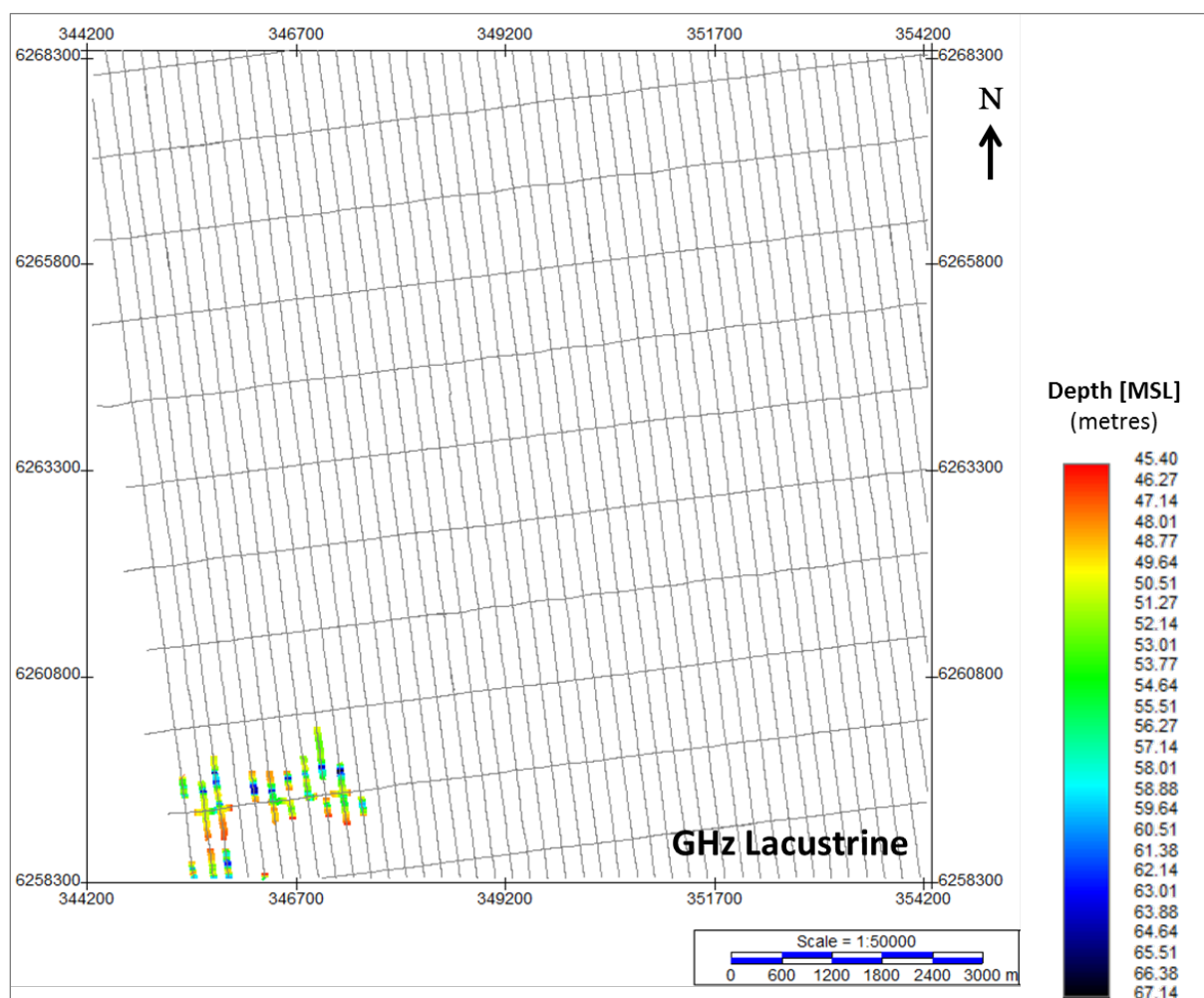


Figure 198 Lateral extent of the interpreted lacustrine deposits (horizon GHZ_Lacustrine). Units in metres below MSL.

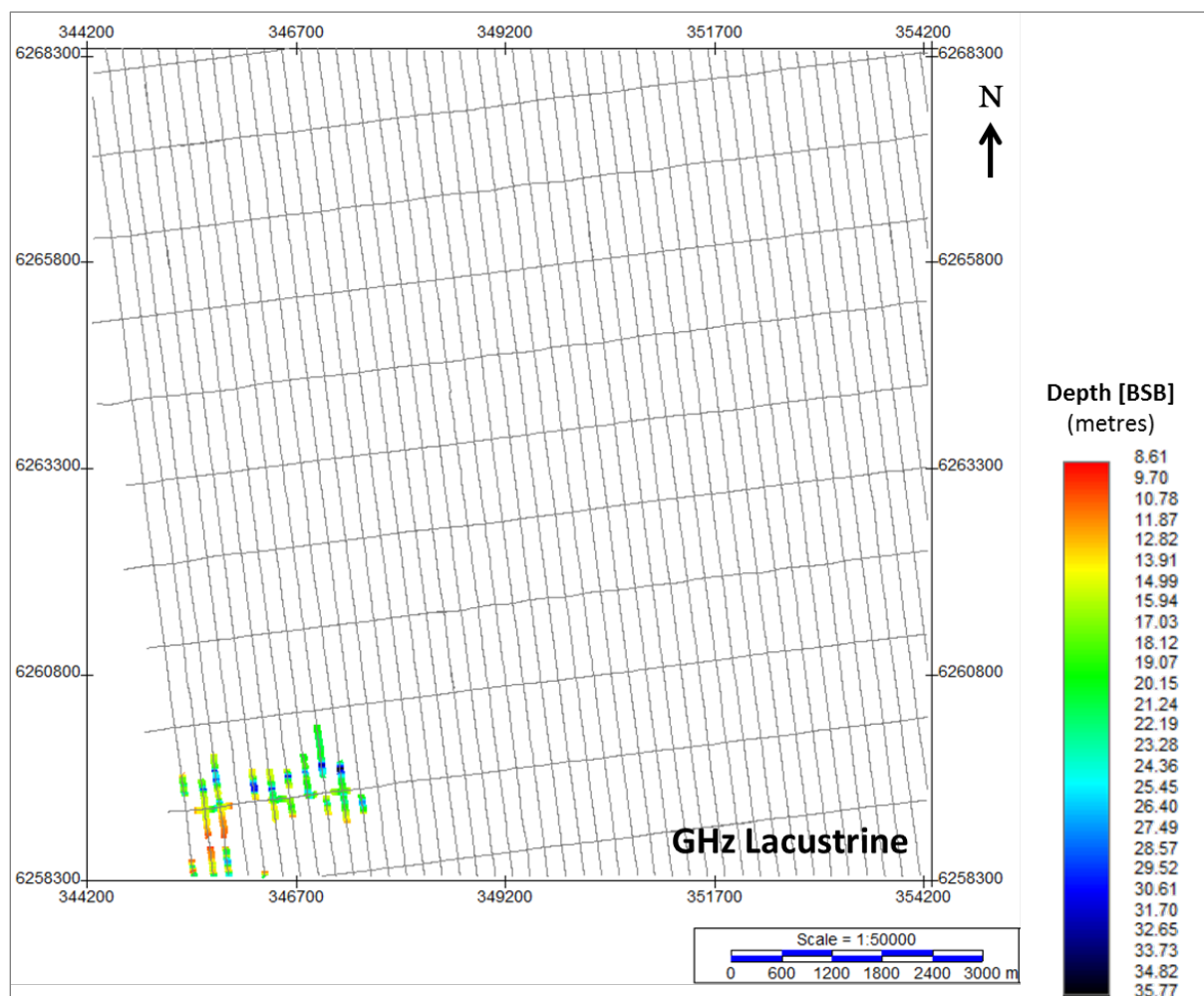


Figure 199 Depth below seabed of horizon GHz_Lacustrine.
 Units in metres below seabed.

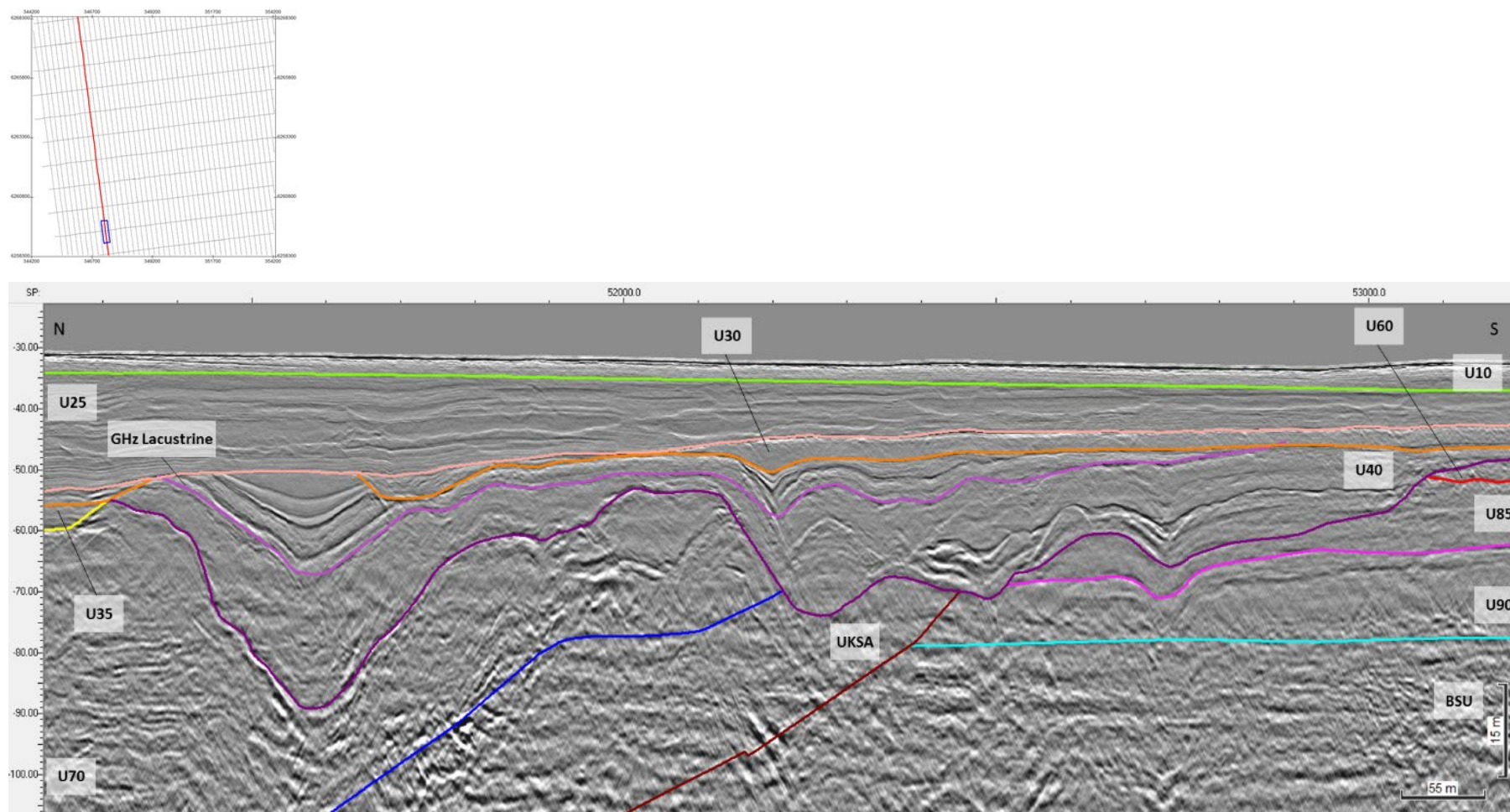


Figure 200 Interpreted glaciolacustrine deposits on the upper levels of Seismic Unit U40.
 Seismic profile BM1_OWF_E_2D_01890

8.9 | ARCHAEOLOGY CONSIDERATIONS

During the survey there was no obvious archaeological findings observed within the Artificial Island survey area.

However, it is suggested that a full archaeology investigation be conducted by professionally qualified archaeologists on the data collected here in order to assess the possibility of paleo landscapes that could have been occupied by early man. This type of analysis is out with the scope for this report.

8.10 | GRAB SAMPLE SUMMARY

The Artificial Island survey area encompasses a variety of seabed conditions. Engineering within investigated depth profile below the seabed should consider the following general observations, which are neither exhaustive or prescriptive, and are related exclusively to the observed material presented in this report:

The results of the grab sampling provide good coverage of the surface seabed conditions, which are dominated by granular sediments, largely SAND with a few samples of GRAVEL in the west of the Artificial Island survey area (Reporting Tiles T13 and T19) and one sample of SILT in the west of the area (Reporting Tile T13), see Figure 201.

Table 29 Grab sample summary

Lithology	Number of Samples
SAND	17
GRAVEL	3
SILT	1
Total	21

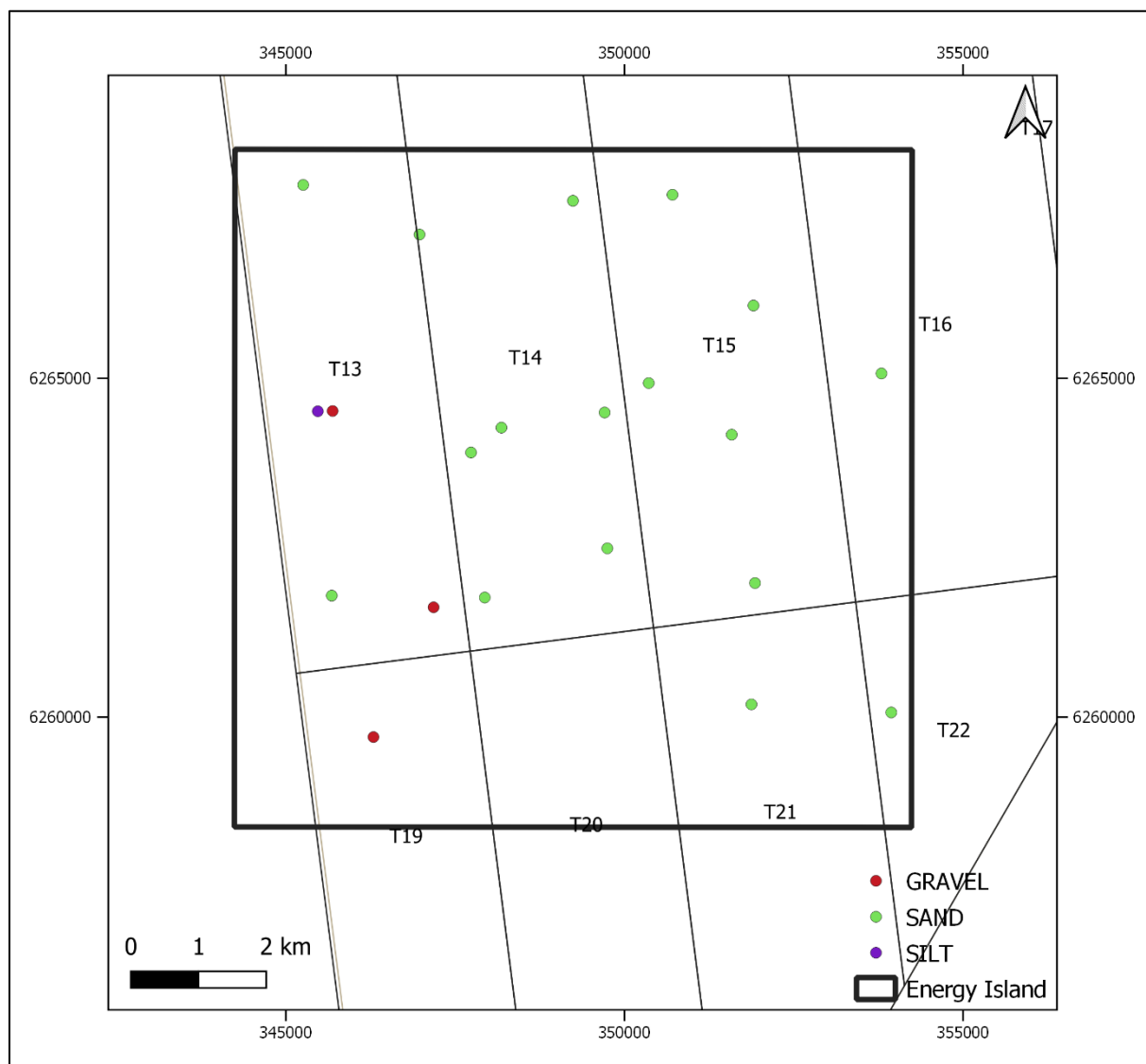


Figure 201 Location plot of grab sample material types within the Artificial Island survey area.

Particular 'exotic' features within a survey area may shallow seabed engineering, i.e., highly organic material, high gravel and/or cobble contents. Within the Artificial Island survey area, GRAVEL is common throughout and COBBLES are encountered at 1 of the 21 locations. Due to the scattered nature of grab sampling, the geophysical data and interpretation should also be consulted as to whether there are significant deposits of coarse GRAVEL and/or COBBLES on the seabed. The presence of organic-rich CLAY and PEAT must also be taken into consideration, due to the undesirable thermal regime which such cohesive material can generate, together with their tendency for compressibility under load and typically low material strength. Whilst there was no presence of PEAT were identified within the sampling sites and no samples were identified fully as CLAY, smaller concentrations of CLAY were found in 3 other samples. As part of the laboratory analysis, 4 of the samples were tested for their total organic matter and total organic carbon which varied between 0.24 - 0.50 % for the total organic matter and 0.41 - 0.86 % for the total organic carbon. Whilst the thermal regime of the seabed has not been a subject of investigation in this report, the potential high thermal resistivities in organic-rich material and low strength cohesive CLAY should be borne in mind, especially with regards to any electrical cable installation activities.

The majority of the seabed sediments sampled were of Recent age, whilst occasional samples were Post Glacial and Late Glacial in age.

For a full description of the grab sample results please refer to the lab report and logs in Appendix C|.

9 | CONCLUSIONS

The results of the bathymetric survey found that the water depths across the site ranged between 25.8 m and 48.2 m with depth generally increasing to the sides of the Artificial Island survey area.

The seabed has a range of natural topographic variability occurring throughout the site with extensive areas of mobile sediments present across much of the Artificial Island survey area. The mobile sediments range from smaller wavelength bedforms such as ripples, large ripples and megaripples to larger scale sediment migration bedforms such as sand waves and sandbars.

Slope angles across the site are typically very gentle ($<1^\circ$) and gentle (1° to 5°).

Very steep slope angles (15° to a maximum of 73°) were observed within the survey area but these were restricted to steep banks on the western side of the Artificial Island survey area.

The seabed sediments in the Artificial Island survey area are dominated by GRAVEL and coarse SAND, often alternating with bands of SAND, both of which are more prominent in the western and central parts of the Artificial Island survey area. Less frequently observed is muddy SAND, predominately in the northeast of the Artificial Island survey area. Infrequent and isolated patches of MUD and sandy MUD are occasionally present in the northwest of the Artificial Island survey area.

Extensive areas of mobile sediments, including ripples, large ripples and megaripples are observed particularly in the west of the Artificial Island survey area and are always associated with GRAVEL and coarse SAND, or SAND. All ripple features have a northeast-southwest orientation indicating a dominating current regime from northwest to southeast. Some sand waves are observed in the central and northern part of the Artificial Island survey area, typically comprising of SAND or GRAVEL and coarse SAND. In the west of the Artificial Island survey area, some larger scale sandbar bedforms are observed, upon which the smaller scale, more mobile and more recent bedforms are often superimposed.

A total of 280 individual seabed contacts (181 MBES contacts and 99 SSS contacts) were detected within the Artificial Island survey area. They were classified as boulders (221) and man-made objects such as debris (51), fishing equipment (1) and wire (1). 6 contacts were classified as other which includes possible sediment mounds. No boulder fields were observed within the Artificial Island survey area, but boulders are of a higher concentration to the west of the Artificial Island survey area.

A total of 128 magnetic anomalies were detected within the Artificial Island survey area. 58 of these were individual discrete anomalies, whilst 70 anomalies were interpreted to form 8 linear anomalies. One of these linear anomalies corresponded to the database position of the buried TAT-14 cable.

Evidence of trawling is found across much of the Artificial Island survey area.

Occasional areas of interest have been identified as unknown features and were assessed for possible biogenic origins. These areas have been evaluated by a senior biologist who determined that these areas of interest are unlikely to be biogenic in nature. The areas have maintained their feature classification in case further investigation to these areas is deemed necessary. These areas are more likely to be erosional features.

Thirteen seismostratigraphic units were interpreted from the MMT OWF survey area UHRS dataset. Taken as a whole, these units represent the structural elements of the site's Geological Ground Model. The seismic units of the model were chosen primarily for their geotechnical significance, resulting from distinct depositional and erosion events, marking relevant environmental changes, and shifts in sediment types.

The seismostratigraphy of the site is complex. The stratal architecture is interpreted as being controlled by the interplay of eustasy-isostasy, autogenic processes, and direct glaciation.

The lower deposits are interpreted to be related to glacial processes, where glaciotectionics have the strongest influence of the seismostratigraphy. Deposits from this mode are interpreted as glacitectorites, glaciofluvial, glaciolacustrine, glacial drift, and outwash accumulations. The sedimentological composition of these deposits is a mixture of unconsolidated, siliciclastic, sediments, i.e., sands, silts, clay, and gravel. The seismic units that represent the glacial processes are positioned above the Pre-Quaternary sequences that comprise the Base Seismic Unit.

The upper deposits comprise the high frequency sequences, where eustatic-isostatic movements have the strongest influence on the depositional environments. These deposits represent fluvial, tidal, estuarine, and coastal marine sediments. The sedimentological composition of these deposits is a mixture of unconsolidated, siliciclastic sediments, i.e., sands, silts, clay, gravel, boulders, and organics.

The variety of sub-surface geohazards identified from the UHRS data is typical for depositional settings at high latitudes. The main interpreted geohazards were: paleo channels, tunnel valleys, glaciotectionized sediments, gravel, faults, soft sediments, organics, amplitude anomalies, and lacustrine sediments.

10 | RESERVATIONS AND RECOMMENDATIONS

The results in this report, both geological descriptions and contact selection, are based on interpretations of geophysical data obtained during the survey. It should be taken into account that there is a natural limitation in the accuracy of interpretation. Results from grab sampling have been used for verification of the geological interpretations and is considered as ground truthing at those locations where collected. Where considered applicable, the sampling results have been extrapolated to constitute a base for verifications also in the surroundings.

Seismic interpretation presented in this report is based solely on seismic interpretation techniques. Unit Thirteen seismostratigraphic units were interpreted from the MMT OWF survey area UHRS dataset. Taken as a whole, these units represent the structural elements of the site's Geological Ground Model. The seismic units of the model were chosen primarily for their geotechnical significance, resulting from distinct depositional and erosion events, marking relevant environmental changes, and shifts in sediment types.

The seismostratigraphy of the site is complex. The stratal architecture is interpreted as being controlled by the interplay of eustasy-isostasy, autogenic processes, and direct glaciation.

The lower deposits are interpreted to be related to glacial processes, where glaciotectionics have the strongest influence of the seismostratigraphy. Deposits from this mode are interpreted as glaciotectionites, glaciofluvial, glaciolacustrine, glacial drift, and outwash accumulations. The sedimentological composition of these deposits is a mixture of unconsolidated, siliciclastic, sediments, i.e., sands, silts, clay, and gravel. The seismic units that represent the glacial processes are positioned above the Pre-Quaternary sequences that comprise the Base Seismic Unit.

The upper deposits comprise the high frequency sequences, where eustatic-isostatic movements have the strongest influence on the depositional environments. These deposits represent fluvial, tidal, estuarine, and coastal marine sediments. The sedimentological composition of these deposits is a mixture of unconsolidated, siliciclastic sediments, i.e., sands, silts, clay, gravel, boulders, and organics.

The variety of sub-surface geohazards identified from the UHRS data is typical for depositional settings at high latitudes. The main interpreted geohazards were: paleo channels, tunnel valleys, glaciotectionized sediments, gravel, faults, soft sediments, organics, amplitude anomalies, and lacustrine sediments definition is based on the identification and mapping of the most prominent reflectors and seismic facies shift that correspond to significant changes on depositional environments and sediment type. Seismic facies identification, internal reflector termination and geometry of the erosive surfaces are the basis for the unit's description, inferred depositional environments and sediment type. No type of subsurface ground truthing was incorporated into the present model. All units display a certain degree of vertical and horizontal variability and heterogeneity. This is due to intrinsic nature of the geological processes that took place, the rapidly changing environment and the great extent of the site. The interpretation derived from the geophysical data should be validated by means of ground sampling (bore hole, cone penetrometer test and any soil inspection technique). Key aspects to be investigated are (1) seismic units inferred soil composition, (2) geotechnical relevance of facies shift (laterally and vertically), (3) geotechnical relevance of internal erosive surfaces, (4) importance of linear features (channels) in terms of mechanical/lithological properties and its variability, (5) mechanical relevance of the identified deformation evidences (glaciotectionics, faults, folds), (6) importance of intra-formational negative impedance contrasts, (7) presence and potential hazard of the identified gas, (8) presence of constrains in engineering and site development (boulders, coarse sediments), (9) accuracy of used depth-conversion velocity model.

Not all existing contacts are detectable in the SSS data due to resolution, material, and orientation of the object.

11 | REFERENCES

- Andersen, L. T. 2004. The Fanø Bugt glaciotectionic thrust fault complex, southeastern Danish North Sea. Ph.D.Thesis 2004. Danmarks og Grønlands Geologiske Undersøgelse Rapport 2004/30: 35-68.
- Anthony, D. and Leth, J. O. 2001. Large-scale bedforms, sediment distribution and sand mobility in the eastern North Sea off the Danish west coast. *Marine Geology* 182 (2002) 247-263
- Anthony, D., Møller, I. 2003. The geological architecture and development of the Holmsland Barrier and Ringkøbing Fjord area, Danish North Sea Coast. *Geografisk Tidsskrift, Danish Journal of Geography* 102 27
- Behre, K-E, 2007. A new Holocene sea-level curve for the southern North Sea. Behre, K.-E. 2007 (January): A new Holocene sea-level curve for the southern North Sea. *Boreas*, Vol. 36, pp. 82-102.
- Bennike, O., Jensen, J.B., Konradi, P., Lemke, W. and Heinemeier, J. 2000. Early Holocene drowned lagoonal deposits from the Kattegat, southern Scandinavia. *Boreas*, Vol. 29, pp. 272-286.
- Bennike, O., Jensen, J.B., 1998. Late- and postglacial shore level changes in the southwestern Baltic Sea. *Bulletin of the Geological Society of Denmark*, Vol. 45, pp. 27-38.
- Dalgas E. 1867-1868. *Geografiske billeder fra Heden* (H. 1 & 2).
- Ehlers, J. 1990. Reconstructing the dynamics of the north-west European Pleistocene ice sheets. *Quaternary Science Reviews* 3: 1-40.
- Fugro 2014. Fugro Seacore Limited, Energinet.dk, April 2014. Preliminary Geotechnical Investigations. Vesterhav Syd Nearshore Wind Farm. Factual Report on Ground Investigation.
- Geoviden 2005. De seneste 150.000 år i Danmark. *Istidslandskabets og Naturens udvikling* , Nr. 2.
- Gregersen, S., Hjelm, J. & Hjortenberg, E.: Earthquakes in Denmark. *Bulletin of the Geological Society of Denmark*, Vol. 44, pp. 115-127. Copenhagen 1998- 02-28.
- Houmark-Nielsen M. 2007. Extent and age of Middle and Late Pleistocene glaciations and periglacial episodes in southern Jutland, Denmark. *Bull. Geol. Soc. Denmark* 55: 9-35.
- Høyer A-S., Jørgensen F., Piotrowski A. J., Jakobsen P. R. 2013. Deeply routed glaciotectionism in the western Denmark. Geological composition, structural characteristics and origin Varde Hill Island. *Jour. of Quat. Science* 28 (7): 683-696.
- Huuse, M., and Lykke-Andersen, H. 2000. Overdeepened Quaternary Valleys in the eastern Danish North Sea: morphology and origin; *Quaternary Science Reviews*, vol 19 (12)
- Huuse, M. and Lykke-Andersen, H. 2000b. Large-Scale glaciotectionic thrust structures in the eastern Danish North Sea Geological Society, London, Special Publications, 1010.1144/GSL.SP,2000.176.01.22. p293-305
- Jakobsen P. R. 2003. GIS based map of glaciotectionic phenomena. *Denmark Geological Quarterly* 47 (4): 331-338
- Japsen, P. 2000. Fra Kidthav til Vesterhav. Nordsobasinets udvikling vurderet ud fra seismiske hastigheder. *Geologisk Tidsskrift, hæfte 2*. pp. 1-36 København
- Japsen, P., Rasmussen, E.S, Green P.F., Nielsen L.H. and Bidstrup T 2008. Cenozoic palaeogeography and isochores predating the Neogene exhumation of the eastern North Sea Basin. *Geological Survey of Denmark and Greenland Bulletin* 15, 25-28.

Johannessen, P. N., Nielsen, L. H., Nielsen, L., Møller, I., Pejrup, M., Andersen, T. J., Korshøj, J., Larsen, B. and Piasecki, S. 2008. Sedimentary facies and architecture of the Holocene to Recent Rømø barrier island in the Danish Wadden Sea. Geological Survey of Denmark and Greenland Bulletin 15, 49–52.

Jørgensen, F., Sandersen, P.B.E. 2006. Buried and open tunnel valleys in Denmark erosion beneath multiple ice sheets. Quaternary Science Reviews 25, 1339–1363

Larsen, B., and Andersen, L. T. Andersen. 2005. Late Quaternary stratigraphy and morphogenesis in the Danish eastern North Sea and its relation to onshore geology. Netherlands Journal of Geosciences 84-2, 113-128.

Leth, J.O. 1996. Late Quaternary geological development of the Jutland Bank and the initiation of the Jutland Current, NE North Sea. Nor. Geol. Unders. Bull. 430, 25-34.

Leth, J.O., Larsen, B., Anthony, D., 2004. Sediment distribution and transport in the shallow coastal waters along the west coast of Denmark Geological Survey of Denmark and Greenland Bulletin 4, 41–44.

Michelsen, O. 1993. Structural development of the Fennoscandian Border Zone, offshore Denmark. Marine and Petroleum Geology Volume 10, 24-134.

Nicolaisen, J. F. 2010. (Editor): Marin råstof- og naturtypekortlægning i Nordsøen, Naturstyrelsen.

Nielsen, L. H. Johannesen, P. 2004. Skagen Odde – et fuldskala, naturligt laboratorium. Nyt Fra GEUS, nr 1.

Nielsen, T., Mathiesen, A. and Bryde-Auken, M. 2008. Base Quaternary in the Danish part of the North Sea and Skagerrak; Geological Survey of Denmark and Greenland Bulletin 15, 37-40

Novak, B. Duarte, H. and Leth J.O. 2015. Glaciotectonic thrust complex offshore Holmsland, the Danish North Sea. Abstract in The Quaternary Geology of the North Sea, Annual discussion Meeting of the Quaternary Research association UK, Edinburgh, January, 71.

Novak B. and Duarte H. 2018. Glaciotectonic thrust complex offshore Holmsland, the Danish North Sea - New Results. Presentation: Nordic Geologic Winter Meeting. DTU, Lyngby, DK 2018.

Novak B., Pedersen G. K. 2000. Sedimentology, seismic facies and stratigraphy of a Holocene spit-platform complex interpreted from high-resolution shallow seismics, Lysegrund, southern Kattegat, Denmark. Marine Geology 162, 317–335.

Novak, B. and Bjørck S. 2002. Late Pleistocene–early Holocene fluvial facies and depositional processes in the Fehmarn Belt, between Germany and Denmark, revealed by high-resolution seismic and lithofacies analysis. Sedimentology, 49, 451–465

Pedersen, S. A. S. 2005. Structural analysis of the Rubjerg Knude glaciotectonic complex, Vendsyssel, Northern. Denmark. Geol. Surv. of Denmark, Bulletin 8.

Rasmussen, E. S., Dybkjær K., Piasecki S. 2010. Lithostratigraphy of the Upper Oligocene–Miocene succession of Denmark. Geological Survey of Denmark and Greenland Bulletin 22: 1–92.

Robertson, P., Campanella, R., Gillespie, D., & Greig, J. (1986). Use of Piezometer Cone. In-situ'86, Use of In-situ testing in Geotechnical Engineering, GSP 6, ASCE, Reston, 1263 - 1280.

Sandersen, P. B. E., Jørgensen F. 2003. Buried Quaternary valleys in western Denmark occurrence and inferred implications for groundwater resources and vulnerability. Journal of Applied Geophysics 53: 229– 248

Sjørring, S., Frederiksen, J. 1980. Glacialstratigrafiske observationer i de vestjyske bakkeøer. Dansk Geologisk Forenings Årsskrift 1979: 63–77.

Smed, P., 1979. Landskabskort over Danmark, Blad 1, Nordjylland. Geografforlaget, Brenderup, Denmark.

Smed, P., 1981. Landskabskort over Danmark, Blad 2, Midtjylland. Geografforlaget, Brenderup, Denmark.

Sorgenfrei, T. & Buch, A.; 1964; Deep Tests in Denmark 1935/1959. Geological Survey of Denmark, III. Series 36, Copenhagen

Vaughan-Hirsch, D.P., Phillips, E.R. 2017. Mid-Pleistocene thin-skinned glaciotectionic thrusting of the Aberdeen Ground Formation, Central Graben region, central North Sea. Journal Of Quaternary Science, 32(2) 196–212

Vejbæk, O. V. 1997. Dybe strukturer i danske sedimentære bassiner. Geologisk Tidsskrift, hæfte 4, pp. 1-31. København, 12-16.

Vejbæk, O.V., Bidstrup, T., Erlström, M, Rasmussen, E. S. and Sivhed, M. 2007. Chalk depth structure map Central to East North Sea, Denmark. GEUS. Geological Survey of Denmark and Greenland Bulletin 13, 9-12.

12 | DATA INDEX

The deliverables listed in Table 30 accompany this report.

Table 30 Deliverables.

Item	Group	Data Product
1	Bathy data	Bathymetry - Un-gridded soundings, (X,Y,Z) values in ASCII format.
2	Bathy data	Bathymetry - Gridded soundings, 0.25m resolution, (X,Y,Z) values in ASCII format (tiled following the UTM grid).
3	Bathy data	Bathymetry - Gridded soundings, 0.25m resolution, GeoTiff stored in esri file geodatabase (untiled).
8	Bathy data	Bathymetry - Bathymetric contour curves with 50cm interval, as TSG object CONTOURS_LIN
9	Bathy data	Bathymetry - Vessel tracks, as TSG object TRACKS_LIN, indicate equipment carrier and equipment type in attributes.
10	Bathy data	Bathymetry - TVU 1.00 m resolution, (X,Y, TVU) values in ASCII format
11	Bathy data	Bathymetry - TVU 1.00 m resolution, GeoTiff stored in esri file geodatabase
12	Bathy data	Bathymetry - THU 1.00 m resolution (X,Y,THU) values in ASCII format
13	Bathy data	Bathymetry - THU 1.00 m resolution, GeoTiff stored in esri file geodatabase
14	Bathy data	Bathymetry - backscatter 32bit GeoTiff stored in esri file geodatabase (amplitude populated channels)
15	Bathy data	SVP - sound velocity profiles as SVP comparison spreadsheet
16	Bathy data	MBES - Anomaly target list, as TSG object MBES_ANOMALY_PTS, anomaly characteristics provided in attributes.
20	SSS data	SSS instrument tracks, as TSG object TRACKS_LIN, indicate equipment carrier and equipment type in attributes
21	SSS data	SSS Anomaly target list, as TSG object SSS_ANOMALY_PTS, anomaly characteristics provided in attributes.
NA	SSS data	Mosaic GeoTiff (also within GIS) - Additional delivery
23	Mag data	MAG measurements, CSV-format
24	Mag data	MAG instrument tracks, as TSG object TRACKS_LIN, indicate equipment carrier and equipment type in attributes
25	Mag data	MAG Anomaly target list, as TSG object MAG_ANOMALY_PTS, anomaly characteristics provided in attributes
29	SBP & 2DUHRS data	SBP and UHRS Anomaly target list, as TSG object SBP_ANOMALY_PTS, anomaly characteristics provided in attributes.
31a	SBP & 2DUHRS data	Generated elevation grids relative to vertical datum for each interpreted horizon in 5 m resolution as GeoTiff grid

Item	Group	Data Product
31b	SBP & 2DUHRS data	Generated elevation grids relative to vertical datum for each interpreted horizon in 5 m resolution as (X,Y,Z) values in ASCII format (Z as the horizon elevation in meter)
32a	SBP & 2DUHRS data	Generated depth below seabed (BSB) grids for each interpreted horizon in 5 m resolution as GeoTiff grid
32b	SBP & 2DUHRS data	Generated depth below seabed (BSB) grids for each interpreted horizon in 5 m resolution as (X,Y,Z) values in ASCII format (Z as the horizon depth BSB in meter)
33a	SBP & 2DUHRS data	Generated Isochore (layer thickness) grids for each interpreted soil unit in 5 m resolution as GeoTiff grid
33b	SBP & 2DUHRS data	Generated Isochore (layer thickness) grids for each interpreted soil unit in 5 m resolution as (X,Y,Z) values in ASCII format (Z as the layer thickness in meter)
35	Grab sampling data	Grab sample positions, as TSG object GEOTECHNIC_PTS, indicate sampling characteristics in attributes.
36	Grab sampling data	Grab sample classification, MS-Excel spread sheet
37	Grab sampling data	Grab sample laboratory analysis, overview table and result tables, MS-Excel spread sheet.
38	Integrated seabed interpretation data	Seabed Surface Geology, as TSG object SEABED_GEOLOGY_POL, indicate surface geological unit in attributes
39	Integrated seabed interpretation data	Seabed Surface Features, as TSG object SEABED_SURFACE_PTS, indicate surface forms in attributes
40	Integrated seabed interpretation data	Seabed Surface Features, as TSG object SEABED_SURFACE_LIN, indicate surface forms in attributes
41	Integrated seabed interpretation data	Seabed Surface Features, as TSG object SEABED_SURFACE_POL, indicate surface forms in attributes
42	Integrated seabed interpretation data	Seabed Substrate type, as TSG object SEABED_SUBSTRATE_POL, indicate substrate type in attributes.
43	Integrated seabed interpretation data	Man-Made-Objects, as TSG object MMO_PTS, indicate MMO type in attributes.
44	Integrated seabed interpretation data	Man-Made-Objects, as TSG object MMO_POL, indicate MMO type in attributes.
45	Integrated seabed interpretation data	Man-Made-Objects, as TSG object MMO_LIN, indicate MMO type in attributes.
47	Report	Geophysical site survey Report (charts as enclosures)

APPENDIX A 	LIST OF PRODUCED CHARTS
APPENDIX B 	CONTACT AND ANOMALY LIST
APPENDIX C 	GRAB SAMPLE LAB REPORT
APPENDIX D 	2D UHRS PROCESSING REPORT